Mathematical modelling of image processing problems : theoretical studies and applications to joint registration and segmentation

Noémie Debroux

▶ **To cite this version:**

Noémie Debroux. Mathematical modelling of image processing problems : theoretical studies and applications to joint registration and segmentation. Modeling and Simulation. Normandie Université, 2018. English. NNT : 2018NORMIR02 . tel-01834573

HAL Id: tel-01834573
https://theses.hal.science/tel-01834573

Submitted on 10 Jul 2018

HAL is a multi-disciplinary open access archive for the deposit and dissemination of scientific research documents, whether they are published or not. The documents may come from teaching and research institutions in France or abroad, or from public or private research centers.

L'archive ouverte pluridisciplinaire **HAL**, est destinée au dépôt et à la diffusion de documents scientifiques de niveau recherche, publiés ou non, émanant des établissements d'enseignement et de recherche français ou étrangers, des laboratoires publics ou privés.

Normandie Université

THESE

Pour obtenir le diplôme de doctorat

Spécialité Mathématiques Appliquées 420004

Préparée au sein de l'Institut National des Sciences Appliquées de Rouen Normandie

Mathematical Modelling of Image Processing Problems : Theoretical Studies and Applications to Joint Registration and Segmentation.

Présentée et soutenue par
Noémie DEBROUX

Thèse soutenue publiquement le 15/03/2018 devant le jury composé de		
M. Simon MASNOU	Professeur, Université de Lyon 1	Rapporteur
Mme Carola SCHÖNLIEB	Professeur, University of Cambridge	Rapporteur
M. Benedikt WIRTH	Professeur, Universität Münster	Rapporteur
Mme Carole LE GUYADER	Professeur, INSA Rouen	Directrice de thèse
M. Christian GOUT	Professeur, INSA Rouen	Examinateur
M. Charles KERVRANN	Directeur de Recherche INRIA, INRIA de Rennes	Examinateur
M. Gabriel PEYRÉ	Directeur de Recherche CNRS, Université Paris-Dauphine et École Normale Supérieure	Président du jury
Mme Luminita VESE	Professeur, University of California, Los Angeles	Examinateur

Thèse dirigée par Mme Carole LE GUYADER, Laboratoire de Mathématiques de l'INSA de Rouen Normandie – LMI (EA 3226)

INSA INSTITUT NATIONAL DES SCIENCES APPLIQUÉES ROUEN NORMANDIE

MI∫IΣ

LMI - EA 3226

Résumé:

Dans cette thèse, nous nous proposons d'étudier et de traiter conjointement plusieurs problèmes phares en traitement d'images incluant le recalage d'images qui vise à apparier deux images via une transformation, la segmentation d'images dont le but est de délimiter les contours des objets présents au sein d'une image, et la décomposition d'images intimement liée au débruitage, partitionnant une image en une version plus régulière de celle-ci et sa partie complémentaire oscillante appelée texture, par des approches variationnelles locales et non locales. Les relations étroites existant entre ces différents problèmes motivent l'introduction de modèles conjoints dans lesquels chaque tâche aide les autres, surmontant ainsi certaines difficultés inhérentes au problème isolé. Le premier modèle proposé aborde la problématique de recalage d'images guidé par des résultats intermédiaires de segmentation préservant la topologie, dans un cadre variationnel. Un second modèle de segmentation et de recalage conjoint est introduit, étudié théoriquement et numériquement puis mis à l'épreuve à travers plusieurs simulations numériques. Le dernier modèle présenté tente de répondre à un besoin précis du CEREMA (Centre d'Études et d'Expertise sur les Risques, l'Environnement, la Mobilité et l'Aménagement) à savoir la détection automatique de fissures sur des images d'enrobés bitumineux. De part la complexité des images à traiter, une méthode conjointe de décomposition et de segmentation de structures fines est mise en place, puis justifiée théoriquement et numériquement, et enfin validée sur les images fournies.

Abstract:

In this thesis, we study and jointly address several important image processing problems including registration that aims at aligning images through a deformation, image segmentation whose goal consists in finding the edges delineating the objects inside an image, and image decomposition closely related to image denoising, and attempting to partition an image into a smoother version of it named cartoon and its complementary oscillatory part called texture, with both local and nonlocal variational approaches. The first proposed model addresses the topology-preserving segmentation-guided registration problem in a variational framework. A second joint segmentation and registration model is introduced, theoretically and numerically studied, then tested on various numerical simulations. The last model presented in this work tries to answer a more specific need expressed by the CEREMA (Centre of analysis and expertise on risks, environment, mobility and planning), namely automatic crack recovery detection on bituminous surface images. Due to the image complexity, a joint fine structure decomposition and segmentation model is proposed to deal with this problem. It is then theoretically and numerically justified and validated on the provided images.

Remerciements

À travers ces quelques mots, je souhaite remercier l'ensemble des personnes qui ont participé à l'élaboration de cette thèse.

Je tiens tout d'abord à exprimer ma plus profonde gratitude à Carole Le Guyader, ma directrice de thèse, sans qui ce manuscrit n'aurait jamais vu le jour. Elle a toujours su me guider au cours de ces trois années de doctorat par sa pédagogie, sa grande culture scientifique, son intestimable expertise et sa rigueur mathématique. J'aimerais aussi souligner ses grandes qualités humaines, sa gentillesse, sa générosité et son soutien inébranlable. Ce fut un réel plaisir de travailler sous sa direction sur des sujets complexes, riches et variés. Pour tout cela, je lui adresse mille mercis.

Je remercie également l'ensemble des rapporteurs Simon Masnou, Carola Schönlieb, et Benedikt Wirth de m'avoir fait cet honneur, et d'avoir pris le temps d'examiner mon travail. Leur expertise et leurs précieux conseils ont permis d'améliorer grandement ce manuscrit. Je suis en outre reconnaissante aux examinateurs qui m'ont fait l'honneur de participer à mon jury : Christian Gout, Charles Kervrann qui m'a fait découvrir le domaine passionnant de la recherche en traitement d'images au cours d'un stage très enrichissant au sein de son équipe, Gabriel Peyré et Luminita Vese.

Par ailleurs, je remercie Nicolas Forcadel et Christian Gout, les directeurs du Laboratoire de Mathématiques de l'INSA de Rouen Normandie, pour leur accueil chaleureux, leur disponibilité et leur soutien. J'adresse ma plus sincère reconnaissance à l'ensemble des membres du laboratoire et particulièrement aux doctorants et post-doctorants qui ont partagé cette expérience avec moi : Wilfredo Salazar pour son écoute, Imène pour sa gentillesse, Adriano pour sa bonne humeur, et Rym pour sa sympathie. J'adresse ma plus grande sympathie à Emmanuelle, Chetna et Marie pour leur enthousiasme, leur amitié et leur dynamisme. Je remercie aussi Solène pour ses précieux conseils et pour ses codes de calculs qui m'ont beaucoup aidée à débuter cette thèse. J'adresse également un merci particulier aux personnes ayant égayé les pauses déjeuner : à Omar dont l'humeur est toujours joviale, à Brigitte dont la prévenance est à toutes épreuves, à Carole dont la sagesse n'a d'égale que sa bonté, à Arnaud et à Bruno dont les discussions passionnées pimentent les déjeuners, et à Samia dont l'enthousiasme et le dynamisme sont admirables.

De plus, j'exprime un merci tout particulier aux membres du centre Becquerel, à Ca-

roline Petitjean, à Su Ruan, ainsi qu'à Cyrille Fauchard, à Denis Jouin, à Rafael Antoine et à l'ensemble des collaborateurs du CEREMA pour leurs discussions enrichissantes, les problèmatiques très intéressantes et pertinentes qu'ils ont pu soulever et qui ont motivé une partie de mes recherches, mais aussi pour les données fournies qui ont permis d'alimenter grandement ces travaux de thèse.

Je témoigne aussi ma plus profonde gratitude à Luminita Vese pour son accueil chaleureux, sa bienveillance, ses précieux et judicieux conseils. J'espère que nous aurons l'occasion de collaborer à nouveau. J'exprime également ma reconnaissance à Patrick Bousquet-Melou et à toute l'équipe du CRIANN dont les suggestions ont grandement optimisé les codes de calcul et aux étudiants Nathan Rouxelin, Timothée Schmoderer, Emeric Quesnel pour leur intérêt scientifique et pour leur participation au hackathon.

Je remercie en outre Isabelle Lamitte pour son aide précieuse dans mes recherches bibliographiques. Brigitte Diarra et Sandra Hague ont toujours su me guider avec efficacité dans les méandres de l'administration française et pour cela je les remercie sincèrement.

D'autre part, je suis particulièrement reconnaissante à l'équipe pédagogique du premier cycle dont Jean-Marc Cabanial, Guillaume Duval, Carole Le Guyader et Antoine Tonnoir pour la confiance qu'ils m'ont accordée pendant mes missions d'enseignements et qui ont rendu avec les étudiants des groupes I, J, C et D cette première experience d'enseignement très enrichissante.

Pour finir, je tiens à remercier ma famille, mes grand-parents, mes parents et ma soeur pour leur soutien inconditionnel, leurs encouragements et leur positivité. Ils ont participé plus qu'ils ne le croient à l'aboutissement de cette thèse et pour cela je leur témoigne ma plus grande affection et toute ma reconnaissance.

Sommaire

1 Introduction **1**
- 1 Digital image processing introduction . . . 1
- 2 Image registration . . . 2
- 3 Image segmentation . . . 9
- 4 Joint image segmentation and image registration . . . 14
- 5 Texture modelling and image decomposition . . . 18
- 6 Contributions and thesis organization . . . 21
- 7 Scientific outreach . . . 22

2 Mathematical background **34**
- 1 Functional spaces . . . 34
  - 1.1 L^p spaces . . . 34
  - 1.2 Sobolev spaces . . . 38
  - 1.3 Fractional Sobolev spaces . . . 42
  - 1.4 BV space and its subsets . . . 45
- 2 Viscosity solution theory . . . 47
  - 2.1 Framework for second order degenerate parabolic equations . . . 47
  - 2.2 General framework for nonlocal and nonlinear parabolic equations . . . 50
- 3 Calculus of variations . . . 52
  - 3.1 Carathéodory, convex, polyconvex, quasiconvex and rank one convex functions . . . 52
  - 3.2 Direct method in the calculus of variations . . . 54
  - 3.3 Γ-convergence . . . 56
- 4 Tridimensional elasticity . . . 57

3 A nonlocal topology-preserving segmentation guided registration model **61**
- 1 Introduction . . . 61
- 2 Mathematical modelling . . . 63
  - 2.1 General mathematical background . . . 63
  - 2.2 Regularization on the deformation . . . 64
  - 2.3 Alignment measure . . . 65
  - 2.4 Overall functional . . . 66
- 3 Theoretical results . . . 67

3.1 Mathematical obstacle and derivation of the associated relaxed problem . . . 67
3.2 Existence of minimizers and relaxation theorem . . . 69
3.3 Well-definedness of $\tilde{\Phi}$ . . . 69
4 Numerical Method of Resolution . . . 72
4.1 Asymptotic behavior of a penalization method in the continuous domain . . . 72
4.2 Discrete counterpart of the quadratic penalty method . . . 73
4.3 Actual algorithm associated with the quadratic penalty method . . . 84
4.4 Augmented Lagrangian method . . . 89
4.5 Actual Augmented Lagrangian algorithm . . . 97
5 Numerical Experiments . . . 99
5.1 Regridding technique and choice of the parameters . . . 99
5.2 Letter C . . . 100
5.3 Mouse brain gene expression data . . . 101
5.4 Slices of the brain . . . 103
5.5 MRI images of cardiac cycle . . . 103
5.6 Tumor . . . 104
6 Conclusion . . . 104

4 A nonlocal joint segmentation/registration model 113
1 Introduction . . . 113
2 Mathematical modelling . . . 115
2.1 Depiction of the model . . . 115
2.2 Theoretical results . . . 121
3 Numerical method of resolution . . . 125
4 Experimental results . . . 152
4.1 Qualitative assessment of the proposed model . . . 152
4.2 Quantitative and qualitative assessment of the functional components 167

5 A second order free discontinuity model for bituminous surfacing crack recovery 177
1 Introduction . . . 177
2 Local mathematical modelling and analysis . . . 180
2.1 Model . . . 180
2.2 Existence of minimizers . . . 182
2.3 Existence of solutions for the Euler-Lagrange equations . . . 184
2.4 Asymptotic results . . . 195
3 A nonlocal version of the modelling and its theoretical analysis . . . 199
3.1 Motivations . . . 199
3.2 Notations and preliminary results . . . 201
3.3 Connection to the local imaging problem . . . 205
4 Numerical Experiments . . . 221
4.1 Sketch of the local algorithm . . . 221

4.2 Sketch of the nonlocal algorithm 224
4.3 MPI parallelization 228
4.4 Numerical simulations 233

6 Conclusion and perspectives **247**

Chapter 1

Introduction

1 Digital image processing introduction

Since the first photograph taken by Joseph Nicéphore Niépce in 1826, imaging has kept developing itself, and the invention of modern computers in the 1940's followed by the apparition of digital images in the 1990's have reached a milestone. We refer the reader to [82] for an insight of the philosophy change it represented and the close connection between mathematics and image processing. Imaging and image processing have thus become an essential field in a growing number of applications including medical imaging, astronomy, astrophysics, surveillance, and video to name a few.
Images are now processed by computer as two-dimensional tables and mathematical modellings have turned out to be requisite (see [7, Introduction], [105, Introduction]). Indeed an image is seen as a discrete function $u : \{1, \dots, M\} \times \{1, \dots, N\} \mapsto \{0, \dots, 255\}^k$ representing the intensity of the image at the pixel location (i, j) with $k = 1$ for a grayscale image (see Figure 1.1 coming from `http://images.math.cnrs.fr/Le-traitement-numerique-des-images.html`, Peyré) and $k = 3$ for a color image (Red Green Blue) (see Figure 1.2 coming from `http://images.math.cnrs.fr/Le-traitement-numerique-des-images.html`, Peyré).

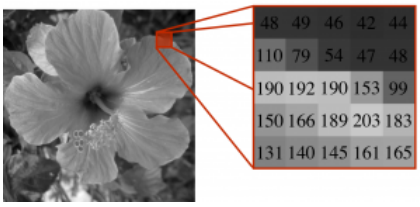

Figure 1.1: Grayscale image representation.

Since the images are usually digital representations of visual perception, they can be as complicated as the scenes they depict and may exhibit several geometrical structures including a wide range of shapes, patterns, scales and even randomness as stressed by

Figure 1.2: Color image representation.

Schaeffer in [91, Introduction]. Following [105], modern image handling can be divided into four categories:

1. image acquisition or sensing (*output: digital image*): it requires physical sensors to catch the energy radiated by the object we want to image, and a digitizer to convert that information into digital form. It often happens that the acquisition produces raw data in a transformed domain such as Fourier domain for Magnetic Resonance Images (MRI) or Radon domain for Computed Tomography (CT) images leading to a reconstruction step (see [82]).

2. image processing or low-level vision (*input: image, output: image*): it includes image enhancing (see [41]), denoising and deblurring (see [89] and [13]), inpainting to fill in the missing data (see [92]), compression and super-resolution (see [33]). The main goal is to improve the quality of the observed data to facilitate further analysis and understanding of the scene.

3. image analysis or mid-level vision (*input: image, output: image components*): it encompasses morphological processing (extracting useful constituents describing shapes) and image segmentation. We will get a closer look at segmentation models in the following.

4. image understanding or high level vision (*input: boundaries, regions, output: image attributes*): it generally follows the previous step and consists in assigning a meaningful label to an object, based on the features and descriptors previously extracted. It is also known as pattern recognition and this field is booming thanks to machine learning algorithms among others.

We now concentrate upon the imaging tasks that constitute the core of this work and highlight the guiding principle of this thesis, namely the combination of two or more processes into a single framework in order to reinforce each of them, using nonlocal methods.

2 Image registration

Image registration, also called image fusion, image matching or image warping according to the applications, aims to align two or more images. In this work, we will focus

on the registration of a pair of images. So given two images called Template (moving image or source; T) and Reference (fixed image or target; R), it consists in determining an optimal transformation/deformation φ in a way to be determined and clarified later, that maps the Template into the Reference. It is an essential tool in image processing when complementary information is encountered in several images, such as images acquired at different times, from different viewpoints, or by different sensors to name a few. Therefore, it has a strong potential clinical impact with a wide range of applications as stressed in [98] and [76]: shape tracking; fusion of anatomical images from Computerized Tomography (CT) or Magnetic Resonance Imaging (MRI) images, with functional images from Positron Emission Tomography (PET), Single-Photon Emission Computed Tomography (SPECT) or Functional Magnetic Resonance Imaging (fMRI), also called multi-modality fusion to facilitate intervention and treatment planning; computer-aided diagnosis and disease follow-up; surgery simulation; atlas generation to integrate anatomic, genetic and physiological observations from multiple patients into a common space and conduct statistical analysis; radiation therapy; assisted/guided surgery; anatomy segmentation; computational model building and image subtraction for contrast enhanced images.

According to the applications, we can distinguish several criteria influencing the modelling such as the modality of the involved images, and the nature of the transformation. Indeed, if the Template and the Reference share the same modality, then the registration process aims at aligning both geometrical features and intensity level distribution, whereas for images acquired through different mechanisms, the goal is to match salient components or shapes while keeping the information contained in both images, impacting then the "optimal" definition. Besides, if the deformation involves only translations and/or rotations, we can proceed to rigid registration, simplifying both the problem and the accuracy quantification by sharply reducing the deformation degrees of freedom (see [76] for an overview of these methods); otherwise we deal with deformable/nonrigid registration and the accuracy evaluation becomes very challenging (see [88]) yielding a drawback for deep-learning inspired methods (see [108]). In the following we will focus on the deformable registration processes.

Many researches have been carried out to address this issue and in a recent survey [98], Sotiras *et al.* provide an extensive overview of existing non-rigid medical image registration models in a systematic manner, by identifying what they believe to be the main components of such models and by thoroughly and independently analyzing them.

In a variational formulation, the aim of registration is to find the best deformation that optimizes a specifically designed cost function encompassing a measure of alignment between the deformed Template and the Reference, and a regularization of the sought deformation. The latter is required since the problem is ill-posed according to Hadamard's definition since the number of unknowns is greater than the number of constraints, leading to an under-constrained problem from a mathematical point of view (see [98]). The mathematical challenges of registration models come also from the non-linearity and the non-convexity of the cost functions and their high dependency to the considered applica-

tion. For instance, different organs do not have the same ability to deform. Also we have already discussed the dependence of the problem definition on the modality of the images involved and finally, the clinical setting greatly influences the modelling since for computer assisted surgery, the registration is to be done between the patient and the image, which is different in nature to the matching of two images. Thus according to Sotiras *et al.* [98], an image registration algorithm consists of three main components:

1. a deformation model delimiting the desirable and acceptable/admissible deformations by describing the setting in which they are viewed and interpreted;

2. an objective function whose description has already been given and in which the regularization is intimately related to the deformation model;

3. an optimization strategy playing an important role in the accuracy of the final results obtained by the algorithm.

Following their strategy, we will now present some registration models.

The deformation model actually motivates the way the transformation φ is built and entails a crucial compromise between computational efficiency and richness of the description. Three main strategies are identified in [98]:

(a) analogy with physical models and following [70], 5 subcategories can be identified:

   i. the elastic body models in which the shapes to be wrapped are considered as observations of the same elastic body before and after being under the influence of forces. For linear models, the Navier-Cauchy partial differential equation (PDE) describes the displacements u ($\mu\nabla^2 u + (\lambda + \mu)\nabla(\nabla.u) + F = 0$), where F is the force field driving the alignment process, λ is the first Lamé's coefficient, and μ is the second one also known as shear modulus measuring the rigidity or the ratio of the shear stress to the shear strain. It is also subject to the validity of Hooke's law imposing proportionality between forces and displacements. In [12], Broit is the first to propose this analogy and the image grid is seen as an elastic membrane constrained by an external force ensuring the matching of shapes, and an internal one enforcing the elastic properties until an equilibrium is reached. Then many alternatives have been proposed including the work of Davatzikos in [26] where the salient features to be matched are considered as an inhomogeneous elastic object allowing some regions to deform more than others thanks to spatially varying elasticity parameters. However, the main drawback of these linear models resides in their assumption of small strains and so small displacements according to Hooke's law. It is thus not suitable when dealing with large deformations and to circumvent this limitation, the linear elasticity framework is changed into the non-linear elasticity one. Especially, hyperelasticity has been widely used as highlighted by Sotiras *et al.* in [98] since rubber, filled elastomers, and biological tissues are often modelled by hyperelastic materials. In [84], the analogy is made with an isotropic (uniformity in all orientations), homogeneous

(same properties at every point), and hyperelastic (ability of undergoing large deformations while keeping elastic behavior ([23])) Saint Venant-Kirchhoff material. The inverse consistency ensuring that when swapping the Template and the Reference the algorithm does actually estimate the inverse transformation, is guaranteed by the use of log-Euclidean metrics leading to Riemannian elasticity. Yanikovsky *et al.* in [115] also use the stored energy function of a Saint Venant-Kirchhoff material and the symmetry is forced by assuming the Jacobian determinant of the deformation follows a log-normal distribution with zero mean after log-transformation. In [34], the authors propose complementing the stored energy function of a Saint Venant-Kirchhoff material by a term controlling the Jacobian determinant of the deformation in order to prevent the deformation map from exhibiting growths or shrinkages that are too large.
In [86], the authors devise a registration model handling large deformations using local linearization and the finite element method to solve the nonlinear equation. In [37], and [90], the authors consider hyperelastic Ogden materials with a polyconvex stored energy function, constraining the length (through $\|\nabla\varphi\|$), the area (thanks to $\|\mathrm{Cof}\nabla\varphi\|$), and the volume (using $\det\nabla\varphi$) of the deformation. A similar regularization is adopted in [14], where Burger *et al.* focus on the numerical implementation employing a discretize-then-optimize approach involving the partitioning of voxels to 24 tetrahedra.

ii. the viscous fluid flow models. The deformation is then built as a viscous fluid ruled by the Navier-Stokes equation in its simplified version with a very low Reynold's number (named viscous fluid flow models): $\mu_f\nabla^2 v + (\mu_f + \lambda_f)\nabla(\nabla.v) + F = 0$, where v is the velocity field related to the displacement field as $v(x,t) = \partial_t u(x,t) + \langle\nabla u(x,t),\, v(x,t)\rangle$ and F the chosen similarity measure. The time is explicitly introduced and an equilibrium is reached. Theoretically, these models can cope with large deformations by integrating v over time. The model developed by Christensen *et al.* in [20] falls within this framework. For each time interval a successive over-relaxation scheme is used and the preservation of topology is achieved by a regridding step. However it is computationally inefficient and the authors propose a highly parallel implementation to overcome this difficulty.

iii. the diffusion models. Inspired by optical flow models and especially Maxwell's demons, some algorithms have been proposed in which the regularization of the deformation is provided by convolutions with the Gaussian kernel corresponding to the Green's function of the diffusion equation $\Delta u + F = 0$. Demons are actually effectors that locally push the image towards its final destination. The standard scheme described in [98] consists in selecting all image elements as demons, computing demon forces using the optical flow constraint, assuming a nonparametric deformation model regularized by applying a Gaussian filter after each iteration and a trilinear interpolation scheme. In [102], Thirion develops an iterative approach encompassing the estimation of the demons forces and the update of the deformation based on the calculated forces. Then a huge amount of variants but still using this iterative scheme has been developed ([43] combination of demons

algorithms with a fully convolutional neural network giving a tight upper bound of the sum of squared differences) despite a lack of theoretical understanding. In [39], Fischer and Modersitzki explain it and give an insight into its working by providing a fast algorithm based on the linearization of the diffusion PDE and connecting it to Thirion's algorithm.

iv. the curvature models in which the deformation satisfies the equilibrium equation $\Delta^2 u + F = 0$. In [40], Fischer *et al.* try to minimize the deformation curvature using this constraint ensuring its smoothness. The biharmonic Euler-Lagrange equation is solved using a semi-implicit iterative finite difference scheme.

v. the flows of diffeomorphisms. The velocity of the deformation over time is assumed to follow the Lagrange transport equation and the regularization term becomes $\int_0^1 \|v(t)\|_V^2 \, dt$ where $\|v\|_V = \|Dv\|_{L^2}$ associated with Gaussian kernels. This framework known as Large Deformation Diffeomorphic Metric Mapping (LDDMM) originally developed in [10] allows large deformations and a distance definition and we refer the reader to [118] for an overview of its evolution. Also Haker *et al.* [48] apply the Monge-Kantorovich theory of optimal mass transport to image registration based on a partial differential equation approach to the minimization of the L^2 Kantorovich-Wasserstein functional under a mass preservation constraint. Recently in [65], Maas *et al.* propose a model for image morphing in an optimal transport framework and with a relaxation on the mass preservation constraint.

(b) interpolation or approximation driven strategy. The deformation is restricted to a parameterizable set. It is considered to be known on a reduced set and then interpolated on the image pixel grid or smoothly approximated by assuming errors can be made in the estimated displacements on the whole domain. The family of interpolation strategy includes: radial basis functions ([119]) but due to their global support a sufficient amount of landmarks is needed; elastic body splines inspired by both interpolation theory and by physical models, introduced by Davis *et al.* in [27] and that appear as solutions to the Navier-Cauchy equilibrium equation for homogeneous isotropic elastic body subject to forces; free-form deformations in which a rectangular grid is superimposed on the image pixel grid and is deformed while the deformation on the finer image pixel grid is recovered using a summation of tensor of univariate splines in [93] and B-splines for their local support and smoothness in [29] and [121]; basis functions from signal image processing inspired by Fourier, Wavelet and Cosine transforms (in [6] a linear combination of Discrete Cosine Transform is used); and piecewise affine model combined with a multiscale approach in [50]. These models are rich enough to describe the transformation while having low degrees of freedom.

(c) inclusion of a-priori knowledge through statistical constraints or through biomechanical/biophysical models. For instance, in [24] a biomechanical model of breast tissue is added to constrain the deformation field.

Further constraints can be added to the model to ensure inverse consistency as in [116], symmetry, topology preservation ([52], [81], [20], [73], [74]), volume preservation ([47]),

lower and upper bounds on the Jacobian determinant ([56]),...

The second fundamental component of a registration algorithm is a matching criterion which can be divided into three groups depending on the way the data are exploited to drive the registration process. Ideally, it should be derived in order to comply with the nature of the observations and the emphasis should be put on the alignment of geometrical structures. It should also be convex for accurate inference and so an important balance should be found between these conditions, as underlined in [98]. Sotiras *et al.* highlighted the three following categories of matching criteria:

(a) geometric methods: they aim to register images based on the alignment of some landmarks which can be reliable anatomical locations for instance (see [22] for a segregation of methods according to their inferences: correspondences, spatial transformations, both). These methods have led to lots of works on the detection of points of interest.

(b) iconic methods: they include intensity-based methods ([34] based on the sum of squared differences between the deformed Template intensity values and the ones of the Reference), attribute-based methods ([94] using a set of moment invariants reflecting the underlying anatomy at different scales), and information-theoretic approaches ([111] aiming at maximizing the mutual information between the deformed Template and the Reference). We refer the reader to [54] for an overview of these matching criteria. Both mono and multi-modal registration frameworks are addressed but monomodal registration is clearly easier to handle. Thus recent works focus on the reduction to monomodal registration. In [19], the authors use image synthesis to create proxy images and then apply a mono-modal registration method. In [2], the authors propose to generate an implicit atlas to which each of the images will be registered in the native image space.

(c) hybrid methods: they summarize both types of approaches as in [56] in which the authors propose a dissimilarity measure based on intensity comparison and landmark alignment via a quasi-conformal map.

Finally, the optimization method plays an important role in the registration accuracy and we can distinguish the following types:

(a) continuous methods in which the variables are assumed to take real values and the objective function to be differentiable including gradient descent ([10]), conjugate gradient ([69]), Newton-type methods ([109]), Levenberg-Marquardt methods ([35]) and stochastic gradient descent methods ([111]).

(b) discrete methods. They perform a global search and exhibit better convergence rates than continuous ones but reduce to problems where the variables take discrete values. They comprise graph-based methods ([101]) and belief propagation approaches([49]).

(c) miscellaneous methods: greedy approaches and evolutionary algorithms.

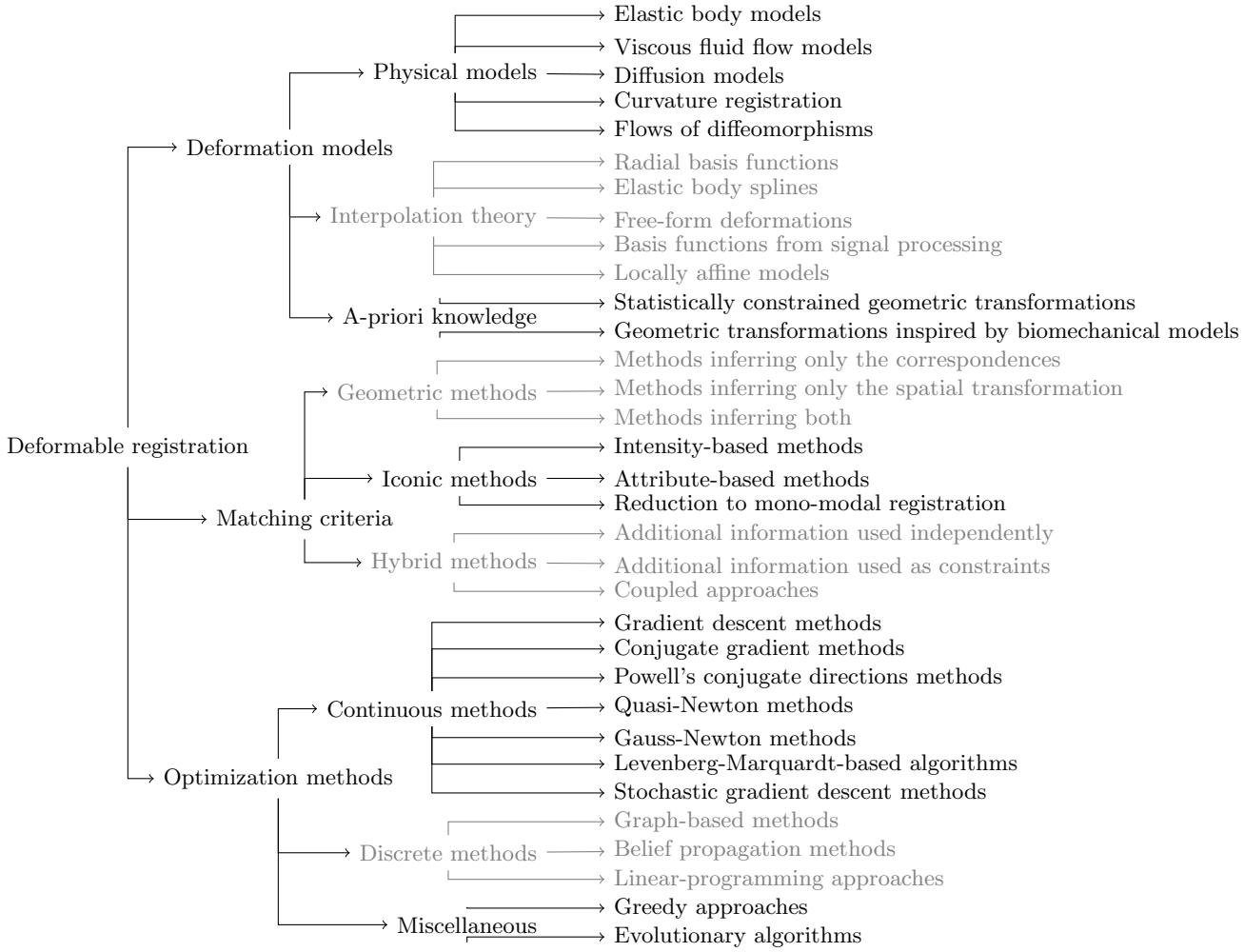

Figure 1.3: Classification of deformable registration processes inspired by [98].

In Figure 1.3, we summarize the classification of deformable registration methods depicted above.
In [54], the authors draw up an inventory of all the open-source registration software available and compare them. However as stressed by Rohlfing in [88], the question of measuring the accuracy of a registration process remains a hard one and image similarity and tissue overlap should be used carefully as such.

Besides, more and more efficient machine learning algorithms addressing the issue of image registration have appeared in the last few years such as the RegNet convolutional neural network architecture developed by Sokooti *et al.* in [97] to directly estimate the displacement vector field of a pair of input images. The training is done using a large set of artificially generated displacement vector fields and does not explicitly define a dissimilarity metric. However, these methods do not constitute the core of this thesis since the emphasis is put on variational methods.

Let us now introduce a closely related fundamental image processing task: image segmentation, that we will propose to connect to the registration step.

3 Image segmentation

Humans have the ability to quickly track down many patterns, and automatically gather them into meaningful and identified structures. Image segmentation aims to imitate this capacity. Indeed, the goal of image segmentation is to partition a given image into significant constituents or to detect the edges of the "objects" it comprises for further analysis and understanding of the image. It represents a critical preliminary step in many applications. However, as emphasized by Zhu *et al.* in [122], image segmentation is a challenging and ill-posed task since the definition of an "object" or a "meaningful constituent" can be ambiguous. Depending on the nature of the image and the application, an "object" can turn out to be a "thing" like a flower, a tree, ..., or a kind of texture like wood, rock, ... or even a stuff like forest, ... and can also be part of other "objects" such as a tumor in a brain MRI image. Moreover, since interpretation is subjective, different human beings may have different visions of what should be an object in an image as illustrated in [122, Fig 1.]. This makes the evaluation of segmentation techniques a very complex issue and remains an open question as highlighted by Zhang *et al.* in [120]. Due to its countless applications such as object detection, reduction complexity, scene parsing, image montage, colorization, organ reconstruction, tumor detection to name a few (see [122] for references), a lot of research has been conducted during the last three decades. We propose overviewing some of them according to Zhu *et al.*'s classification with a more specific focus on unsupervised models.

It includes three main categories:

1. fully supervised methods: they consist in training a segmentation algorithm thanks to fully annotated data —all pixels are labelled as either *boundary* or *no boundary* —and then segmenting an unknown image. They reach high performance but the labelling is very expensive. However, more and more datasets are now available (see [122] for a list of them) with the explosion of machine learning based algorithms and computer abilities in the past few years. To cite just one example among a long list (partly described in [122]), in [68], the authors train a multilayer perceptron neural network to give a binary classification for each pixel assigning a label *boundary* or *no boundary*. This then serves as an energy function for a snake (in reference to the active contour model developed by Kass *et al.* in [53] and described later in this chapter) in order to connect the points and get a continuous closed contour.

2. semi/weakly supervised methods: they usually are interactive methods and require human expertise and intervention. The user labels a few pixels as initial constraints to the segmentation model so that the accuracy of the segmentation is increased in a specific region of interest for instance. In [59], the authors propose a geodesic-active-contour-based model (a description of the geodesic active contour model follows)

under geometrical constraints imposed by the expert, in an approximation framework. In [122], the authors distinguish three subcategories namely contour tracking approaches, label propagation approaches, and local optimization approaches and provide a thorough analysis of referenced models.

3. unsupervised methods: unlike previous methods, unsupervised methods aim to partition the image, based only on low-level features that is to say intensity levels, texture, or curvature for instance, without any training data, nor explicit object models. They can be subdivided into two groups:

   (i) discrete methods: the image is considered as a fixed discrete grid. We can identify three main approaches in this setting:

   (a) filtering approaches: The most famous filters used as edge detector and available in MATLAB are the Robert, the Prewitt, the Sobel and the Canny filters to name a few. As a reminder, the Robert masks ($G_x = \begin{pmatrix} 1 & 0 \\ 0 & -1 \end{pmatrix}$, $G_y = \begin{pmatrix} 0 & 1 \\ -1 & 0 \end{pmatrix}$), the Prewitt masks ($G_x = \begin{pmatrix} -1 & 0 & 1 \\ -1 & 0 & 1 \\ -1 & 0 & 1 \end{pmatrix}$ and $G_y = \begin{pmatrix} -1 & -1 & -1 \\ 0 & 0 & 0 \\ 1 & 1 & 1 \end{pmatrix}$) and the Sobel masks ($G_x = \begin{pmatrix} -1 & 0 & 1 \\ -2 & 0 & 2 \\ -1 & 0 & 1 \end{pmatrix}$ and $G_y = \begin{pmatrix} -1 & -2 & -1 \\ 0 & 0 & 0 \\ 1 & 2 & 1 \end{pmatrix}$) are convolved with the image to estimate the gradient norm and its orientation. The edges lie where the gradient norm is high. The process of Canny edge detection algorithm consists in removing some noise by first applying a smoothing Gaussian filter and then finding the intensity gradient using one of the previous filters and finally thresholding the result to keep only the potential edges. These methods are simple and fast but tend to be sensitive to noise and are inclined to over-segmentation.

   (b) clustering-based approaches: they are mainly inspired and borrowed from the unsupervised classification analysis and map a pixel to a feature vector. They can be either parametric or non-parametric:

   – parametric clustering methods require a prior knowledge of the regions number and the cluster shape. Then the problem amounts to estimating these few parameters. The K-means algorithm is one of the oldest and simplest parametric clustering methods and an effective implementation is available in MATLAB. Given k initial centers, it consists in iteratively assigning each pixel to the closest cluster (defined by its center) using the feature space distance, and then updating the centers until convergence. Clustering based on Gaussian Mixture Models is similar to K-means except that the centers are now replaced by covariance matrices. A version of this model is also available in MATLAB.

The Fuzzy C-Means (FCM) algorithm is implemented in MATLAB and consists in minimizing the following functional $J_m = \sum_i \sum_{j=1}^{N} \mu_{ij}^m \|x_i - c_j\|^2$, where N is the number of cluster, m is the fuzzy partition matrix exponent controlling the degree of fuzzy overlap between regions, c_j are the cluster centers and μ_{ij} is the degree of membership of x_i in the j-th cluster. It is done by a random initialization of the values of μ_{ij} and by iteratively computing the cluster centers and updating the degree of membership until convergence. In [87], the authors model the textured regions by a Gaussian distribution and encode the boundaries by an adaptive chain code. In [21], Chuang *et al.* propose improving the conventional fuzzy C-means algorithm (FCM) by incorporating information into the fuzzy membership function for clustering, leading to a less sensitive to noise model. These methods are quite efficient but often too simplistic for natural images. Besides the region number is a strong a-priori and is usually hard to get.

- non-parametric clustering approaches estimating the number of clusters and their modes have been designed to overcome this difficulty. In [75], a region splitting by thresholding is applied on the image histogram. The underlying assumption is that a region is made of pixels with similar intensities whereas two pixels from two distinct regions have different intensities. Region merging methods also exist as mentioned in [122]. In [25], the mean shift algorithm is proposed. The feature space is seen as a probability density function and the modes of it correspond to the clusters. The modes are located at the zeros of the probability density function and the mean shift procedure is able to find them without explicitly estimating the density function. To do so, an iterative scheme is used in which the modes are updated using a weighted mean. A convergence result is given and the clusters are then formed by grouping the pixels in the basin of attraction of the corresponding convergence points.

(c) graph-based approaches: the image is seen as a graph where the clusters are mapped to the nodes and the edges reflect the similarities between them. The optimization of a cost function over the graph is then carried out and leads to the segmentation of the image. In [38], the authors propose grouping pixels using an internal difference ($Int(C)$) defined by the largest weight, that is to say, the largest intensity level difference in the minimum spanning tree of the group. Then regions (C_1 and C_2) are merged if the in-between edge weight is less than $\min\{Int(C_1) + \frac{k}{|C_1|}, Int(C_2) + \frac{k}{|C_2|}\}$, with k a constant controlling the component size so that a larger k causes a preference for larger components. Normalized cut is a well-known algorithm for segmentation [96]. The segmentation is obtained by minimizing the disassociation between groups $\{S_i\}_{i=1}^k$, and maximizing the association be-

tween groups using the following dissimilarity measure $Ncut(S_1, \ldots, S_k) = \frac{1}{2}\sum_{i=1}^{k} \frac{W(S_i,\bar{S}_i)}{vol(S_i)}$, where $W(S_i, \bar{S}_i)$ is the sum of the boundary edge weights of S_i and $vol(S_i)$, the sum of weights of all edges attached to vertices in S_i. It thus favors clusters with similar volume and so "balanced" clustering. Many works have been done exploiting these ideas and proposing algorithms to solve the related NP-hard problems.

(ii) continuous methods: the image is seen as a continuous surface and tends to present visually more pleasing results. They can be partitioned into two categories:

i. edge-based models: a curve is evolved to match the object edges. There are two ways of representing the curve:
   - explicitly using a parametrized spline curve. The original snake model developed by Kass in [53] detects edges by deforming an initial parametrized spline curve subject to internal regularization forces and external data-driven forces attracting the contour to the edges using image gradient. However, it is not invariant to a change of parametrization, re-parameterization may be needed during the evolution process, topological changes are not automatically handled and it is sensitive to initialization as stressed by Vese and Le Guyader in [105, Introduction]. A lot of research has been conducted to overcome these difficulties (see [105, Chapter 9] for an overview).
   - implicitly as the zero level-line of a Lipschitz continuous level-set function. In [15], Caselles *et al.* introduce the geodesic active contour model. They prove that under some assumptions, the classical active contour model amounts to finding a geodesic curve, i.e. a path of minimal length, in a Riemann space. The associated metric depends on the image content and the evolving contour is considered to be the zero level line of a level-set function ([77]). Topological changes are automatically handled. A lot of variants have been proposed, including [60] in which the authors introduce a topology-preserving model handling concavities in the edges. They introduce an additional nonlocal topology constraint preventing the contour from splitting or merging. This can be required in medical imaging.

   However, they both suffer from boundary leakage problem when weak boundaries with low contrast are present as mentioned by Wang *et al.* in [110].

ii. region-based models: they are essentially based on the extensively studied Mumford-Shah model. In [72], Mumford and Shah introduce the following segmentation problem: $\inf_{u,K} \mu \int_\Omega (u-f)^2\,dx + \int_{\Omega\setminus K} |\nabla u|^2 + \mathcal{H}(K)$ where $\mathcal{H}$ is the Hausdorff measure, u is a piecewise smooth approximation of the initial image f and K the set of discontinuities, based on the idea that f can be partitioned into regions within which f varies smoothly, whereas

it varies discontinuously or quickly across the boundaries represented by K. Theoretical studies and results can be found in [28]. However, due its nonconvexity and the nature of the unknown K, solving this problem is challenging. In order to circumvent this difficulty, Ambrosio and Tortorelli introduce an elliptic approximation within the phase field theory in [4]. They prove that their approximated functional Γ-converges to the initial weak formulation of the Mumford-Shah functional. The boundaries are recovered thanks to an auxiliary variable v acting like an edge-detector being equal to 1 in homogeneous regions and dropping to 0 around edges. Blake and Zisserman ([11]) extend the Mumford-Shah functional to the second-order case in order to detect both the edge set and the crease set, enabling the segmentation of fine structures as discussed in Chapter 5 of this thesis. Coming back to the first order Mumford-Shah functional, an important specific case called problem of minimal partition is obtained when u is restricted to the space of piecewise constant functions. Many works have been addressing this issue using a convexification process as in [16], using ADMM and linear programming in [99], and considering the set K as the zero level line of a Lipschitz continuous level-set function in [17] to name a few. However, region-based methods tend to rely on intensity homogeneity inside regions and are not applicable to images not fulfilling this assumption. Vese and Chan ([106]) propose a piecewise model in which the regions are no longer assumed to have constant intensities but homogeneous textures to overcome the previous drawback. However, the computational cost is expensive and the complex parameter setting limits its use. In [91, Chapter 3], an extension of the level-set segmentation techniques is proposed by defining a more general edge set able to capture free curves. Li *et al.* in [62] propose the Local Binary Fitting (LBF) model where the constant mean values of each region is replaced by a local mean value spatially varying using a Gaussian kernel in the level-set framework. But this locality is responsible for the apparition of local minima and the method is therefore dependent on the initialization. In [71], the authors propose a convexification of this problem leaving the level-set framework and using fuzzy membership functions. It is no longer subject to initialization dependency. In [110], Wang *et al.* propose a model combining both local and global image information using a level-set formulation to allow for more initialization flexibility. Indeed, the local intensity fitting term based on the LBF model becomes dominant around edges and attracts the contour to the object boundaries improving thus accuracy, while the global intensity fitting term inspired by the Chan-Vese model improves robustness since it is dominant far from the edges.

Figure 1.4 summarizes the classification of segmentation methods we have just discussed.

This concludes the overview of a large variety of existing segmentation methods. We

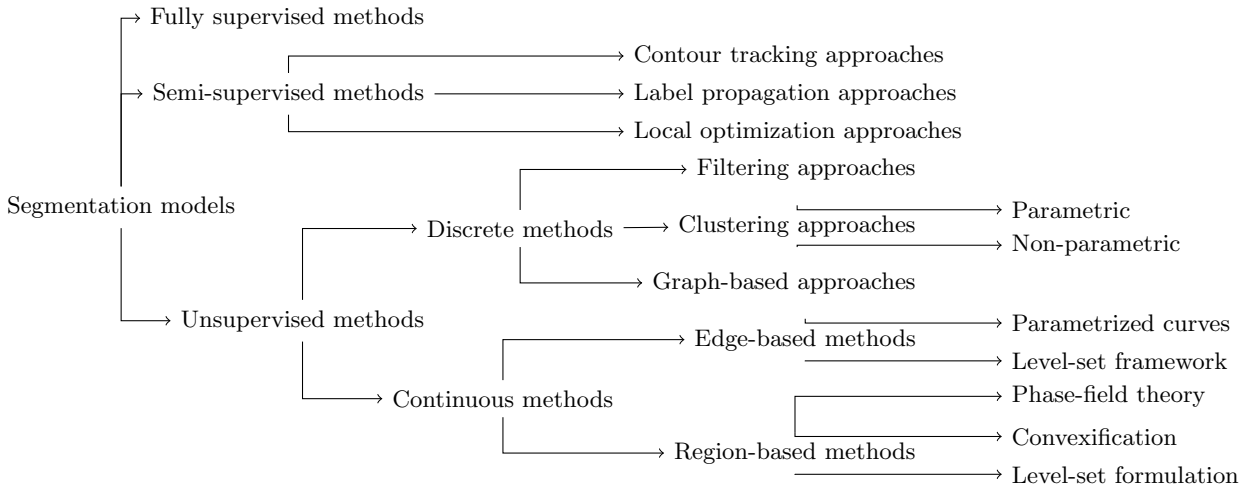

Figure 1.4: Classification of segmentation methods inspired by [122].

now turn to hybrid methods combining multiple tasks into a single framework to increase the accuracy of each of them, while erasing the brakes that may stem when considered individually.

4 Joint image segmentation and image registration

Segmentation and registration are fundamental requirements in many image processing chains. Images need to be registered and then segmented to analyze them jointly and accurately. It is often done linearly, that is to say one after another without correlating them. Yet, as structure matching and intensity distribution comparison drives the registration process, it sounds relevant to treat both segmentation and registration jointly. Indeed, the registration task can be seen as prior information to guide the segmentation process to overcome the difficulty of weak boundary definition, and accurate segmented salient components can drive the registration method correctly. In the following, we give a brief overview of existing joint models.

In [45], the authors propose a simultaneous segmentation and registration with missing data of a probabilistic atlas of healthy population model to brain MRI images exhibiting glioma. It is based on the Expectation-Maximization (EM) algorithm that integrates a glioma growth model for atlas seeding, modifying then the atlas into one with tumor adapted to best match a given set of patient images. This new atlas is then registered into the patient scale and used for estimating the posterior probabilities of various tissue labels. This allows for the segmentation of the tumor.

In [85], Pohl *et al.* present a statistical model combining segmentation and registration. They use an Expectation-Maximization based algorithm to estimate image artifacts,

anatomical label maps and a structure-dependent hierarchical mapping from the atlas to the image space. The deformation is then recovered using an interpolation function.

In [113] and in [36], the authors highlight the increased difficulty of infant image registration and segmentation compared with adults, due to the dynamic appearance change with rapid brain development. To overcome these difficulties, they propose to jointly proceed segmentation and registration and to incorporate the growth trajectories learnt from a large set of training subjects with complete longitudinal data in order to accurately characterize structure changes in infant brain evolution. Assuming a one-year old child's brain image with ground truth tissue segmentation is available and set as the Reference domain, they want to register the infant brain image of a new subject at earlier age. The tissue probability maps are then estimated with a sparse patch-based multi-atlas label-fusion technique where only the training data at the respective age are considered as atlases. These maps are then fused as a good initialization to guide the level-set segmentation along with the learnt growth trajectories whereas the registration process is based on the HAMMER algorithm.

In [114], Wyatt *et al.* apply Markov Random Fields (MRF) in the solution of a Maximum A Posteriori (MAP) model for image segmentation and rigid registration to embed local spatial information. They assess that a joint solution to segmentation and registration is more accurate and robust than a sequential solution. They also demonstrate that the extension to non-rigid registration gives poor results despite its success for rigid ones.

In [83], Parisot *et al.* present a graph-based concurrent brain tumor segmentation and healthy atlas to diseased patient registration model. Both tasks are coupled into a single MRF framework on a sparse grid superimposed on the image domain and then the unknowns are recovered on the pixel image grid thanks to an interpolation function. Segmentation is addressed based on pattern classification techniques, while registration is performed by maximizing the similarity between volumes. The registration process introduces global information on the brain structure helping the segmentation, while the segmentation of the tumor and thus the acknowledgement of its presence improves the quality of the registration by treating this region differently.

A joint segmentation and registration model for time series of cardiac perfusion images is proposed by Mahapatra in [66]. They first decompose the time series into a low rank and a sparse component using a Robust Principle Component Analysis (RPCA). Registration is then achieved by maximizing the smoothness of the intensity in the low rank component, whereas segmentation is obtained by minimizing the sparse component pixel intensity difference with other pixels having the same label as in the K-means algorithm. The Dynamic Contrast Enhanced (DCE) Magnetic Resonance (MR) sequence of images is affinely aligned with the first one. The displacements are computed on control points, then calculated on each pixel using cubic B-splines.

Yezzi *et al.* [117] propose a variational approach for joint segmentation and registra-

tion so that they both take advantage of each other. The segmentation of the Reference is obtained by evolving a closed curve $\mathcal{C}$, while the curve $\hat{\mathcal{C}}$ represents the edges of the Template. They are related by the equality $\hat{\mathcal{C}} = \varphi(\mathcal{C})$, where φ is the deformation inspired by physical models. In their original paper, they restricted φ to a parameterizable set of transformations. The unknowns are then $\mathcal{C}$ and φ. The evolution of $\mathcal{C}$ is based on the active contour without edges model and the regularization of φ relies on the mean curvature flow to ensure the smoothness of $\mathcal{C}$. A generalization of this model can be found in [103].

In [104], Vemuri *et al.* suggest a coupled PDE model to jointly perform segmentation and registration using a level-set formulation. In the first PDE, the level-set functions associated with the Template are evolved along their normal with a speed defined as the intensity difference between the deformed Template and the Reference. The second one allows the explicit recovery of the displacement field.

In [64], Lord *et al.* handle the issue of quantifying the difference between two shapes. Their work falls within the analysis of the hippocampus shape and is motivated by the fact that asymmetry comparison facilitates disease classification. To perform this analysis, the authors propose a joint segmentation and registration model with two unknowns namely the deformation field and the curve modelling the contour. The segmentation is guided by the deformation whose regularity is ensured by minimizing its deviation from an isometry. The fidelity term is based on shape comparison and more precisely on the first fundamental force (derived from the spatial derivatives of the deformation map) and on a homogeneity constraint based on the Chan-Vese model for segmentation.

In [61], Le Guyader and Vese develop a model based on the active contour without edges model and on nonlinear elasticity principles. The shapes to be matched are viewed as an isotropic, homogeneous, hyperelastic Ciarlet-Geymonat material. The Reference segmentation is reached through the zero level line of the composition of a level-set function with the deformation field. The zero level line of the level-set function is assumed to represent the edges of the Template image.

In [5], a variational PDE method for simultaneous image segmentation and deformable registration using prior shape implicitly modelled by level-set functions and intensity information is introduced. The segmentation of the Reference is obtained by finding a non-rigid deformation composed of a global rigid deformation and a local non-rigid transformation and then by taking the zero level-line of the level-set function composed with this deformation. The level-set function gives a segmentation of the Template by extracting its zero level-line which is seen as prior shape.

In [46], Gorthi *et al.* propose a new framework for atlas-based segmentation. They propose a new label function representation of the level sets that are able to model any number of regions and represent various types of registration forces using a single function. The contours do not correspond to the zero level line anymore but to the discontinuities

of a piecewise constant level-set function. A mean curvature regularization is used on the deformation field and a region-based fidelity term inspired by the Chan-Vese model drives the registration process assuming that a manual segmentation of the atlas is available. The atlas is mapped into the target image and a segmentation of it is then produced.

In [100], Swierczynski *et al.* devise a new mathematical formulation to jointly segment and register three-dimensional lung CT volumes based on a level-set formulation. They combine Vemuri *et al.*'s approach with Gorthi *et al.*'s one with a weighting parameter and the smoothness of the deformation field is ensured by the minimization of its curvature. They show that their algorithm improves the accuracy of the results compared to the ones obtained by a sequential application of registration and segmentation on a publicly available lung CT data set.

In [37], Droske and Rumpf introduce a variational model combining the detection of edges, an edge-preserving denoising procedure and a deformable registration of a multimodal pair of images. The morphology of an image is split into 2 components: an edge set and a field of normals on the ensemble of level sets. A phase-field approximation of the Mumford-Shah functional to segment and to match the singular morphology as well as a measure of alignment between deformed normals and normals at deformed positions to match the regular morphology are used as a fidelity term. The regularization of the deformation field is ensured by a nonlinear stored energy function of an Ogden material controlling the change of length, the change of area and the change of volume. For an efficient implementation, they propose a multiscale approach.

More recently, Ozeré *et al.* [80] design a joint segmentation/registration model in a variational framework. A dissimilarity measure based on the weighted total variation to align the edges of the deformed Template with the ones of the Reference and a classical sum of square intensity differences is complemented by a regularizer inspired by the stored energy function of a Saint Venant-Kirchhoff material.

In [112], the author examines the behavior of phase field approximations of the Mumford-Shah model in a joint segmentation and registration framework. Phase fields and deformation fields are coupled and the regularization on the transformation field is based on the stored energy function of Ogden materials, ensuring the deformation map is a bi-Hölder continuous homeomorphism. Both Ambrosio-Tortorelli and Modica-Mortola phase field approximations are considered and many theoretical results are provided regarding their behavior and especially their Γ-convergence.

A new variational method for joint segmentation and registration model extending the ones presented in [80] by adding a region-based dissimilarity measure inspired by the Chan Vese model for segmentation is presented in Chapter 4.

Other methods suggest to use the segmentation result to guide the registration process as in Chapter 3 of this thesis, where we introduce a nonlinear-elasticity-based registration

method guided by topology-preserving segmentation results and in [1], in which they use the error of segmentation as a fidelity term in the registration process of multimodal images.

Let us now introduce another essential image processing task, namely texture modelling and image decomposition inherently related to image restoration.

5 Texture modelling and image decomposition

Following ideas of Meyer [67], image decomposition aims to separate a given image f into a cartoon or geometric component u that is piecewise smooth, and a texture component v that catches the oscillatory patterns and the noise of f. Texture modelling consists in finding the best functional space to represent the oscillatory patterns. We will focus on two dimensional variational minimization models of the form: $\inf_{u\in X_1,\, v\in X_2, u+v=f} F(u,v) = F_1(u) + \lambda F_2(v)$, assuming that $f \in X_1 + X_2$, and present a non-extensive overview of existing decomposition models (see also [105, Chapter 5]). As stressed by Vese and Le Guyader in [105, Chapter 5], a good model is given by a choice of X_1 and X_2 so that $F_1(u) >> F_1(v)$ and $F_2(v) >> F_2(u)$, where F_1 and F_2 are non-negative and finite for any $(u,v) \in X_1 \times X_2$. A classical and appropriate choice for X_1 is the space of functions of bounded variations (BV whose definition and properties will be given in Chapter 2) sometimes restricted to the space of special functions of bounded variations (SBV presented in Chapter 2) and for F_1, the semi-norm of this space called the total variation $|u|_{BV} = \int |Du|$. Indeed it favors constant regions and preserves sharp edges which are good properties for the cartoon component. On the other hand, X_2 should be a rougher space with a small norm for oscillatory functions and its choice has been widely discussed. We can distinguish exact decomposition models in which $v = f - u$ and approximated decomposition model, where v appears explicitly and a residual possibly seen as noise is introduced as $f - u - v$.

The Mumford Shah functional and its weak formulation ([28]) as well as the models approximating it (such as the Ambrosio and Tortorelli's one ([4]) introduced previously) can also be seen as exact decomposition models. Indeed the image $f \in L^2(\Omega)$ where $\Omega \subset \mathbb{R}^2$ is the image domain, is decomposed into $u \in SBV(\Omega)$ a piecewise smooth function with its discontinuity set included in a union of curves whose overall length is finite, and $v = f - u \in L^2(\Omega)$ representing the noise. One of the most famous exact decomposition models addressing deblurring and denoising problems is the one introduced by Rudin, Osher and Fatemi ([89], ROF). They aim at minimizing $\inf_{u\in BV(\Omega)} |u|_{BV} + \|f-u\|^2_{L^2(\Omega)}$ and so here, $X_2 = L^2(\Omega)$ and $F_2 = \|.\|^2_{L^2(\Omega)}$ with v modelling only additive Gaussian noise with zero mean. However it may not be able to recover a function of bounded variations without any noise in u as illustrated in [105, Example 3, Chapter 5]. To overcome this difficulty, Chan and Esedoḡlu in [18] analyze a model in which the $L^2(\Omega)$ norm is replaced by the $L^1(\Omega)$ norm. We refer the reader to [58] for an overview of numerical algorithms

designed to solve this problem and the introduction of a new effective primal-dual one.

Based on the idea that to denoise a pixel it is better to average the nearby pixels with similar structures rather than just similar intensities, Buades *et al.* ([13]) propose a nonlocal filtering algorithm named NL-means to address denoising, thus generalizing the idea of using patch-based methods. Then Osher and Gilboa [44] introduce a variational framework of it by defining nonlocal operators: $\nabla_w u(x,y) = (u(y)-u(x))\sqrt{w(x,y)}$, $|\nabla_w u|(x) = \sqrt{\int_\Omega (u(y)-u(x))^2 w(x,y)\,dy}$, $\mathrm{div}_w v(x) = \int_\Omega (v(x,y)-v(y,x))\sqrt{w(x,y)}\,dy$, $\Delta_w u(x) = \int_\Omega (u(y)-u(x))w(x,y)\,dy$, with w a weight function assumed to be nonnegative and symmetric and often taken as $w(x,y) = \exp\left(-\frac{\int_\Omega G_a(t)|f(x+t)-f(y+t)|^2\,dt}{h^2}\right)$, G_a being the Gaussian kernel with standard deviation a determining the patch size, and h the filtering parameter which corresponds to the noise level. Then nonlocal variants of the previous models are suggested in which $|u|_{BV}$ is replaced by $\int_\Omega |\nabla_w u|(x)\,dx$ (nonlocal ROF and nonlocal TV-L1 models in [44], and nonlocal Mumford-Shah regularizers in [51]). An extension of the nonlocal Mumford-Shah regularizer to the Blake Zisserman model with a texture model based on the G-norm (defined in the following) is proposed in Chapter 5 for denoising and segmentation of fine structures.

In [67], Meyer analyzes further the texture modelling and proposes to refine the ROF model using one of these functional spaces for X_2:

$G = \{\mathrm{div}\vec{g},\ \vec{g} = (g_1,g_2) \in (L^\infty(\Omega))^2\} = W^{-1,1}$ being a good approximation of the dual of BV

and associated with the norm $\|v\|_G = \inf\{\|\sqrt{g_1^2+g_2^2}\|_{L^\infty(\Omega)} | v = \mathrm{div}\vec{g}\}$,

$F = \{\mathrm{div}\vec{g},\ \vec{g} \in BMO^2\} = BMO^{-1}$

with $BMO = \left\{ g \in L^1_{loc}(\Omega) | \exists c \geq 0,\ \forall Q \subset \mathbb{R}^2 \text{ square },\ \frac{1}{|Q|}\int_Q \left| g - \int_Q g\,dx \right| dx \leq c \right\}$,

$\|v\|_{BMO} = \sup_{Q\,\text{square}} \frac{1}{|Q|}\int_Q \left| v - \int_Q v\,dx \right| dx$,

and endowed with the norm $\|v\|_F = \inf_{v=\mathrm{div}\vec{g},\,\vec{g}\in BMO^2} \|g_1\|_{BMO} + \|g_2\|_{BMO}$,

$E = \{\Delta g,\ g \text{ Zygmund function },\ i.e.,\ \exists c \geq 0,\ \forall (x,y) \in \mathbb{R}^4,\ |g(x+y)+g(x-y)-2g(x)| \leq c|y|\}$,

also called generalized homogeneous Besov space $B^{-1}_{\infty,\infty} = \Delta B^1_{\infty,\infty}$ where $B^\alpha_{p,\infty} = \{g \in L^1_{loc}(\Omega) | \exists c \geq 0, \forall y \in \mathbb{R}^2,\ \|g(.+y)-2g(.)+g(.-y)\|_{L^p(\Omega)} \leq c|y|^\alpha\}$. In two dimensions we have $BV \subset L^2 \subset G \subset F \subset E$. These weak spaces encourage oscillatory behavior as their norm decreases while the amount of oscillations increases as illustrated in [105, Chapter 5]. The larger the space X_2 is, the finer the details and the texture caught by v are. However the analysis and discretization of these spaces is not obvious due to their complexity and a rich literature can be found on this subject. Vese and Osher [107] propose to approach the (BV,G) model by minimizing the following approximated decomposition model differentiating the texture from the noise/residual $\inf_{u,\vec{g}}\{|u|_{BV} + \mu\|f-u-\mathrm{div}\vec{g}\|^2_{L^2(\Omega)} + \lambda\|\sqrt{g_1^2+g_2^2}\|_{L^p(\Omega)}\}$ with p going to infinity. This model

is numerically more tractable. It appears in practice that good results are obtained with $p = 1$. In [8], Aujol *et al.* propose to solve the (BV, G) problem using projections on spaces $B_{G(\mu)} = \{v \in G, \|v\|_G \leq \mu\}$. They prove the convergence of their algorithm. Similarly, Aujol *et al.* ([9]) propose an algorithm using projections and including dual formulations to solve the (BV, E) problem. Then Garnett *et al.* [42] reformulate and generalize this (BV, E) problem by considering $\inf_{u,g}\{|u|_{BV} + \mu\|f - u - \Delta g\|^2_{L^2(\Omega)} + \lambda\|g\|_{B^\alpha_{p,\infty}}\}$ with $p \geq 1$, $0 < \alpha < 2$. Theoretical results including existence of minimizers are given along with a numerical algorithm to solve it. Also in [57], Le and Vese address the decomposition issue by solving the following model: $\inf_{u,\vec{g}}\{|u|_{BV} + \mu\|f - u - \mathrm{div}\vec{g}\|^2_{L^2(\Omega)} + \lambda(\|g_1\|_{BMO} + \|g_2\|_{BMO})$ approaching the (BV, F) model. They propose several methods to compute the BMO norm including one exact algorithm using the Fast Fourier Transform (FFT).

Osher *et al.* [78] develop another model based on the Helmotz-Hodge decomposition of $\vec{g} \in (L^2(\Omega))^2$ into $\vec{g} = \nabla P + \vec{Q}$ with $P \in H^1(\Omega)$ and $\vec{Q}$ a divergence free vector field yielding to $v = f - u = \mathrm{div}\vec{g} = \Delta P$. As in [107], the $L^\infty(\Omega)$ norm in (TV, G) model is replaced by an $L^2(\Omega)$ norm and the $\vec{Q}$ component is neglected leading to the following minimization problem: $\inf_u\{|u|_{BV} + \lambda\|\sqrt{g_1^2 + g_2^2}\|^2_{L^2(\Omega)} = |u|_{BV} + \lambda\||\nabla P|\|^2_{L^2(\Omega)} = |u|_{BV} + \lambda\||\nabla(\Delta^{-1})(f - u)|\|^2_{L^2(\Omega)} = |u|_{BV} + \lambda\|f - u\|^2_{H^{-1}(\Omega)}\}$. $H^{-1}(\Omega)$ is the dual space of the Sobolev space $H^1(\Omega)$. Then Lieu and Vese [63] generalize this model by using negative fractional Hilbert-Sobolev spaces $H^{-s}(\mathbb{R}^2)$ whose dual spaces are the fractional Hilbert-Sobolev spaces $H^s(\mathbb{R}^2)$ with $s > 0$. The embedded norm is : $\|v\|_{H^{-s}} = \int_{\mathbb{R}^2}(1 + |\xi|^2)^{-s}|\hat{v}|^2(\xi)\, d\xi$, where $\hat{v}$ is the Fourier transform of v. The smaller s is, the larger the space H^{-s} is and so the finer are the details captured by v. In [55], Kim and Vese extend even more this idea by modelling the textures with the dual of homogeneous Sobolev spaces with pseudo-derivatives $W^{\alpha,p}(\mathbb{R}^2) = \{v|(2\pi|.|)^\alpha\hat{v}(.) \in L^p(\mathbb{R}^2)\}$ with $-2 \leq \alpha < 0$ and $\|v\|_{W^{\alpha,p}(\mathbb{R}^2)} = \|(2\pi|.|)^\alpha\hat{v}(.)\|_{L^p(\mathbb{R}^2)}$. Further details on these spaces will be given in the next chapter. In [91], the author proposes a decomposition model in which the texture lies in an approximation of the dual space to $W^{1,\infty}(\Omega)$. To approach the $L^\infty(\Omega)$ norm, he uses an $L^1(\Omega)$ norm with respect to a measure which concentrates near the maximum. Finally, in [95], the authors propose to couple the decomposition model based on the H^{-1} norm with the Mumford-Shah functional called Mumford-Shah-Sobolev model for segmented decomposition. The alternating scheme can be carried out using level-set functions or the phase-field approximation based Ambrosio-Tortorelli's framework. It relates then image decomposition, texture modelling and image segmentation.

In Table 1.1, we summarize the presented models using a classification based on the one proposed in [58] where $f - u$ is replaced by v if necessary and J_u is the jump set of u. We now present the contributions and the organization of this thesis.

Class	Minimized energy	Name	Texture space	Reference
BV+noise/	$\int_\Omega \lvert Du\rvert^2\,dx + \mathcal{H}^1(J_u) + \int_\Omega \lvert v\rvert^2\,dx$	$SBV - L^2$	L^2	[72], [4]
SBV+noise	$\int_\Omega \lvert Du\rvert + \int_\Omega \lvert v\rvert^2\,dx$	ROF	L^2	[89]
models	$\int_\Omega \lvert Du\rvert + \int_\Omega \lvert v\rvert\,dx$	TV-L^1	L^1	[18], [58]
	$\beta \int_\Omega g^2 \Phi(\lvert\nabla_w u\rvert^2)\,dx + \lVert v\rVert^2_{L^2(\Omega)}$			
NL/BV	$+\alpha \int_\Omega \left(\varepsilon\lvert\nabla g\rvert^2 + \frac{(g-1)^2}{4\varepsilon}\right) dx$	NL/MS-L^2	L^2	[51]
-NL/H^1	$\beta \int_\Omega g^2 \Phi(\lvert\nabla_w u\rvert^2)\,dx + \lVert v\rVert_{L^1(\Omega)}$			
+ noise	$+\alpha \int_\Omega \left(\varepsilon\lvert\nabla g\rvert^2 + \frac{(g-1)^2}{4\varepsilon}\right) dx$	NL/MS-L^1	L^1	[51]
models	$\int_\Omega \lvert\nabla_w u\rvert\,dx + \int_\Omega \lvert v\rvert^2\,dx$	NL/ROF	L^2	[44]
	$\int_\Omega \lvert\nabla_w u\rvert\,dx + \int_\Omega \lvert v\rvert\,dx$	NL/TV-L^1	L^1	[44]
	$\int_\Omega \lvert Du\rvert + \lVert v\rVert_G$	TV-G	G	[67], [107], [8]
Meyer's	$\int_\Omega \lvert Du\rvert + \lVert v\rVert_F$	TV-F	F	[67], [57]
models	$\int_\Omega \lvert Du\rvert + \lVert v\rVert_E$	TV-E	E	[67], [42], [9]
	$\int_\Omega \lvert Du\rvert + \lVert v\rVert_{H^{-1}(\mathbb{R}^2)}$	TV-H^{-1}	H^{-1}	[78], [95]
Negative	$\int_\Omega \lvert Du\rvert + \lVert v\rVert_{H^{-s}(\mathbb{R}^2)}$, $s > 0$	TV-H^{-s}	H^{-s}	[63]
Sobolev	$\int_\Omega \lvert Du\rvert + \lVert v\rVert_{W^{\alpha,p}(\mathbb{R}^2)}$,			
spaces	$-2 \le \alpha < 0$, $1 \le p \le \infty$	TV-NSobolev	$W^{\alpha,p}$	[55]

Table 1.1: Summary of variational decomposition models.

6 Contributions and thesis organization

Chapter 2 introduces some useful mathematical tools that will be referred to throughout the manuscript. It encompasses, among others, properties of some functional spaces, notions on viscosity solution theory, on the theory of calculus of variations, and on nonlinear elasticity.

In Chapter 3, we propose a registration model guided by topology-preserving segmentation that falls within the continuation of [79, Chapter 5]. The shapes to be matched are viewed as Saint Venant-Kirchhoff materials and are implicitly modelled by level-set functions. The alignment of the evolving shape with intermediate topology-preserving segmentation results drives the registration process. The main contributions rely on the study of two numerical methods of resolution, one based on penalization methods, and the other one based on augmented Lagrangian method in a discrete setting. This work brought forth publication [32] and Chapter 3 constitutes an extension of it.

Chapter 4 is dedicated to the study of a new joint segmentation/registration model based on weighted total variation and its nonlocal characterization, on region-based shape descriptors inspired by the Chan-Vese model for segmentation and on nonlinear elasticity principles. It extends a model presented by Ozeré *et al.* in [79, Chapter 4] and [80] by adding a nonlocal shape descriptor. A theoretical analysis has been done and yields the existence of minimizers for both the local and nonlocal problems, a connection with the

segmentation process, a nonlocal characterization of weighted semi-norms and their Γ-convergence to the local ones, and asymptotic results after introducing splitting variables to facilitate the numerical resolution of our problem for the local and nonlocal versions. Chapter 4 is a more detailed version of a paper that has been accepted for publication in SIAM Journal on Imaging Sciences in February 2018 [30].

In Chapter 5, we address the issue of crack detection recovery on bituminous surface images. Cyrille Fauchard and Denis Join from the CEREMA (Centre of analysis and expertise on risks, environment, mobility and planning) provided us with bituminous surface images and set out their desire of designing a model capable of automatically recover cracks for road maintenance. This work is the result of a collaboration with Professor Luminita Vese from the University of California, Los Angeles and a part of it has been accepted for publication in Annals of Mathematical Sciences and Applications [31] and the first part of Chapter 5 is a longer version of this paper. We introduce a second order variational model based on the elliptic approximation of the Blake-Zisserman functional [3] involving an unknown simulating the discontinuity set of the image gradients encoding the geometrical structures. We propose complementing it with a decomposition model in which the texture is assumed to belong to the G space [67]. Existence of minimizers, existence of a unique viscosity solution to the derived evolution problem and a Γ-convergence result relating the elliptic problems to the initial one are given. We then provide a nonlocal version of this model and prove the existence of minimizers, and the Γ-convergence of these nonlocal approximations to the local problem. We derive numerical algorithms for both the local and nonlocal models. A parallelization of the code using MPI has been done with the help of Patrick Bousquet-Melou from the CRIANN (Regional Centre for Computer Sciences and Numerical Simulations of Normandy), and three master students of the Mathematical and Software Engineering Department of the INSA (National Institute of Applied Sciences) of Rouen Normandy: Nathan Rouxelin, Timothée Schmoderer and Emeric Quesnel as part of our participation to the hackathon.

Chapter 6 acts as a conclusion by summarizing our work and giving some perspectives for future works.

7 Scientific outreach

1. **Publications in peer-reviewed international journals:**

   [1] Debroux N. And Le Guyader, C., *A Joint Segmentation/Registration Model Based on a Nonlocal Characterization of Weighted Total Variation and Non-local Shape Descriptors*, SIAM Journal on Imaging Sciences (SIIMS), in revision (2017).

   [2] Debroux N., Le Guyader, C. And Vese, L., A., *A Second Order Free Discontinuity Model for Bituminous Surfacing Crack Recovery and Analysis of a Non-local Version of it*, accepted for publication in Annals of Mathematical

Sciences and Applications, special issue in honor of Professor David Mumford (2017).

[3] Debroux, N., Ozeré, S. And Le Guyader, C., *A Non-local Topology-Preserving Segmentation-Guided Registration Model*, in Journal of Mathematical Imaging and Vision, 1-24, online in January (2017).

[4] Carre, C., Debroux, N., Deneufchâtel, M., Dubernard, J.-P., Hillairet, C., Luque, J.-G., And Mallet, O., *Dirichlet Convolution and Enumeration of Pyramid Polycubes*, in Journal of Integer Sequences, vol. 18 (2015).

2. **Papers in refereed conference proceedings:**

[5] Debroux, N., And Le Guyader, C., *A Unified Hyperelastic Joint Segmentation/Registration Model Based on Weighted Total Variation and Non-local Shape Descriptors*, in Lauze, F., Dong, Y., Dahl, A. B. (eds) Scale Space and Variational Methods in Computer Vision: 6^{th} International Conference, SSVM 2017, Kolding, Denmark, June 4-8, 2017, Proceedings, pp. 614625 (2017).

[6] Fortun, D., Debroux, N., And Kervrann, C., *Spatially-variant kernel for optical flow under low signal-to-noise ratios: application to microscopy*, in IEEE ICCV Workshop - BioImage Computing (BIC), Venice, Italy, October 2017, pp. 9 (2017).

3. **Oral communications:**

- Debroux*, N., And Le Guyader, C., *Joint Segmentation/Registration Model*, in Minisymposium Hybrid Models for Inverse Imaging Problems in Applied Inverse Problems Conference, Hangzhou, China, May 29 - June 2, (2017).
- *A Unified Hyperelastic Joint Segmentation/Registration Model Based on Weighted Total Variation and Nonlocal Shape Descriptors.* Seminar, School of Mathematical Sciences, Monash University, Melbourne, Australia, April 28, (2017).
- *A Unified Hyperelastic Joint Segmentation/Registration Model Based on Weighted Total Variation and Nonlocal Shape Descriptors.* Journe Normastic Mthodes Variationnelles et Statistiques Appliques au Traitement dImages, INSA of Rouen, France, January 27, (2017).
- *Methods for Joint Registration and Segmentation.* Communication at the Level Set collective, Department of Applied Mathematics, UC Los Angeles, U.S.A., July 12, (2016).

4. **Participation to a hackathon within the CRIANN (Centre Régional Informatique et d'Applications Numériques de Normandie / Regional Computer Center and Digital Applications of Normandy).**

Bibliography

[1] I. Aganj and B. Fischl, *Multimodal image registration through simultaneous segmentation*, IEEE Signal Processing Letters, 24 (2017), pp. 1661–1665.

[2] I. Aganj, J. E. Iglesias, M. Reuter, M. R. Sabuncu, and B. Fischl, *Mid-space-independent deformable image registration*, NeuroImage, 152 (2017), pp. 158 – 170.

[3] L. Ambrosio, L. Faina, and R. March, *Variational approximation of a second order free discontinuity problem in computer vision*, SIAM J. Math. Analysis, 32 (2001), pp. 1171–1197.

[4] L. Ambrosio and V. M. Tortorelli, *Approximation of functional depending on jumps by elliptic functional via* Γ*-convergence*, Communications on Pure and Applied Mathematics, 43 (1990), pp. 999–1036.

[5] J.-H. An, Y. Chen, F. Huang, D. Wilson, and E. Geiser, *Medical Image Computing and Computer-Assisted Intervention – MICCAI 2005: 8th International Conference, Palm Springs, CA, USA, October 26-29, 2005, Proceedings, Part I*, Springer Berlin Heidelberg, 2005, ch. A Variational PDE Based Level Set Method for a Simultaneous Segmentation and Non-Rigid Registration, pp. 286–293.

[6] J. Ashburner and K. J. Friston, *Nonlinear spatial normalization using basis functions*, Human brain mapping, 7 (1999), pp. 254–266.

[7] G. Aubert and P. Kornprobst, *Mathematical Problems in Image Processing: Partial Differential Equations and the Calculus of Variations*, Applied Mathematical Sciences, Springer-Verlag, 2001.

[8] J.-F. Aujol, G. Aubert, L. Blanc-Féraud, and A. Chambolle, *Image decomposition into a bounded variation component and an oscillating component*, Journal of Mathematical Imaging and Vision, 22 (2005), pp. 71–88.

[9] J.-F. Aujol and A. Chambolle, *Dual norms and image decomposition models*, International Journal of Computer Vision, 63 (2005), pp. 85–104.

[10] M. Beg, M. Miller, A. Trouvé, and L. Younes, *Computing Large Deformation Metric Mappings via Geodesic Flows of Diffeomorphisms*, International Journal of Computer Vision, 61 (2005), pp. 139–157.

[11] A. Blake and A. Zisserman, *Visual Reconstruction*, MIT Press, Cambridge, 1989.

[12] C. Broit, *Optimal Registration of Deformed Images*, PhD thesis, Computer and Information Science, University of Pennsylvania, 1981.

[13] A. Buades, B. Coll, and J.-M. Morel, *A non-local algorithm for image denoising*, in Computer Vision and Pattern Recognition, 2005. CVPR 2005. IEEE Computer Society Conference, vol. 2, IEEE, 2005, pp. 60–65.

[14] M. Burger, J. Modersitzki, and L. Ruthotto, *A hyperelastic regularization energy for image registration*, SIAM Journal on Scientific Computing, 35 (2013), pp. B132–B148.

[15] V. Caselles, R. Kimmel, and G. Sapiro, *Geodesic Active Contours*, Int. J. Comput. Vis., 22 (1993), pp. 61–87.

[16] A. Chambolle, D. Cremers, and T. Pock, *A convex approach to minimal partitions*, SIAM Journal on Imaging Sciences, 5 (2012), pp. 1113–1158.

[17] T. Chan and L. Vese, *Active Contours Without Edges*, IEEE Trans. Image Process., 10 (2001), pp. 266–277.

[18] T. F. Chan and S. Esedoḡlu, *Aspects of total variation regularized L^1 function approximation*, SIAM Journal on Applied Mathematics, 65 (2005), pp. 1817–1837.

[19] M. Chen, A. Carass, A. Jog, J. Lee, S. Roy, and J. L. Prince, *Cross contrast multi-channel image registration using image synthesis for MR brain images*, Medical Image Analysis, 36 (2017), pp. 2 – 14.

[20] G. Christensen, R. Rabbitt, and M. Miller, *Deformable Templates Using Large Deformation Kinematics*, IEEE Trans. Image Process., 5 (1996), pp. 1435–1447.

[21] K.-S. Chuang, H.-L. Tzeng, S. Chen, J. Wu, and T.-J. Chen, *Fuzzy C-means clustering with spatial information for image segmentation*, computerized medical imaging and graphics, 30 (2006), pp. 9–15.

[22] H. Chui and A. Rangarajan, *A new point matching algorithm for non-rigid registration*, Computer Vision and Image Understanding, 89 (2003), pp. 114–141.

[23] P. Ciarlet, *Elasticité Tridimensionnelle*, Masson, 1985.

[24] O. Clatz, M. Sermesant, P.-Y. Bondiau, H. Delingette, S. K. Warfield, G. Malandain, and N. Ayache, *Realistic simulation of the 3-D growth of brain tumors in MR images coupling diffusion with biomechanical deformation*, Medical Imaging, IEEE Transactions on, 24 (2005), pp. 1334–1346.

[25] D. Comaniciu and P. Meer, *Mean shift: A robust approach toward feature space analysis*, IEEE Transactions on pattern analysis and machine intelligence, 24 (2002), pp. 603–619.

[26] C. Davatzikos, *Spatial transformation and registration of brain images using elastically deformable models*, Computer Vision and Image Understanding, 66 (1997), pp. 207–222.

[27] M. H. Davis, A. Khotanzad, D. P. Flamig, and S. E. Harms, *A physics-based coordinate transformation for 3-D image matching*, Medical Imaging, IEEE Transactions on, 16 (1997), pp. 317–328.

[28] E. De Giorgi, M. Carriero, and A. Leaci, *Existence theorem for a minimum problem with free discontinuity set*, Archive for Rational Mechanics and Analysis, 108 (1989), pp. 195–218.

[29] B. D. de Vos, F. F. Berendsen, M. A. Viergever, M. Staring, and I. Išgum, *End-to-end unsupervised deformable image registration with a convolutional neural network*, arXiv preprint arXiv:1704.06065, (2017).

[30] N. Debroux and C. Le Guyader, *A joint segmentation/registration model based on a nonlocal characterization of weighted total variation and nonlocal shape descriptors*, SIAM Journal on Imaging Sciences, (2017).

[31] N. Debroux, C. Le Guyader, and A. Vese, L., *A second order free discontinuity model for bituminous surfacing crack recovery and analysis of a nonlocal version of it*, Annals of Mathematical Sciences and Applications, (2017).

[32] N. Debroux, S. Ozeré, and C. Le Guyader, *A non-local topology-preserving segmentation-guided registration model*, Journal of Mathematical Imaging and Vision, 59 (2016), pp. 432–455.

[33] Q. Denoyelle, V. Duval, and G. Peyré, *Support recovery for sparse super-resolution of positive measures*, Journal of Fourier Analysis and Applications, 23 (2017), pp. 1153–1194.

[34] R. Derfoul and C. Le Guyader, *A relaxed problem of registration based on the Saint Venant-Kirchhoff material stored energy for the mapping of mouse brain gene expression data to a neuroanatomical mouse atlas*, SIAM Journal on Imaging Sciences, 7 (2014), pp. 2175–2195.

[35] J. Dong, K. Lu, J. Xue, S. Dai, R. Zhai, and W. Pan, *Accelerated nonrigid image registration using improved Levenberg-Marquardt method*, Information Sciences, 423 (2018), pp. 66 – 79.

[36] P. Dong, L. Wang, W. Lin, D. Shen, and G. Wu, *Scalable joint segmentation and registration framework for infant brain images*, Neurocomputing, 229 (2017), pp. 54–62.

[37] M. Droske and M. Rumpf, *Multiscale Joint Segmentation and Registration of Image Morphology*, Pattern Analysis and Machine Intelligence, IEEE Transactions on, 29 (2007), pp. 2181–2194.

[38] P. F. Felzenszwalb and D. P. Huttenlocher, *Efficient graph-based image segmentation*, International journal of computer vision, 59 (2004), pp. 167–181.

[39] B. Fischer and J. Modersitzki, *Fast diffusion registration*, AMS Contemporary Mathematics, Inverse Problems, Image Analysis, and Medical Imaging, 313 (2002), pp. 11–129.

[40] B. Fischer and J. Modersitzki, *Curvature based image registration*, J. Math. Imaging Vis., 18 (2003), pp. 81–85.

[41] A. F. Frangi, W. J. Niessen, K. L. Vincken, and M. A. Viergever, *Multiscale vessel enhancement filtering*, in International Conference on Medical Image Computing and Computer-Assisted Intervention, Springer, 1998, pp. 130–137.

[42] J. B. Garnett, T. M. Le, Y. Meyer, and L. A. Vese, *Image decompositions using bounded variation and generalized homogeneous Besov spaces*, Applied and Computational Harmonic Analysis, 23 (2007), pp. 25–56.

[43] S. Ghosal and N. Ray, *Deep deformable registration: Enhancing accuracy by fully convolutional neural net*, Pattern Recognition Letters, (2017).

[44] G. Gilboa and S. Osher, *Nonlocal operators with applications to image processing*, Multiscale Modeling & Simulation, 7 (2008), pp. 1005–1028.

[45] A. Gooya, K. Pohl, M. Bilello, L. Cirillo, G. Biros, E. Melhem, and C. Davatzikos, *GLISTR: Glioma Image Segmentation and Registration*, Medical Imaging, IEEE Transactions on, 31 (2012), pp. 1941–1954.

[46] S. Gorthi, V. Duay, X. Bresson, M. B. Cuadra, F. J. S. Castro, C. Pollo, A. S. Allal, and J.-P. Thiran, *Active deformation fields: Dense deformation field estimation for atlas-based segmentation using the active contour framework*, Medical Image Analysis, 15 (2011), pp. 787–800.

[47] E. Haber and J. Modersitzki, *Numerical methods for volume preserving image registration*, Inverse Probl., 20 (2004), pp. 1621–1638.

[48] S. Haker, L. Zhu, A. Tannenbaum, and S. Angenent, *Optimal mass transport for registration and warping*, International Journal of Computer Vision, 60 (2004), pp. 225–240.

[49] M. P. Heinrich, I. J. Simpson, B. W. Papież, M. Brady, and J. A. Schnabel, *Deformable image registration by combining uncertainty estimates from supervoxel belief propagation*, Medical image analysis, 27 (2016), pp. 57–71.

[50] P. Hellier, C. Barillot, É. Mémin, and P. Pérez, *Hierarchical estimation of a dense deformation field for 3-D robust registration*, IEEE transactions on medical imaging, 20 (2001), pp. 388–402.

[51] M. Jung, X. Bresson, T. F. Chan, and L. A. Vese, *Nonlocal Mumford-Shah regularizers for color image restoration*, IEEE transactions on image processing, 20 (2011), pp. 1583–1598.

[52] B. Karaçali and C. Davatzikos, *Estimating topology preserving and smooth displacement fields*, IEEE Trans. Med. Imag., 23 (2004), pp. 868–880.

[53] M. Kass, A. Witkin, and D. Terzopoulos, *Snakes: Active contour models*, International journal of computer vision, 1 (1988), pp. 321–331.

[54] A. P. Keszei, B. Berkels, and T. M. Deserno, *Survey of non-rigid registration tools in medicine*, Journal of Digital Imaging, 30 (2017), pp. 102–116.

[55] Y. Kim and L. Vese, *Image recovery using functions of bounded variation and Sobolev spaces of negative differentiability*, Inverse problems and Imaging, 3 (2009), pp. 43–68.

[56] K. C. Lam and L. M. Lui, *Landmark-and intensity-based registration with large deformations via quasi-conformal maps*, SIAM Journal on Imaging Sciences, 7 (2014), pp. 2364–2392.

[57] T. M. Le and L. A. Vese, *Image decomposition using total variation and div (BMO)*, Multiscale Modeling & Simulation, 4 (2005), pp. 390–423.

[58] V. Le Guen, *Cartoon + Texture Image Decomposition by the TV-L^1 Model*, Image Processing On Line, 4 (2014), pp. 204–219.

[59] C. Le Guyader and C. Gout, *Geodesic active contour under geometrical conditions: theory and 3D applications*, Numerical algorithms, 48 (2008), pp. 105–133.

[60] C. Le Guyader and L. Vese, *Self-Repelling Snakes for Topology-Preserving Segmentation Models*, Image Processing, IEEE Transactions on, 17 (2008), pp. 767–779.

[61] C. Le Guyader and L. Vese, *A combined segmentation and registration framework with a nonlinear elasticity smoother*, Computer Vision and Image Understanding, 115 (2011), pp. 1689–1709.

[62] C. Li, C.-Y. Kao, J. C. Gore, and Z. Ding, *Implicit active contours driven by local binary fitting energy*, in Computer Vision and Pattern Recognition, 2007. CVPR'07. IEEE Conference on, IEEE, 2007, pp. 1–7.

[63] L. H. Lieu and L. A. Vese, *Image restoration and decomposition via bounded total variation and negative Hilbert-Sobolev spaces*, Applied Mathematics & Optimization, 58 (2008), pp. 167–193.

[64] N. Lord, J. Ho, B. Vemuri, and S. Eisenschenk, *Simultaneous Registration and Parcellation of Bilateral Hippocampal Surface Pairs for Local Asymmetry Quantification*, IEEE Trans. Med. Imaging, 26 (2007), pp. 471–478.

[65] J. Maas, M. Rumpf, and S. Simon, *Transport Based Image Morphing with Intensity Modulation*, Springer International Publishing, Cham, 2017, pp. 563–577.

[66] D. Mahapatra, Z. Li, F. Vos, and J. Buhmann, *Joint segmentation and groupwise registration of cardiac DCE MRI using sparse data representations*, in Biomedical Imaging (ISBI), 2015 IEEE 12th International Symposium on, IEEE, 2015, pp. 1312–1315.

[67] Y. Meyer, *Oscillating patterns in image processing and nonlinear evolution equations: the fifteenth Dean Jacqueline B. Lewis memorial lectures*, vol. 22, American Mathematical Soc., 2001.

[68] I. Middleton and R. I. Damper, *Segmentation of magnetic resonance images using a combination of neural networks and active contour models*, Medical engineering & physics, 26 (2004), pp. 71–86.

[69] M. I. Miller and L. Younes, *Group actions, homeomorphisms, and matching: A general framework*, International Journal of Computer Vision, 41 (2001), pp. 61–84.

[70] J. Modersitzki, *Numerical Methods for Image Registration*, Oxford University Press, 2004.

[71] B. Mory and R. Ardon, *Fuzzy Region Competition: A Convex Two-Phase Segmentation Framework*, in Scale Space and Variational Methods in Computer Vision 2007. SSVM 2007., vol. 4485/2008 of Lecture Notes in Computer Science, Ischia, Italy, 2007, Springer Berlin / Heidelberg, pp. 214–226.

[72] D. Mumford and J. Shah, *Optimal approximation by piecewise smooth functions and associated variational problems*, Commun. Pure Applied Mathematics, (1989), pp. 577–685.

[73] O. Musse, F. Heitz, and J.-P. Armspach, *Topology preserving deformable image matching using constrained hierarchical parametric models*, IEEE Trans. Image Process., 10 (2001), pp. 1081–1093.

[74] V. Noblet, C. Heinrich, F. Heitz, and J.-P. Armspach, *3-D deformable image registration: a topology preservation scheme based on hierarchical deformation models and interval analysis optimization*, IEEE Trans. Image Process., 14 (2005), pp. 553–566.

[75] R. Ohlander, K. Price, and D. R. Reddy, *Picture segmentation using a recursive region splitting method*, Computer graphics and image processing, 8 (1978), pp. 313–333.

[76] F. P. Oliveira and J. M. R. Tavares, *Medical image registration: a review*, Computer methods in biomechanics and biomedical engineering, 17 (2014), pp. 73–93.

[77] S. Osher and J. A. Sethian, *Fronts propagating with curvature-dependent speed: algorithms based on Hamilton-Jacobi formulations*, Journal of computational physics, 79 (1988), pp. 12–49.

[78] S. Osher, A. Solé, and L. Vese, *Image decomposition and restoration using total variation minimization and the H^{-1} norm*, Multiscale Modeling & Simulation, 1 (2003), pp. 349–370.

[79] S. Ozeré, *Modélisation mathématique de problèmes relatifs au recalage d'images*, PhD thesis, 2015. Thèse de doctorat dirigée par Gout, Christian et Le Guyader, Carole Mathématiques Rouen, INSA 2015.

[80] S. Ozeré, C. Gout, and C. Le Guyader, *Joint Segmentation/Registration Model by Shape Alignment via Weighted Total Variation Minimization and Nonlinear Elasticity*, SIAM Journal on Imaging Sciences, 8 (2015), pp. 1981–2020.

[81] S. Ozeré and C. Le Guyader, *Topology preservation for image-registration-related deformation fields*, Communications in Mathematical Sciences, 13 (2015), pp. 1135–1161.

[82] K. Papafitsoros, *Novel higher order regularisation methods for image reconstruction*, PhD thesis, University of Cambridge, 2015.

[83] S. Parisot, W. Wells, S. Chemouny, H. Duffau, and N. Paragios, *Concurrent tumor segmentation and registration with uncertainty-based sparse non-uniform graphs*, Medical image analysis, 18 (2014), pp. 647–659.

[84] X. Pennec, R. Stefanescu, V. Arsigny, P. Fillard, and N. Ayache, *Medical Image Computing and Computer-Assisted Intervention – MICCAI 2005: 8th International Conference, Palm Springs, CA, USA, October 26-29, 2005, Proceedings, Part II*, Springer Berlin Heidelberg, 2005, ch. Riemannian Elasticity: A Statistical Regularization Framework for Non-Linear Registration, pp. 943–950.

[85] K. M. Pohl, J. Fisher, W. E. L. Grimson, R. Kikinis, and W. M. Wells, *A Bayesian model for joint segmentation and registration*, NeuroImage, 31 (2006), pp. 228–239.

[86] R. Rabbitt, J. Weiss, G. Christensen, and M. Miller, *Mapping of Hyperelastic Deformable Templates Using the Finite Element Method*, in Proceedings SPIE, vol. 2573, SPIE, 1995, pp. 252–265.

[87] S. R. Rao, H. Mobahi, A. Y. Yang, S. S. Sastry, and Y. Ma, *Natural image segmentation with adaptive texture and boundary encoding*, in Asian Conference on Computer Vision, Springer, 2009, pp. 135–146.

[88] T. Rohlfing, *Image similarity and tissue overlaps as surrogates for image registration accuracy: widely used but unreliable*, IEEE transactions on medical imaging, 31 (2012), pp. 153–163.

[89] L. Rudin, S. Osher, and E. Fatemi, *Nonlinear Total Variation Based Noise Removal Algorithms*, Phys. D, 60 (1992), pp. 259–268.

[90] M. Rumpf and B. Wirth, *A Nonlinear Elastic Shape Averaging Approach*, SIAM Journal on Imaging Sciences, 2 (2009), pp. 800–833.

[91] H. Schaeffer, *Variational Models for Fine Structures*, PhD thesis, University of California, Los Angeles, USA, 2013.

[92] C.-B. Schönlieb, *Partial Differential Equation Methods for Image Inpainting*, Cambridge Monographs on Applied and Computational Mathematics, Cambridge University Press, 2015.

[93] T. Sederberg and S. Parry, *Free-form Deformation of Solid Geometric Models*, SIGGRAPH Comput. Graph., 20 (1986), pp. 151–160.

[94] D. Shen and C. Davatzikos, *HAMMER: hierarchical attribute matching mechanism for elastic registration*, Medical Imaging, IEEE Transactions on, 21 (2002), pp. 1421–1439.

[95] J. Shen, *Piecewise $H^{-1} + H^0 + H^1$ images and the Mumford-Shah-Sobolev model for segmented image decomposition*, Applied Mathematics Research Express, 2005 (2005), pp. 143–167.

[96] J. Shi and J. Malik, *Normalized cuts and image segmentation*, IEEE Transactions on pattern analysis and machine intelligence, 22 (2000), pp. 888–905.

[97] H. Sokooti, B. de Vos, F. Berendsen, B. P. F. Lelieveldt, I. Išgum, and M. Staring, *Nonrigid image registration using multi-scale 3d convolutional neural networks*, in Medical Image Computing and Computer Assisted Intervention MICCAI 2017, M. Descoteaux, L. Maier-Hein, A. Franz, P. Jannin, D. L. Collins, and S. Duchesne, eds., Springer International Publishing, 2017, pp. 232–239.

[98] A. Sotiras, C. Davatzikos, and N. Paragios, *Deformable medical image registration: A survey*, Medical Imaging, IEEE Transactions on, 32 (2013), pp. 1153–1190.

[99] M. Storath and A. Weinmann, *Fast partitioning of vector-valued images*, SIAM Journal on Imaging Sciences, 7 (2014), pp. 1826–1852.

[100] P. Swierczynski, B. W. Papież, J. A. Schnabel, and C. Macdonald, *A level-set approach to joint image segmentation and registration with application to ct lung imaging*, Computerized Medical Imaging and Graphics, (2017).

[101] T. W. Tang and A. C. Chung, *Non-rigid image registration using graph-cuts*, in Medical Image Computing and Computer-Assisted Intervention–MICCAI 2007, Springer, 2007, pp. 916–924.

[102] J.-P. Thirion, *Image matching as a diffusion process: an analogy with Maxwell's demons*, Medical image analysis, 2 (1998), pp. 243–260.

[103] G. Unal and G. Slabaugh, *Coupled PDEs for non-rigid registration and segmentation*, in Computer Vision and Pattern Recognition, 2005. CVPR 2005. IEEE Computer Society Conference on, vol. 1, 2005, pp. 168–175.

[104] B. Vemuri, J. Ye, Y. Chen, and C. Leonard, *Image Registration via level-set motion: Applications to atlas-based segmentation*, Medical Image Analysis, 7 (2003), pp. 1–20.

[105] L. Vese and C. Le Guyader, *Variational Methods in Image Processing*, Chapman & Hall/CRC Mathematical and Computational Imaging Sciences Series, Taylor & Francis, 2015.

[106] L. A. Vese and T. F. Chan, *A multiphase level-set framework for image segmentation using the Mumford and Shah model*, International journal of computer vision, 50 (2002), pp. 271–293.

[107] L. A. Vese and S. J. Osher, *Modeling textures with total variation minimization and oscillating patterns in image processing*, Journal of scientific computing, 19 (2003), pp. 553–572.

[108] M. A. Viergever, J. A. Maintz, S. Klein, K. Murphy, M. Staring, and J. P. Pluim, *A survey of medical image registration–under review*, 2016.

[109] F. Wang, B. C. Vemuri, A. Rangarajan, and S. J. Eisenschenk, *Simultaneous nonrigid registration of multiple point sets and atlas construction*, Pattern Analysis and Machine Intelligence, IEEE Transactions on, 30 (2008), pp. 2011–2022.

[110] L. Wang, C. Li, Q. Sun, D. Xia, and C.-Y. Kao, *Active contours driven by local and global intensity fitting energy with application to brain MR image segmentation*, Computerized Medical Imaging and Graphics, 33 (2009), pp. 520–531.

[111] W. M. Wells, P. Viola, H. Atsumi, S. Nakajima, and R. Kikinis, *Multi-modal volume registration by maximization of mutual information*, Medical image analysis, 1 (1996), pp. 35–51.

[112] B. Wirth, *On the Γ-limit of joint image segmentation and registration functionals based on phase fields*, 18 (2016), pp. 441–477.

[113] G. Wu, L. Wang, J. Gilmore, W. Lin, and D. Shen, *Joint Segmentation and Registration for Infant Brain Images*, in Medical Computer Vision: Algorithms for Big Data: International Workshop, MCV 2014, Held in Conjunction with MICCAI 2014, Cambridge, MA, USA, September 18, 2014, Revised Selected Papers, B. Menze, G. Langs, A. Montillo, M. Kelm, H. Müller, S. Zhang, T. W. Cai, and D. Metaxas, eds., Springer International Publishing, 2014, pp. 13–21.

[114] P. P. Wyatt and J. A. Noble, *MAP MRF joint segmentation and registration of medical images*, Medical Image Analysis, 7 (2003), pp. 539–552.

[115] I. Yanovsky, C. Le Guyader, A. Leow, A. Toga, P. Thompson, and L. Vese, *Unbiased volumetric registration via nonlinear elastic regularization*, in 2nd MICCAI Workshop on Mathematical Foundations of Computational Anatomy, 2008.

[116] I. Yanovsky, P. M. Thompson, S. Osher, and A. D. Leow, *Topology preserving log-unbiased nonlinear image registration: Theory and implementation*, in Proc. IEEE Conf. Comput. Vis. Pattern Recognit., 2007, pp. 1–8.

[117] A. Yezzi, L. Zollei, and T. Kapur, *A variational framework for joint segmentation and registration*, in Mathematical Methods in Biomedical Image Analysis, IEEE-MMBIA, 2001, pp. 44–51.

[118] L. Younes, F. Arrate, and M. I. Miller, *Evolution equations in computational anatomy*, NeuroImage, 45 (2009), pp. S40 – S50. Mathematics in Brain Imaging.

[119] L. Zagorchev and A. Goshtasby, *A comparative study of transformation functions for nonrigid image registration*, Image Processing, IEEE Transactions on, 15 (2006), pp. 529–538.

[120] H. Zhang, J. E. Fritts, and S. A. Goldman, *Image segmentation evaluation: A survey of unsupervised methods*, computer vision and image understanding, 110 (2008), pp. 260–280.

[121] F. Zhu, M. Ding, and X. Zhang, *Self-similarity inspired local descriptor for non-rigid multi-modal image registration*, Information Sciences, 372 (2016), pp. 16–31.

[122] H. Zhu, F. Meng, J. Cai, and S. Lu, *Beyond pixels: A comprehensive survey from bottom-up to semantic image segmentation and cosegmentation*, Journal of Visual Communication and Image Representation, 34 (2016), pp. 12–27.

Chapter 2

Mathematical background

In this chapter, we recall some mathematical tools, notions, definitions and properties that are used in the remaining of the manuscript. We will first proceed to a review of some functional spaces and then summarize some relevant facts in the theory of viscosity solutions and in the theory of calculus of variations. Finally, we will give a brief presentation of elasticity and hyperelasticity theory.

1 Functional spaces

1.1 L^p spaces

Let us first recall some basic results in measure theory based on [1].

Definition 1.1 (σ-algebra and measure spaces)**.** *Let X be a non-empty set and let $\mathcal{E}$ be a collection of subsets of X.*

- *We say that $\mathcal{E}$ is an algebra if $\emptyset \in \mathcal{E}$, $E_1 \cup E_2 \in \mathcal{E}$ and $X \setminus E_1 \in \mathcal{E}$ whenever $E_1, E_2 \in \mathcal{E}$.*
- *We say that an algebra $\mathcal{E}$ is a σ-algebra if for any sequence $(E_h) \subset \mathcal{E}$, its union $\underset{h}{\cup} E_h$ belongs to $\mathcal{E}$.*
- *For any collection $\mathcal{G}$ of subsets of X, the σ-algebra generated by $\mathcal{G}$ is the smallest σ-algebra containing $\mathcal{G}$. If (X, τ) is a topological space, we denote by $\mathcal{B}(X)$ the σ-algebra of Borel subsets of X, that is to say, the σ-algebra generated by the open subsets of X.*
- *If $\mathcal{E}$ is a σ-algebra in X, we call the pair $(X,\mathcal{E})$ a measure space.*

Definition 1.2 (measure)**.** *Let $(X,\mathcal{E})$ be a measure space. Let $n \in \mathbb{N}^*$.*

1. *$\mu : X \to \mathbb{R}^n$ is a measure if $\mu(\emptyset) = 0$ and if for any sequence $(E_k)_{k\in\mathbb{N}}$ of pairwise disjoint elements of $\mathcal{E}$, $\mu\left(\underset{k\in\mathbb{N}}{\cup} E_k\right) = \sum\limits_{k\in\mathbb{N}} \mu(E_k)$. If $n = 1$, μ is said to be a real measure, otherwise μ is a vector measure.*

2. If μ is a measure, we define its total variation $|\mu|$ for every $E \in \mathcal{E}$ as follows

$$|\mu|(E) := \sup\left\{\sum_{h=0}^{\infty}|\mu(E_h)| \,|\, E_h \in \mathcal{E} \text{ pairwise disjoint, } E = \bigcup_{h=0}^{\infty} E_h\right\}$$

Theorem 1.1. *If μ is a measure on $(X,\mathcal{E})$, then $|\mu|$ is a positive finite measure ($\mu(X) < \infty$ and $\mu : \mathcal{E} \to [0,\infty]$).*

Definition 1.3 (μ-negligible sets)**.** *Let μ be a positive measure on the measure space $(X,\mathcal{E})$.*

- *We say that $N \subset X$ is μ-negligible if there exists $E \in \mathcal{E}$ such that $N \subset E$ and $\mu(E) = 0$.*
- *We say that the property $P(x)$ depending on the point $x \in X$ holds μ almost everywhere (μ-a.e.) in X if the set where P fails is a μ-negligible set.*
- *Let $\mathcal{E}_\mu$ be the collection of all the subsets of X of the form $F = E \cup N$ with $E \in \mathcal{E}$ and N μ-negligible; then $\mathcal{E}_\mu$ is a σ-algebra which is called the μ-completion of $\mathcal{E}$, and we say that $E \in X$ is μ-measurable if $E \in \mathcal{E}_\mu$. The measure μ extends to $\mathcal{E}_\mu$ by setting, for F as above, $\mu(F) = \mu(E)$.*

Definition 1.4 (Measurable functions)**.** *Let $(X,\mathcal{E})$ be a measure space and (Y,d) a metric space.*

- *A function $f : X \to Y$ is said to be $\mathcal{E}$-measurable if $f^{-1}(A) \in \mathcal{E}$ for every open set $A \subset Y$.*
- *If μ is a positive measure on $(X,\mathcal{E})$, the function f is said to be μ-measurable if it is $\mathcal{E}_\mu$-measurable.*

Let us now recall the definition of an integral and some notions on summable functions. They are then extended to vector-valued functions as well as to vector measures.

Definition 1.5. *Let $(X,\mathcal{E})$ be a measure space.*

- *For $E \subset X$, we define the characteristic function of E, denoted by χ_E, by $\chi_E := \begin{cases} 1 & \text{if } x \in E \\ 0 & \text{if } x \notin E \end{cases}$. We say that $f : X \to \mathbb{R}$ is a simple function if it belongs to the vector space generated by the characteristic functions.*
- *Let μ be a positive measure on $(X,\mathcal{E})$; the integral of a μ-measurable function $u : X \to \mathbb{R}$ is defined by:*

$$\int_X u\,d\mu := \sup\left\{\int_X v\,d\mu = \sum_{z \in v(X)} z\mu(v^{-1}(z)),\ v\ \mu\text{-measurable, simple, } v \le u\right\}.$$

$u : X \to \bar{\mathbb{R}}$ is said to be μ-summable if $\int_X |u|\,d\mu < \infty$.

- *Let μ be a measure on $(X,\mathcal{E})$ and $u : X \to \bar{\mathbb{R}}$ be a $|\mu|$-measurable function. We say that u is μ-summable if u is $|\mu|$-summable. If μ is a $\mathbb{R}^n$-vector measure, we define $\int_X u\, d\mu := \left(\int_X u\, d\mu_1, \ldots, \int_X u\, d\mu_n\right)$.*
- *If μ is a real measure and $u = (u_1, \ldots, u_k) : X \to \mathbb{R}^k$ is $|\mu|$-measurable, we say that u is $|\mu|$-summable if all its components are $|\mu|$-summable and we denote $\int_X u\, d\mu := \left(\int_X u_1\, d\mu, \ldots, \int_X u_k\, d\mu\right)$.*

Let us now introduce Radon measures. Let Ω be an open subset of $\mathbb{R}^n$.

Definition 1.6 (Radon measure)**.** *A positive measure on $(\Omega, \mathcal{B}(\Omega))$ is called a Borel measure. Moreover, if it is finite on every compact subset of Ω, then it is called a positive Radon measure.*
A measure $\mu : \mathcal{B}(\Omega) \to \mathbb{R}^m$, $m \in \mathbb{N}^*$ is called a finite Radon measure (the Lebesgue measure on $(\Omega, \mathcal{B}(\Omega))$ is a positive Radon measure).

Proposition 1.7. *Let μ be a $\mathbb{R}^m$-valued Radon measure on $(\Omega, \mathcal{B}(\Omega))$. Then for every open set $A \subset \Omega$, we have $|\mu|(A) = \sup\left\{\sum_{i=1}^{m} \int_X u_i\, d\mu_i \,|\, u \in \mathcal{C}_c^0(A),\, u(x) \leq 1,\, \forall x \in A\right\}$.*

Theorem 1.2 (Riesz)**.** *Let L be a continuous linear form on $\mathcal{C}^0(\Omega, \mathbb{R}^m)$, $m \in \mathbb{N}$. There exists a unique finite $\mathbb{R}^m$-valued Radon measure on $(\Omega, \mathcal{B}(\Omega))$ such that $L(u) = \sum_{i=1}^{m} \int_\Omega u_i\, d\mu_i$, $\forall u \in \mathcal{C}^0(\Omega, \mathbb{R}^m)$. Furthermore, $\|L\| = |\mu|(\Omega)$.*

Theorem 1.3 (Weak convergence for Radon measures)**.** *Let (μ_k) be a sequence of Radon measures on $\mathbb{R}^n$ and μ be a Radon measure on $\mathbb{R}^n$. The following statements are equivalent:*

- *μ_k weakly converges to μ, $\mu_k \rightharpoonup \mu$.*
- *$\lim_{k\to+\infty} \int_{\mathbb{R}^n} f\, d\mu_k = \int_{\mathbb{R}^n} f\, d\mu$ for all $f \in \mathcal{C}_c^0(\mathbb{R}^n)$.*
- *$\limsup_{k\to+\infty} \mu_k(K) \leq \mu(K)$ for each compact set $K \subset \mathbb{R}^n$ and $\mu(U) \leq \liminf_{k\to+\infty} \mu_k(U)$ for each open set $U \subset \mathbb{R}^n$.*
- *$\lim_{k\to+\infty} \mu_k(B) = \mu(B)$ for each bounded Borel set $B \subset \mathbb{R}^n$ with $\mu(\partial B) = 0$.*

We introduce L^p spaces whose definitions and properties are extracted from [5] and [1].

Definition 1.8. *Let $(X, \mathcal{E})$ be a measure space, μ be a positive measure on it and $u : X \to \mathbb{R}^l$ a μ-measurable function, $l \in \mathbb{N}^*$. We set*

$$\|u\|_{L^p(X,\mathbb{R}^l;\mu)} := \left(\int_X |u|^p\, d\mu\right)^{\frac{1}{p}},$$

if $1 \leq p < \infty$ and

$$\|u\|_{L^\infty(X,\mathbb{R}^l;\mu)} := \inf\{C \in [0,\infty] : |u(x)| \leq C,\ for\, \mu - a.e.\, x \in X\}$$

We say that $u \in L^p(X, \mathbb{R}^l; \mu)$ *if* $\|u\|_{L^p(X,\mathbb{R}^l;\mu)} < \infty$. *The sets* $L^p(X, \mathbb{R}^l; \mu)$ *(in which two functions that agree a.e. as identical are identified) are Banach vector spaces with the norms* $\|u\|_{L^p(X,\mathbb{R}^l;\mu)}$ *defined previously for* $1 \leq p \leq \infty$. *The space* $L^2(X, \mathbb{R}^l; \mu)$ *is a Hilbert space endowed with the inner product* $(u, v)_{L^2(X,\mathbb{R}^l;\mu)} = \int_X < u(x), v(x) >_{\mathbb{R}^l} d\mu$.

We can extend this definition to Banach-space valued functions.

Definition 1.9. *Let* B *be a Banach space and* $T > 0$. *Then* $L^p(0, T; B) = \{f : [0, T] \to B | \int_0^T \|f(t)\|_B^p \, dt < +\infty\}$ *for* $1 \leq p < +\infty$ *and* $L^\infty(0, T; B) = \{f : [0, T] \to B | \sup_{t\in[0,T]} \|f(t)\|_B < +\infty\}$.

Let us now state some important integration results considering $l = 1$, $\mu = dx$ the Lebesgue measure of X, an open set of $\mathbb{R}^N$, and using the simplified notation $L^p(X)$.

Theorem 1.4 (Monotone convergence theorem of Beppo-Levi)**.** *Let* $u_h : X \to \mathbb{R}$ *be an increasing sequence of functions in* $L^1(X)$ *and assume that* $\sup_h \int_\Omega u_h \, dx < +\infty$. *Then* $u_h(x)$ *converges almost everywhere on* X *to a finite limit denoted by* $f(x)$. *Moreover,* $f \in L^1(X)$ *and* $\|u_h - f\|_{L^1(X)} \underset{h\to+\infty}{\longrightarrow} 0$.

Lemma 1.10 (Fatou's lemma)**.** *Let* $u_h : X \to \mathbb{R}$ *be a sequence of functions in* $L^1(X)$ *such that:*

1. *for every* $h \in \mathbb{N}$, $u_h(x) \geq 0$ *almost everywhere on* X,
2. $\sup_{h\in\mathbb{N}} \int_X u_h \, dx < \infty$.

For every $x \in X$, *we set* $u(x) = \liminf_{h\to+\infty} u_h(x)$. *Then* $u \in L^1(X)$ *and* $\int_X u \, dx \leq \liminf_{h\to+\infty} \int_X u_h \, dx$.

Theorem 1.5 (Lebesgue dominated convergence theorem)**.** *Let* $u_h : X \to \mathbb{R}$ *be a sequence of functions in* $L^1(X)$. *We assume that*

1. $u_h(x) \underset{h\to+\infty}{\longrightarrow} u(x)$ *almost everywhere on* X,
2. *there exists a function* $g \in L^1(X)$ *such that for every* $h \in \mathbb{N}$, $|u_h(x)| \leq g(x)$ *almost everywhere on* X.

Then $u \in L^1(X)$ *and* $\|u_h - u\|_{L^1(X)} \underset{h\to+\infty}{\longrightarrow} 0$.

Theorem 1.6 (Hölder's inequality)**.** *Let* $f \in L^p(X)$ *and* $g \in L^q(X)$ *with* $1 \leq p \leq \infty$ *and* $\frac{1}{p} + \frac{1}{q} = 1$. *Then* $fg \in L^1(X)$ *and* $\int_X |fg| \, dx \leq \|f\|_{L^p(X)} \|g\|_{L^q(X)}$.

Theorem 1.7 (Fubini-Tonelli's theorem)**.** *Let* $(X, \mathcal{A}, \mu)$ *and* $(Y, \mathcal{B}, \nu)$ *be two measure spaces such that* μ *and* ν *are* σ*-finite that is to say,* X *is the countable union of measurable sets with finite measure* μ, *and* Y *is the countable union of measurable sets with finite measure* ν. *Let* $(X \times Y, \mathcal{A} \times \mathcal{B}, \mu \times \nu)$ *be the product measure space endowed with the product measure. If* $f : X \times Y \to [0, +\infty]$ *is a* $\mathcal{A} \times \mathcal{B}$*-measurable function, then* $x \mapsto \int_Y f(x, y) \, d\nu(y)$ *and* $y \mapsto \int_X f(x, y) \, d\mu(x)$ *are respectively* $\mathcal{A}/\mathcal{B}$*-measurable functions and* $\int_{X\times Y} f(x, y) \, d(\mu \times \nu)(x, y) = \int_X \left[\int_Y f(x, y) \, d\nu(y)\right] d\mu(x) = \int_Y \left[\int_X f(x, y) \, d\mu(x)\right] d\nu(y)$.

We continue by presenting some properties of these sets.

Theorem 1.8. *Let $u_h : X \to \mathbb{R}$ be a sequence of functions in $L^p(X)$ and $u \in L^p(X)$ such that $\|u_h - u\|_{L^p(X)} \underset{h\to+\infty}{\longrightarrow} 0$. Then there exists a subsequence (u_{h_k}) of (u_h) such that:*

1. *$u_{h_k}(x) \underset{k\to+\infty}{\longrightarrow} u(x)$ for almost every $x \in X$,*
2. *there exists $h \in L^p(X)$ such that $|u_{h_k}|(x) \leq h(x)$ for almost every $x \in X$ and for all $k \in \mathbb{N}$.*

Theorem 1.9. *$L^p(X)$ is a reflexive space for $1 < p < +\infty$ and is a separable space for $1 \leq p < +\infty$. The dual space of $L^1(X)$ can be identified with $L^\infty(X)$.*

Theorem 1.10. *The dual space of $L^p(X)$ with $1 < p < +\infty$ is identified with $L^{\frac{p}{p-1}}(X)$.*

Theorem 1.11 (General compactness properties)**.**

1. *Let Y be a reflexive Banach space and let $C > 0$ be a positive real constant. Let also (u_h) be a sequence of Y such that $\|u_h\|_Y \leq C$ for all $h \in \mathbb{N}$. Then there exist $u \in Y$ and a subsequence (u_{h_k}) of (u_h) such that $u_{h_k} \underset{k\to+\infty}{\overset{Y}{\rightharpoonup}} u$.*
2. *Let Y be a separable Banach space and let $C > 0$ be a positive real constant. Let also (l_n) be a sequence of Y', the dual space of Y, such that $\|l_n\|_{Y'} \leq C$ for all $n \in \mathbb{N}$. Then there exist $l \in Y'$ and a subsequence (l_{n_k}) of (l_n) such that $l_{n_k} \underset{k\to+\infty}{\overset{Y*}{\rightharpoonup}} l$.*

1.2 Sobolev spaces

Definitions and theorems are extracted from [5] and [14]. Let $\Omega \subset \mathbb{R}^N$ be an open set associated with the Lebesgue measure dx.

Definition 1.11. *Assume that $u \in L^1_{loc}(\Omega)$. We say that $v_i \in L^1_{loc}(\Omega)$ is the weak partial derivative of u with respect to x_i in Ω (or the partial derivative in the sense of distributions) if*

$$\int_\Omega u \frac{\partial \phi}{\partial x_i}\, dx = -\int_\Omega v_i \phi\, dx,$$

for all $\phi \in \mathcal{C}^\infty_c(\Omega)$.

Definition 1.12. *Let $1 \leq p \leq +\infty$. The Sobolev space $W^{1,p}(\Omega)$ is defined by*

$$\begin{aligned} W^{1,p}(\Omega) &= \left\{ u \in L^p(\Omega) \;\middle|\; \begin{array}{l} \exists g_1, \ldots, g_N \in L^p(\Omega) \text{ such that} \\ \int_\Omega u \frac{\partial \phi}{\partial x_i}\, dx = -\int_\Omega g_i \phi\, dx,\ \forall \phi \in \mathcal{C}^\infty_c(\Omega),\ \forall i = 1, \ldots, N. \end{array} \right\} \\ &= \left\{ u \in L^p(\Omega) \,\middle|\, \forall i = 1, \ldots, N,\ \frac{\partial u}{\partial x_i},\ \text{the weak derivative of } u \text{ with respect to } x_i, \text{ exists} \right. \\ &\quad \left. \text{and } \frac{\partial u}{\partial x_i} \in L^p(\Omega) \right\}. \end{aligned}$$

The space $W^{1,2}(\Omega)$ is often denoted by $H^1(\Omega)$. Let $m \geq 2$ be an integer. The Sobolev space $W^{m,p}(\Omega)$ is defined by

$$W^{m,p}(\Omega) = \left\{ u \in L^p(\Omega \;\middle|\; \begin{array}{l} \forall \alpha \in \mathbb{N}^N \text{ with } |\alpha| \leq m, \exists g_\alpha \in L^p(\Omega) \text{ such that} \\ \int_\Omega u D^\alpha \phi \, dx = (-1)^{|\alpha|} \int_\Omega g_\alpha \phi \, dx, \forall \phi \in \mathcal{C}_c^\infty(\Omega). \end{array} \right\}$$
$$= \left\{ u \in L^p(\Omega) \middle| \forall \alpha \in \mathbb{N}^N \text{ with } |\alpha| \leq m, D^\alpha u = \frac{\partial^{\alpha_1+\alpha_2+\cdots+\alpha_N} u}{\partial^{\alpha_1} x_1 \partial^{\alpha_2} x_2 \ldots \partial^{\alpha_N} x_N}, \text{ the weak derivative of } u, \text{ exists and } D^\alpha u \in L^p(\Omega) \right\}.$$

The space $W^{m,2}(\Omega)$ is often denoted by $H^m(\Omega)$.

Proposition 1.13. *The spaces $W^{m,p}(\Omega)$ with $m \in \mathbb{N}^*$ and $1 \leq p \leq \infty$ are Banach spaces endowed with the respective norms $\|u\|_{W^{m,p}(\Omega)} = \sum_{0 \leq |\alpha| \leq m} \|D^\alpha u\|_{L^p(\Omega)}$.*
The spaces $W^{m,p}(\Omega)$ with $m \in \mathbb{N}^*$ and $1 < p < \infty$, are reflexive.
The spaces $W^{m,p}(\Omega)$ with $m \in \mathbb{N}^*$ and $1 \leq p < \infty$, are separable.
The spaces $H^m(\Omega)$, $m \in \mathbb{N}^*$, are separable and reflexive Hilbert spaces equipped with the inner product $(u,v)_{H^m(\Omega)} = \sum_{0 \leq |\alpha| \leq m} (D^\alpha u, D^\alpha v)_{L^2(\Omega)}$.

Let us now define some other classical functional spaces before giving more properties of Sobolev spaces.

Definition 1.14.

1. *$\mathcal{C}^0(\Omega) = \mathcal{C}(\Omega)$ is the set of continuous functions $u : \Omega \to \mathbb{R}$ with the norm $\|u\|_{\mathcal{C}^0(\Omega)} = \sup_{x \in \Omega} |u(x)|$.*

2. *$\mathcal{C}^0(\bar{\Omega})$ is the set of continuous functions $u : \Omega \to \mathbb{R}$ which can be extended continuously to $\bar{\Omega}$. The associated norm is defined by $\|u\|_{\mathcal{C}^0(\bar{\Omega})} = \sup_{x \in \bar{\Omega}} |u(x)|$.*

3. *The support of a function $u : \Omega \to \mathbb{R}$ is defined as $\operatorname{supp} u := \overline{\{x \in \Omega \,:\, u(x) \neq 0\}}$.*

4. *$\mathcal{C}_c(\Omega) = \{u \in \mathcal{C}(\Omega) \,|\, \operatorname{supp} u \subset \Omega \text{ is compact}\}$.*

5. *For all $k \in \mathbb{N}$, we denote by $\mathcal{C}^k(\Omega)$ the space of continuous functions with all their partial derivatives up to order k being also continuous. The associated norm is defined by $\|u\|_{\mathcal{C}^k(\Omega)} = \sup_{|\alpha| \leq k} \sup_{x \in \Omega} |D^\alpha u(x)|$.*

6. *Let X be a Banach space and $T > 0$. For all $k \in \mathbb{N}$, we denote by $\mathcal{C}^k(0,T;X)$ the space of continuous functions $u : [0,T] \to X$ with all their partial derivatives up to order k with respect to t being also continuous. The associated norm is defined by $\|u\|_{\mathcal{C}^k(0,T;X)} = \sup_{|\alpha| \leq k} \sup_{t \in [0,T]} \|\frac{\partial^k}{\partial t^k} u(t)\|_X$.*

7. *For all $k \in \mathbb{N}$ and $1 \geq \gamma \geq 0$, we define Hölder spaces by:*

$$\mathcal{C}^{k,\gamma}(\Omega) = \left\{u \in \mathcal{C}^k(\Omega) | \|u\|_{C^{k,\gamma}(\Omega)} = \|u\|_{\mathcal{C}^k(\Omega)} + \sup_{(x,y)\in\Omega^2,\, x\neq y} \left\{ \frac{|u(y)-u(x)|}{|x-y|^\gamma} \right\} < +\infty \right\}.$$

We continue with some interesting properties of Sobolev spaces with $m = 1$.

Theorem 1.12. *Assume that $1 \leq p < +\infty$.*

1. *(***Product rule***) If $(u, v) \in (W^{1,p}(\Omega) \cap L^\infty(\Omega))^2$, then $uv \in W^{1,p}(\Omega) \cap L^\infty(\Omega)$ and $\frac{\partial uv}{\partial x_i} = \frac{\partial u}{\partial x_i} v + \frac{\partial v}{\partial x_i} u$, for all $i = 1, \ldots, N$.*
2. *(***Chain rule***) Let $G \in \mathcal{C}^1(\mathbb{R})$ such that $G(0) = 0$ and $|G'(s)| \leq M$, $\forall s \in \mathbb{R}$. Let $u \in W^{1,p}(\Omega)$, then $G \circ u \in W^{1,p}(\Omega)$ and $\frac{\partial}{\partial x_i} G \circ u = (G' \circ u) \frac{\partial u}{\partial x_i}$, for all $i = 1, \ldots, N$.*

Theorem 1.13 (Trace theorem)**.** *Assume that Ω is a bounded open subset of $\mathbb{R}^N$ of class $\mathcal{C}^1$, and $1 \leq p < \infty$. There exists a bounded linear operator $T : W^{1,p}(\Omega) \to L^p(\partial\Omega)$ such that $Tu = u$ on $\partial\Omega$ for all $u \in W^{1,p}(\Omega) \cap \mathcal{C}(\bar{\Omega})$. Furthermore, for all $\phi \in C_c^\infty(\mathbb{R}^N, \mathbb{R})$ and $u \in W^{1,p}(\Omega)$,*

$$\int_\Omega u \, div\phi \, dx = -\int_\Omega \nabla u . \phi \, dx + \int_{\partial\Omega} (\phi . \nu) Tu \, d\mathcal{H}^{N-1},$$

ν denoting the unit outer normal to $\partial\Omega$ and $\mathcal{H}^{N-1}$ the $N-1$-dimensional Hausdorff measure whose definition follows.

Definition 1.15 (Hausdorff measure [10])**.** *For $K \subset \mathbb{R}^N$, and $n > 0$, we set*

$$\mathcal{H}^n(K) = \sup_{\varepsilon > 0} \mathcal{H}^n_\varepsilon(K),$$

called the n-dimensional Hausdorff measure of the set K, where

$$\mathcal{H}^n_\varepsilon(K) = c_n \inf \left\{ \sum_{i=1}^\infty (diam\, A_i)^n \right\},$$

and the infimum is taken over all countable families $\{A_i\}_{i=1}^\infty$ of closed sets A_i such that $K \subset \bigcup_{i=1}^\infty A_i$ and $diam\, A_i \leq \varepsilon$ for all i. The constant c_n is chosen so that $\mathcal{H}^n$ coincides with the Lebesgue measure on n-planes.

Theorem 1.14 (Generalized Poincaré inequality, [9])**.** *Let Ω be a Lipschitz bounded domain in $\mathbb{R}^N$. Let $p \in [1, \infty)$ and let $\mathcal{N}$ be a continuous semi-norm on $W^{1,p}(\Omega)$, that is, a norm on the constant functions. Let $u \in W^{1,p}(\Omega)$. Then there exists a constant $C > 0$ that depends only on Ω, N, and p, such that*

$$\|u\|_{W^{1,p}(\Omega)} \leq C \left(\left(\int_\Omega |\nabla u|^p \, dx \right)^{\frac{1}{p}} + \mathcal{N}(u) \right).$$

We apply this result to $\mathcal{N}(u) = \int_{\partial\Omega} |u(x)| \, dx$.

Theorem 1.15 (Density). *We assume that Ω is of class $\mathcal{C}^1$. Let $u \in W^{1,p}(\Omega)$ with $1 \leq p < \infty$. Then there exists a sequence $(u_n) \in \mathcal{C}_c^\infty(\mathbb{R}^N)$ such that $u_{n|\Omega} \underset{n\to+\infty}{\longrightarrow} u$ in $W^{1,p}(\Omega)$. In other words, the restrictions to Ω of functions of $\mathcal{C}_c^\infty(\mathbb{R}^N)$ are dense in $W^{1,p}(\Omega)$.*

Theorem 1.16 (Extension operators, [9]). *Let $m \in \mathbb{N}^*$. We assume that Ω is an open set of class $\mathcal{C}^m$, with $\partial\Omega$ bounded (or $\Omega = \mathbb{R}_+^N$). Then it has an (m,p)-extension property for every $p \in [1,\infty[$ that is to say, there exists a linear extension operator $E : W^{m,p}(\Omega) \to W^{m,p}(\mathbb{R}^N)$ such that $\forall u \in W^{m,p}(\Omega)$:*

1. *$Eu_{|\Omega} = u$,*
2. *$\|Eu\|_{L^p(\mathbb{R}^N)} \leq C\|u\|_{L^p(\Omega)}$,*
3. *$\|Eu\|_{W^{m,p}(\mathbb{R}^N)} \leq C\|u\|_{W^{1,p}(\Omega)}$,*

where C depends only on Ω. For $m = 1$, this property is also true for $p = \infty$.

We will now give Sobolev inequalities and embedding theorems.

Theorem 1.17 (Sobolev, Gagliardo, Nirenberg). *Let $1 \leq p < N$, then $W^{1,p}(\mathbb{R}^N) \subset L^{p^*}(\mathbb{R}^N)$ where $\frac{1}{p^*} = \frac{1}{p} - \frac{1}{N}$, and there exists a constant $C = C(p,N)$ such that $\|u\|_{L^{p^*}(\mathbb{R}^N)} \leq C\|\nabla u\|_{L^p(\mathbb{R}^N)}$, $\forall u \in W^{1,p}(\mathbb{R}^N)$.*

Corollary 1.16. *Let $1 \leq p < N$. Then $W^{1,p}(\mathbb{R}^N) \subset L^q(\mathbb{R}^N)$, $\forall q \in [p,p^*]$ with continuous embeddings.*

Corollary 1.17. *In the case where $p = N$, we have $W^{1,N}(\mathbb{R}^N) \subset L^q(\mathbb{R}^N)$, $\forall q \in [N,+\infty[$ with continuous embeddings.*

Theorem 1.18 (Morrey). *Let $p > N$, then $W^{1,p}(\mathbb{R}^N) \subset L^\infty(\mathbb{R}^N)$ with continuous embedding.*
Moreover, for all $u \in W^{1,p}(\mathbb{R}^N)$, we have $|u(x) - u(y)| \leq C|x-y|^\alpha \|\nabla u\|_{L^p(\mathbb{R}^N)}$ for almost every $(x,y) \in \mathbb{R}^{2N}$, with $\alpha = 1 - \frac{N}{p}$ and $C = C(p,N)$ a non-negative constant.

Corollary 1.18. *Let $m \geq 1$ be an integer and $1 \leq p < \infty$. We have*

- *if $\frac{1}{p} - \frac{m}{N} > 0$, then $W^{m,p}(\mathbb{R}^N) \subset L^q(\mathbb{R}^N)$ for all $q \in [p, \frac{Np}{N-mp}]$,*
- *if $\frac{1}{p} - \frac{m}{N} = 0$, then $W^{m,p}(\mathbb{R}^N) \subset L^q(\mathbb{R}^N)$, $\forall q \in [p,\infty[$,*
- *if $\frac{1}{p} - \frac{m}{N} > 0$, then $W^{m,p}(\mathbb{R}^N) \subset L^\infty(\mathbb{R}^N)$,*

with continuous embeddings.
Moreover, if $m - \frac{N}{p} > 0$ is not an integer, we set $k = \left[m - \frac{N}{p}\right]$ where $[.]$ denotes the bracket function and $\theta = m - \frac{N}{p} - k$ $(0 < \theta < 1)$. We have for all $u \in W^{1,p}(\mathbb{R}^N)$, $\|D^\alpha u\|_{L^\infty(\mathbb{R}^N)} \leq C\|u\|_{W^{m,p}(\mathbb{R}^N)}$, $\forall \alpha \in \mathbb{N}^N$ such that $|\alpha| \leq k$ and $|D^\alpha u(x) - D^\alpha u(y)| \leq C\|u\|_{W^{m,p}(\mathbb{R}^N)}|x-y|^\theta$ for almost every $(x,y) \in \mathbb{R}^{2N}$, and $\forall \alpha \in \mathbb{N}^N$ such that $|\alpha| = k$. In particular $W^{m,p}(\mathbb{R}^N) \subset \mathcal{C}^{k,\alpha}(\mathbb{R}^N)$ with continuous embeddings for all $\alpha \in [0,\theta]$.

Corollary 1.19. *Let Ω be an open set of class $\mathcal{C}^1$ with bounded boundary or $\Omega = \mathbb{R}^N$. The conclusions of the previous Corollary remain true if we replace $\mathbb{R}^N$ by Ω.*

Theorem 1.19 (Rellich-Kondrachov theorem)**.** *Let Ω be an open bounded Lipschitz subset of $\mathbb{R}^N$. Let $p \geq 1$.*

- *If $N > mp$ and $N > 1$, the embedding $W^{m,p}(\Omega) \subset L^q(\Omega)$ is compact for all $q \in [p, \frac{Np}{N-mp}[$.*
- *If $p < N$, then $W^{1,p}(\Omega) \subset L^q(\Omega)$ with compact embeddings for all $q \in [1, p^*[$, $\frac{1}{p^*} = \frac{1}{p} - \frac{1}{N}$.*
- *If $p = N$, then $W^{1,p}(\Omega) \subset L^q(\Omega)$ with compact embeddings for all $q \in [1, \infty[$.*
- *If $p > N$, then $W^{1,p}(\Omega) \subset \mathcal{C}^{0,\alpha}(\bar{\Omega})$ with compact embeddings for all $\alpha \in [0, 1 - \frac{N}{p}[$.*
- *If $mp > N$ and with $j = \left[\frac{N}{p}\right] + 1$, $W^{m,p}(\Omega) \subset \mathcal{C}^{m-j,\alpha}(\bar{\Omega})$ with compact embeddings for all $\alpha \in [0, j - \frac{N}{p}[$.*

Lemma 1.20 (Aubin-Lions lemma, extension to Sobolev spaces of Banach space-valued functions)**.** *Let X_0, X and X_1 be three Banach spaces with $X_0 \subseteq X \subseteq X_1$. Suppose that X_0 is compactly embedded in X and that X is continuously embedded in X_1. For $1 \leq p$, $q \leq +\infty$, let*

$$W = \left\{ u \in L^p(0,T;X_0) \,|\, \frac{\partial u}{\partial t} \in L^q(0,T;X_1) \right\}$$

be a generalized Sobolev space of Banach space-valued functions.

1. *If $p < +\infty$, then the embedding of W into $L^p(0,T;X)$ is compact.*
2. *If $p = +\infty$ and $q > 1$, then the embedding of W into $\mathcal{C}^0(0,T;X)$ is compact.*

1.3 Fractional Sobolev spaces

Before introducing fractional Sobolev spaces, we will briefly review tempered distributions and Fourier transform coming from [9] and [14].

Definition 1.21 (Rapidly decreasing functions)**.** *A function ϕ is said to be rapidly decreasing in $\mathbb{R}^N$ if $\phi \in \mathcal{C}^\infty(\mathbb{R}^N)$ and if, when D^j denotes the differentiation operator with respect to the multi-index $j = (j_1, j_2, \ldots, j_N)$, we have:*

$$\begin{aligned} &\forall j \in \mathbb{N}^N, \forall k \in \mathbb{N}, |x|^k D^j \phi \in L^\infty(\mathbb{R}^N). \\ &\Leftrightarrow \forall (j,k) \in \mathbb{N}^N \times \mathbb{N}, |x|^k D^j \phi \in L^1(\mathbb{R}^N). \\ &\Leftrightarrow \forall (j,k) \in \mathbb{N}^N \times \mathbb{N}, \lim_{|x| \to +\infty} |x|^k D^j \phi(x) = 0. \end{aligned}$$

The set of these functions is a vector space denoted by $\mathcal{S}(\mathbb{R}^N)$ having a natural topology generated by the following countable family of semi-norms: $n_{k,j}(\phi) = \| |x|^k D^j \phi \|_{L^\infty(\mathbb{R}^N)}$.

Proposition 1.22. *The space $\mathcal{D}(\mathbb{R}^N) = \mathcal{C}_c^\infty(\mathbb{R}^N)$ is dense in $\mathcal{S}(\mathbb{R}^N)$.*

Definition 1.23 (Tempered distributions)**.** *Let $\mathcal{S}'(\mathbb{R}^N)$ be the topological dual of $\mathcal{S}(\mathbb{R}^N)$. $\mathcal{S}'(\mathbb{R}^N)$ is the space of tempered distributions included in $\mathcal{D}'(\mathbb{R}^N)$, space of all distributions, dual space of $\mathcal{D}(\mathbb{R}^N)$.*

The Fourier transform is a classical tool in image processing and expresses a function in the spatial domain as a function of frequencies. In the following, we define it and present some of its useful properties.

Definition 1.24. *The Fourier transform $\mathcal{F}$ defined by*

$$\forall \xi \in \mathbb{R}^N,\ \forall \phi \in \mathcal{S}(\mathbb{R}^N),\ \mathcal{F}(\phi)(\xi) = \int_{\mathbb{R}^N} e^{-2i\pi\xi.x}\phi(x)\,dx,$$

is an automorphism of $\mathcal{S}(\mathbb{R}^N)$. The inverse operator of $\mathcal{F}$, which we denote by $\bar{\mathcal{F}}$, is defined by $\forall \xi \in \mathbb{R}^N$, $\bar{\mathcal{F}}(\phi)(\xi) = \mathcal{F}(\phi)(-\xi)$. The Fourier transform of $T \in \mathcal{S}'(\mathbb{R}^N)$, defined by $\forall \phi \in \mathcal{S}(\mathbb{R}^N)$, $< \mathcal{F}(T), \phi >=< T, \mathcal{F}(\phi) >$ is a tempered distribution.
We can easily see that if $f \in L^p(\mathbb{R}^N)$ with $p \in [1, \infty]$, then the associated distribution $[f]$ is tempered. In particular, if $f \in L^1(\mathbb{R}^N)$, then the function $\mathcal{F}(f) : \xi \mapsto \int_{\mathbb{R}^N} e^{-2i\pi\xi.x} f(x)\,dx$, which belongs to $L^\infty(\mathbb{R}^N)$, coincides with the transform $\mathcal{F}([f])$.

Proposition 1.25. *The distributions with bounded support which belong to $(\mathcal{C}^\infty(\mathbb{R}^N))'$, the topological dual space of $\mathcal{C}^\infty(\mathbb{R}^N)$ are tempered. The Fourier transform of such a distribution T can be identified with the function defined by $\xi \mapsto < T_{(x)}, e^{(-2i\pi\xi.x)} >$.*

Theorem 1.20 (Plancherel theorem)**.** *$\mathcal{F}_{|L^1(\mathbb{R}^N)\cap L^2(\mathbb{R}^N)}$ extends uniquely to a unitary isomorphism on $L^2(\mathbb{R}^N)$. In particular, if $u \in L^2(\mathbb{R}^N)$, then $\mathcal{F}(u) \in L^2(\mathbb{R}^N)$ and $\|u\|_{L^2(\mathbb{R}^N)} = \|\mathcal{F}(u)\|_{L^2(\mathbb{R}^N)}$.*

Theorem 1.21 (Convolution theorem)**.** *Let $u, v \in L^1(\mathbb{R}^N)$. Then $u * v \in L^1(\mathbb{R}^N)$ and $\mathcal{F}(u * v) = \mathcal{F}(u) \times \mathcal{F}(v)$ where $*$ denotes the convolution operator.*

We continue with the definitions and some properties of fractional Hilbert-Sobolev spaces.

Definition 1.26. *Let s be a real number.*
If $s > 0$, then we define $H^s(\mathbb{R}^N) = \{u \in L^2(\mathbb{R}^N) \,|\, \{\xi \mapsto (1 + |\xi|^2)^{\frac{s}{2}}\mathcal{F}(u)(\xi)\} \in L^2(\mathbb{R}^N)$.
If $s < 0$, then we define $H^s(\mathbb{R}^N) = \{u \in \mathcal{S}'(\mathbb{R}^N) \,|\, \{\xi \mapsto (1 + |\xi|^2)^{\frac{s}{2}}\mathcal{F}(u)(\xi)\} \in L^2(\mathbb{R}^N)$.

Proposition 1.27. *The space $H^s(\mathbb{R}^N)$ endowed with the norm defined by $\|u\|_{H^s(\mathbb{R}^N)} = \|(1 + |\xi|^2)^{\frac{s}{2}}\mathcal{F}(u)\|_{L^2(\mathbb{R}^N)}$ is a Banach space.*

Proposition 1.28. *If $s = m \in \mathbb{N}^*$, then the space $H^s(\mathbb{R}^N)$ coincides with the classical Sobolev space $W^{m,2}(\mathbb{R}^N)$.*

Proposition 1.29. *For $s > 0$, the space $H^{-s}(\mathbb{R}^N)$ coincides with the topological dual $H^s(\mathbb{R}^N)'$.*

Proposition 1.30. *The space $\mathcal{S}(\mathbb{R}^N)$ is dense in $H^s(\mathbb{R}^N)$.*

The following proposition will allow us to show that the spaces $H^s(\mathbb{R}^N)$ coincide with the spaces $W^{s,2}(\mathbb{R}^N)$ whose definitions are given later.

Proposition 1.31. *Let $s \in]0,1[$. Then $u \in H^s(\mathbb{R}^N)$ if and only if $u \in L^2(\mathbb{R}^N)$ and $\int_{\mathbb{R}^N}\int_{\mathbb{R}^N} \frac{|u(x)-u(y)|^2}{|x-y|^{N+2s}}\,dx\,dy < +\infty$.*

Proposition 1.32 (Embedding results)**.** *Let $s > 0$. We have the following continuous embeddings:*

1. *If $\frac{1}{2} < s < \frac{N}{2}$, then $H^s(\mathbb{R}^N) \subset L^q(\mathbb{R}^N)$ for every $q < \frac{2N}{N-2s}$.*
2. *If $s = \frac{N}{2}$, then $H^s(\mathbb{R}^N) \subset L^q(\mathbb{R}^N)$ for every $q < \infty$.*
3. *If $s > \frac{N}{2}$, then $H^s(\mathbb{R}^N) \subset \mathcal{C}^0(\mathbb{R}^N)$.*

We now provide the definition and some properties of fractional Sobolev spaces.

Definition 1.33. *Let $s \in]0,1[$ and let $p \in]1,\infty[$. Let Ω be an open subset of $\mathbb{R}^N$. We define the fractional Sobolev space $W^{s,p}(\Omega)$ as follows:*

$$W^{s,p}(\Omega) = \left\{ u \in L^p(\Omega) \mid \int_\Omega\int_\Omega \frac{|u(x)-u(y)|^p}{|x-y|^{N+sp}}\,dx\,dy < \infty \right\}.$$

Let $s \in \mathbb{R}\setminus\mathbb{N}$ with $s \geq 1$, $p \in [1,\infty[$, and Ω be an open subset of $\mathbb{R}^N$. The space $W^{s,p}(\Omega)$ is defined to be

$$W^{s,p}(\Omega) = \left\{ u \in W^{[s],p}(\Omega) \mid D^j u \in W^{s-[s],p}(\Omega),\ \forall j,\ |j| = [s] \right\}.$$

Proposition 1.34. *Let $s \in]0,1[$, $p \in]1,\infty[$ and Ω be an open subset of $\mathbb{R}^N$. The space $W^{s,p}(\Omega)$ endowed with the norm $\|u\|_{W^{s,p}(\Omega)} = \left(\|u\|^p_{L^p(\Omega)} + \int_\Omega\int_\Omega \frac{|u(x)-u(y)|^p}{|x-y|^{N+sp}}\,dx\,dy\right)^{\frac{1}{p}}$ is a Banach space.*
Let $s \in \mathbb{R}\setminus\mathbb{N}$, $s \geq 1$, $p \in]1,\infty[$ and Ω be an open subset of $\mathbb{R}^N$. It is clear that $W^{s,p}(\Omega)$ endowed with the norm $\|u\|_{W^{s,p}(\Omega)} = \left(\|u\|^p_{W^{[s],p}(\Omega)} + \sum\limits_{j,|j|=[s]} \int_\Omega\int_\Omega \frac{|D^j u(x)-D^j u(y)|^p}{|x-y|^{N+(s-[s])p}}\,dx\,dy\right)^{\frac{1}{p}}$ is a Banach space.

Proposition 1.35. *The space $W^{s_2,p}(\Omega)$ is continuously embedded in $W^{s_1,p}(\Omega)$, when $0 < s_1 \leq s_2 < 1$ and with $p \in]1,\infty[$ and Ω an open subset of $\mathbb{R}^N$.*
Let $p \in]1,\infty[$ and $s \in (0,1)$. Let Ω be a Lipschitz open set in $\mathbb{R}^N$ with bounded boundary and $u : \Omega \to \mathbb{R}$ be a measurable function. Then $W^{1,p}(\Omega) \subset W^{s,p}(\Omega)$ with continuous embedding.
Let $p \in]1,\infty[$ and $s_1 > s_2 > 1$. Let Ω be a Lipschitz open set in $\mathbb{R}^N$ with bounded boundary and $u : \Omega \to \mathbb{R}$ be a measurable function. Then $W^{s_1,p}(\Omega) \subset W^{s_2,p}(\Omega)$ with continuous embedding.

Proposition 1.36 (Continuous embedding results)**.** *Let Ω be a Lipschitz open subset of $\mathbb{R}^N$. Let $p \in]1, \infty[$. Let $s \in \mathbb{R} \setminus \mathbb{N}$. We then have:*

- *If $sp < N$, then $W^{s,p}(\Omega) \subset L^q(\Omega)$ for every $q \leq \frac{Np}{N-sp}$ with continuous embeddings.*
- *If $sp = N$, then $W^{s,p}(\Omega) \subset L^q(\Omega)$ for every $q < \infty$ with continuous embeddings.*
- *If $sp > N$, then we have:*
  - *If $s - \frac{N}{p} \notin \mathbb{N}$, then $W^{s,p}(\Omega) \subset C_b^{\left[s-\frac{N}{p}\right],\lambda}(\Omega) = \left\{ f \in C^{\left[s-\frac{N}{p}\right],\lambda}(\Omega),\ f \text{ bounded} \right\}$ for all $\lambda \leq s - \frac{N}{p} - \left[s - \frac{N}{p}\right]$, with continuous embeddings.*
  - *If $s - \frac{N}{p} \in \mathbb{N}$, then $W^{s,p}(\Omega) \subset C_b^{s-\frac{N}{p}-1,\lambda}(\Omega)$ with continuous embeddings for all $\lambda < 1$.*

Proposition 1.37 (Compact embedding results)**.** *Let Ω be a bounded Lipschitz open subset of $\mathbb{R}^N$. Let $p \in]1, \infty[$. Let $s \in \mathbb{R} \setminus \mathbb{N}$. We then have:*

- *If $sp < N$, then $W^{s,p}(\Omega) \subset L^q(\Omega)$ for every $q < \frac{Np}{N-sp}$ with compact embeddings.*
- *If $sp = N$, then $W^{s,p}(\Omega) \subset L^q(\Omega)$ for every $q < \infty$ with compact embeddings.*
- *If $sp > N$, then we have:*
  - *If $s - \frac{N}{p} \notin \mathbb{N}$, then $W^{s,p}(\Omega) \subset C_b^{\left[s-\frac{N}{p}\right],\lambda}(\Omega)$ for all $\lambda < s - \frac{N}{p} - \left[s - \frac{N}{p}\right]$, with compact embeddings.*
  - *If $s - \frac{N}{p} \in \mathbb{N}$, then $W^{s,p}(\Omega) \subset C_b^{s-\frac{N}{p}-1,\lambda}(\Omega)$ with compact embeddings for all $\lambda < 1$.*

1.4 BV space and its subsets

In this section, we remind the reader of the definition of functions of bounded variation functional space allowing to capture discontinuities along edges in images, as well as basic results. Precise studies of this space of functions are available in [10], [9] and [1]. This section is extracted from these books and we refer the reader to them for proofs of the results.
In the following, Ω is an open set of $\mathbb{R}^N$.

Definition 1.38 ($BV(\Omega)$ space)**.** *Let $u \in L^1(\Omega)$. u is a function of bounded variation on Ω if and only if $\int_\Omega u \frac{\partial \phi}{\partial x_i}\, dx = -\int_\Omega \phi\, dD_i u$, $\forall \phi \in \mathcal{C}_c^1(\Omega)$ with $Du = (D_1 u, D_2 u, \ldots, D_N u)$ a finite $\mathbb{R}^N$-valued Radon measure. The vector space of all functions of bounded variation is called $BV(\Omega)$.*

Definition 1.39 (Total variation)**.** *If $u \in L^1(\Omega)$, its total variation is defined by $|u|_{BV(\Omega)} := \sup\{\int_\Omega u\, div\, \phi\, dx \mid \phi \in \mathcal{C}_c^1(\Omega, \mathbb{R}^N), \|\phi\|_{L^\infty(\Omega)} \leq 1\}$. $u \in BV(\Omega)$ if and only if $|u|_{BV(\Omega)} < \infty$ and then $|u|_{BV(\Omega)} = |Du|(\Omega)$.*

Proposition 1.40. *$BV(\Omega)$ is a Banach space endowed with the norm $\|u\|_{BV(\Omega)} = \|u\|_{L^1(\Omega)} + |u|_{BV(\Omega)}$.*

Definition 1.41 (weak-$*$ convergence in $BV(\Omega)$)**.** *Let $u \in BV(\Omega)$, $(u_n)_{n\in\mathbb{N}}$ be a sequence of functions of bounded variation on Ω. We say that the sequence (u_n) converges weakly-$*$ to $u \in BV(\Omega)$ in $BV(\Omega)$ if $(u_n)_{n\in\mathbb{N}}$ converges to u strongly in $L^1(\Omega)$ and (Du_n) weakly converges to Du in the space of $\mathbb{R}^N$-valued Radon measures, that is to say, $\lim_{n\to+\infty} \|u_n - u\|_{L^1(\Omega)} = 0$ and $\lim_{n\to+\infty} \int_\Omega v Du_n = \int_\Omega v Du$, $\forall v \in \mathcal{C}_c(\Omega, \mathbb{R}^N)$.*

Theorem 1.22 (Lower semi-continuity of total variation)**.** *Assume that $u_n \in BV(\Omega)$ $(n = 1, 2, \dots)$ and $u_n \to u$ strongly in $L^1(\Omega)$. Then $|u|_{BV(\Omega)} \leq \liminf_{n\to+\infty} |u_n|_{BV(\Omega)}$.*

Theorem 1.23 (Compactness)**.** *Let $\Omega \subset \mathbb{R}^N$ be a bounded open set with Lipschitz boundary $\partial\Omega$. Assume that $\{u_n\}_{n=1}^\infty$ is a sequence in $BV(\Omega)$ satisfying $\sup_{n\in\mathbb{N}} \|u_n\|_{BV(\Omega)} < \infty$. Then there exists a subsequence $\{u_{n_j}\}_{j=1}^\infty$ and a function $u \in BV(\Omega)$ such that $u_{n_j} \underset{j\to+\infty}{\longrightarrow} u$ strongly in $L^1(\Omega)$.*

Theorem 1.24 (Regular approximation)**.** *Let Ω be a bounded open subset of $\mathbb{R}^N$. Let $u \in BV(\Omega)$, then there exists a sequence $(u_k)_{k\in\mathbb{N}}$ of $BV(\Omega) \cap \mathcal{C}^\infty(\Omega)$ functions such that:*

1. *$u_k \underset{k\to+\infty}{\longrightarrow} u$ strongly in $L^1(\Omega)$, and*
2. *$|u_k|_{BV(\Omega)} \underset{k\to+\infty}{\longrightarrow} |u|_{BV(\Omega)}$.*

Theorem 1.25 (Embedding theorem)**.** *Let $\Omega \subset \mathbb{R}^N$ be an open and bounded set with a Lipschitz boundary $\partial\Omega$. Then the embedding $BV(\Omega) \subset L^{\frac{N}{N-1}}(\Omega)$ is continuous and the embeddings $BV(\Omega) \subset L^p(\Omega)$ for all $p \in [1, \frac{N}{N-1}[$ are compact.*

Theorem 1.26 (Poincaré-Wirtinger inequality)**.** *Let $\Omega \subset \mathbb{R}^N$ be an open, bounded and connected set with Lipschitz boundary $\partial\Omega$. Then there exists a constant $C > 0$ depending only on N and Ω such that $\|u - \frac{1}{|\Omega|}\int_\Omega u(x)\,dx\|_{L^p(\Omega)} \leq C|u|_{BV(\Omega)}$, $\forall u \in BV(\Omega)$ and $1 \leq p \leq \frac{N}{N-1}$.*

Theorem 1.27 (Coarea formula)**.** *Let $u \in BV(\Omega)$ with Ω an open subset of $\mathbb{R}^N$. Then*

- *$E_t = \{x \in \Omega \,|\, u(x) > t\}$ has finite perimeter that is to say $\chi_{E_t} \in BV(\Omega)$ and $|\chi_{E_t}|_{BV(\Omega)}$ is the perimeter $P_\Omega(E_t)$ of E_t in Ω, for almost every $t \in \mathbb{R}$.*
- *$|u|_{BV(\Omega)} = \int_{-\infty}^{+\infty} |\chi_{E_t}|_{BV(\Omega)}\,dt$*
- *Conversely, if $u \in L^1(\Omega)$ and $\int_{-\infty}^{+\infty} |\chi_{E_t}|_{BV(\Omega)}\,dt < \infty$, then $u \in BV(\Omega)$.*

We briefly introduce the characterization of functions of bounded variations. Indeed, the measure Du of a function u of bounded variation can be decomposed into three terms namely $Du = D^a u + D^c u + D^j u$ where $D^a u$ is the absolutely continuous part of Du and

$D^s u = D^j u + D^c u$ is the singular part with $D^j u$ being the jump part and $D^c u$ being the Cantor part. Moreover, we can express $Du = \nabla u\, dx + (u^+ - u^-)\vec{n}_u\, \mathcal{H}^{N-1}|_{S_u} + D^c u$, where $\nabla u \in L^1(\Omega)$, S_u is of finite $(N-1)$-dimensional Hausdorff measure, $(u^+ - u^-)\vec{n}_u \chi_{S_u} \in L^1(\Omega, \mathbb{R}^N; \mathcal{H}^{N-1}|_{S_u})$ with u^+ and u^- on each side of the jump part S_u, and $\vec{n}_u$ the unit normal to S_u; finally, $D^c u$ satisfies $D^c u(B) = 0$ for all B such that $\mathcal{H}^{N-1}(B) < +\infty$.

Definition 1.42 (SBV space)**.** *We say that $u \in BV(\Omega)$ is a special function of bounded variation and we write $u \in SBV(\Omega)$ if the Cantor part $D^c u$ of its derivative Du is zero.*

Theorem 1.28 (Compactness of SBV)**.** *Let (u_n) be a sequence of special functions of bounded variation such that there exists a constant $C > 0$ with $|u_n(x)| \leq C$ for almost every $x \in \Omega$ open subset of $\mathbb{R}^N$ and $\int_\Omega |\nabla u_n|^2\, dx + \mathcal{H}^{N-1}(S_{u_n}) \leq C$. Then there exists a subsequence (u_{n_k}) converging almost everywhere to a function $u \in SBV(\Omega)$. Moreover, (∇u_{n_k}) weakly converges to ∇u in $L^2(\Omega)$ and $\mathcal{H}^{N-1}(S_u) \leq \liminf_{k \to +\infty} \mathcal{H}^{N-1}(S_{u_{n_k}})$.*

Theorem 1.29. *Let Ω be an open subset of $\mathbb{R}^N$. We have $W^{1,1}(\Omega) \subset SBV(\Omega) \subset BV(\Omega)$.*

Definition 1.43 ($GSBV$ space)**.** *The space of generalized special functions of bounded variation is defined by*

$$GSBV(\Omega) = \{u : \Omega \to \mathbb{R} \,:\, u \text{ Borel function}, \max(-k, \min(u, k)) \in SBV(\Omega),\ \forall k \in \mathbb{N}\}.$$

2 Viscosity solution theory

The theory of viscosity solutions applies to certain partial differential equations and allows merely continuous functions to be solutions of fully nonlinear equations of first and second order. We refer the reader to [2] and [6] for a general introduction. In a first part, we will focus on the theory of viscosity solutions applied to second order degenerate parabolic equations and then to nonlocal and nonlinear parabolic equations.

2.1 Framework for second order degenerate parabolic equations

This section is based on [11] and [12]. Given $T > 0$, we consider the following problem:

$$\begin{cases} u_t + G(x, t, Du, D^2 u) = 0 \text{ in } (0,T) \times \mathbb{R}^n \\ u(x, 0) = u_0(x) \text{ in } \mathbb{R}^n \end{cases}, \tag{2.1}$$

with $G : \mathbb{R}^n \times (0,T) \times \mathbb{R}^n \times \mathcal{S}^n$, $\mathcal{S}^n$ being the set of symmetric $n \times n$ matrices equipped with its natural partial order satisfying the following properties:

(F1) G is continuous on $\mathbb{R}^n \times (0,T) \times \mathbb{R}^n \setminus \{0_{\mathbb{R}^n}\} \times \mathcal{S}^n$. This allows equation (2.1) to be singular at $\nabla u = 0$.

(F2) G is degenerate elliptic that is to say, $G(x,t,p,X+Y) \leq G(x,t,p,X)$ for all $(x,t,p,X) \in \mathbb{R}^n \times (0,T) \times \mathbb{R}^n \times \mathcal{S}^n$ and any $Y \in \mathcal{S}^n$, $Y \geq 0$.

(F3) $-\infty < G_*(x,t,0_{\mathbb{R}^n}, 0_{\mathcal{S}^n}) = G^*(x,t,0_{\mathbb{R}^n}, 0_{\mathcal{S}^n}) < +\infty$ for all $(x,t) \in \mathbb{R}^n \times (0,T)$ where G_* is the lower semicontinuous envelope of G and G_*, the upper semicontinuous one.

Definition 2.1.

$$USC(\mathbb{R}^n \times [0,T)) = \{u : \mathbb{R}^n \times [0,T) \to \mathbb{R} \text{ locally bounded, upper semicontinuous }\}.$$

$$LSC(\mathbb{R}^n \times [0,T)) = \{u : \mathbb{R}^n \times [0,T) \to \mathbb{R} \text{ locally bounded, lower semicontinuous }\}.$$

We then define viscosity solutions.

Definition 2.2 (Viscosity subsolution, supersolution and solution)**.** *A function $u \in USC(\mathbb{R}^N \times [0,T))$ is a viscosity subsolution of (2.1) if it satisfies:*

1. *$u(x,0) \leq u_0(x)$ in $\mathbb{R}^n$,*
2. *for every $(x_0,t_0) \in \mathbb{R}^n \times (0,T)$ and for every test function $\Phi : \mathbb{R}^n \times (0,T) \to \mathbb{R}$, $\mathcal{C}^1$ in time, $\mathcal{C}^2$ in space, that is tangent from above to u at (x_0,t_0), the following holds:*

$$\frac{\partial \Phi}{\partial t}(x_0,t_0) + G_*(x_0,t_0,D\Phi,D^2\Phi) \leq 0.$$

A function $v \in LSC(\mathbb{R}^n \times [0,T))$ is a viscosity supersolution of (2.1) if it satisfies:

1. *$v(x,0) \geq u_0(x)$ in $\mathbb{R}^n$,*
2. *for every $(x_0,t_0) \in \mathbb{R}^n \times (0,T)$ and for every test function $\Phi : \mathbb{R}^n \times (0,T) \to \mathbb{R}$, $\mathcal{C}^1$ in time, $\mathcal{C}^2$ in space, that is tangent from below to v at (x_0,t_0), the following holds:*

$$\frac{\partial \Phi}{\partial t}(x_0,t_0) + G^*(x_0,t_0,D\Phi,D^2\Phi) \geq 0.$$

A function $v \in \mathcal{C}^0(\mathbb{R}^n \times [0,T))$ is a viscosity solution of (2.1) if and only if it is a subsolution and a supersolution of (2.1).

Before giving another definition, we define parabolic sub and superdifferentials of semicontinuous functions.

Definition 2.3 (Parabolic sub/superdifferentials of semicontinuous functions)**.** *Let $u : \mathbb{R}^n \times (0,T) \to \mathbb{R}$.*
The parabolic superdifferential of u, $\mathcal{P}^+u$, is defined as follows: $(a,p,X) \in \mathbb{R} \times \mathbb{R}^n \times \mathcal{S}^n$ belongs to $\mathcal{P}^+u(x,t)$ if $(x,t) \in \mathbb{R}^n \times (0,T)$ and $u(y,s) \leq u(x,t) + a(s-t) + \langle p, y-x\rangle + \frac{1}{2}\langle X(y-x), y-x\rangle + o(|s-t| + |x-y|^2)$, as $(y,s) \in \mathbb{R}^n \times (0,T) \to (x,t)$. Similarly $\mathcal{P}^-u = -\mathcal{P}^+(-u)$. We also define two sets:

$$\bar{\mathcal{P}}^+u(x,t) = \left\{ \begin{array}{l} (a,p,X) \in \mathbb{R} \times \mathbb{R}^n \times \mathcal{S}^n, \\ \exists (x_n,t_n,a_n,p_n,X_n) \in \mathbb{R}^n \times \mathbb{R} \times \mathbb{R} \times \mathbb{R}^n \times \mathcal{S}^n \\ \text{such that } (a_n,p_n,X_n) \in \mathcal{P}^+u(x_n,t_n) \\ \text{and } (x_n,t_n,u(x_n,t_n),a_n,p_n,X_n) \to (x,t,u(x,t),a,p,X) \end{array} \right\}$$

The set $\bar{\mathcal{P}}^-u(x,t)$ is defined in a similar way.

Definition 2.4 (Equivalent definition for viscosity solutions)**.** *A function $u \in USC(\mathbb{R}^n \times [0,T))$ is a viscosity subsolution of (2.1) if it satisfies:*

1. *$u(x,0) \leq u_0(x)$ in $\mathbb{R}^n$,*
2. *for every $(x,t) \in \mathbb{R}^n \times (0,T)$ and for every $(a,p,X) \in \mathcal{P}^+u(x,t)$, we have $a + G_*(x,t,p,X) \leq 0$.*

A function $v \in LSC(\mathbb{R}^n \times [0,T))$ is a viscosity supersolution of (2.1) if it satisfies:

1. *$v(x,0) \geq u_0(x)$ in $\mathbb{R}^n$,*
2. *for every $(x,t) \in \mathbb{R}^n \times (0,T)$ and for every $(a,p,X) \in \mathcal{P}^-v(x,t)$, we have $a + G^*(x,t,p,X) \geq 0$.*

A function $v \in \mathcal{C}^0(\mathbb{R}^n \times [0,T))$ is a viscosity solution of (2.1) if, and only if, it is a subsolution and a supersolution of (2.1).

We recall the parabolic version of Ishii's lemma.

Lemma 2.5 (Parabolic Ishii's lemma)**.** *Let U and V be open sets of $\mathbb{R}^n$, $u \in USC(U \times \mathbb{R}^+)$ and $v \in LSC(V \times \mathbb{R}^+)$. Let $\phi : U \times V \times \mathbb{R}^+ \to \mathbb{R}$ of class $\mathcal{C}^2$. Assume that $(x,y,t) \mapsto u(x,t) - v(y,t) - \phi(x,y,t)$ reaches a local maximum at $(\bar{x},\bar{y},\bar{t}) \in U \times V \times \mathbb{R}_*^+$. We set $\tau = \partial_t\phi(\bar{x},\bar{y},\bar{t})$, $p_1 = D_x\phi(\bar{x},\bar{y},\bar{t})$, $p_2 = -D_y\phi(\bar{x},\bar{y},\bar{t})$. Assume also that u and $-v$ satisfy the compactness assumption, that is to say for every $(z,s) \in \mathbb{R}^n \times \mathbb{R}_*^+$, there exists $r_u, r_{-v} > 0$ such that for every $M > 0$, there exists C_u, C_{-v} such that*

$$\left.\begin{array}{r} |(x,t)-(z,s)| \leq r_u \\ (\tau,p,X) \in \bar{P}^+u(x,t) \\ |u(x,t)| + |p| + |X| \leq M \end{array}\right\} \Rightarrow \tau \leq C_u,$$

$$\left.\begin{array}{r} |(x,t)-(z,s)| \leq r_{-v} \\ (\tau,p,X) \in \bar{P}^+(-v)(x,t) \\ |-v(x,t)| + |p| + |X| \leq M \end{array}\right\} \Rightarrow \tau \leq C_{-v}.$$

Then for every $\alpha > 0$ such that $\alpha A < I$, there exists $\tau_1, \tau_2 \in \mathbb{R}$ and $X, Y \in \mathcal{S}^n$ such that

$$\begin{aligned} \tau = \tau_1 - \tau_2, \\ (\tau_1,p_1,X) \in \bar{\mathcal{P}}^+u(\bar{x},\bar{t}), (\tau_2,p_2,Y) \in \bar{\mathcal{P}}^-v(\bar{x},\bar{t}), \\ \frac{-1}{\alpha}\begin{pmatrix} I & 0 \\ 0 & I \end{pmatrix} \leq \begin{pmatrix} X & 0 \\ 0 & Y \end{pmatrix} \leq (I-\alpha A)^{-1}A. \end{aligned}$$

The strategy is then to get a comparison principle, construct barriers, prove the existence and uniqueness of a viscosity solution based on Perron's method and study the regularity of this solution using additional specific properties of G.

2.2 General framework for nonlocal and nonlinear parabolic equations

We take this general framework from [3] and we follow the same notations. Let us consider the class of nonlocal and nonlinear parabolic equations which can be rewritten as

$$\begin{cases} u_t = H[\mathbb{1}_{\{u\geq 0\}}]\left(x,t,u,Du,D^2u\right) \text{ in } \mathbb{R}^N\times(0,T)\,, \\ u(\cdot,0)=u_0 \text{ in } \mathbb{R}^N\,, \end{cases} \tag{2.2}$$

where u_t, Du and D^2u stand respectively for the time derivative, gradient and Hessian matrix with respect to the space variable x of $u:\mathbb{R}^N\times[0,T]\to\mathbb{R}$ and where $\mathbb{1}_A$ denotes the indicator function of a set A. The initial datum u_0 is a bounded and Lipschitz continuous function on $\mathbb{R}^N$.
For any indicator function $\chi:\mathbb{R}^N\times[0,T]\to\mathbb{R}$, or more generally for any $\chi\in L^\infty(\mathbb{R}^N\times[0,T];[0,1])$, $H[\chi]$ denotes a function of $(x,t,r,p,A)\in\mathbb{R}^N\times[0,T]\times\mathbb{R}\times\mathbb{R}^N\setminus\{0\}\times\mathcal{S}^N$ where $\mathcal{S}^N$ is the set of real $N\times N$ symmetric matrices. For almost any $t\in[0,T]$, $(x,r,p,A)\mapsto H[\chi](x,t,r,p,A)$ is a continuous function on $\mathbb{R}^N\times\mathbb{R}\times\mathbb{R}^N\setminus\{0\}\times\mathcal{S}^N$ with a possible singularity at $p=0$, while $t\mapsto H[\chi](x,t,r,p,A)$ is a bounded measurable function for all $(x,r,p,A)\in\mathbb{R}^N\times\mathbb{R}\times\mathbb{R}^N\setminus\{0\}\times\mathcal{S}^N$. The equation is said to be degenerate elliptic if, for any $\chi\in L^\infty(\mathbb{R}^N\times[0,T];[0,1])$, for any $(x,r,p)\in\mathbb{R}^N\times\mathbb{R}\times\mathbb{R}^N\setminus\{0\}$, for almost every $t\in[0,T]$ and for all $A,B\in\mathcal{S}^N$, one has:

$$H[\chi](x,t,r,p,A)\leq H[\chi](x,t,r,p,B) \text{ if } A\leq B\,,$$

with $\leq$ the usual partial ordering for symmetric matrices.
Such equations arise typically when one aims at describing, through the level-set approach, the motion of a family $\{K(t)\}_{t\in[0,T]}$ of closed subsets of $\mathbb{R}^N$ evolving with a nonlocal velocity. Indeed, following the main idea of the level-set approach, it is natural to introduce a function u such that $K(t)=\{x\in\mathbb{R}^N;\, u(x,t)\geq 0\}$, and this equation can be seen as the level-set equation for u. In this framework, the nonlinearity H corresponds to the velocity and it depends not only on the time, the position of the front, the normal direction and the curvature tensor but also on nonlocal properties of $K(t)$ which are carried by the dependence in $\mathbb{1}_{\{u\geq 0\}}$. The equation would appear as a well-posed equation if we consider the nonlocal dependence (i.e. $\mathbb{1}_{\{u\geq 0\}}$) as being fixed.
The notion of viscosity solutions for equations with a measurable dependence in time (called L^1-viscosity solution) is needed to define weak solutions. For a complete presentation of the theory, the reader may refer to [4]. The following definition of weak solutions is introduced in [3].

Definition 2.6 (extracted from [3])**.**
Let $u:\mathbb{R}^N\times[0,T]\to\mathbb{R}$ be a continuous function. u is said to be a weak solution of (2.2) if there exists $\chi\in L^\infty(\mathbb{R}^N\times[0,T];[0,1])$ such that:

i) u is a L^1-viscosity solution of

$$\begin{cases} u_t(x,t)=H[\chi](x,t,u,Du,D^2u) \text{ in } \mathbb{R}^N\times(0,T)\,, \\ u(\cdot,0)=u_0 \text{ in } \mathbb{R}^N\,. \end{cases} \tag{2.3}$$

ii) For almost all $t \in [0,T]$,

$$\mathbb{1}_{\{u(\cdot,t)>0\}} \leq \chi(\cdot,t) \leq \mathbb{1}_{\{u(\cdot,t)\geq 0\}} \text{ a.e. in } \mathbb{R}^N.$$

Moreover, we say that u *is a classical solution of (2.2) if in addition, for almost every* $t \in [0,T]$,

$$\mathbb{1}_{\{u(\cdot,t)>0\}} = \mathbb{1}_{\{u(\cdot,t)\geq 0\}} \text{ a.e in } \mathbb{R}^N.$$

We now state some assumptions (still following [3]) that are needed to establish the result of existence of at least one weak solution to general problem (2.2).

[A1]

i) For any $\chi \in X \subset L^\infty(\mathbb{R}^N \times [0,T];[0,1])$, equation (2.3) has a bounded uniformly continuous L^1-viscosity solution u. Moreover, there exists a constant $L > 0$ independent of $\chi \in X$ such that $\|u\|_{L^\infty(\mathbb{R}^N\times[0,T])} \leq L$.

ii) For any fixed $\chi \in X$, a comparison principle holds for equation (2.3): if u is a bounded, upper semicontinuous L^1-viscosity subsolution of (2.3) in $\mathbb{R}^N \times (0,T)$ and v is a bounded, lower semicontinuous L^1-viscosity supersolution of (2.3) in $\mathbb{R}^N \times (0,T)$ with $u(\cdot,0) \leq v(\cdot,0)$ in $\mathbb{R}^N$, then $u \leq v$ in $\mathbb{R}^N \times (0,T)$.

[A2]

i) For any compact subset $K \subset \mathbb{R}^N \times \mathbb{R} \times \mathbb{R}^N \setminus \{0\} \times \mathcal{S}^N$, there exists a (locally bounded) modulus of continuity $m_K : [0,T] \times \mathbb{R}^+ \to \mathbb{R}^+$ such that $m_K(\cdot,\varepsilon) \to 0$ in $L^1(0,T)$ as $\varepsilon \to 0$, and

$$\begin{aligned} &|H[\chi](x_1,t,r_1,p_1,A_1) - H[\chi](x_2,t,r_2,p_2,A_2)| \leq \\ &m_K(t, |x_1-x_2| + |r_1-r_2| + |p_1-p_2| + |A_1-A_2|)\,, \end{aligned}$$

for any $\chi \in X$, for almost all $t \in [0,T]$ and all (x_1,r_1,p_1,A_1), $(x_2,r_2,p_2,A_2) \in K$.

ii) There exists a bounded function $h(x,t,r)$, which is continuous in x and r for almost every t and measurable in t, such that: for any neighborhood V of $(0,0)$ in $\mathbb{R}^N \setminus \{0\} \times \mathcal{S}^N$ and any compact subset $K \subset \mathbb{R}^N \times \mathbb{R}$, there exists a modulus of continuity $m_{K,V} : [0,T] \times \mathbb{R}^+ \to \mathbb{R}^+$ such that $m_{K,V}(\cdot,\varepsilon) \to 0$ in $L^1(0,T)$ as $\varepsilon \to 0$, and

$$|H[\chi](x,t,r,p,A) - h(x,t,r)| \leq m_{K,V}(t, |p| + |A|)\,,$$

for any $\chi \in X$, for almost all $t \in [0,T]$, all $(x,r) \in K$ and $(p,A) \in V$.

iii) If $\chi_n \rightharpoonup \chi$ weakly-$*$ in $L^\infty(\mathbb{R}^N \times [0,T];[0,1])$ with $\chi_n, \chi \in X$ for all n, then for all $(x,t,r,p,A) \in \mathbb{R}^N \times [0,T] \times \mathbb{R} \times \mathbb{R}^N \setminus \{0\} \times \mathcal{S}^N$,

$$\int_0^1 H[\chi_n](x,s,r,p,A)\,ds \underset{n\to+\infty}{\longrightarrow} \int_0^1 H[\chi](x,s,r,p,A)\,ds\,,$$

locally uniformly for $t \in [0,T]$.

[A3] For any $\chi \in X$, for almost every $t \in [0,T]$, for all $(x,p,A) \in \mathbb{R}^N \times \mathbb{R}^N \setminus \{0\} \times \mathcal{S}^N$, and for any $r_1 \geq r_2$,

$$H[\chi](x,t,r_1,p,A) \leq H[\chi](x,t,r_2,p,A)\,.$$

The general existence theorem proposed by Barles *et al.* ([3]) is then:

Theorem 2.1 (General existence theorem ([3]))**.** *Assume that [A1], [A2] and [A3] hold. Then there exists at least a weak solution to (2.2).*

3 Calculus of variations

The scope of this section extracted from [7] is to investigate the existence and uniqueness of the following minimization problem:

$$\inf_{u \in X} I(u) = \int_\Omega f(x, u(x), \nabla u(x))\, dx, \tag{2.4}$$

where

- $\Omega \subset \mathbb{R}^N$, $N \geq 1$, is an open bounded set and a point in Ω is denoted by $x = (x_1, \ldots, x_N)$;
- $u : \Omega \to \mathbb{R}^M$, $M \geq 1$ is the unknown function with $\nabla u = \left(\frac{\partial u^j}{\partial x_i}\right)_{1 \leq i \leq N}^{1 \leq j \leq M} \in \mathbb{R}^{M \times N}$;
- X is the space of admissible functions;
- $f : \Omega \times \mathbb{R}^M \times \mathbb{R}^{M \times N} \to \mathbb{R}$ is a given function.

Before giving the main results, we define some specific functions.

3.1 Carathéodory, convex, polyconvex, quasiconvex and rank one convex functions

Definition 3.1 (Carathéodory function)**.** *Let $\Omega \subset \mathbb{R}^N$ be an open set and let $f : \Omega \times \mathbb{R}^L \to \mathbb{R} \cup \{+\infty\}$. Then f is said to be a Carathéodory function if*

1. *$\xi \mapsto f(x,\xi)$ is continuous for almost every $x \in \Omega$,*
2. *$x \mapsto f(x,\xi)$ is measurable for every $\xi \in \mathbb{R}^L$.*

Remark 3.2. *In the following, we consider functions $f : \Omega \times \mathbb{R}^M \times \mathbb{R}^{M \times N} \to \mathbb{R} \cup \{+\infty\}$, $(x,u,\xi) \mapsto f(x,u,\xi)$, When we speak of Carathéodory function in this case, we consider the variable ξ as playing the role of (u,ξ) and $\mathbb{R}^L = \mathbb{R}^M \times \mathbb{R}^{M \times N}$.*

Definition 3.3 (Convex function)**.**

– *A function $f : \mathbb{R}^N \to \mathbb{R} \cup \{+\infty\}$ is said to be convex if*

$$f(tx + (1-t)y) \leq tf(x) + (1-t)f(y),$$

for every $x \in \mathbb{R}^N$, every $y \in \mathbb{R}^N$, and every $t \in [0,1]$.

– *A function $f : E \subset \mathbb{R}^N \to \mathbb{R} \cup \{+\infty\}$ is said to be strictly convex on a convex set E if*

$$f(tx + (1-t)y) < tf(x) + (1-t)f(y)$$

for every $(x,y) \in E^2$, $x \neq y$, and every $t \in (0,1)$.

In the scalar case $M = 1$ or $N = 1$, convexity plays an important role in the existence and uniqueness of minimizers for problem (2.4). However in the vectorial case (when $M > 1$ and $N > 1$), we need to introduce a weaker definition of convexity called quasiconvexity.

Definition 3.4 (Weaker convex functions)**.**

1. *(***Rank one convex***) A function $f : \mathbb{R}^{M\times N} \to \mathbb{R} \cup \{+\infty\}$ is said to be rank one convex if*

$$f(\lambda\xi + (1-\lambda)\eta) \leq \lambda f(\xi) + (1-\lambda)f(\eta),$$

for every $\lambda \in [0,1]$, $\xi \in \mathbb{R}^{M\times N}$, $\eta \in \mathbb{R}^{M\times N}$ with rank $(\xi - \eta) \leq 1$.

2. *(***Quasiconvex***) A Borel measurable and locally bounded function $f : \mathbb{R}^{M\times N} \to \mathbb{R} \cup \{+\infty\}$ is said to be quasiconvex if*

$$f(\xi) \leq \frac{1}{meas(D)} \int_D f(\xi + \nabla\phi(x))\, dx,$$

for every open bounded set $D \subset \mathbb{R}^N$, for every $\xi \in \mathbb{R}^{M\times N}$ and for every $\phi \in W^{1,\infty}(D, \mathbb{R}^M)$.

3. *(***Polyconvex***) A function $f : \mathbb{R}^{M\times N} \to \mathbb{R} \cup \{+\infty\}$ is said to be polyconvex if there exists $F : \mathbb{R}^{\tau(N,M)} \to \mathbb{R} \cup \{+\infty\}$ convex such that $f(\xi) = F(T(\xi))$ where $T : \mathbb{R}^{M\times N} \to \mathbb{R}^{\tau(N,M)}$ is such that $T(\xi) := (\xi, adj_2\xi, \ldots, adj_{\min(N,M)}\xi)$. We recall that $adj_s\xi$ stands for the matrix of all $s \times s$ minors of $\xi \in \mathbb{R}^{M\times N}$, $2 \leq s \leq \min(N,M)$ and $\tau(N,M) = \sum_{i=1}^{\min(N,M)} \sigma(s)$ where $\sigma(s) := \binom{M}{s}\binom{N}{s} = \frac{N!M!}{(s!)^2(M-s)!(N-s)!}$. For $M = N = 2$, $T(\xi) = (\xi, \det\xi)$ and for $M = N = 3$, $T(\xi) = (\xi, Cof\xi, \det\xi)$.*

4. *(***Separately convex***) A function $f : \mathbb{R}^m \to \mathbb{R} \cup \{+\infty\}$ is said to be separately convex, or convex in each variable, if the function $x_i \mapsto f(x_1, \ldots, x_{i-1}, x_i, x_{i+1}, \ldots, x_m)$ is convex for every $i = 1, \ldots, m$ for every fixed $(x_1, \ldots, x_{i-1}, x_{i+1}, \ldots, x_m) \in \mathbb{R}^{m-1}$.*

5. *(***Affine***) A function f is called polyaffine, quasiaffine or rank one affine if f and $-f$ are respectively polyconvex, quasiconvex, rank one convex.*

Definition 3.5 (Quasiconvex envelope)**.** *The quasiconvex envelope of a function* $f : \mathbb{R}^{M\times N} \to \mathbb{R} \cup \{+\infty\}$ *denoted by* Qf *is the quasiconvex function defined by*

$$Qf = \sup_g \{g \leq f,\ g \text{ quasiconvex }\}.$$

Remark 3.6. *In a similar way, we can define the convex envelope, the polyconvex envelope and the rank-one convex envelope of a function* f*.*

Proposition 3.7. *Let* $f : \mathbb{R}^{M\times N} \to \mathbb{R}$*. Then*

$$f \text{ convex} \Rightarrow f \text{ polyconvex} \Rightarrow f \text{ quasiconvex} \Rightarrow f \text{ rank one convex.}$$

If f *is convex, polyconvex, quasiconvex or rank one convex, then* f *is locally Lipschitz.*
If $M = 1$ *or* $N = 1$ *then all these notions are equivalent.*
If $f : \mathbb{R}^{M\times N} \to \mathbb{R} \cup \{+\infty\}$*, then*

$$f \text{ convex} \Rightarrow f \text{ polyconvex} \Rightarrow f \text{ rank one convex.}$$

We now focus on the direct method in the calculus of variations.

3.2 Direct method in the calculus of variations

The direct method of the calculus of variations aims to prove the existence of a solution to the problem (2.4) and relies on the three following steps:

1. One first constructs a minimizing sequence (u_n) of X (which always exists by the sequential definition of the infimum) satisfying $\lim_{n\to+\infty} I(u_n) = \inf_{u\in X} I(u)$ after verifying that $\inf_{u\in X} I(u)$ is finite.

2. One obtains a uniform bound on $\|u_n\|_X$ by deriving a coercivity inequality. Indeed, if I is coercive meaning that $\lim_{\|u\|_X\to+\infty} I(u) = +\infty$, this uniform bound is straightforwardly extracted. (Arguing by contradiction, let us assume that $\forall C > 0$, $\exists n \in \mathbb{N}$, $\|u_n\|_X > C$. We prove, by construction, that there exists a subsequence (u_{n_k}) of (u_n) such that $\lim_{k\to+\infty} I(u_{n_k}) = +\infty$ owing to the coercivity of I, which contradicts the fact that $\lim_{n\to+\infty} I(u_n) = \inf_{u\in X} I(u)$).
   If X is reflexive, then by Theorem 1.11, one can thus find $\bar{u} \in X$ and a subsequence (u_{n_k}) of (u_n) such that $u_{n_k} \underset{k\to+\infty}{\overset{X}{\rightharpoonup}} \bar{u}$.

3. To prove that $\bar{x}$ is a minimizer of I, it suffices to have the inequality

$$I(\bar{u}) \leq \liminf_{k\to+\infty} I(u_{n_k}).$$

The latter property is called weak lower semicontinuity.

Definition 3.8 (Weak lower semicontinuity). *Let $p \geq 1$ and Ω, u, f be as above. We say that I is sequentially weakly lower semicontinuous in X if for every sequence $u_n \underset{n\to+\infty}{\overset{X}{\rightharpoonup}} \bar{u}$, then*

$$I(\bar{u}) \leq \liminf_{n\to+\infty} I(u_n).$$

I is sequentially weak-$*$ lower semicontinuous in X if for every sequence $u_n \underset{n\to+\infty}{\overset{X*}{\rightharpoonup}} \bar{u}$, then

$$I(\bar{u}) \leq \liminf_{n\to+\infty} I(u_n).$$

In the scalar case ($M = 1$ or $N = 1$), the convexity of $\xi \mapsto f(x, u, \xi)$ plays an important role especially in the derivation of a necessary and sufficient condition ensuring the weak lower semicontinuity property (see [14]). In the vectorial case, it is still a sufficient condition but not a necessary one anymore. However, one can prove (see [7])

$$f \text{ quasiconvex} \Leftrightarrow I \text{ weakly lower semicontinuous.}$$

We now give an existence theorem for quasiconvex functions in the vectorial case.

Theorem 3.1 (Existence of minimizers). *Let $p > 1$, $\Omega \subset \mathbb{R}^N$ be a bounded open set with a Lipschitz boundary. Let $f : \Omega \times \mathbb{R}^M \times \mathbb{R}^{M\times N} \to \mathbb{R}$ be a Carathéodory function satisfying for almost every $x \in \Omega$, for every $(u, \xi) \in \mathbb{R}^M \times \mathbb{R}^{M\times N}$,*

$$\xi \to f(x, u, \xi) \text{ is quasiconvex,}$$
$$\alpha_1|\xi|^p + \beta_1|u|^q + \gamma_1(x) \leq f(x, u, \xi) \leq \alpha_2|\xi|^p + \beta_2|u|^r + \gamma_2(x),$$

where $\alpha_2 \geq \alpha_1 > 0$, $\beta_1 \in \mathbb{R}$, $\beta_2 \geq 0$, γ_1, $\gamma_2 \in L^1(\Omega)$, $p > q \geq 1$ and $1 \leq r \leq \frac{Np}{N-p}$ if $p < N$ and $1 \leq r < \infty$ if $p \geq N$. Let

$$\inf\left\{ I(u) = \int_\Omega f(x, u(x), \nabla u(x))\, dx \;\middle|\; u \in u_0 + W_0^{1,p}(\Omega, \mathbb{R}^M) \right\}, \tag{2.5}$$

then (2.5) admits at least one solution.

Now we state an important relaxation theorem after defining a growth condition.

Definition 3.9 (Growth condition). *Let $1 \leq p \leq \infty$ and $f : \Omega \times \mathbb{R}^M \times \mathbb{R}^{M\times N} \to \mathbb{R}$, $f = f(x, u, \xi)$, be a Carathéodory function. We say that f satisfies growth condition (G_p) if there exists a Carathéodory function $g : \Omega \times \mathbb{R}^M \times \mathbb{R}^{M\times N} \to \mathbb{R}$, $g = g(x, u, \xi)$ quasiconvex in the last variable and $g(x, u, \xi) \leq f(x, u, \xi)$ for almost every $x \in \Omega$ and for every $(u, \xi) \in \mathbb{R}^M \times \mathbb{R}^{M\times N}$.*
Moreover, the following inequalities hold for almost every $x \in \Omega$ and for every $(u, \xi) \in \mathbb{R}^M \times \mathbb{R}^{M\times N}$:

1. *when $1 \leq p < \infty$,*

$$|g(x, u, \xi)|, |f(x, u, \xi)| \leq \alpha(1 + |u|^p + |\xi|^p), \tag{Gp}$$

where $\alpha \geq 0$ is a constant;

2. *if* $p = \infty$,

$$|g(x,u,\xi)|, |f(x,u,\xi)| \leq \beta(x) + \alpha(|u|, |\xi|), \tag{Ginfinity}$$

where $\alpha, \beta \geq 0$, $\beta \in L^1(\Omega)$ *and* α *is a continuous and increasing in each argument function.*

Theorem 3.2 (Relaxation theorem)**.** *Let* $1 \leq p \leq \infty$, $\Omega \subset \mathbb{R}^N$ *be a bounded open set and* $f : \Omega \times \mathbb{R}^M \times \mathbb{R}^{M\times N} \to \mathbb{R}$, $f = f(x,u,\xi)$, *be a Carathéodory function satisfying the growth condition* (G_p). *For almost every* $x \in \Omega$ *and for every* $(u,\xi) \in \mathbb{R}^M \times \mathbb{R}^{M\times N}$, *let* Qf *be the quasiconvex envelope with respect to the last variable of* f : $Qf = \inf\left\{\frac{1}{meas(D)}\int_D f(x,u,\xi+\nabla\phi(y))\,dy \,|\, \phi \in W_0^{1,\infty}(D,\mathbb{R}^M)\right\}$, $D \subset \mathbb{R}^N$ *being a bounded open set. Assume that* $Qf : \Omega \times \mathbb{R}^M \times \mathbb{R}^{M\times N} \to \mathbb{R}$ *is a Carathéodory function.*

1. *(***Part 1.***) Let* $p \leq q \leq \infty$ *and* $u \in W^{1,q}(\Omega,\mathbb{R}^M)$, *then there exists a sequence* $\{u_\nu\}_{\nu=1}^{\infty} \subset u + W_0^{1,q}(\Omega,\mathbb{R}^M)$ *such that*

$$u_\nu \underset{\nu\to+\infty}{\longrightarrow} u \text{ strongly in } L^q(\Omega,\mathbb{R}^M),$$
$$\int_\Omega f(x,u_\nu(x),\nabla u_\nu(x))\,dx \underset{\nu\to+\infty}{\longrightarrow} \int_\Omega Qf(x,u(x),\nabla u(x))\,dx.$$

2. *(***Part 2.***) Assume in addition to the hypothesis of Part 1, that* $1 \leq p < \infty$ *and there exist* $\alpha_2 > 0$ *and* $\alpha_3 \in \mathbb{R}$ *such that, for almost every* $x \in \Omega$, *for every* $(u,\xi) \in \mathbb{R}^M \times \mathbb{R}^{M\times N}$, $f(x,u,\xi) \geq \alpha_2|\xi|^p + \alpha_3$.
Then in addition to the conclusions of Part 1, the following holds:

$$u_\nu \underset{\nu\to+\infty}{\rightharpoonup} u \text{ weakly in } W^{1,p}(\Omega,\mathbb{R}^M).$$

3.3 Γ-convergence

The notion of Γ-convergence is fundamental in variational image processing and we refer the reader to [8] (from which this section is taken) for a comprehensive introduction to it.

Definition 3.10 (Γ-convergence)**.** *Let* (X,D) *be a metric space. We say that a sequence* $F_j : X \to [-\infty,+\infty]$ Γ*-converges to* $F : X \to [-\infty,+\infty]$ *(as* $j \to +\infty$*) if for all* $u \in X$ *we have*

1. *(*$\liminf$ **inequality***) for every sequence* $(u_j) \subset X$ *converging to* u, $F(u) \leq \liminf_{j\to+\infty} F_j(u_j)$;

2. *(***recovery sequence***) there exists a sequence* $(u_j) \subset X$ *converging to* u *such that* $F(u) \geq \limsup_{j\to+\infty} F_j(u_j)$.

The function F *is called the* Γ*-limit of* (F_j) *with respect to* D *and we write* $F = \Gamma - \lim_j F_j = F$.

The following theorem is requisite in the convergence of some approximations.

Theorem 3.3 (Fundamental theorem of Γ-convergence)**.** *Let us assume that* $F = \Gamma - \lim_j F_j$*, and let a compact set* $C \subset X$ *exist such that* $\inf_X F_j = \inf_C F_j$ *for all* j*. Then there is a minimum of* F *over* X *such that* $\min_X F = \lim_j \inf_X F_j$*, and if* $(u_j) \subset X$ *is a converging sequence such that* $\lim_j F_j(u_j) = \lim_j \inf_X F_j$*, then its limit is a minimum point of* F*.*

4 Tridimensional elasticity

In this section, we recall some definitions of the theory of tridimensional elasticity taken from [13].

Let Ω be an open bounded connected space of $\mathbb{R}^3$. We consider that the points $x \in \bar{\Omega}$ represent the points of a material. Ω is said to be the reference configuration of the material. The map $\varphi : \bar{\Omega} \to \mathbb{R}^3$ is a deformation. We also introduce the displacements $u = \varphi - Id$. The matrix $(\nabla\varphi)_{ij} = \partial_j \varphi_i$ is called the gradient of the deformation.

Remark 4.1. *The preservation of the orientation corresponds to the condition* $\det \nabla\varphi(x) > 0$*,* $x \in \Omega$*.*

We first introduce and define some basic notions.

Definition 4.2.

1. *The deformation tensor or right Cauchy-Green tensor associated with the deformation* φ *is defined by*

$$C = \nabla\varphi^T \nabla\varphi.$$

   It can be interpreted as a quantifier of the square of local change in distances due to the deformation.

2. *The Green-Saint Venant tensor is defined by*

$$E = \frac{1}{2}(C - I) = \frac{1}{2}(\nabla u + \nabla u^T) + \frac{1}{2}\nabla u^T \nabla u.$$

   It measures the deviation between the deformation φ *and a rigid deformation.*

Definition 4.3 (Rigid deformation)**.** *A deformation* φ *is said to be rigid if it can be written as* $\varphi(x) = a + Qx$*, where* $a \in \mathbb{R}^3$ *and* $Q \in SO(3)$ *are respectively a given vector and a rotation matrix in the group of orthogonal matrices of size* 3×3 *satisfying* $\det Q = 1$*.*

Definition 4.4 (Behavior law)**.** *The behavior law of a material is defined by*

$$\hat{T} : \bar{\Omega} \times \{\textit{deformations}\} \to S_3,$$

where S_3 *is the space of* 3×3 *symmetric matrices, such that for every deformation* φ *and every point* $x \in \Omega$*, we have* $T^\varphi(y) = \hat{T}(x, \varphi)$ *for* $y = \varphi(x)$ *and where* T^φ *is the Cauchy stress tensor.*

Definition 4.5 (Material)**.**

1. *(***Elastic***) A material is said to be elastic if its behavior law can be written by* $\hat{T} : \bar{\Omega} \times M_3^+ \to S_3$ *with* $T^\varphi(y) = \hat{T}(x, \nabla\varphi(x))$ *where* M_3^+ *is the set of* 3×3 *matrices with a positive determinant. In other words, a material is said to be elastic if its behavior law depends only on the gradient of the deformation.*

2. *(***Hyperelastic***) An elastic material is said to be hyperelastic if there exists a function* $\hat{W} : \bar{\Omega} \times M_3^+ \to \mathbb{R}$ *differentiable with respect to its second variable such that*

$$\hat{T}_R(x,F) = \hat{T}(x,F)\,Cof\nabla F(x) = \frac{\partial \hat{W}}{\partial F}(x,F),$$
$$\Leftrightarrow (\hat{T}_R(x,F))_{ij} = (\hat{T}(x,F)\,Cof\nabla F(x))_{ij} = \frac{\partial \hat{W}}{\partial F_{ij}}(x,F),\ \forall (i,j) \in \{1,2,3\}^2$$

   The function $\hat{W}$ *is named elastic energy density of the material.*

3. *(***Isotropic***) A material is said to be isotropic if it has the same mechanical properties in every direction.*

4. *(***Homogeneous***) A material is said to be homogeneous if its behavior law does not depend on* x*.*

Theorem 4.1. *The energy density of an isotropic, homogeneous and hyperelastic material is of the form*

$$\forall x \in \Omega, \forall F \in M_3^+,\ \hat{W}(x,F) = \mathcal{W}(Tr(C), Tr(CofC), detC),$$

where $\mathcal{W} : \mathbb{R}_+^3 \to \mathbb{R}$ *is a function.*

Exemple 4.6 (Homogeneous, isotropic, hyperelastic materials)**.**

- *Saint Venant-Kirchhoff materials:* $\hat{W}(F) = -\frac{3\lambda+2\mu}{4}Tr(C) + \frac{\lambda+2\mu}{8}Tr(C^2) + \frac{\lambda}{4}Tr(CofC) + \frac{6\mu+9\lambda}{8}$*, with* λ *and* μ *being the Lamé coefficients and* $C = F^TF$*. It is the simplest homogeneous isotropic and hyperelastic material.*

- *Ogden materials:* $\hat{W}(F) = \sum_{i=1}^{M} a_i \|F\|^{\gamma_i} + \sum_{j=1}^{N} tr(Cof(F^TF))^{\frac{\delta_j}{2}} + \Gamma(\det F)$*, with* $a_i > 0$, $b_j > 0$, $\gamma_i \geq 1$, $\delta_j \geq 1$ *and* $\Gamma :]0, +\infty[\to \mathbb{R}$ *being convex and satisfying* $\lim_{\delta \to 0^+} \Gamma(\delta) = +\infty$*.*

- *Mooney-Rivlin materials:* $\hat{W}(F) = a\|F\|^2 + b\|CofF\|^2 + \Gamma(\det F)$*, with* $a > 0$, $b > 0$ *and* $\Gamma :]0, +\infty[\to \mathbb{R}$ *being convex and satisfying* $\lim_{\delta \to 0^+} \Gamma(\delta) = +\infty$*.*

Bibliography

[1] L. Ambrosio, N. Fusco, and D. Pallara, *Functions of bounded variation and free discontinuity problems*, vol. 254, Clarendon Press Oxford, 2000.

[2] G. Barles, *Solutions de viscosité et équations elliptiques du deuxième ordre*, (1997).

[3] G. Barles, P. Cardaliaguet, O. Ley, and A. Monteillet, *Existence of weak solutions for general nonlocal and nonlinear second-order parabolic equations*, Nonlinear Analysis: Theory, Methods & Applications, 71 (2009), pp. 2801–2810.

[4] M. Bourgoing, *Viscosity solutions of fully nonlinear second order parabolic equations with L^1 dependence in time and Neumann boundary conditions*, Discrete and Continuous Dynamical Systems, 21 (2008), pp. 763–800.

[5] H. Brezis, *Analyse fonctionelle. Théorie et Applications*, Dunod, Paris, 2005.

[6] M. G. Crandall, H. Ishii, and P.-L. Lions, *User's guide to viscosity solutions of second order partial differential equations*, Bulletin of the American Mathematical Society, 27 (1992), pp. 1–67.

[7] B. Dacorogna, *Direct Methods in the Calculus of Variations*, Applied Mathematical Sciences, Springer New York, 2007.

[8] G. Dal Maso, *An Introduction to* Γ*-Convergence*, Progress in Nonlinear Differential Equations and Their Applications, Birkhäuser Boston, 1993.

[9] F. Demengel, G. Demengel, and R. Erné, *Functional Spaces for the Theory of Elliptic Partial Differential Equations*, Universitext, Springer London, 2012.

[10] L. Evans and R. Gariepy, *Measure Theory and Fine Properties of Functions*, Studies in Advanced Mathematics, Taylor & Francis, 1991.

[11] N. Forcadel, *Contribution à l'analyse d'équations aux dérivées partielles décrivant le mouvement de fronts avec applications à la dynamique des dislocations*, PhD thesis, 2007. Thèse de doctorat dirigée par Monneau, Régis, Informatique et mathématiques Marne-la-vallée, ENPC 2007.

[12] Y. Giga, S. Goto, H. Ishii, and M.-H. Sato, *Comparison principle and convexity preserving properties for singular degenerate parabolic equations on unbounded domains*, Indiana University Mathematics Journal, (1991), pp. 443–470.

[13] H. Le Dret, *Notes de Cours de DEA. Méthodes mathématiques en élasticité*, 2003-2004.

[14] L. Vese and C. Guyader, *Variational Methods in Image Processing*, Chapman & Hall/CRC Mathematical and Computational Imaging Sciences Series, CRC Press, 2015.

Chapter 3

A nonlocal topology-preserving segmentation guided registration model

In this chapter, we address the issue of designing a theoretically well-motivated segmentation guided registration method capable of handling large and smooth deformations. The shapes to be matched are viewed as hyperelastic materials and more precisely as Saint Venant-Kirchhoff ones, and are implicitly modelled by level set functions. These are driven in order to minimize a functional containing both a nonlinear-elasticity-based regularizer prescribing the nature of the deformation, and a criterion that forces the evolving shape to match intermediate topology-preserving segmentation results. Theoretical results encompassing existence of minimizers, existence of a weak viscosity solution of the related evolution problem and asymptotic results are given. The study is then complemented by the derivation of the discrete counterparts of the asymptotic results provided in the continuous domain. Both a pure quadratic penalization method and an augmented Lagrangian technique (involving a related dual problem) are investigated with convergence results.

1 Introduction

While image segmentation aims to partition a given image into meaningful constituents or to find boundaries delineating such objects with the goal to quantify information (see [4, Chapter 4] for instance or [56, Part II], for a relevant analysis of this problem), registration, given two images called Template and Reference (both defined on the open and bounded domain Ω in the plane - a rectangle in practice), consists of determining an optimal diffeomorphic transformation (or deformation) φ mapping the Template into the Reference. This latter technique is encountered in the domain of shape tracking, multi-modality fusion to facilitate diagnosis and treatment planning (see [54]), disease progression evaluation, when comparing an image to its counterpart in a database in order to facilitate the integration of anatomic, genetic and physiological observations from multiple subjects into a common space, or shape averaging as in [52].

According to the modalities of the involved images and on the nature of the study (the registration problem encompassing different aspects), the optimality criterion might differ: for images of same modality, a well-registered Template has geometric features and intensity distribution matched with those of the Reference. When the images have been acquired through different mechanisms and have different modalities, registration aims to match both images in terms of shapes and salient components, while preserving the modality of the Template.

We refer the reader to [54] for an extensive overview of registration techniques in a systematic manner. The sought transformation (or deformation) φ is seen as the optimal solution of a specifically designed cost function, the problem being mathematically hard to solve (see again [54]) due to its ill-posedness (it is underconstrained from a mathematical point of view), to the involved non-linearity, to its non-convexity and to its versatile formulation according to the desired application. Once a deformation model describing the setting in which the objects to be matched are interpreted and viewed (physical models — [7], [18], [12], [25], [26], [5], [9], [21], [23], [38], [52], [47] —, purely geometric models — [62], [19], [53], [3] —, models including a priori knowledge [15]) is selected, the objective function is designed. It generally comprises a term quantifying the degree of alignment between the deformed Template and the Reference, and a term of regularization.

Additional constraints can be prescribed in order that the deformation exhibits suitable properties such as topology or orientation preservation (one-to-one property of the deformation) ([35], [49], [11], [43], [45]), symmetry, inverse consistency (which means that interchanging the Template and the Reference should not impact on the produced result) ([60]), volume preservation ([32]), lower and upper bounds on the Jacobian determinant ([33]), etc.

As structure/salient component/shape/geometrical feature matching and intensity distribution comparison rule registration, it sounds relevant to intertwine the segmentation and registration tasks into a single framework: accurate segmentation results will drive the registration process correctly, providing then a reliable deformation field between encoded structures. This work thus focuses primarily on a registration model guided by segmentation (segmentation results will serve as target to reach and as such are inputs in our model). A joint framework in which segmentation and registration are performed simultaneously has also been investigated (see Remark 4.8). Prior related works suggest to jointly treat these two tasks : [61], [55] (in a level set framework), [38] (registration is achieved using the transfer of edges based on the active contour model without edges), [40] (model based on metric structure comparison), [29] (based on Expectation Maximization algorithm that incorporates a glioma growth model for atlas seeding), [2], [30] (active contour framework combined with dense deformation fields of optical flow), [24] (edges and the normals of the two images are matched by applying a Mumford-Shah type free discontinuity problem), or [47] (based on weighted total variation). We emphasize again that this work focuses on a registration model guided by segmentation.

To summarize, in addition to devising a theoretically well-motivated registration model, we propose defining a geometric dissimilarity measure based on shape comparisons thanks to successive segmentation results that will serve as inputs in our registration model. Segmentation thus influences registration. Let us emphasize that the focus of this chapter is

on the mathematical presentation and well-posedness of a nonlinear elasticity-based registration model in the two dimensional case. Later work may go to higher dimensions.
In [59], the authors propose a similar model in which the shapes are implicitly described as boundary contours of objects, and thus implicitly modelled by level-set functions and the deformation is obtained by finding a geodesic path based on the continuum mechanical notion of viscous dissipation. A time discretization as a sequence of pairwise matching problems ensures invariance with respect to rigid body motions and inverse consistency, and a finite element scheme is used to numerically solve the problems.
Finally, we would like to mention that this work is the continuation of a very preliminary conference proceedings version [48] and [46, Chapter 5]. In particular, the model has been slightly reshaped and a thorough numerical analysis of the proposed algorithm is provided with convergence results, which was not the case in [48] and in [46, Chapter 5].
For additional mathematical material, we refer the reader to Chapter 2, Sections 1.1, 1.2, 2.2, 3.2, and 4.

2 Mathematical modelling

2.1 General mathematical background

There are forward and backward transformations: the former is done in the Lagrangian framework where a forward transformation ψ is sought and grid points x with intensity values $T(x)$ are moved and arrive at non-grid points $y = \psi(x)$ with intensity values $T(x) = T(\psi^{-1}(y))$. In the Eulerian framework (considered here), we find a backward transformation $\varphi = \psi^{-1}$ such that grid points y in the deformed image originate from non-grid points $x = \varphi(y) = \psi^{-1}(y)$ and are assigned intensity values $T(\varphi(y)) = T(\psi^{-1}(y)) = T(x)$. We thus compare a point $(y, R(y))$ (R denoting the Reference image) with $\big(y, T(\psi^{-1}(y)) = T(\varphi(y))\big)$.

More precisely, when the forward mapping is computed, every pixel of the Template image is pushed forward to its assessed position in the deformed image (entailing in practice a problem of scattered data interpolation), while in the backward setting, the pixel value in the deformed configuration is pulled from the Template image, meaning that the intensities can be easily calculated by interpolating the values of the neighboring pixels. We refer the reader to [31] and [54] in which both frameworks are clearly stated.

Let Ω be a connected bounded open subset of $\mathbb{R}^2$ of class $\mathcal{C}^1$. Let us denote by $R : \bar{\Omega} \to \mathbb{R}$ the Reference image assumed to be sufficiently smooth (the expression 'smooth enough' is a convenient way of saying that in a given definition, the smoothness of the involved variables or data is such that all arguments make sense), and by $T : \bar{\Omega} \to \mathbb{R}$ the Template image. The shape contained in the Template image is assumed to be modelled by a Lipschitz continuous function Φ_0 (input of the problem obtained by applying the topology-preserving segmentation model [37]) whose zero level line is the shape boundary. Denoting by $\mathcal{C}$ the zero level set of Φ_0 and by $w \subset \Omega$ the open set it delineates, Φ_0 is chosen such that $\mathcal{C} = \{x \in \Omega \,|\, \Phi_0(x) = 0\}$, $w = \{x \in \Omega \,|\, \Phi_0(x) > 0\}$ and $\Omega \setminus \bar{w} = \{x \in \Omega \,|\, \Phi_0(x) < 0\}$. For theoretical and numerical purposes, we may consider a linear extension operator (see [6, p. 158]) $P : W^{1,\infty}(\Omega) \to W^{1,\infty}(\mathbb{R}^2)$ such that for all $\Phi \in W^{1,\infty}(\Omega)$, (i) $P\Phi_{|\Omega} = \Phi$, (ii)

$\|P\Phi\|_{L^\infty(\mathbb{R}^2)} \leq C\,\|\Phi\|_{L^\infty(\Omega)}$ and (iii) $\|P\Phi\|_{W^{1,\infty}(\mathbb{R}^2)} \leq C\,\|\Phi\|_{W^{1,\infty}(\Omega)}$, with C depending only on Ω. By this extension process, we consider then that $\Phi_0 \in W^{1,\infty}(\mathbb{R}^2)$ to ensure that $\Phi_0 \circ \varphi$ – with φ introduced later – is always defined.
Let $\varphi : \bar{\Omega} \to \mathbb{R}^2$ be the sought deformation (or transformation). (Of course, in practice, the sought transformation φ should be with values in $\bar{\Omega}$ but from a mathematical point of view, if we work with such spaces of functions we lose the structure of vector space). A deformation is a smooth mapping that is orientation-preserving and injective, except possibly on $\partial\Omega$. As stressed by Ciarlet ([14, p. 26]), the reason a deformation may lose its injectivity on the boundary of Ω is that self-contact must be allowed. We also denote by u the associated displacement such that $\varphi = \mathtt{Id} + u$, $\mathtt{Id}$ denoting the identity mapping. The deformation gradient is $\nabla\varphi = I + \nabla u$, $\bar{\Omega} \to M_2(\mathbb{R})$, the set $M_2(\mathbb{R})$ being the set of all real square matrices of order 2 identified to $\mathbb{R}^4$. This sought deformation is seen as the optimal solution of a specifically designed cost function, comprising a regularization on φ prescribing the nature of the deformation, and a term measuring alignment or how the available data are exploited to drive the registration process. These are depicted hereafter.

2.2 Regularization on the deformation

Nonlinear elasticity principles dictate the design of the smoother on φ. The shapes to be matched are viewed as isotropic (uniformity in all orientations), homogeneous (same properties at every point) and hyperelastic materials (materials capable of undergoing large deformations while keeping their elastic behavior), hyperelasticity being a suitable framework when dealing with large and nonlinear deformations: rubber, filled elastomers, and biological tissues are often modelled within this setting. More precisely, the shapes are considered to be Saint Venant-Kirchhoff materials (—see [13] for further details and [9] for an alternative hyperelastic model. For the sake of completeness, we also refer the reader to [50] for a nonlinear elasticity based regularization implemented with the finite element method, [23], [22], [24] in which the general Mumford and Shah functional is used in the minimization, combined with registration of the unknown edge sets, [21] in which basic similarity measures are incorporated and a Saint Venant-Kirchhoff like stored energy function is considered —). A motivation for this choice is that the stored energy function of such materials is the simplest one that agrees with the generic expression of the stored energy of an isotropic, homogeneous, hyperelastic material. Also, to ensure that the distribution of the deformation Jacobian determinants does not exhibit shrinkages or growths, we propose complementing the model by a term controlling that the Jacobian determinant remains close to 1. (The weighting of the determinant component by parameter μ is justified in the proof of Proposition 3.2 in [46, Chapter 5]). At this stage, the considered regularizer would be, setting $F = \nabla\varphi$,

$$W(F) = W_{SVK}(F) + \mu\,(\det F - 1)^2\,,$$

with $W_{SVK}(F) = \dfrac{\lambda}{2}\,(\operatorname{tr} E)^2 + \mu \operatorname{tr} E^2$, the stored energy function of a Saint Venant-Kirchhoff material, λ and μ the Lamé coefficients, $E = \left(F^T F - I\right)/2$ the Green-Saint Venant stress tensor measuring the deviation between φ and a rigid deformation, and

with the following notation $A : B = \mathrm{tr} A^T B$, the matrix inner product, and $\|A\| = \sqrt{A : A}$ the related matrix norm (Frobenius norm). Note that this regularizer has been investigated in prior related works by Derfoul and Le Guyader [21] and Ozeré, Gout and Le Guyader [47]. Nevertheless, it does not constitute the core of the present work, the emphasis being put on the numerical analysis of the proposed algorithm. We refer the reader to Remark 3.3 for the motivation of this choice for regularization.

2.3 Alignment measure

Accurate segmentation results drive the registration process. Recall that the shape contained in the Template image is assumed to be modelled by a Lipschitz continuous function Φ_0 whose zero level line is the shape boundary. We thus aim to find a smooth deformation field φ such that the zero level line of $\Phi_0 \circ \varphi$ gives a relevant partition of the Reference image R. A criterion measuring the distance between $\Phi_0 \circ \varphi$ and an input (a priori knowledge in the model) resulting from the topology-preserving segmentation process of Le Guyader and Vese ([37]) is introduced, with the goal to maximize the overlapping between the shape delineated by the zero level line of $\Phi_0 \circ \varphi$ - shape contained in the deformed Template - and the shape included in the Reference image and defined through the zero level line of an auxiliary level set function.

This measure constitutes an alternative to classical intensity-based/information-theoretic-based matching measures, mutual information – suitable when dealing with images that have been acquired through different sensors –, measures based on the comparison of gradient vector fields of both images, metric structure comparisons, mass-preserving measures, etc. It is defined by

$$W_{\mathrm{al}}(\varphi) = \int_\Omega \left(H_\varepsilon(\Phi_0 \circ \varphi) - H_\varepsilon(\tilde{\Phi}(\cdot, \bar{T})) \right)^2 dx,$$

H_ε denoting a $\mathcal{C}^\infty$ - regularization of the one - dimensional Heaviside function, $\tilde{\Phi}$ being the solution of the evolution equation stemming from the topology-preserving segmentation model by Le Guyader and Vese ([37]) and allowing for a partition of the Reference image:

$$\begin{cases} \dfrac{\partial \tilde{\Phi}}{\partial t} = |\nabla \tilde{\Phi}| \left[\mathrm{div}\left(\tilde{g}(|\nabla R|) \dfrac{\nabla \tilde{\Phi}}{|\nabla \tilde{\Phi}|} \right) + k\tilde{g}(|\nabla R|) \right] + 4\dfrac{\mu'}{d^2} \bar{H}(\tilde{\Phi}(x) + l) \\ \bar{H}(l - \tilde{\Phi}(x)) \displaystyle\int_\Omega \left[\langle x - y, \nabla \tilde{\Phi}(y) \rangle \, e^{-\|x-y\|_2^2/d^2} \bar{H}(\tilde{\Phi}(y) + l) \bar{H}(l - \tilde{\Phi}(y)) \right] dy \,, \\ \tilde{\Phi}(x, 0) = \Phi_0(x) \,, \\ \dfrac{\partial \tilde{\Phi}}{\partial \vec{n}} = 0, \quad \text{on } \partial\Omega \,. \end{cases} \tag{3.1}$$

Φ_0 is naturally taken to be the initial condition of this segmentation process. Function $\tilde{g}$ is an edge-detector function satisfying $\tilde{g}(0) = 1$, $\tilde{g}$ strictly decreasing and $\lim_{r \to +\infty} \tilde{g}(r) = 0$. This evolution equation results from the minimization of functional $J(\tilde{\Phi}) + \mu' L(\tilde{\Phi})$ ($\mu' > 0$,

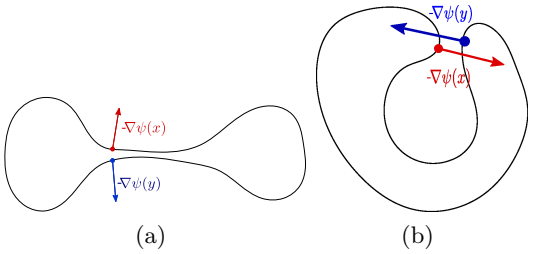

Figure 3.1: Geometrical characterization of points where the curve is to merge (a) or split (b).

tuning parameter), combination of $J(\tilde{\Phi}) = \int_\Omega \tilde{g}(|\nabla R|)|\nabla \bar{H}(\tilde{\Phi})|$ coming from the classical geodesic active contour model ([10]) ($\bar{H}$ being the one - dimensional Heaviside function) and L, related to the topological constraint:

$$L(\tilde{\Phi}) = -\int_\Omega\int_\Omega \Big[\exp\left(-\frac{\|x-y\|_2^2}{d^2}\right)\langle\nabla\tilde{\Phi}(x),\nabla\tilde{\Phi}(y)\rangle\,\bar{H}(\tilde{\Phi}(x)+l)\bar{H}(l-\tilde{\Phi}(x))\bar{H}(\tilde{\Phi}(y)+l)$$
$$\bar{H}(l-\tilde{\Phi}(y))\Big]\,dx\,dy\,. \tag{3.2}$$

The Euclidean scalar product in $\mathbb{R}^2$ is denoted by $\langle\cdot,\cdot\rangle$ and $\|\cdot\|_2$ is the associated norm. A geometrical observation motivates the introduction of L. Indeed, in the case when Φ is a signed-distance function, $|\nabla\Phi| = 1$ and the unit outward normal vector to the zero level line at point x is $-\nabla\Phi(x)$. Let us now consider two points $(x,y) \in \Omega\times\Omega$ belonging to the zero level line of Φ, close enough to each other, and let $-\nabla\Phi(x)$ and $-\nabla\Phi(y)$ be the two unit outward normal vectors to the contour at these points. When the contour is about to merge or split, that is, when the topology of the evolving contour is to change, then $\langle\nabla\Phi(x),\nabla\Phi(y)\rangle \simeq -1$ (see Figure 3.1). This remark justifies the construction of L. In many applications, such as medical imaging, topology preservation is a desirable property: when the shape to be detected has a known topology (e.g. spherical topology for the brain), or when the resulting shape must be homeomorphic to the initial one. In other words, an initial contour should be deformed without change of topology as merging or breaking. Also, as shown in [37], this topology-preserving constraint enables us to delineate properly the thin concavities of the objects. The registration process is then fed by the knowledge of the segmentation of the Reference image at time $\bar{T}$.

2.4 Overall functional

In the end, gathering the smoothing component and the alignment measure yields the following global minimization problem (P) with $\bar{T}$, given fixed artificial time:

$$\inf\Big\{I(\varphi) = \int_\Omega f(x,\varphi(x),\nabla\varphi(x))\,dx, \tag{P}$$
$$= \int_\Omega \left[W(\nabla\varphi(x)) + \frac{\nu}{2}\left(H_\varepsilon(\Phi_0\circ\varphi) - H_\varepsilon(\tilde{\Phi}(\cdot,\bar{T}))\right)^2\right]dx\Big\},$$

with $\varphi \in \mathtt{Id} + W_0^{1,4}(\Omega, \mathbb{R}^2)$ meaning that $\varphi = \mathtt{Id}$ —the identity mapping— on $\partial\Omega$ and $\varphi \in W^{1,4}(\Omega, \mathbb{R}^2)$. With this choice, the boundary is mapped onto the boundary. Note that boundary conditions are of relative importance, provided the images are embedded into a uniform backdrop. Nevertheless, alternative boundary conditions could have been investigated (Dirichlet, Neumann, periodic, sliding, bending boundary conditions —[42]) but in practice, for disease progression evaluation for instance (Figure 3.7), it sounds relevant to assume such boundary conditions. Also, it emphasizes the ability of our model to handle large deformations. Note that from generalized Hölder's inequality, if $\varphi \in W^{1,4}(\Omega, \mathbb{R}^2)$, then $\det \nabla\varphi \in L^2(\Omega)$. Also, in [1], Ambrosio and Dal Maso prove a general chain rule for the distribution derivatives of the composite function $v(x) = f(u(x))$, where $u : \mathbb{R}^n \to \mathbb{R}^m$ has bounded variation and $f : \mathbb{R}^m \to \mathbb{R}^k$ is Lipschitz continuous. A simpler result is given when $u \in W^{1,p}(\Omega, \mathbb{R}^m)$ for some p, $1 \leq p \leq +\infty$ and states that $v = f(u)$ belongs to $W^{1,p}(\Omega, \mathbb{R}^k)$. With these elements in hand (in particular, the data fidelity term is well-defined thanks to the previous result), we have the following remark:

Remark 2.1. *A judicious rewriting of* $W(\xi)$ *into* $W(\xi) = \beta\,\left(\|\xi\|^2 - \alpha\right)^2 + \Psi(det\xi)$ *with* $\alpha = 2\,\frac{\lambda+\mu}{\lambda+2\mu}$ *and* $\beta = \frac{\lambda+2\mu}{8}$, *and* $\Psi : s \mapsto -\frac{\mu}{2}s^2 + \mu\,(s-1)^2 + \underbrace{\frac{\mu(\lambda+\mu)}{2(\lambda+2\mu)}}_{:=\gamma}$ *enables us to see that* $W^{1,4}(\Omega, \mathbb{R}^2)$ *is a suitable functional space for* φ. *Indeed, it can easily be proved that*

$$\begin{cases} \beta\,\left(\|\xi\|^2 - \alpha\right)^2 \leq \beta\,\|\xi\|^4 + \beta\,\alpha^2, \\ \Psi(\det\xi) \leq \mu\,(\det\xi)^2 + 3\mu + \dfrac{\mu\,(\lambda+\mu)}{2(\lambda+2\mu)}, \end{cases}$$

so that if $\varphi \in W^{1,4}(\Omega, \mathbb{R}^2)$, $\displaystyle\int_\Omega f(x, \varphi(x), \nabla\varphi(x))\,dx < \infty$.

3 Theoretical results

3.1 Mathematical obstacle and derivation of the associated relaxed problem

We start by expressing the main technical difficulty related to this problem that led us to introduce the associated relaxed problem.

Proposition 3.1. *Function* f *is not quasi-convex (see [17, Chapter 9] for a complete review of this notion).*

Proof. See proof of [47, Proposition 1.] and [46, Chapter 5] for similar standard arguments. □

Proposition 3.1 raises a drawback of a theoretical nature since we cannot obtain the weak lower semicontinuity of the introduced functional. The idea is thus to replace the original problem (P) by a relaxed one denoted by (QP) formulated in terms of the quasi-convex envelope Qf of f. In what follows, we establish the explicit expression of the

quasi-convex envelope of f and derive the related relaxed problem (the proof is available in [46, Chapter 5]).

Proposition 3.2. *The quasi-convex envelope Qf of f is defined by*

$$Qf(x,\varphi,\xi) = \frac{\nu}{2}\int_\Omega \left(H_\varepsilon(\Phi_0\circ\varphi) - H_\varepsilon(\tilde{\Phi}(\cdot,\bar{T}))\right)^2 dx + QW(\xi),$$

with $QW(\xi) = \begin{cases} W(\xi) \ \text{ if } \|\xi\|^2 \geq \alpha, \\ \Psi(det\,\xi) \ \text{ if } \|\xi\|^2 < \alpha, \end{cases}$ *and Ψ, the convex mapping defined in Remark 2.1. The relaxed problem (QP) is thus defined by:*

$$\inf\left\{\bar{I}(\varphi) = \int_\Omega Qf(x,\varphi(x),\nabla\varphi(x))\,dx\right\}, \tag{QP}$$

with $\varphi \in \mathtt{Id} + W_0^{1,4}(\Omega,\mathbb{R}^2)$.

Remark 3.3. *Note that the stored energy function W_{SVK} alone lacks a term penalizing the determinant: it thus does not preclude deformations with negative Jacobian. Also, it exhibits the same property of non rank-1 convexity (and thus non quasiconvexity), which raises the same theoretical issues as for the existence of minimizers. From our experience, in practice, the Saint Venant-Kirchhoff model alone requires more regridding steps when large deformations are involved compared with the proposed stored energy (see [38] for comparisons). It is also possible to compute the quasiconvex envelope of W_{SVK}. Its expression is more complex than in our case, since including explicitly the singular values of ξ and making its numerical implementation more involved with finite element approximations. This computation was achieved by Le Dret and Raoult in [36]. It is noticeable that, in this case, when the singular values of ξ are lower than 1, the quasiconvex envelope equals 0, which shows bad behavior under compression. In comparison, we see in the expression of QW that when $\|\xi\|^2 < \alpha$, that is, when the sum of the singular values of ξ to the square is lower than α, a penalization on the determinant still remains, function Ψ reaching its minimum for a positive value of its argument.*

Remark 3.4. *We emphasize that the extension of the model to the 3D case is not straightforward. Indeed, in three dimensions, the expression of $W_{SVK}(\xi)$ involves the cofactor matrix denoted by $Cof\xi$ as follows:*

$$W_{SVK}(\xi) = \frac{\lambda}{8}\left(\|\xi\|^2 - \left(3 + \frac{2\mu}{\lambda}\right)\right)^2 + \frac{\mu}{4}\left(\|\xi\|^4 - 2\,\|Cof\xi\|^2\right) - \frac{\mu}{4\lambda}\left(2\mu + 3\lambda\right),$$

and it is not clear that one can derive the explicit expression of the quasiconvex envelope QW of W with $W(\xi) = W_{SVK}(\xi) + \mu(\det\xi - 1)^2$.

In the next subsection, we prove that the infimum of problem (QP) is attained and that if $\bar{\varphi}$ is a solution of problem (P), then there exists a minimizing sequence $\{\varphi_\nu\}$ of problem (P) such that $\{\varphi_\nu\}$ weakly converges to $\bar{\varphi}$ and $I(\varphi_\nu) \to \bar{I}(\bar{\varphi})$. The solutions of (QP) are considered as generalized solutions of (P), in the sense of weak convergence. We also ensure that $\tilde{\Phi}(\cdot,\bar{T})$ is well-defined, using the viscosity solution theoretical framework.

3.2 Existence of minimizers and relaxation theorem

We state the main theoretical result related to the existence of minimizers, following arguments similar to those used in [21] and in [46, Chapter 5].

Theorem 3.1. *The infimum of (QP) is attained. Let then $\bar{\varphi} \in W^{1,4}(\Omega, \mathbb{R}^2)$ be a minimizer of the relaxed problem (QP). Then there exists a sequence $\{\varphi_\nu\}_{\nu=1}^{\infty} \subset \bar{\varphi} + W_0^{1,4}(\Omega, \mathbb{R}^2)$ such that $\varphi_\nu \to \bar{\varphi}$ in $L^4(\Omega, \mathbb{R}^2)$ as $\nu \to \infty$ and $I(\varphi_\nu) \to \bar{I}(\bar{\varphi})$ as $\nu \to \infty$. Moreover, the following holds: $\varphi_\nu \rightharpoonup \bar{\varphi}$ in $W^{1,4}(\Omega, \mathbb{R}^2)$ as $\nu \to \infty$.*
It means in particular that $\inf\limits_{\varphi \in \mathtt{Id} + W_0^{1,4}(\Omega,\mathbb{R}^2)} I(\varphi) = \min\limits_{\varphi \in \mathtt{Id} + W_0^{1,4}(\Omega,\mathbb{R}^2)} \bar{I}(\varphi)$, *as $QW \leq W$. The solutions of (QP) are considered as generalized solutions of problem (P).*

We now investigate the well-definedness of $\tilde{\Phi}(\cdot, \bar{T})$ and ensure that it exhibits sufficient regularity properties.

3.3 Well-definedness of $\tilde{\Phi}$

Problem (3.1) is hard to handle from a theoretical point of view. A suitable setting would be the one of the viscosity solution theory ([16]) (owing to the nonlinearity induced by the modified mean curvature term), but the dependency of the nonlocal term on the gradient $\nabla\tilde{\Phi}(y)$ and the failure to fulfill the monotony property in $\tilde{\Phi}$ make it difficult. For this reason, for the theoretical part, we consider a slightly modified problem: we assume that the topological constraint is only applied to the zero level line. Assuming that $\tilde{\Phi}$ is a signed-distance function, the topological constraint L is then rephrased as

$$L(\tilde{\Phi}) = -\int_\Omega \int_\Omega \Big[\exp\left(-\frac{\|x-y\|_2^2}{d^2}\right) \langle \nabla\tilde{\Phi}(x), \nabla\tilde{\Phi}(y)\rangle \delta(\tilde{\Phi}(x))\delta(\tilde{\Phi}(y))\Big] dx\, dy\,,$$

with δ the Dirac measure. Computing the Euler - Lagrange equation, then applying an L^2 gradient flow method and doing an integration by parts and a rescaling by replacing $\delta(\tilde{\Phi})$ by $|\nabla\tilde{\Phi}|$, yields the following evolution problem (defined on $\mathbb{R}^2$ for the space coordinates for the sake of simplicity)

$$\frac{\partial\tilde{\Phi}}{\partial t} = |\nabla\tilde{\Phi}| \left\{ \operatorname{div}\left(\tilde{g}(|\nabla R|) \frac{\nabla\tilde{\Phi}}{|\nabla\tilde{\Phi}|} \right) + c_0 * \left[\tilde{\Phi}(\cdot,t)\right] + k\tilde{g}(|\nabla R|) \right\}, \tag{3.3}$$

with $\left[\tilde{\Phi}(\cdot,t)\right]$ the characteristic function of the set $\left\{\tilde{\Phi}(\cdot,t) \geq 0\right\}$ and

$$c_0 : \begin{cases} \mathbb{R}^2 \to \mathbb{R} \\ x \mapsto \dfrac{4\mu}{d^2}\left(2 - \dfrac{2}{d^2}\|x\|_2^2\right) \exp\left(-\dfrac{\|x\|_2^2}{d^2}\right) \end{cases} . \tag{3.4}$$

Remark 3.5. *A sample of experiments shows that this simplified model qualitatively performs in a similar way to [37] (see [27] in particular).*

We now derive an existence theorem in the viscosity solutions framework. Note that the proposed result, which is a result of existence of weak solutions to problem (3.3)– with no restriction on time $\bar{T}$ – is different from the one obtained in [27], which is a short-time existence/uniqueness result in the classical sense. Equipped with the theoretical elements introduced in Section 2.2 from Chapter 2, we now state the main theoretical result regarding the existence of at least one weak solution to problem (3.3).

Theorem 3.2. *Assuming that $g := \tilde{g}(|\nabla R|)$, $g^{\frac{1}{2}}$ and ∇g are bounded and Lipschitz continuous on $\mathbb{R}^2$, problem (3.3) admits at least one weak solution.*

Proof. First, one can easily check that setting $C(p) := (I - \frac{p \bigotimes p}{|p|^2})$,

$$H[\chi](x,t,p,A) = g(x)\mathrm{tr}\,(C(p)A) + \langle \nabla g(x), p\rangle + |p| \int_{\mathbb{R}^2} c_0(x-y)\chi(y,t)\,dy + kg(x)|p|\,.$$

We give the sketch of the proof by mainly checking that the assumptions of Theorem 2.1 from Chapter 2 are fulfilled. Assumption [A1] is rather classical and for the sake of conciseness, we do not go into details. Assumption [A3] is obviously fulfilled, $H[\chi]$ being independent of r in the considered problem. Let us now focus on assumption [A2] i). $M > 0$ denotes a positive constant that may change line to line and that may depend on K, g, ∇g, $\|c_0\|_{L^1(\mathbb{R}^2)}$ or $\|\nabla c_0\|_{L^1(\mathbb{R}^2)}$. Recall that (x_i, p_i, A_i) belongs to the compact subset K. One then has

$$\begin{aligned} |\langle \nabla g(x_1), p_1\rangle - \langle \nabla g(x_2), p_2\rangle| =& |\langle \nabla g(x_1) - \nabla g(x_2), p_1\rangle + \langle \nabla g(x_2), p_1 - p_2\rangle| \\ \leq& M\,(|x_1 - x_2| + |p_1 - p_2|)\,, \end{aligned}$$

due to the properties of ∇g. Also,

$$\begin{aligned} \left|k|p_1|g(x_1) - k|p_2|g(x_2)\right| &\leq |k|\,|p_1 - p_2||g(x_1)| + |k|\,|p_2||g(x_1) - g(x_2)|, \\ &\leq M(|p_1 - p_2| + |x_1 - x_2|), \end{aligned}$$

due to the properties of g. Furthermore,

$$\begin{aligned} &\left||p_1| \int_{\mathbb{R}^2} c_0(x_1 - y)\chi(y,t)\,dy - |p_2| \int_{\mathbb{R}^2} c_0(x_2 - y)\chi(y,t)\,dy\right| \\ &\leq\ ||p_1| - |p_2|| \left|\int_{\mathbb{R}^2} c_0(x_1 - y)\chi(y,t)\,dy\right| + |p_2| \left|\int_{\mathbb{R}^2} \left(c_0(x_1 - y) - c_0(x_2 - y)\right)\chi(y,t)\,dy\right|\,, \\ &\leq |p_1 - p_2|\,\|c_0\|_{L^1(\mathbb{R}^2)}\|\chi\|_{L^\infty(\mathbb{R}^2\times[0,T])} + |p_2| \\ &\left|\int_{\mathbb{R}^2} \left(\int_0^1 \langle \nabla c_0((x_2 - y) + s(x_1 - x_2)), x_1 - x_2\rangle\,ds\right)\chi(y,t)\,dy\right|\,. \end{aligned}$$

A change of variable in the integral allows to conclude that

$$\begin{aligned}&\left||p_1|\int_{\mathbb{R}^2} c_0(x_1-y)\chi(y,t)\,dy - |p_2|\int_{\mathbb{R}^2} c_0(x_2-y)\chi(y,t)\,dy\right| \\ &\leq |p_1-p_2|\,\|c_0\|_{L^1(\mathbb{R}^2)}\|\chi\|_{L^\infty(\mathbb{R}^2\times[0,T])} + |p_2|\,|x_1-x_2|\,\|\chi\|_{L^\infty(\mathbb{R}^2\times[0,T])}\,\|\nabla c_0\|_{L^1(\mathbb{R}^2)}\,, \\ &\leq M\,(|p_1-p_2|+|x_1-x_2|)\,.\end{aligned}$$

It remains to estimate $|g(x_1)\mathrm{tr}\,(C(p_1)A_1) - g(x_2)\mathrm{tr}\,(C(p_2)A_2)|$. One has

$$\begin{aligned}|g(x_1)\mathrm{tr}\,(C(p_1)A_1) - g(x_2)\mathrm{tr}\,(C(p_2)A_2)| &\leq |g(x_1)-g(x_2)|\,|\mathrm{tr}\,(C(p_1)A_1)| \\ &\quad + g(x_2)\;|\mathrm{tr}\,(C(p_1)A_1) - \mathrm{tr}\,(C(p_2)A_2)|\,, \\ &\leq M\,|x_1-x_2|\,\|C(p_1)\|_F\|A_1\|_F + g(x_2) \\ &\quad |\mathrm{tr}\,((C(p_1)-C(p_2))\,A_1) + \mathrm{tr}\,(C(p_2)\,(A_1-A_2))|\,,\end{aligned}$$

$\|\cdot\|_F$ denoting the Frobenius norm. Remarking that $\|C(p_1)\|_F = 1$ and that one has $\|A_1\|_F \leq \sqrt{2}\|A_1\|_2 = \sqrt{2}|A_1|$, it yields

$$\begin{aligned}|g(x_1)\mathrm{tr}\,(C(p_1)A_1) - g(x_2)\mathrm{tr}\,(C(p_2)A_2)| &\leq M\;(|x_1-x_2| + |A_1-A_2|) \\ &\quad + g(x_2)\,|\mathrm{tr}\,((C(p_1)-C(p_2))\,A_1)|\,.\end{aligned} \tag{3.5}$$

One can notice that $C(p) = \sigma(p)\sigma(p)^T$ with $\sigma(p) = \begin{pmatrix} \frac{p_{02}}{|p|} & 0 \\ -\frac{p_{01}}{|p|} & 0 \end{pmatrix}$ given $p = (p_{01}, p_{02})^T \neq 0$.

Consequently,

$$\begin{aligned}g(x_2)\;|\mathrm{tr}\,((C(p_1)-C(p_2))\,A_1)| &\leq M\;\left|\mathrm{tr}\left((\sigma(p_1)-\sigma(p_2))\,\sigma(p_1)^T A_1\right)\right. \\ &\quad \left.+\mathrm{tr}\left(\sigma(p_2)\left(\sigma(p_1)^T-\sigma(p_2)^T\right)A_1\right)\right|\,.\end{aligned}$$

Focusing on the first term of the right part of the inequality, the result being similar for the second component, one obtains

$$\begin{aligned}\left|\mathrm{tr}\left((\sigma(p_1)-\sigma(p_2))\,\sigma(p_1)^T A_1\right)\right| &\leq \|A_1\|_F\,\|\sigma(p_1)-\sigma(p_2)\|_F\,\|\sigma(p_1)^T\|_F\,, \\ &\leq M\,\left|\frac{p_1}{|p_1|}-\frac{p_2}{|p_2|}\right| \leq \frac{|p_1-p_2|}{\min\,(|p_1|,|p_2|)}\,,\end{aligned}$$

so

$$\left|\mathrm{tr}\left((\sigma(p_1)-\sigma(p_2))\,\sigma(p_1)^T A_1\right)\right| \leq M\,|p_1-p_2|\,.$$

Including this result in equation (3.5) yields the desired estimation.
The two remaining assumptions are checked using the same arguments as above and taking h the null function for assumption [A2] ii), and by definition of the L^∞-weak $*$ convergence for assumption [A2] iii). □

4 Numerical Method of Resolution

4.1 Asymptotic behavior of a penalization method in the continuous domain

In [44], Negrón Marrero describes and analyzes a numerical method that detects singular minimizers and avoids the Lavrentiev phenomenon for three dimensional problems in nonlinear elasticity. This method consists in decoupling the function φ from its gradient and in formulating a related decoupled problem under inequality constraint. In the same spirit, we introduce an auxiliary variable V simulating the Jacobian deformation field $\nabla\varphi$ (–the underlying idea being to remove the nonlinearity in the derivatives of the deformation–) and derive a functional minimization problem phrased in terms of the two variables φ and V. This problem corresponds in fact to the conversion of the original problem formulated in terms of φ and V under the equality constraint $V = \nabla\varphi$ a.e., into an unconstrained minimization problem via quadratic penalty method.
The decoupled problem is thus defined by means of the following functional:

$$\bar{I}_\gamma(\varphi, V) = \frac{\nu}{2} \|H_\varepsilon(\Phi_0 \circ \varphi) - H_\varepsilon(\tilde{\Phi}(\cdot, \bar{T}))\|^2_{L^2(\Omega)} + \int_\Omega QW(V)\, dx + \frac{\gamma}{2} \|V - \nabla\varphi\|^2_{L^2(\Omega, M_2(\mathbb{R}))}. \tag{3.6}$$

Let us now denote by $\widehat{\mathcal{W}}$ the functional space defined by $\widehat{\mathcal{W}} = \mathtt{Id} + W^{1,2}_0(\Omega, \mathbb{R}^2)$ and by $\widehat{\chi}$, the functional space $\widehat{\chi} = \left\{V \in L^4(\Omega, M_2(\mathbb{R}))\right\}$. The decoupled problem consists in minimizing (3.6) on $\widehat{\mathcal{W}} \times \widehat{\chi}$. Then the following asymptotic theorem holds.

Theorem 4.1. *Let (γ_j) be an increasing sequence of positive real numbers such that $\lim_{j\to+\infty} \gamma_j = +\infty$. Let also $(\varphi_k(\gamma_j), V_k(\gamma_j))$ be a minimizing sequence of the decoupled problem with $\gamma = \gamma_j$. Then there exists a subsequence denoted by $\left(\varphi_{N(\gamma_{\Psi\circ\zeta(j)})}(\gamma_{\Psi\circ\zeta(j)}), V_{N(\gamma_{\Psi\circ\zeta(j)})}(\gamma_{\Psi\circ\zeta(j)})\right)$ of $(\varphi_k(\gamma_j), V_k(\gamma_j))$ and a minimizer $\bar{\varphi}$ of $\bar{I}$ ($\bar{\varphi} \in \mathtt{Id} + W^{1,4}_0(\Omega, \mathbb{R}^2)$) such that:*

$$\lim_{j\to+\infty} \bar{I}_{\gamma_{\Psi\circ\zeta(j)}} \left(\varphi_{N(\gamma_{\Psi\circ\zeta(j)})}(\gamma_{\Psi\circ\zeta(j)}), V_{N(\gamma_{\Psi\circ\zeta(j)})}(\gamma_{\Psi\circ\zeta(j)})\right) = \bar{I}(\bar{\varphi}).$$

Proof. See [21, Theorem 10] and [46, Theorem 5.3.1] for similar arguments. □

Remark 4.1. *When applying the direct method of the calculus of variations to problem (3.6) for fixed γ, we obtain the boundednesss of the minimizing component V_j in $L^4(\Omega, M_2(\mathbb{R}))$, which allows to extract a weakly converging subsequence still denoted V_j. Unfortunately, we cannot say anything about the behaviour of $\det V_j$, preventing us from obtaining any minimizer existence result. That is the reason why the previous asymptotic result involves for each γ_j a minimizing sequence associated with the decoupled problem.*

We now concentrate upon the discrete counterparts of the previous study. Two strategies have been investigated: a purely quadratic penalty method and an augmented Lagrangian technique.

4.2 Discrete counterpart of the quadratic penalty method

Let us introduce some notations first. We now denote by $\tilde{\Omega} = \{1, \dots, N\} \times \{1, \dots, M\}$, N being the number of pixels in the horizontal axis and M the number of pixels in the vertical axis, a fixed rectangular lattice of integral points. We define the counterparts of the previous variables on the discrete domain, $\tilde{\varphi}^1 = \left(\tilde{\varphi}^1_{1,1}, \dots, \tilde{\varphi}^1_{i,j}, \dots, \tilde{\varphi}^1_{N,M}\right)^T \in \mathbb{R}^{N\times M}$ where $\tilde{\varphi}^1_{i,j} = \tilde{\varphi}^1(i,j)$, $\tilde{\varphi}^2 = \left(\tilde{\varphi}^2_{1,1}, \dots, \tilde{\varphi}^2_{i,j}, \dots, \tilde{\varphi}^2_{N,M}\right)^T \in \mathbb{R}^{N\times M}$, where $\tilde{\varphi}^2_{i,j} = \tilde{\varphi}^2(i,j)$, $\tilde{\varphi} = (\tilde{\varphi}^1, \tilde{\varphi}^2) \in \mathcal{F}_1(\tilde{\Omega}) = \{$set of all functions defined on $\tilde{\Omega}$ which are equal to identity on the boundary $\partial\tilde{\Omega}\}$. The discrete gradient $\nabla : \mathbb{R}^{N\times M} \times \mathbb{R}^{N\times M} \to (M_2(\mathbb{R}))^{N\times M}$ with periodic boundary conditions is defined as $\nabla\tilde{\varphi} = (\nabla\tilde{\varphi}_{1,1}, \dots, \nabla\tilde{\varphi}_{i,j}, \dots, \nabla\tilde{\varphi}_{N,M})^T$ with $\nabla\tilde{\varphi}_{i,j} = \begin{pmatrix} \partial_x\tilde{\varphi}^1_{i,j} & \partial_y\tilde{\varphi}^1_{i,j} \\ \partial_x\tilde{\varphi}^2_{i,j} & \partial_y\tilde{\varphi}^2_{i,j} \end{pmatrix}$, $\partial_x\tilde{\varphi}^k_{i,j} = \begin{cases} \tilde{\varphi}^k_{i,j} - \tilde{\varphi}^k_{i-1,j} & \text{if } i > 1 \\ \tilde{\varphi}^k_{1,j} - \tilde{\varphi}^k_{N,j} & \text{if } i = 1 \end{cases}$, $\partial_y\tilde{\varphi}^k_{i,j} = \begin{cases} \tilde{\varphi}^k_{i,j} - \tilde{\varphi}^k_{i,j-1} & \text{if } j > 1 \\ \tilde{\varphi}^k_{i,1} - \tilde{\varphi}^k_{i,M} & \text{if } j = 1 \end{cases}$, $k = 1, 2$. This choice of periodic boundary conditions is purely technical to prove the discrete counterpart of the generalized Poincaré inequality. In practice, as $\varphi = \mathtt{Id}$ on $\partial\Omega$, the discrete approximations $\tilde{\varphi}_{i,j}$ are only updated on internal nodes and the computations do not involve the particular cases $i = 1$ and $j = 1$.

Similarly, $\tilde{V} = \left(\tilde{V}_{1,1}, \dots, \tilde{V}_{i,j}, \dots, \tilde{V}_{N,M}\right)^T \in (M_2(\mathbb{R}))^{N\times M}$, with $\tilde{V}_{i,j} = \begin{pmatrix} \tilde{V}^{1,1}_{i,j} & \tilde{V}^{1,2}_{i,j} \\ \tilde{V}^{2,1}_{i,j} & \tilde{V}^{2,2}_{i,j} \end{pmatrix}$ and $\tilde{V}^{k,l}_{i,j} = \tilde{V}^{k,l}(i,j)$, $k, l = 1, 2$. The discrete norms are defined as $\|q\|_{l^p(\tilde{\Omega}, M_2(\mathbb{R}))} = \left(\sum_{i=1}^{N}\sum_{j=1}^{M} \sqrt{(q^{1,1}_{i,j})^2 + (q^{1,2}_{i,j})^2 + (q^{2,1}_{i,j})^2 + (q^{2,2}_{i,j})^2}^{\,p}\right)^{\frac{1}{p}} = \left(\sum_{i=1}^{N}\sum_{j=1}^{M} \|q_{i,j}\|^p\right)^{\frac{1}{p}}$ with $q \in (M_2(\mathbb{R}))^{N\times M}$ and $\|q\|_{l^p(\tilde{\Omega}, \mathbb{R}^2)} = \left(\sum_{i=1}^{N}\sum_{j=1}^{M} \sqrt{(q^1_{i,j})^2 + (q^2_{i,j})^2}^{\,p}\right)^{\frac{1}{p}}$ for $p \in \mathbb{N}$, $p < +\infty$ with q a $\mathbb{R}^2$-valued function defined on $\tilde{\Omega}$. Finally, $\|q\|_{l^p(\tilde{\Omega})} = \left(\sum_{i=1}^{N}\sum_{j=1}^{M} q^p_{i,j}\right)^{\frac{1}{p}}$ for $p \in \mathbb{N}$, $p < +\infty$ with q a real-valued function defined on $\tilde{\Omega}$. $\|.\|$ still denotes the Frobenius norm for matrices of size 2×2.

Before studying the discrete counterpart of our model, let us introduce the discrete generalized Poincaré inequality. We first recall the continuous generalized Poincaré inequality.

Theorem 4.2 (extracted from [20, p.106])**.** *Let Ω be a bounded Lipschitz domain in $\mathbb{R}^N$. Let $p \in [1, +\infty[$ and let $\mathcal{N}$ be a continuous seminorm on $W^{1,p}(\Omega)$, that is a norm on the constant functions. Suppose that $u \in W^{1,p}(\Omega)$, then there exists a constant $C > 0$ depending only on N, p, Ω such that:*

$$\|u\|_{W^{1,p}(\Omega)} \leq C\left(\left(\int_\Omega |\nabla u|^p \, dx\right)^{\frac{1}{p}} + \mathcal{N}(u)\right),$$

with $\mathcal{N}(u) = \int_{\Gamma_0} |u(x)| \, dx$ when Ω is a $\mathcal{C}^1$ open set and Γ_0 is a subset of $\partial\Omega$ with positive (N-1)-dimensional Lebesgue measure.

Now, we will provide a similar discrete inequality. The following result is an adaption of the one from [58] given for real-valued functions which vanish on the boundary whereas the results presented here stand for $\mathbb{R}^2$-valued functions which are equal to the identity on the boundary.

Lemma 4.2 (adapted from [58, Lemma 3.9]). *Let $f = (f^1, f^2) \in \mathcal{F}(\tilde{\Omega}) = \{f : \tilde{\Omega} \to \mathbb{R}^2\}$. For any $t = (t_1, t_2) \in \tilde{\Omega}$, we have:*

$$\begin{aligned}
&(|f^1(t)|^2 + |f^2(t)|^2)^{\frac{1}{2}} \leq |f^1(t)| + |f^2(t)| \\
&\leq \frac{1}{4}\left(\sum_{u=1}^{N}(|\partial_x f^1(u,t_2)| + |\partial_x f^2(u,t_2)|) + \left|2f^1(N,t_2)\right| + \left|2f^2(N,t_2)\right|\right. \\
&\left.+\sum_{u=1}^{M}(|\partial_y f^1(t_1,u)| + |\partial_y f^2(t_1,u)|) + \left|2f^1(t_1,M)\right| + \left|2f^2(t_1,M)\right|\right).
\end{aligned}$$

Proof. It can be checked easily for $i = 1, 2$ that:

$$\begin{aligned}
f^i(t) - f^i(N,t_2) &= \sum_{u=1}^{t_1}\partial_x f^i(u,t_2) \text{ as } \partial_x f^i(u,t_2) = f^i(u,t_2) - f^i(u-1,t_2),\ u \geq 2, \\
&\qquad \text{and } \partial_x f^i(1,t_2) = f^i(1,t_2) - f^i(N,t_2), \\
f^i(t) - f^i(t_1,M) &= \sum_{u=1}^{t_2}\partial_y f^i(t_1,u) \text{ as } \partial_y f^i(t_1,u) = f^i(t_1,u) - f^i(t_1,u-1),\ u \geq 2, \\
&\qquad \text{and } \partial_y f^i(t_1,1) = f^i(t_1,1) - f^i(t_1,M), \\
f^i(t) - f^i(N,t_2) &= -\sum_{u=t_1+1}^{N}\partial_x f^i(u,t_2) \text{ as } \partial_x f^i(u,t_2) = f^i(u,t_2) - f^i(u-1,t_2),\ u \geq 2, \\
f^i(t) - f^i(t_1,M) &= -\sum_{u=t_2+1}^{M}\partial_y f^i(t_1,u) \text{ as } \partial_y f_2^i(t_1,u) = f^i(t_1,u) - f^i(t_1,u-1),\ u \geq 2.
\end{aligned}$$

Summing the previous inequalities leads to :

$$\begin{aligned}
2f^i(t) &= \sum_{u=1}^{t_1}\partial_x f^i(u,t_2) + \sum_{u=1}^{t_2}\partial_y f^i(t_1,u) + f^i(N,t_2) + f^i(t_1,M), \\
2f^i(t) &= -\sum_{u=t_1+1}^{N}\partial_x f^i(u,t_2) - \sum_{u=t_2+1}^{M}\partial_y f^i(t_1,u) + f^i(N,t_2) + f^i(t_1,M).
\end{aligned}$$

Consequently,

$$2|f^i(t)| \leq \sum_{u=1}^{t_1}|\partial_x f^i(u,t_2)| + \sum_{u=1}^{t_2}|\partial_y f^i(t_1,u)| + |f^i(N,t_2)| + |f^i(t_1,M)|,$$

$$2|f^i(t)| \leq \sum_{u=t_1+1}^{N} |\partial_x f^i(u,t_2)| + \sum_{u=t_2+1}^{M} |\partial_y f^i(t_1,u)| + |f^i(N,t_2)| + |f^i(t_1,M)|,$$

yielding

$$\begin{aligned}\left(|f^1(t)|^2 + |f^2(t)|^2\right)^{\frac{1}{2}} &\leq |f^1(t)| + |f^2(t)| \\ &\leq \frac{1}{4}\sum_{u=1}^{N}\left(|\partial_x f^1(u,t_2)| + |\partial_x f^2(u,t_2)|\right) + \sum_{u=1}^{M}\left(|\partial_y f^1(t_1,u)| + |\partial_y f^2(t_1,u)|\right) \\ &+ 2\left|f^1(N,t_2)\right| + 2\left|f^2(N,t_2)\right| + 2\left|f^1(t_1,M)\right| + 2\left|f^2(t_1,M)\right|.\end{aligned}$$

□

Lemma 4.3 (extracted from [58, Lemme 3.7]). *For any $p_\alpha, c_\alpha, q_\alpha > 0$ with $\alpha = 1, ..., m$, $m \geq 2$ and $\sum_{\alpha=1}^{m} \frac{q_\alpha}{p_\alpha} = 1$,*

$$\prod_{\alpha=1}^{m} c_\alpha^{q_\alpha} \leq \sum_{\alpha=1}^{m} \frac{q_\alpha}{p_\alpha} c_\alpha^{p_\alpha},$$

where the equality holds if and only if $c_1 = c_2 = ... = c_m$.

Lemma 4.4 (extracted from [58, Lemma 3.8]). *For any $r_i \geq 0$ and $s > 0$,*

$$\left(\sum_{i=1}^{2} r_i\right)^s \leq c(s,2)\sum_{i=1}^{2} r_i^s,$$

with $c(s,2) = \begin{cases} 2^{s-1} & \text{if} \quad s > 1 \\ 1 & \text{if} \quad 0 < s \leq 1 \end{cases}$

Lemmas 4.3 and 4.4 are fundamental inequalities easily derivable from the arithmetic-geometric mean inequality. For their proofs, one is referred to, for example, [34] or [41].

Theorem 4.3 (adapted from [58, Theorem 3.1]). *For any $f^\alpha \in \mathcal{F}(\tilde{\Omega})$, any real number $p_\alpha \geq 2$, $q_\alpha \geq 0$, $\alpha = 1, \cdots, m$, $m \geq 2$ with $\sum_{\alpha=1}^{m} \frac{q_\alpha}{p_\alpha} = 1$ and any $c_\alpha > 0$,*

$$\begin{aligned}\|\prod_{\alpha=1}^{m}(\|f^\alpha\|_2(.))^{q_\alpha}\|_1 &\leq \sum_{t\in\tilde{\Omega}}\prod_{\alpha=1}^{m}\left||f^{\alpha,1}(t)| + |f^{\alpha,2}(t)|\right|^{q_\alpha}, \\ &\leq C\sum_{\alpha=1}^{m}\frac{q_\alpha}{p_\alpha}c_\alpha^{p_\alpha}B^{p_\alpha}2^{\frac{3p_\alpha-4}{2}}\left(\|\nabla f^\alpha\|_{p_\alpha}^{p_\alpha} + \left[N\left(\frac{2}{N}\right)^2\sum_{t_2=0}^{M}\left|f^{\alpha,1}(N,t_2)\right|^2\right.\right. \\ &\left.\left. + \left|f^{\alpha,2}(N,t_2)\right|^2 + M\left(\frac{2}{M}\right)^2\sum_{t_1=0}^{N}\left|f^{\alpha,1}(t_1,M)\right|^2 + \left|f^{\alpha,2}(t_1,M)\right|^2\right]^{\frac{p_\alpha}{2}}\right),\end{aligned}$$

where $C = \prod_{\beta=1}^{m} c_\beta^{-q_\beta}$ *and* $B = \max(M, N)$.

Proof. By lemmas 4.2, 4.3 and 4.4 , we have:

$$
\begin{aligned}
&\prod_{\alpha=1}^{m} \left| |f^{\alpha,1}(t)| + |f^{\alpha,2}(t)| \right|^{q_\alpha} = \left(\prod_{\beta=1}^{m} c_\beta^{-q_\beta} \right) \prod_{\alpha=1}^{m} \left| c_\alpha (|f^{\alpha,1}(t)| + |f^{\alpha,2}(t)|) \right|^{q_\alpha}, \\
&\leq C \sum_{\alpha=1}^{m} \frac{q_\alpha}{p_\alpha} c_\alpha^{p_\alpha} \left| |f^{\alpha,1}(t)| + |f^{\alpha,2}(t)| \right|^{p_\alpha}, \\
&\leq C \sum_{\alpha=1}^{m} \frac{q_\alpha}{p_\alpha} c_\alpha^{p_\alpha} \left[\frac{1}{4} \left(\sum_{u=1}^{N} \left| \partial_x f^{\alpha,1}(u, t_2) \right| + \left| \partial_x f^{\alpha,2}(u, t_2) \right| + \sum_{u=1}^{M} \left| \partial_y f^{\alpha,1}(t_1, u) \right| + \left| \partial_y f^{\alpha,2}(t_1, u) \right| \right. \right. \\
&\left. \left. + 2 \left| f^{\alpha,1}(N, t_2) \right| + 2 \left| f^{\alpha,2}(N, t_2) \right| + 2 \left| f^{\alpha,1}(t_1, M) \right| + 2 \left| f^{\alpha,2}(t_1, M) \right| \right) \right]^{p_\alpha}, \\
&\leq C \sum_{\alpha=1}^{m} \frac{q_\alpha}{p_\alpha} c_\alpha^{p_\alpha} \frac{1}{4^{p_\alpha}} c(p_\alpha, 2) \left[\left(\sum_{u=1}^{N} \left| \partial_x f^{\alpha,1}(u, t_2) \right| + \left| \partial_x f^{\alpha,2}(u, t_2) \right| + 2 \left| f^{\alpha,1}(N, t_2) \right| + 2 \left| f^{\alpha,2}(N, t_2) \right| \right)^{p_\alpha} \right. \\
&\left. + \left(\sum_{u=1}^{M} \left| \partial_y f^{\alpha,1}(t_1, u) \right| + \left| \partial_y f^{\alpha,2}(t_1, u) \right| + 2 \left| f^{\alpha,1}(t_1, M) \right| + 2 \left| f^{\alpha,2}(t_1, M) \right| \right)^{p_\alpha} \right].
\end{aligned}
$$

According to lemma 4.4, $\forall t \in \Omega,\ \forall \alpha \in \{1, ..., m\},\ c(p_\alpha, 2) = 2^{p_\alpha - 1}$ so that :

$$
\begin{aligned}
&\prod_{\alpha=1}^{m} \left| |f^{\alpha,1}(t)| + |f^{\alpha,2}(t)| \right|^{q_\alpha} \\
&\leq C \sum_{\alpha=1}^{m} \frac{q_\alpha}{p_\alpha} c_\alpha^{p_\alpha} \frac{1}{2^{p_\alpha + 1}} \left[\left(\sum_{u=1}^{N} \left| \partial_x f^{\alpha,1}(u, t_2) \right| + \left| \partial_x f^{\alpha,2}(u, t_2) \right| + 2 \left| f^{\alpha,1}(N, t_2) \right| + 2 \left| f^{\alpha,2}(N, t_2) \right| \right)^{p_\alpha} \right. \\
&\left. + \left(\sum_{u=1}^{M} \left| \partial_y f^{\alpha,1}(t_1, u) \right| + \left| \partial_y f^{\alpha,2}(t_1, u) \right| + 2 \left| f^{\alpha,1}(t_1, M) \right| + 2 \left| f^{\alpha,2}(t_1, M) \right| \right)^{p_\alpha} \right], \\
&\leq C \sum_{\alpha=1}^{m} \frac{q_\alpha}{p_\alpha} c_\alpha^{p_\alpha} \frac{1}{2^{p_\alpha + 1}} \left[\left[\left(\sum_{u=1}^{N} 1 \right)^{\frac{p_\alpha - 1}{p_\alpha}} \right. \right. \\
&\left. \left. \left(\sum_{u=1}^{N} \left(\left| \partial_x f^{\alpha,1}(u, t_2) \right| + \left| \partial_x f^{\alpha,2}(u, t_2) \right| + \frac{2}{N} \left| f^{\alpha,1}(N, t_2) \right| + \frac{2}{N} \left| f^{\alpha,2}(N, t_2) \right| \right)^{p_\alpha} \right)^{\frac{1}{p_\alpha}} \right]^{p_\alpha}
\end{aligned}
$$

$$
\begin{aligned}
&+\left[\left(\sum_{u=1}^{M}1\right)^{\frac{p_\alpha-1}{p_\alpha}}\left(\sum_{u=1}^{M}\Big(\left|\partial_y f^{\alpha,1}(t_1,u)\right|+\left|\partial_y f^{\alpha,2}(t_1,u)\right|\right.\right.\\
&\left.\left.+\frac{2}{M}\left|f^{\alpha,1}(t_1,M)\right|+\frac{2}{M}\left|f^{\alpha,2}(t_1,M)\right|\Big)^{p_\alpha}\right)^{\frac{1}{p_\alpha}}\right]^{p_\alpha}\Bigg] \text{ (Hölder's inequality),}\\
&\leq C\sum_{\alpha=1}^{m}\frac{q_\alpha}{p_\alpha}c_\alpha^{p_\alpha}\frac{1}{2^{p_\alpha+1}}\left[(N)^{p_\alpha-1}\left(\sum_{u=1}^{N}\left(\left|\partial_x f^{\alpha,1}(u,t_2)\right|+\left|\partial_x f^{\alpha,2}(u,t_2)\right|+\frac{2}{N}\left|f^{\alpha,1}(N,t_2)\right|\right.\right.\right.\\
&\left.\left.+\frac{2}{N}\left|f^{\alpha,2}(N,t_2)\right|\right)^{p_\alpha}\right)+(M)^{p_\alpha-1}\left(\sum_{u=1}^{M}\left(\left|\partial_y f^{\alpha,1}(t_1,u)\right|+\left|\partial_y f^{\alpha,2}(t_1,u)\right|\right.\right.\\
&\left.\left.\left.+\frac{2}{M}\left|f^{\alpha,1}(t_1,M)\right|+\frac{2}{M}\left|f^{\alpha,2}(t_1,M)\right|\right)^{p_\alpha}\right)\right],\\
&\leq C\sum_{\alpha=1}^{m}\frac{q_\alpha}{p_\alpha}c_\alpha^{p_\alpha}\frac{1}{2^{p_\alpha+1}}B^{p_\alpha-1}\left[\left(\sum_{u=1}^{N}\left(\left|\partial_x f^{\alpha,1}(u,t_2)\right|+\left|\partial_x f^{\alpha,2}(u,t_2)\right|+\frac{2}{N}\left|f^{\alpha,1}(N,t_2)\right|\right.\right.\right.\\
&\left.\left.+\frac{2}{N}\left|f^{\alpha,2}(N,t_2)\right|\right)^{p_\alpha}\right)+\left(\sum_{u=1}^{M}\Big(\left|\partial_y f^{\alpha,1}(t_1,u)\right|+\left|\partial_y f^{\alpha,2}(t_1,u)\right|\right.\\
&\left.\left.+\frac{2}{M}\left|f^{\alpha,1}(t_1,M)\right|+\frac{2}{M}\left|f^{\alpha,2}(t_1,M)\right|\Big)^{p_\alpha}\right)\right].
\end{aligned}
$$

Let us now sum on t:

$$
\begin{aligned}
&\sum_{t\in\tilde{\Omega}}\left[\sum_{u=1}^{N}\left(\left|\partial_x f^{\alpha,1}(u,t_2)\right|+\left|\partial_x f^{\alpha,2}(u,t_2)\right|+\left|\frac{2}{N}f^{\alpha,1}(N,t_2)\right|+\left|\frac{2}{N}f^{\alpha,2}(N,t_2)\right|\right)^{p_\alpha}\right.\\
&\left.+\sum_{u=1}^{M}\left(\left|\partial_y f^{\alpha,1}(t_1,u)\right|+\left|\partial_y f^{\alpha,2}(t_1,u)\right|+\left|\frac{2}{M}f^{\alpha,1}(t_1,M)\right|+\left|\frac{2}{M}f^{\alpha,2}(t_1,M)\right|\right)^{p_\alpha}\right],\\
=&\sum_{u=1}^{N}\sum_{t\in\tilde{\Omega}}\left(\left|\partial_x f^{\alpha,1}(u,t_2)\right|+\left|\partial_x f^{\alpha,2}(u,t_2)\right|+\left|\frac{2}{N}f^{\alpha,1}(N,t_2)\right|+\left|\frac{2}{N}f^{\alpha,2}(N,t_2)\right|\right)^{p_\alpha}\\
&+\sum_{u=1}^{M}\sum_{t\in\tilde{\Omega}}\left(\left|\partial_y f^{\alpha,1}(t_1,u)\right|+\left|\partial_y f^{\alpha,2}(t_1,u)\right|+\left|\frac{2}{M}f^{\alpha,1}(t_1,M)\right|+\left|\frac{2}{M}f^{\alpha,2}(t_1,M)\right|\right)^{p_\alpha},\\
=&N\sum_{t\in\tilde{\Omega}}\left(\left|\partial_x f^{\alpha,1}(t_1,t_2)\right|+\left|\partial_x f^{\alpha,2}(t_1,t_2)\right|+\left|\frac{2}{N}f^{\alpha,1}(N,t_2)\right|+\left|\frac{2}{N}f^{\alpha,2}(N,t_2)\right|\right)^{p_\alpha}\\
&+M\sum_{t\in\tilde{\Omega}}\left(\left|\partial_y f^{\alpha,1}(t_1,t_2)\right|+\left|\partial_y f^{\alpha,2}(t_1,t_2)\right|+\left|\frac{2}{M}f^{\alpha,1}(t_1,M)\right|+\left|\frac{2}{M}f^{\alpha,2}(t_1,M)\right|\right)^{p_\alpha},
\end{aligned}
$$

$$\leq B\left(\sum_{t\in\tilde{\Omega}}\left(\left|\partial_x f^{\alpha,1}(t_1,t_2)\right|+\left|\partial_x f^{\alpha,2}(t_1,t_2)\right|+\left|\frac{2}{N}f^{\alpha,1}(N,t_2)\right|+\left|\frac{2}{N}f^{\alpha,2}(N,t_2)\right|\right)^{p_\alpha}\right.$$
$$\left.+\sum_{t\in\tilde{\Omega}}\left(\left|\partial_y f^{\alpha,1}(t_1,t_2)\right|+\left|\partial_y f^{\alpha,2}(t_1,t_2)\right|+\left|\frac{2}{M}f^{\alpha,1}(t_1,M)\right|+\left|\frac{2}{M}f^{\alpha,2}(t_1,M)\right|\right)^{p_\alpha}\right).$$

So we have:

$$\sum_{t\in\tilde{\Omega}}\prod_{\alpha=1}^{m}\left||f^{\alpha,1}(t)|+|f^{\alpha,2}(t)|\right|^{q_\alpha}$$
$$\leq\sum_{t\in\tilde{\Omega}}C\sum_{\alpha=1}^{m}\frac{q_\alpha}{p_\alpha}c_\alpha^{p_\alpha}\frac{1}{2^{p_\alpha+1}}B^{p_\alpha-1}\left[\left(\sum_{u=1}^{N}\left(\left|\partial_x f^{\alpha,1}(u,t_2)\right|+\left|\partial_x f^{\alpha,2}(u,t_2)\right|+\frac{2}{N}\left|f^{\alpha,1}(N,t_2)\right|\right.\right.\right.$$
$$\left.\left.\left.+\frac{2}{N}\left|f^{\alpha,2}(N,t_2)\right|\right)^{p_\alpha}\right)+\left(\sum_{u=1}^{M}\left(\left|\partial_y f^{\alpha,1}(t_1,u)\right|+\left|\partial_y f^{\alpha,2}(t_1,u)\right|+\frac{2}{M}\left|f^{\alpha,1}(t_1,M)\right|\right.\right.\right.$$
$$\left.\left.\left.+\frac{2}{M}\left|f^{\alpha,2}(t_1,M)\right|\right)^{p_\alpha}\right)\right],$$
$$\leq C\sum_{\alpha=1}^{m}\frac{q_\alpha}{p_\alpha}c_\alpha^{p_\alpha}\frac{1}{2^{p_\alpha+1}}B^{p_\alpha-1}\left[\sum_{t\in\tilde{\Omega}}\left(\sum_{u=1}^{N}\left(\left|\partial_x f^{\alpha,1}(u,t_2)\right|+\left|\partial_x f^{\alpha,2}(u,t_2)\right|+\frac{2}{N}\left|f^{\alpha,1}(N,t_2)\right|\right.\right.\right.$$
$$\left.\left.\left.+\frac{2}{N}\left|f^{\alpha,2}(N,t_2)\right|\right)^{p_\alpha}\right)+\sum_{t\in\tilde{\Omega}}\left(\sum_{u=1}^{M}\left(\left|\partial_y f^{\alpha,1}(t_1,u)\right|+\left|\partial_y f^{\alpha,2}(t_1,u)\right|+\frac{2}{M}\left|f^{\alpha,1}(t_1,M)\right|\right.\right.\right.$$
$$\left.\left.\left.+\frac{2}{M}\left|f^{\alpha,2}(t_1,M)\right|\right)^{p_\alpha}\right)\right],$$
$$\leq C\sum_{\alpha=1}^{m}\frac{q_\alpha}{p_\alpha}c_\alpha^{p_\alpha}\frac{1}{2^{p_\alpha+1}}B^{p_\alpha}\left[\sum_{t\in\tilde{\Omega}}4^{p_\alpha}\left(\left|\partial_x f^{\alpha,1}(t_1,t_2)\right|^{p_\alpha}+\left|\partial_x f^{\alpha,2}(t_1,t_2)\right|^{p_\alpha}+\left(\frac{2}{N}\right)^{p_\alpha}\left|f^{\alpha,1}(N,t_2)\right|^{p_\alpha}\right.\right.$$
$$\left.\left.+\left(\frac{2}{N}\right)^{p_\alpha}\left|f^{\alpha,2}(N,t_2)\right|^{p_\alpha}\right)+\sum_{t\in\tilde{\Omega}}4^{p_\alpha}\left(\left|\partial_y f^{\alpha,1}(t_1,t_2)\right|^{p_\alpha}+\left|\partial_y f^{\alpha,2}(t_1,t_2)\right|^{p_\alpha}\right.\right.$$
$$\left.\left.+\left(\frac{2}{M}\right)^{p_\alpha}\left|f^{\alpha,1}(t_1,M)\right|^{p_\alpha}+\left(\frac{2}{M}\right)^{p_\alpha}\left|f^{\alpha,2}(t_1,M)\right|^{p_\alpha}\right)\right],$$
$$\leq C\sum_{\alpha=1}^{m}\frac{q_\alpha}{p_\alpha}c_\alpha^{p_\alpha}2^{p_\alpha-1}B^{p_\alpha}\left[\sum_{t\in\tilde{\Omega}}\left(\left|\partial_x f^{\alpha,1}(t_1,t_2)\right|^{p_\alpha}+\left|\partial_x f^{\alpha,2}(t_1,t_2)\right|^{p_\alpha}+\left(\frac{2}{N}\right)^{p_\alpha}\left|f^{\alpha,1}(N,t_2)\right|^{p_\alpha}\right.\right.$$
$$\left.\left.+\left(\frac{2}{N}\right)^{p_\alpha}\left|f^{\alpha,2}(N,t_2)\right|^{p_\alpha}\right)+\sum_{t\in\tilde{\Omega}}\left(\left|\partial_y f^{\alpha,1}(t_1,t_2)\right|^{p_\alpha}+\left|\partial_y f^{\alpha,2}(t_1,t_2)\right|^{p_\alpha}\right.\right.$$
$$\left.\left.+\left(\frac{2}{M}\right)^{p_\alpha}\left|f^{\alpha,1}(t_1,M)\right|^{p_\alpha}+\left(\frac{2}{M}\right)^{p_\alpha}\left|f^{\alpha,2}(t_1,M)\right|^{p_\alpha}\right)\right],$$

$$\leq C\sum_{\alpha=1}^{m}\frac{q_\alpha}{p_\alpha}c_\alpha^{p_\alpha}2^{p_\alpha-1}B^{p_\alpha}\sum_{t\in\tilde{\Omega}}\left[c\left(\frac{2}{p_\alpha},2\right)\left(\left|\partial_x f^{\alpha,1}(t_1,t_2)\right|^{p_\alpha}+\left|\partial_x f^{\alpha,2}(t_1,t_2)\right|^{p_\alpha}\right.\right.$$
$$\left.+\left(\frac{2}{N}\right)^{p_\alpha}\left|f^{\alpha,1}(N,t_2)\right|^{p_\alpha}+\left(\frac{2}{N}\right)^{p_\alpha}\left|f^{\alpha,2}(N,t_2)\right|^{p_\alpha}\right)^{\frac{2}{p_\alpha}}+c\left(\frac{2}{p_\alpha},2\right)\left(\left|\partial_y f^{\alpha,1}(t_1,t_2)\right|^{p_\alpha}\right.$$
$$\left.\left.+\left|\partial_y f^{\alpha,2}(t_1,t_2)\right|^{p_\alpha}+\left(\frac{2}{M}\right)^{p_\alpha}\left|f^{\alpha,1}(t_1,M)\right|^{p_\alpha}+\left(\frac{2}{M}\right)^{p_\alpha}\left|f^{\alpha,2}(t_1,M)\right|^{p_\alpha}\right)^{\frac{2}{p_\alpha}}\right]^{\frac{p_\alpha}{2}}.$$

As $p_\alpha \geq 2$, we have $c\left(\frac{2}{p_\alpha},2\right)=1$. Then

$$\sum_{t\in\tilde{\Omega}}\prod_{\alpha=1}^{m}\left||f^{\alpha,1}(t)|+|f^{\alpha,2}(t)|\right|^{q_\alpha}$$
$$\leq C\sum_{\alpha=1}^{m}\frac{q_\alpha}{p_\alpha}c_\alpha^{p_\alpha}2^{p_\alpha-1}B^{p_\alpha}\sum_{t\in\tilde{\Omega}}\left[\left(\left|\partial_x f^{\alpha,1}(t_1,t_2)\right|^2+\left|\partial_x f^{\alpha,2}(t_1,t_2)\right|^2+\left(\frac{2}{N}\right)^2\left|f^{\alpha,1}(N,t_2)\right|^2\right.\right.$$
$$\left.+\left(\frac{2}{N}\right)^2\left|f^{\alpha,2}(N,t_2)\right|^2\right)+\left(\left|\partial_y f^{\alpha,1}(t_1,t_2)\right|^2+\left|\partial_y f^{\alpha,2}(t_1,t_2)\right|^2\right.$$
$$\left.\left.+\left(\frac{2}{M}\right)^2\left|f^{\alpha,1}(t_1,M)\right|^2+\left(\frac{2}{M}\right)^2\left|f^{\alpha,2}(t_1,M)\right|^2\right)\right]^{\frac{p_\alpha}{2}},$$
$$\leq C\sum_{\alpha=1}^{m}\frac{q_\alpha}{p_\alpha}c_\alpha^{p_\alpha}2^{p_\alpha-1}B^{p_\alpha}\sum_{t\in\tilde{\Omega}}\left[\left|\partial_x f^{\alpha,1}(t_1,t_2)\right|^2+\left|\partial_x f^{\alpha,2}(t_1,t_2)\right|^2+\left(\frac{2}{N}\right)^2\left|f^{\alpha,1}(N,t_2)\right|^2\right.$$
$$+\left(\frac{2}{N}\right)^2\left|f^{\alpha,1}(N,t_2)\right|^2+\left|\partial_y f^{\alpha,1}(t_1,t_2)\right|^2+\left|\partial_y f^{\alpha,2}(t_1,t_2)\right|^2+\left(\frac{2}{M}\right)^2\left|f^{\alpha,1}(t_1,M)\right|^2$$
$$\left.+\left(\frac{2}{M}\right)^2\left|f^{\alpha,2}(t_1,M)\right|^2\right]^{\frac{p_\alpha}{2}},$$
$$\leq C\sum_{\alpha=1}^{m}\frac{q_\alpha}{p_\alpha}c_\alpha^{p_\alpha}B^{p_\alpha}2^{\frac{3p_\alpha-4}{2}}\sum_{t\in\tilde{\Omega}}\left(\left[\left|\partial_x f^{\alpha,1}(t_1,t_2)\right|^2+\left|\partial_x f^{\alpha,2}(t_1,t_2)\right|^2+\left|\partial_y f^{\alpha,1}(t_1,t_2)\right|^2\right.\right.$$
$$\left.+\left|\partial_y f^{\alpha,2}(t_1,t_2)\right|^2\right]^{\frac{p_\alpha}{2}}+\left[\left(\frac{2}{N}\right)^2\left|f^{\alpha,1}(N,t_2)\right|^2+\left(\frac{2}{N}\right)^2\left|f^{\alpha,2}(N,t_2)\right|^2\right.$$
$$\left.\left.+\left(\frac{2}{M}\right)^2\left|f^{\alpha,1}(t_1,M)\right|^2+\left(\frac{2}{M}\right)^2\left|f^{\alpha,2}(t_1,M)\right|^2\right]^{\frac{p_\alpha}{2}}\right),$$
$$\leq C\sum_{\alpha=1}^{m}\frac{q_\alpha}{p_\alpha}c_\alpha^{p_\alpha}B^{p_\alpha}2^{\frac{3p_\alpha-4}{2}}\left(\|\nabla f^\alpha\|_{p_\alpha}^{p_\alpha}+N\left(\frac{2}{N}\right)^2 2^{\frac{p_\alpha}{2}-1}\sum_{t_2=1}^{M}\left(\left|f^{\alpha,1}(N,t_2)\right|^2+\left|f^{\alpha,2}(N,t_2)\right|^2\right)^{\frac{p_\alpha}{2}}\right.$$

$$+M\left(\frac{2}{M}\right)^2 2^{\frac{p_\alpha}{2}-1}\sum_{t_1=1}^{N}\left(\left|f^{\alpha,1}(t_1,M)\right|^2+\left|f^{\alpha,2}(t_1,M)\right|^2\right)^{\frac{p_\alpha}{2}}\Bigg).$$

And $\|\prod_{\alpha=1}^{m}(\|f^\alpha\|_2(.))^{q_\alpha}\|_1 \leq \sum_{t\in\tilde{\Omega}}\prod_{\alpha=1}^{m}\left||f^{\alpha,1}(t)|+|f^{\alpha,2}(t)|\right|^{q_\alpha}$. □

Remark 4.5. *For any $f^\alpha \in \mathcal{F}_1(\tilde{\Omega})$, any real number $p_\alpha \geq 2$, $q_\alpha \geq 0$, $\alpha = 1, \cdots, m$, $m \geq 2$ with $\sum_{\alpha=1}^{m}\frac{q_\alpha}{p_\alpha} = 1$ and any $c_\alpha > 0$,*

$$\|\prod_{\alpha=1}^{m}(\|f^\alpha\|_2(.))^{q_\alpha}\|_1 \leq C\sum_{\alpha=1}^{m}\frac{q_\alpha}{p_\alpha}c_\alpha^{p_\alpha}B^{p_\alpha}2^{\frac{3p_\alpha-4}{2}}\left(\|\nabla f^\alpha\|_{p_\alpha}^{p_\alpha}+2^{\frac{p_\alpha}{2}-1}\left[\frac{\left(MN^2+\frac{M(M+1)(2M+1)}{6N}\right)^{\frac{p_\alpha}{2}}}{N}\right.\right.$$
$$\left.\left.+\frac{\left(NM^2+\frac{N(N+1)(2N+1)}{6}\right)^{\frac{p_\alpha}{2}}}{M}\right]\right),$$

$$\|\prod_{\alpha=1}^{m}(\|f^\alpha\|_2(.))^{q_\alpha}\|_1 \leq C\sum_{\alpha=1}^{m}\frac{q_\alpha}{p_\alpha}c_\alpha^{p_\alpha}B^{p_\alpha}2^{\frac{3p_\alpha-4}{2}}\|\nabla f^\alpha\|_{p_\alpha}^{p_\alpha}+c_2,$$

where $C = \prod_{\beta=1}^{m}c_\beta^{-q_\beta}$, $B = \max(M,N)$ and

$$c_2 = C\sum_{\alpha=1}^{m}\frac{q_\alpha}{p_\alpha}c_\alpha^{p_\alpha}B^{p_\alpha}2^{2p_\alpha-1}\left[\frac{\left(MN^2+\frac{M(M+1)(2M+1)}{6N}\right)^{\frac{p_\alpha}{2}}}{N}+\frac{\left(NM^2+\frac{N(N+1)(2N+1)}{6}\right)^{\frac{p_\alpha}{2}}}{M}\right].$$

Corollary 4.6. (from [58, Corollary 3.2])*: For any $f^\alpha \in \mathcal{F}_1(\Omega)$ and any real numbers $p_\alpha \geq 2$, $q_\alpha \geq 0$, $\alpha = 1, ..., m$, $m \geq 2$, with $\sum_{\alpha=1}^{m}\frac{q_\alpha}{p_\alpha} = 1$,*

$$\|\prod_{\alpha=1}^{m}(\|f^\alpha\|_2(.))^{q_\alpha}\|_1 \leq \sum_{\alpha=1}^{m}\frac{q_\alpha}{p_\alpha}B^{p_\alpha}2^{\frac{3p_\alpha-4}{2}}\|\nabla f^\alpha\|_{p_\alpha}^{p_\alpha}+c_3,$$

with $c_3 = \sum_{\alpha=1}^{m}\frac{q_\alpha}{p_\alpha}B^{p_\alpha}2^{2p_\alpha-1}\left[\frac{\left(MN^2+\frac{M(M+1)(2M+1)}{6N}\right)^{\frac{p_\alpha}{2}}}{N}+\frac{\left(NM^2+\frac{N(N+1)(2N+1)}{6}\right)^{\frac{p_\alpha}{2}}}{M}\right] = c_2$ setting $c_\alpha = 1, \forall\alpha$.

Proof. This follows immediately from Theorem 4.3 by letting $c_\alpha = 1$, $\alpha = 1, ..., m$. □

Corollary 4.7. (from [58, Corollary 3.5]) *For any $f^\alpha \in \mathcal{F}_1(\Omega)$ and any real numbers $q_\alpha \geq 0$, $\alpha = 1, ..., m$, $m \geq 2$, with $q = \sum_{\alpha=1}^{m}q_\alpha \geq 2$,*

$$\|\prod_{\alpha=1}^{m}(\|f^\alpha\|_2(.))^{q_\alpha}\|_1 \leq B^q 2^{\frac{3q-4}{2}}\sum_{\alpha=1}^{m}\frac{q_\alpha}{q}\|\nabla f^\alpha\|_q^q+c_4,$$

with $c_4 = B^q 2^{2q-1}\left[\frac{\left(MN^2+\frac{M(M+1)(2M+1)}{6N}\right)^{\frac{q}{2}}}{N}+\frac{\left(NM^2+\frac{N(N+1)(2N+1)}{6}\right)^{\frac{q}{2}}}{M}\right] = c_3$ *setting* $p_\alpha = q,\ \alpha = 1, ..., m.$

Proof. This follows immediately from Corollary 4.6 by letting $p_\alpha = q, \forall \alpha = 1, ..., m.$ □

Theorem 4.4 (adapted from [58, Corollary 3.10], discrete generalized Poincaré inequality)**.** *For any* $f \in \mathcal{F}_1(\Omega)$*, and any real number* $q \geq 2$*, we have:*

$$\|f^q\|_1 = \|f\|_q^q \leq B^q 2^{\frac{7q+2}{2}} \|\nabla f\|_q^q + c_4,$$

with $c_4 = B^q 2^{\frac{7q+2}{2}}\left[8NM + \frac{4}{N}\frac{M(M+1)(2M+1)}{6} + \frac{4}{M}\frac{N(N+1)(2N+1)}{6}\right]^{\frac{q}{2}}$*, with* $B = \max\{M, N\}$.

Proof. This follows imediately from Corollary 4.7 by letting $f^\alpha = f$, $\forall \alpha \in \{1, ...m\}$. □

We now introduce the discrete version of the initial problem (QP)

$$\inf_{\tilde{\varphi}\in\mathcal{F}_1(\tilde{\Omega})}\left\{J(\tilde{\varphi}) = \sum_{i=1}^{N}\sum_{j=1}^{M}\left[\frac{\nu}{2}\left(H_\varepsilon(\Phi_0 \circ \tilde{\varphi}_{i,j}) - H_\varepsilon(\tilde{\Phi}(\cdot, \bar{T}))\right)^2 + QW(\nabla\tilde{\varphi}_{i,j})\right]\right\}. \tag{3.7}$$

Theorem 4.5. *Functional* J *is continuous and admits a finite minimum.*

Proof. Let us devise a coercivity inequality. One successively has:

$$\beta(\|\nabla\tilde{\varphi}_{i,j}\|^2 - \alpha)^2 \geq \frac{\beta}{2}\|\nabla\tilde{\varphi}_{i,j}\|^4 - \beta\alpha^2,\ \psi(\det\nabla\tilde{\varphi}_{i,j}) \geq \frac{-\mu(\lambda+3\mu)}{2(\lambda+2\mu)},$$

$$QW(\nabla\tilde{\varphi}_{i,j}) \geq \frac{\beta}{2}\|\nabla\tilde{\varphi}_{i,j}\|^4 - \beta\alpha^2 - \frac{\mu(\lambda+3\mu)}{2(\lambda+2\mu)},$$

$$J(\tilde{\varphi}) \geq \frac{\beta}{2}\|\nabla\tilde{\varphi}\|^4_{l^4(\tilde{\Omega},M_2(\mathbb{R}))} + \sum_{i=1}^{N}\sum_{j=1}^{M}\left(-\beta\alpha^2 - \frac{\mu(\lambda+3\mu)}{2(\lambda+2\mu)}\right).$$

Then from the discrete generalized Poincaré inequality, using the same notations for the constants B and c_4 yields:

$$J(\tilde{\varphi}) \geq \frac{\beta}{2^4 B^4}(\|\tilde{\varphi}\|^4_{l^4(\tilde{\Omega},M_2(\mathbb{R}))} - c_4) + \sum_{i=1}^{N}\sum_{j=1}^{M}\left(-\beta\alpha^2 - \frac{\mu(\lambda+3\mu)}{2(\lambda+2\mu)}\right),$$

and $J(\mathtt{Id}) < +\infty$ so the infimum is finite. Thus J is coercive and continuous, so there exists at least one minimum of J over $\mathcal{F}_1(\tilde{\Omega})$. □

The discrete counterpart of (3.6) (pure quadratic penalization) is given by:

$$\inf_{\tilde{\varphi},\tilde{V}}\left\{J_\gamma(\tilde{\varphi},\tilde{V}) = \sum_{i=1}^{N}\sum_{j=1}^{M}\frac{\nu}{2}\left(H_\varepsilon(\Phi_0(\tilde{\varphi}_{i,j})) - H_\varepsilon(\tilde{\Phi}(\cdot,\bar{T}))\right)^2 + QW(\tilde{V}_{i,j}) + \frac{\gamma}{2}\|\tilde{V}_{i,j} - \nabla\tilde{\varphi}_{i,j}\|^2\right\}.$$

The discrete analogue of Theorem 4.1 is thus stated as:

Theorem 4.6. *Let (γ_j) be an increasing sequence of positive real numbers such that $\lim_{j\to+\infty}\gamma_j = +\infty$. Let also $(\bar{\tilde{\varphi}}(\gamma_j), \bar{\tilde{V}}(\gamma_j))$ be a minimum of the decoupled problem with $\gamma = \gamma_j$. Then there exists a subsequence of $\left(\bar{\tilde{\varphi}}(\gamma_j), \bar{\tilde{V}}(\gamma_j)\right)$ denoted by $\left(\bar{\tilde{\varphi}}(\gamma_{\psi\circ\zeta(j)}), \bar{\tilde{V}}(\gamma_{\psi\circ\zeta(j)})\right)$ and a minimum $\bar{\tilde{\varphi}}$ of J ($\bar{\tilde{\varphi}} \in \mathcal{F}_1(\tilde{\Omega})$) such that*

$$\lim_{j\to+\infty} J_{\gamma_{\psi\circ\zeta(j)}}\left(\bar{\tilde{\varphi}}(\gamma_{\psi\circ\zeta(j)}), \bar{\tilde{V}}(\gamma_{\psi\circ\zeta(j)})\right) = J(\bar{\tilde{\varphi}}).$$

Proof. The proof is divided into two steps: the first one is dedicated to the existence of a minimum for the decoupled problem, while the second shows the convergence result.

– **Existence of a minimum of the decoupled problem for any $\gamma > 0$:**
Let $\gamma > \gamma_0$ ($\gamma_0 > 0$ fixed) be a positive real number. Functional J_γ is continuous and bounded below by $-\frac{\mu(\lambda+3\mu)}{2(\lambda+2\mu)}$. Furthermore, by taking $\tilde{\varphi} = \mathtt{Id}$ and $\tilde{V} = \nabla\tilde{\varphi} = (I_2)^{N\times M}$, I_2 denoting the identity matrix of size 2×2, we have $J_\gamma(\tilde{\varphi}, \tilde{V}) < +\infty$, then the infimum is finite. Let $(\tilde{\varphi}_n(\gamma), \tilde{V}_n(\gamma))$ be a minimizing sequence of J_γ. We have $J_\gamma(\tilde{\varphi}_n(\gamma), \tilde{V}_n(\gamma)) \geq \frac{\beta}{2}\|\tilde{V}_n(\gamma)\|^4_{l^4(\tilde{\Omega},M_2(\mathbb{R}))} - \beta\alpha^2 NM - \frac{\mu(\lambda+3\mu)NM}{2(\lambda+2\mu)}$. As J_γ is proper and $(\tilde{\varphi}_n(\gamma), \tilde{V}_n(\gamma))$ is a minimizing sequence, then for n sufficiently large, $J_\gamma(\mathtt{Id}, (I_2)^{N\times M}) + 1 \geq J_\gamma(\tilde{\varphi}_n(\gamma), \tilde{V}_n(\gamma)) \geq \frac{\beta}{2}\|\tilde{V}_n(\gamma)\|^4_{l^4(\tilde{\Omega},M_2(\mathbb{R}))} - \beta\alpha^2 NM - \frac{\mu(\lambda+3\mu)NM}{2(\lambda+2\mu)}$. So, $(\tilde{V}_n(\gamma))$ is uniformly bounded in $\|.\|_{l^4(\tilde{\Omega},M_2(\mathbb{R}))}$. According to Bolzano-Weierstrass theorem, we can extract a subsequence denoted by $(\tilde{V}_{\psi(n)}(\gamma))$ such that $\tilde{V}_{\psi(n)}(\gamma) \xrightarrow[n\to+\infty]{} \bar{\tilde{V}}(\gamma) \in (M_2(\mathbb{R}))^{N\times M}$. Moreover, for n sufficiently large

$$\begin{aligned}
J_\gamma(\mathtt{Id}, (I_2)^{N\times M}) + 1 &\geq J_\gamma(\tilde{\varphi}_{\psi(n)}(\gamma), \tilde{V}_{\psi(n)}(\gamma)),\\
&\geq -\frac{\mu(\lambda+3\mu)NM}{2(\lambda+2\mu)} + \frac{\gamma}{2}\|\nabla\tilde{\varphi}_{\psi(n)}(\gamma) - \tilde{V}_{\psi(n)}(\gamma)\|^2_{l^2(\tilde{\Omega},M_2(\mathbb{R}))},\\
&\geq -\frac{\mu(\lambda+3\mu)NM}{2(\lambda+2\mu)} + \frac{\gamma}{2}\left|\|\nabla\tilde{\varphi}_{\psi(n)}\|_{l^2(\tilde{\Omega},M_2(\mathbb{R}))} - \|\tilde{V}_{\psi(n)}\|_{l^2(\tilde{\Omega},M_2(\mathbb{R}))}\right|^2,\\
&\geq -\frac{\mu(\lambda+3\mu)NM}{2(\lambda+2\mu)} + \frac{\gamma}{4}\|\nabla\tilde{\varphi}_{\psi(n)}\|^2_{l^2(\tilde{\Omega},M_2(\mathbb{R}))} - \frac{\gamma}{2}\|\tilde{V}_{\psi(n)}\|^2_{l^2(\tilde{\Omega},M_2(\mathbb{R}))}.
\end{aligned}$$

Consequently,

$$\begin{aligned}
&J_\gamma(\mathtt{Id}, (I_2)^{N\times M}) + 1 + \frac{\gamma}{2}\|\tilde{V}_{\psi(n)}(\gamma)\|^2_{l^2(\tilde{\Omega},M_2(\mathbb{R}))} + \frac{\mu(\lambda+3\mu)NM}{2(\lambda+2\mu)}\\
&\geq \frac{\gamma}{4}\|\nabla\tilde{\varphi}_{\psi(n)}(\gamma)\|^2_{l^2(\tilde{\Omega},M_2(\mathbb{R}))} \geq \frac{\gamma}{2^3B^2}(\|\tilde{\varphi}_{\psi(n)}(\gamma)\|^2_{l^2(\tilde{\Omega},\mathbb{R}^2)} - c_4),
\end{aligned}$$

from the discrete generalized Poincaré inequality. The sequence $(\tilde{\varphi}_{\psi(n)}(\gamma))$ is uniformly bounded in $\|.\|_{l^2(\tilde{\Omega},\mathbb{R}^2)}$ and according to Bolzano-Weierstrass theorem, we can extract a subsequence denoted by $(\tilde{\varphi}_{\psi\circ\zeta(n)}(\gamma))$ such that $\tilde{\varphi}_{\psi\circ\zeta(n)}(\gamma) \xrightarrow[n\to+\infty]{} \bar{\tilde{\varphi}}(\gamma) \in \mathcal{F}_1(\tilde{\Omega})$. By continuity of J_γ, $J_\gamma(\tilde{\varphi}_{\psi\circ\zeta(n)}(\gamma), \tilde{V}_{\psi\circ\zeta(n)}(\gamma)) \xrightarrow[n\to+\infty]{} J_\gamma(\bar{\tilde{\varphi}}(\gamma), \bar{\tilde{V}}(\gamma))$

and by uniqueness of the limit $J_\gamma(\bar{\tilde{\varphi}}(\gamma), \bar{\tilde{V}}(\gamma)) = \inf J_\gamma(\tilde{\varphi}, \tilde{V})$ with $\tilde{\varphi} \in \mathcal{F}_1(\tilde{\Omega})$, $\tilde{V} \in (M_2(\mathbb{R}))^{N\times M}$.

– **Convergence of the sequence of minima:**
Let (γ_j) be an increasing sequence of positive real numbers such that $\lim_{j\to+\infty} \gamma_j = +\infty$. Let $\left(\bar{\tilde{\varphi}}(\gamma_j), \bar{\tilde{V}}(\gamma_j)\right)$ be the sequence of minima associated with (J_{γ_j}). Let $\epsilon > 0$ be given, $\epsilon \in]0; \epsilon_0]$, $\epsilon_0 > 0$ fixed. There exists $\hat{\varphi}_\epsilon \in \mathcal{F}_1(\tilde{\Omega})$ such that $J_\gamma(\bar{\tilde{\varphi}}(\gamma), \bar{\tilde{V}}(\gamma)) = \min_{(\tilde{\varphi},\tilde{V})\in\mathcal{F}_1(\tilde{\Omega})\times(M_2(\mathbb{R}))^{N\times M}} J_\gamma(\tilde{\varphi}, \tilde{V}) \leq J_\gamma(\hat{\varphi}_\epsilon, \nabla\hat{\varphi}_\epsilon) = J(\hat{\varphi}_\epsilon) < \inf_{\tilde{\varphi}\in\mathcal{F}_1(\tilde{\Omega})} J(\tilde{\varphi}) + \epsilon \leq \inf_{\tilde{\varphi}\in\mathcal{F}_1(\tilde{\Omega})} J(\tilde{\varphi}) + \epsilon_0$. So, $J_\gamma\left(\bar{\tilde{\varphi}}(\gamma), \bar{\tilde{V}}(\gamma)\right) = \min_{(\tilde{\varphi},\tilde{V})\in\mathcal{F}_1(\tilde{\Omega})\times(M_2(\mathbb{R}))^{N\times M}} J_\gamma(\tilde{\varphi}, \tilde{V}) \leq \inf_{\tilde{\varphi}\in\mathcal{F}_1(\tilde{\Omega})} J(\tilde{\varphi}) + \epsilon$, $\forall\gamma > 0$. Let us take $\epsilon = \frac{1}{\gamma_j}$, we have $J_{\gamma_j}(\bar{\tilde{\varphi}}(\gamma_j), \bar{\tilde{V}}(\gamma_j)) \leq \inf_{\tilde{\varphi}\in\mathcal{F}_1(\tilde{\Omega})} J(\tilde{\varphi}) + \frac{1}{\gamma_j} \leq \inf_{\tilde{\varphi}\in\mathcal{F}_1(\tilde{\Omega})} J(\tilde{\varphi}) + \frac{1}{\gamma_0} < +\infty$. Consequently, $\inf_{\tilde{\varphi}\in\mathcal{F}_1(\tilde{\Omega})} J(\tilde{\varphi}) + \frac{1}{\gamma_0} \geq J_{\gamma_j}(\bar{\tilde{\varphi}}(\gamma_j), \bar{\tilde{V}}(\gamma_j)) \geq \frac{\beta}{2}\|\bar{\tilde{V}}(\gamma_j)\|^4_{l^4(\tilde{\Omega},M_2(\mathbb{R}))} - \beta\alpha^2 NM - \frac{\mu(\lambda+3\mu)}{2(\lambda+2\mu)}NM$. Thus $\left(\bar{\tilde{V}}(\gamma_j)\right)$ is uniformly bounded in $\|.\|_{l^4(\tilde{\Omega},M_2(\mathbb{R}))}$ and according to Bolzano-Weierstrass theorem, we can extract a subsequence $\left(\bar{\tilde{V}}(\gamma_{\psi(j)})\right)$ from $\left(\bar{\tilde{V}}(\gamma_j)\right)$ such that $\bar{\tilde{V}}\left(\gamma_{\psi(j)}\right) \xrightarrow[j\to+\infty]{} \bar{V} \in (M_2(\mathbb{R}))^{N\times M}$. Also we have $\frac{\gamma_{\psi(j)}}{2}\|\bar{\tilde{V}}(\gamma_{\psi(j)}) - \nabla\bar{\tilde{\varphi}}(\gamma_{\psi(j)})\|^2_{l^2(\tilde{\Omega},M_2(\mathbb{R}))} \leq \inf_{\tilde{\varphi}\in\mathcal{F}_1(\tilde{\Omega})} J(\tilde{\varphi}) + \frac{1}{\gamma_0} + \frac{\mu(\lambda+3\mu)}{2(\lambda+2\mu)}NM$ and thus successively:

$$\|\bar{\tilde{V}}(\gamma_{\psi(j)}) - \nabla\bar{\tilde{\varphi}}(\gamma_{\psi(j)})\|^2_{l^2(\tilde{\Omega},M_2(\mathbb{R}))} \leq \frac{2}{\gamma_0}\left(\inf_{\tilde{\varphi}\in\mathcal{F}_1(\tilde{\Omega})} J(\tilde{\varphi}) + \frac{1}{\gamma_0} + \frac{\mu(\lambda+3\mu)}{2(\lambda+2\mu)}NM\right),$$

$$\left|\|\nabla\bar{\tilde{\varphi}}(\gamma_{\psi(j)})\|_{l^2(\tilde{\Omega},M_2(\mathbb{R}))} - \|\bar{\tilde{V}}(\gamma_{\psi(j)})\|_{l^2(\tilde{\Omega},M_2(\mathbb{R}))}\right|^2 \leq \frac{2}{\gamma_0}\left(\inf_{\tilde{\varphi}\in\mathcal{F}_1(\tilde{\Omega})} J(\tilde{\varphi}) + \frac{1}{\gamma_0} + \frac{\mu(\lambda+3\mu)}{2(\lambda+2\mu)}NM\right),$$

$$\frac{\|\nabla\bar{\tilde{\varphi}}(\gamma_{\psi(j)})\|^2_{l^2(\tilde{\Omega},M_2(\mathbb{R}))}}{2} - \|\bar{\tilde{V}}(\gamma_{\psi(j)})\|^2_{l^2(\tilde{\Omega},M_2(\mathbb{R}))} \leq \frac{2}{\gamma_0}\left(\inf_{\tilde{\varphi}\in\mathcal{F}_1(\tilde{\Omega})} J(\tilde{\varphi}) + \frac{1}{\gamma_0} + \frac{\mu(\lambda+3\mu)}{2(\lambda+2\mu)}NM\right),$$

$$\frac{\|\bar{\tilde{\varphi}}(\gamma_{\psi(j)})\|^2_{l^2(\tilde{\Omega},\mathbb{R}^2)} - c_4}{2^9B^2} \leq \frac{2}{\gamma_0}\left(\inf_{\tilde{\varphi}\in\mathcal{F}_1(\tilde{\Omega})} J(\tilde{\varphi}) + \frac{1}{\gamma_0} + \frac{\mu(\lambda+3\mu)}{2(\lambda+2\mu)}NM\right) + \|\bar{\tilde{V}}(\gamma_{\psi(j)})\|^2_{l^2(\tilde{\Omega},M_2(\mathbb{R}))},$$

this last inequality stemming again from the discrete generalized Poincaré inequality. As $\bar{\tilde{V}}(\gamma_{\psi(j)})$ is uniformly bounded and all the norms are equivalent in finite dimension, we can deduce that $(\bar{\tilde{\varphi}}(\gamma_{\psi(j)}))$ is also uniformly bounded in $\|.\|_{l^2(\tilde{\Omega},\mathbb{R}^2)}$. Then, from Bolzano-Weierstrass theorem, we can extract a subsequence $(\bar{\tilde{\varphi}}(\gamma_{\psi\circ\zeta(j)}))$ from $(\bar{\tilde{\varphi}}(\gamma_{\psi(j)}))$ such that $\bar{\tilde{\varphi}}(\gamma_{\psi\circ\zeta(j)}) \xrightarrow[j\to+\infty]{} \bar{\varphi}$. Furthermore, we have $\|\bar{\tilde{V}}(\gamma_{\psi\circ\zeta(j)}) - \nabla\bar{\tilde{\varphi}}(\gamma_{\psi\circ\zeta(j)})\|^2_{l^2(\tilde{\Omega},M_2(\mathbb{R}))} \leq \frac{2}{\gamma_{\psi\circ\zeta(j)}}\left(\inf_{\tilde{\varphi}\in\mathcal{F}_1(\tilde{\Omega})} J(\tilde{\varphi}) + \frac{1}{\gamma_0} + \frac{\mu(\lambda+3\mu)}{2(\lambda+2\mu)}NM\right)$. As $\gamma_{\psi\circ\zeta(j)} \xrightarrow[j\to+\infty]{} +\infty$, we deduce that $\|\bar{\tilde{V}}(\gamma_{\psi\circ\zeta(j)}) - \nabla\bar{\tilde{\varphi}}(\gamma_{\psi\circ\zeta(j)})\|^2_{l^2(\tilde{\Omega},M_2(\mathbb{R}))} \xrightarrow[j\to+\infty]{} 0$. By

continuity of the norm, we get $\|\nabla\bar{\varphi} - \bar{V}\|^2_{l^2(\tilde{\Omega},M_2(\mathbb{R}))} = 0$ and so $\bar{V} = \nabla\bar{\varphi}$. Since $\frac{\nu}{2}\|H_\varepsilon(\Phi_0(\bar{\tilde{\varphi}}(\gamma_{\psi\circ\zeta(j)}))) - H_\varepsilon(\tilde{\Phi}(\cdot,\bar{T}))\|^2_{l^2(\tilde{\Omega})} + \sum_{i=1}^{N}\sum_{l=1}^{M} QW(\bar{\tilde{V}}_{i,l}(\gamma_{\psi\circ\zeta(j)})) \leq J_{\gamma_{\psi\circ\zeta(j)}}(\bar{\tilde{\varphi}}(\gamma_{\psi\circ\zeta(j)}), \bar{\tilde{V}}(\gamma_{\psi\circ\zeta(j)}))$, by continuity, we have $\inf_{\tilde{\varphi}\in\mathcal{F}_1(\tilde{\Omega})} J(\tilde{\varphi}) \leq J(\bar{\varphi}) \leq \liminf_{j\to+\infty} J_{\gamma_{\psi\circ\zeta(j)}}(\bar{\tilde{\varphi}}(\gamma_{\psi\circ\zeta(j)}), \bar{\tilde{V}}(\gamma_{\psi\circ\zeta(j)}))$ and $J_{\gamma_{\psi\circ\zeta(j)}}(\bar{\tilde{\varphi}}(\gamma_{\psi\circ\zeta(j)}), \bar{\tilde{V}}(\gamma_{\psi\circ\zeta(j)})) \leq \inf_{\tilde{\varphi}\in\mathcal{F}_1(\tilde{\Omega})} J(\tilde{\varphi}) + \frac{1}{\gamma_{\psi\circ\zeta(j)}}$. Consequently, $\limsup_{j\to+\infty} J_{\gamma_{\psi\circ\zeta(j)}}(\bar{\tilde{\varphi}}(\gamma_{\psi\circ\zeta(j)}), \bar{\tilde{V}}(\gamma_{\psi\circ\zeta(j)})) \leq \inf_{\tilde{\varphi}\in\mathcal{F}_1(\tilde{\Omega})} J(\tilde{\varphi})$ which yields $\lim_{j\to+\infty} J_{\gamma_{\psi\circ\zeta(j)}}(\bar{\tilde{\varphi}}(\gamma_{\psi\circ\zeta(j)}), \bar{\tilde{V}}(\gamma_{\psi\circ\zeta(j)})) = J(\bar{\varphi}) = \inf_{\tilde{\varphi}\in\mathcal{F}_1(\tilde{\Omega})} J(\tilde{\varphi})$.

□

The previous results justify the use of the following algorithm.

4.3 Actual algorithm associated with the quadratic penalty method

In this section, we introduce the quadratic penalty algorithm. Its main step is divided into 2 important parts: the segmentation step which will guide the registration process and the registration step. The latter one is done thanks to an alternating scheme solving successively the Euler-Lagrange equations in $\tilde{\varphi}$ and $\tilde{V}$.

Remark 4.8. *In practice, it may be relevant to use a couple of intermediate segmentation steps, in particular, when the shapes to be registered exhibit thin concavities. A control on the local curvature of the zero level line of $\tilde{\Phi}$ to detect extrema can be made to identify such regions. In order to comply with the mechanical interpretation of our model, rather than considering a continuum in time, we assume that the problem is sampled in time, and solve sequentially the subproblems :*

$$\inf_{\varphi_i\in \mathtt{Id}+W_0^{1,4}(\Omega,\mathbb{R}^2)} \int_\Omega QW(\nabla\varphi_i)\,dx + \frac{\nu}{2}\int_\Omega \Big(H_\varepsilon(\Phi_0\circ\varphi_1\circ\cdots\circ\varphi_i) - H_\varepsilon(\tilde{\Phi}(\cdot,t_i))\Big)^2\,dx,$$

for $i \in \{1,\cdots\zeta\}$, ζ small in practice. In the end, the overall deformation is given by $\varphi_1\circ\cdots\circ\varphi_\zeta$.

From a purely mathematical point of view, the existence of minimizers for each subproblem is guaranteed: Rellich-Kondrachov's embedding theorem states that weak convergence in $W^{1,4}(\Omega,\mathbb{R}^2)$ leads to uniform convergence in $\bar{\Omega}$, an extension process as before can be applied on all φ_k, $k = 1,\cdots,i-1$ to ensure the well-definedness of the composition, and the continuous injection $W^{1,4}(\mathbb{R}^2,\mathbb{R}^2) \circlearrowleft \mathcal{C}^0(\mathbb{R}^2,\mathbb{R}^2)$ holds, these three elements combined allowing to handle the fidelity term.

A first alternative would consist in introducing explicitly the time variable $t \in [0,\bar{T}]$ in the modelling and in minimizing with respect to now $\varphi = \varphi(x,t)$:

$$J(\varphi) = \iint_V \|\frac{\partial\varphi}{\partial t}(x,t)\|_2^2\,dx\,dt + \iint_V \left[QW(\nabla\varphi(x,t)) + \frac{\nu}{2}\Big(H_\varepsilon(\Phi_0\circ\varphi(x,t)) - H_\varepsilon(\tilde{\Phi}(x,t))\Big)^2\right]dx\,dt,$$

with $V = \Omega \times [0, \bar{T}]$. *A suitable functional space is* $\big\{\varphi \in L^4(0,\bar{T}; W^{1,4}(\Omega,\mathbb{R}^2)) \mid \frac{\partial \varphi}{\partial t} \in L^2(0,\bar{T}; L^2(\Omega,\mathbb{R}^2))\big\}$ *endowed with the norm* $\|\varphi\|_W = \|\varphi\|_{L^4(0,\bar{T};Id+W^{1,4}(\Omega,\mathbb{R}^2))} + \|\frac{\partial \varphi}{\partial t}\|_{L^2(0,\bar{T};L^2(\Omega,\mathbb{R}^2))}$ *and a result of existence of minimizers holds in this space thanks to Aubin-Lions lemma in particular. Indeed, the proof is divided into the following three steps:*

– **Coercivity inequality***: By taking* $\varphi(t) = Id\ \forall t \in [0;\bar{T}]$, *we get* $J(\varphi) < +\infty$ *and the functional is proper. We first derive a coercivity inequality. From what was previously done, we know that:*

$$
\begin{aligned}
QW(\nabla\varphi(x,t)) &\geq \frac{\beta}{2}\|\nabla\varphi(t,x)\|^4 - \beta\alpha^2 - \frac{\mu(\lambda+3\mu)}{2(\lambda+2\mu)} + \gamma,\\
\int_\Omega QW(\nabla\varphi(x,t))\,dx &\geq \frac{\beta}{2}\|\nabla\varphi(t,.)\|^4_{L^4(\Omega,M_2(\mathbb{R}))} + meas(\Omega)\Big(-\beta\alpha^2 - \frac{\mu(\lambda+3\mu)}{2(\lambda+2\mu)} + \gamma\Big),\\
\int_\Omega QW(\nabla\varphi(x,t))\,dx &\geq \frac{\beta}{2(c^4+1)}\|\varphi(t,.)\|^4_{W^{1,4}(\Omega,\mathbb{R}^2)} + meas(\Omega)\Big(-\beta\alpha^2 - \frac{\mu(\lambda+3\mu)}{2(\lambda+2\mu)}\\
&\quad + \gamma\Big) + k \quad \textit{(from generalized Poincaré inequality)},\\
J(\varphi) &\geq \|\frac{\partial\varphi}{\partial t}\|^2_{L^2(]0,\bar{T}[\times\Omega,\mathbb{R}^2)} + \frac{\beta}{2(c^4+1)}\int_0^{\bar{T}}\|\varphi(t,.)\|^4_{W^{1,4}(\Omega,\mathbb{R}^2)}\,dt\\
&\quad - \beta\alpha^2 meas(\Omega)\bar{T} - \frac{\mu(\lambda+3\mu)}{2(\lambda+2\mu)}meas(\Omega)\bar{T} + \gamma meas(\Omega)\bar{T} + k\bar{T},\\
J(\varphi) &\geq \|\frac{\partial\varphi}{\partial t}\|^2_{L^2(]0,\bar{T}[\times\Omega,\mathbb{R}^2)} + \frac{\beta}{2(c^4+1)}\|\varphi\|^4_{L^4(0,\bar{T};W^{1,4}(\Omega,\mathbb{R}^2))}\\
&\quad - \beta\alpha^2 meas(\Omega)\bar{T} - \frac{\mu(\lambda+3\mu)}{2(\lambda+2\mu)}meas(\Omega)\bar{T} + \gamma meas(\Omega)\bar{T} + k\bar{T}.
\end{aligned}
$$

So, the infimum is finite.

– **Convergence of a minimizing sequence***: Let* $\{\varphi^k\}_{k\in\mathbb{N}}$ *be a minimizing sequence. As the functional is proper, there exists* $\hat{\varphi}$ *such that for all* k *large enough,* $J(\varphi^k) \leq J(\hat{\varphi}) + 1 < +\infty$. *Then from the coercivity inequality, we can deduce that* $\{\varphi^k\}_{k\in\mathbb{N}}$ *is uniformly bounded in* $L^4(0,\bar{T};W^{1,4}(\Omega,\mathbb{R}^2))$ *so we can extract a subsequence still denoted* $\{\varphi^k\}$ *such that* $\varphi^k \rightharpoonup \bar{\varphi}$ *in* $L^4(0,\bar{T};W^{1,4}(\Omega,\mathbb{R}^2))$. *Besides,* $\{\frac{\partial\varphi^k}{\partial t}\}_{k\in\mathbb{N}}$ *is uniformly bounded in* $L^2(0,\bar{T};L^2(\Omega,\mathbb{R}^2))$ *so we can extract a subsequence still denoted* $\{\frac{\partial\varphi^k}{\partial t}\}$ *such that* $\frac{\partial\varphi^k}{\partial t} \rightharpoonup \bar{\delta}$ *in* $L^2(0,\bar{T};L^2(\Omega,\mathbb{R}^2))$. *By taking a common subsequence still denoted* $\{\varphi^k\}$, *we know that* $\forall k \in \mathbb{N}$, $\frac{\partial\varphi^k}{\partial t}$ *is the weak derivative of* φ^k *according to the time variable,* $\varphi^k \rightharpoonup \bar{\varphi}$ *in* $L^4(0,\bar{T};W^{1,4}(\Omega,\mathbb{R}^2))$, $\frac{\partial\varphi^k}{\partial t} \rightharpoonup \bar{\delta}$ *in* $L^2(0,\bar{T};L^2(\Omega,\mathbb{R}^2))$ *and we can deduce that* $\bar{\delta} = \frac{\partial\bar{\varphi}}{\partial t}$.
We also notice that $\{\varphi^k\}_{k\in\mathbb{N}}$ *is uniformly bounded in* W *so we can extract a subsequence still denoted* $\{\varphi^k\}$ *such that* $\varphi^k \rightharpoonup \bar{\varphi}_1$ *in* W. *By extracting a common subsequence and thanks to the uniqueness of the weak limit, it yields* $\bar{\varphi}_1 = \bar{\varphi}$.

As $W^{1,4}(\Omega,\mathbb{R}^2)\subset L^2(\Omega,\mathbb{R}^2)$ with compact injection, the Aubin-Lions lemma states that the embedding of W in $L^4(0,\bar{T};L^2(\Omega,\mathbb{R}^2)$ is compact. As $L^4(0,\bar{T};L^2(\Omega,\mathbb{R}^2))\subset L^2(]0,\bar{T}[\times\Omega,\mathbb{R}^2)$ is continuous then the embedding of W into $L^2(]0,\bar{T}[\times\Omega,\mathbb{R}^2)$ is also compact. We can therefore extract a subsequence of $\{\varphi^k\}$ still denoted $\{\varphi^k\}$ such that $\varphi^k\to\bar{\varphi}$ in $L^2(]0,\bar{T}[\times\Omega,\mathbb{R}^2)$.

– **Weak lower semi-continuity**: *$\|.\|_{L^2(]0,\bar{T}[\times\Omega,\mathbb{R}^2)}$ is convex and strongly continuous and so it is weakly lower semi-continuous in $L^2(]0,\bar{T}[\times\Omega,\mathbb{R}^2)$ so $\|\frac{\partial\bar{\varphi}}{\partial t}\|_{L^2(]0,\bar{T}[\times\Omega,\mathbb{R}^2)}\leq\liminf_{k\to+\infty}\|\frac{\partial\varphi^k}{\partial t}\|_{L^2(]0,\bar{T}[\times\Omega,\mathbb{R}^2)}$.*
As, $\varphi^k\to\bar{\varphi}$ in $L^2(]0,\bar{T}[\times\Omega,\mathbb{R}^2)$, up to a subsequence, one has pointwise convergence of $\{\varphi^k\}$ to $\bar{\varphi}$ and the dominated convergence theorem enables us to obtain the weak lower semi-continuity of the data fidelity term.
Let $\{\psi_k\}_{k\in\mathbb{N}}$ be a sequence that strongly converges to $\bar{\psi}$ in $L^4(0,\bar{T};W^{1,4}(\Omega,\mathbb{R}^2))$. Then $\int_0^{\bar{T}}\|\bar{\psi}(t)-\psi_k(t)\|^4_{W^{1,4}(\Omega,\mathbb{R}^2)}\,dt\underset{k\to+\infty}{\longrightarrow}0$. By seeing $\|\bar{\psi}(t)-\psi_k(t)\|^4_{W^{1,4}(\Omega,\mathbb{R}^2)}$ as a real-valued function depending on t defined on $]0,\bar{T}[$ and by applying the reciprocal of dominated convergence theorem, we get that $\|\bar{\psi}(t)-\psi_k(t)\|^4_{W^{1,4}(\Omega,\mathbb{R}^2)}$ converges to 0 for almost every $t\in]0,\bar{T}[$ up to a subsequence. So for almost every $t\in]0,\bar{T}[$, $\psi_k(t)$ strongly converges to $\bar{\psi}(t)$ in $W^{1,4}(\Omega,\mathbb{R}^2)$ and $\det\nabla\psi^k(t)\underset{k\to+\infty}{\to}\det\nabla\bar{\psi}(t)$ in $L^2(\Omega)$. From what was done in the stationary case, we know that $(\Psi,\delta)\mapsto\int_\Omega K(\nabla\Psi,\delta)\,dx$, defined on $W^{1,4}(\Omega,\mathbb{R}^2)\times L^2(\Omega)$, is convex, weakly lower semi-continuous, with $K(\Psi,\delta)=\begin{cases}\beta(\|\nabla\Psi\|^2-\alpha)^2+\psi(\delta), & \text{if } \|\nabla\Psi\|^2>\alpha\\ \psi(\delta), & \text{otherwise.}\end{cases}$. So for almost every $t\in[0,\bar{T}]$,

$$\begin{aligned}&\int_\Omega QW(\nabla\bar{\psi}(t))\,dx=\int_\Omega K(\nabla\bar{\psi}(t),\det\nabla\bar{\psi}(t))\,dx\\&\leq\liminf_{k\to+\infty}\int_\Omega QW(\nabla\psi_k(t))\,dx=\liminf_{k\to+\infty}\int_\Omega K(\nabla\psi_k(t),\det\nabla\psi_k(t))\,dx,\\ \text{and}\ &0\leq\int_\Omega QW(\nabla\bar{\psi}(t))\,dx+meas(\Omega)\Big(\beta\alpha^2+\frac{\mu(\lambda+3\mu}{2(\lambda+2\mu)}-\gamma\Big)\\&\leq\liminf_{k\to+\infty}\int_\Omega QW(\nabla\psi_k(t))\,dx+meas(\Omega)\Big(\beta\alpha^2+\frac{\mu(\lambda+3\mu}{2(\lambda+2\mu)}-\gamma\Big).\end{aligned}$$

So by Fatou's lemma, we get:

$$\begin{aligned}&\int_0^{\bar{T}}\int_\Omega QW(\nabla\bar{\psi}(x,t))\,dx\,dt+meas(\Omega)\Big(\beta\alpha^2\bar{T}+\frac{\mu(\lambda+3\mu)}{2(\lambda+2\mu)}\bar{T}-\gamma\bar{T}\Big)\\&\leq\int_0^{\bar{T}}\liminf_{k\to+\infty}\int_\Omega QW(\nabla\psi_k(x,t))\,dx\,dt+meas(\Omega)\Big(\beta\alpha^2\bar{T}+\frac{\mu(\lambda+3\mu)}{2(\lambda+2\mu)}\bar{T}-\gamma\bar{T}\Big),\\&\leq\liminf_{k\to+\infty}\int_0^{\bar{T}}\int_\Omega QW(\nabla\psi_k(x,t))\,dx\,dt+meas(\Omega)\Big(\beta\alpha^2\bar{T}+\frac{\mu(\lambda+3\mu)}{2(\lambda+2\mu)}\bar{T}-\gamma\bar{T}\Big).\end{aligned}$$

Thus

$$\int_0^{\bar{T}}\int_\Omega QW(\nabla\bar{\psi}(x,t))\,dx\,dt = \int_0^{\bar{T}}\int_\Omega K(\nabla\bar{\psi}(x,t),\det\nabla\bar{\psi}(x,t))\,dx\,dt$$
$$\leq \liminf_{k\to+\infty}\int_0^{\bar{T}}\int_\Omega QW(\nabla\psi_k(x,t))\,dx\,dt = \liminf_{k\to+\infty}\int_0^{\bar{T}}\int_\Omega K(\nabla\psi_k(x,t),\det\nabla\psi_k(x,t))\,dx\,dt.$$

Then it is convex and strongly sequentially lower semi-continuous and so it is weakly lower semi-continuous. We finally have

$$\int_0^{\bar{T}}\int_\Omega QW(\nabla\bar{\varphi}(x,t))\,dx\,dt = \int_0^{\bar{T}}\int_\Omega K(\nabla\bar{\varphi}(x,t),\det\nabla\bar{\varphi}(x,t))\,dx\,dt$$
$$\leq \liminf_{k\to+\infty}\int_0^{\bar{T}}\int_\Omega QW(\nabla\varphi^k(x,t))\,dx\,dt = \liminf_{k\to+\infty}\int_0^{\bar{T}}\int_\Omega K(\nabla\varphi^k(x,t),\det\nabla\varphi^k(x,t))\,dx\,dt,$$

which concludes the proof.

The numerical analysis of this model is still a work in progress.
Another alternative (yielding results comparable to the ones displayed) that we have investigated consists in treating jointly the segmentation and registration tasks by minimizing

$$\inf_{\bar{\Phi},\varphi} J(\bar{\Phi}) + \mu'\,L(\bar{\Phi}) + \int_\Omega QW(\nabla\varphi)\,dx + \frac{\gamma}{2}\,\|\bar{\Phi}-\Phi_0\circ\varphi\|^2_{L^2(\Omega)}.$$

A substitute for $\Phi_0\circ\varphi$ denoted by $\bar{\Phi}$ is thus incorporated in the topology-preserving segmentation model and the coupling is made through the L^2-penalization, entailing mutual influence of both tasks. Note that the question of existence of minimizers is still an open question for this problem. Proceeding as in subsection 3.3 and setting $\widehat{\Phi} = e^{\gamma t}\,\bar{\Phi}$, it is noticeable that the evolution equation satisfied by $\widehat{\Phi}$ is then defined by:

$$\frac{\partial\widehat{\Phi}}{\partial t} = |\nabla\widehat{\Phi}|\left\{ div\left(\tilde{g}(|\nabla R|)\frac{\nabla\widehat{\Phi}}{|\nabla\widehat{\Phi}|}\right) + c_0 * \left[\widehat{\Phi}(\cdot,t)\right] + k\tilde{g}(|\nabla R|)\right\} + \gamma\,\exp(\gamma t)\,\Phi_0\circ\varphi\,,$$

which exhibits the same property of geometrical type, namely the map χ defined in Definition 2.6 from Chapter 2 only depends on the zero level set of the initial condition Φ_0 and not on the initial condition itself. Function Φ_0 being Lipschitz continuous with Lipschitz constant $\mathcal{L}_{\Phi_0}$ and considering φ as a function of time t with values in $W^{1,4}(\mathbb{R}^2,\mathbb{R}^2)$, i.e., $\varphi:\begin{array}{ccc}]0,\bar{T}[& \to & W^{1,4}(\mathbb{R}^2,\mathbb{R}^2)\\ t & \mapsto & \varphi(t)\end{array}$ *, thanks to the continuous Sobolev embedding $W^{1,4}(\mathbb{R}^2,\mathbb{R}^2)\circlearrowleft \mathcal{C}^0(\mathbb{R}^2,\mathbb{R}^2)$, we deduce that $\varphi(t)$ is uniformly continuous on any compact subset of $\mathbb{R}^2$ yielding:*

$$\gamma\,\exp(\gamma t)\,|\Phi_0(\varphi(x_1,t)) - \Phi_0(\varphi(x_2,t))| \leq \gamma\,\exp(\gamma t)\,\mathcal{L}_{\Phi_0}\,|\varphi(x_1,t)-\varphi(x_2,t)|,$$
$$\leq \gamma\,\exp(\gamma t)\,\mathcal{L}_{\Phi_0}\,w_K(t,|x_1-x_2|),$$

w_K modulus of continuity of φ depending on the compact subset considered. If, for instance, we assume that this modulus of continuity is uniform in time, assumption A2 i. is satisfied as well as assumption A2 ii., by taking $h(x,t,r) = \gamma \exp(\gamma t)\, \Phi_0(\varphi(x,t))$.

1: [Initialization step]: $\tilde{V}^0 = (I_2)^{N\times M}$, $\tilde{\varphi}^0 = \mathrm{Id}$ and regrid_count $= 0$ for the registration part;
$\tilde{\Phi}(.,0) = \Phi_0$ (input segmentation of the Template) for the topology preserving segmentation part.
Select λ, μ, γ large enough, and ν.

2: [Main Step]:

(i) Compute $\tilde{\Phi}$, solution of the evolution equation problem (3.1): the discretization of (3.1) is made using an Additive Operator scheme (see [57]), requiring a linear computational cost at each step. A detailed numerical algorithm can be found in [37, Appendix B, pp. 777-778], both to derive the AOS scheme and to reinitialize $\tilde{\Phi}$ since it is assumed to be a signed-distance function in the modelling.

(ii) For $k = 1, 2, \cdots, \zeta$, compute $(\tilde{\varphi}^k, \tilde{V}^k) = \underset{(\tilde{\varphi},\tilde{V})}{\arg\min}\, J_\gamma(\tilde{\varphi}, \tilde{V})$ with $\tilde{\Phi}(.,\bar{T}) = \tilde{\Phi}(.,t_k)$, $t_\zeta = \bar{T}$, $\tilde{\Phi}(.,t_\zeta)$ representing the object inside the Reference and $\Phi_{0,k} = \Phi_0 \circ \tilde{\varphi}_1 \circ \cdots \circ \tilde{\varphi}_{k-1}$, using an alternative scheme:

(a) Solve the Euler-Lagrange equation in $\tilde{\varphi}_{i,j}$ for each $(i,j) \in \{2,\ldots,N-1\} \times \{2,\ldots,M-1\}$: $\nu\delta_\varepsilon(\Phi_{0,k}\circ\tilde{\varphi}_{i,j})\Big(H_\varepsilon(\Phi_{0,k}\circ\tilde{\varphi}_{i,j}) - H_\varepsilon(\tilde{\Phi}(.,t_k))\Big)\nabla\Phi_{0,k}(\tilde{\varphi}_{i,j}) + \gamma\begin{pmatrix} \mathrm{div}\tilde{V}_{1_{i,j}} \\ \mathrm{div}\tilde{V}_{2_{i,j}} \end{pmatrix} - \gamma\Delta\tilde{\varphi}_{i,j} = 0$. To do so, we use an L^2 gradient flow algorithm and an implicit Euler time stepping scheme.

(b) Solve the system of Euler-Lagrange equations in $\tilde{V}_{i,j}$ for each $(i,j) \in \{2,\ldots,N-1\} \times \{2,\ldots,M-1\}$:

$$\begin{cases} 0 = 2\beta\Big(\|\tilde{V}_{i,j}\|^2 - \alpha\Big)\tilde{V}_{11_{i,j}}\Big(2H_\varepsilon(\|\tilde{V}_{i,j}\|^2-\alpha) + (\|\tilde{V}_{i,j}\|^2-\alpha) \\ \qquad \delta_\varepsilon(\|\tilde{V}_{i,j}\|^2-\alpha)\Big) + \mu\tilde{V}_{22_{i,j}}(\det\tilde{V}_{i,j} - 2) + \gamma(\tilde{V}_{11_{i,j}} - \partial_x\tilde{\varphi}^1_{i,j}) \\ 0 = 2\beta\Big(\|\tilde{V}_{i,j}\|^2 - \alpha\Big)\tilde{V}_{12_{i,j}}\Big(2H_\varepsilon(\|\tilde{V}_{i,j}\|^2-\alpha) + (\|\tilde{V}_{i,j}\|^2-\alpha) \\ \qquad \delta_\varepsilon(\|\tilde{V}_{i,j}\|^2-\alpha)\Big) - \mu\tilde{V}_{21_{i,j}}(\det\tilde{V}_{i,j} - 2) + \gamma(\tilde{V}_{12_{i,j}} - \partial_y\tilde{\varphi}^1_{i,j}) \\ 0 = 2\beta\Big(\|\tilde{V}_{i,j}\|^2 - \alpha\Big)\tilde{V}_{21_{i,j}}\Big(2H_\varepsilon(\|\tilde{V}_{i,j}\|^2-\alpha) + (\|\tilde{V}_{i,j}\|^2-\alpha) \\ \qquad \delta_\varepsilon(\|\tilde{V}_{i,j}\|^2-\alpha)\Big) - \mu\tilde{V}_{12_{i,j}}(\det\tilde{V}_{i,j} - 2) + \gamma(\tilde{V}_{21_{i,j}} - \partial_x\tilde{\varphi}^2_{i,j}) \end{cases}$$

2: (following)

(ii) (following)

(b) (following)

$$\begin{cases} 0 &= 2\beta\left(\|\tilde{V}_{i,j}\|^2-\alpha\right)\tilde{V}_{22_{i,j}}\Big(2H_\varepsilon(\|\tilde{V}_{i,j}\|^2-\alpha)+(\|\tilde{V}_{i,j}\|^2-\alpha) \\ & \quad \delta_\varepsilon(\|\tilde{V}_{i,j}\|^2-\alpha)\Big)+\mu\tilde{V}_{11_{i,j}}(\det\tilde{V}_{i,j}-2)+\gamma(\tilde{V}_{22_{i,j}}-\partial_y\tilde{\varphi}_{i,j}^2) \end{cases}.$$

To do so, we use an L^2 gradient flow algorithm and a semi-implicit Euler time stepping scheme.

(c) Control of the Jacobian determinant, see Algorithm 4. Go back to (a) until convergence.

Algorithm 1: A topology preserving segmentation guided registration model - Quadratic Penalization

Remark 4.9. *As the matrices involved in the subproblems of the AOS scheme are monotone and the sum of the coefficients of each row of the inverse matrices is equal to one, then the numerical schemes are unconditionally stable in the L^∞-norm.*

The quadratic penalty method involves the minimization of functional J_γ for ever-larger values of γ, which may create some numerical instabilities. As an alternative, we propose introducing an augmented Lagrangian method (the underlying idea still being to convert the decoupled minimization problem denoted by (DP) under equality constraint $\tilde{V}=\nabla\tilde{\varphi}$ into an unconstrained minimization problem).

$$\begin{cases} \min\limits_{\tilde{\varphi}\in\mathcal{F}_1(\tilde{\Omega}),\tilde{V}\in(M_2(\mathbb{R}))^{N\times M}} & \frac{\nu}{2}\|H_\varepsilon(\Phi_0(\tilde{\varphi}))-H_\varepsilon(\tilde{\Phi}(\cdot,\bar{T}))\|^2_{l^2(\tilde{\Omega})}+\sum\limits_{i=1}^{N}\sum\limits_{j=1}^{M}QW(\tilde{V}_{i,j}) \\ \text{with } \nabla\tilde{\varphi}=\tilde{V} & \end{cases} \tag{DP}$$

Indeed, it has the advantage of solving the problem without having $\gamma\to+\infty$ as shown in the following, and thus the augmented Lagrangian method is numerically more stable.

4.4 Augmented Lagrangian method

In that purpose, we introduce the augmented Lagrangian function:

$$L(\tilde{\varphi},\tilde{V},\lambda,\gamma)=\frac{\nu}{2}\|H_\varepsilon(\Phi_0(\tilde{\varphi}))-H_\varepsilon(\tilde{\Phi}(\cdot,\bar{T}))\|^2_{l^2(\tilde{\Omega})}+\sum_{i=1}^{N}\sum_{j=1}^{M}QW(\tilde{V}_{i,j})+(\lambda,\tilde{V}-\nabla\tilde{\varphi})_{l^2(\tilde{\Omega},M_2(\mathbb{R}))}$$
$$+\frac{\gamma}{2}\|\tilde{V}-\nabla\tilde{\varphi}\|^2_{l^2(\tilde{\Omega},M_2(\mathbb{R}))}, \tag{3.8}$$

λ denoting the Lagrange multiplier. (We think that there is no confusion with the Lamé coeffficient). Now, we will follow the same arguments as in [51]. For the sake of clarity, we introduce the following set notations, $X=\{(\tilde{\varphi},\tilde{V})\in\mathcal{F}_1(\tilde{\Omega})\times(M_2(\mathbb{R}))^{N\times M}\}$,

$C = \{(\tilde{\varphi}, \tilde{V}) \in X, \nabla\tilde{\varphi} = \tilde{V}\}$, $\tilde{Y} = (M_2(\mathbb{R}))^{N\times M} \times (0, +\infty) \sim \mathbb{R}^{4\times N\times M} \times (0, +\infty)$; variable notations, $x = (\tilde{\varphi}, \tilde{V})$, $\tilde{y} = (\lambda, \gamma)$; function notations, $f_0(x) = \frac{\nu}{2}\|H_\varepsilon(\Phi_0(\tilde{\varphi})) - H_\varepsilon(\tilde{\Phi}(\cdot, \bar{T}))\|^2_{l^2(\tilde{\Omega})} + \sum_{i=1}^{N}\sum_{j=1}^{M} QW(\tilde{V}_{i,j})$, and $f_1(x) = \tilde{V} - \nabla\tilde{\varphi}$.

Thus for fixed $x \in X$, we have $L(x, \lambda, \gamma) = f_0(x) + (\lambda, f_1(x))_{l^2(\tilde{\Omega}, M_2(\mathbb{R}))} + \frac{\gamma}{2}\|f_1(x)\|^2_{l^2(\Omega, M_2(\mathbb{R}))}$ and $\sup_{(\lambda,\gamma)\in\tilde{Y}} L(x, \lambda, \gamma) = \begin{cases} f_0(x) & \text{when} \quad x \in C \\ +\infty & \text{when} \quad x \notin C \end{cases}$ since for fixed $x \in X$ and $\lambda \in (M_2(\mathbb{R}))^{N\times M}$, the limit of $L(x, \lambda, \gamma)$ as $\gamma \to +\infty$ already gives $f_0(x)$ when $\|f_1(x)\|_{l^2(\tilde{\Omega}, M_2(\mathbb{R}))} = 0 \Leftrightarrow f_1(x) = 0 \Leftrightarrow x \in C$ but $+\infty$ when $\|f_1(x)\|_{l^2(\tilde{\Omega}, M_2(\mathbb{R}))} \neq 0 \Leftrightarrow f_1(x) \neq 0 \Leftrightarrow x \notin C$. In [51], Rockafellar proved that finding a minimizer of (DP) amounts to finding a saddle point of the augmented Lagrangian function.

Theorem 4.7 (extracted from [51, Theorem 6.3])**.** *A pair of vectors $\bar{x} \in X$ and $(\bar{\lambda}, \bar{\gamma}) \in \tilde{Y}$ furnishes a saddle point of the augmented Lagrangian L on $X \times \tilde{Y}$ if and only if*

$$\begin{cases} \bar{x} \text{ is a (globally) optimal solution to } (DP) \\ p(u) \geq p(0) + (\bar{\lambda}, u)_{l^2(\tilde{\Omega}, M_2(\mathbb{R}))} - \frac{\bar{\gamma}}{2}\|u\|^2_{l^2(\tilde{\Omega}, M_2(\mathbb{R}))} \end{cases}, \tag{3.9}$$

with $(P(u))$: $\inf_{x\in X} f_0(x)$ such that $f_1(x) + u = 0$, $u \in (M_2(\mathbb{R}))^{N\times M} \sim \mathbb{R}^{4\times N\times M}$ and $p(u) = \inf(P(u)) = [$ the optimal value corresponding to $u]$. When this holds, any $\bar{\gamma}' > \bar{\gamma}$ will have the property that

$$[\bar{x} \text{ solves } (DP)] \Leftrightarrow \left[\bar{x} \text{ minimizes } L(x, \bar{\lambda}, \bar{\gamma}') \text{ over } x \in X\right]. \tag{3.10}$$

The following proposition gives another definition of the saddle point.

Proposition 4.10 (extracted from [51, Proposition 5.2])**.** *$(\bar{x}, \bar{\lambda}, \bar{\gamma})$ furnishes a saddle point of $L(x, \lambda, \gamma)$ on $X \times \tilde{Y}$ if and only if*

$$\begin{cases} \bar{x} \text{ is an optimal solution to } (DP), \\ (\bar{\lambda}, \bar{\gamma}) \text{ is an optimal solution to } (D), \\ \inf(DP) = \sup(D). \end{cases} \tag{3.11}$$

Lastly, we introduce the augmented dual problem (D): maximize $g(\lambda, \gamma) = \inf_{x\in X} L(x, \lambda, \gamma)$ over all $(\lambda, \gamma) \in \tilde{Y}$, and prove that the primal and the dual problems are equivalent.

Theorem 4.8. *We have $\inf(DP) = \sup(D)$ and $(\bar{x}, \bar{\lambda}, \bar{\gamma})$ gives a saddle point of L on $X \times \tilde{Y}$ if and only if $\bar{x}$ solves (DP) and $(\bar{\lambda}, \bar{\gamma})$ solves (D). The pairs $(\bar{\lambda}, \bar{\gamma}')$ with the exact penalty property (3.10) are then the ones such that, for some $\bar{\gamma} < \bar{\gamma}'$, $(\bar{\lambda}, \bar{\gamma})$ is an optimal solution to (D). Furthermore in this case, the function g in (D) is finite everywhere on $\tilde{Y}$, so this maximization problem is effectively unconstrained.*

Proof. We concentrate upon the equality $\inf(DP) = \sup(D)$. We know that $\sup_{(\lambda,\gamma)\in\tilde{Y}} L(x,\lambda,\gamma) = \begin{cases} f_0(x) & \text{when} \quad x \in C \\ +\infty & \text{when} \quad x \notin C \end{cases}$. So $\inf(DP) = \inf_{x\in X} \sup_{(\lambda,\gamma)\in\tilde{Y}} L(x,\lambda,\gamma)$ and $\inf(DP) \geq \sup(D)$ holds. We must now demonstrate that the inequality cannot be strict and then the saddle point assertion will likewise be a consequence of Proposition 4.10. Let $(\lambda,\gamma) \in \tilde{Y}$ be fixed. Let $x_n = (\tilde{\varphi}_n, \tilde{V}_n)$ be a minimizing sequence of $L(x,\lambda,\gamma)$.

$$
\begin{aligned}
L(x_n,\lambda,\gamma) &\geq -\beta\alpha^2 NM - \frac{\mu(\lambda+3\mu)}{2(\lambda+2\mu)}NM + \frac{\beta}{2}\|\tilde{V}_n\|^4_{l^4(\tilde{\Omega},M_2(\mathbb{R}))} + \frac{\gamma}{2}\|f_1(x_n)\|^2_{l^2(\tilde{\Omega},M_2(\mathbb{R}))} \\
&\quad - \|\lambda\|_{l^2(\tilde{\Omega},M_2(\mathbb{R}))}\|f_1(x_n)\|_{l^2(\tilde{\Omega},M_2(\mathbb{R}))}, \\
&\geq -\beta\alpha^2 NM - \frac{\mu(\lambda+3\mu)}{2(\lambda+2\mu)}NM + \frac{\beta}{2}\|\tilde{V}_n\|^4_{l^4(\tilde{\Omega},M_2(\mathbb{R}))} + \frac{\gamma}{2}\|f_1(x_n)\|^2_{l^2(\tilde{\Omega},M_2(\mathbb{R}))} \\
&\quad - c_\epsilon\|\lambda\|^2_{l^2(\tilde{\Omega},M_2(\mathbb{R}))} - \epsilon\|f_1(x_n)\|^2_{l^2(\tilde{\Omega},M_2(\mathbb{R}))}, \\
&\geq -\beta\alpha^2 NM - \frac{\mu(\lambda+3\mu)}{2(\lambda+2\mu)}NM + \frac{\beta}{2}\|\tilde{V}_n\|^4_{l^4(\tilde{\Omega},M_2(\mathbb{R}))} + \left(\frac{\gamma}{2}-\epsilon\right)\|f_1(x_n)\|^2_{l^2(\tilde{\Omega},M_2(\mathbb{R}))} \\
&\quad - c_\epsilon\|\lambda\|^2_{l^2(\tilde{\Omega},M_2(\mathbb{R}))}.
\end{aligned}
$$

For ϵ sufficiently small such that $\frac{\gamma}{2} - \epsilon > 0$, $(\tilde{V}_n)$ is uniformly bounded in $\|.\|_{l^4(\tilde{\Omega},M_2(\mathbb{R}))}$ and according to Bolzano-Weiertrass theorem, there exist a subsequence $(\tilde{V}_{\rho(n)})$ and $\bar{\tilde{V}}$ such that $\tilde{V}_{\rho(n)} \xrightarrow[n\to+\infty]{} \bar{\tilde{V}}$. Also,

$$
\begin{aligned}
L(x_{\rho(n)},\lambda,\gamma) &\geq -\frac{\mu(\lambda+3\mu)}{2(\lambda+2\mu)}NM + \left(\frac{\gamma}{2}-\epsilon\right)\|f_1(x_{\rho(n)})\|^2_{l^2(\tilde{\Omega},M_2(\mathbb{R}))} - c_\epsilon\|\lambda\|^2_{l^2(\tilde{\Omega},M_2(\mathbb{R}))}, \\
&\geq -\frac{\mu(\lambda+3\mu)}{2(\lambda+2\mu)}NM - c_\epsilon\|\lambda\|^2_{l^2(\tilde{\Omega},M_2(\mathbb{R}))} + \left(\frac{\gamma}{2}-\epsilon\right)\Big(\|\nabla\tilde{\varphi}_{\rho(n)}\|_{l^2(\tilde{\Omega},M_2(\mathbb{R}))} \\
&\quad -\|\tilde{V}_{\rho(n)}\|_{l^2(\tilde{\Omega},M_2(\mathbb{R}))}\Big)^2, \\
&\geq -\frac{\mu(\lambda+3\mu)}{2(\lambda+2\mu)}NM - c_\epsilon\|\lambda\|^2_{l^2(\tilde{\Omega},M_2(\mathbb{R}))} + \left(\frac{\gamma}{2}-\epsilon\right)\Big(\frac{1}{2}\|\nabla\tilde{\varphi}_{\rho(n)}\|^2_{l^2(\tilde{\Omega},M_2(\mathbb{R}))} \\
&\quad -\|\tilde{V}_{\rho(n)}\|^2_{l^2(\tilde{\Omega},M_2(\mathbb{R}))}\Big), \\
&\geq -\frac{\mu(\lambda+3\mu)}{2(\lambda+2\mu)}NM - c_\epsilon\|\lambda\|^2_{l^2(\tilde{\Omega},M_2(\mathbb{R}))} + \left(\frac{\gamma}{2}-\epsilon\right)\Big(\frac{1}{2^2B^2}\left(\|\tilde{\varphi}_{\rho(n)}\|^2_{l^2(\tilde{\Omega},\mathbb{R}^2)} - c_4\right) \\
&\quad -\|\tilde{V}_{\rho(n)}\|^2_{l^2(\tilde{\Omega},M_2(\mathbb{R}))}\Big).
\end{aligned}
$$

The last step comes again from the discrete generalized Poincaré inequality. As $(\tilde{V}_{\rho(n)})$ is uniformly bounded, $(\tilde{\varphi}_{\rho(n)})$ is also uniformly bounded in $\|.\|_{l^2(\tilde{\Omega},\mathbb{R}^2)}$. Then, according to Bolzano-Weierstrass theorem, there exist a subsequence $(\tilde{\varphi}_{\rho\circ\zeta(n)})$ and $\bar{\tilde{\varphi}}$ such that $\tilde{\varphi}_{\rho\circ\zeta(n)} \xrightarrow[n\to+\infty]{} \bar{\tilde{\varphi}}$ and so $x_{\rho\circ\zeta(n)} \xrightarrow[n\to+\infty]{} \bar{x}$. Then, by continuity of L, $L(x_{\rho\circ\zeta(n)},\lambda,\gamma) \xrightarrow[n\to+\infty]{} L(\bar{x},\lambda,\gamma)$ and $L(\bar{x},\lambda,\gamma) = \inf_{x\in X} L(x,\lambda,\gamma)$. Consequently, the infimum is finite and attained.

Let $\epsilon' > 0$. By definition of the infimum, there exists $\hat{x} \in C$ such that $f_0(\hat{x}) < \inf_{\tilde{x}\in C} f_0(\tilde{x}) + \epsilon'$. Also, $\inf_{x\in X} L(x,\lambda,\gamma) \leq L(\hat{x},\lambda,\gamma) = f_0(\hat{x})$, yielding $\inf_{x\in X} L(x,\lambda,\gamma) \leq f_0(\hat{x}) < \inf_{\tilde{x}\in C} f_0(\tilde{x}) + \epsilon'$. Let (γ_j) be an increasing sequence of positive real numbers such that $\lim_{j\to+\infty} \gamma_j = +\infty$. Let (x_{γ_j}) be the sequence of minimizers of $L(x,\lambda,\gamma_j)$ with λ still being fixed. In the previous inequality, we take $\epsilon' = \frac{1}{\gamma_j}$, so that $L(x_{\gamma_j},\lambda,\gamma_j) \leq \inf_{\tilde{x}\in C} f_0(\tilde{x}) + \frac{1}{\gamma_j} \leq \inf_{\tilde{x}\in C} f_0(\tilde{x}) + \frac{1}{\gamma_0} < +\infty$. Then we have, setting $x_{\gamma_j} = \left(\tilde{\varphi}_{\gamma_j}, \tilde{V}_{\gamma_j}\right)$:

$$\inf_{\tilde{x}\in C} f_0(\tilde{x}) + \frac{1}{\gamma_0} \geq \frac{\beta}{2}\|\tilde{V}_{\gamma_j}\|^4_{l^4(\tilde{\Omega},M_2(\mathbb{R}))} - \beta\alpha^2 NM - \frac{\mu(\lambda+3\mu)}{2(\lambda+2\mu)}NM - c_\epsilon\|\lambda\|^2_{l^2(\tilde{\Omega},M_2(\mathbb{R}))} + \left(\frac{\gamma_j}{2} - \epsilon\right)\|f_1(x_{\gamma_j})\|^2_{l^2(\tilde{\Omega},M_2(\mathbb{R}))}.$$

We take ϵ such that $\frac{\gamma_j}{2} - \epsilon > 0$, $\forall j \in \mathbb{N}$ then $(\tilde{V}_{\gamma_j})$ is uniformly bounded in $\|.\|_{l^4(\tilde{\Omega},M_2(\mathbb{R}))}$ and according to Bolzano - Weierstrass theorem, there exist a subsequence $(\tilde{V}_{\gamma_{\rho(j)}})$ and $\bar{\tilde{V}}$ such that $\tilde{V}_{\gamma_{\rho(j)}} \xrightarrow[j\to+\infty]{} \bar{\tilde{V}}$. Also,

$$\inf_{\tilde{x}\in C} f_0(\tilde{x}) + \frac{1}{\gamma_0} \geq -\frac{\mu(\lambda+3\mu)}{2(\lambda+2\mu)}NM - c_\epsilon\|\lambda\|^2_{l^2(\tilde{\Omega},M_2(\mathbb{R}))} + \left(\frac{\gamma_{\rho(j)}}{2} - \epsilon\right)\|\tilde{V}_{\gamma_{\rho(j)}} - \nabla\tilde{\varphi}_{\gamma_{\rho(j)}}\|^2_{l^2(\tilde{\Omega},M_2(\mathbb{R}))}.$$

Consequently,

$$\|\tilde{V}_{\gamma_{\rho(j)}} - \nabla\tilde{\varphi}_{\gamma_{\rho(j)}}\|^2_{l^2(\tilde{\Omega},M_2(\mathbb{R}))} \leq \left(\inf_{\tilde{x}\in C} f_0(\tilde{x}) + \frac{1}{\gamma_0} + \frac{\mu(\lambda+3\mu)}{2(\lambda+2\mu)}NM + c_\epsilon\|\lambda\|^2_{l^2(\tilde{\Omega},M_2(\mathbb{R}))}\right)\frac{2}{\gamma_{\rho(j)} - 2\epsilon}.$$

Thus $\|f_1(x_{\gamma_{\rho(j)}})\|^2_{l^2(\tilde{\Omega},M_2(\mathbb{R}))} \xrightarrow[j\to+\infty]{} 0$, implying $f_1(x_{\gamma_{\rho(j)}}) \xrightarrow[j\to+\infty]{} 0$. Furthermore, from the previous inequality we get:

$$-\|\tilde{V}_{\gamma_{\rho(j)}}\|^2_{l^2(\tilde{\Omega},M_2(\mathbb{R}))} + \frac{1}{2}\|\nabla\tilde{\varphi}_{\gamma_{\rho(j)}}\|^2_{l^2(\tilde{\Omega},M_2(\mathbb{R}))} \leq \left(\inf_{\tilde{x}\in C} f_0(\tilde{x}) + \frac{1}{\gamma_0} + \frac{\mu(\lambda+3\mu)}{2(\lambda+2\mu)}NM + c_\epsilon\|\lambda\|^2_{l^2(\tilde{\Omega},M_2(\mathbb{R}))}\right)\frac{2}{\gamma_{\rho(j)} - 2\epsilon}.$$

So,

$$-\|\tilde{V}_{\gamma_{\rho(j)}}\|^2_{l^2(\tilde{\Omega},M_2(\mathbb{R}))} + \frac{1}{2^2B^2}\left(\|\tilde{\varphi}_{\gamma_{\rho(j)}}\|^2_{l^2(\tilde{\Omega},\mathbb{R}^2)} - c_4\right) \leq \left(\inf_{\tilde{x}\in C} f_0(\tilde{x}) + \frac{1}{\gamma_0} + \frac{\mu(\lambda+3\mu)}{2(\lambda+2\mu)}NM + c_\epsilon\|\lambda\|^2_{l^2(\tilde{\Omega},M_2(\mathbb{R}))}\right)\frac{2}{\gamma_{\rho(j)} - 2\epsilon},$$

still from the discrete generalized Poincaré inequality. As $(\tilde{V}_{\gamma_{\rho(j)}})$ is uniformly bounded, we deduce that $(\tilde{\varphi}_{\gamma_{\rho(j)}})$ is uniformly bounded in $\|.\|_{l^2(\tilde{\Omega},\mathbb{R}^2)}$. So, according to Bolzano-Weierstrass theorem, there exist a subsequence $(\tilde{\varphi}_{\gamma_{\rho\circ\zeta(j)}})$ of $(\tilde{\varphi}_{\gamma_{\rho(n)}})$ and $\bar{\tilde{\varphi}}$ such that $\tilde{\varphi}_{\gamma_{\rho\circ\zeta(j)}} \xrightarrow[j\to+\infty]{} \bar{\tilde{\varphi}}$. Finally, $x_{\gamma_{\rho\circ\zeta(j)}} \xrightarrow[j\to+\infty]{} \bar{x}$ and $\nabla\bar{\tilde{\varphi}} = \bar{\tilde{V}}$ with $\bar{x} = (\bar{\tilde{\varphi}}, \bar{\tilde{V}})$. Moreover

we have $f_0(x_{\gamma_{\rho\circ\zeta(j)}}) + \left(\lambda, f_1(x_{\gamma_{\rho\circ\zeta(j)}})\right)_{l^2(\tilde{\Omega},M_2(\mathbb{R}))} \leq L(x_{\gamma_{\rho\circ\zeta(j)}}, \lambda, \gamma_{\rho\circ\zeta(j)})$, and by continuity, $\inf_{\tilde{x}\in C} f_0(\tilde{x}) \leq f_0(\bar{x}) \leq \liminf_{j\to+\infty} L(x_{\gamma_{\rho\circ\zeta(j)}}, \lambda, \gamma_{\rho\circ\zeta(j)})$. Also, $\limsup_{j\to+\infty} L(x_{\gamma_{\rho\circ\zeta(j)}}, \lambda, \gamma_{\rho\circ\zeta(j)}) \leq \inf_{\tilde{x}\in C} f_0(\tilde{x})$ and then $\lim_{j\to+\infty} L(x_{\gamma_{\rho\circ\zeta(j)}}, \lambda, \gamma_{\rho\circ\zeta(j)}) = f_0(\bar{x}) = \inf(DP)$. We thus have $\sup(D) = \inf(DP)$. The assertion about the exact penalty property is now immediate from Theorem 4.7. The finiteness of $g(\lambda, \gamma)$ results from the previous arguments. □

The function g is concave and upper semicontinuous as it is the minimum of affine functions of (λ, γ). Furthermore, as it is finite everywhere, we can deduce that g is continuous over $\tilde{Y}$.
As we have proved that the extremal values of the augmented primal and dual problems are equal, we propose focusing on the augmented dual problem for which we provide a convergent algorithm of resolution.
We prove the following theorems by adapting the proofs in [28] and in [8] dedicated to the case of a sharp Lagrangian algorithm, so different from our proposed approach. The first one gives a stopping criterion in the proposed algorithm for the augmented dual problem.

Theorem 4.9 (adapted from [28, Theorem 5])**.** *Suppose that for some* $(\bar{\lambda}, \bar{\gamma}) \in \tilde{Y}$ *and* $\bar{x} \in X$*,*

$$\min_{x\in X} L(x, \bar{\lambda}, \bar{\gamma}) = f_0(\bar{x}) + \left(\bar{\lambda}, f_1(\bar{x})\right)_{l^2(\tilde{\Omega},M_2(\mathbb{R}))} + \frac{\bar{\gamma}}{2}\|f_1(\bar{x})\|^2_{l^2(\tilde{\Omega},M_2(\mathbb{R}))}. \tag{3.12}$$

Then $\bar{x}$ *is a solution to* (DP) *and* $(\bar{\lambda}, \bar{\gamma})$ *is a solution to* (D) *if and only if* $f_1(\bar{x}) = 0$*.*

Proof. Necessity. If (3.12) is satisfied and $\bar{x}$ is a solution to (DP) then $\bar{x}$ is feasible and $f_1(\bar{x}) = 0$.

Sufficiency. We argue by contradiction. In that purpose, suppose that (3.12) holds and $f_1(\bar{x}) = 0$ is satisfied but $\bar{x}$ or $(\bar{\lambda}, \bar{\gamma})$ are not solutions. If $\bar{x}$ is not a solution to (DP) then there exists $\tilde{x} \in C$ such that $f_0(\tilde{x}) < f_0(\bar{x})$. Hence :

$$\begin{aligned} f_0(\tilde{x}) < f_0(\bar{x}) &= f_0(\bar{x}) + \left(\bar{\lambda}, f_1(\bar{x})\right)_{l^2(\tilde{\Omega},M_2(\mathbb{R}))} + \frac{\bar{\gamma}}{2}\|f_1(\bar{x})\|^2_{l^2(\tilde{\Omega},M_2(\mathbb{R}))} = g(\bar{\lambda}, \bar{\gamma}), \\ &= \min_{x\in X} L(x, \bar{\lambda}, \bar{\gamma}) \leq \max_{(\lambda,\gamma)\in\tilde{Y}} \min_{x\in X} L(x, \lambda, \gamma) = \sup(D) = \inf(DP) \leq f_0(\tilde{x}), \end{aligned}$$

which raises a contradiction. If $\bar{x}$ is a solution to (DP) but $(\bar{\lambda}, \bar{\gamma})$ is not a solution to (D), then there exists $(\tilde{\lambda}, \tilde{\gamma}) \in \tilde{Y}$ such that $g(\bar{\lambda}, \bar{\gamma}) \leq g(\tilde{\lambda}, \tilde{\gamma})$. As $\bar{x}$ is a solution to (DP), we have $f_0(\bar{x}) = \inf(DP) = \sup(D) \geq g(\tilde{\lambda}, \tilde{\gamma}) > g(\bar{\lambda}, \bar{\gamma}) = f_0(\bar{x})$, which raises again a contradiction. □

We now consider the augmented dual problem and introduce

$$S(\lambda, \gamma) = \arg\min_{x\in X} \left[f_0(x) + (\lambda, f_1(x))_{l^2(\tilde{\Omega},M_2(\mathbb{R}))} + \frac{\gamma}{2}\|f_1(x)\|^2_{l^2(\tilde{\Omega},M_2(\mathbb{R}))}\right].$$

The following result is a technical one which will serve in the next proofs.

Theorem 4.10 (adapted from [28, Theorem 6])**.** *For any* $(\bar{\lambda}, \bar{\gamma}) \in \tilde{Y}$*, if* $\bar{x} \in S(\bar{\lambda}, \bar{\gamma})$*, then* $\left(f_1(\bar{x}), \frac{\|f_1(\bar{x})\|^2_{l^2(\tilde{\Omega}, M_2(\mathbb{R}))}}{2}\right)$ *is a supergradient (the equivalent notion of subgradient for concave functions) of* g *at* $(\bar{\lambda}, \bar{\gamma})$*.*

Proof. We know from the proof of Theorem 4.8 that for any $(\bar{\lambda}, \bar{\gamma}) \in \tilde{Y}$, $S(\bar{\lambda}, \bar{\gamma})$ is nonempty. Let $\bar{x} \in S(\bar{\lambda}, \bar{\gamma})$. Then $g(\bar{\lambda}, \bar{\gamma}) = f_0(\bar{x}) + \big(\bar{\lambda}, f_1(\bar{x})\big)_{l^2(\tilde{\Omega}, M_2(\mathbb{R}))} + \frac{\bar{\gamma}}{2}\|f_1(\bar{x})\|^2_{l^2(\tilde{\Omega}, M_2(\mathbb{R}))}$. For any $(\lambda, \gamma) \in \tilde{Y}$, we have:

$$
\begin{aligned}
&g(\bar{\lambda}, \bar{\gamma}) + \big(f_1(\bar{x}), \lambda - \bar{\lambda}\big)_{l^2(\tilde{\Omega}, M_2(\mathbb{R}))} + \frac{\|f_1(\bar{x})\|^2_{l^2(\tilde{\Omega}, M_2(\mathbb{R}))}}{2}(\gamma - \bar{\gamma}) \\
&= f_0(\bar{x}) + (\lambda, f_1(\bar{x}))_{l^2(\tilde{\Omega}, M_2(\mathbb{R}))} + \frac{\gamma}{2}\|f_1(\bar{x})\|^2_{l^2(\tilde{\Omega}, M_2(\mathbb{R}))} \\
&\geq \min_{x \in X}\left\{f_0(x) + (\lambda, f_1(x))_{l^2(\tilde{\Omega}, M_2(\mathbb{R}))} + \frac{\gamma}{2}\|f_1(x)\|^2_{l^2(\tilde{\Omega}, M_2(\mathbb{R}))}\right\} = g(\lambda, \gamma).
\end{aligned}
$$

So $\left(f_1(\bar{x}), \frac{\|f_1(\bar{x})\|^2_{l^2(\tilde{\Omega}, M_2(\mathbb{R}))}}{2}\right)$ is a supergradient of g at $(\bar{\lambda}, \bar{\gamma})$. □

Let us now introduce the proposed supergradient algorithm.

1: [Initialization Step] Choose a vector (λ_1, γ_1) with $\gamma_1 > 0$, let $k = 1$, and go to the main step.

2: [Main Step]

1. Given (λ_k, γ_k), solve the following subproblem:

   Minimize $f_0(x) + (\lambda_k, f_1(x))_{l^2(\tilde{\Omega}, M_2(\mathbb{R}))} + \frac{\gamma_k}{2}\|f_1(x)\|^2_{l^2(\tilde{\Omega}, M_2(\mathbb{R}))}$ subject to $x \in X$.

   Let x_k be any solution (x_k exists from Theorem 4.8). If $f_1(x_k) = 0$ then stop; by Theorem 4.9, (λ_k, γ_k) is a solution to (D) and x_k is a solution to (DP). Otherwise go to step 2.

2. Let $\lambda_{k+1} = \lambda_k + s_k f_1(x_k)$, $\gamma_{k+1} = \gamma_k + \frac{(s_k + \epsilon_k)}{2}\|f_1(x_k)\|^2_{l^2(\tilde{\Omega}, M_2(\mathbb{R}))}$, where s_k and ϵ_k are positive scalar stepsizes, replace k by $k + 1$ and repeat step 1.

Algorithm 2: Supergradient algorithm.

The following theorem demonstrates that the distance between the points generated by Algorithm 2 and the solution to the dual problem (if it exists) decreases at each iteration.

Theorem 4.11 (adapted from [28, Theorem 8])**.** *Assume there exists a dual solution* $(\bar{\lambda}, \bar{\gamma})$*. Let* $(\lambda_1, \gamma_1) \in \tilde{Y}$*. We define* $\lambda_{k+1} = \lambda_k + s_k f_1(x_k)$ *and* $\gamma_{k+1} = \gamma_k + \frac{s_k + \epsilon_k}{2}\|f_1(x_k)\|^2_{l^2(\tilde{\Omega}, M_2(\mathbb{R}))}$*, where* x_k *is an exact solution of* $\min_{x \in X} f_0(x) + (\lambda_k, f_1(x))_{l^2(\tilde{\Omega}, M_2(\mathbb{R}))} + \frac{\gamma_k}{2}\|f_1(x)\|^2_{l^2(\tilde{\Omega}, M_2(\mathbb{R}))}$*, and* s_k*,* ϵ_k *are positive scalar stepsizes. Let* (λ_k, γ_k) *be any iteration which is not a solution to the dual problem, so* $f_1(x_k) \neq 0$*. Then, for any dual solution* $(\bar{\lambda}, \bar{\gamma})$*, we have*

$\|(\bar{\lambda},\bar{\gamma})-(\lambda_{k+1},\gamma_{k+1})\|_{\tilde{Y}} < \|(\bar{\lambda},\bar{\gamma})-(\lambda_k,\gamma_k)\|_{\tilde{Y}}$ *for all stepsize* s_k *such that:*

$$0 < s_k < \frac{2\left(g(\bar{\lambda},\bar{\gamma})-g(\lambda_k,\gamma_k)\right)}{\|f_1(x_k)\|^2_{l^2(\tilde{\Omega},M_2(\mathbb{R}))}+\|f_1(x_k)\|^4_{l^2(\tilde{\Omega},M_2(\mathbb{R}))}},$$

and $0<\epsilon_k<s_k$.

Proof. We have:

$$\begin{aligned}
&\|(\bar{\lambda},\bar{\gamma})-(\lambda_{k+1},\gamma_{k+1})\|^2_{\tilde{Y}} = \|\bar{\lambda}-\lambda_{k+1}\|^2_{l^2(\tilde{\Omega},M_2(\mathbb{R}))}+|\bar{\gamma}-\gamma_{k+1}|^2,\\
&= \|\bar{\lambda}-\lambda_k-s_kf_1(x_k)\|^2_{l^2(\tilde{\Omega},M_2(\mathbb{R}))}+\left|\bar{\gamma}-\gamma_k-\frac{(s_k+\epsilon_k)}{2}\|f_1(x_k)\|^2_{l^2(\tilde{\Omega},M_2(\mathbb{R}))}\right|^2,\\
&= \|\bar{\lambda}-\lambda_k\|^2_{l^2(\tilde{\Omega},M_2(\mathbb{R}))}-2s_k\left(\bar{\lambda}-\lambda_k,f_1(x_k)\right)_{l^2(\tilde{\Omega},M_2(\mathbb{R}))}+s_k^2\|f_1(x_k)\|^2_{l^2(\tilde{\Omega},M_2(\mathbb{R}))}\\
&+|\bar{\gamma}-\gamma_k|^2-(\bar{\gamma}-\gamma_k)(s_k+\epsilon_k)\|f_1(x_k)\|^2_{l^2(\tilde{\Omega},M_2(\mathbb{R}))}+\frac{(s_k+\epsilon_k)^2}{4}\|f_1(x_k)\|^4_{l^2(\tilde{\Omega},M_2(\mathbb{R}))},\\
&< \|\bar{\lambda}-\lambda_k\|^2_{l^2(\tilde{\Omega},M_2(\mathbb{R}))}-2s_k\left(\bar{\lambda}-\lambda_k,f_1(x_k)\right)_{l^2(\tilde{\Omega},M_2(\mathbb{R}))}+s_k^2\|f_1(x_k)\|^2_{l^2(\tilde{\Omega},M_2(\mathbb{R}))}\\
&+|\bar{\gamma}-\gamma_k|^2-(\bar{\gamma}-\gamma_k)s_k\|f_1(x_k)\|^2_{l^2(\tilde{\Omega},M_2(\mathbb{R}))}+\frac{(2s_k)^2}{4}\|f_1(x_k)\|^4_{l^2(\tilde{\Omega},M_2(\mathbb{R}))},
\end{aligned}$$

because $\|f_1(x_k)\|_{l^2(\tilde{\Omega},M_2(\mathbb{R}))}>0$ and $0<\epsilon_k<s_k$. We use the supergradient inequality:

$$g(\bar{\lambda},\bar{\gamma})-g(\lambda_k,\gamma_k)\le\left(\bar{\lambda}-\lambda_k,f_1(x_k)\right)_{l^2(\tilde{\Omega},M_2(\mathbb{R}))}+\frac{\bar{\gamma}-\gamma_k}{2}\|f_1(x_k)\|^2_{l^2(\tilde{\Omega},M_2(\mathbb{R}))},$$

in what precedes and get:

$$\begin{aligned}
&\|\bar{\lambda}-\lambda_{k+1}\|^2_{l^2(\tilde{\Omega},M_2(\mathbb{R}))}+|\bar{\gamma}-\gamma_{k+1}|^2\le\|\bar{\lambda}-\lambda_k\|^2_{l^2(\tilde{\Omega},M_2(\mathbb{R}))}+|\bar{\gamma}-\gamma_k|^2-2s_k(g(\bar{\lambda},\bar{\gamma})\\
&-g(\lambda_k,\gamma_k))+s_k^2(\|f_1(x_k)\|^2_{l^2(\tilde{\Omega},M_2(\mathbb{R}))}+\|f_1(x_k)\|^4_{l^2(\tilde{\Omega},M_2(\mathbb{R}))}).
\end{aligned}\tag{3.13}$$

Then for $0<s_k<\frac{2(g(\bar{\lambda},\bar{\gamma})-g(\lambda_k,\gamma_k))}{\|f_1(x_k)\|^2_{l^2(\tilde{\Omega},M_2(\mathbb{R}))}+\|f_1(x_k)\|^4_{l^2(\tilde{\Omega},M_2(\mathbb{R}))}}$ and $0<\epsilon_k<s_k$, we clearly have $\|\bar{\lambda}-\lambda_{k+1}\|^2_{l^2(\tilde{\Omega},M_2(\mathbb{R}))}+|\bar{\gamma}-\gamma_{k+1}|^2<\|\bar{\lambda}-\lambda_k\|^2_{l^2(\tilde{\Omega},M_2(\mathbb{R}))}+|\bar{\gamma}-\gamma_k|^2$. □

The following theorem proves the convergence for a specific stepsize.

Theorem 4.12 (adapted from [28, Theorem 9])**.** *Assume there exists a dual solution* $(\bar{\lambda},\bar{\gamma})$*. Let* (λ_k,γ_k) *be any iteration as defined in the previous theorem. Suppose that each new iteration* $(\lambda_{k+1},\gamma_{k+1})$ *is calculated for the stepwise* $s_k=\frac{g(\bar{\lambda},\bar{\gamma})-g(\lambda_k,\gamma_k)}{\|f_1(x_k)\|^2_{l^2(\tilde{\Omega},M_2(\mathbb{R}))}+\|f_1(x_k)\|^4_{l^2(\tilde{\Omega},M_2(\mathbb{R}))}}$ *and* $0<\epsilon_k<s_k$*, where* $\bar{g}=g(\bar{\lambda},\bar{\gamma})$ *denotes the optimal dual value. Then* $g(\lambda_k,\gamma_k)\to\bar{g}$.

Proof. By taking $s_k=\frac{\bar{g}-g(\lambda_k,\gamma_k)}{\|f_1(x_k)\|^2_{l^2(\tilde{\Omega},M_2(\mathbb{R}))}+\|f_1(x_k)\|^4_{l^2(\tilde{\Omega},M_2(\mathbb{R}))}}$ in the previous recurrence formulae, we have

$$\begin{aligned}
\|\bar{\lambda}-\lambda_{k+1}\|^2_{l^2(\tilde{\Omega},M_2(\mathbb{R}))}+|\bar{\gamma}-\gamma_k|^2&<\|\bar{\lambda}-\lambda_k\|^2_{l^2(\tilde{\Omega},M_2(\mathbb{R}))}+|\bar{\gamma}-\gamma_k|^2\\
&-\frac{(\bar{g}-g(\lambda_k,\gamma_k))^2}{\|f_1(x_k)\|^2_{l^2(\tilde{\Omega},M_2(\mathbb{R}))}+\|f_1(x_k)\|^4_{l^2(\tilde{\Omega},M_2(\mathbb{R}))}},
\end{aligned}$$

which can be rewritten as

$$(\bar{g} - g(\lambda_k, \gamma_k))^2 < \left(\|f_1(x_k)\|^2_{l^2(\tilde{\Omega},M_2(\mathbb{R}))} + \|f_1(x_k)\|^4_{l^2(\tilde{\Omega},M_2(\mathbb{R}))}\right)\left(\|\bar{\lambda} - \lambda_k\|^2_{l^2(\tilde{\Omega},M_2(\mathbb{R}))} + |\bar{\gamma} - \gamma_k|^2 - \|\bar{\lambda} - \lambda_{k+1}\|^2_{l^2(\tilde{\Omega},M_2(\mathbb{R}))} - |\bar{\gamma} - \gamma_{k+1}|^2\right).$$

It is obvious that the sequence $\left\{\|\bar{\lambda} - \lambda_k\|^2_{l^2(\tilde{\Omega},M_2(\mathbb{R}))} + |\bar{\gamma} - \gamma_k|^2\right\}$ is bounded below (by 0 for example) and according to the previous theorem, it is decreasing. So, $\left\{\|\bar{\lambda} - \lambda_k\|^2_{l^2(\tilde{\Omega},M_2(\mathbb{R}))} + |\bar{\gamma} - \gamma_k|^2\right\}$ is a convergent sequence. Thus $\lim_{k\to+\infty}\left[\|\bar{\lambda} - \lambda_k\|^2_{l^2(\tilde{\Omega},M_2(\mathbb{R}))} + |\bar{\gamma} - \gamma_k|^2 - \|\bar{\lambda} - \lambda_{k+1}\|^2_{l^2(\tilde{\Omega},M_2(\mathbb{R}))} - |\bar{\gamma} - \gamma_{k+1}|^2\right] = 0$. Furthermore, we can deduce from the previous result that (λ_k) is uniformly bounded.
On the other hand, $(\|f_1(x_k)\|^2_{l^2(\tilde{\Omega},M_2(\mathbb{R}))} + \|f_1(x_k)\|^4_{l^2(\tilde{\Omega},M_2(\mathbb{R}))})$ is bounded. Indeed, as x_k minimizes $L(x, \lambda_k, \gamma_k)$, from the proof of Theorem 4.8 (coercivity inequality),

$$\|f_1(x_k)\|^2_{l^2(\tilde{\Omega},M_2(\mathbb{R}))} \leq \left(L(x_k, \lambda_k, \gamma_k) + \frac{\mu(\lambda + 3\mu)}{2(\lambda + 2\mu)}NM + c_\epsilon\|\lambda_k\|^2_{l^2(\tilde{\Omega},M_2(\mathbb{R}))}\right)\frac{2}{\gamma_1 + 2\epsilon}.$$

and $L(x_k, \lambda_k, \gamma_k) = \min_{x\in X} L(x, \lambda_k, \gamma_k) \leq \sup_{(\lambda,\gamma)\in\tilde{Y}}\inf_{x\in X} L(x,\ \lambda, \gamma) = \sup(D) = \inf(DP) < +\infty$. Finally, $\|f_1(x_k)\|^2_{l^2(\tilde{\Omega},M_2(\mathbb{R}))}$ is bounded and so is $\|f_1(x_k)\|^4_{l^2(\tilde{\Omega},M_2(\mathbb{R}))}$. In conclusion $g(\lambda_k, \gamma_k) \xrightarrow[k\to+\infty]{} \bar{g}$. □

We can provide even more accurate results, namely convergence of the sequences of dual values based on prior related works by Burachik *et al.* dedicated to modified subgradient algorithm for dual problems via sharp augmented Lagrangian.

Lemma 4.11 (adapted from [8, Lemma 1])**.** *Considering the notations and definitions of Algorithm 2, the following statements are equivalent.*

1. $\sum_{k=1}^{+\infty} s_k\|f_1(x_k)\|_{l^2(\tilde{\Omega},M_2(\mathbb{R}))} < +\infty$ *and* $\sum_{k=1}^{+\infty}\frac{s_k+\epsilon_k}{2}\|f_1(x_k)\|^2_{l^2(\tilde{\Omega},M_2(\mathbb{R}))} < +\infty$.

2. (λ_k, γ_k) *is bounded.*

Proof. From Algorithm 2, we have $\gamma_{m+1} - \gamma_1 = \sum_{k=1}^{m}\frac{s_k+\epsilon_k}{2}\ \|f_1(x_k)\|^2_{l^2(\tilde{\Omega},M_2(\mathbb{R}))}$ and $\|\lambda_{m+1} - \lambda_1\|_{l^2(\tilde{\Omega},M_2(\mathbb{R}))} \leq \sum_{k=1}^{m} s_k\ \|f_1(x_k)\|_{l^2(\tilde{\Omega},M_2(\mathbb{R}))}$. Then it is obvious that the two assertions are equivalent. □

Theorem 4.13 (adapted from [8, Theorem 6])**.** *Let $\bar{g}$ be the optimal dual value (i.e. $\bar{g} = sup(D)$). Assume that (λ_k, γ_k) defined in Theorem 4.11 is bounded and that the*

step size s_k *satisfies* $s_k \geq \eta \frac{\bar{g}-g(\lambda_k,\gamma_k)}{\|f_1(x_k)\|^2_{l^2(\tilde{\Omega},M_2(\mathbb{R}))}+\|f_1(x_k)\|^4_{l^2(\tilde{\Omega},M_2(\mathbb{R}))}}$ *for a fixed* $\eta > 0$. *Then every accumulation point of* (λ_k, γ_k) *is a dual solution. In particular,* $S(D) \neq \emptyset$ *with* $S(D) = \left\{(\lambda,\gamma) \in \tilde{Y},\ g(\lambda,\gamma) = \sup_{(\tilde{\lambda},\tilde{\gamma})\in\tilde{Y}} g(\tilde{\lambda},\tilde{\gamma})\right\}$.

Proof. According to the previous result, as (λ_k, γ_k) is bounded, $\sum_{k=1}^{+\infty} s_k \|f_1(x_k)\|_{l^2(\tilde{\Omega},M_2(\mathbb{R}))} < +\infty$ and $\sum_{k=1}^{+\infty} \frac{s_k+\epsilon_k}{2} \|f_1(x_k)\|^2_{l^2(\tilde{\Omega},M_2(\mathbb{R}))} < +\infty$. Let $(\bar{\lambda},\bar{\gamma})$ be an accumulation point of the sequence (λ_k, γ_k) and let us denote by $\mathcal{K}$ the infinite set of indices such that $\lim_{\substack{k\in\mathcal{K}\\ k\to+\infty}} (\lambda_k,\gamma_k) = (\bar{\lambda},\bar{\gamma})$. According to the proof of Theorem 4.8, and (λ_k, γ_k) being bounded, the sequence (x_k) generated by the algorithm is bounded. We can assume that the whole sequence $(x_k)_{k\in\mathcal{K}}$ converges to some $\bar{x}$ otherwise we can extract a common subsequence. Let us first assume that $f_1(\bar{x}) = 0$. By definition of x_k, we have that $f_0(x_k) + (\lambda_k, f_1(x_k))_{l^2(\tilde{\Omega},M_2(\mathbb{R}))} + \frac{\gamma_k}{2}\|f_1(x_k)\|^2_{l^2(\tilde{\Omega},M_2(\mathbb{R}))} \leq f_0(x) + (\lambda_k, f_1(x))_{l^2(\tilde{\Omega},M_2(\mathbb{R}))} + \frac{\gamma_k}{2}\|f_1(x)\|^2_{l^2(\tilde{\Omega},M_2(\mathbb{R}))}$ for all $x \in X$ and for all $k \in \mathcal{K}$. Passing to the limit for $k \in \mathcal{K}$, $k \to +\infty$ in the previous expression yields $f_0(\bar{x}) + (\bar{\lambda}, f_1(\bar{x}))_{l^2(\tilde{\Omega},M_2(\mathbb{R}))} + \frac{\bar{\gamma}}{2}\|f_1(\bar{x})\|^2_{l^2(\tilde{\Omega},M_2(\mathbb{R}))} \leq f_0(x) + (\bar{\lambda}, f_1(x))_{l^2(\tilde{\Omega},M_2(\mathbb{R}))} + \frac{\bar{\gamma}}{2}\|f_1(x)\|^2_{l^2(\tilde{\Omega},M_2(\mathbb{R}))}$ for all $x \in X$. Hence $\bar{x} \in S(\bar{\lambda},\bar{\gamma})$ and thus $(\bar{\lambda},\bar{\gamma}) \in S(D)$ according to Theorem 4.9. Now, let us assume that $f_1(\bar{x}) \neq 0$. This fact together with $\sum_{k=1}^{+\infty} s_k \|f_1(x_k)\|_{l^2(\tilde{\Omega},M_2(\mathbb{R}))} < +\infty$ implies that the sequence $(s_k)_{k\in\mathcal{K}}$ converges to 0. Using also $s_k \geq \eta \frac{\bar{g}-g(\lambda_k,\gamma_k)}{\|f_1(x_k)\|^2_{l^2(\tilde{\Omega},M_2(\mathbb{R}))}+\|f_1(x_k)\|^4_{l^2(\tilde{\Omega},M_2(\mathbb{R}))}}$ for $k \in \mathcal{K}$, we conclude that the subsequence of dual values $(g(\lambda_k,\gamma_k))_{k\in\mathcal{K}}$ converges to $\bar{g}$. By upper semi-continuity of g, we have that $g(\bar{\lambda},\bar{\gamma}) \geq \limsup_{\substack{k\in\mathcal{K}\\ k\to+\infty}} g(\lambda_k,\gamma_k) = \bar{g}$. This shows that $g(\bar{\lambda},\bar{\gamma})$ has optimal functional value $\bar{g}$ and hence $(\bar{\lambda},\bar{\gamma}) \in S(D)$. □

We are now providing a pseudo-code for the algorithm whose legimity has been proved through the previous theorems.

4.5 Actual Augmented Lagrangian algorithm

In this section, we present the algorithm used to solve the discrete augmented Lagragian problem. It consists of an initialization step and a main step. The latter is divided into two parts: the segmentation step guiding the registration process and the registration step. It is done thanks to an alternating scheme solving successively the Euler-Lagrange equations in $\tilde{\varphi}$ and $\tilde{V}$.

1: [Initialization step]: same as the one for the quadratic penalty method except that we initialize here $(\lambda_0, \gamma_0) \in \tilde{Y}$ and do not select γ large enough.

2: [Main step]:

(i) Compute $\tilde{\Phi}$ as in the quadratic penalty algorithm.

(ii) For $k = 1, 2, \cdots, \zeta$, compute $(\tilde{\varphi}^k, \tilde{V}^k, \lambda_k, \gamma_k)$ the saddle point of the augmented Lagrangian function with $\tilde{\Phi}(., \bar{T}) = \tilde{\Phi}(., t_k)$, $t_\zeta = \bar{T}$, $\tilde{\Phi}(., t_\zeta)$ representing the object contained inside the Reference and $\Phi_{0,k} = \Phi_0 \circ \tilde{\varphi}_1 \circ \cdots \circ \tilde{\varphi}_{k-1}$, using a supergradient algorithm.

(a) Solve the Euler-Lagrange equation in $\tilde{\varphi}_{i,j}$ for each $(i,j) \in \{2, \ldots, N-1\} \times \{2, \ldots, M-1\}$: $\nu \delta_\varepsilon(\Phi_{0,k} \circ \tilde{\varphi}_{i,j}) \Big(H_\varepsilon(\Phi_{0,k} \circ \tilde{\varphi}_{i,j}) - H_\varepsilon(\tilde{\Phi}(., t_k)) \Big) \nabla \Phi_{0,k}\, (\tilde{\varphi}_{i,j})$ $+\gamma \begin{pmatrix} \mathrm{div}\tilde{V}_{1_{i,j}} \\ \mathrm{div}\tilde{V}_{2_{i,j}} \end{pmatrix} - \gamma_l \Delta \tilde{\varphi}_{i,j} + \begin{pmatrix} \mathrm{div}\lambda_{l1} \\ \mathrm{div}\lambda_{l2} \end{pmatrix} = 0$. To do so, we use an implicit Euler time stepping and an L^2 gradient flow algorithm.

(b) Solve the system of Euler-Lagrange equations in $\tilde{V}_{i,j}$ for each $(i,j) \in \{2, \ldots, N-1\} \times \{2, \ldots, M-1\}$:

$$
\begin{cases}
0 = 2\beta \Big(\|\tilde{V}_{i,j}\|^2 - \alpha \Big) \tilde{V}_{11_{i,j}} \Big(2H_\varepsilon(\|\tilde{V}_{i,j}\|^2 - \alpha) + (\|\tilde{V}_{i,j}\|^2 - \alpha) \\
\qquad \delta_\varepsilon(\|\tilde{V}_{i,j}\|^2 - \alpha) \Big) + \mu \tilde{V}_{22_{i,j}} (\det \tilde{V}_{i,j} - 2) + \gamma_l (\tilde{V}_{11_{i,j}} - \partial_x \tilde{\varphi}^1_{i,j}) + \lambda_{l11} \\
0 = 2\beta \Big(\|\tilde{V}_{i,j}\|^2 - \alpha \Big) \tilde{V}_{12_{i,j}} \Big(2H_\varepsilon(\|\tilde{V}_{i,j}\|^2 - \alpha) + (\|\tilde{V}_{i,j}\|^2 - \alpha) \\
\qquad \delta_\varepsilon(\|\tilde{V}_{i,j}\|^2 - \alpha) \Big) - \mu \tilde{V}_{21_{i,j}} (\det \tilde{V}_{i,j} - 2) + \gamma_l (\tilde{V}_{12_{i,j}} - \partial_y \tilde{\varphi}^1_{i,j}) + \lambda_{l12} \\
0 = 2\beta \Big(\|\tilde{V}_{i,j}\|^2 - \alpha \Big) \tilde{V}_{21_{i,j}} \Big(2H_\varepsilon(\|\tilde{V}_{i,j}\|^2 - \alpha) + (\|\tilde{V}_{i,j}\|^2 - \alpha) \\
\qquad \delta_\varepsilon(\|\tilde{V}_{i,j}\|^2 - \alpha) \Big) - \mu \tilde{V}_{12_{i,j}} (\det \tilde{V}_{i,j} - 2) + \gamma_l (\tilde{V}_{21_{i,j}} - \partial_x \tilde{\varphi}^2_{i,j}) + \lambda_{l21} \\
0 = 2\beta \Big(\|\tilde{V}_{i,j}\|^2 - \alpha \Big) \tilde{V}_{22_{i,j}} \Big(2H_\varepsilon(\|\tilde{V}_{i,j}\|^2 - \alpha) + (\|\tilde{V}_{i,j}\|^2 - \alpha) \\
\qquad \delta_\varepsilon(\|\tilde{V}_{i,j}\|^2 - \alpha) \Big) + \mu \tilde{V}_{11_{i,j}} (\det \tilde{V}_{i,j} - 2) + \gamma_l (\tilde{V}_{22_{i,j}} - \partial_y \tilde{\varphi}^2_{i,j}) + \lambda_{l22}
\end{cases}
$$

To do so, we use an L^2 gradient flow algorithm and a semi-implicit Euler time stepping scheme.

(c) Control of the Jacobian determinant, see Algorithm 4. Go back to (a) until convergence and set $x_l = (\tilde{\varphi}^l, \tilde{V}^l)$ after convergence.

(d) **if**: $\|f_1(x_l)\|^2_{l^2(\tilde{\Omega},M_2(\mathbb{R}))} \leq$ threshold **then**: stop and set $(\tilde{\varphi}^k, \tilde{V}^k, \lambda_k, \gamma_k) = (\tilde{\varphi}^l, \tilde{V}^l, \lambda_l, \gamma_l)$.
else: go on to the next step.

(e) Update $\lambda_l = \lambda_l + s_l f_1(x_l)$ and $\gamma_l = \gamma_l + \frac{s_l+\epsilon_l}{2}\|f_1(x_l)\|^2_{l^2(\tilde{\Omega},M_2(\mathbb{R}))}$, with $s_l = \frac{\bar{g}-g(\lambda_l,\gamma_l)}{\|f_1(x_l)\|^2_{l^2(\tilde{\Omega},M_2(\mathbb{R}))}+\|f_1(x_l)\|^4_{l^2(\tilde{\Omega},M_2(\mathbb{R}))}}$ and $\epsilon_l = 0.95 s_l$. $\bar{g}$ is approximated by assessing functional in (DP) with $\tilde{\varphi} = \mathrm{Id}$ and $\tilde{V} = (I_2)^{N\times M}$ since $\sup(D) = \inf(DP)$.

(f) Go back to (a).

Algorithm 3: A topology preserving segmentation guided registration model- Augmented Lagrangian Method.

We now provide some numerical experiments.

5 Numerical Experiments

We first make the parameters we use in practice more explicit. Function H_ε is taken to be $H_\varepsilon : z \mapsto \frac{1}{2}\left(1 + \frac{2}{\pi}\arctan\left(\frac{z}{\varepsilon}\right)\right)$ ($\varepsilon = 1$ in practice) and $\tilde{g} : z \mapsto \frac{1}{1+cz^2}$. For the sake of reproducibility, we provide the values of the tuning parameters in the discretization of the evolution equation. The time step is set to 0.5, parameter c of the edge detector function is between 1 and 5, parameter k is between -0.15 and 0.2, —negative value for inflating and positive value for deflating —, l is set to 1, μ' to 0.2, d to 4.0 and the size of the window to compute the topological constraint is 5×5.
As for the functional minimization problem, both methods - straight quadratic penalization and augmented Lagrangian method - have been investigated and produce similar results. In the proposed supergradient algorithm (augmented Lagrangian method), γ_1 is set to 80000, while in the purely quadratic penalty method, parameter γ is set to this same value and is not increased in practice during the algorithm. As we searched for a suitable trade-off between quality of the obtained results and readability/smaller computational cost, which, we believe, is what prevails in the numerical simulation setting, we did not investigate further, in the numerical simulations, the augmented Lagrangian method. The results presented below are the ones obtained by the purely quadratic penalty method.

5.1 Regridding technique and choice of the parameters

The deformation must remain physically and mechanically meaningful, and reflect material properties: self-penetration of the matter (indicating that the transformation is not injective) should be prohibited. The penalty term $(\det \nabla\varphi - 1)^2$ does not guarantee that the Jacobian determinant remains positive. That is the reason why we have implemented the regridding algorithm proposed by Christensen and his collaborators in [11] to ensure the positivity of the Jacobian. For the sake of completeness, we summarize the outlines

of the regridding algorithm.

1. If at stage $k \in \{1, \cdots, \zeta\}$ and at discrete time t_{q+1} in the L^2 gradient flow method, $\min_{i,j} \det \nabla \tilde{\varphi}_{i,j}^{q+1} < tol$:
   - regrid_count=regrid_count+1
   - $\Phi_{0,k} = \Phi_{0,k} \circ \tilde{\varphi}_{i,j}^{q}$
   - save $tab_\varphi(regrid_count) = \tilde{\varphi}^q$, $\tilde{\varphi}^{q+1} = \mathrm{Id}$, $\tilde{V}^{q+1} = I$
   - continue loop in q
2. At the end of stage k, if regrid_count>0
   $\tilde{\varphi}^k = tab_\varphi(1) \circ \cdots \circ tab_\varphi(\text{regrid_count})$

Algorithm 4: Regridding step.

For each pair, we provide the Reference image together with the zero level line of $\tilde{\Phi}$ at time $\bar{T}$, the Template image, the intermediate segmentation steps that serve as inputs —if any —, the obtained deformed Template, that is to say $T \circ \varphi$, the deformed grid associated with φ (Reference to Template, straightforwardly given by φ) and the deformed grid associated with φ^{-1} (Template to Reference, computed using interpolation techniques).
For all applications, the ranges of the parameters are the same. Parameter ν balancing the L^2-fidelity term is around 100000, while the Lamé coefficient λ is set to 10. The Lamé coefficient μ is between 1500 and 8000. It is the shear modulus, that is to say that μ measures the resistance of the material.
From our experience, the parameter that proves to be the most sensitive is the Lamé parameter μ. It can be seen as a measure of rigidity. The greater parameter μ is, the more rigid the deformation is (which can be relevant if we aim to obtain a smooth and topology-preserving deformation map). The issue is thus to find a proper trade-off between accurate image alignment (which means authorizing large deformations) and topology or orientation preservation (which means monitoring the Jacobian determinant by limiting shrinkage and growth).

5.2 Letter C

First, the method is applied on an academic example (Figure 3.2) taken from [12] for mapping a disk to the letter C, demonstrating the ability of the algorithm to handle large deformations. Note that with linear elasticity model, diffusion model or curvature-based model, registration cannot be successfully accomplished (see [42]). As in [12], the right part of the disk is stretched into the shape of the interior edge of the letter C, and then moves outward to align the interior boundary of the letter C. Nevertheless, our deformation field is smoother (see in particular [12, p. 88]). In [9], the authors also apply their method on a similar example. We can notice that the deformed Template cannot reach the end of the hollow of the C, while our method handles very well deep concavities. At last, compared

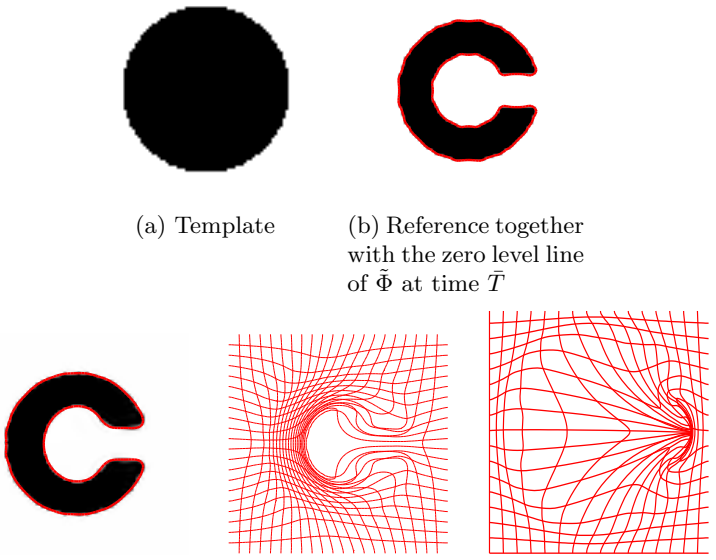

(a) Template

(b) Reference together with the zero level line of $\tilde{\Phi}$ at time $\bar{T}$

(c) Deformed Template $T \circ \varphi$ with the zero level line of $\Phi_0 \circ \varphi$

(d) Deformed grid: Template to Reference

(e) Deformed grid: Reference to Template

Figure 3.2: **Mapping of a disk to letter C**. $\min \det \nabla\varphi = 4.7\,10^{-4}$, $\max \det \nabla\varphi = 4.04$. $\lambda = 10$, $\mu = 8000$, $\nu = 150000$.

to [38], the algorithm requires fewer regridding corrections (3 versus 4 in [38]) and the range of the Jacobian determinant is smaller.

5.3 Mouse brain gene expression data

Then the method was applied on medical images (Figure 3.3) with the goal to map a 2D slice of mouse brain gene expression data (Template T) to its corresponding 2D slice of the mouse brain atlas, in order to facilitate the integration of anatomic, genetic and physiologic observations from multiple subjects in a common space. Since genetic mutations and knock-out strains of mice provide critical models for a variety of human diseases, such linkage between genetic information and anatomical structure is important. The data are provided by the Center for Computational Biology, UCLA. The mouse atlas acquired from the LONI database was pre-segmented. The gene expression data were segmented manually to facilitate data processing in other applications. Some algorithms have been developed to automatically segment the brain area of gene expression data. The non-brain regions have been removed to produce better matching. Our method qualitatively performs as the one in [39] and produces a smooth deformation field. Compared to the results obtained in [38], [39] or [21], the deformation grid is more regular and does not exhibit shrinkage or growth. For instance, for Figure 3.3, the Jacobian determinants mass more around the value 1 (range [0.54,2.24]) versus [0.28,2.09] in [38], [0.15,2.40] in [39] or [0.09,2.47] in [21].

(a) Template

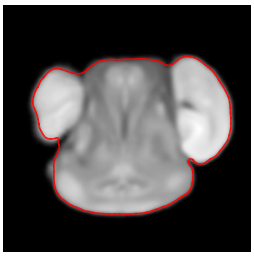

(b) Reference together with the zero level line of $\tilde{\Phi}$ at time $\bar{T}$

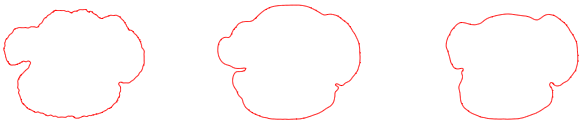

(c) Input: intermediate segmentation results; left: zero level line of $\Phi_0 = \tilde{\Phi}(\cdot, 0)$; middle: zero level line of $\tilde{\Phi}(\cdot, t_1)$; right: zero level line of $\tilde{\Phi}(\cdot, t_2 = \bar{T})$.

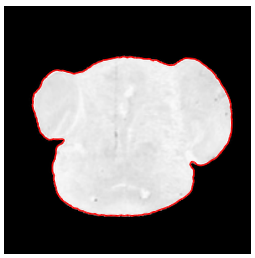

(d) Deformed Template $T \circ \varphi$ with the zero level line of $\Phi_0 \circ \varphi$

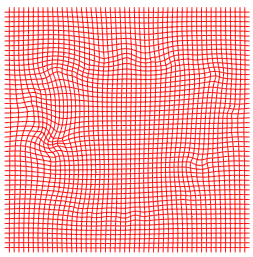

(e) Deformed grid: Template to Reference

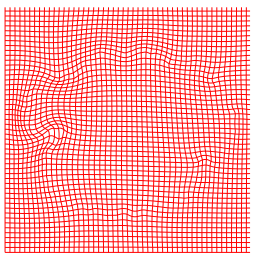

(f) Deformed grid: Reference to Template

Figure 3.3: **Mapping of a 2D slice of mouse brain gene expression data to its counterpart in an atlas**. $\min \det \nabla\varphi = 0.54, \max \det \nabla\varphi = 2.24$. $\lambda = 10$, $\mu = 5000$, $\nu = 100000$.

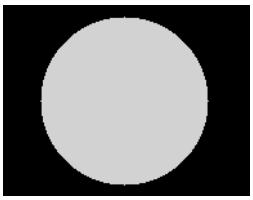

(a) Template

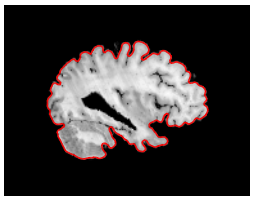

(b) Reference together with the zero level line of $\tilde{\Phi}$ at time $\bar{T}$

(c) Input: intermediate segmentation results; from left to right: zero level line of $\Phi_0 = \tilde{\Phi}(\cdot, 0)$, $\tilde{\Phi}(\cdot, t_1)$, $\tilde{\Phi}(\cdot, t_2)$, $\tilde{\Phi}(\cdot, t_3)$ and $\tilde{\Phi}(\cdot, t_4 = \bar{T})$.

(d) Deformed Template $T \circ \varphi$ with the zero level line of $\Phi_0 \circ \varphi$

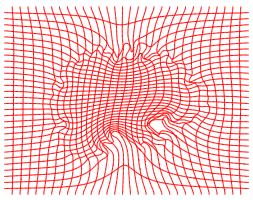

(e) Deformed grid: Template to Reference

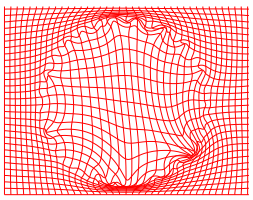

(f) Deformed grid: Reference to Template

(g) Obtained deformed Template when no intermediate segmentation step is included, same parameters

Figure 3.4: **Mapping of a disk to a slice of a brain**. $\min \det \nabla\varphi = 0.079, \max \det \nabla\varphi = 3.07$. $\lambda = 10$, $\mu = 5000$, $\nu = 120000$.

5.4 Slices of the brain

The method has also been applied to complex slices of brain data (Figure 3.4) (courtesy of Laboratory Of Neuro-Imaging, UCLA). We aim to register a disk to the slice of brain with topology preservation to demonstrate the ability of the algorithm to handle complex topologies. The results are very satisfactory on these examples since the deformed Template matches very well the convolutions of the brain. Remark that including intermediate segmentation steps improves the accuracy of the result. At last, the additional topology constraint in the active contour model allows for the delineation of the thin concavities on the Reference image.

5.5 MRI images of cardiac cycle

Numerical simulations on MRI images of a patient cardiac cycle have been carried out (Figs. 3.5,3.6). We were supplied with a whole cardiac MRI examination of a patient (courtesy of the LITIS, University of Rouen, France). It is made of 280 images divided

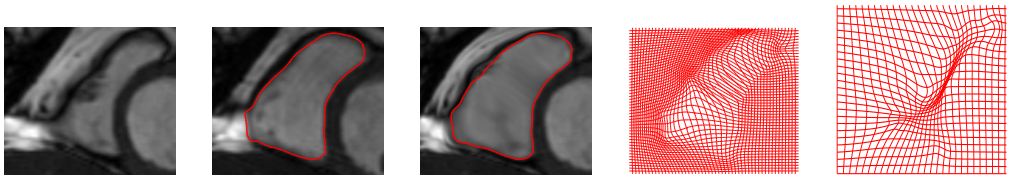

(a) Template (b) Reference together with the zero level line of $\tilde{\Phi}$ at time $\bar{T}$ (c) Deformed Template $T \circ \varphi$ with the zero level line of $\Phi_0 \circ \varphi$ (d) Deformed grid: Template to Reference (e) Deformed grid: Reference to Template

Figure 3.5: **Mapping of MRI images. Reference corresponding to end diastole (ED) and Template corresponding to end systole (ES) of a same sequence**. $\min \det \nabla\varphi = 0.05, \max \det \nabla\varphi = 2.8$. $\lambda = 10$, $\mu = 1500$, $\nu = 100000$.

into 14 levels of slice and 20 images per cardiac cycle. The numbering of the images goes from 0 to 279, and includes both the slice number and the time index. The image 0 is set at the upper part of the heart and the sequence from image 0 to image 19 contains the whole cardiac cycle for this slice. The sequence from images 20 to 39 contains the whole cardiac cycle for the slice underneath the previous one and so on. A cardiac cycle is composed of a contraction phase (40% of the cycle duration), followed by a dilation phase (60% of the cycle duration). The first image of the sequence (frames 0, 20, 40, etc.) is when the heart is most dilated (end diastole - ED) and the 8^{th} of the sequence (end systole - ES) is when the heart is most contracted. It thus seemed relevant, in order to assess the accuracy of the proposed algorithm in handling large deformations, to register a pair of the type: Reference corresponding to end diastole (ED), that is the first image of a sequence, and Template corresponding to end systole (ES), that is the 8^{th} frame of the same sequence. One interest of the proposed algorithm (due to the intrinsic modelling) is that we can focus on the desired target, here the heart, without taking into account the surrounding region. At last, to assess the inverse consistency, we switched the role of the Template and the Reference.

5.6 Tumor

Finally, the algorithm has been tested on brain tumor images (Figure 3.7) taken at different times in order to highlight the ability of the model to handle complex topologies with thin tubes and concavities.

6 Conclusion

This work intended to intertwine segmentation and registration in a single framework including geometrical and topological considerations, and motivated by the fact that shape matching contributes to increase the reliability of the registration process. To overcome the usual limitation of registration models, namely the inability to generate large deformations,

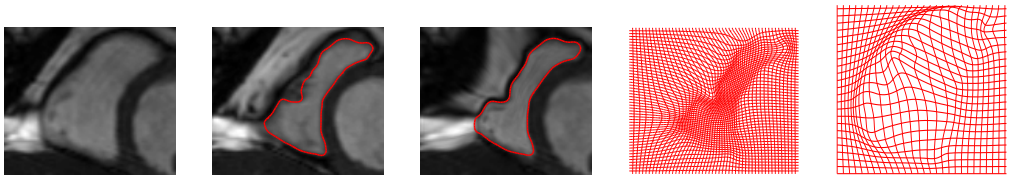

(a) Template (b) Reference together with the zero level line of $\tilde{\Phi}$ at time $\bar{T}$ (c) Deformed Template $T \circ \varphi$ with the zero level line of $\Phi_0 \circ \varphi$ (d) Deformed grid: Template to Reference (e) Deformed grid: Reference to Template

Figure 3.6: **Mapping of MRI images. Reference corresponding to end systole (ES) and Template corresponding to end diastole (ED) of a same sequence**. $\min \det \nabla\varphi = 0.016, \max \det \nabla\varphi = 2.83$. $\lambda = 10$, $\mu = 1500$, $\nu = 100000$.

the nonlinear-elasticity-based framework has been adopted by viewing the shapes to be matched as Saint Venant-Kirchhoff materials. New perspectives have been enlarged, in particular, the explicit introduction of the dynamics in the modelling (instead of a sampled-in-time problem) yielding to a minimization problem defined on a Sobolev space of Banach-space-valued functions, as well as a joint model with mutual influence of segmentation and registration (instead of a segmentation-guided registration problem) that inherits fine theoretical properties in the context of the viscosity solution theory.

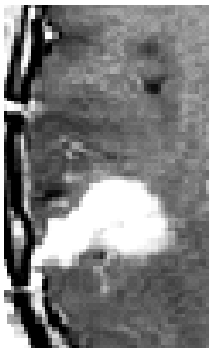

(a) Template

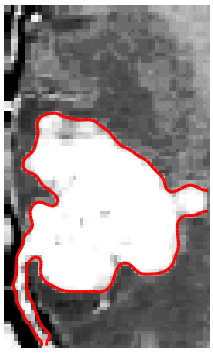

(b) Reference together with the zero level line of $\tilde{\Phi}$ at time $\bar{T}$

(c) Input: intermediate segmentation results; from left to right: zero level line of $\Phi_0 = \tilde{\Phi}(\cdot, 0)$, $\tilde{\Phi}(\cdot, t_1)$, $\tilde{\Phi}(\cdot, t_2)$ and $\tilde{\Phi}(\cdot, t_3 = \bar{T})$.

(d) Deformed Template $T \circ \varphi$ with the zero level line of $\Phi_0 \circ \varphi$

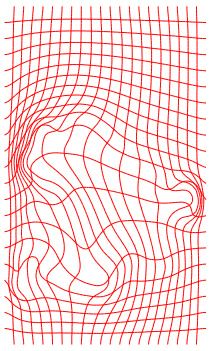

(e) Deformed grid: Template to Reference

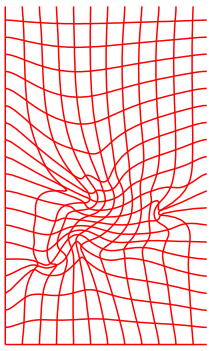

(f) Deformed grid: Reference to Template

Figure 3.7: **Mapping of brain tumor images**. $\min \det \nabla\varphi = 0.09, \max \det \nabla\varphi = 4.2$. $\lambda = 10$, $\mu = 5000$, $\nu = 150000$.

Bibliography

[1] L. Ambrosio and G. Dal Maso, *A general chain rule for distributional derivatives*, Proceedings of the American Mathematical Society, 108 (1990), pp. 691–702.

[2] J.-H. An, Y. Chen, F. Huang, D. Wilson, and E. Geiser, *Medical Image Computing and Computer-Assisted Intervention – MICCAI 2005: 8th International Conference, Palm Springs, CA, USA, October 26-29, 2005, Proceedings, Part I*, Springer Berlin Heidelberg, 2005, ch. A Variational PDE Based Level Set Method for a Simultaneous Segmentation and Non-Rigid Registration, pp. 286–293.

[3] J. Ashburner and K. J. Friston, *Nonlinear spatial normalization using basis functions*, Human brain mapping, 7 (1999), pp. 254–266.

[4] G. Aubert and P. Kornprobst, *Mathematical Problems in Image Processing: Partial Differential Equations and the Calculus of Variations*, Applied Mathematical Sciences, Springer-Verlag, 2001.

[5] M. Beg, M. Miller, A. Trouvé, and L. Younes, *Computing Large Deformation Metric Mappings via Geodesic Flows of Diffeomorphisms*, International Journal of Computer Vision, 61 (2005), pp. 139–157.

[6] H. Brezis, *Analyse fonctionelle. Théorie et Applications*, Dunod, Paris, 2005.

[7] C. Broit, *Optimal Registration of Deformed Images*, PhD thesis, Computer and Information Science, University of Pennsylvania, 1981.

[8] R. S. Burachik, R. N. Gasimov, N. A. Ismayilova, and C. Y. Kaya, *On a modified subgradient algorithm for dual problems via sharp augmented Lagrangian*, Journal of Global Optimization, 34 (2005), pp. 55–78.

[9] M. Burger, J. Modersitzki, and L. Ruthotto, *A hyperelastic regularization energy for image registration*, SIAM Journal on Scientific Computing, 35 (2013), pp. B132–B148.

[10] V. Caselles, R. Kimmel, and G. Sapiro, *Geodesic Active Contours*, Int. J. Comput. Vis., 22 (1993), pp. 61–87.

[11] G. Christensen, R. Rabbitt, and M. Miller, *Deformable Templates Using Large Deformation Kinematics*, IEEE Trans. Image Process., 5 (1996), pp. 1435–1447.

[12] G. E. Christensen, *Deformable shape models for anatomy*, PhD thesis, Washington University, Sever Institute of technology, USA, 1994.

[13] P. Ciarlet, *Elasticité Tridimensionnelle*, Masson, 1985.

[14] P. Ciarlet, *Mathematical Elasticity, Volume I: Three-dimensional elasticity*, Amsterdam etc., North-Holland, 1988.

[15] O. Clatz, M. Sermesant, P.-Y. Bondiau, H. Delingette, S. K. Warfield, G. Malandain, and N. Ayache, *Realistic simulation of the 3-D growth of brain tumors in MR images coupling diffusion with biomechanical deformation*, Medical Imaging, IEEE Transactions on, 24 (2005), pp. 1334–1346.

[16] M. Crandall, H. Ishii, and P.-L. Lions, *User's Guide to Viscosity Solutions of Second Order Partial Differential Equations*, Bull. Amer. Math. Soc., 27 (1992), pp. 1–67.

[17] B. Dacorogna, *Direct Methods in the Calculus of Variations, Second Edition*, Springer, 2008.

[18] C. Davatzikos, *Spatial transformation and registration of brain images using elastically deformable models*, Computer Vision and Image Understanding, 66 (1997), pp. 207–222.

[19] M. H. Davis, A. Khotanzad, D. P. Flamig, and S. E. Harms, *A physics-based coordinate transformation for 3-D image matching*, Medical Imaging, IEEE Transactions on, 16 (1997), pp. 317–328.

[20] F. Demengel, G. Demengel, and R. Erné, *Functional Spaces for the Theory of Elliptic Partial Differential Equations*, Universitext, Springer London, 2012.

[21] R. Derfoul and C. Le Guyader, *A relaxed problem of registration based on the Saint Venant-Kirchhoff material stored energy for the mapping of mouse brain gene expression data to a neuroanatomical mouse atlas*, SIAM Journal on Imaging Sciences, 7 (2014), pp. 2175–2195.

[22] M. Droske, W. Ring, and M. Rumpf, *Mumford–Shah based registration: a comparison of a level set and a phase field approach*, Computing and Visualization in Science, 12 (2008), pp. 101–114.

[23] M. Droske and M. Rumpf, *A Variational Approach to Non-Rigid Morphological Registration*, SIAM J. Appl. Math., 64 (2004), pp. 668–687.

[24] M. Droske and M. Rumpf, *Multiscale Joint Segmentation and Registration of Image Morphology*, Pattern Analysis and Machine Intelligence, IEEE Transactions on, 29 (2007), pp. 2181–2194.

[25] B. Fischer and J. Modersitzki, *Fast diffusion registration*, AMS Contemporary Mathematics, Inverse Problems, Image Analysis, and Medical Imaging, 313 (2002), pp. 11–129.

[26] B. Fischer and J. Modersitzki, *Curvature based image registration*, J. Math. Imaging Vis., 18 (2003), pp. 81–85.

[27] N. Forcadel and C. Le Guyader, *A short time existence/uniqueness result for a nonlocal topology-preserving segmentation model*, Journal of Differential Equations, 253 (2012), pp. 977–995.

[28] R. N. Gasimov, *Augmented Lagrangian duality and nondifferentiable optimization methods in nonconvex programming*, Journal of Global Optimization, 24 (2002), pp. 187–203, http://dx.doi.org/10.1023/A:1020261001771.

[29] A. Gooya, K. Pohl, M. Bilello, L. Cirillo, G. Biros, E. Melhem, and C. Davatzikos, *GLISTR: Glioma Image Segmentation and Registration*, Medical Imaging, IEEE Transactions on, 31 (2012), pp. 1941–1954.

[30] S. Gorthi, V. Duay, X. Bresson, M. B. Cuadra, F. J. S. Castro, C. Pollo, A. S. Allal, and J.-P. Thiran, *Active deformation fields: Dense deformation field estimation for atlas-based segmentation using the active contour framework*, Medical Image Analysis, 15 (2011), pp. 787–800.

[31] E. Haber, S. Heldmann, and J. Modersitzki, *A computational framework for image-based constrained registration*, Linear Algebra and its Applications, 431 (2009), pp. 459–470. Special Issue in honor of Henk van der Vorst.

[32] E. Haber and J. Modersitzki, *Numerical methods for volume preserving image registration*, Inverse Probl., 20 (2004), pp. 1621–1638.

[33] E. Haber and J. Modersitzki, *Image registration method with guaranteed displacement regularity*, Int. J. Comput. Vision, 71 (2007), pp. 361–372.

[34] H. Hardy, G., E. Littlewood, J., and G. Pólya, *Inequalities*, University Press Cambridge, 1952.

[35] B. Karaçali and C. Davatzikos, *Estimating topology preserving and smooth displacement fields*, IEEE Trans. Med. Imag., 23 (2004), pp. 868–880.

[36] H. Le Dret and A. Raoult, *The quasi-convex envelope of the Saint Venant-Kirchhoff stored energy function.*, Proceedings of the Royal Society of Edinburgh: Section A Mathematics, 125 (1995), pp. 1179–1192.

[37] C. Le Guyader and L. Vese, *Self-Repelling Snakes for Topology-Preserving Segmentation Models*, Image Processing, IEEE Transactions on, 17 (2008), pp. 767–779.

[38] C. Le Guyader and L. Vese, *A combined segmentation and registration framework with a nonlinear elasticity smoother*, Computer Vision and Image Understanding, 115 (2011), pp. 1689–1709.

[39] T. Lin, C. Le Guyader, I. Dinov, P. Thompson, A. Toga, and L. Vese, *Gene Expression Data to Mouse Atlas Registration Using a Nonlinear Elasticity Smoother and Landmark Points Constraints*, J. Sci. Comput., 50 (2012), pp. 586–609.

[40] N. Lord, J. Ho, B. Vemuri, and S. Eisenschenk, *Simultaneous Registration and Parcellation of Bilateral Hippocampal Surface Pairs for Local Asymmetry Quantification*, IEEE Trans. Med. Imaging, 26 (2007), pp. 471–478.

[41] S. Mitrinovic, D., *Analytic Inequalities*, Die Grundlehren der mathematischen Wissenschaften, Springer-Verlag, 1970.

[42] J. Modersitzki, *Numerical Methods for Image Registration*, Oxford University Press, 2004.

[43] O. Musse, F. Heitz, and J.-P. Armspach, *Topology preserving deformable image matching using constrained hierarchical parametric models*, IEEE Trans. Image Process., 10 (2001), pp. 1081–1093.

[44] P. Negrón Marrero, *A numerical method for detecting singular minimizers of multidimensional problems in nonlinear elasticity*, Numerische Mathematik, 58 (1990), pp. 135–144.

[45] V. Noblet, C. Heinrich, F. Heitz, and J.-P. Armspach, *3-D deformable image registration: a topology preservation scheme based on hierarchical deformation models and interval analysis optimization*, IEEE Trans. Image Process., 14 (2005), pp. 553–566.

[46] S. Ozeré, *Modélisation mathématique de problèmes relatifs au recalage d'images*, PhD thesis, 2015. Thèse de doctorat dirigée par Gout, Christian et Le Guyader, Carole Mathématiques Rouen, INSA 2015.

[47] S. Ozeré, C. Gout, and C. Le Guyader, *Joint Segmentation/Registration Model by Shape Alignment via Weighted Total Variation Minimization and Nonlinear Elasticity*, SIAM Journal on Imaging Sciences, 8 (2015), pp. 1981–2020.

[48] S. Ozeré and C. Le Guyader, *Scale Space and Variational Methods in Computer Vision: 5th International Conference, SSVM 2015, Lège-Cap Ferret, France, May 31 - June 4, 2015, Proceedings*, Springer International Publishing, Cham, 2015, ch. Nonlocal Joint Segmentation Registration Model, pp. 348–359.

[49] S. Ozeré and C. Le Guyader, *Topology preservation for image-registration-related deformation fields*, Communications in Mathematical Sciences, 13 (2015), pp. 1135–1161.

[50] R. Rabbitt, J. Weiss, G. Christensen, and M. Miller, *Mapping of Hyperelastic Deformable Templates Using the Finite Element Method*, in Proceedings SPIE, vol. 2573, SPIE, 1995, pp. 252–265.

[51] T. Rockafellar, R., *Lagrange multipliers and optimiality*, SIAM, 35 (1993), pp. 183–238.

[52] M. Rumpf and B. Wirth, *A Nonlinear Elastic Shape Averaging Approach*, SIAM Journal on Imaging Sciences, 2 (2009), pp. 800–833.

[53] T. Sederberg and S. Parry, *Free-form Deformation of Solid Geometric Models*, SIGGRAPH Comput. Graph., 20 (1986), pp. 151–160.

[54] A. Sotiras, C. Davatzikos, and N. Paragios, *Deformable medical image registration: A survey*, Medical Imaging, IEEE Transactions on, 32 (2013), pp. 1153–1190.

[55] B. Vemuri, J. Ye, Y. Chen, and C. Leonard, *Image Registration via level-set motion: Applications to atlas-based segmentation*, Medical Image Analysis, 7 (2003), pp. 1–20.

[56] L. Vese and C. Le Guyader, *Variational Methods in Image Processing*, Chapman & Hall/CRC Mathematical and Computational Imaging Sciences Series, Taylor & Francis, 2015.

[57] J. Weickert and G. Kühne, *Geometric Level Set Methods in Imaging, Vision, and Graphics*, Springer New York, 2003, ch. Fast Methods for Implicit Active Contour Models, pp. 43–57.

[58] C. Wing-Sum, *Some discrete Poincaré-type inequalities*, International Journal of Mathematics and Mathematical Sciences, 25 (2001), pp. 479–488.

[59] B. Wirth, L. Bar, M. Rumpf, and G. Sapiro, *A continuum mechanical approach to geodesics in shape space*, International Journal of Computer Vision, 93 (2011), pp. 293–318.

[60] I. Yanovsky, P. M. Thompson, S. Osher, and A. D. Leow, *Topology preserving log-unbiased nonlinear image registration: Theory and implementation*, in Proc. IEEE Conf. Comput. Vis. Pattern Recognit., 2007, pp. 1–8.

[61] A. Yezzi, L. Zollei, and T. Kapur, *A variational framework for joint segmentation and registration*, in Mathematical Methods in Biomedical Image Analysis, IEEE-MMBIA, 2001, pp. 44–51.

[62] L. Zagorchev and A. Goshtasby, *A comparative study of transformation functions for nonrigid image registration*, Image Processing, IEEE Transactions on, 15 (2006), pp. 529–538.

Chapter 4

A nonlocal joint segmentation/registration model

Segmentation and registration are cornerstone steps of many imaging situations: while segmentation aims to identify relevant constituents of an image for visualization or quantitative analysis, registration consists of mapping salient features of an image onto the corresponding ones in another. Instead of treating these tasks linearly one after another, so without correlating them, we propose a unified variational model, in a hyperelasticity setting, processing these two operations simultaneously. The dissimilarity measure relates local and global (or region-based) information, since relying on weighted total variation and nonlocal shape descriptors inspired by the piecewise constant Mumford-Shah model. Theoretical results emphasizing the mathematical and practical soundness of the model are provided, among which existence of minimizers, connection with the segmentation step, nonlocal characterization of weighted semi-norms, asymptotic results and Γ-convergence properties.

1 Introduction

Segmentation and registration are preprocessing steps that prove to be fundamental requirements in many image processing chains: images need to be registered to one another, which means determining an optimal diffeomorphic transformation (or deformation) φ that aligns the structures visible in an image into the corresponding ones in the other, then segmented, that is, partitioned into meaningful constituents in order to identify structures such as homogeneous regions or edges, yielding an accurate quantitative and joint analysis of them. Each step encompasses a large variety of methodologies (see [7, Chapter 4] for instance or [60, Part II], for a relevant analysis of the segmentation problem, and [45], [46], [57] for the registration counterpart) and one might think as a first attempt to address these issues to proceed linearly, one stage after another, without correlating both tasks, which in practice may propagate errors from step to step. Yet, as structure/salient component/shape/geometrical feature matching and intensity distribution comparison rule registration, combining the segmentation and registration tasks into a single framework

sounds relevant. First, the registration operation can be seen as the incorporation of prior information to guide the segmentation process. This allows to overcome the difficulty of weak boundary definition resulting from the amalgamation of several factors such as noise sources in the acquisition device, degradation of the image content during the reconstruction process, or artifacts ([4, Subsection 2.3]). Second, accurate segmented structures allow to drive the registration process correctly, providing then a reliable deformation between the encoded structures, not only based on intensity distribution comparison but also on geometrical and topological features. The primary scope of this chapter is thus to define a suitable joint segmentation/registration model addressed with variational techniques. A difficulty relies in the complexity of the formulation that is generally underconstrained and that involves nonlinearity and non-convexity. If we focus on the registration problem alone for instance, the deformation we aim to reconstruct is usually viewed as a minimal argument (uniqueness defaults in general) of a specifically designed cost function that takes on a versatile appearance according to the desired application and to the nature of the observations ([57]). When the images have been acquired by different modalities, the quality of registration is no longer measured by intensity distribution alignment, but by the assessment of shape, salient component and geometric feature matching, while preserving the modality of each image of the pair. Also, several stances can be adopted to describe the setting in which the objects to be matched are interpreted and viewed (physical models —[11], [17], [18], [21], [26], [30], [32], [35], [42], [49], [54] —, purely geometric ones —[5], [28], [55], [63] —, models including a priori knowledge ([24]), depending on the assumption regarding the properties of the deformation to be recovered) and to devise the measure of alignement (that is, how the available data are exploited to drive the registration process), increasing thus the complexity of the problem. In order to make our model flexible, capable of handling large deformations and reliable in terms of matching quality of the structures encoded in the pair of images, we propose, within the hyperelastic framework, meeting these goals by devising an original dissimilarity measure. It is grounded in weighted total variation (ensuring edge mapping) and in a region-based criterion (inspired by the piecewise constant Mumford-Shah model [47]), so combining local and nonlocal structure comparison. More precisely, the novelty of this work rests upon: (i) an original modelling involving the stored energy function of a Saint Venant-Kirchhoff material, weighted total variation and a region-based criterion; (ii) the introduction of a relaxed problem for which theoretical results are provided; (iii) the derivation of a numerical method of resolution based on the approximation of the weighted total variation by a sequence of integral operators involving a differential quotient, a suitable sequence of radial mollifiers and on a splitting approach leading to Γ-convergence results. This work falls within the continuation of [49] but includes novel aspects both in the modelling (with the integration of a region-based criterion entailing substantial modifications in the mathematical proofs) and more importantly (this is the core of this chapter), in the design of the algorithm (introduction of a nonlocal operator). This latter part required non straightforward extensions of prior related results by Bourgain *et al.* [14], Dávila [27], Ponce [52], and Spector [58] dedicated to new characterizations of semi-norms on Sobolev spaces $W^{1,p}(\Omega)$ or on the space of functions of bounded variation $BV(\Omega)$ to weighted such semi-norms, which takes on various connotations, from theoretical considerations to computational aspects.

The loss of symmetry implies in particular, a substantial mathematical development in the proofs. In addition to its theoretical justification, this modelling yields more accurate segmentation and registration results in comparison to [49] (exemplified in Table 4.1 and Figure 4.2 for instance, empirically/visually, and by computing comparison criteria such as the Dice coefficient ([31]) to assess segmentation and registration accuracy), and also a decomposition of the Reference into a simplified version and an oscillatory part (so achieving decomposition of the Reference image in addition to registration and segmentation in a single framework). Nonlocality thus appears at two levels: in the region-based fidelity term and in the treatment of the weighted total variation. Before depicting in depth our model, we would like to point out that prior related works suggest to jointly perform segmentation and registration: [62], [59] (in a level set framework), [42] (registration is achieved using the transfer of edges based on the active contour model without edges), [44] (model based on metric structure comparison), [37] (based on Expectation Maximization algorithm that incorporates a glioma growth model for atlas seeding), [3], [38] (active contour framework combined with dense deformation fields of optical flow), [33] (edges and the normals of the two images are matched by applying a Mumford-Shah type free discontinuity problem), or [49] (based on weighted total variation). More recently, in [29], a nonlocal topology-preserving segmentation guided registration model is introduced. The shapes to be matched are viewed as hyperelastic materials and are implicitly modelled by level set functions. These are driven in order to minimize a functional containing both a nonlinear-elasticity-based regularizer prescribing the nature of the deformation, and a criterion that forces the evolving shape to match intermediate topology-preserving segmentation results. In [12], a joint segmentation/optimal transport model is analyzed to determine the velocity of blood flow in vascular structures. A convex variational method is used and primal-dual proximal splitting algorithms are implemented. At last, in [61], the author wonders about the behavior of phase field approximations of the Mumford-Shah model when used for joint segmentation and registration.
We now turn to the analysis of the proposed model.
For additional mathematical material, we refer the reader to Chapter 2, Sections 1.1, 1.2, 1.4, 3.2, 3.3, and 4.

2 Mathematical modelling

2.1 Depiction of the model

Let Ω be a connected bounded open subset of $\mathbb{R}^2$ of class $\mathcal{C}^1$. Let us denote by $R : \bar{\Omega} \to \mathbb{R}$ the Reference image assumed to be sufficiently smooth (convenient way of saying that in a given definition, the smoothness of the involved variables or data is such that all arguments make sense) and by $T : \bar{\Omega} \to \mathbb{R}$ the Template image. For theoretical and numerical purposes, we assume that T is compactly supported on Ω to ensure that $T \circ \varphi$ is always defined and we assume that T is Lipschitz continuous. It can thus be considered as an element of the Sobolev space $W^{1,\infty}(\mathbb{R}^2)$. Let $\varphi : \bar{\Omega} \to \mathbb{R}^2$ be the sought deformation. Of course, in practice, the sought transformation φ should be with values in $\bar{\Omega}$ but from a mathematical point of view, if we work with such spaces of functions, we lose the structure

of vector space. A deformation is a smooth mapping that is orientation-preserving and injective, except possibly on $\partial\Omega$. The deformation gradient is $\nabla\varphi : \bar{\Omega} \to M_2(\mathbb{R})$, the set $M_2(\mathbb{R})$ being the set of real square matrices of order 2. The sought deformation φ is seen as the optimal solution of a specifically designed cost function comprising a regularization on φ prescribing the nature of the deformation, and a term measuring alignment or how the available data are exploited to drive the registration process. To allow large deformations, the shapes to be matched are viewed as hyperelastic materials, and more precisely as Saint Venant-Kirchhoff ones ([23, 22]). This outlook dictates the design of the regularization on φ which is thus based on the stored energy function of a Saint Venant-Kirchhoff material.

We recall that the right Cauchy-Green strain tensor (interpreted as a quantifier of the square of local change in distances due to deformation) is defined by $C = \nabla\varphi^T \nabla\varphi = F^T F$. The Green-Saint Venant strain tensor is defined by $E = \frac{1}{2}(C - I)$. Associated with a given deformation φ, it is a measure of the deviation between φ and a rigid deformation. We also need the following notations: $A : B = \mathrm{tr} A^T B$, the matrix inner product and $||A|| = \sqrt{A : A}$, the related matrix norm (Frobenius norm). The stored energy function of a Saint Venant-Kirchhoff material is defined by $W_{SVK}(F) = \widehat{W}(E) = \frac{\lambda}{2}\,(\mathrm{tr}\, E)^2 + \mu\,\mathrm{tr}\, E^2$, λ and μ being the Lamé coefficients. To ensure that the distribution of the deformation Jacobian determinants does not exhibit contractions or expansions that are too large and to avoid singularity as much as possible, we complement the stored energy function W_{SVK} by the term $\mu\,(\det F - 1)^2$ controlling that the Jacobian determinant remains close to 1. The weighting of the determinant component by parameter μ allows to recover a property of convexity for the function Ψ introduced later. (Note that the stored energy function W_{SVK} alone lacks a term penalizing the determinant: it does not preclude deformations with negative Jacobian. The expression of its quasiconvex envelope is more complex since involving explicitly the singular values of F. Also, when they are all lower than 1, the quasiconvex envelope equals 0, which shows bad behavior under compression). Therefore, the regularization can be written, after intermediate computations, as $W(F) = \beta(\|F\|^2 - \alpha)^2 - \frac{\mu}{2}(\det F)^2 + \mu(\det F - 1)^2 + \frac{\mu(\lambda+\mu)}{2(\lambda+2\mu)}$, where $\alpha = 2\frac{\lambda+\mu}{\lambda+2\mu}$ and $\beta = \frac{\lambda+2\mu}{8}$. Although meaningful, function W takes on a drawback since it is not quasiconvex (see [25, Chapter 9] for a complete review of this notion), which raises an issue of a theoretical nature since we cannot obtain the weak lower semi-continuity property. The idea is thus to replace W by its quasiconvex envelope defined by $QW(\xi) = \begin{cases} W(\xi) \text{ if } ||\xi||^2 \geq 2\dfrac{\lambda+\mu}{\lambda+2\mu}, \\ \Psi(\det \xi) \text{ if } ||\xi||^2 < 2\dfrac{\lambda+\mu}{\lambda+2\mu}, \end{cases}$

and Ψ, the convex mapping such that $\Psi : t \mapsto -\dfrac{\mu}{2}\,t^2 + \mu\,(t-1)^2 + \dfrac{\mu(\lambda+\mu)}{2(\lambda+2\mu)}$ (see [49] for the derivation), for which the minimal argument is $t = 2$. This regularizer has been investigated in prior related works by Derfoul and Le Guyader ([30]) and Ozeré, Gout and Le Guyader ([49]). Nevertheless, it does not constitute the core of the present work, the emphasis being put on the nonlocal rephrasing of the model and on its numerical analysis.

The regularizer is now complemented by a dissimilarity measure inspired by the unified model of image segmentation (geodesic active contours [19] and piecewise-constant Mumford-Shah model (PCMSM) [47]) and image denoising (Rudin-Osher-Fatemi model

[53]) into a global minimization framework introduced by Bresson *et al.* ([15]), designed to overcome the limitation of local minima and to deal with global minimum. In that purpose, let $g : \mathbb{R}^+ \to \mathbb{R}^+$ be an edge detector function satisfying $g(0) = 1$, g strictly decreasing and $\lim_{r\to+\infty} g(r) = 0$. From now on, we set $g := g(|\nabla R|)$ and for theoretical purposes, we assume that $\exists c > 0$ such that $0 < c \leq g \leq 1$ and that g is Lipschitz continuous. We then use the generalization of the notion of function of bounded variation to the setting of BV-spaces associated with a Muckenhoupt's weight function depicted in [10]. We follow Baldi's arguments and notations to define the weighted BV-space related to weight g.

For a general weight w, some hypotheses are required (fulfilled here by g). More precisely, Ω_0 being a neighborhood of $\bar{\Omega}$, the positive weight $w \in L^1_{loc}(\Omega_0)$ is assumed to belong to the global Muckenhoupt's $A_1 = A_1(\Omega)$ class of weight functions, i.e., w satisfies the condition:

$$C\, w(x) \geq \frac{1}{|B(x,r)|} \int_{B(x,r)} w(y)\, dy \ \text{ a.e.} \tag{4.1}$$

in any ball $B(x,r) \subset \Omega_0$. Now, denoting by A_1^* the class of weights $w \in A_1$, w lower semi-continuous (lsc) and that satisfy condition (4.1) pointwise, the definition of the weighted BV-space related to weight w is given by:

Definition 2.1 ([10, Definition 2])**.** *Let w be a weight function in the class A_1^*. We denote by $BV(\Omega, w)$ the set of functions $u \in L^1(\Omega, w)$ (set of functions that are integrable with respect to the measure $w(x)\,dx$) such that:*

$$\sup \left\{ \int_\Omega u\, div(\varphi)\, dx \ : \ |\varphi| \leq w \text{ everywhere}, \ \varphi \in Lip_0(\Omega, \mathbb{R}^2) \right\} < \infty, \tag{4.2}$$

with $Lip_0(\Omega, \mathbb{R}^2)$ the space of Lipschitz continuous functions with compact support. We denote by $var_w\, u$ the quantity (4.2).

Remark 2.2. *In [10], Baldi defines the BV-space taking as test functions elements of $Lip_0(\Omega, \mathbb{R}^2)$. Classically in the literature, the test functions are chosen in $\mathcal{C}^1_c(\Omega, \mathbb{R}^2)$. It can be proved that these two definitions coincide thanks to mollifications and density results.*

Proof. Firstly, we clearly have that $\sup \left\{ \int_\Omega u \mathrm{div}\varphi\, dx : |\varphi| \leq 1 \text{ everywhere}, \ \varphi \in \mathcal{C}^1_c(\Omega, \mathbb{R}^2) \right\}$ $\leq \sup \left\{ \int_\Omega u \mathrm{div}\varphi\, dx : |\varphi| \leq 1 \text{ everywhere}, \ \varphi \in Lip_0(\Omega, \mathbb{R}^2) \right\}$ since $\mathcal{C}^1_c(\Omega, \mathbb{R}^2) \subset Lip_0(\Omega, \mathbb{R}^2)$.
Then we prove the second inequality. We assume that $\sup \left\{ \int_\Omega u \mathrm{div}\varphi\, dx : |\varphi| \leq 1 \text{ everywhere}, \ \varphi \in \mathcal{C}^1_c(\Omega, \mathbb{R}^2) \right\} < \infty$, otherwise it is done. To do so, we start off with showing that $\forall u \in BV(\Omega) = BV(\Omega, \mathbb{R})$, $\forall f \in Lip_0(\Omega) = Lip_0(\Omega, \mathbb{R})$, $\int_\Omega u \dfrac{\partial f}{\partial x_i}\, dx = -\int_\Omega f\, dD_i u$.
Let $u \in BV(\Omega)$ and $f \in Lip_0(\Omega)$. Let (ρ_ε) be a sequence of mollifiers as in [34]. For

$\varepsilon > 0$ small enough, we have that $f * \rho_\varepsilon \in C_c^\infty(\Omega)$. Indeed, the support of $f * \rho_\varepsilon$ is included in $\text{supp}\,(f) + \overline{B(0,\varepsilon)}$, so by choosing $\varepsilon \in]0, \varepsilon_0]$, $\varepsilon_0 > 0$ fixed sufficiently small, $\text{supp}\,(f) + \overline{B(0,\varepsilon)} \subset \text{supp}\,(f) + \overline{B(0,\varepsilon_0)} \subset \Omega$. Then $\displaystyle\int_\Omega u \frac{\partial (f * \rho_\varepsilon)}{\partial x_i}\, dx = -\int_\Omega f * \rho_\varepsilon \, dD_i u$. Furthermore, $f * \rho_\varepsilon$ uniformly converges to f ([34, Theorem 1 p.123]) and up to a subsequence, $\dfrac{\partial (f * \rho_\varepsilon)}{\partial x_i} = \dfrac{\partial f}{\partial x_i} * \rho_\varepsilon \underset{\varepsilon \to 0}{\longrightarrow} \dfrac{\partial f}{\partial x_i}$ almost everywhere ([34, Theorem 1 p.123]). Thus the dominated convergence theorem applies and lets us conclude that $\displaystyle\lim_{\varepsilon \to 0} \int_\Omega u \frac{\partial (f * \rho_\varepsilon)}{\partial x_i}\, dx = \int_\Omega u \frac{\partial f}{\partial x_i}\, dx = \lim_{\varepsilon \to 0} -\int_\Omega f * \rho_\varepsilon dD_i u = -\int_\Omega f dD_i u$.
Moreover, it has been proved that for any $f \in Lip_0(\Omega, \mathbb{R}^2)$, there exists a sequence $(f_k) \in \mathcal{C}_c^1(\Omega, \mathbb{R}^2)$ that uniformly converges to f in Ω. Let $\{\psi_k\} \in Lip_0(\Omega, \mathbb{R}^2)$ be a maximizing sequence with $\forall k \in \mathbb{N}$, $|\psi_k| \leq 1$ everywhere. Then for each $k \in \mathbb{N}$, there exists a sequence $\{\psi_{k,j}\}_{j \in \mathbb{N}} \in \mathcal{C}_c^1(\Omega, \mathbb{R}^2)$ such that $\forall j \in \mathbb{N}$, $|\psi_{k,j}| \leq 1$ everywhere, and such that $(\psi_{k,j})$ uniformly converges to ψ_k in Ω when j tends to infinity, that is to say $\forall \varepsilon > 0$, $\exists N_{\varepsilon,k}$, $\forall j \in \mathbb{N}$, $\forall x \in \Omega$, $(j \geq N_{\varepsilon,k} \Rightarrow |\psi_{k,j}(x) - \psi_k(x)| \leq \varepsilon)$. Let us take in particular $\varepsilon = \frac{1}{k}$, then there exists N_k such that $\forall j \in \mathbb{N}, \forall x \in \Omega$, $\left(j \geq N_k \Rightarrow |\psi_{k,j}(x) - \psi_k(x)| \leq \frac{1}{k}\right)$. Let us now take $j = N_k$. Then $\forall x \in \Omega$, $|\psi_{k,N_k}(x) - \psi_k(x)| \leq \frac{1}{k}$. Besides, $\displaystyle\int_\Omega u \text{div} \psi_k \, dx \underset{k \to +\infty}{\longrightarrow} \sup \left\{ u \text{div} \psi \, dx : |\psi| \leq 1, \, \psi \in Lip_0(\Omega, \mathbb{R}^2) \right\}$. Since $\displaystyle\int_\Omega u \text{div} \psi_k \, dx = -\int_\Omega \psi_k dDu$ and $\displaystyle\int_\Omega u \text{div} \psi_{k,N_k} \, dx = -\int_\Omega \psi_{k,N_k} \, dDu$, we get $\displaystyle\left| \int_\Omega u \text{div} \psi_{k,N_k} \, dx - \int_\Omega u \text{div} \psi_k \, dx \right| \leq \|\psi_k - \psi_{k,N_k}\|_{L^\infty(\Omega)} \int_\Omega d|Du|$.
We then derive the following inequality $\displaystyle\left| \int_\Omega u \text{div} \psi_{k,N_k} \, dx - \sup \left\{ \int_\Omega u \text{div}(\psi) \, dx : |\psi| \leq 1, \, \psi \in Lip_0(\Omega, \mathbb{R}^2) \right\} \right| \leq \left| \int_\Omega u \text{div} \psi_{k,N_k} \, dx - \int_\Omega u \text{div} \psi_k \, dx \right| + \left| \int_\Omega u \text{div} \psi_k \, dx - \sup \left\{ \int_\Omega u \text{div}(\psi) \, dx : |\psi| \leq 1, \, \psi \in Lip_0(\Omega, \mathbb{R}^2) \right\} \right|$ with $\displaystyle\left| \int_\Omega u \text{div} \psi_{k,N_k} \, dx - \int_\Omega u \text{div} \psi_k \, dx \right| \underset{k \to +\infty}{\longrightarrow} 0$ and $\displaystyle\left| \int_\Omega u \text{div} \psi_k \, dx - \sup \left\{ \int_\Omega u \text{div}(\psi) \, dx : |\psi| \leq 1, \, \psi \in Lip_0(\Omega, \mathbb{R}^2) \right\} \right| \underset{k \to +\infty}{\longrightarrow} 0$. We eventually end up with $\displaystyle\sup \left\{ \int_\Omega u \text{div}(\psi) \, dx : |\psi| \leq 1, \, \psi \in Lip_0(\Omega, \mathbb{R}^2) \right\} \leq \sup \left\{ \int_\Omega u \ \text{div}(\psi) \, dx : |\psi| \leq 1, \, \psi \in \mathcal{C}_c^1(\Omega, \mathbb{R}^2) \right\}$, which concludes the proof. □

To get a clearer picture of the meaning of (4.2), we give the following result:

Remark 2.3 (Taken from [10, Remark 10])**.** *Given a weight w sufficiently smooth, if E is a regular bounded open set in $\mathbb{R}^2$, with boundary of class $\mathcal{C}^2$, then $|\partial E|(\Omega, w) = var_w \, \chi_E = \int_{\Omega \cap \partial E} w \, dH^1$, which can be interpreted in the case where $w = g$ as a new definition of the curve length with a metric that depends on the Reference image content.*

Equipped with this material (—and due to the properties of function g: it is obviously L^1, continuous and it suffices to take $C = \frac{1}{c}$ to satisfy (4.1) pointwise—), we propose

introducing as dissimilarity measure the following functional:

$$W_{fid}(\varphi) = \mathrm{var}_g\, T\circ\varphi + \frac{\nu}{2}\int_\Omega (T\circ\varphi(x) - R(x))^2\,dx$$
$$+ a\int_\Omega \left[(c_1 - R(x))^2 - (c_2 - R(x))^2\right] T\circ\varphi(x)\,dx, \tag{4.3}$$

with $c_1 = \frac{\int_\Omega R(x)\,H_\varepsilon(T\circ\varphi(x)-\rho)\,dx}{\int_\Omega H_\varepsilon(T\circ\varphi(x)-\rho)\,dx}$ and $c_2 = \frac{\int_\Omega R(x)\,(1-H_\varepsilon(T\circ\varphi(x)-\rho))\,dx}{\int_\Omega (1-H_\varepsilon(T\circ\varphi(x)-\rho))\,dx}$ —we dropped the dependency on φ to lighten the expressions —, H_ε denoting a regularization of the Heaviside function and $\rho \in [0,1]$ being a fixed parameter allowing to partition $T\circ\varphi$ into two phases and yielding a binary version of the Reference. ρ can be estimated by analyzing the Reference histogram to discriminate two relevant regions or phases. For instance, through histogram shape-based methods, clustering-based methods, entropy-based methods, object attribute-based methods, spatial methods, or local methods ([56]). This proposed functional emphasizes the link between the geodesic active contour model ([19]) and the PCMSM: if $\tilde{T}$ is the characteristic function of the set $\Omega_{\mathcal{C}}$, bounded subset of Ω with regular boundary $\mathcal{C}$, $\mathrm{var}_g\,\tilde{T}$ is a new definition of the length of $\mathcal{C}$ with a metric depending on the Reference content (so minimizing this quantity is equivalent to locating the curve on the boundary of the shape contained in the Reference), while $\int_\Omega \left[(c_1 - R(x))^2 - (c_2 - R(x))^2\right] \tilde{T}(x)\,dx$ approximates R in the L^2 sense by two regions $\Omega_{\mathcal{C}}$ and $\Omega\backslash\Omega_{\mathcal{C}}$ with two values c_1 and c_2. Indeed, $\mathrm{var}_g\,\tilde{T} = \int_{\Omega\cap\mathcal{C}} g\,dH^1$, and if c_1 and c_2 are fixed (which is in practice the case in the alternating algorithm), $\int_\Omega \left[(c_1 - R(x))^2 - (c_2 - R(x))^2\right] 1_{\Omega_{\mathcal{C}}}\,dx$ is equivalent to minimizing $\int_\Omega (c_1 - R(x))^2\,1_{\Omega_{\mathcal{C}}}\,dx + \int_\Omega (c_2 - R(x))^2\,1_{\Omega\backslash\Omega_{\mathcal{C}}}\,dx$.

In the end, the global minimization problem denoted by (QP) —that stands for *Quasiconvex Problem*— is stated by:

$$\inf_{\varphi\in\mathcal{W}=\mathrm{Id}+W_0^{1,4}(\Omega,\mathbb{R}^2)} \bar{I}(\varphi) = W_{fid}(\varphi) + \int_\Omega QW(\nabla\varphi)\,dx. \tag{QP}$$

It is a relaxed problem related to problem

(P) : $\inf_{\varphi\in\mathcal{W}=\mathrm{Id}+W_0^{1,4}(\Omega,\mathbb{R}^2)} I(\varphi) = W_{fid}(\varphi) + \int_\Omega W(\nabla\varphi)\,dx$, and we will see the connection between them later on. $\varphi \in \mathrm{Id} + W_0^{1,4}(\Omega,\mathbb{R}^2)$ means that $\varphi = \mathrm{Id}$ on $\partial\Omega$ and $\varphi \in W^{1,4}(\Omega,\mathbb{R}^2)$. $W^{1,4}(\Omega,\mathbb{R}^2)$ denotes the Sobolev space of functions $\varphi \in L^4(\Omega,\mathbb{R}^2)$ with distributional derivatives up to order 1 which also belong to $L^4(\Omega)$. $\mathcal{W}$ is a suitable space due, in particular, to the $\|F\|^4$ component in $W(F)$. Note that from generalized Hölder's inequality, if $\varphi \in W^{1,4}(\Omega,\mathbb{R}^2)$, then $\det\nabla\varphi \in L^2(\Omega)$. Now we justify that $\mathrm{var}_g\,T\circ\varphi$ is well-defined. In [1], Ambrosio and Dal Maso prove a general chain rule for the distribution derivatives of the composite function $v(x) = f(u(x))$, where $u : \mathbb{R}^n \to \mathbb{R}^m$ has bounded variation and $f : \mathbb{R}^m \to \mathbb{R}^k$ is Lipschitz continuous. A simpler result is given when $u \in W^{1,p}(\Omega,\mathbb{R}^m)$ for some p, $1 \le p \le +\infty$, resulting in our case in $T\circ\varphi \in W^{1,4}(\Omega) := W^{1,4}(\Omega,\mathbb{R}) \subset BV(\Omega) \subset BV(\Omega,g)$, since $g \le 1$. A key difference with the model in [49] is the introduction of the nonlocal component

$\int_\Omega \left[(c_1 - R(x))^2 - (c_2 - R(x))^2\right] T \circ \varphi(x)\, dx$ and the treatment of the weighted BV seminorm, for which a nonlocal counterpart is provided, entailing substantial mathematical development. It results in more accurate segmentation results compared to [49], with in particular, the detection of small features.

Remark 2.4. *We point out that the extension of the model to the 3D case is not straightforward. Indeed, the expression of the stored energy function of a 3D Saint Venant-Kirchhoff material involves the cofactor matrix denoted by Cof as follows:* $W_{SVK}(F) = \frac{\lambda}{8}\left(\|F\|^2 - \left(3 + \frac{2\mu}{\lambda}\right)\right)^2 + \frac{\mu}{4}\left(\|F\|^4 - 2\|CofF\|^2\right) - \frac{\mu}{4\lambda}(2\mu+3\lambda)$ *and it is not clear that one can derive the explicit expression of the quasiconvex envelope QW of W in three dimensions as done for the two dimensional case. In particular, it is not sufficient to simply add the quasiconvex envelopes of each of the components. Nevertheless, two lines of research are considered:*

(i) The first one consists in working with the Saint Venant-Kirchhoff stored energy function alone for which it is possible to compute the related quasiconvex envelope. Its expression is complex since including explicitly the singular values of ξ, making its numerical implementation more involved with finite element approximations. Such a kind of implementation was provided in [40] in the case of non-linear elastic membranes. More precisely, the authors consider the nonlinear membrane model obtained by Le Dret and Raoult using Γ-convergence in the case of a Saint Venant-Kirchhoff bulk material, and use conforming P_1 and Q_1 finite element approximations of the membrane problem.
The cons: As already observed, the stored energy function W_{SVK} alone lacks a term penalizing the determinant: it thus does not preclude deformations with negative Jacobian. It is noticeable here that when the singular values of ξ are lower than 1, the quasiconvex envelope equals 0, which shows bad behavior under compression and may yield violation of topology preservation characterization.
The pros: (a) the numerical implementation of the problem in φ no longer requires the introduction of an auxiliary variable V to simulate $\nabla\varphi$ since now based on conforming finite element approximation. —We emphasize that the introduction of the auxiliary variable V makes it possible to move the nonlinearity on V and thus to constrain the L^4 norm of V instead of the L^4 norm of $\nabla\varphi$ (which requires very low values for the time step to obtain stability when using classical L^2 gradient flow method)—In the P_1 case for instance, deformations are approximated by piecewise affine globally continuous functions on a triangulation of the domain. As the problem is highly nonlinear and the stored energy function is only of class $\mathcal{C}^1$, the nonlinear conjugate gradient method would be well-adapted to the problem; (b) the subproblem in $\tilde{T}$ is unchanged.

(ii) A second line of research aim to introduce a polyconvex stored energy function including an explicit control on the Jacobian determinant, e.g., the Ciarlet-Geymonat stored energy. From a numerical viewpoint, a splitting method is still implemented involving the auxiliary variable V simulating $\nabla\varphi$ and the function now involves an

additional quadratic penalization of the form $\|Cof\nabla\varphi - CofV\|^2_{L^2(\Omega,M_3(\mathbb{R}))}$. *We need to investigate more on this side, in particular, whether the asymptotic results hold in this case.*

2.2 Theoretical results

In this subsection, we theoretically analyze the relaxed problem (QP) by showing its well-definedness. We prove that the infimum of (QP) is attained and relate the minimum of (QP) to the infimum of (P) involving W rather than QW in the following theorem. The introduction of (P) is just for theoretical analysis purpose: it will not be considered afterwards.

Theorem 2.1 (Existence of minimizers.)**.** *The infimum of (QP) is attained. Let* $\bar{\varphi}$ *be a minimizer of (QP). Then there exists a sequence* $\{\varphi_n\}_{n=1}^{\infty} \subset Id + W_0^{1,4}(\Omega,\mathbb{R}^2)$ *such that* $\varphi_n \rightharpoonup \bar{\varphi}$ *in* $W^{1,4}(\Omega,\mathbb{R}^2)$ *as* $n \to +\infty$ *and* $\int_\Omega \frac{\nu}{2}(T\circ\varphi_n - R)^2 + a\left[(c_1^n - R)^2 - (c_2^n - R)^2\right] T\circ\varphi_n + W(\nabla\varphi_n)\,dx \to \int_\Omega \frac{\nu}{2}(T\circ\bar{\varphi} - R)^2 + a\left[(\bar{c_1} - R)^2 - (\bar{c_2} - R)^2\right] T\circ\bar{\varphi} + QW(\nabla\bar{\varphi})\,dx$. *Let us assume that* $T \in W^{2,\infty}(\mathbb{R}^2)$, *if moreover* $(\nabla\varphi_n)$ *strongly converges to* $\nabla\bar{\varphi}$ *in* $L^1(\Omega, M_2(\mathbb{R}))$, *then one has* $I(\varphi_n) \to \bar{I}(\bar{\varphi})$, *yielding* $\min QP = \inf QP = \inf(P)$.

Proof. Note that one always has $\inf QP \leq \inf(P)$. We use the notations c_1^n, c_2^n, $\bar{c}_1$, $\bar{c}_2$ to highlight their dependance on φ_n and $\bar{\varphi}$ respectively.
Let us first prove that the infimum of (QP) is attained.
For the sake of simplicity but without loss of generality, we assume $meas(\Omega) = 1$. Let us take $\hat{\varphi} = \mathrm{Id} \in \mathrm{Id} + W_0^{1,4}(\Omega,\mathbb{R}^2)$ then $\nabla\hat{\varphi} = I$, and since $QW(I) = 0$, we have $\bar{I}(\hat{\varphi}) < +\infty$. The first step rests upon the derivation of a coercivity inequality to ensure the infimum is finite. To do so, we first consider these inequalities:

$$c_1 = \frac{\displaystyle\int_\Omega R(x) H_\varepsilon(T\circ\varphi(x) - \rho)\,dx}{\displaystyle\int_\Omega H_\varepsilon(T\circ\varphi(x) - \rho)\,dx} \leq \|R\|_{L^\infty(\Omega)},$$

$$c_2 = \frac{\displaystyle\int_\Omega R(x)(1 - H_\varepsilon(T\circ\varphi(x) - \rho))\,dx}{\displaystyle\int_\Omega (1 - H_\varepsilon(T\circ\varphi(x) - \rho))\,dx} \leq \|R\|_{L^\infty(\Omega)}.$$

For almost every $x \in \Omega$,
$$0 \leq (c_1 - R(x))^2 \leq 4\|R\|^2_{L^\infty(\Omega)}$$
$$0 \leq (c_2 - R(x))^2 \leq 4\|R\|^2_{L^\infty(\Omega)}$$
$$0 \geq -(c_2 - R(x))^2 \geq -4\|R\|^2_{L^\infty(\Omega)}$$
$$\left[(c_1 - R(x))^2 - (c_2 - R(x))^2\right] \geq -4\|R\|^2_{L^\infty(\Omega)} > -\infty.$$

Furthermore, $T \in W^{1,\infty}(\mathbb{R}^2,\mathbb{R})$ so $\|T\|_{L^\infty(\Omega)} < \infty$. Thus we get according to [49]:

$$\bar{I}(\varphi) \geq \frac{\mu}{4}\|\det(\nabla\varphi)\|^2_{L^2(\Omega)} + \frac{\beta}{2}\|\nabla\varphi\|^4_{L^4(\Omega,M_2(\mathbb{R}))} - \beta\alpha^2 - 3\mu + \frac{\mu(\lambda+\mu)}{2(\lambda+2\mu)} - 4a\|R\|^2_{L^\infty(\Omega)}\|T\|_{L^\infty(\Omega)},$$

and the infimum of (QP) is finite.
Then we introduce a minimizing sequence $\{\varphi^k\}_{k\in\mathbb{N}} \in \mathrm{Id} + W^{1,4}_0(\Omega,\mathbb{R}^2)$. We can always assume that for k large enough $\bar{I}(\varphi^k) \leq 1 + \bar{I}(\hat{\varphi})$. From the previous coercivity inequality and the generalized Poincaré inequality $\forall p \in [1,+\infty[$, $\forall u \in W^{1,p}(\Omega)$, $\|u\|_{W^{1,p}(\Omega)} \leq C(\|\nabla u\|_{L^p(\Omega)} + \int_{\partial\Omega}|u(x)|d\sigma)$, it comes that $\{\varphi^k\}$ is uniformly bounded in $W^{1,4}(\Omega,\mathbb{R}^2)$ and $\{\det(\nabla\varphi^k)\}$ is uniformly bounded in $L^2(\Omega)$. We can thus extract a subsequence still denoted by $\{\varphi^k\}$ such that:

$$\begin{cases} \varphi^k \rightharpoonup \bar{\varphi} \in W^{1,4}(\Omega,\mathbb{R}^2) \\ \det(\nabla\varphi^k) \rightharpoonup \bar{\delta} \in L^2(\Omega) \end{cases}.$$

From [25, Theorem 1.14 p.16], if $\varphi^k \rightharpoonup \bar{\varphi}$ in $W^{1,4}(\Omega,\mathbb{R}^2)$, then $\det(\nabla\varphi^k) \rightharpoonup \det(\nabla\bar{\varphi})$ in $L^2(\Omega)$ yielding $\bar{\delta} = \det(\nabla\bar{\varphi})$ by uniqueness of the weak limit in $L^2(\Omega)$.
The last step consists in showing that the functional $\bar{I}$ is weakly lower semi-continuous.
Let us now introduce J : $\begin{array}{ccc} W^{1,4}(\Omega,\mathbb{R}^2)\times L^2(\Omega) & \to & \mathbb{R} \\ (\phi,\delta) & \mapsto & \displaystyle\int_\Omega W^*(\phi,\delta)\,dx \end{array}$ with $W^*(\phi,\delta) = \left|\begin{array}{cc} \beta(\|\nabla\phi\|^2-\alpha)^2+\psi(\delta) & \text{if } \|\nabla\phi\|^2 > \alpha \\ \psi(\delta) & \text{otherwise} \end{array}\right.$. W^* is convex thanks to the polyconvexity of QW (c.f. [49]) and continuous. By classical arguments (see [41]), one can prove that J is convex with respect to (ϕ,δ), strongly sequentially lower semi-continuous and thus weakly lower semi-continuous so that $J(\bar{\varphi},\det(\nabla\bar{\varphi})) \leq \liminf_{k\to+\infty} J(\varphi^k,\det(\nabla\varphi^k))$.
The Rellich-Kondrachov embedding theorem gives that $W^{1,4}(\Omega,\mathbb{R}^2) \overset{c}{\circlearrowleft} \mathcal{C}^0(\Omega,\mathbb{R}^2)$ with compact injection. Thus $\{\varphi^k\}$ uniformly converges to $\bar{\varphi}$ and so in $L^1(\Omega,\mathbb{R}^2)$ as Ω is bounded. Since T is assumed to be Lipschitz continuous, $\{T\circ\varphi^k\}$ strongly converges to $T\circ\bar{\varphi}$ in $L^1(\Omega)$ and so in $L^1(\Omega,g)$ as g is assumed to be bounded by 1. The semicontinuity theorem from [10, Theorem 3.2] enables us to conclude that $var_g\, T\circ\bar{\varphi} \leq \liminf_{k\to+\infty} var_g\, T\circ\varphi^k$.
Now we will successively use the dominated convergence theorem to show that $\lim_{k\to+\infty}\int_\Omega \left[(c_1^k - R)^2 - (c_2^k - R)^2\right] T\circ\varphi^k\,dx = \int_\Omega \left[(\bar{c}_1 - R)^2 - (\bar{c}_2 - R)^2\right] T\circ\bar{\varphi}\,dx$. As $\{\varphi^k\}$ uniformly converges to $\bar{\varphi}$ and T and H_ε are continuous, $R\,H_\varepsilon(T\circ\varphi^k-\rho)$ converges to $R\,H_\varepsilon(T\circ\bar{\varphi}-\rho)$ almost everywhere and $\forall k\in\mathbb{N}$, $R\,H_\varepsilon(T\circ\varphi^k-\rho) \leq \|R\|_{L^\infty(\Omega)} \in L^1(\Omega)$ since Ω is bounded. Therefore, $\int_\Omega R\,H_\varepsilon(T\circ\varphi^k-\rho)\,dx \underset{k\to+\infty}{\longrightarrow} \int_\Omega R\,H_\varepsilon(T\circ\bar{\varphi}-\rho)\,dx$. In a similar way and by noticing that $\forall z\in\mathbb{R}$, $0 < H_\varepsilon(z) < 1$ and $T \in L^\infty(\Omega)$, we get that $\int_\Omega H_\varepsilon(T\circ\varphi^k-\rho)\,dx \underset{k\to+\infty}{\longrightarrow} \int_\Omega H_\varepsilon(T\circ\bar{\varphi}-\rho)\,dx$, $\int_\Omega R\,(1-H_\varepsilon(T\circ\varphi^k-\rho))\,dx \underset{k\to+\infty}{\longrightarrow} \int_\Omega R\,(1-H_\varepsilon(T\circ\bar{\varphi}-\rho))\,dx$ and

$\int_\Omega (1-H_\varepsilon(T\circ\varphi^k-\rho))\,dx \underset{k\to+\infty}{\longrightarrow} \int_\Omega (1-H_\varepsilon(T\circ\bar\varphi-\rho))\,dx$. Hence $c_1^k \underset{k\to+\infty}{\longrightarrow} \bar c_1$ and $c_2^k \underset{k\to+\infty}{\longrightarrow} \bar c_2$. Then we can deduce that $\left[(c_1^k-R)^2-(c_2^k-R)^2\right] T\circ\varphi^k \underset{k\to+\infty}{\longrightarrow} [(\bar c_1-R)^2-(\bar c_2-R)^2]T\circ\bar\varphi$ almost everywhere and for almost every $x\in\Omega$, $\forall k\in\mathbb{N}$, $|[(c_1^k-R)^2-(c_2^k-R)^2]T\circ\varphi^k| \le 4\|R\|^2_{L^\infty(\Omega)}\|T\|_{L^\infty(\Omega)} \in L^1(\Omega)$. So, $\int_\Omega \left[(c_1^k-R)^2-(c_2^k-R)^2\right] T\circ\varphi^k\,dx \underset{k\to+\infty}{\longrightarrow} \int_\Omega \left[(\bar c_1-R)^2-(\bar c_2-R)^2\right] T\circ\bar\varphi\,dx$.
We use a last time the dominated convergence theorem to show that $\|T\circ\varphi^k-R\|^2_{L^2(\Omega)} \underset{k\to+\infty}{\longrightarrow} \|T\circ\bar\varphi-R\|^2_{L^2(\Omega)}$. Indeed, we have $(T\circ\varphi^k-R)^2 \underset{k\to+\infty}{\longrightarrow} (T\circ\bar\varphi-R)^2$ almost everywhere and the result follows from the dominated convergence theorem.
Eventually, $\bar I(\bar\varphi)\le \liminf_{k\to+\infty} \bar I(\varphi^k) = \inf_{\varphi\in \mathrm{Id}+W_0^{1,4}(\Omega,\mathbb{R}^2)} \bar I(\varphi)$. Besides, by continuity of the trace map we get that $\bar\varphi\in \mathrm{Id}+W_0^{1,4}(\Omega,\mathbb{R}^2)$ and so the infimum exists and is attained, which concludes the first part of the proof.
We now recall some results of Dacorogna to prove the second part of the theorem.

Proposition 2.5 (taken from [25])**.** *The relaxed problem in the sense of Dacrorogna associated to*

$$\inf\left\{\mathcal{F}(\varphi)=\int_\Omega f(x,\varphi(x),\nabla\varphi(x))\,dx \,:\, \varphi\in u_0+W_0^{1,p}(\Omega,\mathbb{R}^N)\right\}$$

where $f:\Omega\times\mathbb{R}^N\times\mathbb{R}^{N\times n}\to\mathbb{R}$ is a given non-convex function, is defined by:

$$\inf\left\{\bar{\mathcal{F}}(\varphi)=\int_\Omega Qf(x,\varphi(x),\nabla\varphi(x))\,dx \,:\, \varphi\in u_0+W_0^{1,p}(\Omega,\mathbb{R}^2)\right\},$$

where $Qf(x,\varphi,\nabla\varphi)$ is the quasiconvex envelope of f.

Let us introduce the following supplementary problem:

$$\inf\left\{\mathcal{F}(\varphi)=\int_\Omega f(x,\varphi(x),\nabla\varphi(x))\,dx \,:\, \varphi\in \mathrm{Id}+W_0^{1,4}(\Omega,\mathbb{R}^2)\right\}, \tag{PG}$$

where $f(x,\varphi(x),\nabla\varphi(x)) = a\left[(c_1-R(x))^2-(c_2-R(x))^2\right]T\circ\varphi(x)+\frac{\nu}{2}(T\circ\varphi(x)-R(x))^2+W(\nabla\varphi(x))$ and a relaxed problem associated to it:

$$\inf\left\{\bar{\mathcal{F}}(\varphi)=\int_\Omega Qf(x,\varphi(x),\nabla\varphi(x))\,dx \,:\, \varphi\in \mathrm{Id}+W_0^{1,4}(\Omega,\mathbb{R}^2)\right\}, \tag{QPG}$$

where $Qf(x,\varphi,\nabla\varphi) = a\left[(c_1-R(x))^2-(c_2-R(x))^2\right]T\circ\varphi(x)+\frac{\nu}{2}(T\circ\varphi(x)-R(x))^2+QW(\nabla\varphi(x))$, QW being the quasiconvex envelope of W as defined previously. It has to be noticed that because of the nonlocal terms c_1 and c_2, this is not exactly the relaxed problem in the sense of Dacorogna. We then have the following results.

Theorem 2.2 (adapted from [25])**.** *The infimum of (QPG) is attained. Let then* $\varphi^* \in W^{1,4}(\Omega,\mathbb{R}^2)$ *be a minimizer of the relaxed problem (QPG). Then there exists a sequence* $\{\varphi_\nu\}_{\nu=1}^{\infty} \subset \varphi^* + W_0^{1,4}(\Omega,\mathbb{R}^2)$ *such that* $\varphi_\nu \to \varphi^*$ *in* $L^4(\Omega,\mathbb{R}^2)$ *as* $\nu \to +\infty$ *and* $\mathcal{F}(\varphi_\nu) \to \bar{\mathcal{F}}(\varphi^*)$ *as* $\nu \to +\infty$*, yielding* $\min(QPG) = \inf(PG)$*. Moreover, the following holds:* $\varphi_\nu \rightharpoonup \varphi^*$ *in* $W^{1,4}(\Omega,\mathbb{R}^2)$ *as* $\nu \to +\infty$*.*

Proof. The first part of the proposition is proved using exactly the same arguments as those previously used. Let us now consider the following subproblem:

$$\inf_{\varphi \in \mathrm{Id}+W_0^{1,4}(\Omega,\mathbb{R}^2)} \left\{ \mathcal{F}_1(\varphi) = \int_\Omega \frac{\nu}{2}(T\circ\varphi - R)^2 + W(\nabla\varphi)dx \right\}. \tag{SP}$$

The associated relaxed problem in the sense of Dacorogna is:

$$\inf_{\varphi \in \mathrm{Id}+W_0^{1,4}(\Omega,\mathbb{R}^2)} \left\{ \bar{\mathcal{F}}_1(\varphi) = \int_\Omega \frac{\nu}{2}(T\circ\varphi - R)^2 + QW(\nabla\varphi)dx \right\} \tag{QSP}$$

as $\frac{\nu}{2}(T\circ\varphi - R)^2 + QW(\nabla\varphi)$ is the quasiconvex envelope of $\frac{\nu}{2}(T\circ\varphi - R)^2 + W(\nabla\varphi)$. Since both of the previous functions are Carathéodory functions, and $(\det\zeta)^2 = \det\zeta^T\zeta = \frac{1}{2}\|\zeta\|^4 - \frac{1}{2}\operatorname{tr}(\zeta^T\zeta)^2$ leading to

$$\begin{aligned} &C_1\|\xi\|^4 - C_2 \le \frac{\nu}{2}(T\circ\varphi - R(x))^2 + QW(\xi) \le \frac{\nu}{2}(T\circ\varphi - R(x))^2 + W(\xi) \\ &\le \left(\beta + \frac{\mu}{2}\right)\|\xi\|^4 + C_3\|\varphi\|^2 + C_4, \end{aligned}$$

with C_1, C_2, C_3 and C_4 positive constants, according to [25, Theorem 8.29, p. 404 and Theorem 9.8, p. 432], the infimum of (QSP) is attained and let $4 \le q \le \infty$ and $u \in W^{1,q}(\Omega,\mathbb{R}^2)$, there exists a sequence $\{\varphi_\nu\}_{\nu=1}^{\infty} \subset u + W_0^{1,q}(\Omega,\mathbb{R}^2)$ such that (u_ν) strongly converges to u in $L^q(\Omega,\mathbb{R}^2)$ as ν tends to infinity and $\mathcal{F}_1(u_\nu)$ converges to $\bar{\mathcal{F}}_1(u)$ as ν tends to infinity. In addition, u_ν weakly converges to u in $W^{1,4}(\Omega,\mathbb{R}^2)$ as ν tends to infinity.
Let us take $u = \varphi^* \in W^{1,4}(\Omega,\mathbb{R}^2)$, minimizer of (QPG) in what precedes. Thus there exists a sequence $\{\varphi_\nu\}_{\nu=1}^{\infty} \subset \varphi^* + W_0^{1,4}(\Omega,\mathbb{R}^2) = \mathrm{Id} + W_0^{1,4}(\Omega,\mathbb{R}^2)$ such that:

$$\begin{aligned} \varphi_\nu &\underset{\nu\to+\infty}{\longrightarrow} \varphi^* \text{ in } L^4(\Omega,\mathbb{R}^2), \\ \varphi_\nu &\underset{\nu\to+\infty}{\rightharpoonup} \varphi^* \text{ in } W^{1,4}(\Omega,\mathbb{R}^2), \\ \mathcal{F}_1(\varphi_\nu) &\underset{\nu\to+\infty}{\longrightarrow} \bar{\mathcal{F}}_1(\varphi^*). \end{aligned}$$

So, it remains to prove that $a\displaystyle\int_\Omega \left[(c_1^\nu - R)^2 - (c_2^\nu - R)^2\right] T\circ\varphi_\nu\, dx$ converges to $a\displaystyle\int_\Omega \left[(c_1^* - R)^2 - (c_2^* - R)^2\right] T\circ\varphi^*\, dx$. This was proved by applying several times the dominated convergence theorem in the previous proof as $\varphi_\nu \underset{\nu\to+\infty}{\rightharpoonup} \varphi^*$ in $W^{1,4}(\Omega,\mathbb{R}^2)$. We can conclude

that:

$$\varphi_\nu \underset{\nu\to+\infty}{\longrightarrow} \varphi^* \text{ in } L^4(\Omega,\mathbb{R}^2),$$
$$\varphi_\nu \underset{\nu\to+\infty}{\rightharpoonup} \varphi^* \text{ in } W^{1,4}(\Omega,\mathbb{R}^2),$$
$$\mathcal{F}(\varphi_\nu) = a\int_\Omega \left[(c_1^\nu - R)^2 - (c_2^\nu - R)^2\right] T\circ\varphi_\nu\, dx + \mathcal{F}_1(\varphi_\nu)$$
$$\underset{\nu\to+\infty}{\longrightarrow} \bar{\mathcal{F}}(\varphi^*) = a\int_\Omega \left[(c_1^* - R)^2 - (c_2^* - R)^2\right] T\circ\varphi^*\, dx + \bar{\mathcal{F}}_1(\varphi^*),$$
$$\text{yielding } \min_{\varphi\in \mathrm{Id}+W_0^{1,4}(\Omega,\mathbb{R}^2)}(QPG) = \inf_{\varphi\in \mathrm{Id}+W_0^{1,4}(\Omega,\mathbb{R}^2)}(PG).$$

□

Theorem 2.3 (in [50, Proposition 4.1.10])**.** *Let us assume that $T \in W^{2,\infty}(\mathbb{R}^2,\mathbb{R})$, ∇T being Lipschitz continuous with Lipschitz constant κ'. Let $\bar{\varphi} \in Id + W_0^{1,4}(\Omega,\mathbb{R}^2)$ be a minimizer of the relaxed problem (QP). Due to the previous theorem there exists a sequence $\{\varphi_\nu\}_{\nu=1}^\infty \subset \bar{\varphi} + W_0^{1,4}(\Omega,\mathbb{R}^2)$ such that $\varphi_\nu \rightharpoonup \bar{\varphi}$ in $W^{1,4}(\Omega,\mathbb{R}^2)$ as $\nu\to+\infty$ and $\int_\Omega f(x,\varphi_\nu(x),\nabla\varphi_\nu(x))\,dx \to \int_\Omega Qf(x,\bar{\varphi}(x),\nabla\bar{\varphi}(x))\,dx$. If moreover $\{\nabla\varphi_\nu\}$ strongly converges to $\nabla\bar{\varphi}$ in $L^1(\Omega,M_2(\mathbb{R}))$, then one has $I(\varphi_\nu)\to\bar{I}(\bar{\varphi})$ as $\nu\to+\infty$ and therefore* $\inf(QP) = \min(QP) = \inf(P)$.

This concludes the proof. □

We now investigate an original numerical method for the resolution of (QP).

3 Numerical method of resolution

Inspired by prior works by Dávila [27] and Ponce [52] dedicated to the design of nonlocal counterparts of Sobolev and BV semi-norms, we introduce the sequence $\{\rho_n\}_{n\in\mathbb{N}}$ of radial mollifiers satisfying: $\forall n\in\mathbb{N}, \forall x\in\mathbb{R}^2, \rho_n(x) = \rho_n(|x|)$; $\forall n\in\mathbb{N}, \rho_n \geq 0$; $\forall n\in\mathbb{N}, \int_{\mathbb{R}^2}\rho_n(x)\,dx = 1$; $\forall\delta>0, \lim_{n\to+\infty}\int_\delta^{+\infty}\rho_n(r)rdr = 0$. We would like to point that the qualifying term "nonlocal" might sound inadequate in the sense that the "nonlocal counterpart" includes a parameter n, via the mollifier ρ_n, that is destined to tend to $+\infty$ concentrating the measure around the point of interest and removing in some way the nonlocal nature of the component. Nevertheless, it takes on mathematical interests since, to the best of our knowledge, this kind of approximation for the weighted total variation has not been investigated. It also represents a good compromise between our local model and the actual numerical model we implement which is introduced and motivated later, and falls within the "true nonlocal algorithms". In practice, for "true nonlocal methods", the computations are restricted to a small area around the point of interest (like the NL-means algorithm) and it makes these methods quite similar to our model from our point of view. Then the following approximation of the weighted total variation by a sequence of integral operators involving a differential quotient and the radial mollifiers sequence holds:

Theorem 3.1 (Nonlocal approximation of the weighted total variation)**.** *Let $\Omega \subset \mathbb{R}^2$ be an open bounded set with Lipschitz boundary and let $f \in BV(\Omega, g) \subset BV(\Omega)$ as $0 < c \leq g \leq 1$ everywhere. Consider $\{\rho_n\}$ defined previously. Then*

$$\lim_{n\to+\infty} \int_\Omega g(x) \left[\int_\Omega \frac{|f(x)-f(y)|}{|x-y|}\rho_n(x-y)\,dy\right] dx$$
$$= \left[\frac{1}{|S^1|}\int_0^{2\pi} \left|e.\begin{pmatrix}\cos(\theta)\\ \sin(\theta)\end{pmatrix}\right| d\theta\right] var_g\, f = K_{1,2}\, var_g\, f,$$

with e being any unit vector of $\mathbb{R}^2$ and S^1 being the unit sphere in $\mathbb{R}^2$.

Proof. In the following, the associated total variation measure of a function $f \in BV(\Omega)$ is denoted by $|Df|$, that is to say $var\, f = \int_\Omega d|Df|$. The first step is inspired by Dávila's work [27] and consists in proving that the sequence of Radon measures $\left\{\mu_n = g(x)\left[\int_\Omega \frac{|f(y)-f(x)|}{|x-y|}\rho_n(|x-y|)\,dy\right]dx\right\}$ weakly converges to $K_{1,2}\, g\, |Df|$ in the sense of Radon measures in Ω when n tends to infinity. The second part of the proof is an adaptation of the one of [27, Theorem 1] and is devoted to prove that $\lim_{n\to+\infty} \mu_n(\Omega) = K_{1,2}\, var_g\, f$ using a sequence of auxiliary sets $V_\delta = \{x \in \Omega : dist(x, \partial\Omega) > \delta\}$.
We first introduce the following lemma.

Lemma 3.1 (adapted from [27, Lemma 2])**.** *Assume ρ_n satisfies the previous conditions and let $f \in BV(\Omega, g) \subset BV(\Omega)$. Then $\mu_n \underset{n\to+\infty}{\rightharpoonup} \mu = K_{1,2}\, g\, |Df|$ weakly in the sense of Radon measures in Ω with $\int_\Omega g\, d|Df| = |f|_{BV(\Omega,g)} = var_g\, f$ and $\int_\Omega d|Df| = |f|_{BV(\Omega)} = var\, f$.*

Proof. According to [27, Lemma 2], we get that $\tilde{\mu}_n = \left[\int_\Omega \frac{|f(x)-f(y)|}{|x-y|}\rho_n(x-y)\,dy\right] dx$ weakly converges in the sense of Radon measures to $\tilde{\mu} = K_{1,2}\,|Df|$. According to [34, Theorem 1 p.54], this means that for every $\phi \in \mathcal{C}_0(\Omega)$ with $\mathcal{C}_0(\Omega)$ being the set of all continuous compactly supported functions on Ω, $\int_\Omega \phi\, d\tilde{\mu}_n$ converges to $\int_\Omega \phi\, d\tilde{\mu}$.
Besides, according to [10, Theorem 4.1], as $f \in BV(\Omega, g)$ then $f \in BV(\Omega)$, $g \in L^1(|Df|)$ and $var_g\, f = |f|_{BV(\Omega,g)} = \int_\Omega g\, d|Df|$, $g\,|Df|$ being a Radon measure.
Thus we get that for any $\phi \in \mathcal{C}_0(\Omega)$,

$$\left|\int_\Omega \phi\, d\mu_n - \int_\Omega \phi\, d\mu\right| = \left|\int_\Omega \phi(x)g(x)\left[\int_\Omega \frac{|f(x)-f(y)|}{|x-y|}\rho_n(x-y)\,dy\right] dx - \int_\Omega \phi\, K_{1,2}\, g\, d|Df|\right|,$$
$$= \left|\int_\Omega \phi g\left(\int_\Omega \frac{|f(x)-f(y)|}{|x-y|}\rho_n(x-y)\,dy\,dx - K_{1,2}\, d|Df|\right)\right|,$$
$$\leq \left|\int_\Omega \phi\left(\int_\Omega \frac{|f(x)-f(y)|}{|x-y|}\rho_n(x-y)\,dy\,dx - K_{1,2}\, d|Df|\right)\right|.$$

As $\left|\int_\Omega \phi\left(\int_\Omega \frac{|f(x)-f(y)|}{|x-y|}\rho_n(x-y)\,dy\,dx - K_{1,2}\,d|Df|\right)\right| = \left|\int_\Omega \phi\,(d\tilde{\mu}_n - d\tilde{\mu})\right|$ tends to 0 for every $\phi \in \mathcal{C}_0(\Omega)$ then $\int_\Omega \phi\,d\mu_n$ converges to $\int_\Omega \phi\,d\mu$ for every $\phi \in \mathcal{C}_0(\Omega)$. We can deduce that $\mu_n \underset{n\to+\infty}{\rightharpoonup} \mu$ in the sense of Radon measure. □

Lemma 3.2 (adapted from [27, Lemma 3])**.** *Let E be a Borel set and $R > 0$. Let $E_R = E + B_R(0) = \{x + y \,|\, x \in E,\, y \in B_R(0)\}$, $B_R(0)$ being the ball centered at 0 of radius R, and suppose that $E_R \subset \Omega$. Then* $\int_E d\mu_n \le \frac{K_{1,2}}{c}\,|f|_{BV(E_R,g)} + \frac{2}{R}\|f\|_{L^1(\Omega)}\int_{\mathbb{R}^2\setminus B_R(0)} \rho_n(x)\,dx.$

Proof. From [27, Lemma 3] we get that $\int_E d\tilde{\mu}_n \le K_{1,2}\int_{E_R} d|Df| + \frac{2}{R}\|f\|_{L^1(\Omega)}\int_{\mathbb{R}^2\setminus B_R(0)}$ $\rho_n(x)\,dx$. Thus $\int_E d\mu_n \le \int_E d\tilde{\mu}_n \le K_{1,2}\int_{E_R} d|Df| + \frac{2}{R}\|f\|_{L^1(\Omega)}\int_{\mathbb{R}^2\setminus B_R(0)} \rho_n(x)\,dx \le \frac{K_{1,2}}{c}$ $|f|_{BV(E_R,g)} + \frac{2}{R}\|f\|_{L^1(\Omega)}\int_{\mathbb{R}^2\setminus B_R(0)} \rho_n(x)\,dx$ as $0 < c \le g \le 1$. □

Now let us complete the proof of Theorem 3.1. For $\delta > 0$ and small, let $V_\delta = \{x \in \Omega \,|\, dist(x, \partial\Omega) > \delta\}$. Then $\partial V_\delta = \{x \in \Omega \,|\, dist(x, \partial\Omega) = \delta\}$, and so $\int_{\partial V_\delta} g\,d|Df| = 0$ $\le \int_{\partial V_\delta} d|Df| = 0$ for all but perhaps countably many δ's in an interval $(0, \delta_0)$. Indeed, J_f being the set of jumps of f, is countably $\mathcal{H}^1$-rectifiable according to [2, p. 184]. It can thus be covered with countable many $\mathcal{C}^1$ hypersurfaces. Finally from [2, Lemma 3.76, p.170], we get the result. For any such δ, $\mu_n(V_\delta) \underset{n\to+\infty}{\longrightarrow} K_{1,2}\,|f|_{BV(V_\delta,g)}$, due to [34, Theorem 1, p.54].
To conclude, note that to prove $|f|_{BV(\Omega\setminus V_\delta,g)} \underset{\delta\to 0}{\longrightarrow} 0$, we only need to control $\mu_n(\Omega \setminus V_\delta)$ uniformly as $n \to +\infty$.
Consider $\tilde{f} = Ef$, where $E : BV(\Omega, g) \subset BV(\Omega) \to BV(\mathbb{R}^2) \subset BV(\mathbb{R}^2, g)$ is an extension operator with this additional property: let $U_\delta = \{x \in \mathbb{R}^2 | dist(x, \partial\Omega) < \delta\}$, $|Ef|_{BV(U_\delta,g)} \le \int_{U_\delta} d|D(Ef)| \le C_1 \int_{U_{C_2\delta}\cap\Omega} d|Df| \le \frac{C_1}{c}|f|_{BV(U_{C_2\delta}\cap\Omega,g)}$, with $C_1, C_2 > 0$ depending only on Ω. This can be achieved by a standard reflexion across the boundary, so that $\int_{\partial\Omega} d|D(Ef)| = 0$, that is, E does not create any jump across the boundary of Ω. For more details, please refer to [27, Proof of Theorem 1].
Now, by applying the previous lemma to the function $\tilde{f}$ with $E = \Omega \setminus V_\delta$ we have

$$\mu_n(\Omega \setminus V_\delta) \le \frac{K_{1,2}}{c}|\tilde{f}|_{BV(\Omega\setminus V_\delta + B_R(0),g)} + \frac{2}{R}\|\tilde{f}\|_{L^1(\mathbb{R}^2)}\int_{\mathbb{R}^2\setminus B_R(0)} \rho_n(x)\,dx.$$

Letting $n \to +\infty$, we see that $\limsup_{n\to+\infty} \mu_n(\Omega \setminus V_\delta) \le \frac{K_{1,2}}{c}\,|\tilde{f}|_{BV(\Omega\setminus V_\delta + B_R(0),g)}$ and this holds for any $R > 0$. We take $R = \delta$ and use the property of the extension mapping:

$$\limsup_{n\to+\infty} \mu_n(\Omega \setminus V_\delta) \le \frac{K_{1,2}}{c} C_1 |f|_{BV(\{x\in\Omega \,|\, dist(x,\partial\Omega)<2C_2\delta\},g)},$$

and the right hand side of this inequality has limit 0 as δ tends to 0. □

Motivated by the asymptotic properties of this nonlocal quantity, we propose using this characterization to approximate the weighted total variation of the composite function $T \circ \varphi$ (with n large enough). We replace $\mathrm{var}_g\, T \circ \varphi$ by its nonlocal counterpart that now contains a differential quotient in $T \circ \varphi$. We thus propose minimizing the following nonlocal functional denoted by (NLP) that stands for *NonLocal Problem*:

$$\inf_{\varphi \in \mathrm{Id} + W_0^{1,4}(\Omega,\mathbb{R}^2)} \Bigg\{ E_n(\varphi) = \frac{1}{K_{1,2}} \int_\Omega g(x) \left[\int_\Omega \frac{|T \circ \varphi(y) - T \circ \varphi(x)|}{|x-y|} \rho_n(x-y)\, dy \right] dx$$
$$+ a \int_\Omega \left[(c_1 - R)^2 - (c_2 - R)^2 \right] T \circ \varphi \, dx + \frac{\nu}{2} \|T \circ \varphi - R\|^2_{L^2(\Omega)} + \int_\Omega QW(\nabla \varphi)\, dx \Bigg\}. \tag{NLP}$$

We first state the existence of minimizers for this functional E_n for every $n \in \mathbb{N}^*$.

Theorem 3.2 (Existence of minimizers for E_n)**.** *The problem (NLP) admits at least one solution for any $n \in \mathbb{N}^*$.*

Proof. This proof is divided into three parts. The first one consists of deriving a coercivity inequality. The second one shows the convergence of a minimizing sequence and the last one is dedicated to the lower semi-continuity of the functional.

For the sake of conciseness, we use this notation: $F_n(f) = \int_\Omega g(x) \Big[\int_\Omega \frac{|f(x) - f(y)|}{|x-y|} \rho_n(x-y)\, dy \Big] dx$.

1. **Coercivity inequality**:
   Let $n \in \mathbb{N}^*$, we get the following inequality using the same computations as in Theorem 2.1:

$$\begin{aligned} E_n(\varphi) &\geq a \int_\Omega \left[(c_1(\varphi) - R)^2 - (c_2(\varphi) - R)^2 \right] T \circ \varphi \, dx \\ &\quad + \frac{\nu}{2} \|T \circ \varphi - R\|^2_{L^2(\Omega)} + \int_\Omega QW(\nabla \varphi)\, dx, \\ &\geq \frac{\mu}{4} \|\det(\nabla \varphi)\|^2_{L^2(\Omega)} + \frac{\beta}{2} \|\nabla \varphi\|^4_{L^4(\Omega,M_2)} - \beta \alpha^2 - 3\mu + \frac{\mu(\lambda+\mu)}{2(\lambda+2\mu)} \\ &\quad - 4a \|R\|^2_{L^\infty(\Omega)} \|T\|_{L^\infty(\Omega)}. \end{aligned}$$

   Using the generalized Poincaré inequality, we get $E_n(\varphi) \geq c\|\varphi\|_{W^{1,4}(\Omega,\mathbb{R}^2)} + \kappa$, $\kappa \in \mathbb{R}$. As E_n is proper by taking $\varphi = \mathrm{Id}$, the infimum of the functional E_n is finite.

2. **Convergence of a minimizing sequence**:
   Let $\{\varphi_n^k\}_{k=1}^\infty \in \mathrm{Id} + W_0^{1,4}(\Omega,\mathbb{R}^2)$ be a minimizing sequence of E_n for any $n \in \mathbb{N}^*$. As E_n is proper by taking $\hat{\varphi}_n = \mathrm{Id} \in \mathrm{Id} + W_0^{1,4}(\Omega,\mathbb{R}^2)$, that is to say, $E_n(\hat{\varphi}_n) < \infty$, then for k large enough, we get $E_n(\varphi_n^k) \leq E_n(\hat{\varphi}_n) + 1$. From the previous

coercivity inequality, we deduce that $\{\varphi_n^k\}_k$ is uniformly bounded in $W^{1,4}(\Omega,\mathbb{R}^2)$ and $\{\det\nabla\varphi_n^k\}_k$ is uniformly bounded in $L^2(\Omega)$. We can thus extract subsequences still denoted by $\{\varphi_n^k\}_k$ and $\{\det\nabla\varphi_n^k\}_k$ such that there exist $\bar{\varphi}_n$ and $\bar{\delta}_n$ satisfying:

$$\varphi_n^k \underset{k\to+\infty}{\rightharpoonup} \bar{\varphi}_n \in W^{1,4}(\Omega,\mathbb{R}^2),$$
$$\det\nabla\varphi_n^k \underset{k\to+\infty}{\rightharpoonup} \bar{\delta}_n \in L^2(\Omega).$$

From [25, Theorem 1.14 p.16], if $\varphi_n^k \underset{k\to+\infty}{\rightharpoonup} \bar{\varphi}_n$ in $W^{1,4}(\Omega,\mathbb{R}^2)$ then $\det(\nabla\varphi_n^k) \underset{k\to+\infty}{\rightharpoonup} \det(\nabla\bar{\varphi}_n)$ in $L^2(\Omega)$ and so $\bar{\delta}_n = \det\nabla\bar{\varphi}_n$. Also by continuity of the trace operator, we get $\bar{\varphi}_n = \mathrm{Id}$ on $\partial\Omega$.

3. **Lower semicontinuity**:
Now, we prove the lower semi-continuity of the functional E_n. Let us now introduce the mapping $J : \begin{array}{ll} W^{1,4}(\Omega,\mathbb{R}^2)\times L^2(\Omega) & \to \mathbb{R} \\ (\phi,\delta) & \mapsto \displaystyle\int_\Omega W^*(\phi,\delta)\,dx \end{array}$ with $W^*(\phi,\delta) = \left|\begin{array}{ll} \beta(\|\nabla\phi\|^2-\alpha)^2+\psi(\delta) & \text{if } \|\nabla\phi\|^2>\alpha \\ \psi(\delta) & \text{otherwise} \end{array}\right.$. $W^*(\phi,\delta)$ is convex thanks to the polyconvexity of QW and continuous. By using classical arguments (see [41]), we can show that $J(\phi,\delta)$ is convex strongly lower semi-continuous and so weakly lower semi-continuous. Eventually, we get that $J(\bar{\varphi}_n,\det\nabla\bar{\varphi}_n) \le \liminf_{k\to+\infty} J(\varphi_n^k,\det\nabla\varphi_n^k)$.

Besides, according to Rellich-Kondrachov theorem, we have that $\{\varphi_n^k\}$ converges uniformly to $\bar{\varphi}_n$. As T is assumed to be Lipschitz continuous, we get that $(T\circ\varphi_n^k)$ converges to $T\circ\bar{\varphi}_n$ pointwise. Therefore $g(x)\frac{|T\circ\varphi_n^k(y)-T\circ\varphi_n^k(x)|}{|x-y|}\rho_n(x-y)$ converges to $g(x)\frac{|T\circ\bar{\varphi}_n(y)-T\circ\bar{\varphi}_n(x)|}{|x-y|}\rho_n(x-y)$ almost everywhere and according to Fatou's lemma, $\displaystyle\int_\Omega g(x)\Big[\int_\Omega \frac{|T\circ\bar{\varphi}_n(x)-T\circ\bar{\varphi}_n(y)|}{|x-y|}\,\rho_n(x-y)\,dy\Big]dx \le \liminf_{k\to+\infty}\int_\Omega g(x)\Big[\int_\Omega \frac{|T\circ\varphi_n^k(x)-T\circ\varphi_n^k(y)|}{|x-y|}\rho_n(x-y)\,dy\Big]dx$. We have also proved in what precedes that when $\{\varphi_n^k\}_k$ weakly converges to $\bar{\varphi}_n$ in $W^{1,4}(\Omega,\mathbb{R}^2)$, then $\displaystyle\int_\Omega\big[(c_1(\varphi_n^k)-R)^2-(c_2(\varphi_n^k)-R)^2\big]T\circ\varphi_n^k\,dx = \int_\Omega\big[(c_{1_n}^k-R)^2-(c_{2_n}^k-R)^2\big]T\circ\varphi_n^k\,dx$ converges to $\displaystyle\int_\Omega\big[(c_{1_n}^-R)^2-(c_{2_n}^-R)^2\big]T\circ\bar{\varphi}_n\,dx = \int_\Omega\big[(c_1(\bar{\varphi}_n)-R)^2-(c_2(\bar{\varphi}_n)-R)^2\big]T\circ\bar{\varphi}_n\,dx$ and $\|T\circ\varphi_n^k-R\|^2_{L^2(\Omega)}$ converges to $\|T\circ\bar{\varphi}_n-R\|^2_{L^2(\Omega)}$. To conclude, functional E_n is weakly lower semi-continuous and $E_n(\bar{\varphi}_n) \le \liminf_{k\to+\infty} E_n(\varphi_n^k) = \inf_{\varphi\in\mathrm{Id}+W_0^{1,4}(\Omega,\mathbb{R}^2)} E_n(\varphi)$. So, there exists at least one minimizer for E_n for any $n\in\mathbb{N}^*$ on $\mathrm{Id}+W_0^{1,4}(\Omega,\mathbb{R}^2)$.

□

An important Γ-convergence result relating the approximated problem to the original one (and highlighting thus its interest) is given next.

Theorem 3.3 (Γ-convergence)**.** *Let* $\{\bar{\varphi}_n\}_n \in Id+W_0^{1,4}(\Omega,\mathbb{R}^2)$ *be a sequence of minimizers of* E_n*. Then there exist a subsequence still denoted by* $\{\bar{\varphi}_n\}_n$ *and* $\bar{\varphi} \in Id + W_0^{1,4}(\Omega,\mathbb{R}^2)$ *a minimizer of* $\bar{I}$ *such that* $\bar{\varphi}_n \underset{n\to+\infty}{\rightharpoonup} \bar{\varphi}$ *in* $W^{1,4}(\Omega,\mathbb{R}^2)$*. If we assume that* $g \in \mathcal{C}^1(\bar{\Omega})$ *with* $\|\nabla g\|_{\mathcal{C}^0(\bar{\Omega})} = k < +\infty$*, then one has* $\lim\limits_{n\to+\infty} E_n(\bar{\varphi}_n) = \bar{I}(\bar{\varphi})$.

Proof. The loss of symmetry in the expression of the nonlocal component (due to the g component) raises a technical difficulty. To overcome this issue, an additional assumption is set on g in order to use Taylor's expansion and to recover then some symmetry.
For $n \in \mathbb{N}^*$ fixed, we have proved the existence of a solution $\bar{\varphi_n}$ in $\mathrm{Id} + W_0^{1,4}(\Omega,\mathbb{R}^2)$ to problem (NLP). So for any $n \in \mathbb{N}^*$,

$$\forall v \in \mathrm{Id} + W_0^{1,4}(\Omega,\mathbb{R}^2),\ E_n(\bar{\varphi}_n) \leq E_n(v),$$

and according to the following Proposition :

Proposition 3.3 (taken from [8, Proposition 2.1])**.** *Assume* $1 \leq p \leq +\infty$ *and* $u \in W^{1,p}(\Omega)$ *and* $\rho \in L^1(\mathbb{R}^2)$*,* $\rho > 0$*. Then*

$$\int_\Omega g(x)\left[\int_\Omega \frac{|u(y)-u(x)|^p}{|x-y|^p}\rho(x-y)\,dy\right]dx \leq \int_\Omega \left[\int_\Omega \frac{|u(y)-u(x)|^p}{|x-y|^p}\rho(x-y)\,dy\right]dx,$$
$$\leq C|u|^p_{W^{1,p}(\Omega)}\|\rho\|_{L^1(\mathbb{R}^2)} \leq \frac{C}{c}|u|^p_{W^{1,p}(\Omega,g)}\|\rho\|_{L^1(\mathbb{R}^2)},$$

where C *depends only on* p *and* Ω*, and* $|u|_{W^{1,p}(\Omega)}$ *denotes the semi-norm in* $W^{1,p}(\Omega)$ *that is to say* $|u|_{W^{1,p}(\Omega)} = \|\nabla u\|_{L^p(\Omega)}$.

$E_n(v) \leq \frac{C}{c}|T\circ v|_{W^{1,1}(\Omega,g)} + \frac{\nu}{2}\|T\circ v - R\|^2_{L^2(\Omega,\mathbb{R}^2)} + a\int_\Omega\big[(c_1(v)-R)^2 - (c_2(v)-R)^2\big]T\circ v\,dx + \int_\Omega QW(\nabla v)\,dx$ which is independant of n —take for instance $v = \mathrm{Id}$ and since $T \in W^{1,\infty}(\Omega,\mathbb{R})$, the right-hand side will involve $|T|_{W^{1,1}(\Omega)}$—. Note that as $T\circ v \in W^{1,4}(\Omega,\mathbb{R}) \subset W^{1,1}(\Omega,\mathbb{R})$, $|T\circ v|_{W^{1,1}(\Omega,g)} = \mathrm{var}_g\, T\circ v$, see [10, Remark 5]. Therefore, according to the coercivity inequality, the sequence $\{\bar{\varphi}_n\}_n$ is uniformly bounded in $W^{1,4}(\Omega,\mathbb{R}^2)$ and so there exists $\bar{\varphi} \in \mathrm{Id} + W_0^{1,4}(\Omega,\mathbb{R}^2)$ by continuity of the trace operator, such that up to a subsequence, $\{\bar{\varphi}_n\}_n$ weakly converges to $\bar{\varphi}$ in $W^{1,4}(\Omega,\mathbb{R}^2)$.
We would like to prove that $E_n(\bar{\varphi}_n)$ converges to $\bar{I}(\bar{\varphi})$ when n tends to $+\infty$.
By definition of $\{\bar{\varphi}_n\}$, one has $E_n(\bar{\varphi}_n) \leq E_n(\bar{\varphi})$, for all $n \in \mathbb{N}^*$. Thus by taking the upper

limit when n tends to $+\infty$,

$$\begin{aligned}
\limsup_{n\to+\infty} E_n(\bar\varphi_n) &\le \limsup_{n\to+\infty} E_n(\bar\varphi),\\
&\le \limsup_{n\to+\infty} \frac{1}{K_{1,2}} \int_\Omega g(x)\left[\int_\Omega \frac{|T\circ\bar\varphi(x)-T\circ\bar\varphi(y)|}{|x-y|}\rho_n(x-y)\,dy\right]dx\\
&+ \frac{\nu}{2}\|R-T\circ\bar\varphi\|^2_{L^2(\Omega)} + a\int_\Omega \left[(c_1(\bar\varphi)-R)^2-(c_2(\bar\varphi)-R)^2\right]T\circ\bar\varphi\,dx\\
&+ \int_\Omega QW(\nabla\bar\varphi)\,dx,\\
&\le var_g(T\circ\bar\varphi) + \frac{\nu}{2}\|T\circ\bar\varphi-R\|^2_{L^2(\Omega)}\\
&+ a\int_\Omega \left[(c_1(\bar\varphi)-R)^2-(c_2(\bar\varphi)-R)^2\right]T\circ\bar\varphi\,dx + \int_\Omega QW(\nabla\bar\varphi)\,dx,\\
&\le \bar I(\bar\varphi).
\end{aligned}$$

So, $\limsup_{n\to+\infty} E_n(\bar\varphi_n) \le \bar I(\bar\varphi)$.
It remains to prove that

$$\bar I(\bar\varphi) \le \liminf_{n\to+\infty} E_n(\bar\varphi_n).$$

Due to what was done previously and to compactness properties, it suffices to prove that $var_g(T\circ\bar\varphi) \le \liminf_{n\to+\infty} F_n(T\circ\bar\varphi_n)$.
In that purpose, let us introduce some notations. For $r>0$, we define the two following sets:

$$\begin{aligned}
\Omega_r &= \{x\in\Omega \,:\, dist(x,\partial\Omega) > r\},\\
\Omega^r &= \{x\in\mathbb{R}^2 \,:\, dist(x,\Omega) < r\}.
\end{aligned}$$

Let $\eta\in\mathcal{C}_0^\infty(\mathbb{R}^2)$ be a nonnegative radial function such that $\int_\Omega \eta = 1$, $Supp\,\eta \subset B_1(0)$ where the notation $B_r(c)$ refers to the ball of radius r and centered at c, and let us define

$$f_\delta(x) = \frac{1}{\delta^2}\int_\Omega f(y)\eta(\frac{x-y}{\delta})\,dy = \frac{1}{\delta^2}\int_{B(x,\delta)} f(y)\eta(\frac{x-y}{\delta})\,dy\ \forall x\in\Omega_\delta,$$

a regularization of f.
For the sake of clarity, we set $f = T\circ\bar\varphi$, and due to the properties of T, $f_n = T\circ\bar\varphi_n$ strongly converges to $f = T\circ\bar\varphi$ in $L^1(\Omega)$ since T is Lipschitz continuous.
From an adaptation of [52, Lemma 4], for each $r>0$, $\delta\in(0,r)$:

$$F_n(f_n)+k\delta C \ge \int_{\Omega_{2r}} g(x)\left[\int_{\Omega_{2r}} \frac{|f_{n,\delta}(y)-f_{n,\delta}(x)|}{|x-y|}\rho_n(x-y)\,dy\right]dx,\ \forall\delta\in(0,r).$$

Indeed,

$$\begin{aligned}
&\int_{\Omega_{2r}} g(x)\left[\int_{\Omega_{2r}} \frac{|f_{n,\delta}(x)-f_{n,\delta}(y)|}{|x-y|}\rho_n(x-y)\,dy\right]dx\\
&=\int_{\Omega_{2r}} g(x)\left[\int_{\Omega_{2r}} \frac{|\int_{B_\delta(0)}\frac{f_n(x-z)}{\delta^2}\eta(\frac{z}{\delta})\,dz-\int_{B_\delta(0)}\frac{f_n(y-z)}{\delta^2}\eta(\frac{z}{\delta})\,dz|}{|x-y|}\rho_n(x-y)\,dy\right]dx,\\
&\leq \int_{\Omega_{2r}}\int_{\Omega_{2r}}\int_{B_\delta(0)} g(x)\frac{|f_n(x-z)-f_n(y-z)|}{\delta^2|x-y|}\eta(\frac{z}{\delta})\rho_n(x-y)\,dz\,dy\,dx.
\end{aligned}$$

Now, we use the following change of variables: $w=x-z$ and $v=y-z$ keeping in mind $\delta<r$:

$$\leq \int_{\Omega_r}\int_{\Omega_r}\int_{B_\delta(0)} g(w+z)\frac{|f_n(w)-f_n(v)|}{\delta^2|w-v|}\eta(\frac{z}{\delta})\rho_n(w-v)\,dz\,dv\,dw.$$

Since we have assumed that $g\in\mathcal{C}^1(\bar{\Omega})$ with $\|\nabla g\|_{L^\infty(\bar{\Omega})}=k<\infty$, we get that $g(w+z)=g(w)+\int_0^1\langle\nabla g(w+sz),z\rangle\,ds$. We now integrate this to the previous inequality:

$$\begin{aligned}
&\int_{\Omega_{2r}} g(x)\left[\int_{\Omega_{2r}} \frac{|f_{n,\delta}(x)-f_{n,\delta}(y)|}{|x-y|}\rho_n(x-y)\,dy\right]dx\\
&\leq \int_{\Omega_r}\int_{\Omega_r}\int_{B_\delta(0)}\left[g(w)+\int_0^1\langle\nabla g(w+sz),z\rangle\,ds\right]\frac{|f_n(w)-f_n(v)|}{\delta^2|w-v|}\eta(\frac{z}{\delta})\rho_n(w-v)\,dz\,dv\,dw,\\
&\leq \int_{\Omega_r}\int_{\Omega_r}\int_{B_\delta(0)} g(w)\frac{|f_n(w)-f_n(v)|}{\delta^2|w-v|}\eta(\frac{z}{\delta})\rho_n(w-v)\,dz\,dv\,dw\\
&+\int_{\Omega_r}\int_{\Omega_r}\int_{B_\delta(0)}\int_0^1\langle\nabla g(w+sz),z\rangle\frac{|f_n(w)-f_n(v)|}{\delta^2|w-v|}\eta(\frac{z}{\delta})\rho_n(w-v)\,ds\,dz\,dv\,dw,
\end{aligned}$$

By noticing that $\Omega_r\subset\Omega$ and that $g(w)\frac{|f_n(w)-f_n(v)|}{\delta^2|w-v|}\eta(\frac{z}{\delta})\rho_n(w-v)$ is non-negative, and by using Cauchy-Schwarz inequality:

$$\begin{aligned}
&\int_{\Omega_{2r}} g(x)\left[\int_{\Omega_{2r}} \frac{|f_{n,\delta}(x)-f_{n,\delta}(y)|}{|x-y|}\rho_n(x-y)\,dy\right]dx\\
&\leq \int_{\Omega}\int_{\Omega}\int_{B_\delta(0)} g(w)\frac{|f_n(w)-f_n(v)|}{\delta^2|w-v|}\eta(\frac{z}{\delta})\rho_n(w-v)\,dz\,dv\,dw\\
&+\int_{\Omega_r}\int_{\Omega_r}\int_{B_\delta(0)}\int_0^1|\nabla g(w+sz)||z|\frac{|f_n(w)-f_n(v)|}{\delta^2|w-v|}\eta(\frac{z}{\delta})\rho_n(w-v)\,ds\,dz\,dv\,dw.
\end{aligned}$$

As $w\in\Omega_r$, $z\in B_\delta(0)$, $s\in[0;1]$ and $\delta\in(0,r)$, then $w+sz\in\Omega$,
and by integrating the first part with respect to z, we get:

$$\int_{\Omega_{2r}} g(x)\left[\int_{\Omega_{2r}} \frac{|f_{n,\delta}(x)-f_{n,\delta}(y)|}{|x-y|}\rho_n(x-y)\,dy\right]dx$$
$$\leq \int_{\Omega} g(w)\left[\int_{\Omega} \frac{|f_n(w)-f_n(v)|}{|w-v|}\rho_n(w-v)\,dv\right]dw$$
$$+\|\nabla g\|_{L^\infty(\Omega)}\int_{\Omega_r}\int_{\Omega_r}\int_{B_\delta(0)}\int_0^1 |z|\frac{|f_n(w)-f_n(v)|}{\delta^2|w-v|}\eta(\frac{z}{\delta})\rho_n(w-v)\,ds\,dz\,dv\,dw,$$

We use the change of variable: $u=\dfrac{z}{\delta}$ in the second part. So,

$$\int_{\Omega_{2r}} g(x)\left[\int_{\Omega_{2r}} \frac{|f_{n,\delta}(x)-f_{n,\delta}(y)|}{|x-y|}\rho_n(x-y)\,dy\right]dx$$
$$\leq F_n(f_n)+\|\nabla g\|_{L^\infty(\bar{\Omega})}\int_{\Omega_r}\int_{\Omega_r}\int_{B_1(0)}\delta|u|\frac{|f_n(w)-f_n(v)|}{|w-v|}\eta(u)\rho_n(w-v)\,du\,dv\,dw.$$

Besides, $\displaystyle\int_{B_1(0)}|u|\eta(u)\,du\leq\int_{B_1(0)}\eta(u)\,du=1$ and as $f_n\in W^{1,4}(\Omega)\subset BV(\Omega)$, from [27, Lemma 3], we get $\displaystyle\int_{\Omega_r}\int_{\Omega_r}\frac{|f_n(x)-f_n(y)|}{|x-y|}\rho_n(x-y)\,dx\,dy\leq K_{1,2}var\,f_n+\frac{2}{r}\|f_n\|_{L^1(\Omega)}\leq C<+\infty$ with C independant of n. Then

$$\int_{\Omega_{2r}} g(x)\left[\int_{\Omega_{2r}} \frac{|f_{n,\delta}(x)-f_{n,\delta}(y)|}{|x-y|}\rho_n(x-y)\,dy\right]dx\leq F_n(f_n)+k\delta C. \tag{4.4}$$

We first aim to prove that $\displaystyle\lim_{n\to+\infty}\int_{\Omega_{2r}} g(x)\left[\int_{\Omega_{2r}} \frac{|f_{n,\delta}(x)-f_{n,\delta}(y)|}{|x-y|}\rho_n(x-y)\,dy\right]dx = K_{1,2}\int_{\Omega_{2r}} g\,d|Df_\delta|$.
We start by proving that

$$\lim_{n\to+\infty}\left|\int_{\Omega_{2r}}\int_{\Omega_{2r}} g(x)\left(\frac{|f_{n,\delta}(x)-f_{n,\delta}(y)|}{|x-y|}-\nabla f_\delta(x).\frac{x-y}{|x-y|}\right)\rho_n(x-y)\,dy\,dx\right|=0.$$

It is easily seen that

$$\lim_{n\to+\infty}\left|\int_{\Omega_{2r}} g(x)\left[\int_{\Omega_{2r}}\left(\frac{|f_{n,\delta}(x)-f_{n,\delta}(y)|}{|x-y|}-\left|\nabla f_\delta(x).\frac{x-y}{|x-y|}\right|\right)\rho_n(x-y)\,dy\right]dx\right|$$
$$\leq\lim_{n\to+\infty}\int_{\Omega_{2r}}\left[\int_{\Omega_{2r}}\left|\frac{|f_{n,\delta}(x)-f_{n,\delta}(y)|}{|x-y|}-\left|\nabla f_\delta(x).\frac{x-y}{|x-y|}\right|\right|\rho_n(x-y)\,dy\right]dx,$$
$$\leq\lim_{n\to+\infty}\int_{\Omega_{2r}}\left[\int_{\Omega_{2r}}\frac{|f_{n,\delta}(x)-f_{n,\delta}(y)-\nabla f_\delta(x).(x-y)|}{|x-y|}\rho_n(x-y)\,dy\right]dx,$$
$$\leq\lim_{n\to+\infty}\int_{\Omega_r}\left[\int_{\Omega_r}\frac{|f_{n,\delta}(x)-f_{n,\delta}(y)-\nabla f_\delta(x).(x-y)|}{|x-y|}\rho_n(x-y)\,dy\right]dx,$$

since $\Omega_{2r}\subset\Omega_r$ and the function is non-negative. Let us take s such that $s\in(0,r-\delta)$. Then if $x\in\Omega_r$ and $y\in(\Omega_r)^s$ and if $|x-y|<s$, the segment of endpoints x and y is

contained in $(\Omega_r)^s$ so that, $f_{n,\delta}$ being sufficiently smooth, from Taylor's expansion:

$$f_{n,\delta}(y) - f_{n,\delta}(x) = \int_0^1 (y-x).\nabla f_{n,\delta}(x + s(y-x))\, ds.$$

Then

$$f_{n,\delta}(x) - f_{n,\delta}(y) - \nabla f_\delta(x).(x-y) = \int_0^1 (x-y).(\nabla f_{n,\delta}(x + s(y-x)) - \nabla f_\delta(x))\, ds,$$

and keeping in mind that $|x-y| < s$,

$$\begin{aligned}
|f_{n,\delta}(x) - f_{n,\delta}(y) - \nabla f_\delta(x).(x-y)| &\le |x-y| \int_0^1 |\nabla f_{n,\delta}(x + s(y-x)) - \nabla f_\delta(x)|\, ds, \\
&\le |x-y| \int_0^1 |\nabla f_{n,\delta}(x + s(y-x)) - \nabla f_\delta(x + s(y-x)) \\
&+ \nabla f_\delta(x + s(y-x)) - \nabla f_\delta(x)|\, ds, \\
&\le |x-y| \|\nabla f_{n,\delta} - \nabla f_\delta\|_{L^\infty((\Omega_r)^s)} \\
&+ |x-y| \int_0^1 |\nabla f_\delta(x + s(y-x)) - \nabla f_\delta(x)|\, ds, \\
&\le |x-y| \|\nabla f_{n,\delta} - \nabla f_\delta\|_{L^\infty((\Omega_r)^s)} \\
&+ \frac{1}{2}|x-y|^2 \|\nabla^2 f_\delta\|_{L^\infty(\Omega_\delta)}.
\end{aligned}$$

Thus

$$\frac{|f_{n,\delta}(x) - f_{n,\delta}(y) - \nabla f_\delta(x).(x-y)|}{|x-y|} \le \|\nabla f_{n,\delta} - \nabla f_\delta\|_{L^\infty((\Omega_r)^s)} + \frac{1}{2}|x-y| \|\nabla^2 f_\delta\|_{L^\infty(\Omega_\delta)}.$$

Now,

$$\begin{aligned}
&\int_{\Omega_r}\int_{\Omega_r} \frac{|f_{n,\delta}(x) - f_{n,\delta}(y) - \nabla f_\delta(x).(x-y)|}{|x-y|} \rho_n(x-y)\, dy\, dx \\
&\le \int_{\Omega_r}\int_{(\Omega_r)^s} \frac{|f_{n,\delta}(x) - f_{n,\delta}(y) - \nabla f_\delta(x).(x-y)|}{|x-y|} \rho_n(x-y)\, dy\, dx, \text{ since } \Omega_r \subset (\Omega_r)^s, \\
&\le \int_{\Omega_r}\int_{(\Omega_r)^s \cap |x-y|<s} \frac{|f_{n,\delta}(x) - f_{n,\delta}(y) - \nabla f_\delta(x).(x-y)|}{|x-y|} \rho_n(x-y)\, dy\, dx \\
&+ \int_{\Omega_r}\int_{(\Omega_r)^s \cap |x-y|\ge s} \frac{|f_{n,\delta}(x) - f_{n,\delta}(y) - \nabla f_\delta(x).(x-y)|}{|x-y|} \rho_n(x-y)\, dy\, dx,
\end{aligned}$$

We consider each component of the right hand side of the inequality.

$$\int_{\Omega_r}\int_{(\Omega_r)^s\cap|x-y|<s}\frac{|f_{n,\delta}(x)-f_{n,\delta}(y)-\nabla f_\delta(x).(x-y)|}{|x-y|}\rho_n(x-y)\,dy\,dx$$
$$\leq\int_{\Omega_r}\int_{(\Omega_r)^s\cap|x-y|<s}\left(\|\nabla f_{n,\delta}-\nabla f_\delta\|_{L^\infty((\Omega_r)^s)}+\frac{1}{2}|x-y|\|\nabla^2 f_\delta\|_{L^\infty(\Omega_\delta)}\right)\rho_n(x-y)\,dy\,dx,$$
$$\leq|\Omega_r|\|\nabla f_{n,\delta}-\nabla f_\delta\|_{L^\infty((\Omega_r)^s)}+\left(\frac{|\Omega_r|}{2}\|\nabla^2 f_\delta\|_{L^\infty(\Omega_\delta)}\right)\int_{|h|<s}|h|\rho_n(h)\,dh,$$

$\forall x\in(\Omega_r)^s$,

$$\begin{aligned}|f_{n,\delta}(x)-f_\delta(x)|&\leq\frac{1}{\delta^2}\int_{B(x,\delta)}\eta(\frac{x-y}{\delta})\,|f_n(y)-f(y)|\,dy,\\&\leq\int_{B(0,1)}\eta(z)\,|f_n(x-\delta z)-f(x-\delta z)|\,dy,\\&\leq\|\eta\|_{L^\infty(B_0(1))}\,\|f_n-f\|_{L^1(\Omega)}.\end{aligned}$$

Also, $\frac{\partial f_{n,\delta}}{\partial x_i}(x)=\int_\Omega\frac{\partial\eta_\delta}{\partial x_i}(x-y)\,f_n(y)\,dy=\frac{1}{\delta^3}\int_\Omega\frac{\partial\eta}{\partial x_i}(\frac{x-y}{\delta})\,f_n(y)\,dy$ and $\frac{\partial f_\delta}{\partial x_i}(x)=\int_\Omega\frac{\partial\eta_\delta}{\partial x_i}(x-y)\,f(y)\,dy=\frac{1}{\delta^3}\int_\Omega\frac{\partial\eta}{\partial x_i}(\frac{x-y}{\delta})\,f_n(y)\,dy$ resulting in, $\forall x\in(\Omega_r)^s\subset\Omega_\delta$,

$$|\frac{\partial f_{n,\delta}}{\partial x_i}(x)-\frac{\partial f_\delta}{\partial x_i}(x)|\leq\frac{1}{\delta^3}\int_\Omega|\frac{\partial\eta}{\partial x_i}(\frac{x-y}{\delta})|\,|f_n(y)-f(y)|\,dy,\quad\leq\frac{1}{\delta^3}\,\|\frac{\partial\eta}{\partial x_i}\|_{L^\infty(B_0(1))}\,\|f_n-f\|_{L^1(\Omega)}.$$

As a consequence, $|\Omega_r|\|\nabla f_{n,\delta}-\nabla f_\delta\|_{L^\infty((\Omega_r)^s)}\underset{n\to+\infty}{\longrightarrow}0$, since f_n converges strongly in $L^1(\Omega)$ to f and $\frac{|\Omega_r|}{2}\|\nabla^2 f_\delta\|_{L^\infty(\Omega_\delta)}<\infty$, independent of n since $f_\delta\in\mathcal{C}^\infty(\Omega_\delta)$.
Besides, due to the result by D. Spector [58], $\lim_{n\to+\infty}\int_{|h|<s}|h|\rho_n(h)\,dh=0$. So, $\int_{\Omega_r}\int_{(\Omega_r)^s\cap|x-y|<s}\frac{|f_{n,\delta}(x)-f_{n,\delta}(y)-\nabla f_\delta(x).(x-y)|}{|x-y|}\rho_n(x-y)\,dy\,dx\underset{n\to+\infty}{\longrightarrow}0$. Furthermore,

$$\int_{\Omega_r}\int_{(\Omega_r)^s\cap|x-y|\geq s}\frac{|f_{n,\delta}(x)-f_{n,\delta}(y)-\nabla f_\delta(x).(x-y)|}{|x-y|}\rho_n(x-y)\,dy\,dx$$
$$\leq\frac{1}{s}\int_{\Omega_r}\int_{(\Omega_r)^s\cap|x-y|\geq s}|f_{n,\delta}(x)-f_{n,\delta}(y)|\rho_n(x-y)\,dy\,dx$$
$$+\int_{\Omega_r}\int_{(\Omega_r)^s\cap|x-y|\geq s}\left|\nabla f_\delta(x).\frac{x-y}{|x-y|}\right|\rho_n(x-y)\,dy\,dx,$$
$$\leq\frac{1}{s}\int_{\Omega_r}\int_{(\Omega_r)^s\cap|x-y|\geq s}(|f_{n,\delta}(x)-f_\delta(x)|+|f_\delta(x)-f_\delta(y)|+|f_\delta(y)-f_{n,\delta}(y)|)\,\rho_n(x-y)\,dy\,dx$$
$$+\|\nabla f_\delta\|_{L^\infty(\Omega_\delta)}\int_{\Omega_r}\int_{(\Omega_r)^s\cap|x-y|\geq s}\rho_n(x-y)\,dy\,dx,$$

$$\leq \frac{2}{s}\|f_{n,\delta} - f_\delta\|_{L^\infty((\Omega_r)^s)}|\Omega_r| \int_{|h|\geq s} \rho_n(h)\,dh + \frac{2}{s}\|f_\delta\|_{L^\infty(\Omega_\delta)}|\Omega_r| \int_{|h|\geq s} \rho_n(h)\,dh$$
$$+ \|\nabla f_\delta\|_{L^\infty(\Omega_\delta)}|\Omega_r| \int_{|h|\geq s} \rho_n(h)\,dh.$$

We thus have proved that

$$\lim_{n\to+\infty} \Big| \int_{\Omega_{2r}} g(x) \left[\int_{\Omega_{2r}} \frac{|f_{n,\delta}(x) - f_{n,\delta}(y)|}{|x-y|} \rho_n(x-y)\,dy \right] dx$$
$$- \int_{\Omega_{2r}} g(x) \left[\int_{\Omega_{2r}} \left| \nabla f_\delta(x).\frac{x-y}{|x-y|} \right| \rho_n(x-y)\,dy \right] dx \Big| = 0.$$

Now it suffices to prove that the limit of $\displaystyle\int_{\Omega_{2r}} g(x) \left[\int_{\Omega_{2r}} \left| \nabla f_\delta(x).\frac{x-y}{|x-y|} \right| \rho_n(x-y)\,dy \right] dx$ when n tends to infinity exists and to compute it.

$$\int_{\Omega_{2r}} g(x) \left[\int_{\mathbb{R}^2} \left| \nabla f_\delta(x)\frac{x-y}{|x-y|} \right| \rho_n(x-y)\,dy \right] dx = \int_{\Omega_{2r}} g(x) \left[\int_{\Omega_{2r}} \left| \nabla f_\delta(x).\frac{x-y}{|x-y|} \right| \rho_n(x-y)\,dy \right] dx$$
$$+ \int_{\Omega_{2r}} g(x) \left[\int_{\mathbb{R}^2\setminus\Omega_{2r}} \left| \nabla f_\delta(x).\frac{x-y}{|x-y|} \right| \rho_n(x-y)\,dy \right] dx.$$

Fixing $\lambda > 0$,

$$\int_{\Omega_{2r}} g(x) \left[\int_{\mathbb{R}^2\setminus\Omega_{2r}} \left| \nabla f_\delta(x).\frac{x-y}{|x-y|} \right| \rho_n(x-y)\,dy \right] dx$$
$$\leq \int_{\Omega_{2r}} \int_{\mathbb{R}^2\setminus\Omega_{2r}} \left| \nabla f_\delta(x).\frac{x-y}{|x-y|} \right| \rho_n(x-y)\,dy\,dx$$
$$\leq |\Omega_{2r}|\|\nabla f_\delta\|_{L^\infty(\Omega_\delta)} \int_{|h|>\lambda} \rho_n(h)\,dh + \|\nabla f_\delta\|_{L^\infty(\overline{\Omega_r})} \int_{\Omega_{2r}\setminus\Omega_{2r+\lambda}} \int_{|x-y|\leq\lambda} \rho_n(x-y)\,dy\,dx,$$
$$\leq |\Omega_{2r}|\|\nabla f_\delta\|_{L^\infty(\Omega_\delta)} \int_{|h|>\lambda} \rho_n(h)\,dh + \|\nabla f_\delta\|_{L^\infty(\Omega_\delta)}|\Omega_{2r}\setminus\Omega_{2r+\lambda}| \int_{|h|\leq\lambda} \rho_n(h)\,dh.$$

By letting n tend to $+\infty$, and then λ tend to 0, it follows that:

$$\lim_{n\to+\infty} \int_{\Omega_{2r}} g(x) \left[\int_{\mathbb{R}^2\setminus\Omega_{2r}} \left| \nabla f_\delta(x).\frac{x-y}{|x-y|} \right| \rho_n(x-y)\,dy \right] dx = 0,$$

(using again the properties of ρ_n).
Now,

$$\int_{\Omega_{2r}} g(x) \left[\int_{\mathbb{R}^2} \left| \nabla f_\delta(x).\frac{x-y}{|x-y|} \right| \rho_n(x-y)\,dy \right] dx = \int_{\Omega_{2r}} g(x) \Big[\int_0^{2\pi} \int_0^{+\infty} \left| \nabla f_\delta(x).\begin{pmatrix} cos(\theta) \\ sin(\theta) \end{pmatrix} \right|$$
$$\rho_n(r) r\,dr\,d\theta \Big] dx$$

with the change of variables $\left\{ \begin{array}{l} y_1 = x_1 + r\,\cos(\theta) \\ y_2 = x_2 + r\,\sin(\theta) \end{array} \right.$, $\theta \in [0; 2\pi]$ and $r \in [0; +\infty[$. That is,

$$\begin{aligned} &\int_{\Omega_{2r}} g(x) \left[\int_{\mathbb{R}^2} \left| \nabla f_\delta(x). \frac{x-y}{|x-y|} \right| \rho_n(x-y)\, dy \right] dx \\ &= \int_{\Omega_{2r}} g(x) |\nabla f_\delta(x)| \left[\int_0^{+\infty} \left[\int_0^{2\pi} \left| e. \begin{pmatrix} \cos(\theta) \\ \sin(\theta) \end{pmatrix} \right| d\theta \right] r \rho_n(r)\, dr \right] dx, \end{aligned}$$

with e any unit vector in $\mathbb{R}^2$.
In the end,

$$\begin{aligned} &\lim_{n\to+\infty} \int_{\Omega_{2r}} g(x) \left[\int_{\mathbb{R}^2} \left| \nabla f_\delta(x). \frac{x-y}{|x-y|} \right| \rho_n(x-y)\, dy \right] dx \\ &= \lim_{n\to+\infty} \int_{\Omega_{2r}} g(x) \left[\int_{\Omega_{2r}} \left| \nabla f_\delta(x). \frac{x-y}{|x-y|} \right| \rho_n(x-y)\, dy \right] dx, \\ &= \frac{1}{|S^1|} \int_0^{2\pi} \left| e. \begin{pmatrix} \cos(\theta) \\ \sin(\theta) \end{pmatrix} \right| d\theta \int_{\Omega_{2r}} g(x)\, |\nabla f_\delta(x)|\, dx, \\ &= K_{1,2} \int_{\Omega_{2r}} g(x) |\nabla f_\delta(x)|\, dx, \\ &= K_{1,2} |f_\delta|_{BV(\Omega_{2r},g)}. \end{aligned}$$

By gathering the previous results including (4.4), we prove that:

$$\begin{aligned} K_{1,2} \int_{\Omega_{2r}} g(x) |\nabla f_\delta(x)|\, dx &= \liminf_{n\to+\infty} \int_{\Omega_{2r}} g(x) \left[\int_{\Omega_{2r}} \frac{|f_{n,\delta}(x) - f_{n,\delta}(y)|}{|x-y|} \rho_n(x-y)\, dy \right] dx, \\ &\leq \liminf_{n\to+\infty} F_n(f_n) + C''\delta \end{aligned}$$

with $C'' = kC$ a constant independant of n and of δ. Using the fact that f_δ strongly converges to f in $L^1(\Omega_r)$ and so in $L^1(\Omega_{2r})$, when $\delta \to 0^+$, we get:

$$\begin{aligned} K_{1,2}\, |T \circ \bar{\varphi}|_{BV(\Omega_{2r},g)} &\leq K_{1,2} \liminf_{\delta\to0^+} \int_{\Omega_{2r}} g(x) |\nabla f_\delta(x)|\, dx, \\ &\leq \liminf_{\delta\to0^+} \left(\liminf_{n\to+\infty} F_n(f_n) + C''\delta \right) = \liminf_{n\to+\infty} F_n(f_n). \end{aligned}$$

Following Ponce [52] based on Beppo-Levi, we obtain that $\sup_{A\subset\subset\Omega} |f|_{BV(A,g)} = |f|_{BV(\Omega,g)}$, then

$$\liminf_{n\to+\infty} F_n(f_n) \geq K_{1,2}\, |T \circ \bar{\varphi}|_{BV(\Omega,g)}.$$

Combining the two previous results allows us to conclude that $\lim_{n\to+\infty} E_n(\bar{\varphi}_n) = \bar{I}(\bar{\varphi})$.
Besides, for any $v \in \mathrm{Id} + W_0^{1,4}(\Omega, \mathbb{R}^2)$, we get:

$$E_n(\bar{\varphi}_n) \leq E_n(v),$$

and by taking the limit when n tends to infinity, we get: $\bar{I}(\bar{\varphi}) \leq \bar{I}(v), \forall v \in \mathrm{Id} + W_0^{1,4}(\Omega, \mathbb{R}^2)$. Therefore $\bar{\varphi}$ is a minimizer of $\bar{I}$. □

A first limitation of this theoretical model (NLP) emerges, due to the nonlinearity in the nonlocal component and in the nonlocal shape descriptor. The proposed treatment of the nonlocal operator is dictated by an asymptotic result obtained when introducing splitting variables: $\tilde{T}$ simulating $T\circ\varphi$ to deal with the approximation of the weighted total variation and V simulating $\nabla\varphi$, the underlying idea being to transfer the nonlinearity on V as in [48]. We then turn the related optimization problem under equality constraints into an unconstrained one by means of L^2/L^1 penalizations. We finally come up with the minimization with respect to $\varphi \in \mathrm{Id}+W_0^{1,2}(\Omega,\mathbb{R}^2)$, $\tilde{T}\in BV(\Omega,g)$ and $V\in L^4(\Omega,M_2(\mathbb{R}))$ of the following nonlocal decoupled functional denoted by (NLDP) that stands for *NonLocal Decoupled Problem*:

$$\begin{aligned} E_{n,\gamma}(\varphi,\tilde{T},V) = \frac{1}{K_{1,2}}\int_\Omega g(x)\left[\int_\Omega \frac{|\tilde{T}(y)-\tilde{T}(x)|}{|x-y|}\rho_n(|x-y|)\,dy\right]dx \\ + a\int_\Omega \left[(c_1-R)^2-(c_2-R)^2\right]\tilde{T}\,dx + \gamma\|\tilde{T}-T\circ\varphi\|_{L^1(\Omega)} \\ + \frac{\nu}{2}\|T\circ\varphi-R\|^2_{L^2(\Omega)} + \int_\Omega QW(V)\,dx + \frac{\gamma}{2}\|V-\nabla\varphi\|^2_{L^2(\Omega,M_2(\mathbb{R}))}. \quad \text{(NLDP)} \end{aligned}$$

We observe that we moved some nonlinearity on V: instead of minimizing the L^4-norm of $\nabla\varphi$ —it is known that treating problems involving $W^{1,p}$ norms with high $p's$ is still a challenging issue requiring low time steps if one works in the finite difference setting —, we minimize the L^4-norm of V.

Theorem 3.4 (Asymptotic result)**.** *Assume $g\in\mathcal{C}^1(\bar{\Omega})$ with $\|\nabla g\|_{\mathcal{C}^0(\bar{\Omega})}=k<+\infty$. Let us also suppose that the functions $t\mapsto\rho_n(t)$ and $t\mapsto t^{q+1}\rho_n(t)$ are non-increasing for $t\geq 0$ and any $q\in(0.5,1)$. Let (γ_j) be an increasing sequence of positive real numbers such that $\lim_{j\to+\infty}\gamma_j=+\infty$ with $\gamma_0>4a\|R\|^2_{L^\infty(\Omega)}$. Let (n_l) be a sequence of natural integers such that $\lim_{l\to+\infty} n_l=+\infty$ and such that for all $l\in\mathbb{N}^*$, there exists $\varphi_l\in Id+W_0^{1,4}(\Omega,\mathbb{R}^2)$ such that $\bar{I}(\varphi_l)\leq \inf_{\varphi\in Id+W_0^{1,4}(\Omega,\mathbb{R}^2)}\bar{I}(\varphi)+\frac{1}{l}$ and $\forall n\in\mathbb{N}$, $n\geq n_l\Rightarrow$ $\left|\frac{1}{K_{1,2}}\int_\Omega g(x)\left[\int_\Omega\frac{|T\circ\varphi_l(y)-T\circ\varphi_l(x)|}{|y-x|}\rho_n(x-y)\,dy\right]dx - var_g(T\circ\varphi_l)\right|\leq\frac{1}{l}$ since $T\circ\varphi_l\in BV(\Omega,g)$ (it is always possible to build). Let also $(\varphi_k(n_l,\gamma_j),V_k(n_l,\gamma_j),\tilde{T}_k(n_l,\gamma_j))$ be a minimizing sequence of (NLDP) with $\gamma=\gamma_j$ and $n=n_l$. Then there exists a subsequence denoted by $\big(\varphi_{N(n_{\psi(l)},\gamma_{\zeta(j)})}(n_{\psi(l)},\gamma_{\zeta(j)}),V_{N(n_{\psi(l)},\gamma_{\zeta(j)})}(n_{\psi(l)},\gamma_{\zeta(j)}),\tilde{T}_{N(n_{\psi(l)},\gamma_{\zeta(j)})}(n_{\psi(l)},\gamma_{\zeta(j)})\big)$ of $(\varphi_k(n_l,\gamma_j),V_k(n_l,\gamma_j),\tilde{T}_k(n_l,\gamma_j))$ and a minimizer $\bar{\varphi}$ of $\bar{I}$ such that:*
$\lim_{l\to+\infty}\lim_{j\to+\infty} E_{n_{\psi(l)},\gamma_{\zeta(j)}}(\varphi_{N(n_{\psi(l)},\gamma_{\zeta(j)})}(n_{\psi(l)},\gamma_{\zeta(j)}),V_{N(n_{\psi(l)},\gamma_{\zeta(j)})}(n_{\psi(l)},\gamma_{\zeta(j)}),\tilde{T}_{N(n_{\psi(l)},\gamma_{\zeta(j)})}(n_{\psi(l)},\gamma_{\zeta(j)}))=\bar{I}(\bar{\varphi})$.

Remark 3.4. *The previous asymptotic result involves a minimizing sequence associated with (NLDP) for each n_l and γ_j because we can only obtain weak convergence in $L^4(\Omega,M_2(\mathbb{R}))$ of a subsequence of (V_{n_l,γ_j}), preventing us from knowing anything about the behavior of the determinant of this subsequence and from obtaining any minimizer existence result.*

Proof. For any $n \in \mathbb{N}^*$ and for any $\gamma > 0$, we have the following inequality:

$$\begin{aligned}
E_{n,\gamma}(\varphi, V, \tilde{T}) &\geq a \int_\Omega [(c_1(\tilde{T}) - R)^2 - (c_2(\tilde{T}) - R)^2]\tilde{T}\, dx + \frac{\nu}{2}\|T \circ \varphi - R\|^2_{L^2(\Omega)} \\
&+ \int_\Omega QW(V)\, dx + \gamma\|\tilde{T} - T \circ \varphi\|_{L^1(\Omega)} + \frac{\gamma}{2}\|\nabla\varphi - V\|^2_{L^2(\Omega, M_2(\mathbb{R}))}, \\
&\geq -4a\|R\|^2_{L^\infty(\Omega)}\|\tilde{T}\|_{L^1(\Omega)} + \frac{\mu}{4}\|\det V\|^2_{L^2(\Omega)} + \frac{\beta}{2}\|V\|^4_{L^4(\Omega, M_2(\mathbb{R}))} - \beta\alpha^2 \\
&- 3\mu + \frac{\mu(\lambda+\mu)}{2(\lambda+2\mu)} + \gamma\|\tilde{T}\|_{L^1(\Omega)} - \gamma\|T\|_{L^\infty(\Omega)} + \frac{\gamma}{4}\|\nabla\varphi\|^2_{L^2(\Omega, M_2(\mathbb{R}))} \\
&- \frac{\gamma}{2}\|V\|^2_{L^2(\Omega, M_2(\mathbb{R}))}, \\
&\geq (\gamma - 4a\|R\|^2_{L^\infty(\Omega)})\|\tilde{T}\|_{L^1(\Omega, g)} + \frac{\mu}{4}\|\det V\|^2_{L^2(\Omega)} + \frac{\beta}{2}\|V\|^4_{L^4(\Omega, M_2(\mathbb{R}))} \\
&- \beta\alpha^2 - 3\mu + \frac{\mu(\lambda+\mu)}{2(\lambda+2\mu)} - \gamma\|T\|_{L^\infty(\Omega)} + \frac{\gamma}{4(1+2c'^2)}\|\varphi\|^2_{W^{1,2}(\Omega, \mathbb{R}^2)} \\
&- \frac{\gamma\sqrt{\text{meas}(\Omega)}}{2}\|V\|^2_{L^4(\Omega, M_2(\mathbb{R}))} - \frac{\gamma c''^2}{2(1+c'^2)}.
\end{aligned}$$

We assume $\gamma > 4a\|R\|^2_{L^\infty(\Omega)}$, then

$$\begin{aligned}
E_{n,\gamma}(\varphi, V, \tilde{T}) &\geq (\gamma - 4a\|R\|^2_{L^\infty(\Omega)})\|\tilde{T}\|_{L^1(\Omega)} + \frac{\mu}{4}\|\det V\|^2_{L^2(\Omega)} + \frac{\beta}{4}\|V\|^4_{L^4(\Omega, M_2(\mathbb{R}))} \\
&- \beta\alpha^2 - 3\mu + \frac{\mu(\lambda+\mu)}{2(\lambda+2\mu)} - \gamma\|T\|_{L^\infty(\Omega)} + \frac{\gamma}{4(1+2c'^2)}\|\varphi\|^2_{W^{1,2}(\Omega, \mathbb{R}^2)} \\
&- \frac{\gamma^2\,\text{meas}(\Omega)}{4\beta} - \frac{\gamma c''^2}{2(1+c'^2)},
\end{aligned}$$

since $\frac{\beta}{2}\|V\|^4_{L^4(\Omega, M_2(\mathbb{R}))} - \frac{\gamma\sqrt{\text{meas}(\Omega)}}{2}\|V\|^2_{L^4(\Omega, M_2(\mathbb{R}))} \geq \frac{\beta}{4}\|V\|^4_{L^4(\Omega, M_2(\mathbb{R}))} - \frac{\gamma^2\text{meas}(\Omega)}{4\beta}$ and with c' and c'' some constants depending only on Ω, $p = 2$ and $N = 2$. So, $E_{n,\gamma}$ is coercive for $n \in \mathbb{N}^*$and for any $\gamma > 4a\|R\|^2_{L^\infty(\Omega)}$. Besides, by taking $\varphi = \text{Id}$, $V = I_2$ and $\tilde{T} = T$ then $E_{n,\gamma}(\varphi, V, \tilde{T})$ is finite and for any $n \in \mathbb{N}^*$ and any $\gamma > 4a\|R\|^2_{L^\infty(\Omega)}$ the functional is proper. We can deduce that the infimum is finite.
Let (γ_j) be an increasing sequence of positive real numbers such that $\lim\limits_{j\to+\infty}\gamma_j = +\infty$ and $\gamma_0 > 4a\|R\|^2_{L^\infty(\Omega)}$. Let (n_l) be a sequence of natural integers such that $\lim\limits_{l\to+\infty} n_l = +\infty$ and such that for all $l \in \mathbb{N}^*$, there exists $\varphi_l \in \text{Id} + W^{1,4}_0(\Omega, \mathbb{R}^2)$ such that $\bar{I}(\varphi_l) \leq \inf\limits_{\varphi\in\text{Id}+W^{1,4}_0(\Omega,\mathbb{R}^2)} \bar{I}(\varphi) + \frac{1}{l}$ and $\forall n \in \mathbb{N}$, $n \geq n_l \Rightarrow \left|\frac{1}{K_{1,2}}\int_\Omega g(x)\left[\int_\Omega \frac{|T\circ\varphi_l(y) - T\circ\varphi_l(x)|}{|y-x|}\right.\right.$ $\left.\left.\rho_n(x-y)\,dy\right]\, dx - var_g(T\circ\varphi_l)\right| \leq \frac{1}{l}$ since $T \circ \varphi_l \in BV(\Omega, g)$. Then we consider a minimizing sequence denoted by $\Big(\varphi_k(n_l, \gamma_j), V_k(n_l, \gamma_j), \tilde{T}_k(n_l, \gamma_j)\Big)$ of the decoupled pro-

blem (NLDP) with $\gamma = \gamma_j$ and $n = n_l$: $\lim\limits_{k\to+\infty} E_{n_l,\gamma_j}(\varphi_k(n_l,\gamma_j),\, V_k(n_l,\gamma_j),\, \tilde{T}_k(n_l,\gamma_j)) = \inf\limits_{\varphi\in \mathrm{Id}+W^{1,2}(\Omega,\mathbb{R}^2), V\in L^4(\Omega,M_2(\mathbb{R})),\tilde{T}\in BV(\Omega,g)} E_{n_l,\gamma_j}\,(\varphi,\, V,\, \tilde{T})$. Besides, from what precedes there exists $\varphi_l \in \mathrm{Id} + W^{1,4}(\Omega,\mathbb{R}^2)$ such that: $\inf\limits_{\varphi\in \mathrm{Id}+W_0^{1,2}(\Omega,\mathbb{R}^2),\, V\in L^4(\Omega,M_2(\mathbb{R})),\, \tilde{T}\in BV(\Omega,g)} E_{n_l,\gamma_j}\,(\varphi,\, V,\, \tilde{T}) \le E_{n_l,\gamma_j}\,(\varphi_l,\, \nabla\varphi_l,\, T\circ\varphi_l) \le \bar{I}(\varphi_l) + \frac{1}{l} \le \inf\limits_{\varphi\in \mathrm{Id}+W_0^{1,4}(\Omega,\mathbb{R}^2)} \bar{I}(\varphi) + \frac{2}{l}$. Then there exists $N(n_l,\gamma_j) > 0$ such that for all $k \in \mathbb{N}$, $k \ge N(n_l,\gamma_j) \Rightarrow \Big(E_{n_l,\gamma_j}(\varphi_k(n_l,\gamma_j), V_k(n_l,\gamma_j), \tilde{T}_k(n_l,\gamma_j)) \le \inf\limits_{\varphi\in \mathrm{Id}+W_0^{1,4}(\Omega,\mathbb{R}^2)} \bar{I}(\varphi) + \frac{2}{l} + \frac{1}{\gamma_j} \le \inf\limits_{\varphi\in \mathrm{Id}+W_0^{1,4}(\Omega,\mathbb{R}^2)} \bar{I}(\varphi) + 2 + \frac{1}{\gamma_0} < +\infty$ and $\forall \varphi \in \mathrm{Id}+W_0^{1,4}(\Omega,\mathbb{R}^2)$, $E_{n_l,\gamma_j}(\varphi_k(n_l,\gamma_j),\, V_k(n_l,\gamma_j),\, \tilde{T}_k(n_l,\gamma_j)) \le E_{n_l,\gamma_j}(\varphi, \nabla\varphi, T\circ\varphi) + \frac{1}{\gamma_j} = E_{n_l}(\varphi) + \frac{1}{\gamma_j}\Big)$. Now, we take $k = N(n_l,\gamma_j)$.
So according to the previous coercivity inequality, we have that for each n_l, $(\varphi_{N(n_l,\gamma_j)}(n_l,\gamma_j))$ is uniformly bounded according to j in $W^{1,2}(\Omega,\mathbb{R}^2)$, $(V_{N(n_l,\gamma_j)}(n_l,\gamma_j))$ is uniformly bounded according to j in $L^4(\Omega, M_2(\mathbb{R}))$ and $(\det(V_{N(n_l,\gamma_j)}(n_l,\gamma_j))$ is uniformly bounded according to j in $L^2(\Omega)$. Let ψ be a common extractor, then we get

$$\begin{cases} \varphi_{N(n_l,\gamma_{\psi(j)})}(n_l,\gamma_{\psi(j)}) \underset{j\to+\infty}{\rightharpoonup} \bar{\varphi}_{N(n_l)}(n_l) \text{ in } W^{1,2}(\Omega,\mathbb{R}^2) \\ V_{N(n_l,\gamma_{\psi(j)})}(n_l,\gamma_{\psi(j)}) \underset{j\to+\infty}{\rightharpoonup} \bar{V}_{N(n_l)}(n_l) \text{ in } L^4(\Omega, M_2(\mathbb{R})) \\ \det V_{N(n_l,\gamma_{\psi(j)})}(n_l,\gamma_{\psi(j)}) \underset{j\to+\infty}{\rightharpoonup} \bar{\delta}(n_l) \text{ in } L^2(\Omega) \end{cases}.$$

Besides, one can prove that $(\tilde{T}_{N(n_l,\gamma_{\psi(j)})}(n_l,\gamma_{\psi(j)}))$ is uniformly bounded with respect to j in the fractional Sobolev space $W^{q,1}(\Omega)$ with $q \in (0.5, 1)$ thanks to the hypotheses on the functions ρ_n and to [9, Section 4.]. Using the 2D Rellich-Kondrachov theorem $W^{1,q}(\Omega) \subset L^r(\Omega)$ with compact embedding for $1 \le r < \dfrac{2}{2-q}$ with $\dfrac{4}{3} < \dfrac{2}{2-q} < 2$, we can extract a subsequence of $(\tilde{T}_{N(n_l,\gamma_{\psi(j)})}(n_l,\gamma_{\psi(j)}))$ still denoted $(\tilde{T}_{N(n_l,\gamma_{\psi(j)})}(n_l,\gamma_{\psi(j)}))$ strongly converging to $\bar{\tilde{T}}_{N(n_l)}(n_l)$ in $L^1(\Omega)$ and so almost everywhere in Ω up to a subsequence. Let us set $x_j = \tilde{T}_{N(n_l,\gamma_{\psi(j)})}(n_l,\gamma_{\psi(j)}) - T\circ\varphi_{N(n_l,\gamma_{\psi(j)})}(n_l,\gamma_{\psi(j)})$. We have the following inequality

$$\begin{aligned} \|x_j\|_{L^1(\Omega)} \le \frac{1}{\gamma_{\psi(j)}} \Big| & \beta\alpha^2 + 3\mu - \frac{\mu(\lambda+\mu)}{2(\lambda+2\mu)} \\ & + \inf_{\varphi\in \mathrm{Id}+W_0^{1,4}(\Omega,\mathbb{R}^2)} \bar{I}(\varphi) + 2 + \frac{1}{\gamma_0} + \frac{4a\|R\|^2_{L^\infty(\Omega)}}{\gamma_0 + 4a\|R\|^2_{L^\infty(\Omega)}} \\ & \Big(\beta\alpha^2 + 3\mu - \frac{\mu(\lambda+\mu)}{2(\lambda+2\mu)} + \inf_{\varphi\in \mathrm{Id}+W_0^{1,4}(\Omega,\mathbb{R}^2)} \bar{I}(\varphi) + 2 + \gamma_0\|T\|_{L^\infty(\Omega)} + \frac{1}{\gamma_0}\Big)\Big| \\ & \underset{j\to+\infty}{\longrightarrow} 0, \end{aligned}$$

and $\|\tilde{T}_{N(n_l,\gamma_{\psi(j)})}(n_l,\gamma_{\psi(j)}) - T\circ\bar{\varphi}_{N(n_l)}(n_l)\|_{L^1(\Omega)}$
$\leq \|x_j\|_{L^1(\Omega)} + \|T\circ\varphi_{N(n_l,\gamma_{\psi(j)})}(n_l,\gamma_{\psi(j)}) - T\circ\bar{\varphi}_{N_l}(n_l)\|_{L^1(\Omega)}$,
$\leq \|x_j\|_{L^1(\Omega)} + \kappa_T\|\varphi_{N(n_l,\gamma_{\psi(j)})}(n_l,\gamma_{\psi(j)}) - \bar{\varphi}_{N(l)}(n_l)\|_{L^1(\Omega)}$,
since T is Lipschitz continuous.

Eventually, thanks to the Sobolev embedding theorem stating that $(\varphi_{N(n_l,\gamma_{\psi(j)})}(n_l,\gamma_{\psi(j)}))$ strongly converges to $\bar{\varphi}_{N(n_l)}(n_l)$ in $L^1(\Omega)$, we obtain $\tilde{T}_{N(n_l,\gamma_{\psi(j)})}(n_l,\gamma_{\psi(j)}) \underset{j\to+\infty}{\longrightarrow} T\circ\bar{\varphi}_{N(n_l)}(n_l)$ in $L^1(\Omega)$. By uniqueness of the limit, $\bar{\tilde{T}}_{N(n_l)}(n_l) = T\circ\bar{\varphi}_{N(n_l)}(n_l)$. Then $(\tilde{T}_{N(n_l,\gamma_{\psi(j)})}(n_l,\gamma_{\psi(j)}))$ converges almost everywhere up to a subsequence to $T\circ\bar{\varphi}_{N(n_l)}(n_l)$ when j tends to infinity and so $g(x)\frac{|\tilde{T}_{N(n_l,\gamma_{\psi(j)})}(n_l,\gamma_{\psi(j)})(y)-\tilde{T}_{N(n_l,\gamma_{\psi(j)})}(n_l,\gamma_{\psi(j)})(x)|}{|x-y|}\rho_{n_l}(x-y)$ converges almost everywhere to $g(x)\frac{|T\circ\bar{\varphi}_{N(n_l)}(n_l)(y)-T\circ\bar{\varphi}_{N(n_l)}(n_l)(x)|}{|x-y|}\rho_{n_l}(x-y)$ as j tends to infinity. By Fatou's lemma, we get

$$\liminf_{j\to+\infty}\int_\Omega g(x)\left[\int_\Omega \frac{|\tilde{T}_{N(n_l,\gamma_{\psi(j)})}(n_l,\gamma_{\psi(j)})(y) - \tilde{T}_{N(n_l,\gamma_{\psi(j)})}(n_l,\gamma_{\psi(j)})(x)|}{|x-y|}\rho_{n_l}(x-y)\,dy\right]dx$$
$$\geq \int_\Omega g(x)\left[\int_\Omega \frac{|T\circ\bar{\varphi}_{N(n_l)}(n_l)(y) - T\circ\bar{\varphi}_{N(n_l)}(n_l)(x)|}{|x-y|}\rho_{n_l}(x-y)\,dy\right]dx.$$

Let us now set $z_j = \nabla\varphi_{N(n_l,\gamma_{\psi(j)})}(n_l,\gamma_{\psi(j)}) - V_{N(n_l,\gamma_{\psi(j)})}(n_l,\gamma_{\psi(j)})$. We have $z_j \underset{j\to+\infty}{\longrightarrow} 0$ in $L^2(\Omega)$ since $\|z_j\|^2_{L^2(\Omega,M_2(\mathbb{R}))} \leq \frac{2}{\gamma_{\psi(j)}}\Big(\beta\alpha^2 + 3\mu - \frac{\mu(\lambda+\mu)}{2(\lambda+2\mu)} + \inf_{\varphi\in\mathrm{Id}+W_0^{1,4}(\Omega,\mathbb{R}^2)}\bar{I}(\varphi) + 2 + \frac{1}{\gamma_0} + \gamma_0\|T\|_{L^\infty(\Omega)}\Big)$ and so $\nabla\varphi_{N(n_l,\gamma_{\psi(j)})}(n_l,\gamma_{\psi(j)}) \underset{j\to+\infty}{\rightharpoonup} \bar{V}_{N(l)}(n_l)$ in $L^2(\Omega,M_2(\mathbb{R}))$. Indeed, $\forall\Phi\in L^2(\Omega,M_2(\mathbb{R}))$, $\int_\Omega z_j : \Phi\,dx \underset{j\to+\infty}{\longrightarrow} 0$. So, $\int_\Omega(\nabla\varphi_{N(n_l,\gamma_{\psi(j)})}(n_l,\gamma_{\psi(j)}) - V_{N(n_l,\gamma_{\psi(j)})}(n_l,\gamma_{\psi(j)})) : \Phi\,dx \underset{j\to+\infty}{\longrightarrow} 0$. But $V_{N(n_l,\gamma_{\psi(j)})}(n_l,\gamma_{\psi(j)}) \underset{j\to+\infty}{\rightharpoonup} \bar{V}_{N(n_l)}(n_l)$ in $L^4(\Omega,M_2(\mathbb{R}))$ and so in $L^2(\Omega,M_2(\mathbb{R}))$ and $\forall\Phi\in L^2(\Omega,M_2(\mathbb{R}))$, $\int_\Omega \nabla\varphi_{N(n_l,\gamma_{\psi(j)})}(n_l,\gamma_{\psi(j)}) : \Phi\,dx \underset{j\to+\infty}{\longrightarrow} \int_\Omega \bar{V}_{N(n_l)}(n_l) : \Phi\,dx$. Besides, $\nabla\varphi_{N(n_l,\gamma_{\psi(j)})}(n_l,\gamma_{\psi(j)}) \underset{j\to+\infty}{\rightharpoonup} \nabla\bar{\varphi}_{N(n_l)}(n_l)$ in $L^2(\Omega,M_2(\mathbb{R}))$ and by uniqueness of the weak limit, $\nabla\bar{\varphi}_{N(n_l)}(n_l) = \bar{V}_{N(n_l)}(n_l) \in L^4(\Omega,M_2(\mathbb{R}))$. Thus $\bar{\varphi}_{N(n_l)}(n_l)\in W^{1,4}(\Omega,\mathbb{R}^2)$ and by continuity of the trace operator, $\bar{\varphi}_{N(n_l)}(n_l) = \mathrm{Id}$ on $\partial\Omega$.

Furthermore, since $\varphi_{N(n_l,\gamma_{\psi(j)})}(n_l,\gamma_{\psi(j)}) \underset{j\to+\infty}{\rightharpoonup} \bar{\varphi}_{N(n_l)}(n_l)$ in $W^{1,2}(\Omega,\mathbb{R}^2)$, $\det(\varphi_{N(n_l,\gamma_{\psi(j)})}(n_l,\gamma_{\psi(j)})) \underset{j\to+\infty}{\rightharpoonup} \det(\bar{\varphi}_{N(n_l)}(n_l))$ in the sense of distributions. As $\det(V_{N(n_l,\gamma_{\psi(j)})}(n_l,\gamma_{\psi(j)})) \underset{j\to+\infty}{\rightharpoonup} \bar{\delta}(n_l)$ in $L^2(\Omega)$, $\forall\Phi\in\mathcal{D}(\Omega)$, $\int_\Omega \det(V_{N(n_l,\gamma_{\psi(j)})}(n_l,\gamma_{\psi(j)}))\Phi\,dx \underset{j\to+\infty}{\longrightarrow} \int_\Omega \bar{\delta}(n_l)\Phi\,dx$. Let us set $\det(V_{N(n_l,\gamma_{\psi(j)})}(n_l,\gamma_{\psi(j)})) = \det(\nabla\varphi_{N(n_l,\gamma_{\psi(j)})}(n_l,\gamma_{\psi(j)})) + d_j$ with $d_j = (z_j)_{11}(z_j)_{22} - (z_j)_{12}(z_j)_{21} - (z_j)_{22}\frac{\partial\varphi^1_{N(n_l,\gamma_{\psi(j)})}(n_l,\gamma_{\psi(j)})}{\partial x_1} - (z_j)_{11}\frac{\partial\varphi^2_{N(n_l,\gamma_{\psi(j)})}(n_l,\gamma_{\psi(j)})}{\partial x_2} + (z_j)_{21}\frac{\partial\varphi^1_{N(n_l,\gamma_{\psi(j)})}(n_l,\gamma_{\psi(j)})}{\partial x_2} + (z_j)_{12}\frac{\partial\varphi^2_{N(n_l,\gamma_{\psi(j)})}(n_l,\gamma_{\psi(j)})}{\partial x_1}$. Then $\forall\Phi\in\mathcal{D}(\Omega)$, $\int_\Omega \det(V_{N(n_l,\gamma_{\psi(j)})}(n_l,\gamma_{\psi(j)}))\Phi\,dx = \int_\Omega \det(\nabla\varphi_{N(n_l,\gamma_{\psi(j)})}$

$(n_l, \gamma_{\psi(j)}))\Phi\, dx + \int_\Omega d_j\, \Phi\, dx$, with $\int_\Omega \det(\nabla\varphi_{N(n_l,\gamma_{\psi(j)})}\,(n_l, \gamma_{\psi(j)}))\Phi\, dx \underset{j\to+\infty}{\longrightarrow} \int_\Omega \det(\nabla\bar{\varphi}_{N(n_l)}\,(n_l))\Phi\, dx$ and $\int_\Omega d_j\Phi\, dx \leq \|d_j\|_{L^1(\Omega)}\|\Phi\|_{\mathcal{C}^0(\bar{\Omega})}$ from Hölder's inequality. From what precedes, we get $\|d_j\|_{L^1(\Omega)} \leq \frac{1}{2}\|z_j\|^2_{L^2(\Omega,M_2(\mathbb{R}))} + \|z_j\|_{L^2(\Omega,M_2(\mathbb{R}))}\,\|\nabla\varphi_{N(n_l,\gamma_{\psi(j)})}\,(n_l, \gamma_{\psi(j)})\|_{L^2(\Omega,M_2(\mathbb{R}))}$ with $(\nabla\varphi_{N(n_l,\gamma_{\psi(j)})}(n_l, \gamma_{\psi(j)}))$ uniformly bounded according to j (by taking $\gamma = \gamma_0$ in the first coercivity inequality used in this proof) in $L^2(\Omega, M_2(\mathbb{R}))$ and $\lim_{j\to+\infty} \|z_j\|_{L^2(\Omega,M_2(\mathbb{R}))} = 0$. So, $\lim_{j\to+\infty} \|d_j\|_{L^1(\Omega)}\|\Phi\|_{\mathcal{C}^0(\bar{\Omega})} = 0$ and $\lim_{j\to+\infty} \int_\Omega \det(V_{N(n_l,\gamma_{\psi(j)})}\,(n_l, \gamma_{\psi(j)}))\Phi\, dx = \int_\Omega \bar{\delta}(n_l)\Phi\, dx = \int_\Omega \det(\nabla\bar{\varphi}_{N(n_l)}(n_l))\Phi\, dx$. Thus $\bar{\delta}(n_l) = \det(\nabla\bar{\varphi}_{N(n_l)}(n_l))$ in the sense of distributions and since $\det(\nabla\bar{\varphi}_{N(n_l)}(n_l)) \in L^2(\Omega)$ and $\bar{\delta}(n_l) \in L^2(\Omega)$, it comes $\det(\nabla\bar{\varphi}_{N(n_l)}(n_l)) = \bar{\delta}(n_l)$ almost everywhere.

The mapping $J(V, \delta) = \int_\Omega W^*(V, \delta)\, dx$ is convex and strongly lower semi-continuous on $L^4(\Omega, M_2(\mathbb{R})) \times L^2(\Omega)$ since W^* is continuous and convex. It is thus weakly lower semi-continuous and $\int_\Omega QW(\nabla\bar{\varphi}_{N(n_l)}(n_l))\, dx = \int_\Omega W^*(\nabla\bar{\varphi}_{N(n_l)}(n_l), \det(\nabla\bar{\varphi}_{N(n_l)}(n_l)))\, dx$ $\leq \liminf_{j\to+\infty} \int_\Omega W^*(V_{N(n_l,\gamma_{\psi(j)})}\,(n_l, \gamma_{\psi(j)}), \det V_{N(n_l,\gamma_{\psi(j)})}(n_l, \gamma_{\psi(j)}))\, dx$.

From Rellich-Kondrachov's embedding theorem, we get that $W^{1,2}(\Omega, \mathbb{R}^2) \underset{c}{\circlearrowleft} L^q(\Omega, \mathbb{R}^2)$, $\forall q \in [1; +\infty[$. In particular, $(\varphi_{N(n_l,\gamma_{\psi(j)})}(n_l, \gamma_{\psi(j)}))$ strongly converges to $\bar{\varphi}_{N(n_l)}(n_l)$ in $L^2(\Omega, \mathbb{R}^2)$. As T is assumed to be Lipschitz continuous with κ_T the Lipschitz constant, we have $\lim_{j\to+\infty} \int_\Omega (T \circ \varphi_{N(n_l,\gamma_{\psi(j)})}(n_l, \gamma_{\psi(j)}) - R)^2\, dx = \int_\Omega (T \circ \bar{\varphi}_{N(n_l)}(n_l) - R)^2\, dx$.

As $(\tilde{T}_{N(n_l,\gamma_{\psi(j)})}(n_l, \gamma_{\psi(j)}))$ strongly converges to $T \circ \bar{\varphi}_{N(n_l)}(n_l)$ in $L^1(\Omega)$, we can extract a subsequence of $\left(\tilde{T}_{N(n_l,\gamma_{\psi(j)})}(n_l, \gamma_{\psi(j)})\right)$ denoted by $\left(\tilde{T}_{N(n_l,\gamma_{\zeta(j)})}(n_l, \gamma_{\zeta(j)})\right)$ such that $\tilde{T}_{N(n_l,\gamma_{\zeta(j)})}$ $(n_l, \gamma_{\zeta(j)})(x) \underset{j\to+\infty}{\longrightarrow} T \circ \bar{\varphi}_{N(n_l)}(n_l)(x)$ almost everywhere.

By continuity of H_ε, we have:

$$R(x)H_\varepsilon(\tilde{T}_{N(n_l,\gamma_{\zeta(j)})}(n_l, \gamma_{\zeta(j)})(x) - \rho) \underset{j\to+\infty}{\longrightarrow} R(x)H_\varepsilon(T \circ \bar{\varphi}_{N(n_l)}(n_l)(x) - \rho) \text{ a.e.},$$

$$H_\varepsilon(\tilde{T}_{N(n_l,\gamma_{\zeta(j)})}(n_l, \gamma_{\zeta(j)})(x) - \rho) \underset{j\to+\infty}{\longrightarrow} H_\varepsilon(T \circ \bar{\varphi}_{N(n_l)}(n_l)(x) - \rho) \text{ a.e.},$$

$$R(x)(1 - H_\varepsilon(\tilde{T}_{N(n_l,\gamma_{\zeta(j)})}(n_l, \gamma_{\zeta(j)})(x) - \rho)) \underset{j\to+\infty}{\longrightarrow} R(x)(1 - H_\varepsilon(T \circ \bar{\varphi}_{N(n_l)}(n_l)(x) - \rho)) \text{ a.e.},$$

$$1 - H_\varepsilon(\tilde{T}_{N(n_l,\gamma_{\zeta(j)})}(n_l, \gamma_{\zeta(j)})(x) - \rho) \underset{j\to+\infty}{\longrightarrow} 1 - H_\varepsilon(T \circ \bar{\varphi}_{N(n_l)}(n_l)(x) - \rho) \text{ a.e.},$$

and

$$R(x)H_\varepsilon(\tilde{T}_{N(n_l,\gamma_{\zeta(j)})}(n_l, \gamma_{\zeta(j)})(x) - \rho) < \|R\|_{L^\infty(\Omega)} \in L^1(\Omega),\ \forall j \in \mathbb{N},\ \text{as } \Omega \text{ is bounded},$$

$$H_\varepsilon(\tilde{T}_{N(n_l,\gamma_{\zeta(j)})}(n_l, \gamma_{\zeta(j)})(x) - \rho) < 1 \in L^1(\Omega),\ \forall j \in \mathbb{N},$$

$$R(x)(1 - H_\varepsilon(\tilde{T}_{N(n_l,\gamma_{\zeta(j)})}(n_l, \gamma_{\zeta(j)})(x) - \rho)) < \|R\|_{L^\infty(\Omega)} \in L^1(\Omega),\ \forall j \in \mathbb{N},$$

$$1 - H_\varepsilon(\tilde{T}_{N(n_l,\gamma_{\zeta(j)})}(\gamma_{n_l,\zeta(j)})(x) - \rho) < 1 \in L^1(\Omega),\ \forall j \in \mathbb{N}.$$

Thus, according to the dominated convergence theorem, we get that:

$$\int_\Omega R(x)H_\varepsilon(\tilde{T}_{N(n_l,\gamma_{\zeta(j)})}(n_l,\gamma_{\zeta(j)})(x)-\rho)\,dx \underset{j\to+\infty}{\longrightarrow} \int_\Omega R(x)H_\varepsilon(T\circ\bar{\varphi}_{N(n_l)}(n_l)(x)-\rho)\,dx,$$
$$\int_\Omega H_\varepsilon(\tilde{T}_{N(n_l,\gamma_{\zeta(j)})}(n_l,\gamma_{\zeta(j)})(x)-\rho)\,dx \underset{j\to+\infty}{\longrightarrow} \int_\Omega H_\varepsilon(T\circ\bar{\varphi}_{N(n_l)}(n_l)(x)-\rho)\,dx,$$
$$\int_\Omega R(x)(1-H_\varepsilon(\tilde{T}_{N(n_l,\gamma_{\zeta(j)})}(n_l,\gamma_{\zeta(j)})(x)-\rho))\,dx \underset{j\to+\infty}{\longrightarrow} \int_\Omega R(x)(1-H_\varepsilon(T\circ\bar{\varphi}_{N(n_l)}(n_l)(x)-\rho))\,dx,$$
$$\int_\Omega 1-H_\varepsilon(\tilde{T}_{N(n_l,\gamma_{\zeta(j)})}(n_l,\gamma_{\zeta(j)})(x)-\rho)\,dx \underset{j\to+\infty}{\longrightarrow} \int_\Omega 1-H_\varepsilon(T\circ\bar{\varphi}_{N(n_l)}(n_l)(x)-\rho)\,dx,$$
$$\Rightarrow c_1\left(\tilde{T}_{N(n_l,\gamma_{\zeta(j)})}(n_l,\gamma_{\zeta(j)})\right) \underset{j\to+\infty}{\longrightarrow} c_1\left(\bar{\varphi}_{N(n_l)}(n_l)\right),$$
$$c_2\left(\tilde{T}_{N(n_l,\gamma_{\zeta(j)})}(n_l,\gamma_{\zeta(j)})\right) \underset{j\to+\infty}{\longrightarrow} c_2\left(\bar{\varphi}_{N(n_l)}(n_l)\right).$$

We can derive $\left[\left(c_1\left(\tilde{T}_{N(n_l,\gamma_{\zeta(j)})}(n_l,\gamma_{\zeta(j)})\right)-R\right)^2-\left(c_2\left(\tilde{T}_{N(n_l,\gamma_{\zeta(j)})}(n_l,\gamma_{\zeta(j)})\right)-R\right)^2\right]\tilde{T}_{N(n_l,\gamma_{\zeta(j)})}(n_l,\gamma_{\zeta(j)}) \underset{j\to+\infty}{\longrightarrow} \left[\left(c_1\left(\bar{\varphi}_{N(n_l)}(n_l)\right)-R\right)^2-\left(c_2\left(\bar{\varphi}_{N(n_l)}(n_l)\right)-R\right)^2\right]T\circ\bar{\varphi}_{N(n_l)}(n_l)$ almost everywhere and from [16, Theorem IV.9], there exists $h_{n_l}\in L^1(\Omega)$ such that $\forall j\in\mathbb{N}$, $\left[\left(c_1(\tilde{T}_{N(n_l,\gamma_{\zeta(j)})}(n_l,\gamma_{\zeta(j)}))-R\right)^2-\left(c_2\left(\tilde{T}_{N(n_l,\gamma_{\zeta(j)})}(n_l,\gamma_{\zeta(j)})\right)-R\right)^2\right]\tilde{T}_{N(n_l,\gamma_{\zeta(j)})}(n_l,\gamma_{\zeta(j)})\le 4\|R\|_{L^\infty(\Omega)}h_{n_l}\in L^1(\Omega)$. So, according to the dominated convergence theorem we get

$$\int_\Omega\left[\left(c_1(\varphi_{N(n_l,\gamma_{\zeta(j)})}(n_l,\gamma_{\zeta(j)}))-R\right)^2-\left(c_2(\varphi_{N(n_l,\gamma_{\zeta(j)})}(n_l,\gamma_{\zeta(j)}))-R\right)^2\right]T\circ\varphi_{N(n_l,\gamma_{\zeta(j)})}(n_l,\gamma_{\zeta(j)})\,dx$$
$$\underset{j\to+\infty}{\longrightarrow}\int_\Omega\left[\left(c_1(\bar{\varphi}_{N(n_l)}(n_l))-R\right)^2-\left(c_2(\bar{\varphi}_{N(n_l)}(n_l))-R\right)^2\right]T\circ\bar{\varphi}_{N(n_l)}(n_l)\,dx.$$

By combining all the results, we have that $E_{n_l}(\bar{\varphi}_{N(n_l)}(n_l))\le\liminf_{j\to+\infty}E_{n_l,\gamma_{\zeta(j)}}(\varphi_{N(n_l,\gamma_{\zeta(j)})}(n_l,\gamma_{\zeta(j)}),V_{N(n_l,\gamma_{\zeta(j)})}(n_l,\gamma_{\zeta(j)}),\tilde{T}_{N(n_l,\gamma_{\zeta(j)})}(n_l,\gamma_{\zeta(j)}))\le\limsup_{j\to+\infty}E_{n_l,\gamma_{\zeta(j)}}(\varphi_{N(n_l,\gamma_{\zeta(j)})}(n_l,\gamma_{\zeta(j)}),V_{N(n_l,\gamma_{\zeta(j)})}(n_l,\gamma_{\zeta(j)}),\tilde{T}_{N(n_l,\gamma_{\zeta(j)})}(n_l,\gamma_{\zeta(j)}))\le\limsup_{j\to+\infty}\inf_{\varphi\in\mathrm{Id}+W_0^{1,4}(\Omega,\mathbb{R}^2)}\bar{I}(\varphi)+\frac{2}{l}+\frac{1}{\gamma_j}=\inf_{\varphi\in\mathrm{Id}+W_0^{1,4}(\Omega,\mathbb{R}^2)}\bar{I}(\varphi)+\frac{2}{l}$.

However $\forall\varphi\in\mathrm{Id}+W_0^{1,4}(\Omega,\mathbb{R}^2)$, we have $E_{n_l}(\bar{\varphi}_{N(n_l)}(n_l))\le\liminf_{j\to+\infty}E_{n_l,\gamma_{\zeta(j)}}(\varphi_{N(n_l,\gamma_{\zeta(j)})}(n_l,\gamma_{\zeta(j)}),\ V_{N(n_l,\gamma_{\zeta(j)})}(n_l,\gamma_{\zeta(j)}),\ \tilde{T}_{N(n_l,\gamma_{\zeta(j)})}(n_l,\gamma_{\zeta(j)}))\le\liminf_{j\to+\infty}E_{n_l}(\varphi)+\frac{1}{\gamma_j}=E_{n_l}(\varphi)$.

Therefore, $\bar{\varphi}_{N(n_l)}(n_l)\in\mathrm{Id}+W_0^{1,4}(\Omega,\mathbb{R}^2)$, is a minimizer of E_{n_l} and from the previous theorem we can deduce that there exists a subsequence of $(\bar{\varphi}_{N(n_l)}(n_l))$ denoted by $(\bar{\varphi}_{N(n_{\psi(l)})}(n_{\psi(l)}))$ and $\bar{\varphi}\in\mathrm{Id}+W_0^{1,4}(\Omega,\mathbb{R}^2)$ a minimizer of $\bar{I}$ such that $\bar{\varphi}_{N(n_{\psi(l)})}(n_{\psi(l)})\rightharpoonup\bar{\varphi}$ in $W^{1,4}(\Omega,\mathbb{R}^2)$ and $\lim_{l\to+\infty}E_{n_{\psi(l)}}(\bar{\varphi}_{N(n_{\psi(l)})}(n_{\psi(l)}))=\bar{I}(\bar{\varphi})$ as the assumptions on g are fulfilled here. By taking the limit when l tends to infinity in the previous inequality, we have: $\inf_{\varphi\in\mathrm{Id}+W_0^{1,4}(\Omega,\mathbb{R}^2)}\bar{I}(\varphi)=\bar{I}(\bar{\varphi})=\lim_{l\to+\infty}E_{n_{\psi(l)}}(\bar{\varphi}_{N(n_{\psi(l)})}(n_{\psi(l)})\le\lim_{l\to+\infty}\liminf_{j\to+\infty}E_{n_{\psi(l)},\gamma_{\zeta(j)}}(\varphi_{N(n_{\psi(l)},\gamma_{\zeta(j)})}(n_{\psi(l)},\gamma_{\zeta(j)}),V_{N(n_{\psi(l)},\gamma_{\zeta(j)})}(n_{\psi(l)},\gamma_{\zeta(j)}),\tilde{T}_{N(n_{\psi(l)},\gamma_{\zeta(j)})}(n_{\psi(l)},\gamma_{\zeta(j)}))\le\lim_{l\to+\infty}$

$\limsup_{j\to+\infty} E_{n_{\psi(l)},\gamma_{\zeta(j)}}(\varphi_{N(n_{\psi(l)},\gamma_{\zeta(j)})}(n_{\psi(l)},\gamma_{\zeta(j)}), V_{N(n_{\psi(l)},\gamma_{\zeta(j)})}(n_{\psi(l)},\gamma_{\zeta(j)}), \tilde{T}_{N(n_{\psi(l)},\gamma_{\zeta(j)})}(n_{\psi(l)},\gamma_{\zeta(j)})) \leq \lim_{l\to+\infty} \inf_{\varphi\in \mathrm{Id}+W_0^{1,4}(\Omega,\mathbb{R}^2)} \bar{I}(\varphi) + \frac{2}{l} = \inf_{\varphi\in \mathrm{Id}+W_0^{1,4}(\Omega,\mathbb{R}^2)} \bar{I}(\varphi).$ □

We now solve (NLDP) using an alternating framework. Indeed, we split the problem into three subproblems of one unknown by fixing the others. We thus consider the subproblem according to $\tilde{T}$:

$$\inf_{\tilde{T}}\Bigg\{ E_n(\tilde{T}) = \int_\Omega g(x)\left[\int_\Omega \frac{|\tilde{T}(y)-\tilde{T}(x)|}{|x-y|}\rho_n(|x-y|)\,dy\right]dx + a\int_\Omega \left[(c_1-R)^2-(c_2-R)^2\right]\tilde{T}\,dx + \gamma\,\|T\circ\varphi-\tilde{T}\|_{L^1(\Omega)}\Bigg\}, \tag{PT}$$

for large enough γ and n and fixed φ and V, so that it approximates well

$$\inf_{\tilde{T}} E(\tilde{T}) = var_g\,\tilde{T} + a\int_\Omega \left[(c_1-R)^2-(c_2-R)^2\right]\tilde{T}\,dx + \gamma\,\|T\circ\varphi-\tilde{T}\|_{L^1(\Omega)}. \tag{PT1}$$

We separately solve for fixed $\tilde{T}$ the subproblem in (φ, V) using implicit and semi-implicit Euler time stepping schemes. A remarkable result relating again registration and segmentation is stated next.

Theorem 3.5 (Segmentation of the Reference)**.** *Suppose that $g \in [0,1]$, $R \in [0,1]$ and that $T\circ\varphi$ is a characteristic function of a bounded open subset $\tilde{\Omega}\subset\Omega$ with boundary of class $\mathcal{C}^2$ —with the assumptions on T, it is not theoretically the case —. Then for any c_1, c_2, a, γ, if $0\leq u\leq 1$ is a minimizer of E, for almost every $\kappa\in[0,1]$, the characteristic function $\chi_{\widehat{\Omega}(\kappa)=\{x\,|\,u(x)>\kappa\}}$ is a global minimizer of E.*

Proof. The proof is based on the coarea formula and on the work of Chan *et al.* in [20]. We first prove the existence of minimizers for the problem (PT1) for any c_1, $c_2\in\mathbb{R}$ and any $a\in\mathbb{R}^+$, $\gamma\in\mathbb{R}^+$.
Let c_1, $c_2\in\mathbb{R}$ and γ, $a\in\mathbb{R}^+$. By taking $\tilde{T}=\mathbb{1}_{\tilde{\Omega}}$ in $E(\tilde{T})$, we get $E(\tilde{T}) = var_g\mathbb{1}_{\tilde{\Omega}} + \int_\Omega \left[(c_1-R)^2-(c_2-R)^2\right]\mathbb{1}_{\tilde{\Omega}}\,dx < +\infty$ as $g\in[0,1]$, $\tilde{\Omega}\subset\Omega$, c_1, $c_2\in\mathbb{R}$ and $\|R\|_{L^\infty(\Omega)} < +\infty$.
Furthermore, as $0\leq\tilde{T}\leq 1$ almost everywhere, we have that $E(\tilde{T}) \geq var_g\,\tilde{T} + \min\{0, meas(\Omega)\,\min_{x\in\Omega}\{(c_1-R(x))^2-(c_2-R(x))^2\}\} \geq var_g\,\tilde{T} + \|\tilde{T}\|_{L^1(\Omega,g)} - meas(\Omega) + \min\{0, meas(\Omega)\min_{x\in\Omega}\{(c_1-R(x))^2-(c_2-R(x))^2\}\}$ as $0\leq\|\tilde{T}\|_{L^1(\Omega,g)}\leq meas(\Omega)$ and thus the functional is coercive as $\min_{x\in\Omega}\{(c_1-R(x))^2-(c_2-R(x))^2\}$ is finite and Ω bounded. Thus the infimum is finite.
Let $\{\tilde{T}_n\}\in BV(\Omega,g)\cap L^\infty(\Omega)$ be a minimizing sequence. It is uniformly bounded in $L^\infty(\Omega)$ so in $L^1(\Omega)$ and according to the previous inequalities, $var_g\,\tilde{T}_n$ is uniformly bounded. From [10, Theorem 3.4], for each $n\in\mathbb{N}$, there exists $\{g_n\}$ such that $g_n\in C^\infty(\Omega)\cap BV(\Omega,g)$

and

$$\begin{cases} \int_\Omega g|\tilde{T}_n - g_n|\,dx \leq \dfrac{1}{n} & \text{, for each } n \in \mathbb{N} \\ \sup\limits_{n\in\mathbb{N}} \int_\Omega g|\nabla g_n|\,dx < \infty \end{cases}.$$

As g satisfies $0 < c \leq g$ and $0 \leq \tilde{T}_n \leq 1 \Rightarrow \|\tilde{T}_n\|_{L^1(\Omega)} \leq meas(\Omega) < +\infty$ since Ω is bounded, it follows that $\begin{cases} \int_\Omega |\tilde{T}_n - g_n|\,dx \leq \dfrac{1}{cn} & \text{, for each } n \in \mathbb{N} \\ \sup\limits_{n\in\mathbb{N}} \int_\Omega |\nabla g_n|\,dx < \infty \end{cases}$. Therefore, there exist $\bar{\tilde{T}} \in BV(\Omega) \subset BV(\Omega, g)$ and a subsequence of $\{g_n\}$ still denoted by $\{g_n\}$ such that $g_n \to \bar{\tilde{T}}$ in $L^1(\Omega)$ and so in $L^1(\Omega, g)$.
However, $\|\tilde{T}_n - \bar{\tilde{T}}\|_{L^1(\Omega,g)} \leq \|\tilde{T}_n - g_n\|_{L^1(\Omega,g)} + \|g_n - \bar{\tilde{T}}\|_{L^1(\Omega,g)}$. So, $\tilde{T}_n \to \bar{\tilde{T}}$ in $L^1(\Omega, g)$ and so in $L^1(\Omega)$.
Furthermore, $\tilde{T}_n \in BV(\Omega, g)$, $\bar{\tilde{T}} \in BV(\Omega, g)$ and $\tilde{T}_n \to \bar{\tilde{T}}$ in $L^1(\Omega, g)$ then $var_g\, \bar{\tilde{T}} \leq \liminf\limits_{n\to+\infty} var_g\, \tilde{T}_n$.
As $\tilde{T}_n \to \bar{\tilde{T}}$ in $L^1(\Omega)$, there exists a subsequence of $\{\tilde{T}_n\}$ still denoted by $\{\tilde{T}_n\}$ such that $\tilde{T}_n \to \bar{\tilde{T}}$ almost everywhere. Thus $\left[(c_1 - R)^2 - (c_2 - R)^2\right] \tilde{T}_n \underset{n\to+\infty}{\longrightarrow} \left[(c_1 - R)^2 - (c_2 - R)^2\right] \bar{\tilde{T}}$ almost everywhere and for every $n \in \mathbb{N}$, $|[(c_1-R)^2-(c_2-R)^2]\tilde{T}_n| \leq |\left[(c_1 - R)^2 - (c_2 - R)^2\right]|$ $\leq \left[(|c_1| + \|R\|_{L^\infty(\Omega)})^2 + (|c_2| + \|R\|_{L^\infty(\Omega)})^2\right] \in L^1(\Omega)$ since $\tilde{T}_n \in [0, 1]$ and Ω is bounded.
Then according to the dominated convergence theorem, we get $\lim\limits_{n\to+\infty} \int_\Omega \left[(c_1 - R)^2 - (c_2 - R)^2\right] \tilde{T}_n\, dx = \int_\Omega \left[(c_1 - R)^2 - (c_2 - R)^2\right] \bar{\tilde{T}}\, dx$.
Moreover, $\tilde{T}_n - \mathbb{1}_{\tilde{\Omega}} \to \bar{\tilde{T}} - \mathbb{1}_{\tilde{\Omega}}$ almost everywhere and $|\tilde{T}_n - \mathbb{1}_{\tilde{\Omega}}| \leq 1 + \mathbb{1}_{\tilde{\Omega}} \in L^1(\Omega)$ as $\tilde{\Omega} \subset \Omega$. Therefore, according to the dominated convergence theorem, we get $\lim\limits_{n\to+\infty} \|\tilde{T}_n - \mathbb{1}_{\tilde{\Omega}}\|_{L^1(\Omega)} = \|\bar{\tilde{T}} - \mathbb{1}_{\tilde{\Omega}}\|_{L^1(\Omega)}$.
Thus by combining the previous results, we get $\liminf\limits_{n\to+\infty} E(\tilde{T}_n) \geq E(\bar{\tilde{T}})$ and so $\inf\limits_{0\leq\tilde{T}\leq1} E(\tilde{T}) \geq E(\bar{\tilde{T}})$ for any $c_1, c_2 \in \mathbb{R}$. But, for every $n \in \mathbb{N}$, $\tilde{T}_n \in [0, 1]$ almost everywhere and there exists a subsequence of $\{\tilde{T}_n\}$ still denoted by $\{\tilde{T}_n\}$ such that $\tilde{T}_n \to \bar{\tilde{T}}$ almost everywhere which implies $\bar{\tilde{T}} \in [0, 1]$ almost everywhere. So $E(\bar{\tilde{T}}) = \inf\limits_{0\leq\tilde{T}\leq1} E(\tilde{T})$. We thus have proved the existence of minimizers for the problem (PT1) and the infimum is attained for any c_1, $c_2 \in \mathbb{R}$ and any γ, $a \in \mathbb{R}^+$.
Let us now introduce the geometric functional $MS(\Sigma) = Per_g(\Sigma; \Omega) + a \int_\Sigma (c_1 - R)^2\, dx + a \int_{\Omega\setminus\Sigma} (c_2 - R)^2\, dx + \gamma|\Sigma\Delta\tilde{\Omega}|$ with $Per_g(\Sigma; \Omega) = \int_{\Omega\cap\partial\Sigma} g\, ds = |\partial\Sigma|(\Omega; g)$ with the notation of [10, Remark 10] and Δ denoting the symmetric difference. We aim to find a relation between $E(.)$ and $MS(.)$. Let c_1, $c_2 \in \mathbb{R}$ and γ, $a \in \mathbb{R}^+$. To do so, we express each term

of $E(u)$ in a geometrical way keeping in mind that $0 \leq u \leq 1$:

$$\begin{aligned}
var_g\, u &= \int_\Omega g\, d|Du|, \\
&= \int_0^1 \left(\int_\Omega g\, d|D\, \mathbb{1}_{\Sigma_\kappa := \{x\,:\,u(x)>\kappa\}}| \right) d\kappa, \\
&\quad \text{since } g \text{ is continuous so is a Borel function and } u \in BV(\Omega, g) \subset BV(\Omega)\ , \\
&= \int_0^1 var_g\, \mathbb{1}_{\Sigma_\kappa := \{x\,:\,u(x)>\kappa\}}\, d\kappa, \\
&= \int_0^1 |\partial \Sigma_\kappa|(\Omega; g)\, d\kappa, \\
&= \int_0^1 \left(\int_{\Omega \cap \partial \Sigma_\kappa} g\, ds \right) d\kappa, \\
&= \int_0^1 Per_g(\Sigma_\kappa := \{x\,:\,u(x) > \kappa\}; \Omega)\, d\kappa,
\end{aligned}$$

according to Baldi's work in [10] and [10, Remark 10] and using the coarea formula from [6, Theorem 10.3.3]. Considering $0 \leq u(x) \leq 1$, for almost every $x \in \Omega$, we get:

$$\begin{aligned}
\int_\Omega (c_1 - R(x))^2 u(x) dx &= \int_\Omega (c_1 - R(x))^2 \int_0^1 \mathbb{1}_{[0;u(x))}(\kappa)\, d\kappa\, dx, \\
&= \int_0^1 \int_\Omega (c_1 - R(x))^2 \mathbb{1}_{[0;u(x))}(\kappa)\, dx\, d\kappa \text{ by Fubini-Tonelli theorem}, \\
&= \int_0^1 \int_{\Omega \cap \{x\,:\,u(x)>\kappa\}} (c_1 - R(x))^2\, dx\, d\kappa. \\
\int_\Omega (c_2 - R(x))^2 u(x)\, dx &= \int_\Omega (c_2 - R(x))^2 \int_0^1 \mathbb{1}_{[0;u(x))}(\kappa)\, d\kappa\, dx, \\
&= \int_0^1 \int_{\Omega \cap \{x\,:\,u(x)>\kappa\}} (c_2 - R(x))^2\, dx\, d\kappa \text{ by Fubini-Tonelli theorem}, \\
&= c - \int_0^1 \int_{\Omega \cap \{x\,:\,u(x)>\kappa\}^c} (c_2 - R(x))^2\, dx\, d\kappa, \\
\text{with } c &= \int_\Omega (c_2 - R(x))^2\, dx \text{ independent of } u.
\end{aligned}$$

With $s = \mathbb{1}_{\tilde{\Omega}}$,

$$\begin{aligned}
\int_\Omega |u(x) - s(x)|\, dx &= \int_{\Omega \cap \{x\,:\,u(x)>s(x)\}} |u(x) - s(x)|\, dx, \\
&+ \int_{\Omega \cap \{x\,:\,u(x)<s(x)\}} |u(x) - s(x)|\, dx,
\end{aligned}$$

$$= \int_{\Omega\cap\{x\,:\,u(x)>s(x)\}}\int_{s(x)}^{u(x)} d\kappa\,dx + \int_{\Omega\cap\{x:u(x)<s(x)\}}\int_{u(x)}^{s(x)} d\kappa\,dx,$$

$$= \int_0^1\int_\Omega \mathbb{1}_{\{x\,:\,u(x)>s(x)\}}(x)\mathbb{1}_{[s(x),u(x))}(\kappa) + \mathbb{1}_{\{x\,:\,u(x)<s(x)\}}(x)\mathbb{1}_{[u(x),s(x))}(\kappa)\,dx\,d\kappa \text{ by Fubini-Tonelli theorem.}$$

Furthermore, the following equalities hold:

$$\mathbb{1}_{\{x\,:\,u(x)>s(x)\}}(x)\mathbb{1}_{[s(x);u(x))}(\kappa) = \begin{cases} 1, & \text{if and only if } x\in\{x:u(x)>s(x)\} \\ & \qquad\cap\{x:s(x)>\kappa\}^c \\ & \qquad\cap\{x:u(x)>\kappa\} \\ 0, & \text{otherwise} \end{cases},$$

$$\text{and } \mathbb{1}_{\{x\,:\,u(x)<s(x)\}}(x)\mathbb{1}_{[u(x);s(x))}(\kappa) = \begin{cases} 1, & \text{if and only if } x\in\{x:u(x)<s(x)\} \\ & \qquad\cap\{x:s(x)>\kappa\} \\ & \qquad\cap\{x:u(x)>\kappa\}^c \\ 0, & \text{otherwise} \end{cases}.$$

It means that $\mathbb{1}_{\{x\,:\,u(x)>s(x)\}}(x)\mathbb{1}_{[s(x);u(x))}(\kappa)+\mathbb{1}_{\{x\,:\,u(x)<s(x)\}}(x)\mathbb{1}_{[u(x);s(x))}(\kappa) = \mathbb{1}_{\{x\,:\,u(x)>\kappa\}\Delta\{x\,:\,s(x)>\kappa\}}(x) = \mathbb{1}_{(\{x\,:\,u(x)>\kappa\}\setminus\{x\,:\,s(x)>\kappa\})\cup(\{x\,:\,s(x)>\kappa\}\setminus\{x\,:\,u(x)>\kappa\})}(x)$. Then it follows that:

$$\int_\Omega |u(x)-s(x)|\,dx = \int_0^1 |\{x\,:\,u(x)>\kappa\}\,\Delta\,\{x\,:\,s(x)>\kappa\}|\,d\kappa = \int_0^1 |\{x\,:\,u(x)>\kappa\}\,\Delta\,\tilde{\Omega}|\,d\kappa.$$

By gathering the previous equations and setting $\Sigma_\kappa = \{x\,:\,u(x)>\kappa\}$, we get that $\forall u\in BV(\Omega)$ such that $0\le u(x)\le 1\,a.e.$, $E(u) = var_g\,u + a\int_\Omega \big[(c_1-R(x))^2-(c_2-R(x))^2\big]u(x)\,dx+\gamma\|u-s\|_{L^1(\Omega)} = \int_0^1\Big[Per_g(\Sigma_\kappa;\Omega)+a\int_{\Sigma_\kappa}(c_1-R(x))^2\,dx+a\int_{\Omega\setminus\Sigma_\kappa}(c_2-R(x))^2\,dx+\gamma|\Sigma_\kappa\Delta\tilde{\Omega}|\Big]\,d\kappa - c = \int_0^1 MS(\Sigma_\kappa)\,d\kappa - c.$

Let us now consider the following geometric problem for any c_1, $c_2\in\mathbb{R}$ and γ, $a\in\mathbb{R}^+$.

$$\min_\Sigma MS(\Sigma) \tag{PG}$$

Let u_{c_1,c_2} be a minimizer of $E(.)$ and $\Sigma_\kappa = \{x : u_{c_1,c_2}(x)>\kappa\}$ for almost every $\kappa\in[0,1]$. According to this equality $E(u) = \int_0^1 MS(\Sigma_\kappa)\,d\kappa - c$, if u_{c_1,c_2} is a minimizer of $E(.)$ then necessarily for almost every $\kappa\in[0,1]$, the set Σ_κ is a minimizer of (PG). As for any c_1, $c_2\in\mathbb{R}$ and γ, $a\in\mathbb{R}^+$ there exists at least one minimizer for (PT1) then necessarily, there exists at least one minimizer for (PG). Let Σ^* be one of them. Then, for almost every $\kappa\in[0,1]$, we have $MS(\Sigma_\kappa)\ge MS(\Sigma^*)$. It yields $E(u_{c_1,c_2})\ge E(\mathbb{1}_{\Sigma^*})$. As u_{c_1,c_2} is a minimizer of $E(.)$ then $\mathbb{1}_{\Sigma^*}$ is also a minimizer of $E(.)$ and $E(\mathbb{1}_{\Sigma^*}) = E(u_{c_1,c_2})$.
Eventually, $\mathbb{1}_{\Sigma_\kappa}$ is a minimizer of $E(.)$ for almost every $\kappa\in[0,1]$. □

In practice, it means that once $\tilde{T}$ is computed, for almost every $\kappa\in[0,1]$, the characteristic function $\chi_{\{x\,|\,\tilde{T}(x)>\kappa\}}$ provides a segmentation of the Reference image. It also

justifies the use of an L^1-penalization term to ensure that $\tilde{T}$ remains close to $T \circ \varphi$. We now concentrate upon the minimization problem in $\tilde{T}$ for fixed φ.

Following the same strategy as Bresson *et al.* in [15], we introduce another auxiliary variable f such that the problem in $\tilde{T}$ amounts to minimizing

$$\inf_{\tilde{T},f} \int_\Omega g(x) \left[\int_\Omega \frac{|\tilde{T}(y) - \tilde{T}(x)|}{|x-y|} \rho_n(|x-y|)\, dy \right] dx + a \int_\Omega \left[(c_1 - R(x))^2 - (c_2 - R(x))^2 \right] \tilde{T}(x)\, dx + \gamma \|f\|_{L^1(\Omega)} + \frac{1}{2\theta} \|\tilde{T} - T \circ \varphi + f\|^2_{L^2(\Omega)}.$$

As for the minimization in $\tilde{T}$, two lines of research have been investigated. First, a standard subgradient descent approach has been considered as in [9], based on a finite element type scheme inspired by estimations appearing in electromagnetism. (The function $t \mapsto |t|$ being not differentiable but subdifferentiable with subdifferential $[-1, 1]$, a differential inclusion must be solved for fixed n). Because of the singularity of the kernel, classical finite difference schemes would fail to provide a suitable approximation. The image domain is thus discretized using a triangulation. Interpolation schemes allow to derive explicit expressions of the contribution on each triangle for given x, and then, summing these contributions over each triangle for given x yields an estimation of the integral (see [9, Section 5] for additional comments). However, this kind of implementation raises some issues :

(i) first, it is computationally expensive as stressed in [9];

(ii) second, while the last three properties of the kernel ρ_n are consistent with the discrete setting —the weights are non-negative in practice, normalized and concentrated near the current window center, the radial symmetry of the kernel ρ_n is not relevant for imaging problems (see [51, Subsection 5.7]): we would like to define a nonlocal version of the weighted BV semi-norm at given point x that grants more weight to points that belong to the same region as x (not only based on the difference between intensities, but for instance on the difference between patches around those points and not favouring spatial proximity). This is the second limitation of the theoretical model we identified that pushed us to reconsider the definition of the weights and to find a numerical compromise.

We stress that an implementation of the above algorithm based on a finite element type scheme as in [9] has been made, but it does not provide satisfactory results, which again strenghtened the necessity of redefining the weights. We also would like to point out that to the best of our knowledge, this assumption of radiality cannot be removed (see in particular [27], [52] or [58]). The computation code can be made available if required. At last and for the sake of completeness, we would like to point that in [13], Boulanger *et al.* have generated numerical schemes for the computation of the nonlocal BV semi-norm in an implementation of a standard steepest gradient algorithm for one-dimensional total variation minimization. It is based on the derivation of a particular sequence of kernel functions, and for the transition to the discrete setting, on the approximation of any L^1-function by piecewise constant functions. No extension and applications to higher dimensions are investigated.

Equipped with these observations and arguments, and remarking that our nonlocal term has strong similarities with the contribution by Jung *et al.* ([39]) dedicated to the derivation of a nonlocal version of Mumford-Shah regularizers (the scalar-valued edge map v stemming from the Ambrosio-Tortorelli elliptic approximation can be related to our function g), we propose an implementation that encompasses this requirement of putting more weight to points that have similar geometrical configurations. Motivated by the definition of the nonlocal gradient by Gilboa and Osher [36] and by the contribution [39], we suggest considering the following nonlocal regularizer (which satisfies the properties of a semi-norm) $\int_\Omega g(x) \sqrt{\int_\Omega (\tilde{T}(y) - \tilde{T}(x))^2 \, w(x,y) \, dy} \, dx$, with $w : \Omega \times \Omega \to \mathbb{R}$ a nonnegative, symmetric weight function chosen to depend on $R : \bar{\Omega} \to \mathbb{R}$ by $w(x,y) = \exp - \left(\frac{d_a(R(x),R(y))}{h^2} \right)$, with $d_a(R(x), R(y)) = \int_{\mathbb{R}^2} G_a(t) |R(x+t) - R(y+t)|^2 \, dt$, G_a being a Gaussian kernel with standard deviation a determinining the patch size, and h the filtering parameter. For a fixed pixel $x \in \Omega$, the search window $S(x) = \{y \in \Omega \,|\, |x-y| \leq r\}$ is considered rather than the whole domain Ω to compute $w(x,y)$.

This leads to the introduction of Algorithm 5 provided on the next page.

1. Define $k := 1$, $T :=$ Template image, $R :=$ Reference image, $\tilde{T} := T$, $V = \begin{pmatrix} V_{11} & V_{12} \\ V_{21} & V_{22} \end{pmatrix} := I$, $g := \frac{1}{1+c|\nabla R|^2}$, a, ν, λ, μ, ρ, γ, $nbIter$, θ, $w :=$ window size, $p :=$ patch size, $h := 0.25$, $\varphi = (\varphi_1, \varphi_2) :=$ Id.

2. Compute the nonlocal weights: $\frac{\rho_n(|x-y|)}{|x-y|} \approx w(x,y) = \exp\left\{\frac{-\int_\Omega G_h(z)|R(x+z)-R(y+z)|^2\,dz}{h^2}\right\}$, with G_h, Gaussian kernel of mean 0 and standard deviation h (see 9 for the computation of theses weights).

while $k < nbIter$ **do**

3.1. For each pixel (i,j), update V using the following equations:

$$\begin{cases} V_{11}(i,j) &= (\frac{1}{1+dt\gamma})\Big(V_{11}(i,j) + dt\Big(-\mu(\det V(i,j)-2)V_{22}(i,j) \\ &\quad -2\beta\, c_0\, V_{11}(i,j)\,(c_0\,\delta_\varepsilon(c_0) + 2H_\varepsilon(c_0)) + \gamma\frac{\partial\varphi_1}{\partial x}(i,j)\Big)\Big) \\ V_{12}(i,j) &= (\frac{1}{1+dt\gamma})\Big(V_{12}(i,j) + dt\Big(\mu(\det V(i,j)-2)V_{21}(i,j) \\ &\quad -2\beta\, c_0\, V_{12}(i,j)\,(c_0\,\delta_\varepsilon(c_0) + 2H_\varepsilon(c_0)) + \gamma\frac{\partial\varphi_1}{\partial y}(i,j)\Big)\Big) \\ V_{21}(i,j) &= (\frac{1}{1+dt\gamma})\Big(V_{21}(i,j) + dt\Big(\mu(\det V(i,j)-2)V_{12}(i,j) \\ &\quad -2\beta\, c_0\, V_{21}(i,j)\,(c_0\,\delta_\varepsilon(c_0) + 2H_\varepsilon(c_0)) + \gamma\frac{\partial\varphi_2}{\partial x}(i,j)\Big)\Big) \\ V_{22}(i,j) &= (\frac{1}{1+dt\gamma})\Big(V_{22}(i,j) + dt\Big(-\mu(\det V(i,j)-2)V_{11}(i,j) \\ &\quad -2\beta\, c_0\, V_{22}(i,j)\,(c_0\,\delta_\varepsilon(c_0) + 2H_\varepsilon(c_0)) + \gamma\frac{\partial\varphi_2}{\partial y}(i,j)\Big)\Big) \end{cases},$$

with $c_0 := c_0(i,j) = \|V\|^2(i,j) - \alpha$.

3.2. Update $c_1 := \frac{\sum_{i,j} R(i,j)H_\varepsilon(\tilde{T}(i,j)-\rho)}{\sum_{i,j} H_\varepsilon(\tilde{T}(i,j)-\rho)}$ and $c_2 := \frac{\sum_{i,j} R(i,j)(1-H_\varepsilon(\tilde{T}(i,j)-\rho))}{\sum_{i,j}(1-H_\varepsilon(\tilde{T}(i,j)-\rho))}$.

3.3. Solve the Euler-Lagrange equation in φ using an L^2 gradient flow scheme with an implicit Euler time stepping: $0 = \nu(T\circ\varphi - R)\nabla T(\varphi) - \gamma\Delta\varphi + \gamma\begin{pmatrix}\mathrm{div}V_1\\ \mathrm{div}V_2\end{pmatrix} - \frac{1}{\theta}(f - T\circ\varphi + \tilde{T})\nabla T(\varphi)$, where V_i stands for the i^{th} row of V.

3.4. Compute the norm $N(x) := \sqrt{\int_\Omega |\tilde{T}(y) - \tilde{T}(x)|^2 w(x,y)\,dy}$.

3.5. Update $\tilde{T}$ with the following equation: $\tilde{T}(x) = \tilde{T}(x) + dt\int_\Omega (\tilde{T}(y) - \tilde{T}(x))\left(\frac{g(y)}{N(y)} + \frac{g(x)}{N(x)}\right) w(x,y)\,dy - \frac{dt}{\theta}(\tilde{T}(x) - T\circ\varphi(x) + f(x)) - adt\big[(c_1 - R(x))^2 - (c_2 - R(x))^2\big]$.

3.6. Update $f := \begin{cases} T\circ\varphi - \tilde{T} - \theta\gamma & \text{if} \quad T\circ\varphi - \tilde{T} \geq \theta\gamma, \\ T\circ\varphi - \tilde{T} + \theta\gamma & \text{if} \quad T\circ\varphi - \tilde{T} \leq -\theta\gamma, \\ 0 & \text{otherwise.} \end{cases}$

if $\min_{i,j} \det\nabla\varphi(i,j) < \text{tol}$ **then**

3.7.1. Apply a regridding step (see Algorithm 7).

end if

3.8. $k := k + 1$.

end while

return $T\circ\varphi$, V, $\tilde{T}$, c_1, c_2, f.

Algorithm 5: Alternating scheme of resolution.

In Algorithm 6, we illustrate the computation of the nonlocal weights inspired by the NL-means algorithm.

1. Define $w :=$ window size, $p :=$ patch size, $h := 0.25$, $NbNeigh :=$ number of actual required neighbors including the four closest ones, $Nx :=$ number of horizontal pixels, $Ny :=$ number of vertical pixels.
2. Compute the extended image by symmetry.
for all pixels x **do**
  3.1. Compute the distance $d_h(R(x), R(y))$ between all patches centered at y of size p inside the window with size w centered at the current x and the patch centered at the current x.
end for
for all pixels x **do**
  4.1. Sort the previous distances in ascending order and keep only the lowest $NbNeigh - 4$ values with the corresponding coordinates.
  4.2. Add the four closest neighbors in a geographical sense to make the weights $w(x, y)$ more similar to the theoretical ones $\dfrac{\rho(|x-y|)}{|x-y|}$.
end for
for all pixels x **do**
  5.1. Compute w by the following formula: $w(x, y) = 0$ if y does not belong to the previous list of neighbors, $w(x, y) = \exp\left\{-\frac{d_h(R(x),R(y))}{h^2}\right\}$ otherwise.
end for
return w.

Algorithm 6: Computation of the nonlocal weights following Bresson *et al.* [39].

Besides, even if we added a term penalizing the determinant of the Jacobian of the deformation, there is no guaranty that it remains positive. That is why we introduce a regridding step to ensure the preservation of the topology whose algorithm follows (Algorithm 7).

if at stage k, $\det \nabla\varphi < \text{tol}$ **then**
  1. $regrid_count = regrid_count + 1$.
  2. $T = T \circ \varphi^{k-1}$.
  3. Save $\text{tab}_\varphi(regrid_count) = \varphi^{k-1}$, $\varphi^k = \text{Id}$, $V^k = \text{I}$.
  4. Continue the loop on k.
end if
if at the end of the loop on k, $regrid_count > 0$ **then**
  5. $\varphi^{\text{final}} = \text{tab}_\varphi(1) \circ \cdots \circ \text{tab}_\varphi(regrid_count)$
end if

Algorithm 7: Regridding step.

The next section is devoted to the analysis of numerical experiments on a toy example and then on medical images. The computations have been made on a quad-core computer with 2.0 GHz Intel(R) Xeon(X) CPU E5-2620 processor and 32 GB memory, using OpenMP and the package MUMPS (MUltifrontal Massively Parallel Solver). The question of assessing the proposed model encompasses several levels of discussion and angles of inquiry : the evaluation of the method accuracy according to some qualitative criteria and with respect to comparable joint segmentation/registration models, and the evaluation of each novel component of the introduced functional in comparison to classical ones. These two main levels of discussion dictate the structure of the section.

The first subsection is dedicated to the evaluation of the method accuracy and to the quantification of the gain related to the inclusion of the nonlocal shape descriptor compared with the prior work [49]. Two implementations of the weighted total variation are analyzed: first, in terms of segmentation accuracy and second, in terms of computational cost and convergence speed.

The second subsection allows to highlight the relevance of the nonlinear elasticity based regularizer compared to classical regularizers leading to linear terms with respect to derivatives in the Euler-Lagrange equation and the relevance of the dissimilarity measure combining the weighted total variation and a nonlocal shape descriptor (both in terms of accuracy and in terms of convergence speed).

4 Experimental results

4.1 Qualitative assessment of the proposed model

The proposed method has been evaluated on a toy (geometrical) example and on medical images. In order to fairly compare our method with the one in [49], in addition to the implementation of the nonlocal version of the weighted total variation, a local implementation based on the dual formulation of the weighted total variation and on a decoupling principle (yielding asymptotic results) has been investigated. In the remainder of the manuscript, 'our method L' will refer to the local implementation, while 'our method NL' will stand for the nonlocal numerical scheme depicted above. To assess the intrinsic performance of our algorithms (*i.e.* registration and segmentation accuracy), two measurements have been performed. First, we computed the Dice coefficient ([31]) which measures set agreement (after binarizing R, $T \circ \varphi$ and $\tilde{T}$ by thresholding) between R and $T \circ \varphi$ to estimate the quality of registration, and then between R and $\tilde{T}$ to appraise the accuracy of segmentation. This coefficient is a quantification of spatial overlap widely used for comparing segmentation results. The closest it is to 1, the better the matching is between two sets, emphasizing thus in our case segmentation and registration accuracy. Second, the mutual information was computed to measure image alignment. The mutual information between two random variables quantifies their dependence: larger mutual information indicates better matching (see Table 4.2). As this work primarily focuses on a combined registration/segmentation model, which means in particular that accurate segmentation results drive the registration process, providing a reliable deformation field between encoded structures based on shape pairing, it sounded relevant for us to assess the accuracy

of the method with a tool measuring the degree of overlap of the shapes. We thus favored in the study the Dice coefficient that encompasses both this notion of set agreement (rather than pointwise intensity comparison) and nonlocality, to the detriment of mutual information, which to our point of view is more based on local intensity comparison (since it uses the pixel intensities themselves) and does not take into account the geometry of the structures.

Both implementations of our method give similar numerical results and outperform those in [49] (the best obtained result is always used for comparison) in terms of segmentation and registration accuracy with in particular the capture of small details and thin structures (as exemplified in Figure 4.2 (g) (m) (s), where method [49] fails to delineate small details, or in Figure 4.9 (s) where method [49] fails to correctly capture the fine excrescence), and the restitution of a more faithful simplified version of the Reference image (yielding a more relevant decomposition of the Reference image with an oscillating part containing suitable features as in Figure 4.2 (f), (l)). These elements are corroborated visually first, and by the computation of the Dice coefficient demonstrating that the inclusion of the nonlocal information provides better results. An exhaustive analysis and a systematic comparison with the prior work [49] has been carried out and are summarized in Table 4.1. In order to obtain the segmentation of the Reference image, the contour corresponding to the level line $\left\{\tilde{T} = 0.3\right\}$ of $\tilde{T}$ is displayed. Note also that if the introduced model is highly non convex (yielding potentially many local minima), in practice nevertheless, the algorithm has the tendency to compute a global minimizer.

For the sake of reproducibility, we provide in Table 4.3 the values of the tuning parameters involved. The ranges of these parameters are rather stable for all the experiments. Parameter ν balancing the L^2-fidelity term is between 0.5 and 10, while parameter a weighting the nonlocal shape descriptor is between 1 and 100. They should be optimized according to each image content, taking into account the complexity of the image and the similarity to binary images. When a binary criterion emerges naturally, we value the nonlocal shape descriptor by assigning a larger value to a over ν, whereas ν is set to bigger values when complex topologies are involved. The Lamé coefficient λ is set for general images to 10 (it has no physical meaning but is related to Poisson's ratio, measure of Poisson's effect which can be regarded as the ability of a material compressed in one direction to expand in the other —this choice of λ is not physically inconsistent —) so as ρ and c set to 0.5 and 10 to discriminate two regions in images with intensity values between 0 and 1 and to stabilize the computation of the weight g. Coefficients θ, γ_1 and γ_2 ensuring the proximity between auxiliary variables and the original ones vary in small ranges, namely 0.1/1, 80000/90000 and 0.05/0.25 respectively and can be set for each class of images. Parameter θ is small so that we almost have $T \circ \varphi = \tilde{T} + f$, $\tilde{T}$ representing the geometric information of $T \circ \varphi$, while f captures the texture information. Coefficients p between 3 and 7 and w between 9 and 15 are related to the nonlocal algorithm and should be optimized according to the level of noise and the scale of fine details in images. From our experience, one of the parameters that proves to be the most sensitive is the Lamé coefficient μ between 750 and 5000. It can be viewed as a measure of rigidity. The greater parameter μ is, the more rigid the deformation is, which is relevant if we aim to obtain

a smooth and topology-preserving deformation map. This observation also encompasses intrinsically the main difficulty related to parameter tuning, namely, how to find a proper trade-off between accurate image alignment (which means authorizing large deformations) and topology or orientation preservation (which means monitoring the Jacobian determinant by limiting shrinkage and growth). Indeed, if μ is chosen too small, the deformation may lose its injectivity property, which manifests through overlaps/folds on the deformation grid, while if chosen too big, the registration accuracy may be impaired. In addition to the parameter setting, we have reported in the last column of 4.3 the minimum of the Jacobian determinant to ensure mechanic soundness of the obtained deformation. As for the layout of the figures, we choose a row-wise representation of the results for each method, with a column-wise alignment of the corresponding results for each method, except in Figure 4.3 where we compare the results component by component. We now go through each numerical simulation in depth.

As a preamble and to validate the algorithm, the model has been applied on a toy geometrical example (Figure 4.1) to emphasize the ability of the model to generate large deformations and to handle data corrupted by noise. In addition to a smooth deformation field, the algorithm (the nonlocal implementation here) produces a restored version of the Reference, restitutes the angles as well as the straight lines more accurately than with [49]. The method has then been applied on MRI images of a patient cardiac cycle (4.2, Figure 4.3, Figure 4.4 and Figure 4.5). We were supplied with a whole cardiac MRI examination of a patient (courtesy of the LITIS, University of Rouen, France). It is made of 280 images divided into 14 levels of slice and 20 images per cardiac cycle. The numbering of the images goes from 0 to 279, and includes both the slice number and the time index. The image 0 is set at the upper part of the heart and the sequence from image 0 to image 19 contains the whole cardiac cycle for this slice. The sequence from images 20 to 39 contains the whole cardiac cycle for the slice underneath the previous one and so on. A cardiac cycle is composed of a contraction phase (40% of the cycle duration), followed by a dilation phase (60% of the cycle duration). The first image of the sequence (frames 0, 20, 40, etc.) is when the heart is most dilated (end diastole - ED) and the 8^{th} of the sequence (end systole - ES) is when the heart is most contracted. It thus seemed relevant, in order to assess the accuracy of the proposed algorithm in handling large deformations, to register a pair of the type: Reference corresponding to end diastole (ED), that is the first image of a sequence, and Template corresponding to end systole (ES), that is the 8^{th} frame of the same sequence. This corresponds to the results depicted in Figure 4.2, Figure 4.4 and Figure 4.5. For each example and for each model (our algorithm with the nonlocal implementation of the weighted total variation, our algorithm with the local implementation and the algorithm in [49]), we provide the Reference R, the Template T, the binary Reference obtained thanks to c_1 and c_2 which is rescaled to $0-1$ from the nonlocal numerical method, the deformed template, the deformation grid which does not exhibit any overlap (yielding thus the physical well-definedness of the deformation), $\tilde{T}$ the simplified version of the deformed Template, the segmentation of the Reference obtained thanks to $\tilde{T}$ and the oscillatory part resulting from $R-\tilde{T}$. As previously mentioned, the obtained results outperform those in [49], both in terms of segmentation and registration accuracy. Visually first, with the capture of small details and thin/long structures, in

Toy example	Dice(R,T)	Dice(R, $T\circ\varphi$)	Dice(R, $\bar{T}$)
Our method NL	0.76517	**0.9783**	0.98016
Heart ED(108)-ES(100)	Dice(R,T)	Dice(R, $T\circ\varphi$)	Dice(R, $\bar{T}$)
Our method NL	0.54366	**0.95304**	0.99131
Our method L	0.54366	0.93833	**0.99137**
Method in [49]	0.54366	0.93322	0.95372
Method $L^2 - QW$	0.54366	0.94844	x
Method $L^2 - H^2$	0.54366	0.9161	x
Heart ES(100)-ED(108) *(inverse consistency)*	Dice(R,T)	Dice(R, $T\circ\varphi$)	Dice(R, $\bar{T}$)
Our method NL	0.4915	**0.95032**	**0.9749**
Our method L	0.4915	0.93361	0.97643
Heart ED(128)-ES(120)	Dice(R,T)	Dice(R, $T\circ\varphi$)	Dice(R, $\bar{T}$)
Our method NL	0.48222	0.9566	**0.98107**
Our method L	0.48222	**0.95744**	0.97563
Method in [49]	0.48222	0.95608	0.95806
Method $L^2 - QW$	0.48222	0.95408	x
Method $L^2 - H^2$	0.48222	0.94417	x
Heart ED(148)-ES(140)	Dice(R,T)	Dice(R, $T\circ\varphi$)	Dice(R, $\bar{T}$)
Our method NL	0.46821	0.96274	0.99206
Our method L	0.46821	**0.96372**	**0.99557**
Method in [49]	0.46821	0.95563	0.94701
Method $L^2 - QW$	0.546821	0.96005	x
Method $L^2 - H^2$	0.46821	0.93735	x
Slice of brain 1	Dice(R,T)	Dice(R, $T\circ\varphi$)	Dice(R, $\bar{T}$)
Our method NL	0.68524	**0.96778**	**0.99642**
Our method L	0.68524	0.96273	0.9888
Method in [49]	0.68524	0.96499	0.96637
Method $L^2 - QW$	0.68524	0.96451	x
Method $L^2 - H^2$	0.68524	0.82455	x
Slice of brain 1 *(inverse consistency)*	Dice(R,T)	Dice(R, $T\circ\varphi$)	Dice(R, $\bar{T}$)
Our method NL	0.71571	0.97161	**1**
Our method L	0.71571	**0.97536**	**1**
Method in [49]	0.71571	0.97284	0.99036
Slice of brain 2	Dice(R,T)	Dice(R, $T\circ\varphi$)	Dice(R, $\bar{T}$)
Our method NL	0.93595	**0.98357**	**0.98509**
Our method L	0.93595	0.98341	0.98087
Method in [49]	0.93595	0.9818	0.78033
Brain tumor	Dice(R,T)	Dice(R, $T\circ\varphi$)	Dice(R, $\bar{T}$)
Our method NL	0.59918	**0.94309**	0.98262
Our method L	0.59918	0.94302	**0.98432**
Method in [49]	0.59918	0.94213	0.9548
Method $L^2 - QW$	0.59918	0.93708	x
Method $L^2 - H^2$	0.59918	0.84553	x

Table 4.1: Dice coefficients.

Toy example	MI(R, T)	MI(R, $T\circ\varphi$)
Our method NL	0.5140	0.7433
Heart ED(108)-ES(100)	MI(R, T)	MI(R, $T\circ\varphi$)
Our method NL	0.9313	1.1930
Our method L	0.9313	1.1857
Heart ES(100)-ED(108) *(inverse consistency)*	MI(R, T)	MI(R, $T\circ\varphi$)
Our method NL	0.9313	1.2067
Our method L	0.9313	1.2021
Heart ED(128)-ES(120)	MI(R, T)	MI(R, $T\circ\varphi$)
Our method NL	0.9871	1.2960
Our method L	0.9871	1.2920
Heart ED(148)-ES(140)	MI(R, T)	MI(R, $T\circ\varphi$)
Our method NL	1.0479	1.3034
Our method L	1.0479	1.3020
Slice of brain 1	MI(R, T)	MI(R, $T\circ\varphi$)
Our method NL	0.6282	0.9689
Our method L	0.6282	0.9668
Slice of brain 1 *(inverse consistency)*	MI(R, T)	MI(R, $T\circ\varphi$)
Our method NL	0.6282	0.8332
Our method L	0.6282	0.8364
Slice of brain 2	MI(R, T)	MI(R, $T\circ\varphi$)
Our method NL	1.4617	1.5076
Our method L	1.4617	1.5062
Brain tumor	MI(R, T)	MI(R, $T\circ\varphi$)
Our method NL	0.3336	0.3953
Our method L	0.3336	0.3984

Table 4.2: Mutual information.

Toy example	ν	θ	γ_1	γ_2	μ	λ	c	a	ρ	w	p	$\min\{\det \nabla\varphi\}$
Our method NL	1	1	0.1	80000	1000	10	10	1	0.5	11	5	0.0686
Heart ED(108)-ES(100)	ν	θ	γ_1	γ_2	μ	λ	c	a	ρ	w	p	$\min\{\det \nabla\varphi\}$
Our method NL	2	1	0.25	90000	1000	10	10	40	0.5	11	5	0.0430
Our method L	9	0.1	0.25	90000	3500	10	10	40	0.5	x	x	0.0264
Method in [49]	2	0.25	0.1	90000	3500	10	10	x	x	x	x	0.0024
Heart ES(100)-ED(108)	ν	θ	γ_1	γ_2	μ	λ	c	a	ρ	w	p	$\min\{\det \nabla\varphi\}$
Our method NL	2	1	0.25	90000	2000	10	10	20	0.5	11	5	0.0517
Our method L	10	0.1	0.1	90000	1000	10	10	20	0.5	x	x	0.0678
Heart ED(128)-ES(120)	ν	θ	γ_1	γ_2	μ	λ	c	a	ρ	w	p	$\min\{\det \nabla\varphi\}$
Our method NL	4	1	0.08	90000	1000	10	10	10	0.5	11	5	0.0372
Our method L	4	1	0.1	90000	1000	10	10	10	0.5	x	x	0.0359
Method in [49]	10	0.1	0.1	90000	1000	10	10	x	x	x	x	0.0233
Heart ED(148)-ES(140)	ν	θ	γ_1	γ_2	μ	λ	c	a	ρ	w	p	$\min\{\det \nabla\varphi\}$
Our method NL	2	1	0.25	90000	1000	10	10	50	0.5	11	5	0.0380
Our method L	2	1	0.25	90000	1000	10	10	50	0.5	x	x	0.0445
Method in [49]	5	0.1	0.1	90000	1000	10	10	x	x	x	x	0.0554
Slice of brain 1	ν	θ	γ_1	γ_2	μ	λ	c	a	ρ	w	p	$\min\{\det \nabla\varphi\}$
Our method NL	1.2	1	0.1	80000	750	10	10	100	0.5	9	7	0.0290
Our method L	1.5	1	0.05	80000	1000	10	10	1	0.5	x	x	0.0388
Method in [49]	1	0.1	0.1	80000	1000	10	10	x	x	x	x	0.0635
Slice of brain 1 *(inverse consistency)*	ν	θ	γ_1	γ_2	μ	λ	c	a	ρ	w	p	$\min\{\det \nabla\varphi\}$
Our method NL	3	1	0.1	80000	5000	10	10	100	0.5	11	5	0.0012
Our method L	2.5	1	0.1	80000	5000	10	10	10	0.5	x	x	0.0039
Method in [49]	2	1	0.1	80000	4000	10	10	x	x	x	x	0.0058
Slice of brain 2	ν	θ	γ_1	γ_2	μ	λ	c	a	ρ	w	p	$\min\{\det \nabla\varphi\}$
Our method NL	0.5	1	0.1	80000	1000	10	10	1.5	0.5	11	5	0.6152
Our method L	0.5	1	0.1	80000	1000	10	10	1.5	0.5	x	x	0.6142
Method in [49]	0.5	1	0.1	80000	1000	10	10	x	x	x	x	0.6733
Brain tumor	ν	θ	γ_1	γ_2	μ	λ	c	a	ρ	w	p	$\min\{\det \nabla\varphi\}$
Our method NL	2.5	1	0.1	80000	820	10	10	2.7	0.5	15	3	0.0124
Our method L	2	1	0.1	80000	900.05	10	10	3	0.5	x	x	0.0953
Method in [49]	2.3	1	0.1	80000	802.9	10	10	x	x	x	x	0.0488

Table 4.3: Parameters.

the restitution of a more faithful simplified version of the Reference image yielding a more relevant oscillatory part in the decomposition phase, and at last, in a more regular distribution of the Jacobian determinants particularly with the nonlocal algorithm. These observations are then corroborated by the computation of the Dice coefficient leading systematically to better results (see again Table 4.1). To assess the inverse consistency, we switched the role of the Template and the Reference in Figure 4.3. The deformed grid associated with φ (Reference to Template, straightforwardly given by φ) is naturally depicted. To fairly assess inverse consistency, we also depicted the deformed grid associated with φ^{-1} (Template to Reference, computed using interpolation techniques) and displayed $R \circ \varphi^{-1}$, to be compared with T.

(a) R (b) T (c) Binary Reference (rescaled) NL (d) $T \circ \varphi$ NL (e) Deformation grid NL (f) $\tilde{T}$ NL (g) Segmented Reference NL

Figure 4.1: Toy example (size : 200 × 200), NL execution time : 137s.

The method has also been applied to complex slices of brain data (Figure 4.6) (courtesy of Laboratory Of NeuroImaging, UCLA). We aim to register a tore to the slice of brain with topology preservation to demonstrate the ability of the algorithm to handle complex topologies. This illustration constitutes a preamble to the extension of the model to 3D. Due to the spherical topology of the human cortex, a relevant application would consist in applying the method to a human cortex and a sphere, in making the desired computations and numerical analysis on the sphere (rather than on the cortex), and in recovering the desired quantifiers for the cortex thanks to the inverse mapping. The results are very satisfactory on these examples since the deformed Template matches very well the convolutions of the brain and the thin concavities. The model also allows for the delineation of small holes and thin structures as the larger hole inside the slice more accurately than with [49], for which the inside hole exhibits a bump and is not as thin as it should be in the right extremity.

To assess again inverse consistency, we switched the role of the Template and the Reference in Figure 4.7, resulting in a more accurate alignment of R and $T \circ \varphi$ with the proposed method and fewer artifacts on $T \circ \varphi$ in the central hole, unlike method [49].

In Figure 4.8, we aim to map a slice of a brain to another one (courtesy of Laboratory Of NeuroImaging, UCLA). The obtained simplified version $\tilde{T}$ of R is more faithful to reality with the proposed model including the nonlocal shape descriptor and restitutes better the fine details of the complex topology: the segmentation delineates well the long and thin concavities.

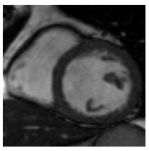

(a) R

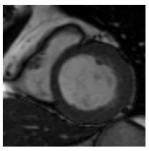

(b) T

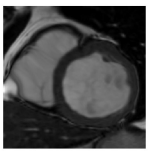

(c) $T \circ \varphi$ NL

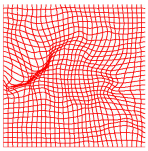

(d) Deformation grid NL

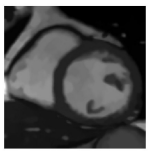

(e) $\tilde{T}$ NL

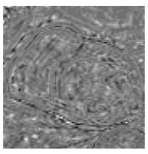

(f) $R - \tilde{T}$ NL

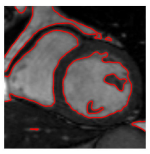

(g) Segmented Reference NL

(h) Binary Reference (rescaled) NL

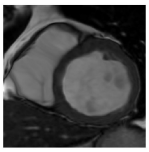

(i) $T \circ \varphi$ L

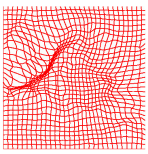

(j) Deformation grid L

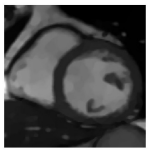

(k) $\tilde{T}$ L

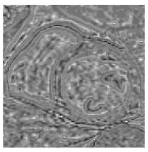

(l) $R - \tilde{T}$ L

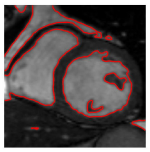

(m) Segmented Reference L

(n) Binary Reference (rescaled) L

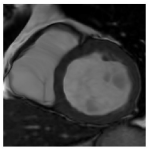

(o) $T \circ \varphi$ from [49]

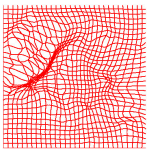

(p) Deformation grid from [49]

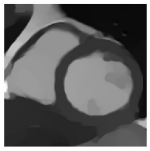

(q) $\tilde{T}$ from [49]

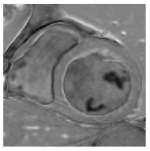

(r) $R - \tilde{T}$ from [49]

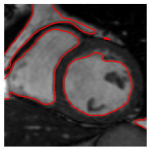

(s) Segmented Reference from [49]

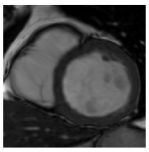

(t) $T \circ \varphi$ with $L^2 - QW$

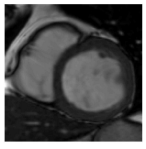

(u) $T \circ \varphi$ with $L^2 - H^2$

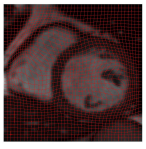

(v) R and the deformation grid with $L^2 - H^2$

Figure 4.2: Mapping of cardiac MRI images (ED(108)-ES(100)) (size : 150 × 150), NL execution time : 123s, L execution time : 891s.

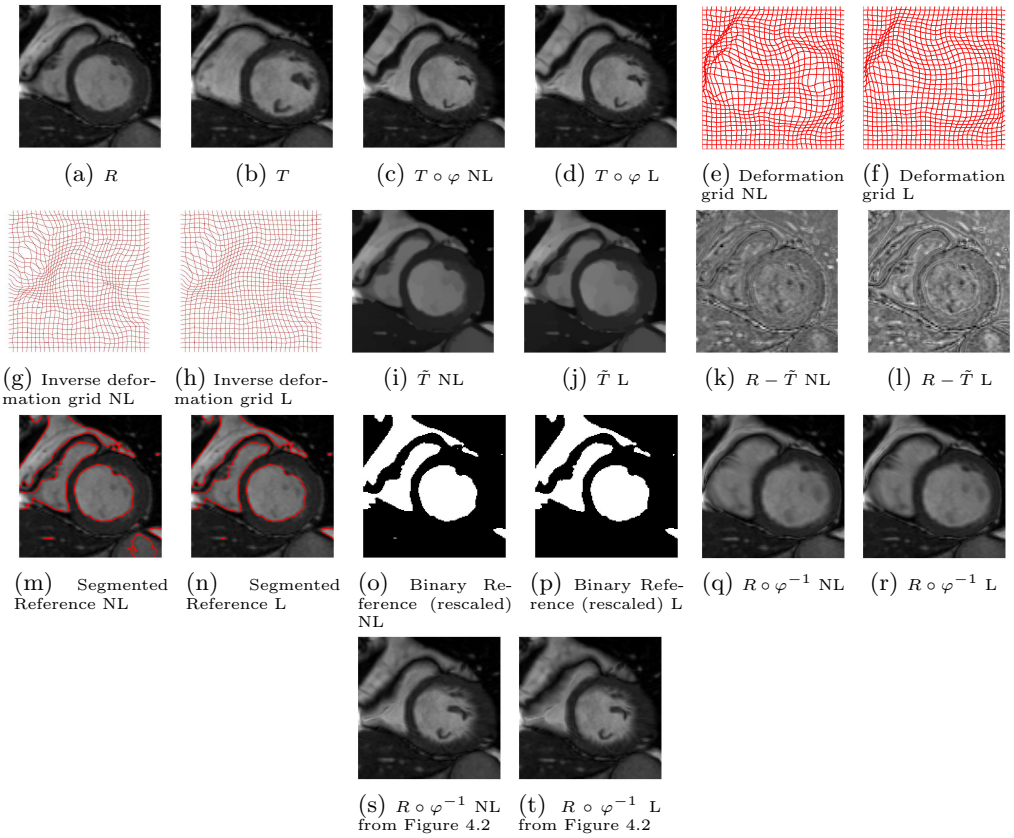

(a) R (b) T (c) $T \circ \varphi$ NL (d) $T \circ \varphi$ L (e) Deformation grid NL (f) Deformation grid L

(g) Inverse deformation grid NL (h) Inverse deformation grid L (i) $\tilde{T}$ NL (j) $\tilde{T}$ L (k) $R - \tilde{T}$ NL (l) $R - \tilde{T}$ L

(m) Segmented Reference NL (n) Segmented Reference L (o) Binary Reference (rescaled) NL (p) Binary Reference (rescaled) L (q) $R \circ \varphi^{-1}$ NL (r) $R \circ \varphi^{-1}$ L

(s) $R \circ \varphi^{-1}$ NL from Figure 4.2 (t) $R \circ \varphi^{-1}$ L from Figure 4.2

Figure 4.3: Mapping of cardiac MRI images (ES(100)-ED(108)) (size : 150 × 150), NL execution time : 123s, L execution time : 891s.

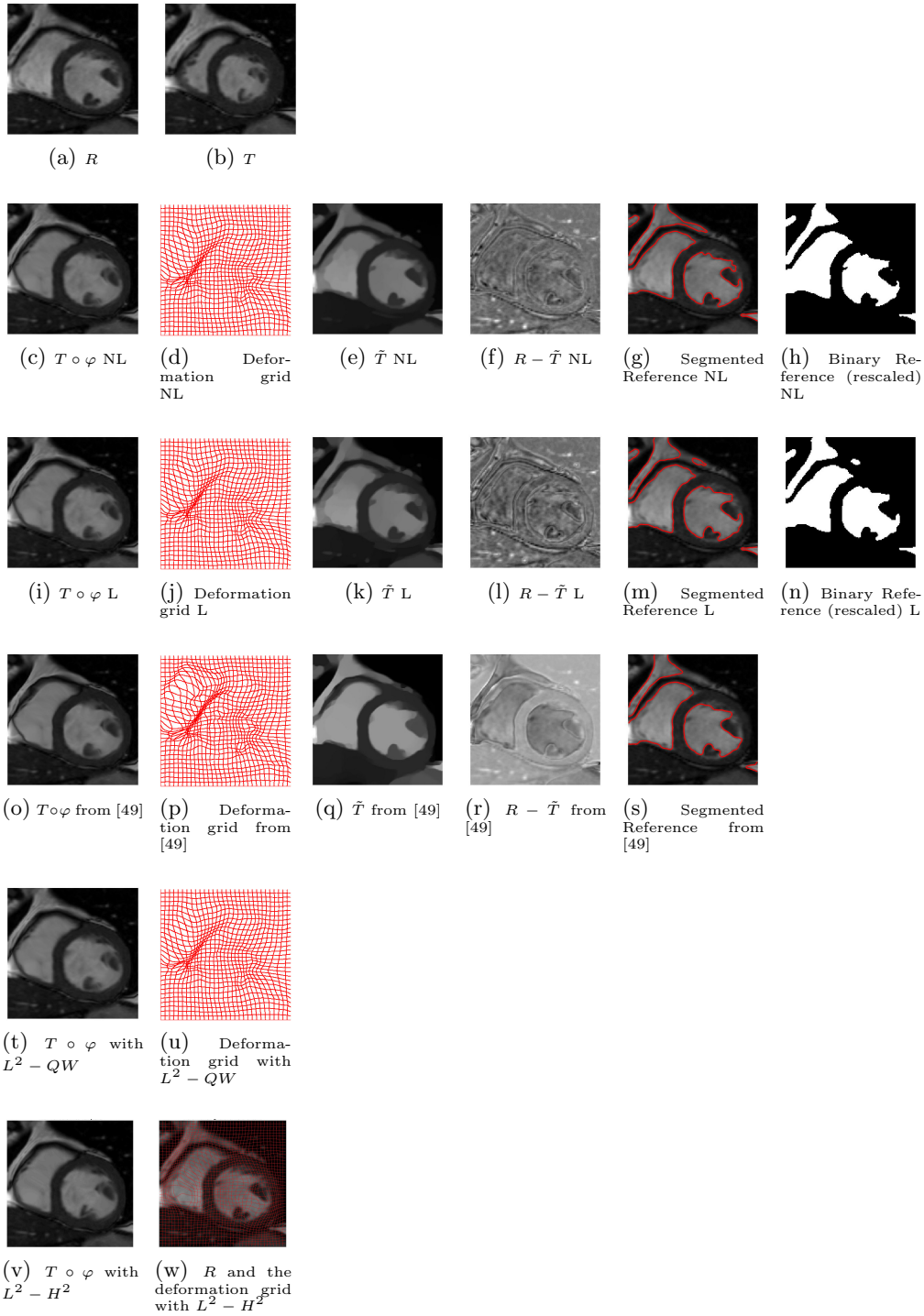

(a) R (b) T

(c) $T \circ \varphi$ NL (d) Deformation grid NL (e) $\tilde{T}$ NL (f) $R - \tilde{T}$ NL (g) Segmented Reference NL (h) Binary Reference (rescaled) NL

(i) $T \circ \varphi$ L (j) Deformation grid L (k) $\tilde{T}$ L (l) $R - \tilde{T}$ L (m) Segmented Reference L (n) Binary Reference (rescaled) L

(o) $T \circ \varphi$ from [49] (p) Deformation grid from [49] (q) $\tilde{T}$ from [49] (r) $R - \tilde{T}$ from [49] (s) Segmented Reference from [49]

(t) $T \circ \varphi$ with $L^2 - QW$ (u) Deformation grid with $L^2 - QW$

(v) $T \circ \varphi$ with $L^2 - H^2$ (w) R and the deformation grid with $L^2 - H^2$

Figure 4.4: Mapping of cardiac MRI images (ED(128)-ES(120)) (size : 150 × 150), NL execution time : 123s, L execution time : 891s.

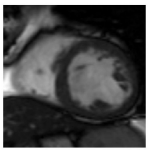

(a) R

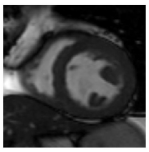

(b) T

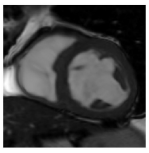

(c) $T \circ \varphi$ NL

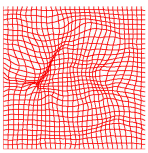

(d) Deformation grid NL

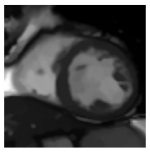

(e) $\tilde{T}$ NL

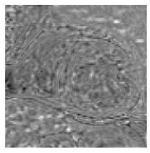

(f) $R - \tilde{T}$ NL

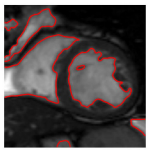

(g) Segmented Reference NL

(h) Binary Reference (rescaled) NL

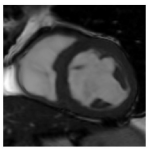

(i) $T \circ \varphi$ L

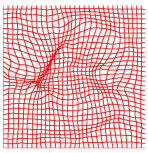

(j) Deformation grid L

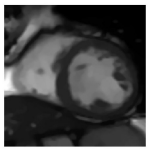

(k) $\tilde{T}$ L

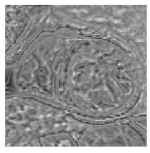

(l) $R - \tilde{T}$ L

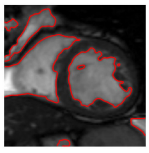

(m) Segmented Reference L

(n) Binary Reference (rescaled) L

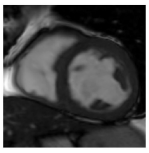

(o) $T \circ \varphi$ from [49]

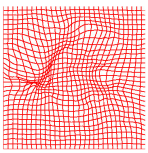

(p) Deformation grid from [49]

(q) $\tilde{T}$ from [49]

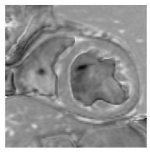

(r) $R - \tilde{T}$ from [49]

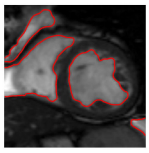

(s) Segmented Reference from [49]

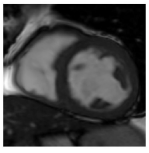

(t) $T \circ \varphi$ with $L^2 - QW$

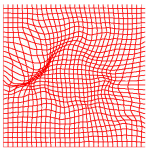

(u) Deformation grid with $L^2 - QW$

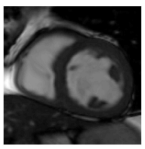

(v) $T \circ \varphi$ with $L^2 - H^2$

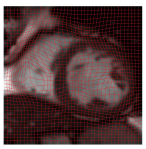

(w) R and the deformation grid with $L^2 - H^2$

Figure 4.5: Mapping of cardiac MRI images (ED(148)-ES(140)) (size : 150 × 150), NL execution time : 123s, L execution time : 891s.

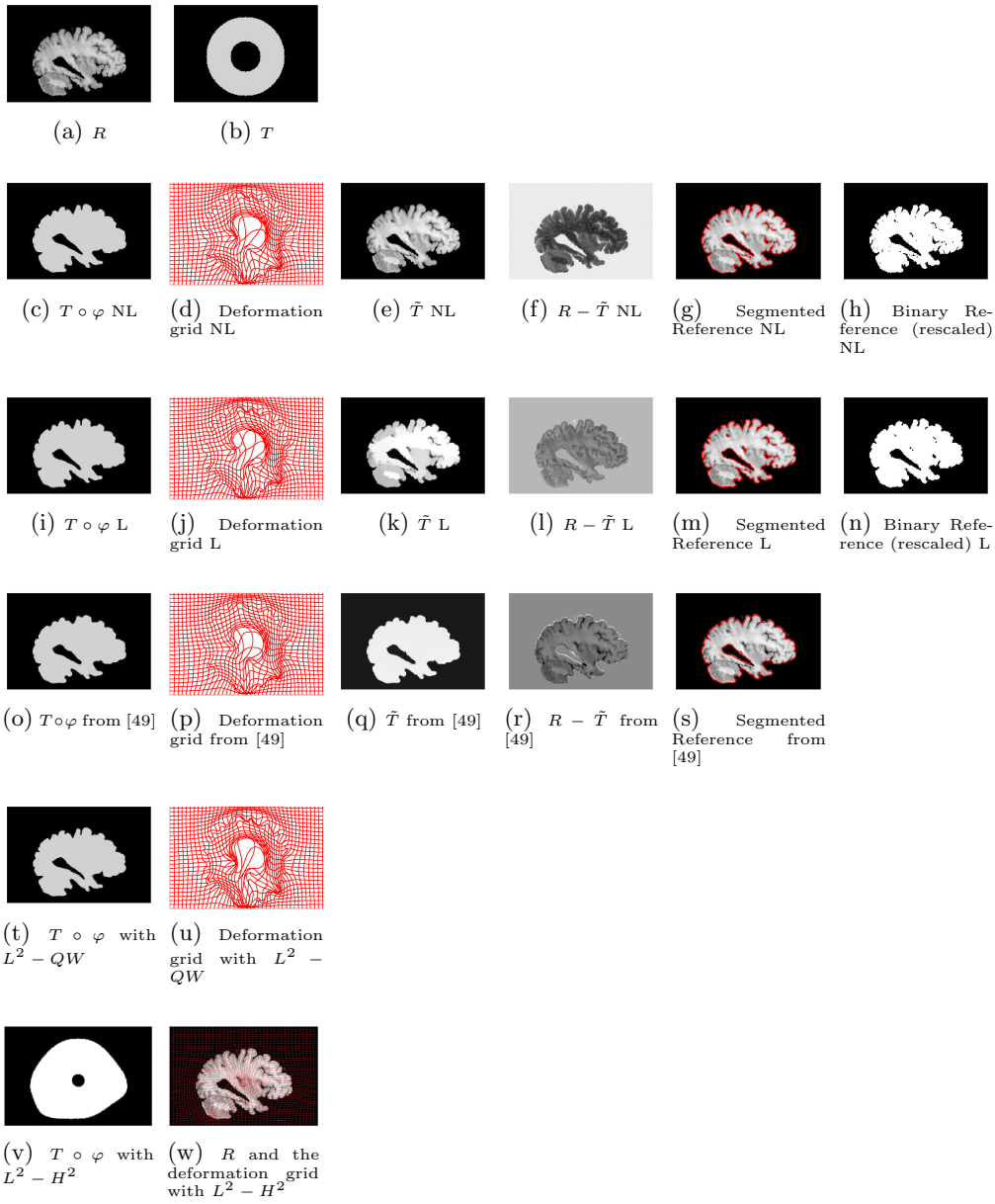

(a) R (b) T

(c) $T \circ \varphi$ NL (d) Deformation grid NL (e) $\tilde{T}$ NL (f) $R - \tilde{T}$ NL (g) Segmented Reference NL (h) Binary Reference (rescaled) NL

(i) $T \circ \varphi$ L (j) Deformation grid L (k) $\tilde{T}$ L (l) $R - \tilde{T}$ L (m) Segmented Reference L (n) Binary Reference (rescaled) L

(o) $T \circ \varphi$ from [49] (p) Deformation grid from [49] (q) $\tilde{T}$ from [49] (r) $R - \tilde{T}$ from [49] (s) Segmented Reference from [49]

(t) $T \circ \varphi$ with $L^2 - QW$ (u) Deformation grid with $L^2 - QW$

(v) $T \circ \varphi$ with $L^2 - H^2$ (w) R and the deformation grid with $L^2 - H^2$

Figure 4.6: Mapping of a tore to a slice of a human brain (1) (size : 128×192), NL execution time : 55s, L execution time : 361s.

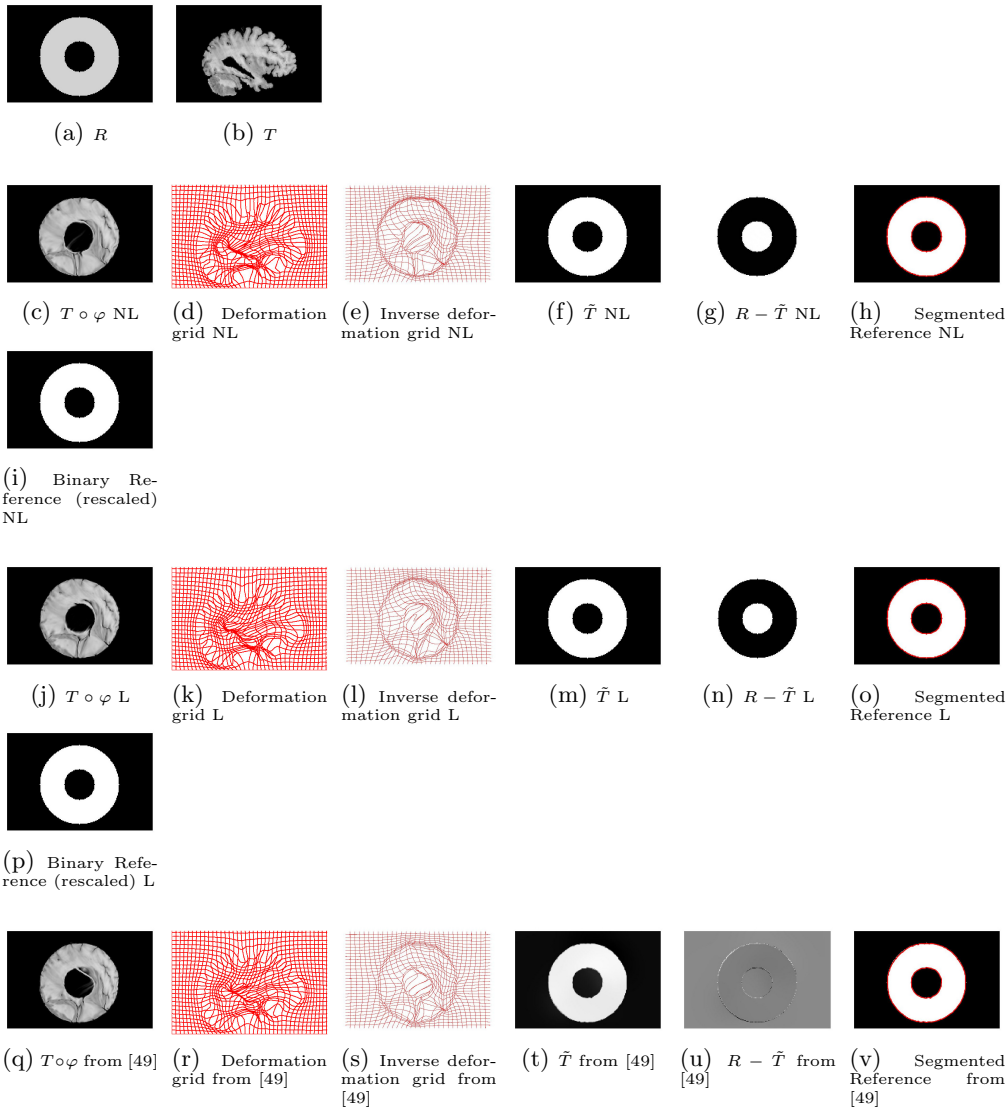

(a) R (b) T

(c) $T \circ \varphi$ NL (d) Deformation grid NL (e) Inverse deformation grid NL (f) $\tilde{T}$ NL (g) $R - \tilde{T}$ NL (h) Segmented Reference NL

(i) Binary Reference (rescaled) NL

(j) $T \circ \varphi$ L (k) Deformation grid L (l) Inverse deformation grid L (m) $\tilde{T}$ L (n) $R - \tilde{T}$ L (o) Segmented Reference L

(p) Binary Reference (rescaled) L

(q) $T \circ \varphi$ from [49] (r) Deformation grid from [49] (s) Inverse deformation grid from [49] (t) $\tilde{T}$ from [49] (u) $R - \tilde{T}$ from [49] (v) Segmented Reference from [49]

Figure 4.7: Mapping of a slice of a human brain to a tore (1 inverse consistency) (size : 128×192), NL execution time : 83s, L execution time : 328s.

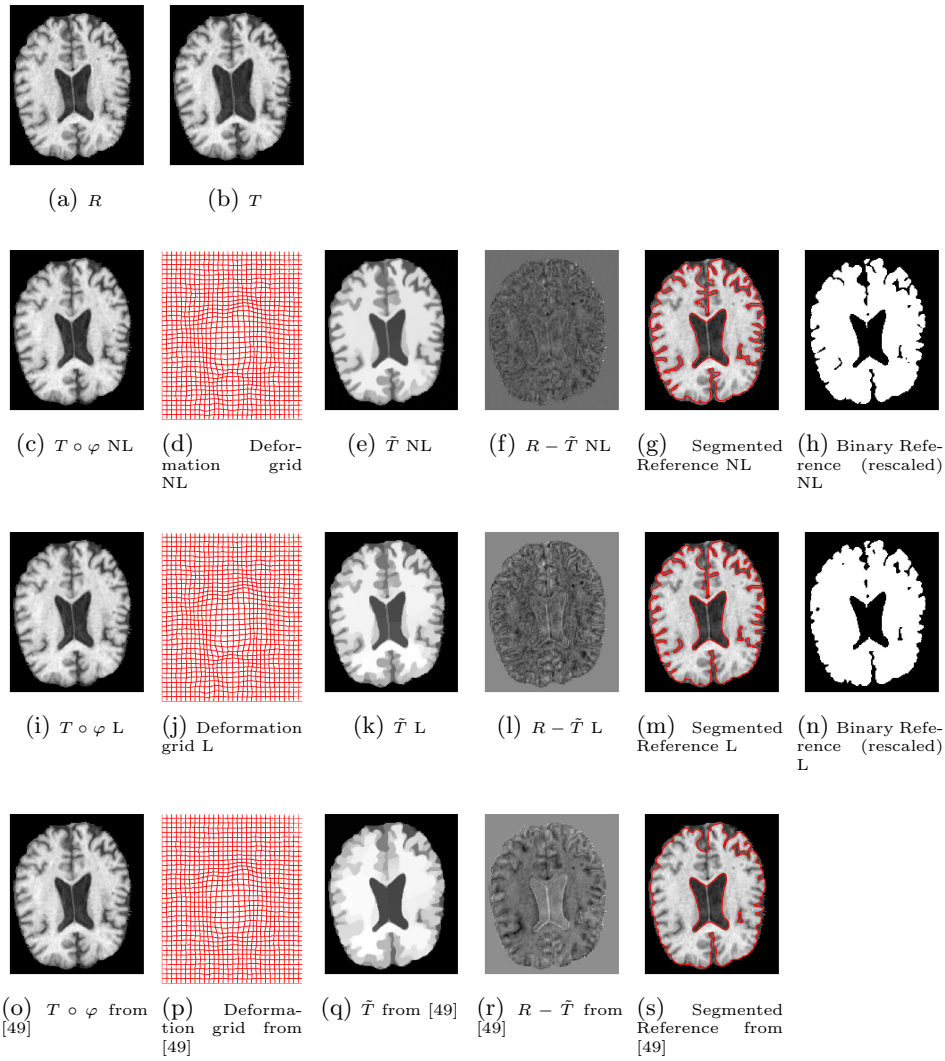

(a) R (b) T

(c) $T \circ \varphi$ NL (d) Deformation grid NL (e) $\tilde{T}$ NL (f) $R - \tilde{T}$ NL (g) Segmented Reference NL (h) Binary Reference (rescaled) NL

(i) $T \circ \varphi$ L (j) Deformation grid L (k) $\tilde{T}$ L (l) $R - \tilde{T}$ L (m) Segmented Reference L (n) Binary Reference (rescaled) L

(o) $T \circ \varphi$ from [49] (p) Deformation grid from [49] (q) $\tilde{T}$ from [49] (r) $R - \tilde{T}$ from [49] (s) Segmented Reference from [49]

Figure 4.8: Mapping of a slice of a human brain to another one (2) (size : 180×150), NL execution time : 304s, L execution time : 378s.

The last numerical experiment is made of brain tumor images (Figure 4.9) taken at different times in order to highlight the ability of the model to handle complex topologies with thin tubes and concavities. The registration and segmentation accuracy are visually better with the proposed model, in particular, in the restitution of the right excrescence that is more faithful to reality and in the accuracy of the delineation of the left tube at the bottom of the image (that is not divided into several pieces, contrary to the result produced by method [49]).

(a) R

(b) T

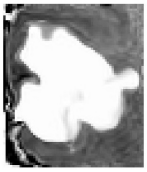

(c) $T \circ \varphi$ NL

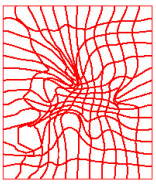

(d) Deformation grid NL

(e) $\tilde{T}$ NL

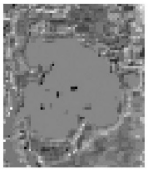

(f) $R - \tilde{T}$ NL

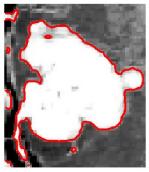

(g) Segmented Reference NL

(h) Binary Reference (rescaled) NL

(i) $T \circ \varphi$ L

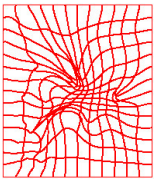

(j) Deformation grid L

(k) $\tilde{T}$ L

(l) $R - \tilde{T}$ L

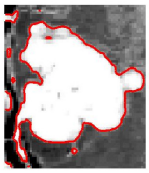

(m) Segmented Reference L

(n) Binary Reference (rescaled) L

(o) $T \circ \varphi$ from [49]

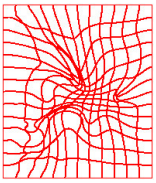

(p) Deformation grid from [49]

(q) $\tilde{T}$ from [49]

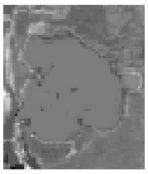

(r) $R - \tilde{T}$ from [49]

(s) Segmented Reference from [49]

(t) $T \circ \varphi$ with $L^2 - QW$

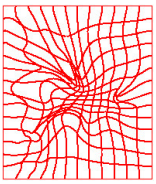

(u) Deformation grid with $L^2 - QW$

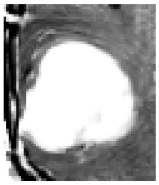

(v) $T \circ \varphi$ with $L^2 - H^2$

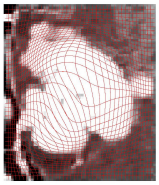

(w) R and the deformations grid with $L^2 - H^2$

Figure 4.9: Mapping of tumor brain images (size : 71×61), NL execution time : 18s, L execution time : 167s.

4.2 Quantitative and qualitative assessment of the functional components

The question of assessing the relevance of the novel components constituting the considered functional is legitimate and takes on two main aspects: the relevance of the nonlinear elasticity based regularizer compared to classical ones (such as diffusion, biharmonic, linear elasticity) that lead to linear terms with respect to the derivatives in φ_i, $i \in \{1, 2\}$ in the Euler-Lagrange equations, and the relevance of the dissimilarity measure based on a combination of weighted total variation and nonlocal shape descriptors. For the study of the relevance of the regularizer, we proceeded like in [49]. Due to the large amount of literature in the field of registration, we had to make a choice as for the alternating methods to be compared with our model. First, we decided to focus on non parametric registration methods, category of methods we are familiar with (keeping in mind that we implement the computer codes ex-nihilo by ourselves). In [43], Lin *et al.* first review the most common and simplest regularization terms (diffusion, biharmonic, linear elasticity models) that lead to linear terms with respect to derivatives in the Euler-Lagrange equations. Then they introduce a nonlinear elasticity regularization based on the basic Saint Venant-Kirchhoff stored energy function in order to allow for larger and smoother deformations. The first conclusion is that, by comparison with image registration models involving linear regularization, the nonlinear-elasticity-based model renders better ground truth, produces larger mutual information and requires fewer numerical corrections such as regridding steps. The second conclusion is that the biharmonic model is more comparable to the nonlinear elasticity model, which motivated us to further examine its behaviour compared with our model.

The first kind of experiment consisted of tuning off the dissimilarity measure, that is, the combination of the weighted total variation and the nonlocal shape descriptor, model denoted by $L^2 - QW$ in each case. In terms of quantitative accuracy, the proposed method gives better results with higher Dice coefficients (see Table 4.1). Visually, this is particularly remarkable in Figure 4.5 (t), where the thin details inside the left ventricular cavity are not as accurately recovered as with the proposed method (in particular in terms of thickness and sharpness), in Figure 4.6 (t) in which inside the larger hole the right extremity becomes finer than it should be, in Figure 4.9 (t), where the excrescences on the right-hand side, on the bottom left hand corner (particularly the upper part of the tube that is not faithfully restored as in Figure 4.9 (i)) and on the top (particularly the round shape and the sharp concavity not as faithfully restored as in 4.9 (c)) are not as well recovered as with the proposed model. Besides, considering Figure 4.10–Figure 4.12, we see that including the dissimilarity measure increases the speed of convergence: for the same number of iterations (300), the L^2-fidelity term alone cannot achieve registration accurately. We observe that the L^2-fidelity term decreases fastest with the nonlocal version of the proposed algorithm. After a bigger number of iterations, the L^2-fidelity term is always slightly greater than the quantity obtained with the proposed model or with [49]. We conducted a second kind of experiment, consisting both in replacing the nonlinear elasticity-based regularizer by the biharmonic one and in removing the dissimilarity measure (so keeping only the L^2-fidelity term), model denoted by $L^2 - H^2$. In the case of

MRI images of a cardiac cycle(Figure 4.2, 4.4, 4.5), our algorithm produces larger deformations and the obtained deformed Template aligns more accurately with the Reference particularly in the left hand side and restitutes better the fine details. In Figure 4.6 (v), for a comparable number of iterations, registration cannot be achieved successfully. In the case of the brain tumor Figure 4.9, the obtained deformed Template (Figure 4.9 (v)) does not capture the details of the tumor boundary, resulting in a significantly smaller Dice coefficient. The right excrescence is not satisfactorily reproduced.

(a) R

(b) T

(c) $T \circ \varphi$ NL

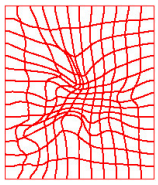

(d) Deformation grid NL

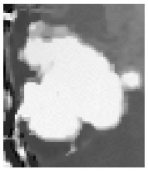

(e) $\tilde{T}$ NL

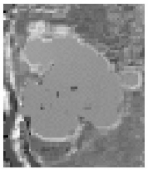

(f) $R - \tilde{T}$ NL

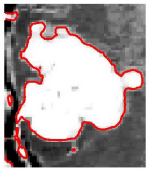

(g) Segmented Reference NL

(h) Binary Reference (rescaled) NL

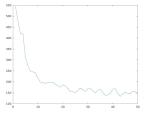

(i) $\|R - T \circ \varphi\|^2_{L^2(\Omega)}$ NL

(j) $T \circ \varphi$ L

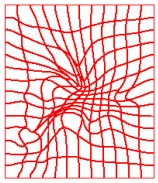

(k) Deformation grid L

(l) $\tilde{T}$ L

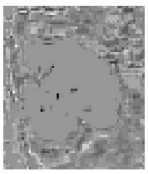

(m) $R - \tilde{T}$ L

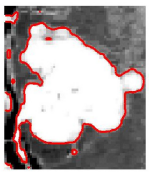

(n) Segmented Reference L

(o) Binary Reference (rescaled) L

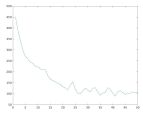

(p) $\|R - T \circ \varphi\|^2_{L^2(\Omega)}$ L

(q) $T \circ \varphi$ from [49]

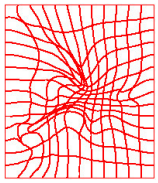

(r) Deformation grid from [49]

(s) $\tilde{T}$ from [49]

(t) $R - \tilde{T}$ from [49]

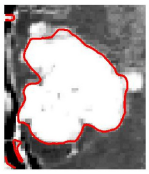

(u) Segmented Reference from [49]

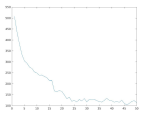

(v) $\|R - T \circ \varphi\|^2_{L^2(\Omega)}$ from [49]

(w) $T \circ \varphi$ with $L^2 - QW$

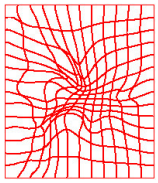

(x) Deformation grid with $L^2 - QW$

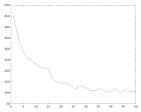

(y) $\|R - T \circ \varphi\|^2_{L^2(\Omega)}$ with $L^2 - QW$

Figure 4.10: Mapping of tumor brain images with 50 iterations (size : 71 × 61), NL execution time : 1s, L execution time : 16s.

(a) R

(b) T

(c) $T \circ \varphi$ NL

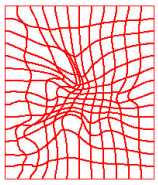

(d) Deformation grid NL

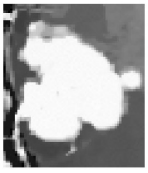

(e) $\tilde{T}$ NL

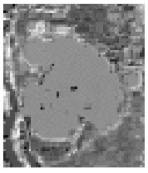

(f) $R - \tilde{T}$ NL

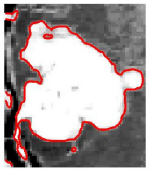

(g) Segmented Reference NL

(h) Binary Reference (rescaled) NL

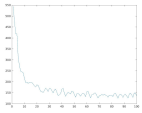

(i) $\|R - T \circ \varphi\|^2_{L^2(\Omega)}$ NL

(j) $T \circ \varphi$ L

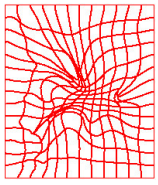

(k) Deformation grid L

(l) $\tilde{T}$ L

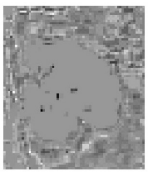

(m) $R - \tilde{T}$ L

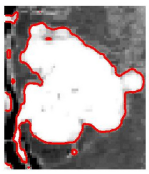

(n) Segmented Reference L

(o) Binary Reference (rescaled) L

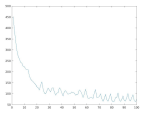

(p) $\|R - T \circ \varphi\|^2_{L^2(\Omega)}$ L

(q) $T \circ \varphi$ from [49]

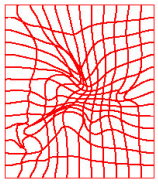

(r) Deformation grid from [49]

(s) $\tilde{T}$ from [49]

(t) $R - \tilde{T}$ from [49]

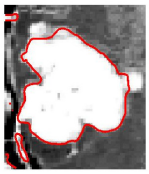

(u) Segmented Reference from [49]

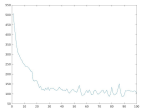

(v) $\|R - T \circ \varphi\|^2_{L^2(\Omega)}$ from [49]

(w) $T \circ \varphi$ with $L^2 - QW$

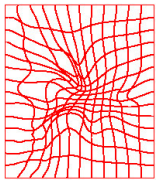

(x) Deformation grid with $L^2 - QW$

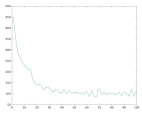

(y) $\|R - T \circ \varphi\|^2_{L^2(\Omega)}$ with $L^2 - QW$

Figure 4.11: Mapping of tumor brain images with 100 iterations (size : 71 × 61), NL execution time : 2s, L execution time : 32s.

(a) R

(b) T

(c) $T \circ \varphi$ NL

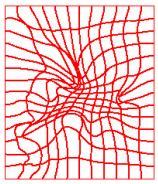

(d) Deformation grid NL

(e) $\tilde{T}$ NL

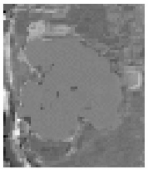

(f) $R - \tilde{T}$ NL

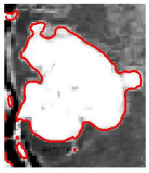

(g) Segmented Reference NL

(h) Binary Reference (rescaled) NL

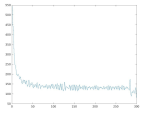

(i) $\|R - T \circ \varphi\|^2_{L^2(\Omega)}$ NL

(j) $T \circ \varphi$ L

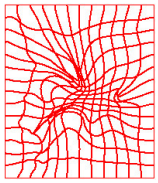

(k) Deformation grid L

(l) $\tilde{T}$ L

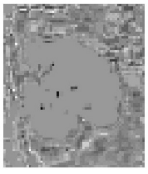

(m) $R - \tilde{T}$ L

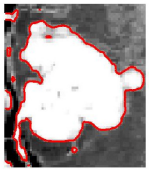

(n) Segmented Reference L

(o) Binary Reference (rescaled) L

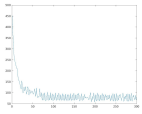

(p) $\|R - T \circ \varphi\|^2_{L^2(\Omega)}$ L

(q) $T \circ \varphi$ from [49]

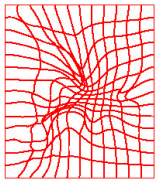

(r) Deformation grid from [49]

(s) $\tilde{T}$ from [49]

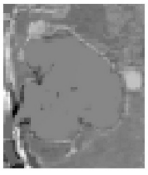

(t) $R - \tilde{T}$ from [49]

(u) Segmented Reference from [49]

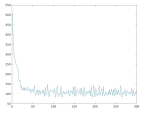

(v) $\|R - T \circ \varphi\|^2_{L^2(\Omega)}$ from [49]

(w) $T \circ \varphi$ with $L^2 - QW$

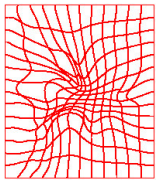

(x) Deformation grid with $L^2 - QW$

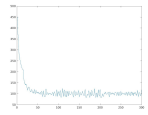

(y) $\|R - T \circ \varphi\|^2_{L^2(\Omega)}$ with $L^2 - QW$

Figure 4.12: Mapping of tumor brain images with 300 iterations (size : 71 × 61), NL execution time : 11s, L execution time : 98s.

Bibliography

[1] L. Ambrosio and G. Dal Maso, *A general chain rule for distributional derivatives*, Proc. Amer. Math. Soc., 108 (1990), pp. 691–702.

[2] L. Ambrosio, N. Fusco, and D. Pallara, *Functions of Bounded Variation and Free Discontinuity Problems*, Oxford university press, 2000.

[3] J.-H. An, Y. Chen, F. Huang, D. Wilson, and E. Geiser, *Medical Image Computing and Computer-Assisted Intervention – MICCAI 2005: 8th International Conference, Palm Springs, CA, USA, October 26-29, 2005, Proceedings, Part I*, Springer Berlin Heidelberg, 2005, ch. A Variational PDE Based Level Set Method for a Simultaneous Segmentation and Non-Rigid Registration, pp. 286–293.

[4] E. Angelini, Y. Jin, and A. Laine, *State of the Art of Level Set Methods in Segmentation and Registration of Medical Imaging Modalities*, Springer US, 2005, pp. 47–101.

[5] J. Ashburner and K. J. Friston, *Nonlinear spatial normalization using basis functions*, Hum. Brain Mapp., 7 (1999), pp. 254–266.

[6] H. Attouch, G. Buttazzo, and G. Michaille, *Variational Analysis in Sobolev and BV Spaces: Applications to PDEs and Optimization*, MOS-SIAM Series on Optimization, Society for Industrial and Applied Mathematics, 2014.

[7] G. Aubert and P. Kornprobst, *Mathematical Problems in Image Processing: Partial Differential Equations and the Calculus of Variations*, Applied Mathematical Sciences, Springer-Verlag, 2001.

[8] G. Aubert and P. Kornprobst, *New algorithm for solving variational problems in $W^{1,p}$ and BV: Application to image restoration*, Research Report RR-6245, INRIA, 2007.

[9] G. Aubert and P. Kornprobst, *Can the nonlocal characterization of Sobolev spaces by Bourgain et al. be useful for solving variational problems?*, SIAM J. Numer. Anal., 47 (2009), pp. 844–860.

[10] A. Baldi, *Weighted BV functions*, Houston J. Math., 27 (2001), pp. 683–705.

[11] M. Beg, M. Miller, A. Trouvé, and L. Younes, *Computing large deformation metric mappings via geodesic flows of diffeomorphisms*, Int. J. Comput. Vis., 61 (2005), pp. 139–157.

[12] Y. Boink, *Combined modelling of optimal transport and segmentation revealing vascular properties*, 2016.

[13] J. Boulanger, P. Elbau, C. Pontow, and O. Scherzer, *Non-Local Functionals for Imaging*, Springer New York, 2011, pp. 131–154.

[14] J. Bourgain, H. Brezis, and P. Mironescu, *Another look at Sobolev spaces*, in Optimal Control and Partial Differential Equations, In honour of Professor Alain Bensoussan's 60^{th} Birthday, A. S. J. L. Menaldi, E. Rofman, ed., 2001, pp. 439–455.

[15] X. Bresson, S. Esedoḡlu, P. Vandergheynst, J.-P. Thiran, and S. Osher, *Fast global minimization of the active contour/snake model*, J. Math. Imaging Vis., 28 (2007), pp. 151–167.

[16] H. Brezis, *Analyse Fonctionelle. Théorie et Applications*, Dunod, Paris, 2005.

[17] C. Broit, *Optimal Registration of Deformed Images*, PhD thesis, Computer and Information Science, University of Pennsylvania, 1981.

[18] M. Burger, J. Modersitzki, and L. Ruthotto, *A hyperelastic regularization energy for image registration*, SIAM J. Sci. Comput., 35 (2013), pp. B132–B148.

[19] V. Caselles, R. Kimmel, and G. Sapiro, *Geodesic Active Contours*, Int. J. Comput. Vis., 22 (1993), pp. 61–87.

[20] T. F. Chan, S. Esedoḡlu, and M. Nikolova, *Algorithms for finding global minimizers of image segmentation and denoising models*, SIAM J. Appl. Math., 66 (2006), pp. 1632–1648.

[21] G. E. Christensen, *Deformable Shape Models for Anatomy*, PhD thesis, Washington University, Sever Institute of technology, USA, 1994.

[22] P. Ciarlet, *Elasticité Tridimensionnelle*, Masson, 1985.

[23] P. Ciarlet, *Mathematical Elasticity, Volume I: Three-dimensional elasticity*, Amsterdam etc., North-Holland, 1988.

[24] O. Clatz, M. Sermesant, P.-Y. Bondiau, H. Delingette, S. K. Warfield, G. Malandain, and N. Ayache, *Realistic simulation of the 3-D growth of brain tumors in MR images coupling diffusion with biomechanical deformation*, IEEE Trans. Med. Imaging, 24 (2005), pp. 1334–1346.

[25] B. Dacorogna, *Direct Methods in the Calculus of Variations, Second Edition*, Springer, 2008.

[26] C. Davatzikos, *Spatial transformation and registration of brain images using elastically deformable models*, Comput. Vis. Image Underst., 66 (1997), pp. 207–222.

[27] J. Dávila, *On an open question about functions of bounded variation*, Calc. Var. Partial Differential Equations, 15 (2002), pp. 519–527.

[28] M. H. Davis, A. Khotanzad, D. P. Flamig, and S. E. Harms, *A physics-based coordinate transformation for 3-D image matching*, IEEE Trans. Med. Imaging, 16 (1997), pp. 317–328.

[29] N. Debroux, S. Ozeré, and C. Le Guyader, *A non-local topology-preserving segmentation guided registration model*, J. Math. Imaging Vision, (2017), pp. 1–24.

[30] R. Derfoul and C. Le Guyader, *A relaxed problem of registration based on the Saint Venant-Kirchhoff material stored energy for the mapping of mouse brain gene expression data to a neuroanatomical mouse atlas*, SIAM J. Imaging Sci., 7 (2014), pp. 2175–2195.

[31] L. R. Dice, *Measures of the amount of ecologic association between species*, Ecology, 26 (1945), pp. 297–302.

[32] M. Droske and M. Rumpf, *A variational approach to non-rigid morphological registration*, SIAM J. Appl. Math., 64 (2004), pp. 668–687.

[33] M. Droske and M. Rumpf, *Multiscale joint segmentation and registration of image morphology*, IEEE Trans. Pattern Anal. Mach. Intell., 29 (2007), pp. 2181–2194.

[34] L. Evans and R. Gariepy, *Measure Theory and Fine Properties of Functions*, CRC Press, 1992.

[35] B. Fischer and J. Modersitzki, *Curvature based image registration*, J. Math. Imaging Vis., 18 (2003), pp. 81–85.

[36] G. Gilboa and S. Osher, *Nonlocal operators with applications to image processing*, Multiscale Model. Simul., 7 (2009), pp. 1005–1028.

[37] A. Gooya, K. Pohl, M. Bilello, L. Cirillo, G. Biros, E. Melhem, and C. Davatzikos, *GLISTR: Glioma Image Segmentation and Registration*, IEEE Trans. Med. Imaging, 31 (2012), pp. 1941–1954.

[38] S. Gorthi, V. Duay, X. Bresson, M. B. Cuadra, F. J. S. Castro, C. Pollo, A. S. Allal, and J.-P. Thiran, *Active deformation fields: Dense deformation field estimation for atlas-based segmentation using the active contour framework*, Med. Image Anal., 15 (2011), pp. 787–800.

[39] M. Jung, X. Bresson, T. F. Chan, and L. A. Vese, *Nonlocal Mumford-Shah regularizers for color image restoration*, IEEE Trans. Image Process., 20 (2011), pp. 1583–1598.

[40] N. Kerdid, H. Le Dret, and A. Saidi, *Numerical approximation for a non-linear membrane problem*, Int J. Non Linear Mech., 43 (2008), pp. 908–914.

[41] H. Le Dret, *Notes de Cours de DEA. Méthodes mathématiques en élasticité*, 2003-2004.

[42] C. Le Guyader and L. Vese, *A combined segmentation and registration framework with a nonlinear elasticity smoother*, Comput. Vis. Image Underst., 115 (2011), pp. 1689–1709.

[43] T. Lin, C. Le Guyader, I. Dinov, P. Thompson, A. Toga, and L. Vese, *Gene expression data to mouse atlas registration using a nonlinear elasticity smoother and landmark points constraints*, J. Sci. Comput., 50 (2012), pp. 586–609.

[44] N. Lord, J. Ho, B. Vemuri, and S. Eisenschenk, *Simultaneous registration and parcellation of bilateral hippocampal surface pairs for local asymmetry quantification*, IEEE Trans. Med. Imaging, 26 (2007), pp. 471–478.

[45] J. Modersitzki, *Numerical Methods for Image Registration*, Oxford University Press, 2004.

[46] J. Modersitzki, *FAIR: Flexible Algorithms for Image Registration*, Society for Industrial and Applied Mathematics (SIAM), 2009.

[47] D. Mumford, *Optimal approximation by piecewise smooth functions and associated variational problems*, Commun. Pure Appl. Anal., (1989), pp. 577–685.

[48] P. Negrón Marrero, *A numerical method for detecting singular minimizers of multidimensional problems in nonlinear elasticity*, Numer. Math., 58 (1990), pp. 135–144.

[49] S. Ozeré, C. Gout, and C. Le Guyader, *Joint segmentation/registration model by shape alignment via weighted total variation minimization and nonlinear elasticity*, SIAM J. Imaging Sci., 8 (2015), pp. 1981–2020.

[50] S. Ozeré and C. Le Guyader, *Topology preservation for image-registration-related deformation fields*, Commun. Math. Sci., 13 (2015), pp. 1135–1161.

[51] K. Papafitsoros, *Novel Higher Order Regularization Methods for Image Reconstruction*, PhD thesis, University of Cambridge, U.K., 2014.

[52] A. C. Ponce, *A new approach to Sobolev spaces and connections to* Γ*-convergence*, Calc. Var. Partial Differential Equations, 19 (2004), pp. 229–255.

[53] L. Rudin, S. Osher, and E. Fatemi, *Nonlinear total variation based noise removal algorithms*, Phys. D, 60 (1992), pp. 259–268.

[54] M. Rumpf and B. Wirth, *A nonlinear elastic shape averaging approach*, SIAM J. Imaging Sci., 2 (2009), pp. 800–833.

[55] T. Sederberg and S. Parry, *Free-form deformation of solid geometric models*, SIGGRAPH Comput. Graph., 20 (1986), pp. 151–160.

[56] M. Sezgin and B. Sankur, *Survey over image thresholding techniques and quantitative performance evaluation*, J. Electron. Imaging, 13 (2004), pp. 146–168.

[57] A. Sotiras, C. Davatzikos, and N. Paragios, *Deformable medical image registration: A survey*, IEEE Trans. Med. Imaging, 32 (2013), pp. 1153–1190.

[58] D. Spector, *Characterization of Sobolev and BV Spaces*, PhD thesis, Carnegie Mellon University, 2011.

[59] B. Vemuri, J. Ye, Y. Chen, and C. Leonard, *Image registration via level-set motion: applications to atlas-based segmentation*, Med. Image Anal., 7 (2003), pp. 1–20.

[60] L. Vese and C. Le Guyader, *Variational Methods in Image Processing*, Chapman & Hall/CRC Mathematical and Computational Imaging Sciences Series, Taylor & Francis, 2015.

[61] B. Wirth, *On the Γ-limit of joint image segmentation and registration functionals based on phase fields*, Interfaces Free Bound., 18 (2016), pp. 441–477.

[62] A. Yezzi, L. Zollei, and T. Kapur, *A variational framework for joint segmentation and registration*, in Mathematical Methods in Biomedical Image Analysis, IEEE-MMBIA, 2001, pp. 44–51.

[63] L. Zagorchev and A. Goshtasby, *A comparative study of transformation functions for nonrigid image registration*, IEEE Trans. Image Process., 15 (2006), pp. 529–538.

Chapter 5

A second order free discontinuity model for bituminous surfacing crack recovery

We consider a second order variational model dedicated to crack detection on bituminous surfacing. It is based on a variant of the weak formulation of the Blake-Zisserman functional that involves the discontinuity set of the gradient of the unknown, set that encodes the geometrical thin structures we aim to recover, as suggested by Drogoul et al. ([30], [8]). Following Ambrosio, Faina and March ([2]), an approximation of this cost function by elliptic functionals is provided. Theoretical results including existence of minimizers, existence of a unique viscosity solution to the derived evolution problem, and a Γ-convergence result relating the elliptic functionals to the initial weak formulation are given. Extending then the ideas developed in the case of first order nonlocal regularization to higher order derivatives, we provide and analyze a nonlocal version of the model.

1 Introduction

The scope of this work is to propose a novel variational method to detect thin structures, namely cracks on bituminous surfacing. If classically, singularities related to edges are associated with a discontinuity of gray level intensities across edges (and are thus detected using spatial gradient information carried by the image), this characterization proves to be unsuitable when dealing with points, cracks or filaments. Indeed, while for an edge the singularity is associated with a jump of the intensity across this edge, for filaments, such a jump does not occur (see [30, p. 2]). As an illustration, on the crossplot of Figure 5.1, the crack is represented by a very thin peak and so the spatial gradient is unable to seize this singularity. In [30], Drogoul provides a heuristic illustration of this fact by considering an approximation of the 1D function defined by $f(x) = 0$ if $x \neq 0$ and $f(0) = 1$ as follows: $f_\eta(x) = 0$ if $|x| \geq \eta$ and $f_\eta(x) = \frac{2}{\eta^3}|x|^3 - \frac{3}{\eta^2}|x|^2 + 1$ if $|x| \leq \eta$. It is not difficult to see that $f'_\eta(0) = 0$, showing that the differential operator of order 1 does not capture the singularity at 0. On the other hand, as $f''_\eta(0) = -\frac{6}{\eta^2}$, f''_η clearly exhibits a

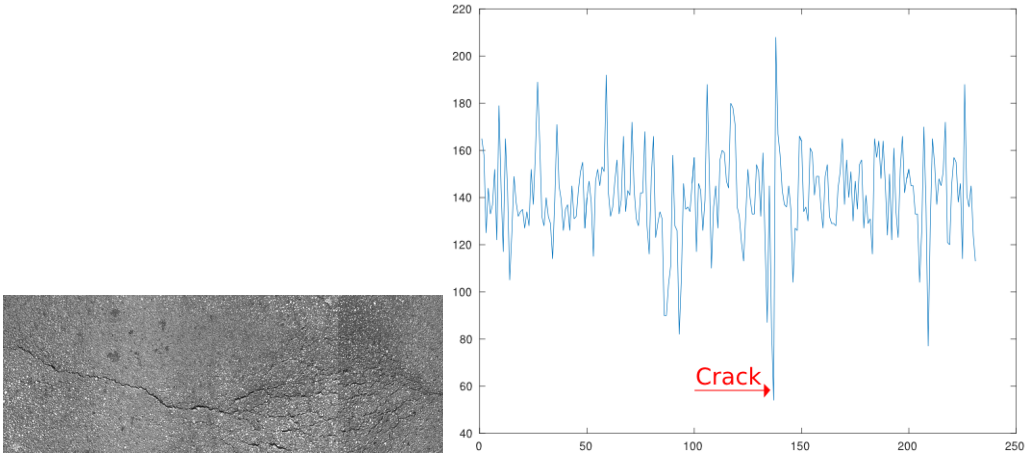

Figure 5.1: A bituminous surfacing image and a crossplot going through the crack.

singularity at 0 when η becomes small. This exemplifies the fact that in order to detect fine structures or filaments, higher order differential operators should be considered. This intuitive illustration is then mathematically formalized in 2D in [30] through Lemma 2.1, and states in substance the following: assuming that a crack can be modelled by an indicator function supported by a smooth curve Γ, it can be approximated by a sequence of smooth functions whose Hessian matrices blow up in the perpendicular direction to Γ, while their gradient is null. Motivated by these observations showing that a suitable model should involve higher order derivatives, the crack recovery model we propose falls within second order variational models. It is based on the Blake-Zisserman functional (see [14]) (recalled in (5.1)) for computer vision problems that depends on free discontinuities, free gradient discontinuities and second order derivatives, and more precisely, on its approximation by elliptic functionals defined on Sobolev spaces ([2]) —(note that the Blake-Zisserman functional was successfully applied to segmentation as in [44] for the segmentation of a digital model of a mixed urban-agricultural area, or image inpainting as in [22])—. This approximation appears as the counterpart for the second order case of the elliptic approximations designed by Ambrosio and Tortorelli ([3, 4]) to approximate Mumford-Shah functional ([36]), and takes place in a variational sense, namely, the De Giorgi Γ-convergence. The qualifying terms "free discontinuities", "free gradient discontinuities" mean that the functional is minimized over three variables: two unknown sets K_0, K_1 with $K_0 \cup K_1$ closed, and u, a smooth function on $\Omega \setminus (K_0 \cup K_1)$ as follows

$$F(u, K_0, K_1) = \int_{\Omega \setminus (K_0 \cup K_1)} \left(|\nabla^2 u|^2 + \Phi(x, u) \right) dx + \alpha \, \mathcal{H}^{n-1}(K_0 \cap \Omega) + \beta \, \mathcal{H}^{n-1}((K_1 \setminus K_0) \cap \Omega), \tag{5.1}$$

α and β being two positive parameters. The set K_0 represents the set of jump points for u, and $K_1 \setminus K_0$ is the set of crease points of u, those points where u is continuous but ∇u is not. Under certain conditions, the existence of minimizers for Blake-Zisserman functional is en-

sured over the space $\left\{u : \Omega \subset \mathbb{R}^n \to \mathbb{R} \,|\, u \in L^2(\Omega),\, u \in GSBV(\Omega),\, \nabla u \in (GSBV(\Omega))^n\right\}$, based on a weak formulation of the problem ($GSBV(\Omega)$ being the space of generalized special functions of bounded variation), see [21]. Ambrosio, Faina and March ([2]) introduce a family of elliptic functionals defined on Sobolev spaces, with in particular, a variable encoding the discontinuity set of ∇u which is exactly the structure we aim to recover. This family of functionals is defined by

$$F_\varepsilon(u,s,\sigma) = \int_\Omega \left(\sigma^2 + \kappa_\varepsilon\right) |\nabla^2 u|^2 \, dx + \int_\Omega \Phi(x,u)\, dx + (\alpha - \beta)\, \mathcal{G}_\varepsilon(s) + \beta\, \mathcal{G}_\varepsilon(\sigma) + \xi_\varepsilon \int_\Omega \left(s^2 + \zeta_\varepsilon\right) |\nabla u|^2 \, dx, \tag{5.2}$$

for suitable infinitesimals κ_ε, ξ_ε and ζ_ε, and with $\mathcal{G}_\varepsilon(l) = \int_\Omega \left[\varepsilon\, |\nabla l|^2 + \frac{(l-1)^2}{4\varepsilon}\right] dx$.

Before depicting in depth the proposed model and its relation to (5.2), we review some prior related works dedicated to thin pattern recovery. In [8, 30], Aubert and Drogoul introduce a topological-gradient-based method for the detection of fine structures in 2D. Given a PDE depending on a domain Ω, and u_Ω the solution of this PDE, topological asymptotic methods aim to study the variations of a cost function $j(\Omega) = j(\Omega, u_\Omega)$ when a topological modification such as the creation of a small hole or a crack measured by a parameter ϵ is applied to the domain Ω, resulting in Ω_ϵ. The expansion of $j(\Omega_\epsilon)$ with respect to ϵ shows that if one intends to minimize $j(\Omega_\epsilon)$, it is relevant to create holes or cracks at points x_0 where the topological gradient is the most negative. Aubert and Drogoul motivate the construction of their cost function involving second order derivatives by showing that a filament can be approximated by a sequence of smooth functions whose Hessian matrices blow up in the perpendicular direction to the filament, while their gradient is null as already mentioned. The proposed cost function is inspired by the Kirchhoff thin static plate model subject to pure bending with a Poisson ratio $\nu = 0$. A major difference with our model lies in the introduction of a variable that encodes the crack-type singularities. In [12], Bergounioux and Vicente propose a variational model to perform the segmentation of tube-like structures with small diameter in MRI images. It is derived from the Mumford-Shah functional (more precisely, on its approximation by elliptic functionals) and includes geometrical priors prescribing the topology of the solution (tube-like structures defined by thickening a parameterized curve to get a symmetric object of diameter $\alpha > 0$). The keypoint is that the 2D/3D problems involved are equivalent to 1D ones formulated in a weighted Sobolev space where the weight is related to the geometry of the tube. A limitation of this model is that it does not handle junctions of tubes. For another method dedicated to the detection and completion of fine structures in an image and relying on tubular structures, we refer to [37].

Other variational models have been investigated, dedicated to particular applications. In [39], Rochery et al. aim to track thin long objects, with applications to the automatic extraction of road networks in remote sensing images. They propose interesting nonlocal regularizers that enforce straightness on the sought parameterized curve. In [10], Baudour et al. propose a new algorithm for the detection and completion of thin filaments (defined as structures of codimension $n-1$ in an ambient space of dimension n) in noisy blurred 2D

or 3D images. To detect such structures, the authors build a 3D vector field lying in the orthogonal plane to the filament, while the completion phase relies on the minimization of a Ginzburg-Landau energy. In [7], Aubert et al. propose detecting image singularities of codimension greater or equal to 2, inspired again by Ginzburg-Landau models.
The spectrum of the methods that address the issue of fine structure recovery is of course not limited to variational ones. Morphological approaches can be found in [43] for automatic detection of vessel-like patterns, but prove to be sensitive to the noise type and time-consuming, as well as wavelet methods. In [41], stochastic methods are developed in which a thin network is simulated by a point process penalizing disconnected segments and favoring aligned pieces.
The next section is dedicated to the depiction of our modelling and its numerical analysis, encompassing existence of minimizers, existence of a unique viscosity solution to the resulting evolution equation, Γ-convergence results and convergence analysis, as well as the derivation of a nonlocal version of it (section 3). In section 4, we show some numerical simulations.
For additional mathematical material, we refer the reader to Chapter 2, Sections 1.2, 1.3, 1.4, 2.1, and 3.3.

2 Local mathematical modelling and analysis

2.1 Model

Let Ω be a connected bounded open subset of $\mathbb{R}^2$ of class $\mathcal{C}^1$. Let us denote by $f : \bar{\Omega} \to \mathbb{R}$ the 2D image representing bituminous surfacing assumed to be in $L^\infty(\Omega)$. Such an image naturally exhibits dense and highly oscillatory texture, reflecting its intrinsic nonlocal nature. This oscillatory component, although relevant in many applications since providing details and making the image more realistic, proves to be unnecessary for the task to accomplish. This observation motivates the introduction of a mixed decomposition/thin-structure-recognition model in which the crack recovery process operates only on that component of the image denoted by u that does not contain these small features captured in v. A geometrical justification relies on the notion of scale (for an individual constant-valued image feature $E \subset \Omega$, $\text{scale}(\vec{x}) = |E|/|\partial E|$ for $\vec{x} \in E$; a rectangle of $k_1 \times k_2$ pixels on a $n \times n$ discretized grid of the unit square would have a scale of $\frac{k_1 \times k_2}{2n(k_1+k_2)}$). Cracks on bituminous surfacing can be compared to long and thin filaments displaying junctions. The scale of such structures (the geometric scale of an object being basically the ratio of an area divided by a perimeter) differs from the scale of small oscillatory patterns present in the image : if the image domain is the $n \times n$ discretized unit square and if, for the sake of simplicity and as an illustration, the crack is modelled as a rectangle of $1 \times k$ pixels with $k \gg 1$, its scale behaves like $\frac{1}{2n}$, while a small feature of a pixel size will have a scale of $\frac{1}{4n}$, so twice as less. By choosing accurately the parameters involved in the modelling, these two features can be properly discriminated : small-scale features related to texture will be removed and captured by component v, while larger-scale features such as cracks will be kept in u. In [35], Meyer introduces the space $G(\mathbb{R}^2)$ (he works on $\mathbb{R}^2$ to remove the problem of boundary conditions) of distributions v that can be written as $v = \operatorname{div} \vec{g}$,

where $\vec{g} = (g_1, g_2) \in \left(L^\infty(\mathbb{R}^2)\right)^2$, and equipped with the norm defined by

$$\|v\|_{G(\mathbb{R}^2)} = \inf\left\{ \|\sqrt{g_1^2 + g_2^2}\|_{L^\infty(\mathbb{R}^2)} \mid v = \operatorname{div} \vec{g} \right\} \tag{5.3}$$

to capture the oscillatory nature of texture (highly oscillatory patterns have a small G-norm). A further justification of the use of this space is the link between the G-norm and the notion of scale provided by Strang ([42]): if $v \in G$, then $\|v\|_G = \sup_{E \subset \Omega} \frac{\int_E v}{P(E,\Omega)}$, with Ω the image domain and $P(E, \Omega)$ denoting the perimeter of E in Ω, showing that the stronger the penalization of $\|v\|_G$ is, the smaller the scale of the details kept in v is. Although mathematically relevant (as it resembles the dual space of BV), the G-space is hard to handle from a numerical point of view. To approximate the G-norm, we introduce an auxiliary variable that naturally stems from the Helmholtz-Hodge decomposition as follows: $\vec{g} = \nabla Q + \vec{P}$, with $\vec{P}$ a divergence-free vector that we disregard afterwards. The coupling between $\vec{g}$ and ∇Q is achieved through a quadratic penalization and the minimization of the L^∞-norm is now applied to ∇Q, yielding a problem related to the absolutely minimizing Lipschitz extensions and to the infinity Laplacian.
Equipped with this material, we propose, in a single variational framework, a mixed decomposition/free discontinuity and free gradient discontinuity model, first in its weak formulation, $\mathcal{H}^1$ denoting the Hausdorff 1-dimensional measure

$$\begin{aligned} \inf \bar{F}(u, \vec{g}, Q) = \; & \|f - u - \operatorname{div} \vec{g}\|^2_{L^2(\Omega)} + \mu \, \||\nabla Q|\|_{L^\infty(\Omega)} + \frac{\gamma}{2} \, \||\vec{g} - \nabla Q|\|^2_{L^2(\Omega)} \\ & + \rho \int_\Omega |\nabla^2 u|^2 \, dx + (\alpha - \beta) \, \mathcal{H}^1(S_u) + \beta \, \mathcal{H}^1(S_{\nabla u} \cup S_u), \end{aligned} \tag{5.4}$$

$\nabla^2 u$ being the Hessian matrix, and with ∇u denoting the approximate differential, S_u, the discontinuity set of u, and $S_{\nabla u}$, the discontinuity set of ∇u. The three first penalizing terms are related to the decomposition of f into $u + v$ with v belonging to G, while the last components are devoted to the crack detection process. The component $\int_\Omega |\nabla^2 u|^2 \, dx$ enables us to control the smoothness of u, while the remaining components monitor the size of the jump/crease sets. Second, phrased in terms of elliptic functionals inspired by [2], with two new auxiliary variables v_1 and v_2 encoding respectively the set of jumps of u and the set of jumps of ∇u, with $\mathcal{G}_\varepsilon$ defined above, and with suitable infinitesimals κ_ε, ξ_ε and ζ_ε

$$\begin{aligned} \inf \mathcal{F}_\varepsilon(u, \vec{g}, Q, v_1, v_2) = \; & \|f - u - \operatorname{div} \vec{g}\|^2_{L^2(\Omega)} + \mu \, \||\nabla Q|\|_{L^\infty(\Omega)} \\ & + \frac{\gamma}{2} \, \||\vec{g} - \nabla Q|\|^2_{L^2(\Omega)} + \rho \int_\Omega (v_2^2 + \kappa_\varepsilon) \, |\nabla^2 u|^2 \, dx \\ & + \xi_\varepsilon \int_\Omega (v_1^2 + \zeta_\epsilon) \, |\nabla u|^2 \, dx + (\alpha - \beta) \, \mathcal{G}_\varepsilon(v_1) + \beta \, \mathcal{G}_\varepsilon(v_2). \end{aligned} \tag{5.5}$$

The different parameters are introduced in order to properly discriminate small features (related to the intrinsic oscillatory nature of the image) from larger scale features such as cracks, and to properly fit the characteristics of the minimizers. The component $\|f - u -$

$\operatorname{div}\vec{g}\|^2_{L^2(\Omega)}$ forces the original image to be close to $u+\operatorname{div}\vec{g}$ with appropriate smoothness on u, and $v=\operatorname{div}\vec{g}$ lives in a suitable functional space. Indeed, if $\gamma\to+\infty$, we formally get $f\simeq u+\operatorname{div}\vec{g}$ with $\vec{g}\in(L^\infty(\Omega))^2$. The variable v_1 (resp. v_2) with range $[0,1]$ is related to the set of jumps (resp. creases). A minimizing $v_{1,\varepsilon}$ (resp. $v_{2,\varepsilon}$) is in particular close to 0 in a neighborhood of the jump (resp. crease) set, and far from it, is close to 1. Function u is thus a smooth approximation of the observed image f, this smoothing effect being localized only on homogeneous parts. The representation of each auxiliary variable forms a partition of the data. Now looking closer at the components $\int_\Omega (v_2^2+\kappa_\varepsilon)\,|\nabla^2 u|^2\,dx$ and $\mathcal{G}_\varepsilon(v_2)$, letting ε become small induces that v_2 should be 1 almost everywhere on Ω, except where $|\nabla^2 u|^2$ blows up. This observation supports the crack characterization we gave, and ensures that v_2 encodes the structures we aim to recover.

We now provide several theoretical results.

2.2 Existence of minimizers

Theorem 2.1. *With $\kappa_\varepsilon,\xi_\varepsilon,\zeta_\varepsilon>0$, $\alpha>\beta>0$, problem (5.5) admits minimizers $(u=u_\varepsilon,\vec{g}=\vec{g_\varepsilon},Q=Q_\varepsilon,v_1=v_{1,\varepsilon},v_2=v_{2,\varepsilon})$ on $\mathcal{D}(\Omega)=\left\{u\in W^{2,2}(\Omega)\,|\,\int_\Omega u\,dx=\int_\Omega f\,dx\right\}\times H(div)\times\left\{Q\in W^{1,\infty}(\Omega)\;|\;\int_\Omega Q\,dx=0\right\}\times W^{1,2}(\Omega,[0,1])\times W^{1,2}(\Omega,[0,1])$, with $H(div)$, the Hilbert space defined by $H(div)=\left\{\sigma\in(L^2(\Omega))^2\,|\,div\,\sigma\in L^2(\Omega)\right\}$ endowed with the inner product*

$$\langle\vec{\sigma_1},\vec{\sigma_2}\rangle_{H(div)}:=\langle\vec{\sigma_1},\vec{\sigma_2}\rangle_{(L^2(\Omega))^2}+\langle div\,\vec{\sigma_1},div\,\vec{\sigma_2}\rangle_{L^2(\Omega)},$$

$\forall(\vec{\sigma_1},\vec{\sigma_2})\in(H(div))^2$.

Remark 2.1. *Condition $\int_\Omega Q\,dx=0$ is not restrictive. An argument to include the constraint $\int_\Omega u\,dx=\int_\Omega f\,dx$ is that the space $G(\Omega)$ defined by $G(\Omega)=\left\{v\in L^2(\Omega)\,|\,v=div\,\vec{g},\,\vec{g}\in L^\infty(\Omega,\mathbb{R}^2),\,\vec{g}\cdot\vec{n}=0\text{ on }\partial\Omega\right\}$ coincides with the space $\left\{v\in L^2(\Omega)\,|\,\int_\Omega v\,dx=0\right\}$ (see [6, Proposition 2.1]).*

Proof. By taking $u\equiv\frac{1}{meas(\Omega)}\int_\Omega f\,dx$, $v_1\equiv1$, $v_2\equiv1$, $\vec{g}\equiv\vec{0}$, $Q\equiv0$, then $\mathcal{F}_\varepsilon(u,\vec{g},Q,v_1,v_2)=\|f-\frac{1}{meas(\Omega)}\int_\Omega f\,dx\|^2_{L^2(\Omega)}<+\infty$ with f assumed to be sufficiently smooth. Thus the functional is proper and positive and the infimum is finite. Let us now extract a converging subsequence of a minimizing sequence.

1. **Extraction of convergent subsequences**: Let $(u_n,\vec{g}_n,Q_n,v_{1,n},v_{2,n})$ be a minimizing sequence of $\mathcal{F}_\varepsilon$. For n large enough, we thus have $\mathcal{F}_\varepsilon(u_n,\vec{g}_n,Q_n,v_{1,n},v_{2,n})\le\inf\mathcal{F}_\varepsilon(u,\vec{g},Q,v_1,v_2)+1<+\infty$.
   - $\mathcal{F}_\varepsilon(u_n,\vec{g}_n,Q_n,v_{1,n},v_{2,n})\ge\mu\||\nabla Q_n|\|_{L^\infty(\Omega)}$. As $\int_\Omega Q_n\,dx=0$ for all $n\in\mathbb{N}$, we can use Poincaré-Wirtinger inequality and get a uniform bound on $\|Q_n\|_{W^{1,\infty}(\Omega)}$. [18, Remark (ii) p. 65] gives us the existence of a subsequence of (Q_n) still denoted by (Q_n) converging weakly-$*$ to $\bar{Q}$ in $W^{1,\infty}(\Omega)$. As the weak-$*$ convergence in $W^{1,\infty}(\Omega)$ implies uniform convergence, then $\int_\Omega\bar{Q}\,dx=0$.
   - $\mathcal{F}_\varepsilon(u_n,\vec{g}_n,Q_n,v_{1,n},v_{2,n})\ge(\alpha-\beta)\varepsilon\||\nabla v_{1,n}|\|^2_{L^2(\Omega)}$. By noticing that $v_{1,n}\in L^\infty(\Omega)$ with $0\le v_{1,n}\le1$ almost everywhere, we have $\int_\Omega v_{1,n}\,dx\le meas(\Omega)<$

$+\infty$ for all $n \in \mathbb{N}$. The Poincaré-Wirtinger inequality gives us the existence of a subsequence of $(v_{1,n})$ still denoted by $(v_{1,n})$ weakly converging to $\overline{v_1}$ in $W^{1,2}(\Omega)$. Since $W^{1,2}(\Omega) \underset{c}{\circlearrowleft} L^2(\Omega)$, $(v_{1,n})$ strongly converges to $\overline{v_1}$ in $L^2(\Omega)$ and so pointwise almost everywhere up to a subsequence. We conclude that $\overline{v_1} \in W^{1,2}(\Omega, [0,1])$.

- $\mathcal{F}_\varepsilon(u_n, \vec{g}_n, Q_n, v_{1,n}, v_{2,n}) \geq \beta\varepsilon \||\nabla v_{2,n}|\|^2_{L^2(\Omega)}$. By noticing that $v_{2,n} \in L^\infty(\Omega)$ with $0 \leq v_{2,n} \leq 1$ almost everywhere, we get $\int_\Omega v_{2,n}\, dx \leq meas(\Omega) < +\infty$ for all $n \in \mathbb{N}$. The Poincaré-Wirtinger inequality gives us the existence of a subsequence of $(v_{2,n})$ still denoted by $(v_{2,n})$ weakly converging to $\overline{v_2}$ in $W^{1,2}(\Omega)$. Since $W^{1,2}(\Omega) \underset{c}{\circlearrowleft} L^2(\Omega)$, $(v_{2,n})$ strongly converges to $\overline{v_2}$ in $L^2(\Omega)$ and so pointwise almost everywhere up to a subsequence. We conclude that $\overline{v_2} \in W^{1,2}(\Omega, [0,1])$.
- $\mathcal{F}_\varepsilon(u_n, \vec{g}_n, Q_n, v_{1,n}, v_{2,n}) \geq \rho\kappa_\varepsilon \|\nabla^2 u_n\|^2_{L^2(\Omega)} + \xi_\varepsilon\zeta_\varepsilon \||\nabla u_n|\|^2_{L^2(\Omega)}$. As $\int_\Omega u_n\, dx = \int_\Omega f\, dx$ for all $n \in \mathbb{N}$, the Poincaré-Wirtinger inequality gives us the existence of a subsequence of (u_n) still denoted by (u_n) weakly converging to $\overline{u}$ in $W^{2,2}(\Omega)$. Since $W^{2,2}(\Omega) \underset{c}{\circlearrowleft} L^2(\Omega)$, (u_n) strongly converges to $\overline{u}$ in $L^2(\Omega)$ and so pointwise almost everywhere up to a subsequence with $\int_\Omega u_n\, dx = \int_\Omega f\, dx < +\infty$. We conclude with the dominated convergence theorem that $\int_\Omega \bar{u}\, dx = \int_\Omega f\, dx$.
- $\mathcal{F}_\varepsilon(u_n, \vec{g}_n, Q_n, v_{1,n}, v_{2,n}) \geq \frac{1}{4}\|\mathrm{div}\vec{g}_n\|^2_{L^2(\Omega)} - \|f\|^2_{L^2(\Omega)} - \frac{1}{2}\|u_n\|^2_{L^2(\Omega)} + \frac{\gamma}{4}\||\vec{g}_n|\|^2_{L^2(\Omega)} - \frac{\gamma}{2}\|\nabla Q_n\|^2_{L^2(\Omega)}$. Since (Q_n) is uniformly bounded in $W^{1,\infty}(\Omega)$ and (u_n) uniformly bounded in $W^{2,2}(\Omega)$ then $(\vec{g}_n)$ is uniformly bounded in $H(div)$ and we extract a subsequence still denoted by $(\vec{g}_n)$ such that $(\vec{g}_n)$ weakly converges to $\vec{\bar{g}}$ in $H(div)$.

2. **Lower semi-continuity of the functional**:

- Since $\nabla Q_n \overset{*}{\rightharpoonup} \nabla\bar{Q}$ in $L^\infty(\Omega)$ then $\liminf_{n\to+\infty} \||\nabla Q_n|\|_{L^\infty(\Omega)} \geq \||\nabla\bar{Q}|\|_{L^\infty(\Omega)}$ ([18, Proposition III.12]).
- Weak-$*$ convergence in $L^\infty(\Omega)$ implying weak convergence in $L^2(\Omega)$, then $\||\nabla\overline{Q} - \vec{\bar{g}}|\|^2_{L^2(\Omega)} \leq \liminf_{n\to+\infty} \||\nabla Q_n - \vec{g}_n|\|^2_{L^2(\Omega)}$.
- $\mathcal{G}_\varepsilon$ is convex and strongly lower semi-continuous in $H^1(\Omega)$ and so weakly lower semi-continuous in $H^1(\Omega)$.
- Since $u_n \underset{n\to+\infty}{\rightharpoonup} \bar{u}$ in $W^{2,2}(\Omega) \underset{c}{\circlearrowleft} L^2(\Omega)$ and $\mathrm{div}\vec{g}_n \underset{n\to+\infty}{\rightharpoonup} \mathrm{div}\vec{\bar{g}}$ in $L^2(\Omega)$ then $\|f - \bar{u} - \mathrm{div}\vec{\bar{g}}\|^2_{L^2(\Omega)} \leq \liminf_{n\to+\infty} \|f - u_n - \vec{g}_n\|^2_{L^2(\Omega)}$.
- Let us consider $h : \Omega \times \mathbb{R} \times \mathbb{R}^2 \to \mathbb{R}$, $(x, v, w) \mapsto (v(x)^2 + \zeta_\varepsilon)|w(x)|^2$. Since $v_{1,n} \underset{n\to+\infty}{\rightharpoonup} \overline{v_1}$ in $W^{1,2}(\Omega) \underset{c}{\circlearrowleft} L^2(\Omega)$ then $v_{1,n} \underset{n\to+\infty}{\longrightarrow} \overline{v_1}$ in $L^2(\Omega)$. Besides, since $u_n \underset{n\to+\infty}{\rightharpoonup} \bar{u}$ in $W^{2,2}(\Omega)$ then $\nabla u_n \underset{n\to+\infty}{\rightharpoonup} \nabla\bar{u}$ in $L^2(\Omega, \mathbb{R}^2)$. h is continuous in (v, w) for almost every $x \in \Omega$, h is measurable on Ω for almost every $(v, w) \in \mathbb{R} \times \mathbb{R}^2$, for any $(x, v) \in \Omega \times \mathbb{R}$, h is convex with respect to w, and for all $(v, w) \in \mathbb{R} \times$

$\mathbb{R}^2$ and for almost every $x \in \Omega$, $h(x,v,w) \geq 0 \in L^1(\Omega)$. Thanks to [13, Theorem 1], we can conclude that $\liminf_{n\to+\infty} \int_\Omega h(x, v_{1,n}, \nabla u_n)\, dx \geq \int_\Omega h(x, \overline{v_1}, \nabla \bar{u})$.

– Let us consider $h : \Omega \times \mathbb{R} \times M_2(\mathbb{R}) \to \mathbb{R}$, $(x,v,w) \mapsto (v(x)^2 + \kappa_\varepsilon)|w(x)|^2$. Since $v_{2,n} \underset{n\to+\infty}{\rightharpoonup} \overline{v_2}$ in $W^{1,2}(\Omega) \overset{c}{\circlearrowleft} L^2(\Omega)$ then $v_{2,n} \underset{n\to+\infty}{\longrightarrow} \overline{v_2}$ in $L^2(\Omega)$. Besides, since $u_n \underset{n\to+\infty}{\rightharpoonup} \bar{u}$ in $W^{2,2}(\Omega)$ then $\nabla^2 u_n \underset{n\to+\infty}{\rightharpoonup} \nabla^2 \bar{u}$ in $L^2(\Omega, M_2(\mathbb{R}))$. h is continuous in (v,w) for almost every $x \in \Omega$, h is measurable on Ω for almost every $(v,w) \in \mathbb{R} \times M_2(\mathbb{R})$, for any $(x,v) \in \Omega \times \mathbb{R}$, h is convex with respect to w, and for all $(v,w) \in \mathbb{R} \times M_2(\mathbb{R})$ and for almost every $x \in \Omega$, $h(x,v,w) \geq 0 \in L^1(\Omega)$. Thanks to [13, Theorem 1], we can conclude that $\liminf_{n\to+\infty} \int_\Omega h(x, v_{2,n}, \nabla^2 u_n)\, dx \geq \int_\Omega h(x, \overline{v_2}, \nabla^2 \bar{u})$.

As the lim inf of the sum of functions is greater than the sum of the lim inf of these functions, then $\mathcal{F}_\varepsilon(\bar{u}, \vec{\bar{g}}, \bar{Q}, \overline{v_1}, \overline{v_2}) \leq \liminf_{n\to+\infty} \mathcal{F}_\varepsilon(u_n, \vec{g}_n, Q_n, v_{1,n}, v_{2,n})$ which concludes the proof.

□

Remark 2.2. *It is possible to set $\xi_\varepsilon = 0$ in (5.5) (the existence theorem still holds), but a suitable functional space for u becomes $W^{2,2}_{loc}(\Omega) \cap L^\infty(\Omega)$. For instance, with the condition $\|u\|_{L^\infty(\Omega)} \leq \|f\|_{L^\infty(\Omega)}$, which is reasonable in virtue of the smoothing properties of the functional. Indeed, [2, Proposition 4.6] provides a uniform bound on $\|\nabla u\|_{L^2(A)}$ once a uniform bound is extracted for $\|u\|_{L^2(B)}$ and $\|\nabla^2 u\|_{L^2(B)}$ with $A, B \subset \mathbb{R}^2$ open sets and $(A_{2r}) \subsetneq B$.*

Remark 2.3. *The case $\kappa_\varepsilon = 0$ can also be considered (an existence theorem still holds) but requires more care and applies to a problem no longer phrased in terms of a L^2-penalization for ∇u, but with a L^γ-penalization, $\gamma > 2$. The unknown u should be searched in the subspace of $W^{1,2}(\Omega)$ defined by $\left\{u \in W^{1,2}(\Omega) \,|\, v_2 \nabla u \in W^{1,p}(\Omega, \mathbb{R}^2)\right\}$, with $p = \frac{2\gamma}{\gamma+2} \in]1,2[$. The boundedness of v_2 in $W^{1,2}(\Omega)$ as well as the boundedness of $|\nabla u|$ in $L^\gamma(\Omega)$, and the fact that $\nabla(v_2 \nabla u) = v_2 \nabla^2 u + \nabla v_2 \bigotimes \nabla u$ show that $v_2 \nabla u$ is bounded in $W^{1,p}(\Omega, \mathbb{R}^2)$ using Hölder's inequality.*

Remark 2.4. *Functional $\mathcal{F}_\varepsilon$ is convex in each variable (which yields a natural alternating framework for the numerical resolution) but not in the joint variable $(u, \vec{g}, Q, v_1, v_2)$. Nevertheless, for v_1, v_2 fixed, if $(u_1, \vec{g_1}, Q_1)$ and $(u_2, \vec{g_2}, Q_2)$ denote two minimizing elements, it can be proved that $u_1 = u_2$ a.e., $div\, \vec{g_1} = div\, \vec{g_2}$ a.e., and $\vec{g_1} - \vec{g_2} = \nabla Q_1 - \nabla Q_2$ a.e.. Consequently, $div(\nabla Q_1 - \nabla Q_2) = \Delta(Q_1 - Q_2) \in L^2(\Omega) = 0$ a.e.. By the generalized Green's formula [29, Proposition 3.58], $\int_\Omega |\nabla(Q_1 - Q_2)|^2\, dx = \langle \nabla(Q_1 - Q_2) \cdot \vec{n}, \gamma_0(Q_1 - Q_2) \rangle$, the linear functional $\nabla(Q_1 - Q_2) \cdot \vec{n}$ belonging to the dual $H^{-1/2}(\partial\Omega)$ of the space of traces $H^{1/2}(\partial\Omega)$. If we assume that $\nabla(Q_1 - Q_2) \cdot \vec{n} = 0$ on $\partial\Omega$, then $Q_1 = Q_2$ a.e..*

2.3 Existence of solutions for the Euler-Lagrange equations

We now focus on the elliptic functional which is the one we solve in practice. Note that, in the numerical simulations, we have dropped the constants κ_ε and ζ_ε. We first

derive the Euler-Lagrange equations according to each unknown, with $x = (x_1, x_2)$ and $\vec{n} = (n_{x_1}, n_{x_2})$, the unit outward normal to the boundary. Making use of the absolutely minimizing Lipschitz extensions ([5]) for the equation in Q, we get:

$$\begin{cases} v_1 = \dfrac{\frac{\alpha-\beta}{2\varepsilon} + 2(\alpha-\beta)\varepsilon\Delta v_1}{2\xi_\varepsilon|\nabla u|^2 + \frac{\alpha-\beta}{2\varepsilon}}, \;\; v_2 = \dfrac{\frac{\beta}{2\varepsilon} + 2\beta\varepsilon\Delta v_2}{2\rho|\nabla^2 u|^2 + \frac{\beta}{2\varepsilon}}, \\ g_1 = \partial_{x_1} Q - \frac{2}{\gamma}\,\partial_{x_1}\left(f - u - \operatorname{div}\vec{g}\right), \;\; g_2 = \partial_{x_2} Q - \frac{2}{\gamma}\,\partial_{x_2}\left(f - u - \operatorname{div}\vec{g}\right), \\ u = (f - \operatorname{div}\vec{g}) - \rho\,\frac{\partial^2}{\partial x_1^2}\left(v_2^2\,\frac{\partial^2 u}{\partial x_1^2}\right) - \rho\,\frac{\partial^2}{\partial x_2^2}\left(v_2^2\,\frac{\partial^2 u}{\partial x_2^2}\right) \\ -2\rho\,\frac{\partial^2}{\partial x_1 \partial x_2}\left(v_2^2\,\frac{\partial^2 u}{\partial x_1 \partial x_2}\right) + \xi_\varepsilon \operatorname{div}\left(v_1^2\,\nabla u\right), \\ -\mu\Delta_\infty Q - \gamma\Delta Q + \gamma \operatorname{div}\vec{g} = 0, \end{cases}$$

combined with the boundary conditions $\nabla v_1 \cdot \vec{n} = 0$, $\nabla v_2 \cdot \vec{n} = 0$, $(f - u - \operatorname{div}\vec{g}) n_{x_1} = 0$, $(f - u - \operatorname{div}\vec{g}) n_{x_2} = 0$, $v_1^2 \nabla u \cdot \vec{n} = 0$, $v_2^2 \partial^2_{x_1 x_1} u\, n_{x_1} = 0$, $\partial_{x_1}\left(v_2^2 \partial^2_{x_1 x_1} u\right) n_{x_1} = 0$, $v_2^2 \partial^2_{x_2 x_2} u\; n_{x_2} = 0$, $\partial_{x_2}\left(v_2^2 \partial^2_{x_2 x_2} u\right) n_{x_2} = 0$, $v_2^2 \partial^2_{x_1 x_2} u\; n_{x_1} = 0$, $\partial_{x_1}\left(v_2^2 \partial^2_{x_1 x_2} u\right) n_{x_2} = 0$ and $(\vec{g} - \nabla Q) \cdot \vec{n} = 0$ on $\partial\Omega$. Let us now embed the last equation in a time-dependent setting. Let $T > 0$ be given. The evolution equation in the unknown Q is thus given by

$$\begin{cases} \dfrac{\partial Q}{\partial t} = \mu\Delta_\infty Q + \gamma\Delta Q - \gamma \operatorname{div}\vec{g} \text{ on } \mathbb{R}^2 \times (0,T), \\ Q(x,0) = Q_0(x) \text{ on } \mathbb{R}^2, \end{cases} \tag{EE}$$

with $Q_0 \in W^{1,\infty}(\mathbb{R}^2)$ and B_0 its Lipschitz constant. (To remove the problem of boundary conditions, we work on $\mathbb{R}^2$ for the spatial domain). We now give an existence/uniqueness result for the PDE in Q in the viscosity solution theory framework. To do so, we first need the additional following assumption

$$\begin{aligned} &\operatorname{div}\vec{g} \text{ is bounded and is Lipschitz continuous uniformly in time} \\ &\text{with } \kappa_{\vec{g}} \text{ its Lipschitz constant independent of time.} \end{aligned} \tag{H}$$

For the sake of conciseness and using the normalized version of the infinity Laplacian, the evolution equation is now written in the form

$$\frac{\partial Q}{\partial t} + G(x, t, \nabla Q, \nabla^2 Q) = 0,$$

with $G : \mathbb{R}^2 \times [0,T) \times \mathbb{R}^2 \times \mathcal{S}^2$ ($\mathcal{S}^2$ being the set of symmetric 2×2 matrices equipped with its natural partial order) defined by

$$\begin{aligned} G(x,t,\vec{p},X) &= -\gamma \operatorname{trace}(X) - \mu\Big\langle \frac{\vec{p}}{|\vec{p}|}, X\frac{\vec{p}}{|\vec{p}|}\Big\rangle + \gamma \operatorname{div}\vec{g} \\ &= -\gamma \operatorname{trace}(X) - \mu \operatorname{trace}\Big(\frac{\vec{p}\otimes\vec{p}}{|\vec{p}|^2} X\Big) + \gamma \operatorname{div}\vec{g}, \\ &= E(X) + F(\vec{p}, X) + \gamma \operatorname{div}\vec{g}, \end{aligned}$$

and with the following properties

1. The operators G, $E : X \mapsto -\gamma \text{trace}(X)$ and $F : (\vec{p}, X) \mapsto -\mu \,\text{trace}\Big(\frac{\vec{p}\otimes\vec{p}}{|\vec{p}|^2}\ X\Big)$ are independent of Q and are elliptic, *i.e.* $\forall X, Y \in \mathcal{S}^2$, $\forall \vec{p} \in \mathbb{R}^2 \setminus \{\vec{0}_{\mathbb{R}^2}\}$, if $X \leq Y$ then $F(\vec{p}, X) \geq F(\vec{p}, Y)$ since $F(\vec{p}, X) - F(\vec{p}, Y) = -\mu\text{trace}\Big(\frac{\vec{p}\otimes\vec{p}}{|\vec{p}|^2}X\Big) + \mu\text{trace}\Big(\frac{\vec{p}\otimes\vec{p}}{|\vec{p}|^2}Y\Big) = -\mu\text{trace}\Big(\frac{\vec{p}\otimes\vec{p}}{|\vec{p}|^2}(X-Y)\Big) = -\mu\Big\langle \frac{\vec{p}}{|\vec{p}|}, (X-Y)\frac{\vec{p}}{|\vec{p}|}\Big\rangle \geq 0$ as $X \leq Y$.

2. F is locally bounded on $\mathbb{R}^2 \times \mathcal{S}^2$, continuous on $\mathbb{R}^2 \setminus \{\vec{0}_{\mathbb{R}^2}\} \times \mathcal{S}^2$, and $F^*(0,0) = F_*(0,0) = 0$, where F^* (resp. F_*) is the upper semicontinuous (usc) envelope (resp. lower semicontinuous (lsc) envelope) of F. Indeed, using Rayleigh quotient and its properties, it is not difficult to see that for nonzero vector $\vec{p}$, $\lambda_{min}(X) \leq \text{trace}\Big(\frac{\vec{p}\otimes\vec{p}}{|\vec{p}|^2}X\Big) = \frac{\langle \vec{p}, X\vec{p}\rangle}{\langle \vec{p}, \vec{p}\rangle} = R(X, \vec{p}) \leq \lambda_{max}(X)$, λ_{min} (resp. λ_{max}) denoting the smallest (resp. biggest) eigenvalue of X.

The first important result is a comparison principle which states that if a sub-solution and a super-solution are ordered at initial time then they are ordered at any time.

Theorem 2.2 (Comparison principle, adapted from [32])**.** *Assume (H) and let $u : \mathbb{R}^2 \times [0,T) \to \mathbb{R}$ be a bounded upper semicontinuous sub-solution and $v : \mathbb{R}^2 \times [0,T) \to \mathbb{R}$ be a bounded lower semicontinuous super-solution of (EE). Assume that $u(x,0) \leq Q_0(x) \leq v(x,0)$ in $\mathbb{R}^2$, then $u \leq v$ in $\mathbb{R}^2 \times [0,T)$.*

Proof. This proof is rather classical and we follow the arguments of [27] for parabolic equations and of [32]. We first remark that for any $\lambda > 0$, $\tilde{u} = u - \frac{\lambda}{T-t}$ is also a sub-solution of (EE) and satisfies:

$$\tilde{u}_t + G_*(x, t, D\tilde{u}, D^2\tilde{u}) \leq \frac{-\lambda}{(T-t)^2} \leq \frac{-\lambda}{T^2},$$

since $\tilde{u}_t = u_t - \frac{\lambda}{(T-t)^2}$, $D\tilde{u} = Du$ and $D^2\tilde{u} = D^2u$. As $u \leq v$ comes from $\tilde{u} \leq v$ in the limit when λ tends to 0, it is sufficient to prove the comparison under the additional assumption:

$$\begin{cases} \text{(i)} & u_t + G_*(x, t, Du, D^2u) \leq \frac{-\lambda}{T^2} \\ \text{(ii)} & \lim\limits_{t\to T} u(x,t) = -\infty \end{cases}.$$

Let us set $M = \sup\limits_{(x,t)\in\mathbb{R}^2\times[0,T)} u(x,t) - v(x,t)$. We want to prove that $M \leq 0$. To do so, we will use a *reductio ad absurdum* reasoning and we assume that $M > 0$ so there exists $(x^*, t^*) \in \mathbb{R}^2 \times [0,T)$ such that $u(x^*,t^*) - v(x^*,t^*) > 0$.
We introduce M_0 defined by $M_0 = \sup\limits_{(x,y,t)\in\mathbb{R}^2\times\mathbb{R}^2\times[0,T)} \big\{f(x,y,t) = u(x,t) - v(y,t) - \frac{1}{4\epsilon}|x - y|^4 - \frac{\alpha}{2}(|x|^2 + |y|^2)\big\}$, $\epsilon > 0$. We notice that $M_0 \geq u(x^*,t^*) - v(x^*,t^*) - \alpha|x^*|^2 > 0$ and so $M_0 > 0$ for α small enough. This supremum is reached owing to the term $\frac{\alpha}{2}(|x|^2 + |y|^2)$, M_u the bound above of u and $-m_v$ the bound above of $-v$, the upper semicontinuity

of f, the fact that f is proper and $\lim_{t\to T,|x|\to+\infty,|y|\to+\infty} f(x,y,t) = -\infty$ since $f(x,y,t) \leq M_u - m_v - \frac{\alpha}{2}(|x|^2+|y|^2)$. We denote by $(x_0,y_0,t_0) \in \mathbb{R}^2\times\mathbb{R}^2\times[0,T)$ a maximum. Consequently, we get the following lemma:

Lemma 2.5 (adapted from [32]). *Let* $M' = \lim_{h\to 0} \sup_{|x-y|\leq h, t\in[0,T)} (u(x,t)-u(y,t))$. *Then*

1. $\lim_{\alpha\to 0} \alpha x_0 = \lim_{\alpha\to 0} \alpha y_0 = 0$.
2. $\lim_{\epsilon\to 0} |x_0-y_0|^4 = 0$.
3. $\lim_{\epsilon\to 0}\lim_{\alpha\to 0} M_0 = M'$.
4. $\lim_{\epsilon\to 0}\lim_{\alpha\to 0} \frac{1}{\epsilon}|x_0-y_0|^4 = 0$.
5. $\lim_{\epsilon\to 0}\lim_{\alpha\to 0} \alpha(|x_0|^2+|y_0|^2) = 0$.

Proof. By boundedness of u and v, then the function $(x,y)\mapsto u(x,t)-v(y,t)$ is bounded for any $t\in[0,T)$. Besides, we assume that $M_0 > 0$. We also have $\frac{|x_0-y_0|^4}{4\epsilon} + \frac{\alpha}{2}(|x_0|^2+|y_0|^2) \leq C$. We deduce that $\frac{\alpha}{2}(|x_0|^2+|y_0|^2) \leq C$ and $|x_0-y_0|^4 \leq 4C\epsilon$ leading to $\lim_{\epsilon\to 0}|x_0-y_0| = 0$ and $\lim_{\alpha\to 0}\alpha x_0 = \lim_{\alpha\to 0}\alpha y_0 = 0$.
Let us now set $M_h = \sup_{|x-y|\leq h, t\in[0,T)} (u(x,t)-u(y,t))$. Let $(x_n^h, y_n^h, t_n^h) \in \mathbb{R}^2\times\mathbb{R}^2\times[0,T)$ be a sequence such that $\forall n\in\mathbb{N}^*$, $u(x_n^h,t_n^h) - v(y_n^h,t_n^h) \geq M_h - \frac{1}{n}$ with $|x_n^h - y_n^h| \leq h$. This sequence is independent of α. We then get $M_h - \frac{1}{n} - \frac{h^4}{4\epsilon} - \frac{\alpha}{2}(|x_n^h|^2+|y_n^h|^2) \leq u(x_n^h,t_n^h) - v(y_n^h,t_n^h) - \frac{|x_n^h-y_n^h|^4}{4\epsilon} - \frac{\alpha}{2}(|x_n^h|^2+|y_n^h|^2) \leq M_0 \leq u(x_0,t_0) - v(y_0,t_0)$. Let α tend to 0 in what precedes, then $M_h - \frac{1}{n} - \frac{h^4}{4\epsilon} \leq \liminf_{\alpha\to 0}(u(x_0,t_0)-v(y_0,t_0)) \leq \limsup_{\alpha\to 0}(u(x_0,t_0)-v(y_0,t_0))$. Now let h tend to 0, we get $M' - \frac{1}{n} \leq \liminf_{\alpha\to 0}(u(x_0,t_0)-v(y_0,t_0)) \leq \limsup_{\alpha\to 0}(u(x_0,t_0) - v(y_0,t_0))$. Finally, we let ϵ tend to 0 and obtain $M' - \frac{1}{n} \leq \liminf_{\epsilon\to 0}\liminf_{\alpha\to 0}(u(x_0,t_0) - v(y_0,t_0)) \leq \liminf_{\epsilon\to 0}\limsup_{\alpha\to 0}(u(x_0,t_0)-v(y_0,t_0)) \leq \limsup_{\epsilon\to 0}\limsup_{\alpha\to 0}(u(x_0,t_0)-v(y_0,t_0)) \leq \limsup_{\epsilon\to 0}\limsup_{\alpha\to 0}\sup_{|x-y|\leq C\epsilon^{\frac{1}{4}},t\in[0,T)}(u(x,t)-v(y,t)) \leq \limsup_{h\to 0}\sup_{|x-y|\leq h,t\in[0,T)}(u(x,t)-v(y,t)) = M'$. So, $\lim_{\epsilon\to 0}\lim_{\alpha\to 0}(u(x_0,t_0)-v(y_0,t_0)) = M'$. In the same way, we get $\lim_{\epsilon\to 0}\lim_{\alpha\to 0} M_0 = M'$. Thus $\lim_{\epsilon\to 0}\lim_{\alpha\to 0}\left(\frac{|x_0-y_0|^4}{4\epsilon} + \frac{\alpha}{2}(|x_0|^2+|y_0|^2)\right) = \lim_{\epsilon\to 0}\lim_{\alpha\to 0}(u(x_0,t_0)-v(x_0,y_0)-M_0) = 0$. So
$$\begin{cases} \lim_{\epsilon\to 0}\lim_{\alpha\to 0}\frac{|x_0-y_0|^4}{4\epsilon} = 0 \\ \lim_{\epsilon\to 0}\lim_{\alpha\to 0}\frac{\alpha}{2}(|x_0|^2+|y_0|^2) = 0 \end{cases}.$$
□

We then distinguish two cases.

1. $\forall\epsilon>0$, $\exists\alpha\in(0,\epsilon)$ such that $t_0 = 0$. Then there exists $\epsilon_n \underset{n\to+\infty}{\longrightarrow} 0$ and $\alpha_n \underset{n\to+\infty}{\longrightarrow} 0$ with $t_n = 0$ and $0 < M_0 \leq u(x_{0,n},0) - v(y_{0,n},0) \leq Q_0(x_{0,n}) - Q_0(y_{0,n}) \leq B_0|x_{0,n} -$

$y_{0,n}|$ where B_0 is the Lipschitz constant of Q_0. We obtain a contradiction since $\lim_{n\to+\infty} |x_{0,n} - y_{0,n}| = 0$.

2. $\exists \epsilon > 0$ such that $\forall \alpha \in (0, \epsilon)$, $t_0 > 0$. We can choose ϵ big enough otherwise we use the first argument, i.e., such that $\frac{|x_0-y_0|^4}{4\epsilon} \leq \frac{\lambda}{2T^2\gamma\kappa_{\vec{g}}}$. We consider $\tilde{u}(x,t) = u(x,t) - \frac{\alpha}{2}|x|^2$ and $\tilde{v}(x,t) = v(x,t) + \frac{\alpha}{2}|x|^2$ and so $M_0 = \sup_{(x,y,t)\in\mathbb{R}^2\times\mathbb{R}^2\times[0,T)} \{\tilde{u}(x,t) - \tilde{v}(y,t) - \frac{|x-y|^4}{4\epsilon}\}$.
Let us take the test function $\psi(x,y,t) = \frac{|x-y|^4}{4\epsilon}$ and set $p_0 = x_0 - y_0$. By using the parabolic version of Ishii's lemma with the same notations, it comes that $\tau = 0$, $p_1 = \frac{|p_0|^2 p_0}{\epsilon} = p_2$, $A = \frac{2}{\epsilon}|p_0|^2 \begin{pmatrix} Z & -Z \\ -Z & Z \end{pmatrix}$ with $Z = \frac{I}{2} + \frac{p_0 \otimes p_0}{|p_0|^2}$ and for each $\beta > 0$ such that $\beta A < I$, there exist $(X, Y) \in (S^2)^2$ and two reals τ_1 and τ_2 such that

$$\begin{aligned}
&\tau_1 - \tau_2 = 0,\\
&(\tau_1, \frac{|p_0|^2 p_0}{\epsilon}, X) \in \bar{\mathcal{P}}^+ \tilde{u}(x_0, t_0),\\
&(\tau_2, \frac{|p_0|^2 p_0}{\epsilon}, Y) \in \bar{\mathcal{P}}^- \tilde{v}(y_0, t_0),\\
&\frac{-1}{\beta}\begin{pmatrix} I & 0 \\ 0 & I \end{pmatrix} \leq \begin{pmatrix} X & 0 \\ 0 & -Y \end{pmatrix} \leq (I - \beta A)^{-1} A.
\end{aligned}$$

The last inequality implies that $X \leq Y$. We then use the following lemma.

Lemma 2.6 (adapted from [32])**.** *We have the following estimations on the matrix A:*

$$\begin{aligned}
&\frac{1}{\|A\|} A < I,\\
&\|A\| \leq \frac{6|p_0|^2}{\epsilon},\\
&\text{If } \delta = \frac{1}{2\|A\|}, \text{ then } (I - \delta A)^{-1} A \leq 2\|A\| I \leq \frac{12}{\epsilon}|p_0|^2 I,
\end{aligned}$$

with $\|A\| = \sup_{\xi\in\mathbb{R}^4} \frac{|A\xi.\xi|}{\xi.\xi}$.

Proof. By definition of $\|A\|$, we have $\frac{A\xi.\xi}{\xi.\xi} \leq \|A\|$ for any $\xi \in \mathbb{R}^4$ and so $\frac{A\xi.\xi}{\|A\|} \leq I\xi.\xi$ which gives the fist result of the lemma.
Let $\xi = \begin{pmatrix} \xi_1 \\ \xi_2 \end{pmatrix} \in \mathbb{R}^4$. we have:

$$\begin{aligned}
A\xi.\xi &= \frac{2}{\epsilon}|p_0|^2 Z(\xi_1 - \xi_2).(\xi_1 - \xi_2),\\
&\leq \frac{4}{\epsilon}|p_0|^2 Z(\xi_1.\xi_1 + \xi_2.\xi_2),\\
&\leq \frac{4}{\epsilon}|p_0|^2 \|Z\||\xi|^2.
\end{aligned}$$

So it suffices to show that $\|Z\| \leq \frac{3}{2}$.

$$\begin{aligned} Z\xi_1.\xi_1 &= \frac{\xi_1^2}{2} + \frac{p_0 \otimes p_0}{|p_0|^2}\xi_1.\xi_1 \\ &\leq \frac{\xi_1^2}{2} + \xi_1^2, \\ &\leq \frac{3}{2}\xi_1^2. \end{aligned}$$

For the last point, it suffices to notice that if $B \geq 0$ and $C \geq 0$ with $B, C \in S^2$ such that $BC = CB$ then $CB \geq 0$. Indeed, $CB\xi.\xi = CB^{\frac{1}{2}}\xi.B^{\frac{1}{2}}\xi \geq 0$ since C is non-negative and B is symmetric non-negative. So, if $B \geq C$ and $D \geq 0$ with $D(B-C) = (B-C)D$ then $DB \geq DC$. It thus suffices to prove that $A \leq 2\|A\|(I - \delta A) = 2\|A\|I - A$, i.e. $A \leq \|A\|I$ which is true by definition of the norm. □

By using this lemma with $\beta = \frac{1}{2\|A\|}$, the inequality becomes $\frac{-12|p_0|^2}{\epsilon}\begin{pmatrix} I & 0 \\ 0 & I \end{pmatrix} \leq \begin{pmatrix} X & 0 \\ 0 & -Y \end{pmatrix} \leq \frac{12|p_0|^2}{\epsilon}\begin{pmatrix} I & 0 \\ 0 & I \end{pmatrix}$. Thus X and Y are bounded independently of α which is also the case for p_0 according to $\frac{|x_0-y_0|^4}{4\epsilon} \leq \frac{\lambda}{2T^2\gamma\kappa_{\vec{g}}}$. In particular, we have $\frac{-12|p_0|^2}{\epsilon}I \leq X \leq \frac{12|p_0|^2}{\epsilon}I$. So there exists a sequence (α_n) such that $\alpha_n \underset{n\to+\infty}{\longrightarrow} 0$, $t_0 \underset{n\to+\infty}{\longrightarrow} t_\infty$, $p_0 \underset{n\to+\infty}{\longrightarrow} p_\infty$, $X \underset{n\to+\infty}{\longrightarrow} X_\infty$ and $Y \underset{n\to+\infty}{\longrightarrow} Y_\infty$. Furthermore, since u is a sub-solution, v is a super-solution and using the additional assumption, we get:

$$\begin{aligned} \tau_1 + G_*(x_0, t_0, \frac{|p_0|^2 p_0}{\epsilon} + \alpha_n x_0, X + \alpha_n I) &\leq \frac{-\lambda}{T^2}, \\ \tau_2 + G^*(y_0, t_0, \frac{|p_0|^2 p_0}{\epsilon} - \alpha_n y_0, Y - \alpha_n I) &\geq 0. \end{aligned}$$

Then using the matrix inequality $X \leq Y$ and the ellipticity of the equation, we obtain $\tau_2 + G^*(y_0, t_0, \frac{|p_0|^2 p_0}{\epsilon} - \alpha_n y_0, X - \alpha_n I) \geq 0$. Subtracting these two inequalities gives us

$$\begin{aligned} &\frac{\lambda}{T^2} + G_*\Big(x_0, t_0, \frac{|p_0|^2 p_0}{\epsilon} + \alpha_n x_0, X + \alpha_n I\Big) \leq G^*\Big(y_0, t_0, \frac{|p_0|^2 p_0}{\epsilon} - \alpha_n y_n, X - \alpha_n I\Big), \\ &- \gamma \mathrm{div}\vec{g}(x_0, t_0) + \gamma \mathrm{div}\vec{g}(y_0, t_0) - E(X + \alpha_n I) - F_*\Big(\frac{|p_0|^2 p_0}{\epsilon} + \alpha_n x_0, X + \alpha_n I\Big) \\ &+ E(X - \alpha_n I) + F^*\Big(\frac{|p_0|^2 p_0}{\epsilon} - \alpha_n y_0, X - \alpha_n I\Big) \geq \frac{\lambda}{T^2}. \end{aligned}$$

Let n tend to infinity. As $\mathrm{div}\vec{g}$ is Lipschitz continuous uniformly in time with $\kappa_{\vec{g}}$ the Lipschitz constant, we get:

$$\gamma\kappa_{\vec{g}}|p_\infty| - E(X_\infty) - F_*\Big(\frac{|p_\infty|^2 p_\infty}{\epsilon}, X_\infty\Big) + E(X_\infty) + F^*\Big(\frac{|p_\infty|^2 p_\infty}{\epsilon}, X_\infty\Big) \geq \frac{\lambda}{T^2}$$

Since $|p_0| \leq \frac{\lambda}{2T^2\gamma\kappa_{\vec{g}}}$ and so $|p_\infty| \leq \frac{\lambda}{2T^2\gamma\kappa_{\vec{g}}}$, hence

$$\frac{\lambda}{2T^2} - F_*\Big(\frac{|p_\infty|^2 p_\infty}{\epsilon}, X_\infty\Big) + F^*\Big(\frac{|p_\infty|^2 p_\infty}{\epsilon}, X_\infty\Big) \geq \frac{\lambda}{T^2}.$$

We distinguish here two cases:

- First case: $p_\infty = 0$. From the matrix inequality $\frac{-12|p_0|^2}{\epsilon}\begin{pmatrix} I & 0 \\ 0 & I \end{pmatrix} \leq \begin{pmatrix} X & 0 \\ 0 & -Y \end{pmatrix} \leq \frac{12|p_0|^2}{\epsilon}\begin{pmatrix} I & 0 \\ 0 & I \end{pmatrix}$, it yields $X_\infty = Y_\infty = 0$. Having $F^*(0,0) = F_*(0,0) = 0$ leads to $0 \geq \frac{\lambda}{2T^2}$ which is absurd.
- Second case: $p_\infty \neq 0$. Since F is continuous on $\mathbb{R}^2\backslash\{\vec{0}\}\times\mathcal{S}^2$, then $F_*\Big(\frac{|p_\infty|^2 p_\infty}{\epsilon}, X_\infty\Big) = F^*\Big(\frac{|p_\infty|^2 p_\infty}{\epsilon}, X_\infty\Big) = F\Big(\frac{|p_\infty|^2 p_\infty}{\epsilon}, X_\infty\Big)$, yielding $0 \geq \frac{\lambda}{2T^2}$ which is absurd.

□

We now turn to the existence of a solution. To do so, we use the classical Perron's method and need to construct barriers.

Theorem 2.3 (Construction of barriers, adapted from [32])**.** *Assume (H) and let $Q_0 \in W^{1,\infty}(\mathbb{R}^2)$. Then $u^+ = \sup_{x\in\mathbb{R}^2} Q_0(x) + \gamma\|div\,\vec{g}\|_{L^\infty(\mathbb{R}^2\times[0,T))}t$ and $u^- = \inf_{x\in\mathbb{R}^2} Q_0(x) - \gamma\|div\,\vec{g}\|_{L^\infty(\mathbb{R}^2\times[0,T))}t$ are respectively super- and sub-solution of (EE).*

Proof. The proof of this theorem is straightforward. Indeed since $Q_0 \in W^{1,\infty}(\mathbb{R}^2)$ then u^- and u^+ are twice differentiable in space and once differentiable in time and are bounded. Besides $u^-(x,0) = \inf_{x\in\mathbb{R}^2} Q_0(x) \leq Q_0(x)$, $u^+(x,0) = \sup_{x\in\mathbb{R}^2} Q_0(x) \geq Q_0(x)$, $\forall x \in \mathbb{R}^2$. Furthermore, $\forall (x,t) \in \mathbb{R}^2 \times [0,T)$, $u_t^-(x,t) = -\gamma\|\mathrm{div}\,\vec{g}\|_{L^\infty(\mathbb{R}^2\times[0,T))}$, $Du^-(x,t) = \vec{0}$ and $D^2u^-(x,t) = 0$; $u_t^+(x,t) = \gamma\|\mathrm{div}\,\vec{g}\|_{L^\infty(\mathbb{R}^2\times[0,T))}$, $Du^+(x,t) = \vec{0}$ and $D^2u^+(x,t) = 0$. It follows then $\forall (x,t) \in \mathbb{R}^2 \times [0,T)$, $u_t^-(x,t) + G_*(t,x,u^-(x,t),Du^-(x,t),D^2u^-(x,t)) = -\gamma\|\mathrm{div}\,\vec{g}\|_{L^\infty(\mathbb{R}^2\times[0,T))} + \gamma\mathrm{div}\vec{g}(x,t) \leq 0$ and $u_t^+(x,t) + G^*(t,x,u^+(x,t),Du^+(x,t),D^2u^+(x,t)) = \gamma\|\mathrm{div}\,\vec{g}\|_{L^\infty(\mathbb{R}^2\times[0,T))} + \gamma\mathrm{div}\vec{g}(x,t) \geq 0$. Hence u^- is a sub-solution and u^+ a super-solution of (EE). □

A direct consequence of the two previous results is the following existence theorem.

Theorem 2.4 (Existence and uniqueness of a solution)**.** *Assume (H) and $Q_0 \in W^{1,\infty}(\mathbb{R}^2)$. Then there exists a unique bounded continuous solution of (EE) in $\mathbb{R}^2 \times [0,T)$.*

Proof. We follow Perron's method here ([27, Theorem 4.1]). Indeed, we have constructed a bounded sub-solution and a bounded super-solution which fall within the comparison principle. Then $Q = \sup\{w,\ w \text{ sub-solution of (EE) and } \forall (x,t) \in \mathbb{R}^2 \times [0,T),\ u^-(x,t) \leq w(x,t) \leq u^+(x,t)\}$ is a solution of (EE) potentially discontinuous. Clearly, Q is bounded since u^+ and u^- are bounded and since Q is a solution of (EE) then Q_* is a super-solution

and Q^* is a sub-solution and so applying the comparison principle gives us $Q^* \leq Q_*$. But by definition, $Q_* \leq Q^*$ and we finally get $Q = Q^* = Q_*$ meaning that Q is continuous on $\mathbb{R}^2 \times [0,T)$. □

Let us now focus on the regularity of the solution. Let us first consider the regularity in space.

Theorem 2.5 (Lipschitz regularity in space, adapted from [32])**.** *Assume (H) and that* $\|\nabla Q_0\|_{L^\infty(\mathbb{R}^2)} \leq B_0$ *with* $B_0 > 0$*. Then the solution of (EE) is Lipschitz continuous in space and satisfies*

$$\|\nabla Q(.,t)\|_{L^\infty(\mathbb{R}^2)} \leq B(t),$$

with $B(t) = \gamma \kappa_{\vec{g}} t + B_0$.

Proof. We will follow arguments of [32, Lemma 4.15]. We have proved that Q is bounded and continuous on $\mathbb{R}^2 \times [0,T)$. Let us set $\Phi^\epsilon(x,y,t) = B(t)(|x-y|^2+\epsilon^2)^{\frac{1}{2}}$ and we aim to show that $Q(x,t) - Q(y,t) \leq \Phi^\epsilon(x,y,t)$ for any $(x,y,t) \in \mathbb{R}^2 \times \mathbb{R}^2 \times [0,T)$. We introduce $M = \sup_{(x,y)\in\mathbb{R}^2\times\mathbb{R}^2, t\in[0,T)} (Q(x,t) - Q(y,t) - \Phi^\epsilon(x,y,t))$.
We assume that $M > 0$. We denote by $\bar{M} = \sup_{(x,y)\in\mathbb{R}^2\times\mathbb{R}^2, t\in[0,T)} \{Q(x,t) - Q(y,t) - \frac{\alpha}{2}(|x|^2 + |y|^2) - \frac{\lambda}{T-t} - \Phi^\epsilon(x,y,t)\}$. For λ small enough and α small enough, we have $\bar{M} > 0$. As Q is bounded and continuous with $\lim_{|x|\to+\infty, |y|\to+\infty, t\to T} Q(x,t) - Q(y,t) - \frac{\alpha}{2}(|x|^2+|y|^2) - \frac{\lambda}{T-t} - \Phi^\epsilon(x,y,t) = -\infty$, the maximum is attained at $(\bar{x},\bar{y},\bar{t})$ with $\bar{x} \neq \bar{y}$ and $\frac{\alpha}{2}(|\bar{x}|^2+|\bar{y}|^2) \leq C$ owing to $\bar{M} > 0$ and Q bounded. Therefore, $\lim_{\alpha\to 0} \alpha|\bar{x}| = \lim_{\alpha\to 0} \alpha|\bar{y}| = 0$.
We now prove that $\bar{t} > 0$ by contradiction. We assume that $\bar{t} = 0$, then $Q(\bar{x},0) - Q(\bar{y},0) - \Phi^\epsilon(\bar{x},\bar{y},0) > 0$ that is to say $Q_0(\bar{x}) - Q_0(\bar{y}) > B(0)(|\bar{x}-\bar{y}|^2+\epsilon^2)^{\frac{1}{2}}) > B_0|\bar{x}-\bar{y}|$ which is absurd since $\|\nabla Q_0\|_{L^\infty(\mathbb{R}^2)} \leq B_0$.
We set $\bar{p} = D_x\Phi^\epsilon(\bar{x},\bar{y},\bar{t}) = -D_y\Phi^\epsilon(\bar{x},\bar{y},\bar{t}) = B(\bar{t})(\bar{x}-\bar{y})(|\bar{x}-\bar{y}|^2+\epsilon^2)^{-\frac{1}{2}} \neq 0$, $Z = D_x^2\Phi^\epsilon(\bar{x},\bar{y},\bar{t}) = D_y^2\Phi^\epsilon(\bar{x},\bar{y},\bar{t}) = B(\bar{t})\Big((|\bar{x}-\bar{y}|^2+\epsilon^2)^{-\frac{1}{2}} I - (|\bar{x}-\bar{y}|^2+\epsilon^2)^{-\frac{3}{2}}(\bar{x}-\bar{y})\otimes(\bar{x}-\bar{y})\Big)$ and $A = \begin{pmatrix} Z & -Z \\ -Z & Z \end{pmatrix}$. Then by the parabolic version of Ishii's lemma applied to $\tilde{u}(x,t) = Q(x,t) - \frac{\alpha}{2}|x|^2$, $\tilde{v}(x,t) = Q(x,t) + \frac{\alpha}{2}|x|^2$, and $\Phi(x,y,t) = \Phi^\epsilon(x,y,t) + \frac{\lambda}{T-t}$, for every β such that $\beta A < I$, there exist $\tau_1 \in \mathbb{R}$, $\tau_2 \in \mathbb{R}$ and $X \in \mathcal{S}^2$, $Y \in \mathcal{S}^2$ such that

$$\tau_1 - \tau_2 = \frac{\lambda}{(T-\bar{t})^2} + B'(\bar{t})(|\bar{x}-\bar{y}|^2+\epsilon^2)^{\frac{1}{2}} = \frac{\lambda}{(T-\bar{t})^2} + \gamma\kappa_{\vec{g}}(|\bar{x}-\bar{y}|^2+\epsilon^2)^{\frac{1}{2}},$$
$$(\tau_1, \bar{p} + \alpha\bar{x}, X + \alpha I) \in \bar{\mathcal{P}}^+ Q(\bar{x},\bar{t}),$$
$$(\tau_2, \bar{p} - \alpha\bar{y}, Y - \alpha I) \in \bar{\mathcal{P}}^- Q(\bar{y},\bar{t}),$$
$$\frac{-1}{\beta}\begin{pmatrix} I & 0 \\ 0 & I \end{pmatrix} \leq \begin{pmatrix} X & 0 \\ 0 & -Y \end{pmatrix} \leq (I - \beta A)^{-1} A.$$

Thus we have

$$\tau_1 + \mathrm{div}\vec{g}(\bar{x},\bar{t}) + E(X+\alpha I) + F_*(\bar{p}+\alpha\bar{x}, X+\alpha I) \leq 0,$$
$$\tau_2 + \mathrm{div}\vec{g}(\bar{y},\bar{t}) + E(Y-\alpha I) + F^*(\bar{p}-\alpha\bar{y}, Y-\alpha I) \geq 0.$$

As the matrix inequality implies $X \leq Y$ and using the ellipticity of the equation, we deduce that

$$\tau_2 + \mathrm{div}\vec{g}(\bar{y},\bar{t}) + E(X-\alpha I) + F^*(\bar{p}-\alpha\bar{y}, X-\alpha I) \geq 0.$$

Subtracting both inequalities, we get

$$\frac{\lambda}{(T-\bar{t})^2} + \gamma\kappa_{\vec{g}}(|\bar{x}-\bar{y}|^2+\epsilon^2)^{\frac{1}{2}} + \gamma\mathrm{div}\vec{g}(\bar{x}) - \gamma\mathrm{div}\vec{g}(\bar{y}) + E(X+\alpha I) - E(X-\alpha I)$$
$$+ F_*(\bar{p}+\alpha\bar{x}, X+\alpha I) - F^*(\bar{p}-\alpha\bar{y}, X-\alpha I) \leq 0.$$

Let α tend to 0 ($\bar{p}$ and X are bounded independently of α so we can extract convergent subsequences whose limits are still denoted by $\bar{p}$ and X), then:

$$\frac{\lambda}{(T-\bar{t})^2} + \lim_{\alpha\to 0}\big(\gamma\kappa_{\vec{g}}(|\bar{x}-\bar{y}|^2+\epsilon^2)^{\frac{1}{2}} + \gamma\mathrm{div}\vec{g}(\bar{x}) - \gamma\mathrm{div}\vec{g}(\bar{y})\big) + F_*(\bar{p},X) - F^*(\bar{p},X) \leq 0.$$

Since $\bar{p} \neq \vec{0}$ then $F^*(\bar{p},X) = F_*(\bar{p},X) = F(\bar{p},X)$. Besides

$$\gamma\kappa_{\vec{g}}(|\bar{x}-\bar{y}|^2+\epsilon^2)^{\frac{1}{2}} + \gamma\mathrm{div}\vec{g}(\bar{x}) - \gamma\mathrm{div}\vec{g}(\bar{y}) \geq \gamma\kappa_{\vec{g}}(|\bar{x}-\bar{y}|^2+\epsilon^2)^{\frac{1}{2}} - \gamma\kappa_{\vec{g}}|\bar{x}-\bar{y}| \geq 0.$$

Therefore $\frac{\lambda}{(T-\bar{t})^2} \leq 0$ which is absurd.
Then $Q(x,t) - Q(y,t) \leq \Phi^\epsilon(x,y,t)$. Let ϵ tend to 0, we get $Q(x,t) - Q(y,t) \leq B(t)|x-y|$. By exchanging x and y in what precedes, we get $|Q(x,t) - Q(y,t)| \leq B(t)|x-y|$ which concludes the proof. □

Besides, we can show that this solution is also uniformly continuous in time.

Theorem 2.6 (adapted from [32])**.** *Assume (H), and that div $\vec{g}$ is uniformly continuous in time with $\omega_{div\,\vec{g}}$ its modulus of continuity. Then the solution of (EE) is uniformly continuous in time.*

Proof. We follow again the arguments of [32, Lemma 4.15]. Let us set $\delta > 0$. For any $(x,t) \in \mathbb{R}^2 \times (0,T)$ such that $t+\delta \leq T$, we set $v(x,t) = Q(x,t+\delta)$. Then v is a sub-solution of $w_t - \omega_{\mathrm{div}\,\vec{g}}(\delta) + \mathrm{div}(\vec{g})(x,t) + E(D^2w) + F(Dw, D^2w) = 0$ on $\mathbb{R}^2 \times (0, T-\delta)$ with $w(x,0) = Q(x,\delta)$ on $\mathbb{R}^2$ in the sense of viscosity solutions theory. Indeed, we have $v_t = Q_t$, $v_t + \mathrm{div}\vec{g}(x,t+\delta) + E(D^2v) + F(Dv, D^2v) = 0$ and $\mathrm{div}\vec{g}(x,t+\delta) \geq -\omega_{\mathrm{div}\vec{g}}(\delta) + \mathrm{div}\vec{g}(x,t)$ leading to $v_t - \omega_{\mathrm{div}\vec{g}}(\delta) + \mathrm{div}\vec{g}(x,t) + E(D^2v) + F(Dv, D^2v) \leq 0$. Besides, $\tilde{u} = Q + \sup_{x\in\mathbb{R}^2}((Q(x,\delta) - Q_0(x))^+) + \omega_{\mathrm{div}\vec{g}}(\delta)t$ ($(\alpha)^+ = \max\{0,\alpha\}$) is a super-solution with $v(x,0) \leq \tilde{u}(x,0)$ for any $x \in \mathbb{R}^2$. Using the comparison principle, we get $\forall (x,t) \in$

$\mathbb{R}^2 \times (0, T-\delta)$, $Q(x,t+\delta) - Q(x,t) \leq \sup_{x\in\mathbb{R}^2}((Q(x,\delta) - Q_0(x))^+) + \omega_{\mathrm{div}\vec{g}}(\delta)t$.
We will now focus on an auxiliary problem. Let us first assume that $Q_0 \in C_b^2(\mathbb{R}^2)$. We set $u^{+/-} = Q_0(x) + / - C_1 t$ with $C_1 = \inf_{x\in\mathbb{R}^2}\{-E(D^2Q_0) - F^*(DQ_0, D^2Q_0), E(D^2Q_0) + F_*(DQ_0, D^2Q_0)\}$. We easily check that u^+ is a super-solution and u^- a sub-solution of (SP): $u_t + E(D^2u) + F(Du, D^2u) = 0$, $u(x,0) = Q_0(x)$. Then there exists a unique solution u of this problem and by the comparison principle, the following holds: $\forall t \in [0,T)$, $\forall x \in \mathbb{R}^2$, $|u(x,t) - Q_0(x)| \leq C_1 t$. We then set $v(x,t) = u(x,t+h)$. So v is also a solution to the problem (SP) with $v(x,0) = u(x,h)$, $\forall x \in \mathbb{R}^2$ and by the comparison principle, we get $u(x,t+h) - u(x,t) \leq \sup_{x\in\mathbb{R}^2}\{u(x,h) - Q_0(x)\} \leq C_1 h$. Similarly, we have $u(x,t) - u(x,t+h) \leq \sup_{x\in\mathbb{R}^2}\{u(x,h) - Q_0(x)\} \leq C_1 h$ and so $|u(x,t+h) - u(x,t)| \leq \sup_{x\in\mathbb{R}^2}\{u(x,h) - Q_0(x)\} \leq C_1 h$. We now assume that $Q_0 \in W^{1,\infty}(\mathbb{R}^2)$. We set $Q_\epsilon^0 = Q_0 * \rho_\epsilon$, where ρ_ϵ is a regularizing sequence satisfying $\rho_\epsilon = \frac{1}{\epsilon^2}\rho(\frac{1}{\epsilon})$, $\rho \in C_c^\infty(\mathbb{R}^2, \mathbb{R})$, $\rho \geq 0$, $\mathrm{supp}(\rho) \subset \bar{B}(0,1)$, and $\int_{\mathbb{R}^2} \rho(x)\,dx = 1$. Then $Q_\epsilon^0 \in C_c^2(\mathbb{R}^2)$ and $\|DQ_\epsilon^0\|_{L^\infty(\mathbb{R}^2)} \leq B_0$, $\|D^2Q_\epsilon^0\|_{L^\infty(\mathbb{R}^2)} \leq \frac{B_0C_2}{\epsilon}$. Indeed using properties stated in [31, Theorem 1, p.123], we have

$$\begin{aligned}
|DQ_\epsilon^0(x)| &= |DQ_0 * \rho_\epsilon(x)|,\\
&= |\int_{\mathbb{R}^2} DQ_0(x-y)\rho_\epsilon(y)\,dy|,\\
&\leq \int_{\mathbb{R}^2} |DQ_0(x-y)\rho_\epsilon(y)|\,dy,\\
&\leq B_0 \int_{\mathbb{R}^2} \rho_\epsilon(y)\,dy,\\
&\leq B_0,
\end{aligned}$$

and

$$\begin{aligned}
|D^2Q_\epsilon^0(x)| &= |DQ_0 * D\rho_\epsilon(x)|,\\
&= |\int_{\mathbb{R}^2} DQ_0(x-y)D\rho_\epsilon(y)\,dy|,\\
&\leq \int_{\mathbb{R}^2} |DQ_0(x-y)D\rho_\epsilon(y)|\,dy,\\
&\leq \frac{B_0}{\epsilon}\int_{\mathbb{R}^2} \frac{1}{\epsilon^2}\left|D\rho\left(\frac{y}{\epsilon}\right)\right|\,dy,\\
&\leq \frac{B_0}{\epsilon}\|D\rho\|_{L^1(\mathbb{R}^2)}.
\end{aligned}$$

Moreover, $\|Q_0 - Q_\epsilon^0\|_{L^\infty(\mathbb{R}^2)} \leq B_0\epsilon$ since

$$\begin{aligned}
|Q_0(x) - Q_\epsilon^0(x)| &\leq \int_{\mathbb{R}^2} |Q_0(x) - Q_0(x-y)|\rho_\epsilon(y)\,dy,\\
&\leq B_0 \int_{\bar{B}(0,\epsilon)} |y|\rho_\epsilon(y)\,dy,
\end{aligned}$$

$$\leq B_0\epsilon \int_{\bar{B}(0,\epsilon)} \rho_\epsilon(y)\, dy = B_0\epsilon.$$

We denote by u_ϵ the solution with initial condition Q^0_ϵ. Then, by the comparison principle, $\|u_{\epsilon'}(.,t) - u_\epsilon(.,t)\|_{L^\infty(\mathbb{R}^2)} \leq \|Q^0_{\epsilon'} - Q^0_\epsilon\|_{L^\infty(\mathbb{R}^2)}$, and so (u_ϵ) converges uniformly to u the solution of (SP) with initial condition Q_0 since (Q^0_ϵ) converges uniformly to Q_0. We then have by the comparison principle that $\|u_\epsilon(.,t) - u(.,t)\|_{L^\infty(\mathbb{R}^2)} \leq \|Q^0_\epsilon - Q_0\|_{L^\infty(\mathbb{R}^2)}$ and deduce that

$$\begin{aligned}\|u(.,t+h) - u(.,t)\|_{L^\infty(\mathbb{R}^2)} &\leq 2\|Q^0_\epsilon - Q_0\|_{L^\infty(\mathbb{R}^2)} + \|u_\epsilon(.,t+h) - u(.,t)\|_{L^\infty(\mathbb{R}^2)},\\ &\leq 2B_0\epsilon + C_1\left(B_0, \frac{B_0C_2}{\epsilon}\right)h.\end{aligned}$$

By taking the minimum on ϵ, we obtain the modulus of continuity of u, called ω_F which depends only on B_0. And so u satisfies $Q_0(x) - \omega_F(t) \leq u(x,t) \leq Q_0(x) + \omega_F(t)$. We now prove that $\|Du\|_{L^\infty(\mathbb{R}^2\times(0,T))} \leq \|DQ_0\|_{L^\infty(\mathbb{R}^2)}$. Indeed, let us consider the function $u^h(x,t) = u(x+h,t) + \|DQ_0\|_{L^\infty(\mathbb{R}^2)}|h|$. Then u^h is still a solution of (SP) with initial condition $u^h(x,0) = Q_0(x+h) + \|DQ_0\|_{L^\infty(\mathbb{R}^2)}|h| \geq Q_0(x)$. So, by the comparison principle, we have $u^h \geq u$. We deduce that for every $h \in \mathbb{R}^2$, $u(x,t) - u(x+h,t) \leq \|DQ_0\|_{L^\infty(\mathbb{R}^2)}|h|$, and so $\|Du\|_{L^\infty(\mathbb{R}^2\times(0,T))} \leq \|DQ_0\|_{L^\infty(\mathbb{R}^2)}$. We then set $U^+(x,t) = u(x,t) + \|\mathrm{div}\vec{g}\|_{L^\infty(\mathbb{R}^2\times[0,T))}t$ and come back to the initial problem. Then $\|DU^+\|_{L^\infty(\mathbb{R}^2\times(0,T))} \leq \|Du\|_{L^\infty(\mathbb{R}^2\times(0,T))} \leq B_0$ and U^+ is a super-solution of (EE) since $U^+(x,0) = u(x,0) = Q_0(x)$ and $U^+_t(x,t) + G^*(x,t,U^+,DU^+,D^2U^+) = u_t(x,t) + \|\mathrm{div}\vec{g}\|_{L^\infty(\mathbb{R}^2\times[0,T))} + \mathrm{div}\vec{g}(x,t) + E(D^2u(x,t)) + F^*(Du(x,t), D^2u(x,t)) = \|\mathrm{div}\vec{g}\|_{L^\infty(\mathbb{R}^2\times[0,T))} + \mathrm{div}\vec{g}(x,t) \geq 0$ and satisfies $U^+(x,t) \leq Q_0(x) + \omega_F(t) + \|\mathrm{div}\vec{g}\|_{L^\infty(\mathbb{R}^2\times[0,T))}t$. Similarly, we construct a sub-solution U^- such that $U^-(x,t) \geq Q_0(x) - \omega_F(t) - \|\mathrm{div}\vec{g}\|_{L^\infty(\mathbb{R}^2\times[0,T))}t$ by setting $U^-(x,t) = u(x,t) - \|\mathrm{div}\vec{g}\|_{L^\infty(\mathbb{R}^2\times[0,T))}t$. By applying the comparison principle, we get that

$$\begin{aligned}Q_0(x) - \omega_F(t) - \|\mathrm{div}\vec{g}\|_{L^\infty(\mathbb{R}^2\times[0,T))}t \leq U^-(x,t) \leq Q(x,t) &\leq U^+(x,t)\\ &\leq Q_0(x) + \omega_F(t) + \|\mathrm{div}\vec{g}\|_{L^\infty(\mathbb{R}^2\times[0,T))}t.\end{aligned}$$

Thus $\sup_{x\in\mathbb{R}^2}((Q(x,\delta) - Q_0(x))^+) \leq \omega_F(\delta) + \|\mathrm{div}\vec{g}\|_{L^\infty(\mathbb{R}^2\times[0,T))}\delta$ and so $Q(x,t+\delta) - Q(x,t) \leq \omega_F(\delta) + \|\mathrm{div}\vec{g}\|_{L^\infty(\mathbb{R}^2\times[0,T))}\delta + \omega_{\mathrm{div}\vec{g}}(\delta)T$. Similarly, v is a super-solution of $w_t + \omega_{\mathrm{div}\vec{g}}(\delta) + \mathrm{div}\vec{g}(x,t) + E(D^2w) + F(Dw, D^2w) = 0$ BLACKwith $w(x,0) = Q(x,\delta)$ on $\mathbb{R}^2$ and $\tilde{u} = Q(x,t) - \sup_{x\in\mathbb{R}^2}((Q(x,\delta) - Q_0(x))^-) - \omega_{\mathrm{div}\vec{g}}(\delta)t$ $((\alpha)^- = \min\{0,\alpha\})$ is a sub-solution. So, by the comparison principle, we have

$$\begin{aligned}Q(x,t) - Q(x,t+\delta) &\leq \sup_{x\in\mathbb{R}^2}((Q(x,\delta) - Q_0(x))^-) + \omega_{\mathrm{div}\vec{g}}(\delta)t,\\ &\leq \omega_F(\delta) + \|\mathrm{div}\vec{g}\|_{L^\infty(\mathbb{R}^2\times[0,T))}\delta + \omega_{\mathrm{div}\vec{g}}(\delta)T.\end{aligned}$$

And so

$$|Q(x,t) - Q(x,t+\delta)| \leq \omega_F(\delta) + \|\mathrm{div}\vec{g}\|_{L^\infty(\mathbb{R}^2\times[0,T))}\delta + \omega_{\mathrm{div}\vec{g}}(\delta)T.$$

which achieves the proof. □

This concludes this section on the existence of a well-defined and smooth solution of the evolution equation derived for Q. Let us now turn to a Γ-convergence result.

2.4 Asymptotic results

In that purpose, an additional condition is set on u to get a uniform bound on $\|u\|_{L^2(\Omega)}$. We assume that $u \in L^\infty(\Omega)$, which is rather a non-restrictive and natural requirement in image processing since at every pixel the light intensity has finite energy. For instance, we introduce the condition $\|u\|_{L^\infty(\Omega)} \leq \|f\|_{L^\infty(\Omega)}$, which is reasonable in the context of image decomposition and in virtue of the smoothing properties of the functional.
We first give a result of existence of minimizers for the non-elliptic problem (5.4).

Theorem 2.7 (Existence of minimizers, adapted from [21])**.** *Let us set* $X(\Omega) = \{u \in GSBV^2(\Omega) \cap L^\infty(\Omega)$ *with* $\|u\|_{L^\infty(\Omega)} \leq C_2\} \times H(div) \times \{Q \in W^{1,\infty}(\Omega) \mid \int_\Omega Q\,dx = 0\}$, *with* C_2 *a positive constant that depends only on* $\|f\|_{L^\infty(\Omega)}$. *Assuming* $\beta \leq \alpha \leq 2\beta$, $\gamma > 0$, $\mu > 0$ *and* $\beta > 0$, *there exists a minimizer* $(\bar{u}, \vec{\bar{g}}, \bar{Q}) \in X(\Omega)$ *of* $\bar{F}$.

Proof. The proof is based on an adaptation of arguments provided in [21].
By choosing $u \equiv 0$, $\vec{g} \equiv \vec{0}$, $Q \equiv 0$, then $F(u, \vec{g}, Q) = \int_\Omega f^2\,dx < +\infty$. And since $\forall (u, \vec{g}, Q) \in X(\Omega)$, $\bar{F}(u, \vec{g}, Q) \geq 0$, then the infimum is finite. Let $(u_h, \vec{g}_h, Q_h) \subset X(\Omega)$ be a minimizing sequence for $\bar{F}$. Then there exists $N \in \mathbb{N}$ such that $\sup_{h \geq N} \bar{F}(u_h, \vec{g}_h, Q_h) \leq \inf_{(u,\vec{g},Q) \in X(\Omega)} \bar{F}(u, \vec{g}, Q) + 1 < +\infty$.

Then (∇Q_h) is uniformly bounded in $L^\infty(\Omega)$. Besides, $\int_\Omega Q_h\,dx = 0$ for all $h \in \mathbb{N}$ and so using the Poincaré-Wirtinger inequality, we get a uniform bound for (Q_h) in $W^{1,\infty}(\Omega)$. We can thus extract a subsequence denoted by (Q_{h_m}) converging weakly-$*$ to $Q_0 \in W^{1,\infty}(\Omega)$. As the weak-$*$ convergence implies uniform convergence then $\int_\Omega Q_0\,dx = 0$. Let us now show that $(\vec{g}_h)$ is uniformly bounded in $H(div)$ using the fact that $\|u_h\|_{L^\infty(\Omega)} \leq C_2$ for all $h \in \mathbb{N}$. Indeed, we have

$$
\begin{aligned}
+\infty > \sup_{h \geq N} \bar{F}(u_h, \vec{g}_h, Q_h) &\geq \|f - u_h - \mathrm{div}\vec{g}_h\|^2_{L^2(\Omega)} + \frac{\gamma}{2}\||\vec{g}_h - \nabla Q_h|\|^2_{L^2(\Omega)}, \\
&\geq \frac{1}{2}\|\mathrm{div}\vec{g}_h\|^2_{L^2(\Omega)} - \|f - u_h\|^2_{L^2(\Omega)} + \frac{\gamma}{4}\||\vec{g}_h|\|^2_{L^2(\Omega)} - \frac{\gamma}{2}\||\nabla Q_h|\|^2_{L^2(\Omega)}, \\
+\infty > \frac{1}{2}\|\mathrm{div}\vec{g}_h\|^2_{L^2(\Omega)} &+ \frac{\gamma}{4}\||\vec{g}_h|\|^2_{L^2(\Omega)}
\end{aligned}
$$

for any $h \geq N$ since $\||\nabla Q_h|\|_{L^\infty(\Omega)}$ is uniformly bounded and so is $\||\nabla Q_h|\|^2_{L^2(\Omega)}$ and $\|f - u_h\|^2_{L^2(\Omega)} \leq (\|f\|_{L^\infty(\Omega)} + C_2)^2 meas(\Omega) < +\infty$ for any $h \in \mathbb{N}$. Therefore there exist a subsequence $(\vec{g}_{h_m})$ of $(\vec{g}_h)$ and $\vec{g}_0$ such that $\vec{g}_{h_m} \underset{m \to +\infty}{\rightharpoonup} \vec{g}_0$ in $H(div)$.
We also note that

$$
\begin{aligned}
+\infty > \sup_{h \geq N} \bar{F}(u_h, \vec{g}_h, Q_h) \geq \sup_{h \geq N} &\rho\|\nabla^2 u_h\|^2_{L^2(\Omega)} + \|f - u_h - \mathrm{div}\vec{g}_h\|^2_{L^2(\Omega)} + \alpha\mathcal{H}^1(S_{u_h}) \\
&+ \beta\mathcal{H}^1(S_{\nabla u_h} \setminus S_{u_h}),
\end{aligned}
$$

$$\geq \sup_{h\geq N} \rho\|\nabla^2 u_h\|^2_{L^2(\Omega)} + \frac{1}{2}\|f-u_h\|^2_{L^2(\Omega)} - \|\mathrm{div}\vec{g}_h\|^2_{L^2(\Omega)} + \alpha\mathcal{H}^1(S_{u_h})$$
$$+ \beta\mathcal{H}^1(S_{\nabla u_h}\setminus S_{u_h}),$$
$$+\infty > \sup_{h\geq N} \rho\|\nabla^2 u_h\|^2_{L^2(\Omega)} + \frac{1}{2}\|f-u_h\|^2_{L^2(\Omega)} + \alpha\mathcal{H}^1(S_{u_h}) + \beta\mathcal{H}^1(S_{\nabla u_h}\setminus S_{u_h}),$$

from what precedes. We can now apply [21, Theorem 8].

Theorem 2.8 (taken from [21, Theorem 8])**.** *Let $\Omega\subset\mathbb{R}^2$ be a bounded open set, $\alpha,\beta,\mu>0$ and let $(u_h)\subset GSBV^2(\Omega)$ be such that $\sup_h \|\nabla^2 u_h\|^2_{L^2(\Omega)} + \mu\|f-u_h\|^2_{L^2(\Omega)} + \alpha\mathcal{H}^1(S_{u_h}) + \beta\mathcal{H}^1(S_{\nabla u_h}\setminus S_{u_h}) < +\infty$. Then there are a subsequence (u_{h_m}) and $u_0\in GSBV^2(\Omega)\cap L^2(\Omega)$ such that, as $m\to+\infty$,*

$$u_{h_m}\to u_0 \text{ almost everywhere in } \Omega \text{ and weakly in } L^2(\Omega),$$
$$u_{h_m}\to u_0 \text{ strongly in } L^q(\Omega),\ 1\leq q<2,$$
$$\nabla u_{h_m}\to\nabla u_0 \text{ almost everywhere in } \Omega,$$
$$\nabla^2 u_{h_m}\rightharpoonup\nabla^2 u_0 \text{ weakly in } [L^2(\Omega)]^{2\times 2}.$$

Since $u_{h_m}\to u_0$ almost everywhere in Ω, we deduce that $\|u_0\|_{L^\infty(\Omega)}\leq C_2$ and so $(u_0,\vec{g}_0,Q_0)\in X(\Omega)$.
It remains to prove the lower semicontinuity of the functional. Since $\sup_{h\geq N}\|\nabla^2 u_h\|^2_{L^2(\Omega)} + \mu\|f-u_h\|^2_{L^2(\Omega)} + \alpha\mathcal{H}^1(S_{u_h}) + \beta\mathcal{H}^1(S_{\nabla u_h}\setminus S_{u_h}) < +\infty$ and $u_{h_m}\underset{m\to+\infty}{\longrightarrow} u_0$ almost everywhere in Ω, we can apply [21, Theorem 10].

Theorem 2.9 (taken from [21, Theorem 10])**.** *Let $\Omega\subset\mathbb{R}^2$ be a bounded open set, $0<\beta\leq\alpha\leq 2\beta$ and $f\in L^2(\Omega)$. Let $u_0, u_h\in GSBV^2(\Omega)$ $(h\in\mathbb{N})$, such that $\sup_h \|\nabla^2 u_h\|^2_{L^2(\Omega)} + \mu\|f-u_h\|^2_{L^2(\Omega)} + \alpha\mathcal{H}^1(S_{u_h}) + \beta\mathcal{H}^1(S_{\nabla u_h}\setminus S_{u_h}) < +\infty$ and $u_h\to u_0$ almost everywhere in Ω. Then $\|\nabla^2 u_0\|^2_{L^2(\Omega)} + \mu\|f-u_0\|^2_{L^2(\Omega)} + \alpha\mathcal{H}^1(S_{u_0}) + \beta\mathcal{H}^1(S_{\nabla u_0}\setminus S_{u_0}) \leq \liminf_{h\to+\infty}\|\nabla^2 u_h\|^2_{L^2(\Omega)} + \mu\|f-u_h\|^2_{L^2(\Omega)} + \alpha\mathcal{H}^1(S_{u_h}) + \beta\mathcal{H}^1(S_{\nabla u_h}\setminus S_{u_h})$ and $\alpha\mathcal{H}^1(S_{u_0}) + \beta\mathcal{H}^1(S_{\nabla u_0}\setminus S_{u_0}) \leq \liminf_{h\to+\infty}\alpha\mathcal{H}^1(S_{u_h}) + \beta\mathcal{H}^1(S_{\nabla u_h}\setminus S_{u_h})$.*

Besides, from the proof of Theorem 2.1, and the weak lower semicontinuity of the L^2-norm, we have $\rho\|\nabla^2 u_0\|^2_{L^2(\Omega)} + \|f-u_0-\mathrm{div}\vec{g}_0\|^2_{L^2(\Omega)} + \mu\||\nabla Q_0|\|_{L^\infty(\Omega)} + \frac{\gamma}{2}\||\vec{g}_0-\nabla Q_0|\|^2_{L^2(\Omega)} \leq \liminf_{m\to+\infty}\rho\|\nabla^2 u_{h_m}\|^2_{L^2(\Omega)} + \|f-u_{h_m}-\mathrm{div}\vec{g}_{h_m}\|^2_{L^2(\Omega)} + \mu\||\nabla Q_{h_m}|\|_{L^\infty(\Omega)} + \frac{\gamma}{2}\||\vec{g}_{h_m}-\nabla Q_{h_m}|\|^2_{L^2(\Omega)}$. Since "$\liminf\sum\geq\sum\liminf$", then $\bar{F}(u_0,\vec{g}_0,Q_0)\leq\liminf_{m\to+\infty}\bar{F}(u_{h_m},\vec{g}_{h_m},Q_{h_m})$. This concludes the proof by taking $(\bar{u},\vec{g},\bar{Q})=(u_0,\vec{g}_0,Q_0)$. □

We now give a Γ-convergence result.

Theorem 2.10 (Γ-convergence, adapted from [2, Theorem 3.1, 3.2, 3.3])**.** *Assume that $\alpha=\beta$, $\kappa_\varepsilon>0$ with $\kappa_\varepsilon=o(\varepsilon^4)$, $\xi_\varepsilon=\zeta_\varepsilon=0$ and Ω is strictly star-shaped. Then the family $(\mathcal{F}_\varepsilon)$ Γ-converges to $\bar{F}$ in the $L^1(\Omega)\times H(div)\times W^{1,\infty}(\Omega)\times L^1(\Omega)\times L^1(\Omega)$ topology (strong*

topology for $L^1(\Omega)$ and weak/weak-$*$ topology for $H(div)$ and $W^{1,\infty}(\Omega)$) as $\varepsilon \to 0^+$. Besides, the limit point of $(\bar{u}_\varepsilon, \bar{\vec{g}}_\varepsilon, \bar{Q}_\varepsilon, \bar{v}_{1,\varepsilon}, \bar{v}_{2,\varepsilon})$, a pair of minimizers of $\mathcal{F}_\varepsilon$, when ε tends to 0^+ is of the form $(\bar{u}, \bar{\vec{g}}, \bar{Q}, 1, 1)$ with $(\bar{u}, \bar{\vec{g}}, \bar{Q}) \in X(\Omega)$ assuming $\forall \varepsilon > 0$, $\|\bar{u}_\varepsilon\|_{L^\infty(\Omega)} \leq C_2$. It means in particular that $\lim\limits_{\varepsilon \to 0^+} \left(\mathcal{F}_\varepsilon(\bar{u}_\varepsilon, \bar{\vec{g}}_\varepsilon, \bar{Q}_\varepsilon, \bar{v}_{1,\varepsilon}, \bar{v}_{2,\varepsilon}) - \bar{F}(\bar{u}, \bar{\vec{g}}, \bar{Q})\right) = 0$.

Remark 2.7. *Under the assumptions of this theorem, then $\mathcal{D}(\Omega) = \{u \in W^{2,2}_{loc}(\Omega) \cap L^\infty(\Omega) | \|u\|_{L^\infty(\Omega)} \leq C_2\} \times H(div) \times \{Q \in W^{1,\infty}(\Omega) | \int_\Omega Q\, dx = 0\} \times W^{1,2}(\Omega; [0,1]) \times W^{1,2}(\Omega; [0,1])$ is the set of admissible solutions.*

Proof. [2, Theorem 3.1, 3.2 and 3.3] will structure our proof. Let us first recall [2, Theorem 3.1].

Theorem 2.11 (taken from [2, Theorem 3.1])**.** *Assume that $\gamma \geq 2$, that $\lim\limits_{\varepsilon \to 0^+} \frac{\xi_\varepsilon}{\varepsilon^{\gamma-1}} = +\infty$, and that $\kappa_\varepsilon > 0$ for ε small enough, $\zeta_\varepsilon \geq 0$ for ε small enough. Then for every triple $(u, s, \sigma) \in L^2(\Omega) \times L^\infty(\Omega; [0,1]) \times L^\infty(\Omega; [0,1])$ and for every family $(u_\varepsilon, s_\varepsilon, \sigma_\varepsilon) \in W^{2,2}_{loc}(\Omega) \times W^{1,2}(\Omega; [0,1]) \times W^{1,2}(\Omega; [0,1])$ converging to (u, s, σ) strongly in $[L^1(\Omega)]^3$ as $\varepsilon \to 0^+$, we have $\liminf\limits_{\varepsilon \to 0^+} \int_\Omega (\sigma_\varepsilon^2 + \kappa_\varepsilon)|\nabla^2 u_\varepsilon|^2\, dx + \mu \int_\Omega |u_\varepsilon - g|^2\, dx + (\alpha - \beta)\mathcal{G}_\varepsilon(s_\varepsilon) + \beta \mathcal{G}_\varepsilon(\sigma_\varepsilon) + \xi_\varepsilon \int_\Omega (s_\varepsilon^2 + \zeta_\varepsilon)|\nabla u_\varepsilon|^\gamma\, dx \geq \mathcal{F}_1(u, s, \sigma)$ with*

$$\mathcal{F}_1(u, s, \sigma) = \begin{cases} \int_\Omega (|\nabla^2 u|^2 + \mu |u - g|^2)\, dx + (\alpha - \beta)\mathcal{H}^1(S_u) + \beta \mathcal{H}^1(S_u \cup S_{\nabla u}) \\ \qquad \text{if } u \in GSBV^2(\Omega),\ s \equiv 1,\ \sigma \equiv 1, \\ +\infty \text{ otherwise} \end{cases};$$

and $\liminf\limits_{\varepsilon \to 0^+} \int_\Omega (\sigma_\varepsilon^2 + \kappa_\varepsilon)|\nabla^2 u_\varepsilon|^2\, dx \geq \int_\Omega (|\nabla^2 u|^2)\, dx$ if $u \in GSBV^2(\Omega)$, $s \equiv 1$, $\sigma \equiv 1$; and $\liminf\limits_{\varepsilon \to 0^+} (\alpha - \beta)\mathcal{G}_\varepsilon(s_\varepsilon) + \beta \mathcal{G}_\varepsilon(\sigma_\varepsilon) \geq (\alpha - \beta)\mathcal{H}^1(S_u) + \beta \mathcal{H}^1(S_u \cup S_{\nabla u})$ if $u \in GSBV^2(\Omega)$, $s \equiv 1$, $\sigma \equiv 1$. Moreover the condition on ξ_ε can be replaced by $\xi_\varepsilon \geq 0$ in the case $\alpha = \beta$.

It thus remain to prove the lower semicontinuity of the other terms that is to say $\liminf\limits_{\varepsilon \to 0^+} \|f - u_\varepsilon - \mathrm{div}\vec{g}_\varepsilon\|_{L^2(\Omega)} \geq \|f - u - \mathrm{div}\vec{g}\|_{L^2(\Omega)}$, $\liminf\limits_{\varepsilon \to 0^+} \||\nabla Q_\varepsilon|\|_{L^\infty(\Omega)} \geq \||\nabla Q|\|_{L^\infty(\Omega)}$ and $\liminf\limits_{\varepsilon \to 0^+} \|\vec{g}_\varepsilon - \nabla Q_\varepsilon|\|^2_{L^2(\Omega)} \geq \|\vec{g} - \nabla Q|\|^2_{L^2(\Omega)}$ for any $(u_\varepsilon, \vec{g}_\varepsilon, Q_\varepsilon) \in \mathcal{D}(\Omega)$ converging to $(u, \vec{g}, Q) \in GSBV^2(\Omega) \times H(div) \times W^{1,\infty}(\Omega)$ strongly in $L^1(\Omega)$, weakly in $H(div)$ and weakly-$*$ in $W^{1,\infty}(\Omega)$. Since $\forall \varepsilon > 0$, $\|u_\varepsilon\|_{L^\infty(\Omega)} \geq C_2$, then $\|u_\varepsilon\|_{L^2(\Omega)} \leq C_2 meas(\Omega) < +\infty$ and so (u_ε) converges weakly to u in $L^2(\Omega)$ by uniqueness of the weak limit up to a subsequence. Since $(\vec{g}_\varepsilon)$ weakly converges to $\vec{g}$ in $H(div)$ then $(\mathrm{div}\vec{g}_\varepsilon)$ converges weakly to $\mathrm{div}\vec{g}$ in $L^2(\Omega)$. Therefore $\liminf\limits_{\varepsilon \to 0^+} \|f - u_\varepsilon - \mathrm{div}\vec{g}_\varepsilon\|_{L^2(\Omega)} \geq \|f - u - \mathrm{div}\vec{g}\|^2_{L^2(\Omega)}$. Since (Q_ε) converges weakly-$*$ to Q in $W^{1,\infty}(\Omega)$ then (∇Q_ε) converges weakly-$*$ to ∇Q in $L^\infty(\Omega)$ and so $\liminf\limits_{\varepsilon \to 0^+} \||\nabla Q_\varepsilon|\|_{L^\infty(\Omega)} \geq \||\nabla Q|\|_{L^\infty(\Omega)}$. Also as the weak-$*$ convergence in $W^{1,\infty}(\Omega)$ implies uniform convergence then $\int_\Omega Q\, dx = 0$. Finally, weak-$*$ convergence in $L^\infty(\Omega)$ implying weak convergence in $L^2(\Omega)$ and weak convergence in $H(div)$ implying weak convergence in $L^2(\Omega)$ yields $\liminf\limits_{\varepsilon \to 0^+} \|\vec{g}_\varepsilon - \nabla Q_\varepsilon|\|^2_{L^2(\Omega)} \geq \|\vec{g} - \nabla Q|\|^2_{L^2(\Omega)}$. This concludes the first part of the proof which gives us:
for any sequence $(u_\varepsilon, \vec{g}_\varepsilon, Q_\varepsilon, s_\varepsilon, \sigma_\varepsilon) \in \mathcal{D}(\Omega)$ converging to $(u, \vec{g}, Q, s, \sigma) \in L^2(\Omega) \times H(div) \times W^{1,\infty}(\Omega) \times L^\infty(\Omega; [0,1]) \times L^\infty(\Omega; [0,1])$ in $L^1(\Omega) \times H(div) \times W^{1,\infty}(\Omega) \times L^1(\Omega) \times L^1(\Omega)$

(strong convergence in $L^1(\Omega)$, weak convergence in $H(div)$ and weak-$*$ convergence in $W^{1,\infty}(\Omega)$) as $\varepsilon \to 0^+$, we have

$$\liminf_{\varepsilon\to 0^+} \mathcal{F}_\varepsilon(u_\varepsilon, \vec{g}_\varepsilon, Q_\varepsilon, s_\varepsilon, \sigma_\varepsilon) \geq \bar{F}(u, \vec{g}, Q, s, \sigma),$$

with $\bar{F}(u, \vec{g}, Q, s, \sigma) = \bar{F}(u, \vec{g}, Q, s, \sigma)$ if $(u, \vec{g}, Q) \in GSBV^2(\Omega)\times H(div)\times\{Q \in W^{1,\infty}(\Omega) | \int_\Omega Q\, dx = 0\}$, $s \equiv 1$, $\sigma \equiv 1$, and $+\infty$ otherwise.
The second part of the proof is based on the following theorem.

Theorem 2.12 (taken from [2, Theorem 3.2])**.** *Let $(u_\varepsilon, s_\varepsilon, \sigma_\varepsilon) \in W^{2,2}_{loc}(\Omega)\times W^{1,2}(\Omega; [0,1])\times W^{1,2}(\Omega; [0,1])$ be such that $\sup_{\varepsilon>0} \int_\Omega (\sigma_\varepsilon^2 + \kappa_\varepsilon)|\nabla^2 u_\varepsilon|^2\, dx + \mu \int_\Omega |u_\varepsilon - g|^2\, dx + (\alpha-\beta)\mathcal{G}_\varepsilon(s_\varepsilon) + \beta\mathcal{G}_\varepsilon(\sigma_\varepsilon) + \xi_\varepsilon \int_\Omega (s_\varepsilon^2 + \zeta_\varepsilon)|\nabla u_\varepsilon|^\gamma\, dx < +\infty$. Then the family $(u_\varepsilon, s_\varepsilon, \sigma_\varepsilon)$ is relatively compact in the $[L^1(\Omega)]^3$ topology as $\varepsilon \to 0^+$ and any limit point is of the form $(u, 1, 1)$ with $u \in GSBV^2(\Omega) \cap L^2(\Omega)$.*

We will now adapt this result to our problem. So let $(u_\varepsilon, \vec{g}_\varepsilon, Q_\varepsilon, s_\varepsilon, \sigma_\varepsilon) \in \mathcal{D}(\Omega)$ be such that $\sup_{\varepsilon>0} \mathcal{F}_\varepsilon(u_\varepsilon, \vec{g}_\varepsilon, Q_\varepsilon, s_\varepsilon, \sigma_\varepsilon) < +\infty$. Then we can extract a subsequence from $(u_\varepsilon, \vec{g}_\varepsilon, Q_\varepsilon, s_\varepsilon, \sigma_\varepsilon)$ converging to $(u, \vec{g}, Q, 1, 1)$ in $L^1(\Omega)\times H(div)\times W^{1,\infty}(\Omega)\times L^1(\Omega)\times L^1(\Omega)$ (strong convergence in $L^1(\Omega)$, weak convergence in $H(div)$ and weak-$*$ convergence in $W^{1,\infty}(\Omega)$), with $(u, \vec{g}, Q) \in X(\Omega)$ assuming that $\|u_\varepsilon\|_{L^\infty(\Omega)} \leq C_2$ for any $\varepsilon > 0$.
Indeed, the following holds

$$+\infty > \sup_{\varepsilon>0} \mathcal{F}_\varepsilon(u_\varepsilon, \vec{g}_\varepsilon, Q_\varepsilon, s_\varepsilon, \sigma_\varepsilon),$$
$$\forall \varepsilon > 0,\ +\infty > C \geq \||\nabla Q_\varepsilon|\|_{L^\infty(\Omega)}.$$

Since $\forall \varepsilon > 0$, $\int_\Omega Q_\varepsilon\, dx = 0$, then by the Poincaré-Wirtinger inequality we deduce that there exist a subsequence still denoted by (Q_ε) and $Q \in W^{1,\infty}(\Omega)$ such that $Q_\varepsilon \underset{\varepsilon\to 0}{\overset{*}{\rightharpoonup}} Q$ in $W^{1,\infty}(\Omega)$. As weak-$*$ convergence in $W^{1,\infty}(\Omega)$ implies uniform convergence we get that $\int_\Omega Q\, dx = 0$. Furthermore,

$$+\infty > \sup_{\varepsilon>0} \mathcal{F}_\varepsilon(u_\varepsilon, \vec{g}_\varepsilon, Q_\varepsilon, s_\varepsilon, \sigma_\varepsilon),$$
$$\forall \varepsilon > 0,$$
$$+\infty > C \geq \frac{1}{2}\|\mathrm{div}\vec{g}_\varepsilon\|^2_{L^2(\Omega)} - 2\|f\|^2_{L^\infty(\Omega)} meas(\Omega) - 2C_2^2 meas(\Omega) + \frac{\gamma}{4}\||\vec{g}_\varepsilon|\|^2_{L^2(\Omega)} - \frac{\gamma}{2}C^2 meas(\Omega),$$

since $\forall \varepsilon > 0$, $\|u_\varepsilon\|_{L^\infty(\Omega)} \leq C_2 < +\infty$ and $\||\nabla Q_\varepsilon|\|^2_{L^2(\Omega)} \leq \||\nabla Q_\varepsilon|\|^2_{L^\infty(\Omega)} meas(\Omega) \leq C^2 meas(\Omega)$. Thus there exist a subsequence still denoted by $(\vec{g}_\varepsilon)$ and $\vec{g} \in H(div)$ such that $\vec{g}_\varepsilon \underset{\varepsilon\to 0^+}{\rightharpoonup} \vec{g}$ in $H(div)$. Moreover, we get

$$+\infty > \sup_{\varepsilon>0} \mathcal{F}_\varepsilon(u_\varepsilon, \vec{g}_\varepsilon, Q_\varepsilon, s_\varepsilon, \sigma_\varepsilon),$$
$$\geq \sup_{\varepsilon>0} \rho \int_\Omega (\sigma_\varepsilon^2 + \kappa_\varepsilon)|\nabla^2 u_\varepsilon|^2\, dx + \|f - u_\varepsilon - \mathrm{div}\vec{g}_\varepsilon\|^2_{L^2(\Omega)} + (\alpha-\beta)\mathcal{G}_\varepsilon(s_\varepsilon) + \beta\mathcal{G}_\varepsilon(\sigma_\varepsilon),$$

$$\geq \sup_{\varepsilon>0} \rho \int_\Omega (\sigma_\varepsilon^2 + \kappa_\varepsilon)|\nabla^2 u_\varepsilon|^2 \, dx + \frac{1}{2}\|f - u_\varepsilon\|^2_{L^2(\Omega)} - \|\mathrm{div}\vec{g}_\varepsilon\|^2_{L^2(\Omega)} + (\alpha-\beta)\mathcal{G}_\varepsilon(s_\varepsilon) + \beta\mathcal{G}_\varepsilon(\sigma_\varepsilon),$$

$$\geq \sup_{\varepsilon>0} \rho \int_\Omega (\sigma_\varepsilon^2 + \kappa_\varepsilon)|\nabla^2 u_\varepsilon|^2 \, dx + \frac{1}{2}\|f - u_\varepsilon\|^2_{L^2(\Omega)} - 2C - 4\|f\|^2_{L^\infty(\Omega)} meas(\Omega) - 4C_2^2 meas(\Omega)$$

$$- \gamma C^2 meas(\Omega) + (\alpha-\beta)\mathcal{G}_\varepsilon(s_\varepsilon) + \beta\mathcal{G}_\varepsilon(\sigma_\varepsilon).$$

Therefore according to [2, Theorem 3.2], there exist a subsequence of $(u_\varepsilon, s_\varepsilon, \sigma_\varepsilon)$ still denoted by $(u_\varepsilon, s_\varepsilon, \sigma_\varepsilon)$ and $u \in GSBV^2(\Omega) \cap L^2(\Omega)$ such that $(u_\varepsilon, s_\varepsilon, \sigma_\varepsilon) \underset{\varepsilon\to 0}{\longrightarrow} (u, 1, 1)$ strongly in $[L^1(\Omega)]^3$. Since the strong convergence in $L^1(\Omega)$ implies the convergence almost everywhere and that $\|u_\varepsilon\|_{L^\infty(\Omega)} \leq C_2$ for any $\varepsilon > 0$, we can deduce that $\|u\|_{L^\infty(\Omega)} \leq C_2$ and so $(u, \vec{g}, Q) \in X(\Omega)$.
The last part of the proof comes from the following theorem.

Theorem 2.13 (taken from [2, Theorem 3.3])**.** *Assume $n = \gamma = 2$, $\alpha = \beta$ and Ω is strictly star-shaped. Assume that $\kappa_\varepsilon > 0$ and $\kappa_\varepsilon = o(\varepsilon^4)$, while $\xi_\varepsilon = \zeta_\varepsilon = 0$. Then the family $(\tilde{\mathcal{F}}_\varepsilon)$ Γ-converges to $\tilde{\mathcal{F}}$ in the $[L^1(\Omega)]^3$ topology for $\varepsilon \to 0^+$, where $\tilde{\mathcal{F}}_\varepsilon(u_\varepsilon, s_\varepsilon, \sigma_\varepsilon) = \int_\Omega (\sigma_\varepsilon^2 + \kappa_\varepsilon)|\nabla u_\varepsilon|^2 \, dx + \mu \int_\Omega |u_\varepsilon - g|^2 \, dx + (\alpha-\beta)\mathcal{G}_\varepsilon(s_\varepsilon) + \beta\mathcal{G}_\varepsilon(\sigma_\varepsilon) + \xi_\varepsilon \int_\Omega (s_\varepsilon^2 + \zeta_\varepsilon)|\nabla u_\varepsilon|^2 \, dx$ and $\tilde{\mathcal{F}}(u) = \int_\Omega (|\nabla^2 u|^2 + \mu|u-g|^2) \, dx + (\alpha-\beta)\mathcal{H}^1(S_u) + \beta\mathcal{H}^1(S_u \cup S_{\nabla u})$.*

The proof consists in showing the existence of a sequence $(u_\varepsilon, s_\varepsilon, \sigma_\varepsilon) \in \mathcal{D}(\Omega)$ and $u \in GSBV^2(\Omega) \cap L^2(\Omega)$ such that $(u_\varepsilon, s_\varepsilon, \sigma_\varepsilon) \underset{\varepsilon\to 0^+}{\longrightarrow} (u, 1, 1)$ strongly in $[L^1(\Omega)]^3$ and $\limsup_{\varepsilon\to 0^+} \tilde{\mathcal{F}}_\varepsilon(u_\varepsilon, s_\varepsilon, \sigma_\varepsilon) \leq \tilde{\mathcal{F}}(u)$. We are now going to adapt this result to our functional and show that there exist a sequence $(u_\varepsilon, \vec{g}_\varepsilon, Q_\varepsilon, s_\varepsilon, \sigma_\varepsilon) \in \mathcal{D}(\Omega)$ and $(u, \vec{g}, Q) \in X(\Omega)$ such that $(u_\varepsilon, \vec{g}_\varepsilon, Q_\varepsilon, s_\varepsilon, \sigma_\varepsilon) \underset{\varepsilon\to 0^+}{\longrightarrow} (u, \vec{g}, Q, 1, 1)$ in $L^1(\Omega) \times H(div) \times W^{1,\infty}(\Omega) \times L^1(\Omega) \times L^1(\Omega)$ (strong convergence in $L^1(\Omega)$, weak convergence in $H(div)$ and weak-$*$ convergence in $W^{1,\infty}(\Omega)$) and $\limsup_{\varepsilon\to 0^+} \mathcal{F}_\varepsilon(u_\varepsilon, \vec{g}_\varepsilon, Q_\varepsilon, s_\varepsilon, \sigma_\varepsilon) \leq \bar{F}(u, \vec{g}, Q)$.
Let $(u, \vec{g}, Q) \in X(\Omega)$. Actually, we take $\vec{g}_\varepsilon = \vec{g}$ for all $\varepsilon > 0$, and $Q_\varepsilon = Q$ for all $\varepsilon > 0$ so that we neglect the terms $\||\nabla Q|\|_{L^\infty(\Omega)}$ and $\||\nabla Q - \vec{g}|\|^2_{L^2(\Omega)}$ and the remaining problem falls exactly in the framework of [2, Theorem 3.3]. Then the construction of $(u_\varepsilon, s_\varepsilon, \sigma_\varepsilon)$ is exactly the same as the one in [2, Theorem 3.3] which concludes the proof since it ensures that $\forall \varepsilon > 0$, $\|u_\varepsilon\|_{L^\infty(\Omega)} \leq C_2$, $\|u\|_{L^\infty(\Omega)} \leq C_2$ so that $(u_\varepsilon, \vec{g}_\varepsilon, Q_\varepsilon, s_\varepsilon, \sigma_\varepsilon) \in \mathcal{D}(\Omega)$. □

Let us now introduce a nonlocal version of our model.

3 A nonlocal version of the modelling and its theoretical analysis

3.1 Motivations

Inspired by prior related works by Bourgain, Brezis and Mironescu [16] (—first concerned with the study of the limiting behavior of the norms of fractional Sobolev spaces $W^{s,p}$, $0 < s < 1$, $1 < p < \infty$ as $s \to 1$ and to a new characterization of the Sobolev spaces $W^{1,p}$, $1 < p < \infty$—), Aubert and Kornprobst [9] (—they question whether this characterization

can be useful to solve variational problems —), Boulanger and co-authors [15] (—in which the authors address the question of the calculus of variations for nonlocal functionals —), Dávila [28], and Ponce [38] (—dedicated to expressing the semi-norms of first order Sobolev spaces and the BV space thanks to a nonlocal operator —), we introduce a sequence of radial mollifiers $\{\rho_n\}_{n\in\mathbb{N}}$ satisfying: $\forall n \in \mathbb{N}$, $\forall x \in \mathbb{R}$, $\rho_n(x) = \rho_n(|x|)$; $\forall n \in \mathbb{N}$, $\rho_n \geq 0$; $\forall n \in \mathbb{N}$, $\int_{\mathbb{R}} \rho_n(x)\,dx = 1$; $\forall \delta > 0$, $\lim\limits_{n\to+\infty} \int_{\delta}^{+\infty} \rho_n(r)\,dr = 0$, and an associated sequence of functionals $\overline{\mathcal{F}_{\varepsilon,n}}$ depending on n and such that the component $\int_\Omega (v_2^2 + \kappa_\varepsilon)\,|\nabla^2 u|^2\,dx$ is approximated by an integral operator involving a differential quotient and the radial mollifier depicted above. It is shown that the approximated formulation admits minimizers for which regularity results are provided in a fractional Sobolev space. This theoretical study will lead to the derivation of a numerically tractable implementation described in the following section.

This part is thus motivated by the idea of extending the concept of nonlocal gradients ([33]) to higher derivatives, of analyzing its theoretical properties and in particular, its convergence to classical second-order regularizers, and of deriving a nonlocal counterpart of the local model (5.5), with the underlying intention of devising a model numerically tractable and improving the overall quality of the local algorithm (by explaining second-order derivatives of u in terms of nonlocal quantities). Our model is also deeply inspired by [34] dedicated to a formulation of a nonlocal Hessian that combines the ideas of higher-order and nonlocal regularization for image restoration, and more largely to a novel characterization of higher Sobolev and BV-spaces. In this paper, the authors connect in particular the finiteness of $\liminf\limits_{n\to\infty} \int_{\mathbb{R}^N} |\mathfrak{H}_n\,u(x)|^p\,dx$ (—$\mathfrak{H}_n\,u(x) := \frac{N(N+2)}{2} \int_{\mathbb{R}^N} \frac{u(x+h)-2u(x)+u(x-h)}{|h|^2} \frac{h\bigotimes h - \frac{|h|^2}{N+2} I_N}{|h|^2}\,\rho_n(h)\,dh$—) with the inclusion of $u \in L^p(\mathbb{R}^N)$, $1 < p < \infty$, in $W^{2,p}(\mathbb{R}^N)$. They thus introduce a nonlocal Hessian that is derivative free, only requiring the considered function u to belong to an L^p-space. As in [34], our model is derivative free, involving a built-in symmetry that associates triples of points; the main difference lies in the independent treatment of the directional derivatives, yielding a nonlocal version not of $\int_{\mathbb{R}^2} |\nabla^2 u|^2\,dx$, but of $\int_{\mathbb{R}^2} \left(\frac{\partial^2 u}{\partial x_1^2}\right)^2 + \left(\frac{\partial^2 u}{\partial x_2^2}\right)^2 dx$ ($x = (x_1, x_2) \in \mathbb{R}^2$), thus removing the control of the L^2-norm of $\frac{\partial^2 u}{\partial x_1 \partial x_2}$. We will show nevertheless with the theory of tempered distributions that if u, $\frac{\partial^2 u}{\partial x_1^2}$, $\frac{\partial^2 u}{\partial x_2^2} \in L^2(\mathbb{R}^2)$, then $u \in W^{2,2}(\mathbb{R}^2)$. This modelling inherits fine analytical properties, has the advantage of being numerically more tractable compared to [34], particularly in the derivation of the Euler-Lagrange equation satisfied by u, and is straightforwardly connected to our imaging problem, which is not the case in [34].

At last, for the sake of completeness, we refer the interested reader to other papers dealing with higher-order regularizations: [24] (—in which the authors propose higher-order models by means of an infimal convolution of two convex regularizers —), [26] (—in which a weighted version of the Laplacian is provided —), [25] (—introducing the Euler-elastica functional), [17] (—proposing the total generalized variation —), or [11] (—bounded Hessian regularization —).

3.2 Notations and preliminary results

Let (e_1, e_2) be the canonical basis of $\mathbb{R}^2$. We use dx ($x = (x_1, x_2)$) for integration with respect to the Lebesgue measure on $\mathbb{R}^2$ and dt, ds, dh for various integrations with respect to the Lebesgue measure on $\mathbb{R}$. The differentiation indices will be a pair $\alpha = (\alpha_1, \alpha_2)$, where α_i is the order of the partial derivative in the variable x_i, and the total order of the derivative is denoted by $|\alpha| = \alpha_1 + \alpha_2$. We will use the shortened notation $D^\alpha u = \frac{\partial^{|\alpha|} u}{\partial {x_1}^{\alpha_1} \partial {x_2}^{\alpha_2}}$.

Given an integer $j \geq 0$, we define the family of spaces $\mathcal{C}_b^j(\mathbb{R}^2)$ ([29, Definition 2.2.1, p. 69]) by setting

$$\mathcal{C}_b^j(\mathbb{R}^2) = \left\{ u \in \mathcal{C}^j(\mathbb{R}^2) \,|\, \forall \alpha \in \mathbb{N}^2,\, |\alpha| \leq j,\, \exists K_\alpha,\, \|D^\alpha u\|_{L^\infty(\mathbb{R}^2)} \leq K_\alpha \right\}.$$

For a positive real number λ, the subspace $\mathcal{C}_b^{j,\lambda}(\mathbb{R}^2)$ consists of the functions in $\mathcal{C}_b^j(\mathbb{R}^2)$ such that if $|\alpha| \leq j$, then

$$\exists C_{\alpha,\lambda},\, \forall x, y \in \mathbb{R}^2,\, |D^\alpha u(x) - D^\alpha u(y)| \leq C_{\alpha,\lambda}\, |x - y|^\lambda.$$

At last, the properties of the considered kernel ρ_n are those depicted above, and we will use several times the following generalized result of Spector ([40, p. 58]):

Lemma 3.1. *If $E \subset \mathbb{R}$ is bounded and measurable, then $\forall p \in \mathbb{N}^*$,*

$$\lim_{n \to +\infty} \int_E |x|^p \, \rho_n(x)\, dx = 0. \tag{5.6}$$

Proof. Fixing $\delta > 0$,

$$\begin{aligned}
\limsup_{n \to +\infty} \int_E |x|^p \, \rho_n(x)\, dx \leq & \limsup_{n \to +\infty} \int_{\{|x| > \delta\} \cap E} |x|^p \, \rho_n(x)\, dx \\
& + \limsup_{n \to +\infty} \int_{\{|x| \leq \delta\}} |x|^p \, \rho_n(x)\, dx, \\
\leq & C_{\delta,E,p} \lim_{n \to +\infty} \int_{|x| > \delta} \rho_n(x)\, dx + \delta^p.
\end{aligned}$$

The result follows from the properties of ρ_n and by sending δ to 0. □

Equipped with this material, we now propose a derivative free nonlocal formulation of the L^2-norms $\int_{\mathbb{R}^2} |D^{(2,0)}u|^2\, dx$ and $\int_{\mathbb{R}^2} |D^{(0,2)}u|^2\, dx$ respectively. We start off with the definition of such a nonlocal version for smooth functions.

Theorem 3.1. *Let $u \in \mathcal{C}_c^4(\mathbb{R}^2)$. Then*

$$\begin{aligned}
& \int_{\mathbb{R}^2} \int_{\mathbb{R}} \frac{|u(x + he_i) - 2u(x) + u(x - he_i)|^2}{|h|^4} \, \rho_n(h)\, dh\, dx \\
& \underset{n \to +\infty}{\longrightarrow} \begin{cases} \int_{\mathbb{R}^2} |D^{(2,0)}u|^2\, dx & \text{if } i = 1 \\ \int_{\mathbb{R}^2} |D^{(0,2)}u|^2\, dx & \text{if } i = 2 \end{cases}.
\end{aligned}$$

Proof. We deal with the case $i = 1$.
Let us define $H_1u(x) := \displaystyle\int_{\mathbb{R}} \frac{|u(x+he_1) - 2u(x) + u(x-he_1)|^2}{|h|^4}\,\rho_n(h)\,dh$. Let $R > 0$ be fixed.

$$\begin{aligned} H_1u(x) = &\int_{\{|h|\le R\}} \frac{|u(x+he_1) - 2u(x) + u(x-he_1)|^2}{|h|^4}\,\rho_n(h)\,dh \\ &+ \int_{\{|h|>R\}} \frac{|u(x+he_1) - 2u(x) + u(x-he_1)|^2}{|h|^4}\,\rho_n(h)\,dh. \end{aligned}$$

But $u(x+he_1) - 2u(x) + u(x-he_1) = h^2 \int_0^1 \int_0^1 D^{(2,0)}u(x+h(s+t-1)e_1)\,dt\,ds$ and from Taylor's expansion $\frac{u(x+he_1)-2u(x)+u(x-he_1)}{h^2} = D^{(2,0)}u(x) + \frac{h^2}{12}\,D^{(4,0)}\,u(\zeta_{x_1,h}, x_2)$, so that

$$\begin{aligned} &\int_{\{|h|>R\}} \left[\int_0^1 \int_0^1 D^{(2,0)}u(x+h(s+t-1)e_1)\,dt\,ds\right]^2 \rho_n(h)\,dh \\ &\le \|D^{(2,0)}u\|^2_{L^\infty(\mathbb{R}^2)} \int_{\{|h|>R\}} \rho_n(h)\,dh \underset{n\to+\infty}{\longrightarrow} 0. \end{aligned}$$

Using the previous Taylor's expansion, the properties of ρ_n and lemma 3.1 yields

$$\int_{\{|h|\le R\}} \frac{|u(x+he_1) - 2u(x) + u(x-he_1)|^2}{|h|^4}\,\rho_n(h)\,dh \underset{n\to+\infty}{\longrightarrow} |D^{(2,0)}u(x)|^2$$

and therefore $H_1u(x)$ converges to $|D^{(2,0)}u(x)|^2$ everywhere. We now aim to prove that $\int_{\mathbb{R}^2} |H_1u(x) - |D^{(2,0)}u(x)|^2|\,dx \underset{n\to+\infty}{\longrightarrow} 0$. We assume without loss of generality that $\operatorname{supp} u \subset B(0,R)$. We first show that $\forall \epsilon > 0$, $\exists L = L(\epsilon) > 1$ such that

$$\sup_{n\in\mathbb{N}} \int_{B(0,LR)^c} |H_1u(x)|\,dx \le \epsilon.$$

One has, making a change of variable,

$$\begin{aligned} &\int_{B(0,LR)^c} |H_1u(x)|\,dx \\ &= \int_{B(0,LR)^c} \int_{\mathbb{R}} \frac{|u(x+he_1) + u(x-he_1)|^2}{|h|^4}\,\rho_n(h)\,dh\,dx, \\ &\le 2\int_{B(0,LR)^c} \int_{\mathbb{R}} \frac{|u(x+he_1)|^2 + |u(x-he_1)|^2}{|h|^4}\,\rho_n(h)\,dh\,dx, \\ &\le 4\int_{B(0,LR)^c} \int_{\{h\,|\,x+he_1\in B(0,R)\}} \frac{|u(x+he_1)|^2}{|h|^4}\,\rho_n(h)\,dh\,dx, \\ &\le \frac{4}{(L-1)^4R^4} \int_{B(0,LR)^c} \int_{\{h\,|\,x+he_1\in B(0,R)\}} |u(x+he_1)|^2\,\rho_n(h)\,dh\,dx, \\ &\le \frac{4}{(L-1)^4R^4}\,\|u\|^2_{L^2(\mathbb{R}^2)}\,\|\rho_n\|_{L^1(\mathbb{R})} = \frac{4}{(L-1)^4R^4}\,\|u\|^2_{L^2(\mathbb{R}^2)}. \end{aligned}$$

Thus $\forall \epsilon > 0$, $\exists L = L(\epsilon) > 1$, $\forall n \in \mathbb{N}$, $\int_{B(0,LR)^c} |H_1 u(x)|\, dx \leq \epsilon$, which means

$$\sup_{n\in\mathbb{N}} \int_{B(0,LR)^c} |H_1 u(x)|\, dx \leq \epsilon.$$

As

$$\begin{aligned}\int_{\mathbb{R}^2} |H_1 u(x) - |D^{(2,0)}u(x)|^2|\, dx = &\int_{B(0,LR)} |H_1 u(x) - |D^{(2,0)}u(x)|^2|\, dx \\ &+ \int_{B(0,LR)^c} |H_1 u(x)|\, dx,\end{aligned}$$

$$\limsup_{n\to+\infty} \int_{\mathbb{R}^2} |H_1 u(x) - |D^{(2,0)}u(x)|^2|\, dx \leq \limsup_{n\to+\infty} \int_{B(0,LR)} |H_1 u(x) - |D^{(2,0)}u(x)|^2|\, dx + \epsilon.$$

Now, $H_1 u$ converges pointwise to $|D^{(2,0)}u(x)|^2$ and on $B(0, LR)$, $H_1 u(x) \leq \|D^{(2,0)}u\|^2_{L^\infty(\mathbb{R}^2)}$, which is integrable on $B(0, LR)$. It follows from the dominated convergence theorem that

$$\int_{B(0,LR)} |H_1 u(x) - |D^{(2,0)}u(x)|^2|\, dx \underset{n\to+\infty}{\longrightarrow} 0,$$

yielding

$$\limsup_{n\to+\infty} \int_{\mathbb{R}^2} |H_1 u(x) - |D^{(2,0)}u(x)|^2|\, dx \leq \epsilon,$$

and in the end,

$$\lim_{n\to+\infty} \int_{\mathbb{R}^2} |H_1 u(x) - |D^{(2,0)}u(x)|^2|\, dx = 0.$$

□

In fact, we have an analogous convergence result for $u \in W^{2,2}(\mathbb{R}^2)$ that we establish with the following lemma.

Lemma 3.2. *Suppose that* $u \in W^{2,2}(\mathbb{R}^2)$. *Then* $\int_{\mathbb{R}^2}\int_{\mathbb{R}} \frac{|u(x+he_i) - 2u(x) + u(x-he_i)|^2}{|h|^4}$ $\rho_n(h)\, dh\, dx$ *is well-defined and*

$$\int_{\mathbb{R}^2}\int_{\mathbb{R}} \frac{|u(x+he_i) - 2u(x) + u(x-he_i)|^2}{|h|^4}\rho_n(h)\, dh\, dx \leq \begin{cases} \|D^{(2,0)}u\|^2_{L^2(\mathbb{R}^2)} & \text{if } i = 1 \\ \|D^{(0,2)}u\|^2_{L^2(\mathbb{R}^2)} & \text{if } i = 2 \end{cases}.$$

Proof. We focus on the case $i = 1$.
Let us begin by estimates for a function $u \in \mathcal{C}^\infty(\mathbb{R}^2) \cap W^{2,2}(\mathbb{R}^2)$. Using Fubini-Tonelli's

theorem and Jensen's inequality,

$$\begin{aligned}
&\int_{\mathbb{R}^2}\int_{\mathbb{R}} \frac{|u(x+he_1)-2u(x)+u(x-he_1)|^2}{|h|^4}\rho_n(h)\,dh\,dx\\
&\leq \int_{\mathbb{R}^2}\int_{\mathbb{R}} \left[\int_0^1\int_0^1 |D^{(2,0)}u(x+(t+s-1)he_1)|^2\,ds\,dt\right]\rho_n(h)\,dh\,dx,\\
&\leq \|D^{(2,0)}u\|^2_{L^2(\mathbb{R}^2)}.
\end{aligned}$$

Consider now a sequence $(u_k)_{k\in\mathbb{N}}$ in $\mathcal{C}^\infty(\mathbb{R}^2)\cap W^{2,2}(\mathbb{R}^2)$ approximating u in $W^{2,2}(\mathbb{R}^2)$ (see [29, Proposition 2.12, p. 60] for a density result). From the above,

$$\int_{\mathbb{R}^2}\int_{\mathbb{R}} \frac{|u_k(x+he_1)-2u_k(x)+u_k(x-he_1)|^2}{|h|^4}\rho_n(h)\,dh\,dx \leq \|D^{(2,0)}u_k\|^2_{L^2(\mathbb{R}^2)}.$$

As $(u_k)_{k\in\mathbb{N}}$ converges to u in $W^{2,2}(\mathbb{R}^2)\circlearrowleft \mathcal{C}_b^{0,\lambda}(\mathbb{R}^2)$ for every $\lambda<1$ ([29, Theorem 2.31, p. 69]), $(u_k)_{k\in\mathbb{N}}$ uniformly converges to u, so pointwise everywhere. Fatou's lemma allows us to conclude that

$$\begin{aligned}
&\int_{\mathbb{R}} \frac{|u(x+he_1)-2u(x)+u(x-he_1)|^2}{|h|^4}\rho_n(h)\,dh\\
&\leq \liminf_{k\to+\infty}\int_{\mathbb{R}} \frac{|u_k(x+he_1)-2u_k(x)+u_k(x-he_1)|^2}{|h|^4}\rho_n(h)\,dh,
\end{aligned}$$

and

$$\begin{aligned}
&\int_{\mathbb{R}^2}\int_{\mathbb{R}} \frac{|u(x+he_1)-2u(x)+u(x-he_1)|^2}{|h|^4}\rho_n(h)\,dh\,dx\\
&\leq \int_{\mathbb{R}^2}\liminf_{k\to+\infty}\int_{\mathbb{R}} \frac{|u_k(x+he_1)-2u_k(x)+u_k(x-he_1)|^2}{|h|^4}\rho_n(h)\,dh\,dx.
\end{aligned}$$

Setting $F_k(x) := \displaystyle\int_{\mathbb{R}} \frac{|u_k(x+he_1)-2u_k(x)+u_k(x-he_1)|^2}{|h|^4}\rho_n(h)\,dh$, $(F_k)_{k\in\mathbb{N}}$ is a sequence of functions of $L^1(\mathbb{R}^2)$ such that $\sup_k \int_{\mathbb{R}^2} F_k < \infty$, so applying Fatou's lemma a second time yields

$$\begin{aligned}
&\int_{\mathbb{R}^2}\int_{\mathbb{R}} \frac{|u(x+he_1)-2u(x)+u(x-he_1)|^2}{|h|^4}\rho_n(h)\,dh\,dx\\
&\leq \liminf_{k\to+\infty}\int_{\mathbb{R}^2}\int_{\mathbb{R}} \frac{|u_k(x+he_1)-2u_k(x)+u_k(x-he_1)|^2}{|h|^4}\rho_n(h)\,dh\,dx,\\
&\leq \liminf_{k\to+\infty} \|D^{(2,0)}u_k\|^2_{L^2(\mathbb{R}^2)} = \|D^{(2,0)}u\|^2_{L^2(\mathbb{R}^2)}.
\end{aligned}$$

□

With this preliminary lemma, we now state the main result.

Theorem 3.2. *Let $u \in W^{2,2}(\mathbb{R}^2)$. Then*

$$\int_{\mathbb{R}^2}\int_{\mathbb{R}} \frac{|u(x+he_i)-2u(x)+u(x-he_i)|^2}{|h|^4}\rho_n(h)\,dh\,dx \underset{n\to+\infty}{\longrightarrow} \begin{cases} \|D^{(2,0)}u\|^2_{L^2(\mathbb{R}^2)} & \text{if } i=1, \\ \|D^{(0,2)}u\|^2_{L^2(\mathbb{R}^2)} & \text{if } i=2 \end{cases}.$$

Proof. We restrict ourselves to the case $i=1$.
Let $\epsilon>0$. By density, there exists $v_\epsilon \in \mathcal{C}^\infty_c(\mathbb{R}^2)$ such that

$$\|D^{(2,0)}u - D^{(2,0)}v_\epsilon\|_{L^2(\mathbb{R}^2)} \le \epsilon.$$

Let us set $u_n(x,h) = \frac{u(x+he_1)-2u(x)+u(x-he_1)}{h^2}\,\rho_n^{\frac{1}{2}}(h)$. $u_n \in L^2(\mathbb{R}^2\times\mathbb{R})$ and $\|u_n\|_{L^2(\mathbb{R}^2\times\mathbb{R})} \le \|D^{(2,0)}u\|_{L^2(\mathbb{R}^2)}$. Denoting by $v_{n,\epsilon} := \frac{v_\epsilon(x+he_1)-2v_\epsilon(x)+v_\epsilon(x-he_1)}{h^2}\,\rho_n^{\frac{1}{2}}(h)$, we thus have

$$\|u_n - v_{n,\epsilon}\|_{L^2(\mathbb{R}^2\times\mathbb{R})} \le \|D^{(2,0)}u - D^{(2,0)}v_\epsilon\|_{L^2(\mathbb{R}^2)} \le \epsilon,$$

and from the second triangle inequality,

$$\left|\|u_n\|_{L^2(\mathbb{R}^2\times\mathbb{R})} - \|v_{n,\epsilon}\|_{L^2(\mathbb{R}^2\times\mathbb{R})}\right| \le \epsilon.$$

To conclude,

$$\begin{aligned}\left|\|u_n\|_{L^2(\mathbb{R}^2\times\mathbb{R})} - \|D^{(2,0)}u\|_{L^2(\mathbb{R}^2)}\right| &\le \left|\|u_n\|_{L^2(\mathbb{R}^2\times\mathbb{R})} - \|v_{n,\epsilon}\|_{L^2(\mathbb{R}^2\times\mathbb{R})}\right| \\ &\quad + \left|\|v_{n,\epsilon}\|_{L^2(\mathbb{R}^2\times\mathbb{R})} - \|D^{(2,0)}v_\epsilon\|_{L^2(\mathbb{R}^2)}\right| \\ &\quad + \left|\|D^{(2,0)}v_\epsilon\|_{L^2(\mathbb{R}^2)} - \|D^{(2,0)}u\|_{L^2(\mathbb{R}^2)}\right|, \\ &\le 2\epsilon + \left|\|v_{n,\epsilon}\|_{L^2(\mathbb{R}^2\times\mathbb{R})} - \|D^{(2,0)}v_\epsilon\|_{L^2(\mathbb{R}^2)}\right|.\end{aligned}$$

It leads to $\limsup_{n\to+\infty}\left|\|u_n\|_{L^2(\mathbb{R}^2\times\mathbb{R})} - \|D^{(2,0)}u\|_{L^2(\mathbb{R}^2)}\right| \le 2\epsilon$ and then $\|u_n\|_{L^2(\mathbb{R}^2\times\mathbb{R})} \underset{n\to+\infty}{\longrightarrow} \|D^{(2,0)}u\|_{L^2(\mathbb{R}^2)}$. □

Equipped with these theoretical results and characterization, we reformulate our local problem into a nonlocal form.

3.3 Connection to the local imaging problem

Owing to the independent treatment of the directional derivatives in the previous nonlocal formulations, we slightly modify the local problem into

$$\begin{aligned}\inf \overline{\mathcal{F}_\varepsilon}(u,\vec{g},Q,v_1,v_2) = {} & \|f-u-\operatorname{div}\vec{g}\|^2_{L^2(\Omega)} + \mu\,\||\nabla Q|\|_{L^\infty(\Omega)} \\ & + \frac{\gamma}{2}\,\||\vec{g}-\nabla Q|\|^2_{L^2(\Omega)} \\ & + \rho\int_\Omega (v_2^2+\kappa_\varepsilon)\left(|D^{(2,0)}u|^2 + |D^{(0,2)}u|^2\right)dx \\ & + \xi_\varepsilon\int_\Omega (v_1^2+\zeta_\epsilon)\,|\nabla u|^2\,dx + (\alpha-\beta)\,\mathcal{G}_\varepsilon(v_1) + \beta\,\mathcal{G}_\varepsilon(v_2). \qquad (5.7)\end{aligned}$$

While the functional spaces for Q, $\vec{g}$, and v_1 are unchanged, the unknowns u and v_2 are now searched in the functional spaces $W_0^{1,2}(\Omega) \cap W^{2,2}(\Omega)$ and $\left\{v_2 \in W^{1,2}(\Omega,[0,1]) \,|\, \gamma_0\, v_2 = 1\right\}$ respectively, γ_0 denoting the trace operator. The reasons for such requirements will be made clearer in the following. Nevertheless, these assumptions are reasonable and not restrictive if we assume for instance that the observed image f is with compact support. Existence of minimizers is still guaranteed as stated below.

Theorem 3.3. *Let Ω be a regular bounded open subset of $\mathbb{R}^2$. With $\kappa_\varepsilon, \xi_\varepsilon, \zeta_\varepsilon > 0$, problem (5.7) admits minimizers $(\overline{u} = \overline{u_\varepsilon}, \overline{\vec{g}} = \overline{\vec{g_\varepsilon}}, \overline{Q} = \overline{Q_\varepsilon}, \overline{v_1} = \overline{v_{1,\varepsilon}}, \overline{v_2} = \overline{v_{2,\varepsilon}})$ on $W_0^{1,2}(\Omega) \cap W^{2,2}(\Omega) \times H(div) \times \left\{Q \in W^{1,\infty}(\Omega) \,|\, \int_\Omega Q\, dx = 0\right\} \times W^{1,2}(\Omega,[0,1]) \times \left\{v_2 \in W^{1,2}(\Omega,[0,1]) \,|\, \gamma_0\, v_2 = 1\right\}$.*

Proof. The proof rests upon two major facts: (i) the space $W_0^{1,2}(\Omega)$ is a strongly closed convex subspace of $W^{1,2}(\Omega)$ by continuity of the trace map, so according to [18, Theorem III.7, p. 38], it is a weakly closed convex subspace. (ii) the mapping $\widehat{\|\cdot\|} : u \mapsto \left(\|D^{(2,0)}u\|^2_{L^2(\Omega)} + \|D^{(0,2)}u\|^2_{L^2(\Omega)}\right)^{\frac{1}{2}}$ is a norm on $W_0^{1,2}(\Omega) \cap W^{2,2}(\Omega)$ equivalent to the usual norm on $W^{2,2}(\Omega)$ that we denote by $\|\cdot\|_{2,\Omega}$. The homogeneity axiom as well as the triangle inequality are straightforwardly obtained. Let $u \in W_0^{1,2}(\Omega) \cap W^{2,2}(\Omega)$ be such that $\widehat{\|u\|} = 0$. Then from Green's formula, $\int_\Omega |\nabla u|^2\, dx = 0$ and from Poincaré's inequality, $u = 0$ almost everywhere on Ω.
Now let us denote by $\mathcal{A}$ the mapping $\mathcal{A} : W_0^{1,2}(\Omega) \cap W^{2,2}(\Omega) \to L^2(\Omega)$ such that $\forall u \in W_0^{1,2}(\Omega) \cap W^{2,2}(\Omega)$, $\mathcal{A}(u) = \Delta u$. For every $f \in L^2(\Omega)$, let us introduce the unique solution (Lax-Milgram theorem) $u \in W_0^{1,2}(\Omega)$ of the variational problem: $\forall v \in W_0^{1,2}(\Omega)$,

$$\int_\Omega \langle \nabla u, \nabla v \rangle_{\mathbb{R}^2}\, dx = -\int_\Omega f\, v\, dx.$$

As the boundary of Ω is sufficiently smooth, a regularity result (see [18, Section IX.6, p. 181] for instance) gives that $u \in W^{2,2}(\Omega)$. As $\Delta u = f$, it follows that $\mathcal{A}$ (which is a continuous mapping since $\|\Delta u\|_{L^2(\Omega)} \leq \sqrt{2}\, \|u\|_{2,\Omega}$) is a bijection from $W_0^{1,2}(\Omega) \cap W^{2,2}(\Omega)$ to $L^2(\Omega)$. The bounded inverse theorem enables us to conclude that the inverse mapping is continuous as well, implying the existence of a constant $C > 0$ such that $\forall u \in W_0^{1,2}(\Omega) \cap W^{2,2}(\Omega)$, $\|u\|_{2,\Omega} \leq C\, \|\Delta u\|_{L^2(\Omega)} \leq \sqrt{2} C\, \widehat{\|u\|}$. □

Our mathematical material being formulated on $\mathbb{R}^2$ rather than Ω, in our nonlocal model, we propose searching for u in a subspace of $W_0^{1,2}(\Omega)$ and for v_2 in $W^{1,2}(\Omega,[0,1])$ such that $\gamma_0\, v_2 = 1$.

Theorem 3.4. *Let Ω be a regular bounded open subset of $\mathbb{R}^2$ with boundary of class $\mathcal{C}^2$. Let us assume that the functions $t \mapsto \rho_n(t)$, $t \mapsto t^q \rho_n(t)$ are non-increasing for $t \geq 0$ and $q \in]0,1[$. (Such a function ρ_n exists : for instance, with $q \in]0,1[$, $\rho(t) = \frac{e^{-|t|}}{|t|^q}$ and*

$\rho_n(t) = C\,n\,\rho(nt)$ *with* $C = \frac{1}{\int_{\mathbb{R}} \rho(t)\,dt}$*). With* $\kappa_\varepsilon, \xi_\varepsilon, \zeta_\varepsilon > 0$*, for any* $n \in \mathbb{N}^*$*, problem*

$$\begin{aligned}\inf \overline{\mathcal{F}_{\varepsilon,n}}(u,\vec{g},Q,v_1,v_2) = {} & \|f - u - div\,\vec{g}\|^2_{L^2(\Omega)} + \mu\,\||\nabla Q|\|_{L^\infty(\Omega)} \\ & + \rho \int_{\mathbb{R}^2} (v_{2,e}^2(x) + \kappa_\varepsilon) \sum_{i=1}^{2} \int_{\mathbb{R}} \frac{|u_e(x+he_i) - 2u_e(x) + u_e(x-he_i)|^2}{|h|^4} \rho_n(h)\,dh \\ & + \frac{\gamma}{2}\,\||\vec{g} - \nabla Q|\|^2_{L^2(\Omega)} + \xi_\varepsilon \int_\Omega (v_1^2 + \zeta_\epsilon)\,|\nabla u|^2\,dx + (\alpha - \beta)\,\mathcal{G}_\varepsilon(v_1) + \beta\,\mathcal{G}_\varepsilon(v_2), \qquad (5.8)\end{aligned}$$

where $v_{2,e}$ *and* u_e *are respectively the extensions of* v_2 *according to [18, Theorem IX.7, p. 158] —by construction,* $0 \le v_{2,e} \le 1$ *a.e. — and of* u *on* $\mathbb{R}^2$ *by* 0 *(—with the regularity assumed on* Ω*,* $v_{2,e}$ *and* u_e *are in* $W^{1,2}(\mathbb{R}^2)$ *—), admits minimizers* $(\overline{u_n} = \overline{u_{\varepsilon,n}}, \overrightarrow{\overline{g_n}} = \overrightarrow{\overline{g_{\varepsilon,n}}}, \overline{Q_n} = \overline{Q_{\varepsilon,n}}, \overline{v_{1,n}} = \overline{v_{1,\varepsilon,n}}, \overline{v_{2,n}} = \overline{v_{2,\varepsilon,n}})$ *on* $W_0^{1,2}(\Omega) \cap W^{s,2}(\Omega) \times H(div) \times \left\{Q \in W^{1,\infty}(\Omega) \,|\, \int_\Omega Q\,dx = 0\right\} \times W^{1,2}(\Omega,[0,1]) \times \left\{v_2 \in W^{1,2}(\Omega,[0,1]) \,|\, \gamma_0\, v_2 = 1\right\}$*, with* $s \in \left[\frac{3}{2}, 2\right[$.

Proof. The functional is proper, take $v_1 \equiv 1$, $v_2 \equiv 1$, $\vec{g} \equiv \vec{0}$, $Q \equiv 0$, and $u \equiv 0$, since f is assumed to be sufficiently smooth (i.e. at least $L^2(\Omega)$) on Ω which is bounded. Let us now consider a minimizing sequence $(u_n^l, \vec{g_n}^l, Q_n^l, v_{1,n}^l, v_{2,n}^l)$ on $W_0^{1,2}(\Omega) \times H(div) \times \left\{Q \in W^{1,\infty}(\Omega) \,|\, \int_\Omega Q\,dx = 0\right\} \times W^{1,2}(\Omega,[0,1]) \times \left\{v_2 \in W^{1,2}(\Omega,[0,1]) \,|\, \gamma_0\, v_2 = 1\right\}$ (the dependency on ε is not explicitly mentioned here for compactness). We will show that in fact, $u_n^l \in W_0^{1,2}(\Omega) \cap W^{s,2}(\Omega)$.

1. **Extraction of convergent subsequences**:
   - $\overline{\mathcal{F}_{\varepsilon,n}}(u_n^l, \vec{g_n}^l, Q_n^l, v_{1,n}^l, v_{2,n}^l) \ge \mu\,\||\nabla Q_n^l|\|_{L^\infty(\Omega)}$. As $\int_\Omega Q_n^l\,dx = 0$ for all $l \in \mathbb{N}$, we can use Poincaré-Wirtinger inequality, which leads us to the existence of a subsequence of (Q_n^l) still denoted by (Q_n^l) weakly-$*$ converging to $\overline{Q_n}$ in $W^{1,\infty}(\Omega)$. As the weak-$*$ convergence in $W^{1,\infty}(\Omega)$ implies uniform convergence, $\int_\Omega \overline{Q_n}(x)\,dx = 0$.
   - $\overline{\mathcal{F}_{\varepsilon,n}}(u_n^l, \vec{g_n}^l, Q_n^l, v_{1,n}^l, v_{2,n}^l) \ge (\alpha - \beta)\varepsilon\|\nabla v_{1,n}^l\|^2_{L^2(\Omega)}$. By noticing that $v_{1,n}^l \in L^\infty(\Omega)$ with $0 \le v_{1,n}^l \le 1$ a.e., $\int_\Omega v_{1,n}^l\,dx \le 1$ and Poincaré-Wirtinger inequality gives us the existence of a subsequence of $(v_{1,n}^l)$ still denoted by $(v_{1,n}^l)$ weakly converging to $\overline{v_{1,n}}$ in $W^{1,2}(\Omega)$. Since $W^{1,2}(\Omega) \underset{c}{\circlearrowleft} L^2(\Omega)$, $(v_{1,n}^l)$ strongly converges to $\overline{v_{1,n}}$ in $L^2(\Omega)$ and so pointwise almost everywhere up to a subsequence. We deduce that $\overline{v_{1,n}} \in W^{1,2}(\Omega,[0,1])$.
   - In the same way, we have $(v_{2,n}^l)$ weakly converging to $\overline{v_{2,n}}$ in $W^{1,2}(\Omega)$ with $\overline{v_{2,n}} \in W^{1,2}(\Omega,[0,1])$ and $\gamma_0\,\overline{v_{2,n}} = 1$ by continuity of the trace operator.
   - $\overline{\mathcal{F}_{\varepsilon,n}}(u_n^l, \vec{g_n}^l, Q_n^l, v_{1,n}^l, v_{2,n}^l) \ge \xi_\varepsilon\zeta_\varepsilon\|\nabla u_n^l\|^2_{L^2(\Omega)}$. By Poincaré inequality and the continuity of the trace operator, we get the existence of a subsequence of (u_n^l) still denoted by (u_n^l) weakly converging to $\overline{u_n} \in W_0^{1,2}(\Omega)$ in $W^{1,2}(\Omega)$.

Let us set $E_n^l(h) = \int_{\mathbb{R}^2} |u_{n,e}^l(x+he_1) - 2u_{n,e}^l(x) + u_{n,e}^l(x-he_1)|^2\,dx$ where $u_{n,e}^l$ denotes the extension by 0 of u_n^l on $\mathbb{R}^2$. Here again, due to the assumption on Ω, $u_{n,e}^l$ belongs to $W^{1,2}(\mathbb{R}^2)$. One can prove that $E_n^l(2h) \leq 16E_n^l(h)$. By using Fubini-Tonelli theorem, we have $\displaystyle\int_{\mathbb{R}^2}\int_{\mathbb{R}} \frac{|u_{n,e}^l(x+he_1) - 2u_{n,e}^l(x) + u_{n,e}^l(x-he_1)|^2}{|h|^4}$ $\rho_n(h)\,dh\,dx = \displaystyle\int_{\mathbb{R}} \frac{E_n^l(h)}{|h|^4}\rho_n(h)\,dh = 2\int_0^\infty \frac{E_n^l(h)}{|h|^4}\,\rho_n(h)\,dh \leq \overline{\mathcal{F}_{\varepsilon,n}}(u_n^l, \vec{g}_n^l, Q_n^l, v_{1,n}^l,$ $v_{2,n}^l)$. We then apply [9, Lemma 3.2] by taking $M = \delta = 1$, $g(t) = \dfrac{E_n^l(t)}{t^{q+1}}$, $k(t) = t^{q-3}\rho_n(t)$ and we get:

$$\int_0^1 \frac{E_n^l(h)}{|h|^4}\rho_n(h)\,dh \geq C(1)\int_0^1 \frac{E_n^l(t)}{|t|^{q+1}}\,dt \int_0^1 t^{q-3}\rho_n(t)\,dt.$$

(We will see further that the condition of monotonicity on k is fulfilled). We now need g to verify the assumption of this lemma, that is to say, $g(\frac{t}{2}) \geq g(t)$. We know that $g(\frac{t}{2}) = \dfrac{E_n^l(\frac{t}{2})2^{q+1}}{t^{q+1}} \geq 2^{q-3}g(t)$. Thus if $q \geq 3$, this condition is fulfilled. By using the properties of ρ_n, we deduce first that $\displaystyle\int_0^1 \frac{E_n^l(t)}{|t|^{q+1}}\,dt \leq C$ with C independent of l. Then $\displaystyle\int_1^\infty \frac{E_n^l(t)}{|t|^{q+1}}\,dt \leq C'\,\|u_{n,e}^l\|_{L^2(\mathbb{R}^2)}^2 \int_1^\infty \frac{dt}{|t|^{q+1}}$, C' being a constant and the last integral being convergent since $q \geq 3$, resulting in the uniform boundedness of $\displaystyle\int_0^\infty \frac{E_n^l(t)}{|t|^{q+1}}\,dt$. Besides, $\displaystyle\int_{\mathbb{R}} \frac{E_n^l(t)}{|t|^{q+1}}\,dt =$ $\displaystyle\int_{\mathbb{R}} \frac{1}{|h|^{q+1}}\int_{\mathbb{R}^2} |u_{n,e}^l(x+he_1) - 2u_{n,e}^l(x) + u_{n,e}^l(x-he_1)|^2\,dx\,dh = \int_{\mathbb{R}} \frac{1}{|h|^{q+1}}\|\tau_{he_1}u_{n,e}^l -$ $2u_{n,e}^l + \tau_{-he_1}u_{n,e}^l\|_{L^2(\mathbb{R}^2)}^2\,dh = \displaystyle\int_{\mathbb{R}} \frac{1}{|h|^{q+1}}\int_{\mathbb{R}^2} |e^{2i\pi h\xi_1} - 2 + e^{-2i\pi h\xi_1}|^2 |\mathcal{F}(u_{n,e}^l)(\xi)|^2\,d\xi\,dh$ by Plancherel theorem ($\tau_\cdot$ denoting the usual translation operator). Then one can prove that $\displaystyle\int_{\mathbb{R}} \frac{E_n^l(t)}{|t|^{q+1}}\,dt = C''\int_{\mathbb{R}^2} |\mathcal{F}(u_{n,e}^l)(\xi)|^2 |\xi_1|^q \int_{\mathbb{R}} \frac{\sin^4(u)}{|u|^{q+1}}\,du\,d\xi \leq C$, (the constant C may change line to line). The generalized integral in u converges if and only if $q \in [3,4[$. By using the same arguments in the other direction (e_2), we get that $|\xi|^{\frac{q}{2}}\mathcal{F}(u_{n,e}^l) \in L^2(\mathbb{R}^2)$ and so $u_{n,e}^l \in H^{\frac{q}{2}}(\mathbb{R}^2)$ (being a Hilbert space) and is uniformly bounded for the associated norm with $q \in [3,4[$. There exists a subsequence still denoted by $(u_{n,e}^l)$ weakly converging to $\tilde{u}_n$ in $H^s(\mathbb{R}^2)$ with $s = \frac{q}{2}$. Besides, we know that $u_{n,e}^l = u_n^l$ on Ω and $D^{(1,0)}u_{n,e}^l = (D^{(1,0)}u_n^l)_e = D^{(1,0)}u_n^l$ on Ω, and $D^{(0,1)}u_{n,e}^l = (D^{(0,1)}u_n^l)_e = D^{(0,1)}u_n^l$ on Ω. Thus, $\|u_n^l\|_{W^{s,2}(\Omega)}^2 = \|u_n^l\|_{W^{1,2}(\Omega)}^2 + \displaystyle\int_\Omega\int_\Omega \frac{|\nabla u_n^l(x) - \nabla u_n^l(y)|^2}{|x-y|^{2s}}\,dx\,dy \leq C$ $+ \displaystyle\int_{\mathbb{R}^2}\int_{\mathbb{R}^2} \frac{|\nabla u_{n,e}^l(x) - \nabla u_{n,e}^l(y)|^2}{|x-y|^{2s}}\,dx\,dy$ with C independent of l. From [29,

Lemma 4.33, p. 200], we know that $\int_{\mathbb{R}^2}\int_{\mathbb{R}^2} \frac{|\nabla u^l_{n,e}(x)-\nabla u^l_{n,e}(y)|^2}{|x-y|^{2s}}\,dx\,dy < \infty \Leftrightarrow \int_{\mathbb{R}}\int_{\mathbb{R}^2} \frac{|\nabla u^l_{n,e}(x)-\nabla u^l_{n,e}(x+he_1)|^2}{|h|^{2s-1}}\,dx\,dh < \infty$ and $\int_{\mathbb{R}}\int_{\mathbb{R}^2} \frac{|\nabla u^l_{n,e}(x)-\nabla u^l_{n,e}(x+he_2)|^2}{|h|^{2s-1}}\,dx\,dh < \infty$. Let us now prove that $\int_{\mathbb{R}}\int_{\mathbb{R}^2} \frac{|\nabla u^l_{n,e}(x)-\nabla u^l_{n,e}(x+he_1)|^2}{|h|^{2s-1}}\,dx\,dh < \infty$ and $\int_{\mathbb{R}}\int_{\mathbb{R}^2} \frac{|\nabla u^l_{n,e}(x)-\nabla u^l_{n,e}(x+he_2)|^2}{|h|^{2s-1}}\,dx\,dh < \infty$ independently of l.
We have $\int_{\mathbb{R}} \frac{1}{|h|^{2s-1}}\|\tau_{he_1}\nabla u^l_{n,e}-\nabla u^l_{n,e}\|^2_{L^2(\mathbb{R}^2)}\,dh = \bar{C}\int_{\mathbb{R}} \frac{\sin^2(u)}{|u|^{2s-1}}\int_{\mathbb{R}^2} |\xi_1|^{2s-2}\,(|\xi_1|^2+|\xi_2|^2)|\mathcal{F}(u^l_{n,e})(\xi)|^2\,d\xi\,du \le C\|u^l_{n,e}\|^2_{H^s(\mathbb{R}^2)}$ by using Plancherel theorem and with C independent of l. By doing the same computations in the other direction, we prove that $\|u^l_n\|_{W^{s,2}(\Omega)}$ is uniformly bounded and so up to a subsequence, $u^l_n \underset{l\to+\infty}{\rightharpoonup} \overline{u_n}$ in $W^{s,2}(\Omega)\subset W^{1,2}(\Omega)$. As $W^{s,2}(\Omega) \underset{c}{\circlearrowleft} \mathcal{C}^{0,\lambda}_b(\Omega)$ with $\lambda < s-1$, then (u^l_n) strongly converges to $\overline{u_n}$ in $\mathcal{C}^{0,\lambda}_b(\Omega)$ and so pointwise everywhere on Ω. Then $\tilde{u}_n = \overline{u_n}$ on Ω and $\overline{u_n}=0$ on $\partial\Omega$, by uniqueness of the weak limit.
Now, $H^s(\mathbb{R}^2)\circlearrowleft L^2(\mathbb{R}^2)\circlearrowleft \mathcal{S}'(\mathbb{R}^2)\circlearrowleft \mathcal{D}'(\mathbb{R}^2)$ with continuous imbeddings. $\forall\varphi\in\mathcal{D}(\mathbb{R}^2)$, $\underbrace{\int_{\mathbb{R}^2}(u^l_{n,e}-\tilde{u}_n)\,\varphi\,dx}_{\underset{l\to+\infty}{\longrightarrow}0} = \underbrace{\int_{\Omega}(u^l_n-\overline{u_n})\,\varphi\,dx}_{\underset{l\to+\infty}{\longrightarrow}0} + \int_{\mathbb{R}^2\setminus\Omega}(u^l_{n,e}-\tilde{u}_n)\,\varphi\,dx$. Consequently, $\forall\varphi\in\mathcal{D}(\mathbb{R}^2)$, $\int_{\mathbb{R}^2\setminus\Omega}\tilde{u}_n\,\varphi\,dx = \int_{\mathbb{R}^2\setminus\bar{\Omega}}\tilde{u}_n\,\varphi\,dx = 0$, since $\tilde{u}_n\in H^s(\mathbb{R}^2)\circlearrowleft \mathcal{C}^0(\mathbb{R}^2)$. In particular, $\forall\varphi\in\mathcal{D}(\mathbb{R}^2\setminus\bar{\Omega})$, $\int_{\mathbb{R}^2\setminus\bar{\Omega}}\tilde{u}_n\,\varphi\,dx=0$, meaning that $\tilde{u}_n=0$ on $\mathbb{R}^2\setminus\bar{\Omega}$ in the sense of distributions. Due to the continuity of $\tilde{u}_n$, we deduce that $\tilde{u}_n=0$ everywhere on $\mathbb{R}^2\setminus\Omega$ and so $\tilde{u}_n=(\overline{u_n})_e$. By combining the previous results, we can say that $(u^l_{n,e})$ converges pointwise everywhere to $(\overline{u_n})_e$ on $\mathbb{R}^2$.

– Classical arguments enable us to conclude that there exists a subsequence still denoted by $\vec{g_n}^{\,l}$ weakly converging to $\overline{\vec{g_n}}$ in $H(div)$.

2. **Lower semicontinuity of the functional**:

– Since $\nabla Q^l_n \overset{*}{\rightharpoonup} \nabla\overline{Q}_n$ in $L^\infty(\Omega)$ then $\|\nabla\overline{Q}_n\|_{L^\infty(\Omega)} \le \liminf_{l\to+\infty}\|\nabla Q^l_n\|_{L^\infty(\Omega)}$.

– Weak-$*$ convergence in $L^\infty(\Omega)$ implying weak convergence in $L^2(\Omega)$, $\|\nabla\overline{Q_n}-\overline{\vec{g_n}}\|^2_{L^2(\Omega)} \le \liminf_{l\to+\infty}\|\nabla Q^l_n-\vec{g_n}^{\,l}\|^2_{L^2(\Omega)}$.

– $\mathcal{G}_\varepsilon$ is convex and strongly lower semi-continuous in $H^1(\Omega)$ and so weakly lower semicontinuous in $H^1(\Omega)$.

– $\|f-\overline{u_n}-\operatorname{div}\overline{\vec{g_n}}\|^2_{L^2(\Omega)} \le \liminf_{l\to+\infty}\|f-u^l_n-\operatorname{div}\vec{g_n}^{\,l}\|^2_{L^2(\Omega)}$.

– Let us consider $h:\Omega\times\mathbb{R}\times\mathbb{R}^2\to\mathbb{R}$, $(x,v,w)\mapsto(v(x)^2+\lambda_\varepsilon)|w(x)|^2$. Since

$v_{1,n}^l \underset{l\to+\infty}{\longrightarrow} \overline{v_{1,n}}$ in $L^2(\Omega)$, $\nabla u_n^l \underset{l\to+\infty}{\rightharpoonup} \nabla\overline{u_n}$ in $L^2(\Omega,\mathbb{R}^2)$, since h is continuous with respect to (v,w) and measurable on Ω for almost every $(v,w)\in\mathbb{R}\times\mathbb{R}^2$, for each (x,v), h is convex with respect to w, $\forall (v,w)\in\mathbb{R}\times\mathbb{R}^2$, $\forall x\in\Omega$ a.e., $h(x,v,w)\geq 0\in L^1(\Omega)$ and $\liminf_{l\to+\infty}\int_\Omega((v_{1,n}^l(x))^2+\lambda_\varepsilon)|\nabla u_n^l|^2\,dx<+\infty$, then $\int_\Omega(\overline{v_{1,n}}^2+\lambda_\varepsilon)|\nabla\overline{u_n}|^2\,dx\leq\liminf_{l\to+\infty}\int_\Omega((v_{1,n}^l)^2+\lambda_\varepsilon)|\nabla u_n^l|^2\,dx$ (see [13]).

– $v_{2,n}^l \underset{l\to+\infty}{\longrightarrow} \overline{v_{2,n}}$ in $L^2(\Omega)$, therefore $v_{2,n,e}^l \underset{l\to+\infty}{\longrightarrow} (\overline{v_{2,n}})_e$ in $L^2(\mathbb{R}^2)$ (since from [18, Theorem IX.7, (ii), p. 158], $\|v_{2,n,e}^l-(\overline{v_{2,n}})_e\|_{L^2(\mathbb{R}^2)}\leq\tilde{C}\,\|v_{2,n}^l-\overline{v_{2,n}}\|_{L^2(\Omega)}$, $\tilde{C}$ depending only on Ω) and so pointwise almost everywhere in $\mathbb{R}^2$ (up to a subsequence). We deduce that $((v_{2,n,e}^l(x))^2+\kappa_\varepsilon)\frac{|u_{n,e}^l(x+he_i)-2u_{n,e}^l(x)+u_{n,e}^l(x-he_i)|^2}{|h|^4}\rho_n(h)$ $\underset{l\to+\infty}{\longrightarrow}((\overline{v_{2,n}})_e(x)^2+\kappa_\varepsilon)\frac{|(\overline{u_n})_e(x+he_i)-2(\overline{u_n})_e(x)+(\overline{u_n})_e(x-he_i)|^2}{|h|^4}\rho_n(h)$, $i\in\{1,2\}$, for all $h\in\mathbb{R}$ and almost all $x\in\mathbb{R}^2$.
Using Fatou's lemma twice, we deduce that $\int_{\mathbb{R}^2}\int_{\mathbb{R}}((\overline{v_{2,n}})_e(x)^2+\kappa_\varepsilon)$ $\frac{|(\overline{u_n})_e(x+he_i)-2(\overline{u_n})_e(x)+(\overline{u_n})_e(x-he_i)|^2}{|h|^4}\rho_n(h)\,dh\,dx\leq\liminf_{l\to+\infty}\int_{\mathbb{R}^2}\int_{\mathbb{R}}$ $((v_{2,n,e}^l(x))^2+\kappa_\varepsilon)\frac{|u_{n,e}^l(x+he_1)-2u_{n,e}^l(x)+u_{n,e}^l(x-he_1)|^2}{|h|^4}\rho_n(h)\,dh\,dx$, $i\in\{1,2\}$.

This concludes the proof.

□

Theorem 3.5 (Γ-convergence)**.** *Let $(u_n,\vec{g}_n,Q_n,v_{1,n},v_{2,n})\in H_0^1(\Omega)\cap W^{s,2}(\Omega)\times H(div)\times\{Q\in W^{1,\infty}(\Omega)|\int_\Omega Q\,dx=0\}\times W^{1,2}(\Omega,[0,1])\times\{v_2\in W^{1,2}(\Omega,[0,1])|\gamma_0 v_2=1\}$ with $s\in[\frac{3}{2},2[$ be a sequence of minimizers of (5.8) for each $n\in\mathbb{N}^*$. Let us assume additionally for technical purposes, that $v_2\in\{v_2\in W^{1,2}(\Omega,[0,1])|\gamma_0 v_2=1\}\cap W^{1,\infty}(\Omega)$ with $\sup_{n\in\mathbb{N}^*}\|\nabla v_{2,n}\|_{L^\infty(\Omega)}\leq C_1<\infty$. Then there exist a subsequence still denoted by $(u_n,\vec{g}_n,Q_n,v_{1,n},v_{2,n})$ and a minimizer $(\bar{u},\bar{\vec{g}},\bar{Q},\bar{v}_1,\bar{v}_2)\in H^2(\Omega)\cap H_0^1(\Omega)\times H(div)\times\{Q\in W^{1,\infty}(\Omega)|\int_\Omega Q\,dx=0\}\times W^{1,2}(\Omega,[0,1])\times\{v_2\in W^{1,2}(\Omega,[0,1])|\gamma_0 v_2=1\}$ of (5.7) such that $u_n\underset{n\to+\infty}{\rightharpoonup}\bar{u}$ in $W^{\frac{3}{2},2}(\Omega)$, $\vec{g}_n\underset{n\to+\infty}{\rightharpoonup}\bar{\vec{g}}$ in $H(div)$, $Q_n\underset{n\to+\infty}{\overset{*}{\rightharpoonup}}\bar{Q}$ in $W^{1,\infty}(\Omega)$, $v_{1,n}\underset{n\to+\infty}{\rightharpoonup}\bar{v}_1$ in $W^{1,2}(\Omega)$, $v_{2,n}\underset{n\to+\infty}{\rightharpoonup}\bar{v}_2$ in $W^{1,2}(\Omega)$ and $\bar{\mathcal{F}}_{n,\varepsilon}(u_n,\vec{g}_n,Q_n,v_{1,n},v_{2,n})\underset{n\to+\infty}{\longrightarrow}\bar{\mathcal{F}}_\varepsilon(\bar{u},\bar{\vec{g}},\bar{Q},\bar{v}_1,\bar{v}_2)$.*

Proof. We have proved in what precedes that for any $n\in\mathbb{N}^*$, there exists a solution to (5.8). Let us consider a sequence of such minimizers $(u_n,\vec{g}_n,Q_n,v_{1,n},v_{2,n})\in H^s(\Omega)\cap H_0^1(\Omega)\times H(div)\times\{Q\in W^{1,\infty}(\Omega)|\int_\Omega Q\,dx=0\}\times W^{1,2}(\Omega,[0,1])\times\{v_2\in W^{1,2}(\Omega,[0,1])|\gamma_0 v_2=1\}$, with $s\in[\frac{3}{2},2[$. Let $u\in W^{2,2}(\Omega)\cap W_0^{1,2}(\Omega),\vec{g}\in H(div),Q\in\{Q\in W^{1,\infty}(\Omega)|\int_\Omega Q\,dx=0\}$, $v_1\in W^{1,2}(\Omega,[0,1])$, $v_2\in W^{1,2}(\Omega,[0,1])|\gamma_0 v_2=1\}$, then $\forall n\in\mathbb{N}^*$, $\mathcal{F}_n(u_n,\vec{g}_n,Q_n,v_{1,n},v_{2,n})\leq\bar{\mathcal{F}}_{n,\varepsilon}(u,\vec{g},Q,v_1,v_2)\leq\rho(1+\kappa_\varepsilon)\|u\|_{W^{2,2}(\Omega)}^2+\xi_\varepsilon\int_\Omega(v_1^2(x)+\zeta_\varepsilon)|\nabla u(x)|^2\,dx+\|f-u-div\vec{g}\|_{L^2(\Omega)}^2+\mu\|\nabla Q\|_{L^\infty(\Omega)}+\frac{\gamma}{2}\|\vec{g}-\nabla Q\|_{L^2(\Omega)}^2+(\alpha-\beta)\int_\Omega\frac{(v_1(x)-1)^2}{4\varepsilon}+\varepsilon|\nabla v_1(x)|^2\,dx+\beta\int_\Omega\frac{(v_2(x)-1)^2}{4\varepsilon}+\varepsilon|\nabla v_2(x)|^2\,dx=C<+\infty$ using Lemma 3.2.
We deduce that:

– $\|\nabla Q_n\|_{L^\infty(\Omega)}$ is uniformly bounded with respect to n and since $\int_\Omega Q_n\,dx = 0$ for any $n \in \mathbb{N}^*$, then using Poincaré-Wirtinger inequality, we get that (Q_n) is uniformly bounded in $W^{1,\infty}(\Omega)$. Thus we can extract a subsequence still denoted by (Q_n) weakly-$*$ converging to $\bar{Q}$ in $W^{1,\infty}(\Omega)$. Besides, the compact embedding $W^{1,\infty}(\Omega) \underset{c}{\circlearrowleft} \mathcal{C}_0(\bar{\Omega})$ leads to $\int_\Omega \bar{Q}\,dx = 0$.

– $\|\nabla v_{1,n}\|_{L^2(\Omega)}$ is uniformly bounded with respect to n and since $v_{1,n} \in W^{1,2}(\Omega,[0,1])$ for any $n \in \mathbb{N}^*$ and Ω being bounded, then by using Poincaré-Wirtinger inequality, we get that $(v_{1,n})$ is uniformly bounded in $W^{1,2}(\Omega)$. We can therefore extract a subsequence still denoted by $(v_{1,n})$ weakly converging to $\bar{v_1}$ in $W^{1,2}(\Omega)$ and thanks to the compact embedding $W^{1,2}(\Omega) \underset{c}{\circlearrowleft} L^2(\Omega)$, the convergence is also pointwise almost everywhere up to a subsequence, leading to $\bar{v_1} \in W^{1,2}(\Omega,[0,1])$.

– Using the same arguments, we get that $v_{2,n} \underset{n\to+\infty}{\rightharpoonup} \bar{v_2}$ in $W^{1,2}(\Omega)$ with $\bar{v_2} \in W^{1,2}(\Omega,[0,1])$ and by continuity of the trace operator, $\gamma_0\bar{v_2} = 1$.

– $\|\nabla u_n\|_{L^2(\Omega)}$ is uniformly bounded with respect to n and since $u_n \in W_0^{1,2}(\Omega)$ for any $n \in \mathbb{N}^*$, then using Poincaré inequality, we can extract a subsequence still denoted by (u_n) weakly converging in $W^{1,2}(\Omega)$ to $\bar{u}$. By continuity of the trace operator, we have $\bar{u} \in W_0^{1,2}(\Omega)$.

– $C \geq \frac{1}{4}\|div\vec{g}_n\|^2_{L^2(\Omega)} - \frac{1}{2}\|u_n\|^2_{L^2(\Omega)} - \|f\|^2_{L^2(\Omega)} + \frac{\gamma}{4}\|\vec{g}_n\|^2_{L^2(\Omega)} - \frac{\gamma}{2}\|\nabla Q_n\|^2_{L^2(\Omega)}$. So, $(\vec{g}_n)$ is uniformly bounded in $H(div)$ and we can extract a subsequence still denoted by $(\vec{g}_n)$ weakly converging to $\vec{\bar{g}}$ in $H(div)$.

Now, let us show that $(u_{n,e})$ weakly converges in $H^{\frac{3}{2}}(\mathbb{R}^2)$ to $\bar{u}_e$.
We set $E_n(h) = \int_{\mathbb{R}^2} |u_{n,e}(x+he_1) - 2u_{n,e}(x) + u_{n,e}(x-he_1)|^2\,dx$. It satisfies $E_n(2h) \leq 16E_n(h)$, $\forall h \in \mathbb{R}$. By using Fubini-Tonelli theorem, we have
$\int_{\mathbb{R}^2}\int_{\mathbb{R}} \frac{|u_{n,e}(x+he_1) - 2u_{n,e}(x) + u_{n,e}(x-he_1)|^2}{|h|^4}\rho_n(h)\,dh\,dx = \int_{\mathbb{R}} \frac{E_n(h)}{|h|^4}\rho_n(h)\,dh = 2\int_0^\infty \frac{E_n(h)}{|h|^4}\rho_n(h)\,dh \leq C$. We then apply [9, Lemma 3.1] with $M = \delta = 1$, $g(t) = \frac{E_n(t)}{t^{q+1}}, k(t) = t^{q-3}\rho_n(t)$ and we get $C(1)\int_0^1 t^{q-3}\rho_n(t)\,dt \int_0^1 \frac{E_n(t)}{t^{q+1}}\,dt \leq \int_0^1 \frac{E_n(t)}{t^4}\rho_n(t)\,dt$. (We will see further that the condition of monotonicity on k is fulfilled). We now need g to verify the assumption of this lemma, that is to say, $g(\frac{t}{2}) \geq g(t)$. We know that $g(\frac{t}{2}) = \frac{E_n(\frac{t}{2})}{t^{q+1}}2^{q+1} \geq 2^{q-3}g(t)$. Thus if $q \geq 3$, this condition is fulfilled. By using the properties of ρ_n, we deduce first that $\int_0^1 \frac{E_n(t)}{t^{q+1}}\,dt \leq C$ with C independent of n for $q = 3$ and n large enough since then $\int_0^1 t^{q-3}\rho_n(t)\,dt = \int_0^1 \rho_n(t)\,dt = 1 - \int_1^\infty \rho_n(t)\,dt$, $\forall n \in \mathbb{N}^*$ with $\lim_{n\to+\infty}\int_1^\infty \rho_n(t)\,dt = 0$ and so for n large enough, $\int_0^1 \rho_n(t)\,dt \in \left[\frac{1}{2},1\right]$. Then $\int_1^\infty \frac{E_n(t)}{t^{q+1}}\,dt \leq C'\|u_{n,e}\|^2_{L^2(\mathbb{R}^2)}\int_1^\infty \frac{1}{t^{q+1}}\,dt$, C' being a constant and the last integral being convergent since $q = 3$, resulting in the uniform boundedness of $\int_0^\infty \frac{E_n(t)}{t^{q+1}}\,dt$. Besides, $\int_{\mathbb{R}} \frac{E_n(t)}{|t|^{q+1}}\,dt = \int_{\mathbb{R}} \frac{1}{|h|^{q+1}}\int_{\mathbb{R}^2} |u_{n,e}(x+he_1) - 2u_{n,e}(x) + u_{n,e}(x-he_1)|^2\rho_n(h)\,dx\,dh = \int_{\mathbb{R}} \frac{1}{|h|^{q+1}}\|\tau_{he_1}u_{n,e} -$

$2u_{n,e} + \tau_{-he_1}u_{n,e}\|^2_{L^2(\mathbb{R}^2)}\,dh = \int_{\mathbb{R}} \frac{1}{|h|^{q+1}} \int_{\mathbb{R}^2} |e^{2i\pi h\xi_1} - 2 + e^{-2i\pi h\xi_1}|^2 |\mathcal{F}(u_{n,e})|^2(\xi)\,d\xi\,dh$ by Plancherel theorem (τ denoting the usual translation operator and $\xi = (\xi_1, \xi_2)$). Then one can prove that $\int_{\mathbb{R}} \frac{E_n(t)}{|t|^{q+1}}\,dt = C'' \int_{\mathbb{R}^2} |\mathcal{F}(u_{n,e})(\xi)|^2 |\xi_1|^q \int_{\mathbb{R}} \frac{\sin^4(u)}{|u|^{q+1}}\,du\,d\xi \leq C''$, (the constant C'' may change line to line). The generalized integral in u converges if and only if $q \in [3, 4[$ so for $q = 3$. By using the same arguments in the other direction (e_2), we get that $|\cdot|^{\frac{q}{2}}\mathcal{F}(u_{n,e})(\cdot) \in L^2(\mathbb{R}^2)$ and so $u_{n,e} \in H^{\frac{3}{2}}(\mathbb{R}^2)$ (being a Hilbert space) and is uniformly bounded for the associated norm for n large enough. There exists a subsequence still denoted by $(u_{n,e})$ weakly converging to $\tilde{u}$ in $H^{\frac{3}{2}}(\mathbb{R}^2)$. Besides, we know that $u_{n,e} = u_n$ on Ω and $D^{(1,0)}u_{n,e} = (D^{(1,0)}u_n)_e = D^{(1,0)}u_n$ on Ω, and $D^{(0,1)}u_{n,e} = (D^{(0,1)}u_n)_e = D^{(0,1)}u_n$ on Ω. Thus, $\|u_n\|^2_{W^{\frac{3}{2},2}(\Omega)} = \|u_n\|^2_{W^{1,2}(\Omega)} + \int_\Omega \int_\Omega \frac{|\nabla u_n(y) - \nabla u_n(x)|^2}{|x-y|^3}\,dx\,dy \leq C + \int_{\mathbb{R}^2}\int_{\mathbb{R}^2} \frac{|\nabla u_{n,e}(y) - \nabla u_{n,e}(x)|^2}{|x-y|^3}\,dx\,dy$, with C independent of n. From [29, Lemma 4.33, p. 200], we know that $\int_{\mathbb{R}^2}\int_{\mathbb{R}^2} \frac{|\nabla u_{n,e}(x) - \nabla u_{n,e}(y)|^2}{|x-y|^3}\,dx\,dy < \infty$
$\Leftrightarrow \int_{\mathbb{R}}\int_{\mathbb{R}^2} \frac{|\nabla u_{n,e}(x) - \nabla u_{n,e}(x+he_1)|^2}{|h|^2}\,dx\,dh < \infty$ and
$\int_{\mathbb{R}}\int_{\mathbb{R}^2} \frac{|\nabla u_{n,e}(x) - \nabla u_{n,e}(x+he_2)|^2}{|h|^2}\,dx\,dh < \infty$. Let us now prove that
$\int_{\mathbb{R}}\int_{\mathbb{R}^2} \frac{|\nabla u_{n,e}(x) - \nabla u_{n,e}(x+he_1)|^2}{|h|^2}\,dx\,dh < \infty$ and $\int_{\mathbb{R}}\int_{\mathbb{R}^2} \frac{|\nabla u_{n,e}(x) - \nabla u_{n,e}(x+he_2)|^2}{|h|^2}\,dx\,dh$
$< \infty$ independently of n. We have $\int_{\mathbb{R}} \frac{1}{|h|^2}\|\tau_{he1}(\nabla u_{n,e}) - \nabla u_{n,e}\|^2_{L^2(\mathbb{R}^2)}\,dh = \bar{C}\int_{\mathbb{R}} \frac{\sin^2(u)}{|u|^2} \int_{\mathbb{R}^2} |\xi_1|$ $(|\xi_1|^2 + |\xi_2|^2)|\mathcal{F}(u_{n,e})(\xi)|^2\,d\xi\,du \leq C\|u_{n,e}\|^2_{H^{\frac{3}{2}}(\mathbb{R}^2)}$ by using Plancherel theorem and with C independent of n. By doing the same computations in the other direction, we prove that $\|u_n\|_{W^{\frac{3}{2},2}(\Omega)}$ is uniformly bounded and so up to a subsequence, $u_n \underset{n\to+\infty}{\rightharpoonup} \bar{u}$ in $W^{\frac{3}{2},2}(\Omega)$, since $W^{\frac{3}{2},2}(\Omega) \subset W^{1,2}(\Omega)$ and the mapping $T : W^{\frac{3}{2},2}(\Omega) \to W^{1,2}(\Omega)$, $u \mapsto Tu = u$ is linear and continuous for the strong topology, so for the weak topology ([29, Theorem III.9, p. 39]). As $W^{\frac{3}{2},2}(\Omega) \underset{c}{\circlearrowleft} \mathcal{C}^{0,\lambda}_b(\Omega)$, with $\lambda < \frac{1}{2}$, then (u_n) strongly converges to $\bar{u}$ in $\mathcal{C}^{0,\lambda}_b(\Omega)$ and so pointwise everywhere on Ω. Then $\tilde{u} = \bar{u}$ on Ω and $\bar{u} = 0$ on $\partial\Omega$, by uniqueness of the weak limit. Now, $H^{\frac{3}{2}}(\mathbb{R}^2) \circlearrowleft L^2(\mathbb{R}^2) \circlearrowleft \mathcal{S}'(\mathbb{R}^2) \circlearrowleft \mathcal{D}'(\mathbb{R}^2)$ with continuous embeddings. $\forall \varphi \in \mathcal{D}(\mathbb{R}^2)$, $\underbrace{\int_{\mathbb{R}^2} (u_{n,e} - \tilde{u})\varphi\,dx}_{\underset{n\to+\infty}{\longrightarrow} 0} = \underbrace{\int_\Omega (u_n - \bar{u})\varphi\,dx}_{\underset{n\to+\infty}{\longrightarrow} 0} + \int_{\mathbb{R}^2\setminus\Omega} (u_{n,e} - \tilde{u})\varphi\,dx.$

Consequently, $\forall \varphi \in \mathcal{D}(\mathbb{R}^2)$, $\int_{\mathbb{R}^2\setminus\Omega} \tilde{u}dx = \int_{\mathbb{R}^2\setminus\bar{\Omega}} \tilde{u}dx = 0$ since $\tilde{u} \in H^{\frac{3}{2}}(\mathbb{R}^2) \circlearrowleft \mathcal{C}(\mathbb{R}^2)$. In particular, $\forall \varphi \in \mathcal{D}(\mathbb{R}^2 \setminus \bar{\Omega})$, $\int_{\mathbb{R}^2\setminus\bar{\Omega}} \tilde{u}\varphi\,dx = 0$, meaning that $\tilde{u} = 0$ on $\mathbb{R}^2 \setminus \bar{\Omega}$ in the sense of distributions. Due to the continuity of $\tilde{u}$, we deduce that $\tilde{u} = 0$ everywhere on $\mathbb{R}^2 \setminus \Omega$ and so $\tilde{u} = \bar{u}_e \in H^{\frac{3}{2}}(\mathbb{R}^2)$.
Now, let us prove that $\bar{u} \in H^2(\Omega) \cap H^1_0(\Omega)$ and $\bar{u}_e \in H^2(\mathbb{R}^2)$. Since $u_n \underset{n\to+\infty}{\longrightarrow} \bar{u}$ in $L^2(\Omega)$

then $u_{n,e} \underset{n\to+\infty}{\longrightarrow} \bar{u}_e$ in $L^2(\mathbb{R}^2)$.
Let $\varphi \in \mathcal{C}_0^\infty(\mathbb{R}^2)$. We denote by $\bar{u}_e$ and by $u_{n,e}$ the extensions by 0 of $\bar{u}$ and u_n for any $n \in \mathbb{N}^*$ on $\mathbb{R}^2$. Since Ω is of class $\mathcal{C}^2$ then $\bar{u}_e, u_{n,e} \in W^{1,2}(\mathbb{R}^2)$, for any $n \in \mathbb{N}^*$. We have

$$\Big| \int_{\mathbb{R}^2}\int_{\mathbb{R}} \frac{\varphi(x+he_1)-2\varphi(x)+\varphi(x-he_1)}{h^2}\rho_n(h)\,dh(u_{n,e}(x)+(\bar{u}_e(x)-u_{n,e}(x)))\,dx\Big|,$$
$$\leq \Big| \int_{\mathbb{R}^2}\int_{\mathbb{R}} \frac{\varphi(x+he_1)-2\varphi(x)+\varphi(x-he_1)}{h^2}\rho_n(h)\,dh(u_{n,e}(x))\,dx\Big|$$
$$+ \Big| \int_{\mathbb{R}^2}\int_{\mathbb{R}} \frac{\varphi(x+he_1)-2\varphi(x)+\varphi(x-he_1)}{h^2}\rho_n(h)\,dh(\bar{u}_e(x)-u_{n,e}(x))\,dx\Big|,$$
$$\leq \Big(\int_{\mathbb{R}^2}\int_{\mathbb{R}} \frac{(\varphi(x+he_1)-2\varphi(x)+\varphi(x-he_1))^2}{h^4}\rho_n(h)\,dh\,dx\Big)^{\frac{1}{2}}.$$
$$\Big(\int_{\mathbb{R}^2}\int_{\mathbb{R}} |u_{n,e}(x)-\bar{u}_e(x)|^2\rho_n(h)\,dh\,dx\Big)^{\frac{1}{2}}$$
$$+ \Big| \int_{\mathbb{R}^2}\int_{\mathbb{R}} \frac{u_{n,e}(x+he_1)-2u_{n,e}(x)+u_{n,e}(x-he_1)}{h^2}\rho_n(h)\,dh(\varphi(x))\,dx\Big|,$$

Hölder's inequality with respect to the measure $\rho_n(h)\,dh\,dx$. Since $\varphi \in \mathcal{C}_0^\infty(\mathbb{R}^2)$ (justification of the integrability and the possibility to change the order of integration is postponed),

$$\leq \|D^{(2,0)}\varphi\|_{L^2(\mathbb{R}^2)}\|u_{n,e}-\bar{u}_e\|^2_{L^2(\mathbb{R}^2)}$$
$$+ \Big(\int_{\mathbb{R}^2}\int_{\mathbb{R}} \frac{(u_{n,e}(x+he_1)-2u_{n,e}(x)+u_{n,e}(x-he_1))^2}{h^4}\rho_n(h)\,dh\,dx\Big)^{\frac{1}{2}}\Big(\int_{\mathbb{R}^2}\int_{\mathbb{R}} \varphi^2(x)\rho_n(h)\,dh\,dx\Big)^{\frac{1}{2}},$$
$$\leq \|D^{(2,0)}\varphi\|_{L^2(\mathbb{R}^2)}\|u_{n,e}-\bar{u}_e\|^2_{L^2(\mathbb{R}^2)}$$
$$+ \Big(\int_{\mathbb{R}^2}\int_{\mathbb{R}} \frac{(u_{n,e}(x+he_1)-2u_{n,e}(x)+u_{n,e}(x-he_1))^2}{h^4}\rho_n(h)\,dh\,dx\Big)^{\frac{1}{2}}\|\varphi\|_{L^2(\mathbb{R}^2)}$$
$$\leq \|D^{(2,0)}\varphi\|_{L^2(\mathbb{R}^2)}\|u_{n,e}-\bar{u}_e\|^2_{L^2(\mathbb{R}^2)} + \sqrt{C}\|\varphi\|_{L^2(\mathbb{R}^2)}.$$

Since $\varphi \in \mathcal{C}_0^\infty(\mathbb{R}^2)$, then for almost every $x \in \mathbb{R}^2$, $\displaystyle\int_{\mathbb{R}} \frac{\varphi(x+he_1)-2\varphi(x)+\varphi(x-he_1)}{h^2}\rho_n(h)\,dh\,\bar{u}_e(x)$ $\underset{n\to+\infty}{\longrightarrow} D^{(2,0)}\varphi(x)\bar{u}_e(x)$ thanks to Theorem 3.1. Besides, $\forall n \in \mathbb{N}^*$ and almost every $x \in \mathbb{R}^2$,
$\displaystyle\Big| \int_{\mathbb{R}} \frac{\varphi(x+he_1)-2\varphi(x)+\varphi(x-he_1)}{h^2}\rho_n(h)\,dh\bar{u}_e(x)\Big| \leq |\bar{u}_e(x)|$
$\displaystyle\int_{\mathbb{R}} \frac{|\varphi(x+he_1)-2\varphi(x)+\varphi(x-he_1)|}{|h|^2}\rho_n(h)\,dh$ by applying Jensen's inequality with respect to the measure $\rho_n(h)\,dh$ (see [40, Theorem 139, p. 56]). But $\bar{u}_e \in L^2(\mathbb{R}^2)$ with $\|\bar{u}_e\|_{L^2(\mathbb{R}^2)} = \|\bar{u}\|_{L^2(\Omega)} \geq c\|\bar{u}\|_{L^1(\Omega)} = c\|\bar{u}_e\|_{L^1(\mathbb{R}^2)}$, since $\bar{u}$ is extended by 0 outside Ω. As $\varphi \in \mathcal{C}_0^\infty(\mathbb{R}^2)$, then
$\displaystyle\int_{\mathbb{R}} \frac{|\varphi(x+he_1)-2\varphi(x)+\varphi(x-he_1)|}{|h|^2}\rho_n(h)\,dh \in L^1(\mathbb{R}^2)$ and
$\displaystyle\int_{\mathbb{R}} \frac{|\varphi(x+he_1)-2\varphi(x)+\varphi(x-he_1)|}{|h|^2}\rho_n(h)\,dh \leq \int_{\mathbb{R}}\int_0^1\int_0^1 |D^{(2,0)}\varphi(x+(t+s-1)he_1)|\rho_n(h)\,ds\,dt\,dh$

$\leq \|D^{(2,0)}\varphi\|_{L^\infty(\mathbb{R}^2)}$. We also have $\int_{\mathbb{R}^2}\left(\int_{\mathbb{R}}\frac{\varphi(x+he_1)-2\varphi(x)+\varphi(x-he_1)}{h^2}\rho_n(h)\,dh\right)^2 dx$ $\leq \int_{\mathbb{R}^2}\int_{\mathbb{R}}\frac{(\varphi(x+he_1)-2\varphi(x)+\varphi(x-he_1))^2}{h^4}\rho_n(h)\,dh\,dx \leq \|D^{(2,0)}\varphi\|^2_{L^2(\mathbb{R}^2)} < +\infty$. Thus $\int_{\mathbb{R}}\frac{\varphi(x+he_1)-2\varphi(x)+\varphi(x-he_1)}{h^2}\rho_n(h)\,dh \in L^2(\mathbb{R}^2)$, and $\bar{u}_e$ being $L^2(\mathbb{R}^2)$, it leads to $\int_{\mathbb{R}}\frac{\varphi(x+he_1)-2\varphi(x)+\varphi(x-he_1)}{h^2}\rho_n(h)\,dh\,\bar{u}_e(x) \in L^1(\mathbb{R}^2)$ with $\left|\int_{\mathbb{R}}\frac{\varphi(x+he_1)-2\varphi(x)+\varphi(x-he_1)}{h^2}\rho_n(h)\,dh\,\bar{u}_e(x)\right| \leq |\bar{u}_e(x)|\|D^{(2,0)}\varphi\|_{L^\infty(\mathbb{R}^2)} \in L^1(\mathbb{R}^2)$. From the dominated convergence theorem, we can conclude that $\lim_{n\to+\infty}\int_{\mathbb{R}^2}\bar{u}_e(x)\int_{\mathbb{R}}\frac{\varphi(x+he_1)-2\varphi(x)+\varphi(x-he_1)}{h^2}\rho_n(h)\,dh\,dx = \int_{\mathbb{R}^2}\bar{u}_e(x)D^{(2,0)}\varphi(x)\,dx$. By letting n tend to infinity in the previous inequality, we get:

$$\int_{\mathbb{R}^2}\bar{u}_e(x)D^{(2,0)}\varphi(x)\,dx \leq \sqrt{C}\|\varphi\|_{L^2(\mathbb{R}^2)}.$$

Eventually, $D^{(2,0)}\bar{u}_e \in L^2(\mathbb{R}^2)$ using [18, Proposition VIII.3]. By applying the same reasoning we also get $D^{(0,2)}\bar{u}_e \in L^2(\mathbb{R}^2)$. Since $\bar{u}_e \in L^2(\mathbb{R}^2)$ then it is a tempered distribution so are its successive derivatives. We can now take the Fourier transform:

$$\widehat{D^{(1,1)}\bar{u}_e}(\xi) = -\xi_1\xi_2 4\pi^2\widehat{\bar{u}_e}(\xi),$$
$$\widehat{D^{(0,2)}\bar{u}_e}(\xi) = -\xi_2\xi_2 4\pi^2\widehat{\bar{u}_e}(\xi),$$
$$\widehat{D^{(2,0)}\bar{u}_e}(\xi) = -\xi_1\xi_1 4\pi^2\widehat{\bar{u}_e}(\xi).$$

Since $D^{(0,2)}\bar{u}_e \in L^2(\mathbb{R}^2)$ and $D^{(2,0)}\bar{u}_e \in L^2(\mathbb{R}^2)$, then $-\xi_2\xi_2\widehat{\bar{u}_e}(\xi) \in L^2(\mathbb{R}^2)$ and $-\xi_1\xi_1\widehat{\bar{u}_e}(\xi) \in L^2(\mathbb{R}^2)$. But

$$\int_{\mathbb{R}^2}4\pi^2\xi_1^2\xi_2^2\widehat{\bar{u}_e}^2(\xi)\,d\xi \leq 2\pi^2\int_{\mathbb{R}^2}\xi_1^4\widehat{\bar{u}_e}^2(\xi)\,d\xi + 2\pi^2\int_{\mathbb{R}^2}\xi_2^4\widehat{\bar{u}_e}^2(\xi)\,d\xi < +\infty,$$

which means that $\widehat{D^{(1,1)}\bar{u}_e}(\xi) \in L^2(\mathbb{R}^2)$ and by Plancherel's theorem we can conclude that $D^{(1,1)}\bar{u}_e \in L^2(\mathbb{R}^2)$. This proves that $\bar{u}_e \in W^{2,2}(\mathbb{R}^2)$ since $\bar{u}_e \in W^{1,2}(\mathbb{R}^2)$ by construction. As $\Omega \in \mathcal{C}^2$ and $\bar{u}_e$ is the extension of $\bar{u}$ by 0 outside Ω, then $\bar{u} \in W^{2,2}(\Omega) \cap W_0^{1,2}(\Omega)$.

By definition of the sequence $(u_n, \vec{g}_n, Q_n, v_{1,n}, v_{2,n})$, we have $\forall n \in \mathbb{N}^*$, $\bar{\mathcal{F}}_{n,\varepsilon}(u_n, \vec{g}_n, Q_n, v_{1,n}, v_{2,n})$ $\leq \bar{\mathcal{F}}_{n,\varepsilon}(\bar{u}, \vec{\bar{g}}, \bar{Q}, \bar{v}_1, \bar{v}_2)$ and by taking the lim sup when n tends to infinity, $\limsup_{n\to+\infty}\bar{\mathcal{F}}_{n,\varepsilon}(u_n, \vec{g}_n,$ $Q_n, v_{1,n}, v_{2,n}) \leq \mathcal{F}(\bar{u}, \vec{\bar{g}}, \bar{Q}, \bar{v}_1, \bar{v}_2)$. Indeed, thanks to Theorem 3.1., we know that $(\bar{v}_{2,e}^2(x)+\kappa_\varepsilon)\int_{\mathbb{R}}\frac{|u(x+he_1)-2u(x)+u(x-he_1)|^2}{|h|^4}\rho_n(h)\,dh \underset{n\to+\infty}{\longrightarrow} (\bar{v}_{2,e}^2(x)+\kappa_\varepsilon)|D^{(2,0)}u|^2(x)$ everywhere in $\mathbb{R}^2$ and for all $u \in \mathcal{C}_c^4(\mathbb{R}^2)$. Without loss of generality, we assume that $supp(u) \subset B(0,R)$ with $R > 0$. We now aim to prove that $\forall\varepsilon > 0, \exists L = L(\varepsilon) > 1$ (we believe that the confusion with the ε from the elliptic approximation is not possible) such

that $\sup_n \int_{B(0,LR)^c} \left|(\bar{v}_{2,e}^2(x)+\kappa_\varepsilon)\int_{\mathbb{R}} \frac{|u(x+he_1)-2u(x)+u(x-he_1)|^2}{|h|^4}\,\rho_n(h)\,dh\right| dx \le \varepsilon$.
We have that $\int_{B(0,LR)^c} \left|(\bar{v}_{2,e}^2(x)+\kappa_\varepsilon)\int_{\mathbb{R}} \frac{|u(x+he_1)-2u(x)+u(x-he_1)|^2}{|h|^4}\,\rho_n(h)\,dh\right| dx \le$
$(1+\kappa_\varepsilon)\int_{B(0,LR)^c}\left|\int_{\mathbb{R}} \frac{|u(x+he_1)-2u(x)+u(x-he_1)|^2}{|h|^4}\,\rho_n(h)\,dh\right| dx \le \frac{(1+\kappa_\varepsilon)4}{(L-1)^4R^4}\|u\|^2_{L^2(\mathbb{R}^2)}$
and the conclusion follows. As

$$
\begin{aligned}
&\int_{\mathbb{R}^2}\left|(\bar{v}_{2,e}^2(x)+\kappa_\varepsilon)\int_{\mathbb{R}}\frac{|u(x+he_1)-2u(x)+u(x-he_1)|^2}{|h|^4}\rho_n(h)\,dh\right.\\
&\left.-(\bar{v}_{2,e}^2(x)+\kappa_\varepsilon)|D^{(2,0)}u(x)|^2\right| dx\\
&=\int_{B(0,LR)}\left|(\bar{v}_{2,e}^2(x)+\kappa_\varepsilon)\int_{\mathbb{R}}\frac{|u(x+he_1)-2u(x)+u(x-he_1)|^2}{|h|^4}\rho_n(h)\,dh\right.\\
&\left.-(\bar{v}_{2,e}^2(x)+\kappa_\varepsilon)|D^{(2,0)}u(x)|^2\right| dx\\
&+\int_{B(0,LR)^c}\left|(\bar{v}_{2,e}^2(x)+\kappa_\varepsilon)\int_{\mathbb{R}}\frac{|u(x+he_1)-2u(x)+u(x-he_1)|^2}{|h|^4}\rho_n(h)\,dh\right.\\
&\left.-(\bar{v}_{2,e}^2(x)+\kappa_\varepsilon)|D^{(2,0)}u(x)|^2\right| dx,\\
&\le\int_{B(0,LR)}\left|(\bar{v}_{2,e}^2(x)+\kappa_\varepsilon)\int_{\mathbb{R}}\frac{|u(x+he_1)-2u(x)+u(x-he_1)|^2}{|h|^4}\rho_n(h)\,dh\right.\\
&\left.-(\bar{v}_{2,e}^2(x)+\kappa_\varepsilon)|D^{(2,0)}u(x)|^2\right| dx+\varepsilon.
\end{aligned}
$$

We know that $(\bar{v}_{2,e}^2(x)+\kappa_\varepsilon)\int_{\mathbb{R}}\frac{|u(x+he_1)-2u(x)+u(x-he_1)|^2}{|h|^4}\rho_n(h)\,dh \underset{n\to+\infty}{\longrightarrow} (\bar{v}_{2,e}^2(x)+$
$\kappa_\varepsilon)|D^{(2,0)}u|^2(x)$ everywhere in $B(0,LR)$ and $\left|(\bar{v}_{2,e}^2(x)+\kappa_\varepsilon)\int_{\mathbb{R}}\frac{|u(x+he_1)-2u(x)+u(x-he_1)|^2}{|h|^4}\right.$
$\left.\rho_n(h)\,dh-(\bar{v}_{2,e}^2(x)+\kappa_\varepsilon)|D^{(2,0)}u|^2(x)\right| \le 2(1+\kappa_\varepsilon)\|D^{(2,0)}u\|^2_{L^\infty(\mathbb{R}^2)} \in L^1(B(0,LR))$. Using
the dominated convergence theorem, we get that
$\int_{B(0,LR)}\left|(\bar{v}_{2,e}^2(x)+\kappa_\varepsilon)\int_{\mathbb{R}}\frac{|u(x+he_1)-2u(x)+u(x-he_1)|^2}{|h|^4}\rho_n(h)\,dh-(\bar{v}_{2,e}^2(x)+\kappa_\varepsilon)|D^{(2,0)}u(x)|^2\right|$
$dx \underset{n\to+\infty}{\longrightarrow} 0$ and by letting ε tend to 0, we conclude that $\int_{\mathbb{R}^2}\left|(\bar{v}_{2,e}^2(x)+\kappa_\varepsilon)\right.$
$\left.\int_{\mathbb{R}}\frac{|u(x+he_1)-2u(x)+u(x-he_1)|^2}{|h|^4}\rho_n(h)\,dh-(\bar{v}_{2,e}^2(x)+\kappa_\varepsilon)|D^{(2,0)}u(x)|^2\right| dx \underset{n\to+\infty}{\longrightarrow} 0.$
We now extend this result to $u\in H^2(\mathbb{R}^2)$. Let $\varepsilon>0$. By density, there exists $v_\varepsilon\in\mathcal{C}_0^\infty(\mathbb{R}^2)$ such that $\|D^{(2,0)}u-D^{(2,0)}v_\varepsilon\|_{L^2(\mathbb{R}^2)}\le\varepsilon$. We set $u_n(x,h)=\frac{u(x+he_1)-2u(x)+u(x-he_1)}{h^2}\rho_n^{\frac{1}{2}}(h)\in$
$L^2(\mathbb{R}^2\times\mathbb{R})$ and $v_{n,\varepsilon}(x,h)=\frac{v_\varepsilon(x+he_1)-2v_\varepsilon(x)+v_\varepsilon(x+he_1)}{h^2}\rho_n^{\frac{1}{2}}(h)\in L^2(\mathbb{R}^2\times\mathbb{R})$. We then

have the following inequalities $\int_{\mathbb{R}^2}\int_{\mathbb{R}}(\bar{v}_{2,e}^2(x)+\kappa_\varepsilon)|u_n(x,h)|^2\,dh\,dx \leq \|u_n\|^2_{L^2(\mathbb{R}^2\times\mathbb{R})}(1+\kappa_\varepsilon) \leq (1+\kappa_\varepsilon)\|D^{(2,0)}u\|^2_{L^2(\mathbb{R}^2)}$ and $\int_{\mathbb{R}^2}\int_{\mathbb{R}}(\bar{v}_{2,e}^2(x)+\kappa_\varepsilon)|v_{n,\varepsilon}(x,h)-u_n(x,h)|^2\,dh\,dx \leq \|u_n - v_{n,\varepsilon}\|^2_{L^2(\mathbb{R}^2\times\mathbb{R})}(1+\kappa_\varepsilon) \leq (1+\kappa_\varepsilon)\|D^{(2,0)}u - D^{(2,0)}v_\varepsilon\|^2_{L^2(\mathbb{R}^2)} \leq (1+\kappa_\varepsilon)\varepsilon^2$ using Lemma 3.2. Then $|\int_{\mathbb{R}^2}\int_{\mathbb{R}}(\bar{v}_{2,e}^2(x)+\kappa_\varepsilon)|u_n(x,h)|^2\,dh\,dx - \int_{\mathbb{R}^2}(\bar{v}_{2,e}^2(x)+\kappa_\varepsilon)|D^{(2,0)}u(x)|^2\,dx| \leq (1+\kappa_\varepsilon)|\int_{\mathbb{R}^2}\int_{\mathbb{R}}|u_n(x,h)|^2\,dh\,dx - \int_{\mathbb{R}^2}|D^{(2,0)}u(x)|^2\,dx| \leq (1+\kappa_\varepsilon)|\int_{\mathbb{R}^2}\int_{\mathbb{R}}|u_n(x,h)|^2\,dh\,dx - \int_{\mathbb{R}^2}|D^{(2,0)}u(x)|^2\,dx - \int_{\mathbb{R}^2}|D^{(2,0)}v_\varepsilon(x)|^2\,dx| \leq (1+\kappa_\varepsilon)|2\int_{\mathbb{R}^2}\int_{\mathbb{R}}|v_{n,\varepsilon}(x,h)-u_n(x,h)|^2\,dh\,dx| + (1+\kappa_\varepsilon)|2\int_{\mathbb{R}^2}\int_{\mathbb{R}}|v_{n,\varepsilon}(x,h)|^2\,dh\,dx - 2\int_{\mathbb{R}^2}|D^{(2,0)}v_\varepsilon(x)|^2\,dx| + (1+\kappa_\varepsilon)|\int_{\mathbb{R}^2}(|D^{(2,0)}v_\varepsilon(x)|^2 - |D^{(2,0)}u(x)|^2)\,dx|$ and so $\limsup_{n\to+\infty}|\int_{\mathbb{R}^2}\int_{\mathbb{R}}(\bar{v}_{2,e}^2(x)+\kappa_\varepsilon)|u_n(x,h)|^2\,dh\,dx - \int_{\mathbb{R}^2}(\bar{v}_{2,e}^2(x)+\kappa_\varepsilon)|D^{(2,0)}u(x)|^2\,dx| \leq 2(1+\kappa_\varepsilon)\varepsilon^2$. Let ε tend to 0 and we get $\int_{\mathbb{R}^2}\int_{\mathbb{R}}(\bar{v}_{2,e}^2(x)+\kappa_\varepsilon)|u_n(x,h)|^2\,dh\,dx \underset{n\to+\infty}{\longrightarrow} \int_{\mathbb{R}^2}(\bar{v}_{2,e}^2(x)+\kappa_\varepsilon)|D^{(2,0)}u(x)|^2\,dx$ and since $\Omega \in \mathcal{C}^2$, then $\bar{u}_e$ is the extension by 0 of $\bar{u}$ from $W^{2,2}(\Omega)$ to $W^{2,2}(\mathbb{R}^2)$. So, $D^{(2,0)}\bar{u}_e = (D^{(2,0)}\bar{u})_e$ and $D^{(2,0)}\bar{u}_e(x) = 0$ almost everywhere on $\mathbb{R}^2\setminus\bar{\Omega}$. We finally have $\int_{\mathbb{R}^2}\int_{\mathbb{R}}(\bar{v}_{2,e}(x)^2+\kappa_\varepsilon)|\bar{u}_{e,n}(x,h)|^2\,dh\,dx \underset{n\to+\infty}{\longrightarrow} \int_{\mathbb{R}^2}(\bar{v}_{2,e}(x)^2+\kappa_\varepsilon)|D^{(2,0)}\bar{u}_e(x)|^2\,dx \leq \int_\Omega(\bar{v}_{2,e}(x)^2+\kappa_\varepsilon)|D^{(2,0)}\bar{u}(x)|^2\,dx$.

It remains to prove that $\bar{\mathcal{F}}_\varepsilon(\bar{u},\vec{\bar{g}},\bar{Q},\bar{v}_1,\bar{v}_2) \leq \liminf_{n\to+\infty}\bar{\mathcal{F}}_{n,\varepsilon}(u_n,\vec{g}_n,Q_n,v_{1,n},v_{2,n})$. From what precedes, it suffices to prove that $\int_\Omega(\bar{v}_2(x)^2+\kappa_\varepsilon)|D^{(2,0)}\bar{u}(x)|^2\,dx \leq \liminf_{n\to+\infty}\int_{\mathbb{R}^2}(v_{2,n,e}^2(x)+\kappa_\varepsilon)\int_{\mathbb{R}}\frac{|u_{n,e}(x+he_1)-2u_{n,e}(x)+u_{n,e}(x-he_1)|^2}{h^4}\rho_n(h)\,dh\,dx$ and $\int_\Omega(\bar{v}_2^2(x)+\kappa_\varepsilon)|D^{(0,2)}\bar{u}(x)|^2\,dx \leq \liminf_{n\to+\infty}\int_{\mathbb{R}^2}(v_{2,n,e}^2(x)+\kappa_\varepsilon)\int_{\mathbb{R}}\frac{|u_{n,e}(x+he_2)-2u_{n,e}(x)+u_{n,e}(x-he_2)|^2}{h^4}\rho_n(h)\,dh\,dx$. Let $\eta\in\mathcal{C}_0^\infty(\mathbb{R}^2)$ be a non-negative radial function satisfying $\int_{\mathbb{R}^2}\eta\,dx=1$, $supp(\eta)\subset B(0,1)$. We then define a regularized function associated with f by $f_\delta(x)=\frac{1}{\delta^2}\int_{\mathbb{R}^2}f(y)\eta(\frac{x-y}{\delta})\,dy$, $\forall x\in\mathbb{R}^2$. We focus on the direction e_1 and compute with $\delta>0$ and $\delta'>0$:

$$\int_{\mathbb{R}^2}(v_{2,n,e,\delta'}^2(x)+\kappa_\varepsilon)\int_{\mathbb{R}}\frac{|u_{n,e,\delta}(x+he_1)-2u_{n,e,\delta}(x)+u_{n,e,\delta}(x-he_1)|^2}{|h|^4}\rho_n(h)\,dh\,dx$$
$$=\int_{\mathbb{R}^2}(v_{2,n,e,\delta'}^2(x)+\kappa_\varepsilon)\int_{\mathbb{R}}\frac{|\int_{B(0,\delta)}\frac{u_{n,e}(x+he_1-z)-2u_{n,e}(x-z)+u_{n,e}(x-he_1-z)}{\delta^2}\eta(\frac{z}{\delta})\,dz|^2}{|h|^4}\rho_n(h)\,dh\,dx.$$

We apply Jensen's inequality with respect to the measure $\frac{\eta(\frac{z}{\delta})}{\delta^2}\,dz$, yielding

$$\leq\int_{\mathbb{R}^2}(v_{2,n,e,\delta'}^2(x)+\kappa_\varepsilon)\int_{\mathbb{R}}\int_{B(0,\delta)}\frac{|u_{n,e}(x+he_1-z)-2u_{n,e}(x-z)+u_{n,e}(x-he_1-z)|^2}{\delta^2|h|^4}$$
$$\eta(\frac{z}{\delta})\rho_n(h)\,dz\,dh\,dx.$$

We make the following change of variable: $v = x - z$,

$$\leq \int_{\mathbb{R}^2}\int_{\mathbb{R}}\int_{B(0,\delta)} (v^2_{2,n,e,\delta'}(v+z)+\kappa_\varepsilon)\frac{|u_{n,e}(v+he_1)-2u_{n,e}(v)+u_{n,e}(v-he_1)|^2}{\delta^2|h|^4}$$
$$\eta(\frac{z}{\delta})\rho_n(h)\,dz\,dh\,dv.$$

Since $v_{2,n,e,\delta'} \in C_0^\infty(\mathbb{R}^2)$, then $v^2_{2,n,e,\delta'}(v+z) = v^2_{2,n,e,\delta'}(v) + \int_0^1 \langle \nabla v^2_{2,n,e,\delta'}(v+sz), z\rangle\, ds$ and by introducing it in the previous inequality, we get:

$$\leq \int_{\mathbb{R}^2}\int_{\mathbb{R}}\int_{B(0,\delta)} (v^2_{2,n,e,\delta'}(v)+\kappa_\varepsilon)\frac{|u_{n,e}(v+he_1)-2u_{n,e}(v)+u_{n,e}(v-he_1)|^2}{\delta^2|h|^4}\eta(\frac{z}{\delta})\rho_n(h)\,dz\,dh\,dv$$
$$+\int_{\mathbb{R}^2}\int_{\mathbb{R}}\int_{B(0,\delta)}\int_0^1 (\langle\nabla v^2_{2,n,e,\delta'}(v+sz),z\rangle)\,ds\frac{|u_{n,e}(v+he_1)-2u_{n,e}(v)+u_{n,e}(v-he_1)|^2}{\delta^2|h|^4}$$
$$\eta(\frac{z}{\delta})\rho_n(h)\,dz\,dh\,dv.$$

We now integrate with respect to z in the first integral and use Cauchy-Schwarz inequality, and the change of variable $u = \frac{z}{\delta}$ in the second one, after bounding the component above by $\|\nabla v^2_{2,n,e,\delta'}\|_{L^\infty(\mathbb{R}^2)}$:

$$\leq \int_{\mathbb{R}^2}\int_{\mathbb{R}} (v^2_{2,n,e,\delta'}(v)+\kappa_\varepsilon)\frac{|u_{n,e}(v+he_1)-2u_{n,e}(v)+u_{n,e}(v-he_1)|^2}{|h|^4}\rho_n(h)\,dh\,dv$$
$$+\int_{\mathbb{R}^2}\int_{\mathbb{R}}\int_{B(0,1)} (\|\nabla v^2_{2,n,e,\delta'}\|_{L^\infty(\mathbb{R}^2)}\delta|u|)\frac{|u_{n,e}(v+he_1)-2u_{n,e}(v)+u_{n,e}(v-he_1)|^2}{|h|^4}$$
$$\eta(u)\rho_n(h)\,du\,dh\,dv,$$
$$\leq \int_{\mathbb{R}^2}\int_{\mathbb{R}} (v^2_{2,n,e,\delta'}(v)+\kappa_\varepsilon)\frac{|u_{n,e}(v+he_1)-2u_{n,e}(v)+u_{n,e}(v-he_1)|^2}{|h|^4}\rho_n(h)\,dh\,dv$$
$$+\|\nabla v^2_{2,n,e,\delta'}\|_{L^\infty(\mathbb{R}^2)}\delta\int_{\mathbb{R}^2}\int_{\mathbb{R}}\frac{|u_{n,e}(v+he_1)-2u_{n,e}(v)+u_{n,e}(v-he_1)|^2}{|h|^4}\rho_n(h)\,dh\,dv,$$
$$\leq \int_{\mathbb{R}^2}\int_{\mathbb{R}} (v^2_{2,n,e,\delta'}(v)+\kappa_\varepsilon)\frac{|u_{n,e}(v+he_1)-2u_{n,e}(v)+u_{n,e}(v-he_1)|^2}{|h|^4}\rho_n(h)\,dh\,dv$$
$$+\|\nabla v^2_{2,n,e,\delta'}\|_{L^\infty(\mathbb{R}^2)}\delta C, \text{ from the coercivity inequality.}$$

Since we assumed that $v_{2,n} \in W^{1,\infty}(\Omega,[0,1])$ such that $\gamma_0 v_{2,n} = 1$ for all $n \in \mathbb{N}^*$ with $\sup_{n\in\mathbb{N}^*}\|v_{2,n,e}\|_{W^{1,\infty}(\mathbb{R}^2)} \leq \sup_{n\in\mathbb{N}^*}\|v_{2,n}\|_{W^{1,\infty}(\Omega)} \leq C_1 < \infty$ and so $\sup_{n\in\mathbb{N}^*}\|\nabla v_{2,n,e}\|_{L^\infty(\mathbb{R}^2)} \leq C_1+1$ where $v_{2,n,e}$ is the extension of $v_{2,n}$ from $W^{1,2}(\Omega,[0,1])\cap W^{1,\infty}(\Omega)$ to $W^{1,2}(\mathbb{R}^2,[0,1])\cap W^{1,\infty}(\mathbb{R}^2)$ and $\bar{v}_{2,e}$ is the extension of $\bar{v}_2$ from $W^{1,2}(\Omega,[0,1])$ to $W^{1,2}(\mathbb{R}^2,[0,1])$, then we have thanks to [31, Theorem 1 p.123] that $\forall x \in \mathbb{R}^2$, $D^{(1,0)}v_{2,n,e,\delta'}(x) = \eta_{\delta'} * D^{(1,0)}v_{2,n,e}(x) = \int_{\mathbb{R}^2}\frac{1}{\delta'^2}D^{(1,0)}v_{2,n,e}(y)\eta(\frac{x-y}{\delta'})\,dy \leq \|D^{(1,0)}v_{2,n,e}\|_{L^\infty(\mathbb{R}^2)}$, $D^{(0,1)}v_{2,n,e,\delta'}(x) = \eta_{\delta'} * D^{(0,1)}v_{2,n,e}(x) =$

$\int_{\mathbb{R}^2} \frac{1}{\delta'^2} D^{(0,1)} v_{2,n,e}(y) \eta(\frac{x-y}{\delta'})\, dy \leq \|D^{(0,1)} v_{2,n,e}\|_{L^\infty(\mathbb{R}^2)}$ and so $\|\nabla v_{2,n,e,\delta'}\|_{L^\infty(\mathbb{R}^2)} \leq \|\nabla v_{2,n,e}\|_{L^\infty(\mathbb{R}^2)}$ $\leq C_1 + 1$. Eventually, we get:

$$\int_{\mathbb{R}^2} (v_{2,n,e,\delta'}(x)^2 + \kappa_\varepsilon) \int_{\mathbb{R}} \frac{|u_{n,e,\delta}(x+he_1) - 2u_{n,e,\delta}(x) + u_{n,e,\delta}(x-he_1)|^2}{|h|^4} \rho_n(h)\, dh\, dx$$
$$\leq \int_{\mathbb{R}^2} \int_{\mathbb{R}} (v^2_{2,n,e,\delta'}(v) + \kappa_\varepsilon) \frac{|u_{n,e}(v+he_1) - 2u_{n,e}(v) + u_{n,e}(v-he_1)|^2}{|h|^4} \rho_n(h)\, dh\, dv$$
$$+ 2(C_1+1)\delta C$$

As $W^{1,\infty}(\mathbb{R}^2) \circlearrowleft \mathcal{C}(\mathbb{R}^2)$, then $v_{2,n,e} \in \mathcal{C}(\mathbb{R}^2)$ and [31, Theorem 1 p.123] gives us that $v_{2,n,e,\delta'} \underset{\delta' \to 0}{\longrightarrow} v_{2,n,e}$ uniformly on compact subsets of $\mathbb{R}^2$ and so pointwise almost everywhere on $\mathbb{R}^2$ as $\mathbb{R}^2$ is locally compact. We thus have $(v^2_{2,n,e,\delta'}(v)+\kappa_\varepsilon) \frac{|u_{n,e}(v+he_1)-2u_{n,e}(v)+u_{n,e}(v-he_1)|^2}{|h|^4} \rho_n(h) \underset{\delta' \to 0}{\longrightarrow}$ $(v^2_{2,n,e}(v) + \kappa_\varepsilon) \frac{|u_{n,e}(v+he_1)-2u_{n,e}(v)+u_{n,e}(v-he_1)|^2}{|h|^4} \rho_n(h)$ and $(v^2_{2,n,e,\delta'}(v) + \kappa_\varepsilon) \frac{|u_{n,e,\delta}(v+he_1)-2u_{n,e,\delta}(v)+u_{n,e,\delta}(v-he_1)|^2}{|h|^4} \rho_n(h) \underset{\delta' \to 0}{\longrightarrow}$ $(v^2_{2,n,e}(v) + \kappa_\varepsilon) \frac{|u_{n,e,\delta}(v+he_1)-2u_{n,e,\delta}(v)+u_{n,e,\delta}(v-he_1)|^2}{|h|^4} \rho_n(h)$ almost everywhere on $\mathbb{R}^2$ and everywhere on $\mathbb{R}$. Besides, $\int_{\mathbb{R}} (v^2_{2,n,e,\delta'}(v)+\kappa_\varepsilon) \frac{|u_{n,e}(v+he_1) - 2u_{n,e}(v) + u_{n,e}(v-he_1)|^2}{|h|^4} \rho_n(h)\, dh \leq$ $(1+\kappa_\varepsilon) \int_{\mathbb{R}} \frac{|u_{n,e}(v+he_1) - 2u_{n,e}(v) + u_{n,e}(v-he_1)|^2}{|h|^4}\, \rho_n(h)\, dh \in L^1(\mathbb{R}^2)$ from the coercivity inequality, and $\int_{\mathbb{R}} (v^2_{2,n,e,\delta'}(v) + \kappa_\varepsilon) \frac{|u_{n,e,\delta}(v+he_1) - 2u_{n,e,\delta}(v) + u_{n,e,\delta}(v-he_1)|^2}{|h|^4} \rho_n(h)\, dh \leq$ $(1 + \kappa_\varepsilon) \int_{\mathbb{R}} \frac{|u_{n,e,\delta}(v+he_1) - 2u_{n,e,\delta}(v) + u_{n,e,\delta}(v-he_1)|^2}{|h|^4}\, \rho_n(h)\, dh \in L^1(\mathbb{R}^2)$ from Theorem 3.1. We can thus apply the dominated convergence theorem and get

$$\lim_{\delta' \to 0} \int_{\mathbb{R}^2} (v_{2,n,e,\delta'}(x)^2 + \kappa_\varepsilon) \int_{\mathbb{R}} \frac{|u_{n,e,\delta}(x+he_1) - 2u_{n,e,\delta}(x) + u_{n,e,\delta}(x-he_1)|^2}{|h|^4} \rho_n(h)\, dh\, dx$$
$$\leq \lim_{\delta' \to 0} \Bigg(\int_{\mathbb{R}^2} \int_{\mathbb{R}} (v^2_{2,n,e,\delta'}(v) + \kappa_\varepsilon) \frac{|u_{n,e}(v+he_1) - 2u_{n,e}(v) + u_{n,e}(v-he_1)|^2}{|h|^4} \rho_n(h)\, dh\, dv$$
$$+ 2(C_1+1)\delta C \Bigg),$$
$$\int_{\mathbb{R}^2} (v_{2,n,e}(x)^2 + \kappa_\varepsilon) \int_{\mathbb{R}} \frac{|u_{n,e,\delta}(x+he_1) - 2u_{n,e,\delta}(x) + u_{n,e,\delta}(x-he_1)|^2}{|h|^4} \rho_n(h)\, dh\, dx,$$
$$\leq \int_{\mathbb{R}^2} \int_{\mathbb{R}} (v^2_{2,n,e}(v) + \kappa_\varepsilon) \frac{|u_{n,e}(v+he_1) - 2u_{n,e}(v) + u_{n,e}(v-he_1)|^2}{|h|^4} \rho_n(h)\, dh\, dv$$
$$+ 2(C_1+1)\delta C.$$

Let us first show that $\lim_{n \to +\infty} \int_{\mathbb{R}^2} \int_{\mathbb{R}} (v^2_{2,n,e}(x)+\kappa_\varepsilon) \frac{|u_{n,e,\delta}(x+he_1) - 2u_{n,e,\delta}(x) + u_{n,e,\delta}(x-he_1)|^2}{|h|^4}$ $\rho_n(h)\, dh\, dx = \int_{\mathbb{R}^2} (\bar{v}^2_{2,e}(x)+\kappa_\varepsilon) |D^{(2,0)} \bar{u}_{e,\delta}(x)|^2\, dx$. To do so, we consider $\lim_{n \to +\infty} \Big| \int_{\mathbb{R}^2} \int_{\mathbb{R}} \big((v^2_{2,n,e}(x)+$

$$\kappa_\varepsilon)\frac{|u_{n,e,\delta}(x+he_1)-2u_{n,e,\delta}(x)+u_{n,e,\delta}(x-he_1)|^2}{|h|^4}-(\bar{v}^2_{2,e}(x)+\kappa_\varepsilon)|D^{(2,0)}\bar{u}_{e,\delta}(x)|^2\big)\rho_n(h)\,dh\,dx\Big| =$$
$$\lim_{n\to+\infty}\Big|\int_{\mathbb{R}^2}\int_{\mathbb{R}}(v^2_{2,n,e}(x)+\kappa_\varepsilon)\big(\frac{|u_{n,e,\delta}(x+he_1)-2u_{n,e,\delta}(x)+u_{n,e,\delta}(x-he_1)|^2}{|h|^4}-|D^{(2,0)}\bar{u}_{e,\delta}(x)|^2\big)$$
$$\rho_n(h)\,dh\,dx+\int_{\mathbb{R}^2}(\bar{v}^2_{2,e}(x)-v^2_{2,n,e,\delta}(x))|D^{(2,0)}\bar{u}_{e,\delta}(x)|^2\,dx\Big|.$$ We have

$$\int_{\mathbb{R}^2}\int_{\mathbb{R}}(v^2_{2,n,e}(x)+\kappa_\varepsilon)\frac{|u_{n,e,\delta}(x+he_1)-2u_{n,e,\delta}(x)+u_{n,e,\delta}(x-he_1)-h^2D^{(2,0)}\bar{u}_{e,\delta}(x)|^2}{|h|^4}\rho_n(h)\,dh\,dx$$
$$\le 2\int_{\mathbb{R}^2}\int_0^R\Big|\int_0^1\int_0^1 D^{(2,0)}u_{n,e,\delta}(x+(t+s-1)he_1)-D^{(2,0)}\bar{u}_{e,\delta}(x)\,ds\,dt\Big|^2\rho_n(h)\,dh\,dx$$
$$+2\int_{\mathbb{R}^2}\int_R^{+\infty}(v^2_{2,n,e}(x)+\kappa_\varepsilon)\frac{|u_{n,e,\delta}(x+he_1)-2u_{n,e,\delta}(x)+u_{n,e,\delta}(x-he_1)-h^2D^{(2,0)}\bar{u}_{e,\delta}(x)|^2}{|h|^4}$$
$$\rho_n(h)\,dh\,dx.$$

Using Jensen's inequality, we get

$$\int_{\mathbb{R}^2}\int_0^R\Big|\int_0^1\int_0^1 D^{(2,0)}u_{n,e,\delta}(x+(t+s-1)he_1)-D^{(2,0)}\bar{u}_{e,\delta}(x)\,ds\,dt\Big|^2\rho_n(h)\,dh\,dx$$
$$\le\int_{\mathbb{R}^2}\int_0^R\int_0^1\int_0^1|D^{(2,0)}u_{n,e,\delta}(x+(t+s-1)he_1)-D^{(2,0)}\bar{u}_{e,\delta}(x)|^2\,ds\,dt\rho_n(h)\,dh\,dx,$$
$$\le 2\int_{\mathbb{R}^2}\int_0^R\int_0^1\int_0^1|D^{(2,0)}u_{n,e,\delta}(x+(t+s-1)he_1)-D^{(2,0)}\bar{u}_{e,\delta}(x+(t+s-1)he_1)|^2\,ds\,dt$$
$$\rho_n(h)\,dh\,dx+2\int_{\mathbb{R}^2}\int_0^R\int_0^1\int_0^1|D^{(2,0)}\bar{u}_{e,\delta}(x+(t+s-1)he_1)-D^{(2,0)}\bar{u}_{e,\delta}(x)|^2\,ds\,dt$$
$$\rho_n(h)\,dh\,dx.$$

We then use Fubini's theorem, Jensen's inequality, and a Taylor's development, and get

$$\le 2\int_0^R\int_0^1\int_0^1\int_{\mathbb{R}^2}|D^{(2,0)}u_{n,e,\delta}(x+(t+s-1)he_1)-D^{(2,0)}\bar{u}_{e,\delta}(x+(t+s-1)he_1)|^2\,ds\,dt$$
$$\rho_n(h)\,dh\,dx+2\int_{\mathbb{R}^2}\int_0^R\int_0^1\int_0^1\int_0^1|D^{(3,0)}\bar{u}_{e,\delta}(x+k(t+s-1)he_1)|^2|h|^2|t+s-1|^2\,dk\,ds\,dt$$
$$\rho_n(h)\,dh\,dx,$$
$$\le 2\|D^{(2,0)}_{n,e,\delta}-D^{(2,0)}\bar{u}_{e,\delta}\|^2_{L^2(\mathbb{R}^2)}+\frac{1}{3}\|D^{(3,0)}\bar{u}_{e,\delta}\|^2_{L^2(\mathbb{R}^2)}\int_0^R h^2\rho_n(h)\,dh,$$
$$\le 2\|D^{(2,0)}_{n,e,\delta}-D^{(2,0)}\bar{u}_{e,\delta}\|^2_{L^2(\mathbb{R}^2)}+\frac{R^2}{3}\|D^{(3,0)}\bar{u}_{e,\delta}\|^2_{L^2(\mathbb{R}^2)}.$$

As $u_{n,e}\underset{n\to+\infty}{\longrightarrow}\bar{u}_e$ in $L^2(\mathbb{R}^2)$ and $D^{(2,0)}u_{n,e,\delta}=D^{(2,0)}\eta_\delta*u_{n,e}$, then $\|D^{(2,0)}_{n,e,\delta}-D^{(2,0)}\bar{u}_{e,\delta}\|_{L^2(\mathbb{R}^2)}$

$\underset{n\to+\infty}{\longrightarrow} 0$. Also by letting R tend to 0, $\lim_{n\to+\infty}\int_{\mathbb{R}^2}\int_0^R\left|\int_0^1\int_0^1 D^{(2,0)}u_{n,e,\delta}(x+(t+s-1)he_1)-D^{(2,0)}\bar{u}_{e,\delta}(x)\,ds\,dt\right|^2\rho_n(h)\,dh\,dx=0$. Furthermore,

$$\int_{\mathbb{R}^2}\int_R^{+\infty}(v_{2,n,e}^2(x)+\kappa_\varepsilon)\frac{|u_{n,e,\delta}(x+he_1)-2u_{n,e,\delta}(x)+u_{n,e,\delta}(x-he_1)-h^2D^{(2,0)}\bar{u}_{e,\delta}(x)|^2}{|h|^4}$$
$$\rho_n(h)\,dh\,dx$$
$$\leq 2\int_{\mathbb{R}^2}\int_R^{+\infty}(1+\kappa_\varepsilon)\frac{|u_{n,e,\delta}(x+he_1)-2u_{n,e,\delta}(x)+u_{n,e,\delta}(x-he_1)|^2}{|h|^4}\rho_n(h)\,dh\,dx$$
$$+2\int_{\mathbb{R}^2}\int_R^{+\infty}(1+\kappa_\varepsilon)|D^{(2,0)}\bar{u}_{e,\delta}(x)|^2\rho_n(h)\,dh\,dx,$$
$$\leq 2\int_{\mathbb{R}^2}\int_R^{+\infty}(1+\kappa_\varepsilon)\frac{1}{|h|^4}\Big(|u_{n,e,\delta}(x+he_1)-\bar{u}_{e,\delta}(x+he_1)-2u_{n,e,\delta}(x)+2\bar{u}_{e,\delta}(x)$$
$$+u_{n,e,\delta}(x-he_1)-\bar{u}_{e,\delta}(x-he_1)+\bar{u}_{e,\delta}(x+he_1)-2\bar{u}_{e,\delta}(x)+\bar{u}_{e,\delta}(x-he_1)|^2\Big)\rho_n(h)\,dh\,dx$$
$$+2(1+\kappa_\varepsilon)\|D^{(2,0)}\bar{u}_{e,\delta}(x)\|^2_{L^2(\mathbb{R}^2)}\int_R^{+\infty}\rho_n(h)\,dh,$$
$$\leq 4\int_{\mathbb{R}^2}\int_R^{+\infty}(1+\kappa_\varepsilon)\frac{1}{|h|^4}\Big(|u_{n,e,\delta}(x+he_1)-\bar{u}_{e,\delta}(x+he_1)|^2+4|u_{n,e,\delta}(x)-\bar{u}_{e,\delta}(x)|^2$$
$$+4|u_{n,e,\delta}(x-he_1)-\bar{u}_{e,\delta}(x-he_1)|^2+4|\bar{u}_{e,\delta}(x+he_1)-2\bar{u}_{e,\delta}(x)+\bar{u}_{e,\delta}(x-he_1)|^2\Big)$$
$$\rho_n(h)\,dh\,dx+2(1+\kappa_\varepsilon)\|D^{(2,0)}\bar{u}_{e,\delta}(x)\|^2_{L^2(\mathbb{R}^2)}\int_R^{+\infty}\rho_n(h)\,dh,$$
$$\leq\left(\frac{36(1+\kappa_\varepsilon)}{R^4}\|u_{n,e,\delta}-\bar{u}_{e,\delta}\|^2_{L^\infty(\mathbb{R}^2)}+16(1+\kappa_\varepsilon)\|D^{(2,0)}\bar{u}_{e,\delta}\|^2_{L^2(\mathbb{R}^2)}\right.$$
$$\left.+2(1+\kappa_\varepsilon)\|D^{(2,0)}\bar{u}_{e,\delta}(x)\|^2_{L^2(\mathbb{R}^2)}\right)\int_R^{+\infty}\rho_n(h)\,dh.$$

Since $\int_R^{+\infty}\rho_n(h)\,dh\underset{n\to+\infty}{\longrightarrow}0$, then

$$\int_{\mathbb{R}^2}\int_R^{+\infty}(v_{2,n,e}^2(x)+\kappa_\varepsilon)\frac{|u_{n,e,\delta}(x+he_1)-2u_{n,e,\delta}(x)+u_{n,e,\delta}(x-he_1)-h^2D^{(2,0)}\bar{u}_{e,\delta}(x)|^2}{|h|^4}$$
$$\rho_n(h)\,dh\,dx\underset{n\to+\infty}{\longrightarrow}0.$$

We also have that $\left|\int_{\mathbb{R}^2}\int_{\mathbb{R}}(v_{2,n,e}^2(x)-\bar{v}_{2,e}^2(x))|D^{(2,0)}\bar{u}_{e,\delta}(x)|^2\rho_n(h)\,dh\,dx\right|\leq\|D^{(2,0)}\bar{u}_{e,\delta}\|^2_{L^\infty(\mathbb{R}^2)}$ $2\|v_{2,n,e}-\bar{v}_{2,e}\|_{L^1(\mathbb{R}^2)}\leq 2\|v_{2,n,e}-\bar{v}_{2,e}\|_{L^2(\mathbb{R}^2)}$ with $\|v_{2,n,e}-\bar{v}_{2,e}\|_{L^2(\mathbb{R}^2)}\leq\|v_{2,n,e}-\bar{v}_{2,e}\|_{L^2(\Omega)}$ by construction of the extension and $(v_{2,n})$ strongly converges to $\bar{v}_2$ in $L^2(\Omega)$.

We thus have proved that $\lim_{n\to+\infty}\left|\int_{\mathbb{R}^2}\int_{\mathbb{R}}\left((v_{2,n,e}(x)^2+\kappa_\varepsilon)\right.\right.$

$$\frac{|u_{n,e,\delta}(x+he_1)-2u_{n,e,\delta}(x)+u_{n,e,\delta}(x-he_1)|^2}{|h|^4}-(\bar{v}_{2,e}(x)^2+\kappa_\varepsilon)|D^{(2,0)}\bar{u}_{e,\delta}(x)|^2\big)\rho_n(h)\,dh\,dx\Big| =$$

0 using the second triangle inequality.
Eventually, we have

$$\begin{aligned}
&\int_{\mathbb{R}^2}\int_{\mathbb{R}}(\bar{v}_{2,e}^2(x)+\kappa_\varepsilon)|D^{(2,0)}\bar{u}_{e,\delta}(x)|^2\rho_n(h)\,dh\,dx\\
&=\liminf_{n\to+\infty}\int_{\mathbb{R}^2}\int_{\mathbb{R}}\big((v_{2,n,e}^2(x)+\kappa_\varepsilon)\frac{|u_{n,e,\delta}(x+he_1)-2u_{n,e,\delta}(x)+u_{n,e,\delta}(x-he_1)|^2}{|h|^4}\rho_n(h)\,dh\,dx,\\
&\le\liminf_{n\to+\infty}\int_{\mathbb{R}^2}\int_{\mathbb{R}}\big((v_{2,n,e}^2(x)+\kappa_\varepsilon)\frac{|u_{n,e}(x+he_1)-2u_{n,e}(x)+u_{n,e}(x-he_1)|^2}{|h|^4}\rho_n(h)\,dh\,dx\\
&+2C(1+C_1)\delta.
\end{aligned}$$

Since $\bar{u}_e\in W^{2,2}(\mathbb{R}^2)$ then $D^{(2,0)}\bar{u}_{e,\delta}\underset{\delta\to0}{\longrightarrow}D^{(2,0)}\bar{u}_e$ in $L^2(\mathbb{R}^2)$ and we deduce by letting δ tend to 0 that

$$\begin{aligned}
&\int_{\mathbb{R}^2}(\bar{v}_{2,e}^2(x)+\kappa_\varepsilon)|D^{(2,0)}\bar{u}_e(x)|^2\,dx\\
&\le\liminf_{n\to+\infty}\int_{\mathbb{R}^2}\int_{\mathbb{R}}\big((v_{2,n,e}^2(x)+\kappa_\varepsilon)\frac{|u_{n,e}(x+he_1)-2u_{n,e}(x)+u_{n,e}(x-he_1)|^2}{|h|^4}\rho_n(h)\,dh\,dx.
\end{aligned}$$

We finally get $\lim_{n\to+\infty}\bar{\mathcal{F}}_{n,\varepsilon}(u_n,\vec{g}_n,Q_n,v_{1,n},v_{2,n})=\mathcal{F}(\bar{u},\vec{\bar{g}},\bar{Q},\bar{v}_1,\bar{v}_2)$ and $\forall(u,\vec{g},Q,v_1,v_2)\in W^{2,2}(\Omega)\cap W_0^{1,2}(\Omega)\times H(div)\times\{Q\in W^{1,\infty}(\Omega)|\int_\Omega Q\,dx=0\}\times W^{1,2}(\Omega)\times\{v_2\in W^{1,2}(\Omega)|\gamma_0 v_2=1\}$, $\bar{\mathcal{F}}_{n,\varepsilon}(u_n,\vec{g}_n,Q_n,v_{1,n},v_{2,n})\le\bar{\mathcal{F}}_{n,\varepsilon}(u,\vec{g},Q,v_1,v_2)$, and by letting n tend to infinity $\mathcal{F}(\bar{u},\vec{\bar{g}},\bar{Q},\bar{v}_1,\bar{v}_2)\le\mathcal{F}(u,\vec{g},Q,v_1,v_2)$ thanks to Theorem 3.2. This concludes the proof. □

We now turn to the part dedicated to numerical experiments.

4 Numerical Experiments

4.1 Sketch of the local algorithm

In this section, we briefly describe the main steps of our algorithm for the sake of reproducibility, and make qualitative comments. We recall that

$$\begin{cases}
v_1 &= \frac{\frac{\alpha-\beta}{2\varepsilon}+2(\alpha-\beta)\varepsilon\Delta v_1}{2\xi_\varepsilon|\nabla u|^2+\frac{\alpha-\beta}{2\varepsilon}},\quad v_2=\frac{\frac{\beta}{2\varepsilon}+2\beta\varepsilon\Delta v_2}{2\rho|\nabla^2u|^2+\frac{\beta}{2\varepsilon}},\\
u &= (f-\operatorname{div}\vec{g})-\rho\frac{\partial^2}{\partial x_1^2}\left(v_2^2\frac{\partial^2u}{\partial x_1^2}\right)-\rho\frac{\partial^2}{\partial x_2^2}\left(v_2^2\frac{\partial^2u}{\partial x_2^2}\right)\\
&\quad -2\rho\frac{\partial^2}{\partial x_1\partial x_2}\left(v_2^2\frac{\partial^2u}{\partial x_1\partial x_2}\right)+\xi_\varepsilon\operatorname{div}(v_1^2\nabla u).
\end{cases}$$

These equations can be interpreted as follows: when v_1 (respectively v_2) is close to 0 at some point, the role of the diffusion term $\operatorname{div}(v_1^2\nabla u)$ (resp. $\frac{\partial^2}{\partial x_i\partial x_j}\left(v_2^2\frac{\partial^2u}{\partial x_i\partial x_j}\right)$, $i,j\in\{1,2\}$) is cut, yielding not oversmoothed regions along edges or fine structures. If on the

contrary v_1 or v_2 is close to 1 at some point, there is diffusion in u at that point to obtain a smooth approximation. If $|\nabla u|$ is close to 0 at some point (resp. $|\nabla^2 u|^2$), then v_1 (resp. v_2) is close to 1, enhancing the regularization process. If on the contrary $|\nabla^2 u|$ is large, v_2 is close to 0 with a very small diffusion coefficient ($\simeq \frac{\beta\,\varepsilon}{\rho\,|\nabla^2 u|^2}$).
The Algorithm 8 consists in alternatively solving the Euler-Lagrange equations related to each unknown and presented in Section 2. We use a time-dependent scheme in $u = u(x_1, x_2, t)$ and $Q = Q(x_1, x_2, t)$ (nonlinear over-relaxation method, see [23, Section 4]), and a stationary semi-implicit fixed-point scheme in $v_1 = v_1(x_1, x_2)$, $v_2 = v_2(x_1, x_2)$ and $\vec{g} = \vec{g}(x_1, x_2)$. At the boundary, we extend u by reflection outside the domain, and a simple boundary condition for $\vec{g}$, $v_1 - 1$, and $v_2 - 1$ would be Dirichlet boundary conditions (and so Neumann boundary condition for Q), which appears to work well in practice.
Let $\Delta x_1 = \Delta x_2 = h = 1$ be the space step , let Δt be the time step, and let $f_{i,j}$, $u^n_{i,j}$, $Q^n_{i,j}$, $v^n_{1,i,j}$, $v^n_{2,i,j}$, $\vec{g}^n_{i,j} = (g^n_{1,i,j}, g^n_{2,i,j})^t$ be the discrete versions of f, u, Q, v_1, v_2 and $\vec{g}$ at iteration $n \geq 0$, for $1 \leq i \leq M$, $1 \leq j \leq N$.

1. [Initialization step]:

$u^0 = f$, $\vec{g}^0 = \vec{0}$, $Q^0 = 0$, $v^0_1 = 1$ and $v^0_2 = 1$.

2. [Main step]:

For $n \geq 1$, compute and **repeat to steady state** for all pixels (i, j):

$$
\begin{aligned}
&|\nabla u^n|^2_{i,j} = (u^n_{i+1,j} - u^n_{i,j})^2 + (u^n_{i,j+1} - u^n_{i,j})^2,\\
&v^{n+1}_{1,i,j} = \frac{\frac{(\alpha-\beta)}{2\varepsilon} + 2(\alpha-\beta)\varepsilon\,(v^n_{1,i+1,j} + v^n_{1,i-1,j} + v^n_{1,i,j+1} + v^n_{1,i,j-1} - 4v^{n+1}_{1,i,j})}{2\xi_\varepsilon\,|\nabla u^n|^2_{i,j} + \frac{(\alpha-\beta)}{2\varepsilon}},\\
&|\nabla^2 u^n|^2_{i,j} = (u^n_{i+1,j} - 2u^n_{i,j} + u^n_{i-1,j})^2 + 2\,(u^n_{i+1,j+1} - u^n_{i+1,j} - u^n_{i,j+1} + u^n_{i,j})^2\\
&+ (u^n_{i,j+1} - 2u^n_{i,j} + u^n_{i,j-1})^2,\\
&v^{n+1}_{2,i,j} = \frac{\frac{\beta}{2\varepsilon} + 2\beta\varepsilon\,(v^n_{2,i+1,j} + v^n_{2,i-1,j} + v^n_{2,i,j+1} + v^n_{2,i,j-1} - 4v^{n+1}_{2,i,j})}{2\rho\,|\nabla^2 u^n|^2_{i,j} + \frac{\beta}{2\varepsilon}},\\
&\frac{u^{n+1}_{i,j} - u^n_{i,j}}{\Delta t} = (f_{i,j} - u^n_{i,j} - \frac{g^n_{1,i,j+1} - g^n_{1,i,j-1}}{2} - \frac{g^n_{2,i+1,j} - g^n_{2,i-1,j}}{2})\\
&+ \xi_\varepsilon\,\left[(v^{n+1}_{1,i,j})^2\,(u^n_{i,j+1} - u^n_{i,j}) - (v^{n+1}_{1,i,j-1})^2\,(u^n_{i,j} - u^n_{i,j-1})\right]\\
&+ \xi_\varepsilon\,\left[(v^{n+1}_{1,i,j})^2\,(u^n_{i+1,j} - u^n_{i,j}) - (v^{n+1}_{1,i-1,j})^2\,(u^n_{i,j} - u^n_{i-1,j})\right]\\
&- \rho\,\left[(v^{n+1}_{2,i,j+1})^2\,(u^n_{i,j+2} - 2u^n_{i,j+1} + u^n_{i,j}) - 2\,(v^{n+1}_{2,i,j})^2\,(u^n_{i,j+1} - 2u^n_{i,j} + u^n_{i,j-1})\right.\\
&\left.+\ (v^{n+1}_{2,i,j-1})^2\,(u^n_{i,j} - 2u^n_{i,j-1} + u^n_{i,j-2})\right] - \rho\,\left[(v^{n+1}_{2,i+1,j})^2\,(u^n_{i+2,j} - 2u^n_{i+1,j} + u^n_{i,j})\right.
\end{aligned}
$$

$$
\begin{aligned}
&-2\,(v_{2,i,j}^{n+1})^2\,(u_{i+1,j}^n - 2u_{i,j}^n + u_{i-1,j}^n) + (v_{2,i-1,j}^{n+1})^2\,(u_{i,j}^n - 2u_{i-1,j}^n + u_{i-2,j}^n)\Big] \\
&- 2\,\rho\,\Big[(v_{2,i+1,j+1}^{n+1})^2\,(u_{i+2,j+2}^n - u_{i+1,j+2}^n - u_{i+2,j+1}^n + u_{i+1,j+1}^n) \\
&- (v_{2,i,j+1}^{n+1})^2\,(u_{i+1,j+2}^n - u_{i,j+2}^n - u_{i+1,j+1}^n + u_{i,j+1}^n) \\
&- (v_{2,i+1,j}^{n+1})^2\,(u_{i+2,j+1}^n - u_{i+1,j+1}^n - u_{i+2,j}^n + u_{i+1,j}^n) \\
&+ (v_{2,i,j}^{n+1})^2\,(u_{i+1,j+1}^n - u_{i,j+1}^n - u_{i+1,j}^n + u_{i,j}^n)\Big],
\end{aligned}
$$

and equations derived in the same way for g_1^n, g_2^n and Q^n.

Algorithm 8: Local alternating algorithm for crack recovery.

An alternating minimization procedure is thus performed as stressed in Algorithm 8, yielding convergence properties (see [20]). More precisely, starting with initial guess $v_1^0 \in S \subset \mathbb{R}^{M\times N}$, $v_2^0 \in S \subset \mathbb{R}^{M\times N}$, $u^0 \in X \subset \mathbb{R}^{M\times N}$, $\vec{g}^0 \in Z \subset (\mathbb{R}^{M\times N})^2$ and $Q^0 \in Y \subset \mathbb{R}^{M\times N}$, we successively obtain the sequence of conditional minimizers by solving

$$
\begin{aligned}
v_1^{(k+1)} &\in \arg\min_{v_1\in S} \mathcal{F}_\varepsilon(u^{(k)}, \vec{g}^{(k)}, Q^{(k)}, v_1, v_2^{(k)}), \\
v_2^{(k+1)} &\in \arg\min_{v_2\in S} \mathcal{F}_\varepsilon(u^{(k)}, \vec{g}^{(k)}, Q^{(k)}, v_1^{(k+1)}, v_2), \\
u^{(k+1)} &\in \arg\min_{u\in X} \mathcal{F}_\varepsilon(u, \vec{g}^{(k)}, Q^{(k)}, v_1^{(k+1)}, v_2^{(k+1)}), \\
\vec{g}^{(k+1)} &\in \arg\min_{\vec{g}\in Z} \mathcal{F}_\varepsilon(u^{(k+1)}, \vec{g}, Q^{(k)}, v_1^{(k+1)}, v_2^{(k+1)}), \\
Q^{(k+1)} &\in \arg\min_{Q\in Y} \mathcal{F}_\varepsilon(u^{(k+1)}, \vec{g}^{(k+1)}, Q, v_1^{(k+1)}, v_2^{(k+1)}),
\end{aligned}
$$

for $k \geq 0$. We consecutively prove :

(i) The monotonicity property

$$
\mathcal{F}_\varepsilon(u^{(k+1)}, \vec{g}^{(k+1)}, Q^{(k+1)}, v_1^{(k+1)}, v_2^{(k+1)}) \leq \mathcal{F}_\varepsilon(u^{(k)}, \vec{g}^{(k)}, Q^{(k)}, v_1^{(k)}, v_2^{(k)}),
$$

$\forall k \in \mathbb{N}$, ensuring that the sequence $\left\{\mathcal{F}_\varepsilon(u^{(k)}, \vec{g}^{(k)}, Q^{(k)}, v_1^{(k)}, v_2^{(k)})\right\}$ converges.

(ii) For any converging subsequence $(u^{(\Psi(k))}, \vec{g}^{(\Psi(k))}, Q^{(\Psi(k))}, v_1^{(\Psi(k))}, v_2^{(\Psi(k))})$ of $(u^{(k)}, \vec{g}^{(k)}, Q^{(k)}, v_1^{(k)}, v_2^{(k)})$ generated by the algorithm with

$$
(u^{(\Psi(k))}, \vec{g}^{(\Psi(k))}, Q^{(\Psi(k))}, v_1^{(\Psi(k))}, v_2^{(\Psi(k))}) \underset{k\to+\infty}{\longrightarrow} (u^*, \vec{g}^*, Q^*, v_1^*, v_2^*),
$$

the following holds :

$$
\begin{aligned}
&\forall u \in X,\ \mathcal{F}_\varepsilon(u^*, \vec{g}^*, Q^*, v_1^*, v_2^*) \leq \mathcal{F}_\varepsilon(u, \vec{g}^*, Q^*, v_1^*, v_2^*), \\
&\forall Q \in Y,\ \mathcal{F}_\varepsilon(u^*, \vec{g}^*, Q^*, v_1^*, v_2^*) \leq \mathcal{F}_\varepsilon(u^*, \vec{g}^*, Q, v_1^*, v_2^*), \\
&\forall \vec{g} \in Z,\ \mathcal{F}_\varepsilon(u^*, \vec{g}^*, Q^*, v_1^*, v_2^*) \leq \mathcal{F}_\varepsilon(u^*, \vec{g}, Q^*, v_1^*, v_2^*),
\end{aligned}
$$

$$\forall v_1 \in S,\ \mathcal{F}_\varepsilon(u^*, \vec{g}^*, Q^*, v_1^*, v_2^*) \leq \mathcal{F}_\varepsilon(u^*, \vec{g}^*, Q^*, v_1, v_2^*),$$
$$\forall v_2 \in S,\ \mathcal{F}_\varepsilon(u^*, \vec{g}^*, Q^*, v_1^*, v_2^*) \leq \mathcal{F}_\varepsilon(u^*, \vec{g}^*, Q^*, v_1^*, v_2),$$

making $(u^*, \vec{g}^*, Q^*, v_1^*, v_2^*)$ a partial minimizer.

(iii) If $(u^{(k)}, \vec{g}^{(k)}, Q^{(k)}, v_1^{(k)}, v_2^{k)}) \underset{k\to+\infty}{\longrightarrow} (u^*, \vec{g}^*, Q^*, v_1^*, v_2^*)$, then $(u^*, \vec{g}^*, Q^*, v_1^*, v_2^*)$ belongs to the set of all partial minimizers of the problem.
If $(u^{(k)}, \vec{g}^{(k)}, Q^{(k)}, v_1^{(k)}, v_2^{k)})$ does not converge, there exists a subsequence that converges to a partial minimizer of the problem.

4.2 Sketch of the nonlocal algorithm

Let us first derive the nonlocal Euler-Lagrange equation with respect to the variable u. Let η be a test function and $\epsilon \in \mathbb{R}$. We set

$$\begin{aligned}
J(\epsilon) &= \|f - u - \epsilon\eta - \operatorname{div}\vec{g}\|^2_{L^2(\Omega)} + \rho \int_{\mathbb{R}^2} (v_{2,e}^2(x) + \kappa_\varepsilon) \\
&\sum_{i=1}^{2} \int_{\mathbb{R}} \frac{|u_e(x+he_i) + \epsilon\eta(x+he_i) - 2u_e(x) - 2\epsilon\eta(x) + u_e(x-he_i) + \epsilon\eta(x-he_i)|^2}{|h|^4} \rho_n(h)\, dh\, dx \\
&+ \xi_\varepsilon \int_\Omega (v_1^2 + \zeta_\epsilon)\, |\nabla u + \epsilon\nabla\eta|^2\, dx, \\
J'(\epsilon) &= -2\int_\Omega (f - u - \epsilon\eta - \operatorname{div}\vec{g})\eta\, dx + \rho \int_{\mathbb{R}^2} (v_{2,e}^2(x) + \kappa_\varepsilon) \\
&\sum_{i=1}^{2} \int_{\mathbb{R}} \frac{2(u_e(x+he_i) + \epsilon\eta(x+he_i) - 2u_e(x) - 2\epsilon\eta(x) + u_e(x-he_i) + \epsilon\eta(x-he_i))}{|h|^4} \\
&(\eta(x+he_i) - 2\eta(x) + \eta(x-he_i))\rho_n(h)\, dh\, dx \\
&+ \xi_\varepsilon \int_\Omega (v_1^2 + \zeta_\epsilon) 2(\nabla u + \epsilon\nabla\eta)\nabla\eta\, dx, \\
J'(0) &= -\int_\Omega 2(f - u - \operatorname{div}\vec{g})\eta\, dx + \rho \int_{\mathbb{R}^2} (v_{2,e}^2(x) + \kappa_\varepsilon) \\
&\sum_{i=1}^{2} \int_{\mathbb{R}} \frac{2(u_e(x+he_i) - 2u_e(x) + u_e(x-he_i))(\eta(x+he_i) - 2\eta(x) + \eta(x-he_i))}{|h|^4} \rho_n(h)\, dh\, dx \\
&+ \xi_\varepsilon \int_\Omega (v_1^2 + \zeta_\epsilon) 2(\nabla u)\nabla\eta\, dx = 0, \\
J'(0) &= -\int_\Omega (f - u - \operatorname{div}\vec{g})\eta\, dx \\
&+ \rho \int_{\mathbb{R}^2} \sum_{i=1}^{2} \int_{\mathbb{R}} \Bigg(\frac{-2(v_{2,e}^2(x) + \kappa_\varepsilon)(u_e(x+he_i) - 2u_e(x) + u_e(x-he_i))}{|h|^4} \\
&+ \frac{(v_{2,e}^2(x-he_i)) + \kappa_\varepsilon)(u(x) - 2u(x-he_i) + u(x-2he_i))}{|h|^4}
\end{aligned}$$

$$+\frac{(v_{2,e}^2(x+he_i)+\kappa_\varepsilon)(u(x+2he_i)-2u(x+he_i)+u(x))}{|h|^4}\Big)\eta\rho_n(h)\,dh\,dx$$
$$-\xi_\varepsilon\int_\Omega \mathrm{div}((v_1^2+\zeta_\epsilon)\nabla u)\eta\,dx=0.$$

Besides, the equation for v_2 becomes $v_2=\dfrac{\frac{\beta}{2\varepsilon}+2\beta\varepsilon\Delta v_2}{2\rho\sum\limits_{i=1}^{2}\int_{\mathbb{R}}\frac{|u_e(x+he_i)-2u_e(x)+u_e(x-he_i)|^2}{|h|^4}\rho_n(h)\,dh+\frac{\beta}{2\varepsilon}}$.

The equations related to the other variables remain unchanged.

We now introduce the nonlocal weights inspired by the NL-means algorithm ([19]). Indeed, we believe that integrating additional information related to the content of the image I is pertinent here. We thus want to put more weights to neighbors that have similar edges/creases and to geographically close neighbors. We consider the following nonlocal weights $\frac{\rho_n(h)}{|h|^4}\approx w_{I,i,x}(h)=\exp\left(-\frac{d_{I,x,i}(h)}{\alpha^2}\right)$ where $d_{I,x,i}(h)=\int_{\mathbb{R}^2}G_a(t)\|\nabla I(x+t)-\nabla I(x+t+he_i)\|^2\,dt$ or $d_{I,x,i}(h)=\int_{\mathbb{R}^2}G_a(t)\|\nabla^2 I(x+t)-\nabla^2 I(x+t+he_i)\|^2\,dt$ where G_a is a Gaussian kernel with standard deviation a controlling the patch size and α is the filtering parameter. Below is the pseudo-code associated with the computation of the nonlocal weights (Algorithm 9).

Input :
Initial image I
Output:

Weights in the first direction $w_{I,x,1}$, the shifts of the selected neighbors in the first direction $indice_1$, weights in the second direction $w_{I,x,2}$, the shifts of the selected neighbors in the second direction $indice_2$.

1. Define $w :=$ window size, $p :=$ patch size, $h := 0.25$, $NbNeigh :=$ number of actual required neighbors including the closest one, $Nx :=$ number of horizontal pixels, $Ny :=$ number of vertical pixels.
2. Compute the extended image by symmetry.
for all pixels $x=(x_1,x_2)$ **do**
3. Compute the distance

$$d_{I,x,1}(y)=\sum_{i=-\frac{p-1}{2}}^{\frac{p-1}{2}}\sum_{j=-\frac{p-1}{2}}^{\frac{p-1}{2}}\Big(\frac{\|\nabla I(x_1+i,x_2+j)-\nabla I(x_1+y+i,x_2+j)\|^2}{2}$$
$$+\frac{\|\nabla I(x_1+i,x_2+j)-\nabla I(x_1+(i-y),x_2+j)\|^2}{2}\Big)$$

between all patches centered at $x+ye_1$ of size p with $0\le y\le\frac{iw-1}{2}$ and the patch centered at the current x.
end for

for all pixels $x = (x_1, x_2)$ **do**

3.(following) or

$$d_{I,x,1}(y) = \sum_{i=-\frac{p-1}{2}}^{\frac{p-1}{2}} \sum_{j=-\frac{p-1}{2}}^{\frac{p-1}{2}} \left(\frac{\|\nabla^2 I(x_1+i, x_2+j) - \nabla^2 I(x_1+y+i, x_2+j)\|^2}{2} + \frac{\|\nabla^2 I(x_1+i, x_2+j) - \nabla^2 I(x_1+(i-y), x_2+j)\|^2}{2} \right)$$

between all patches centered at $x + ye_1$ of size p with $0 \leq y \leq \frac{iw-1}{2}$ and the patch centered at the current x. Compute the distance

$$d_{I,x,2}(y) = \sum_{i=-\frac{p-1}{2}}^{\frac{p-1}{2}} \sum_{j=-\frac{p-1}{2}}^{\frac{p-1}{2}} \left(\frac{\|\nabla I(x_1+i, x_2+j) - \nabla I(x_1+i, x_2+(y+j))\|^2}{2} + \frac{\|\nabla I(x_1+i, x_2+j) - \nabla I(x_1+i, x_2+(j-y))\|^2}{2} \right).$$

or

$$d_{I,x,2}(y) = \sum_{i=-\frac{p-1}{2}}^{\frac{p-1}{2}} \sum_{j=-\frac{p-1}{2}}^{\frac{p-1}{2}} \left(\frac{\|\nabla^2 I(x_1+i, x_2+j) - \nabla^2 I(x_1+i, x_2+(y+j))\|^2}{2} + \frac{\|\nabla^2 I(x_1+i, x_2+j) - \nabla^2 I(x_1+i, x_2+(j-y))\|^2}{2} \right).$$

between all patches centered at $x + ye_2$ of size p with $0 \leq y \leq \frac{iw-1}{2}$ and the patch centered at the current x.

end for

for all pixels x **do**

4.1. Sort the previous distances in ascending order for each direction and keep only the lowest $NbNeigh - 1$ values with the corresponding shift (y) for the first direction in $indice_1$ and for the second direction in $indice_2$.

4.2. Add the closest neighbor in geographical sense and in each direction to make the weights more similar to the theoretical ones.

end for

for all pixels x **do**

5.1. Compute $w_{I,x,1}$ by the following formula: $w_{I,x,1}(y) = 0$ if y does not belong to the previous list of neighbors, $w_{I,x,1}(y) = \exp\left\{-\frac{d_{I,x,1}(y)}{h^2}\right\}$ otherwise. Compute $w_{I,x,2}$ by the following formula: $w_{I,x,2}(y) = 0$ if $x + ye_2$ does not belong to the previous list of neighbors, $w_{I,x,2}(y) = \exp\left\{-\frac{d_{I,x,2}(y)}{h^2}\right\}$ otherwise.

end for

return $w_{I,x,1}$, $w_{I,x,2}$, $indice_1$, $indice_2$.

Algorithm 9: Computation of the nonlocal weights inspired by the NL-means algorithm.

The nonlocal algorithm also relies on an alternating strategy in which we solve the Euler-Lagrange equations related to each unknown using the same schemes as in the local one. Neumann boundary conditions for u and Q and Dirichlet boundary conditions for $v_1 - 1$, $v_2 - 1$ and $\vec{g}$ are applied. We use the same notations as previously done and get the following Algorithm 10.

1. [Initialization step]:
$u^0 = f$, $\vec{g}^0 = \vec{0}$, $Q^0 = 0$, $v_1^0 = 1$ and $v_2^0 = 1$.
2. [Main step]:
for n=1 to n=500 **do**
if n%100==0 **then**
2.1 Compute the nonlocal weights associated to u^n:
$[w_{I,x,1}, w_{I,x,2}, indice_1, indice_2] = compute_weights(u^n)$.
end if
2.2 Compute for all pixels (i, j):

$$|\nabla u^n|^2_{i,j} = (u^n_{i+1,j} - u^n_{i,j})^2 + (u^n_{i,j+1} - u^n_{i,j})^2,$$

$$v^{n+1}_{1,i,j} = \frac{\frac{(\alpha-\beta)}{2\varepsilon} + 2(\alpha-\beta)\varepsilon\,(v^n_{1,i+1,j} + v^n_{1,i-1,j} + v^n_{1,i,j+1} + v^n_{1,i,j-1} - 4v^n_{1,i,j})}{2\xi_\varepsilon\,|\nabla u^n|^2_{i,j} + \frac{(\alpha-\beta)}{2\varepsilon}},$$

$$nlnormu^2_{i,j} = \sum_{h\in indice_1} (u^n(i+h,j) - 2u^n(i,j) + u^n(i-h,j))^2 w_{I,i,j,1}(h))$$
$$+ \sum_{h\in indice_2} (u^n(i,j+h) - 2u^n(i,j) + u^n(i,j-h))^2 w_{I,i,j,2}(h),$$

$$v^{n+1}_{2,i,j} = \frac{\frac{\beta}{2\varepsilon} + 2\beta\varepsilon\,(v^n_{2,i+1,j} + v^n_{2,i-1,j} + v^n_{2,i,j+1} + v^n_{2,i,j-1} - 4v^n_{2,i,j})}{2\rho\, nlnormu^2_{i,j} + \frac{\beta}{2\varepsilon}},$$

$$\frac{u^{n+1}_{i,j} - u^n_{i,j}}{\Delta t} = (f_{i,j} - u^n_{i,j} - \frac{g^n_{1,i,j+1} - g^n_{1,i,j-1}}{2} - \frac{g^n_{2,i+1,j} - g^n_{2,i-1,j}}{2})$$
$$+ \xi_\varepsilon\,\left[(v^n_{1,i,j})^2\,(u^n_{i,j+1} - u^n_{i,j}) - (v^n_{1,i,j-1})^2\,(u^n_{i,j} - u^n_{i,j-1})\right]$$
$$+ \xi_\varepsilon\,\left[(v^n_{1,i,j})^2\,(u^n_{i+1,j} - u^n_{i,j}) - (v^n_{1,i-1,j})^2\,(u^n_{i,j} - u^n_{i-1,j})\right]$$
$$- \rho\left[\sum_{h\in indice_1} (v^n_{2,i+h,j})^2\,(u^n_{i+2h,j} - 2u^n_{i+h,j} + u^n_{i,j}) - 2\,(v^n_{2,i,j})^2\,(u^n_{i,j+h} - 2u^n_{i,j} + u^n_{i,j-h})\right.$$
$$\left. + (v^n_{2,i-h,j})^2\,(u^n_{i,j} - 2u^n_{i-h,j} + u^n_{i-2h,j})\right] w_{I,i,j,1}(h) - \rho w_{I,i,j,2}(h)\left[(v^n_{2,i,j-h})^2\,(u^n_{i,j} - 2u^n_{i,j-h}\right.$$
$$\left. + u^n_{i,j-2h}) + \sum_{h\in indice_2} (v^n_{2,i,j+h})^2\,(u^n_{i,j+2h} - 2u^n_{i,j+h} + u^n_{i,j}) - 2\,(v^n_{2,i,j})^2\,(u^n_{i,j+h} - 2u^n_{i,j} + u^n_{i,j-h})\right],$$

using symmetry if it does not belong to the image domain, and equations derived in the same way for g^n_1, g^n_2 and Q^n.
end for

Algorithm 10: Nonlocal alternating algorithm for crack recovery.

In order to improve the computation efficiency, we propose an MPI parallelization of our code, which motivates our choice of a rather simple alternating minimization method for which a decomposition domain approach is well-suited.

4.3 MPI parallelization

The parallelization of the C code is motivated by the natural geometry of the problem —an image is defined on a rectangle domain Ω —making the partition of the image domain into subdomains supporting simultaneous local computations relevant. Note also that the computational complexity increases with the image size (in practice we have worked with some images of size 2248×4000), requiring more memory to store the data and the results, this fact being particularly marked in the nonlocal model that involves the resolution of a nonlocal partial differential equation.

The meshing is made of ntx interior points in the row direction (we removed the first and last two layers of points for the local case and the first and last layers of points for the nonlocal case) and nty interior points in the column direction (we removed the two leftmost and rightmost columns of points for the local case and the leftmost and rightmost column of points for the nonlocal case). The implementation revolves around the following steps:

(i) we generate a Cartesian topology (see Figure 5.2 for an example), each subdomain comprising two/$w-1$ (local/nonlocal, where w is the window size) rows of ghost cells above, two/$w-1$ rows of ghost cells below, and similarly for the columns, in order to store the data exchanged with neighboring subdomains. Either the developer selects the number of nodes in each direction, or it is left to the MPI library. Some latitude is also given to the user in terms of periodicity (—a periodicity can be applied on the grid in each direction if required thanks to the array **periods** —) and reorganization (—if the user wants the processes to keep the same rank as in the original communicator —).

(ii) For each subdomain, we recover the bounds with respect to the original image reference frame of the indices i and j that are then stored in the 1d array **tab_bounds**: tab_bounds[0]=sx, tab_bounds[1]=ex, tab_bounds[2]=sy and tab_bounds[3]=ey). The numbering of the original image reference frame starts at 0 and the origin is the top left corner. The indices $(sx-2,\ sx-1,\ ex+1,\ ex+2,\ sy-2,\ sy-1,\ ey+1,\ ey+2)/(sx-w+1,\ \ldots,\ sx-1,\ ex+1,\ \ldots,ex+w-1,\ sy-w+1,\ \ldots,\ sy-1,\ ey+1,\ \ldots,\ ey+w-1)$ are used to store the data sent by the 8-connected neighboring subdomains.
Created function : **void domaine(MPI_Comm comm2d,int rang,int * coords,int ntx,int nty,int * dims,int * tab_bounds,int * periods,int reorganization,int nb_procs)**

(iii) For each subdomain, the neighboring subdomain ranks are returned. This is achieved thanks to the routine **voisinage** and these ranks are stored respectively in the 1d array voisin (for the 4-connected blocks) and voisin_diagonale (for the diagonally

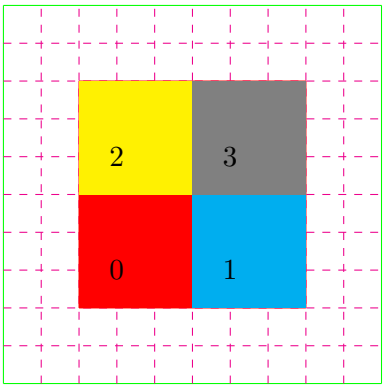

Figure 5.2: Cartesian topology in the local case with 4 processes on a (10×10) image:
Process 0 : $(sx = 2, ex = 4, sy = 5, ey = 7)$;
Process 1 : $(sx = 5, ex = 7, sy = 5, ey = 7)$;
Process 2 : $(sx = 2, ex = 4, sy = 2, ey = 4)$;
Process 3 : $(sx = 5, ex = 7, sy = 5, ey = 7)$.

connected blocks). The necessity of storing the ranks of diagonally connected blocks arises from the numerical schemes used to discretize the partial differential equations satisfied by u, Q, g_1 and g_2 that involve for instance components like $u_{i+2,j+2}$, $Q_{i-1,j+1}$, $v_{2,i-1,j-1}$ or $g_{2,i+1,j-1}$.
Created function: **void voisinage(MPI_Comm comm2d,int * voisin, int * voisin_diagonale,int * coords, int * dims)**

(iv) Once the Cartesian topology is created, one needs to distribute the data file (image data) to each subdomain in parallel (more precisely, the portion of the data file that must be visible for the related process). The general file manipulation function **MPI_File_open** is called. We then create a datatype **MPI_Datatype mysubarray** describing a two-dimensional subarray (the portion of the image related to the current subdomain) of a bigger two-dimensional array (the image here) (routine **MPI_Type_create_subarray**). The **MPI_File_set_view** routine allows to change the process view of the data in the file: the beginning of the data accessible in the file through that view is set to 0, the type of data is set to MPI_DOUBLE, and the distribution of data to processes is set to mysubarray. Then the **MPI_File_read** routine enables us to read the file starting at the specified location.

(v) Derived datatypes are created, describing the rows, columns and 2×2 diagonal arrays involved in the MPI communications : **MPI_Datatype type_2colonnes/type_(w-1)colonnes, type_ligne, type_colonne_mono, type_2lignes/type_(w-1)lignes, type_ligne, type_colonne_mono, type_(w-1)lignes** among others. In that purpose, the routines **MPI_Type_contiguous** —creating a contiguous datatype, here a single row of data —and **MPI_Type_vector** —general constructor that allows replication of a datatype into locations that consist of equally spaced blocks, here a single column, a group of two/(w-1) adjacent columns and a group of two/(w-1)

adjacent rows —are used. For the communications with diagonally connected subdomains, a datatype describing a two-dimensional subarray of size 2×2 of a bigger two-dimensional array is created for each spatial configuration: top left corner, top right corner, bottom left corner and bottom right corner.

(vi) The communications are then handled with the routine **MPI_Sendrecv**. This send-receive operation combines in one call the sending of a message to one destination and the receiving of another message from another process. As an illustration (see also Figure 5.3), *u_local_mat* denoting the local array describing u :

(a) $u_local_mat(sx : sx+1, :)/u_local_mat(sx : sx+w-2, :)$ is sent to the northern neighbor that receives data in $u_local_mat(ex+1 : ex+2, :)/u_local_mat(ex+1 : ex+w-1, :)$;

(b) $u_local_mat(ex-1 : ex, :)/u_local_mat(ex-w+2 : ex, :)$ is sent to the southern neighbor that receives data in $u_local_mat(sx-2 : sx-1, :)/u_local_mat(sx-w+1 : sx-1, :)$;

(c) $u_local_mat(:, sy : sy+1)/u_local_mat(:, sy : sy+w-2)$ is sent to the western neighbor that receives data in $u_local_mat(:, ey+1 : ey+2)/u_local_mat(:, ey+1 : ey+w-1)$;

(d) $u_local_mat(:, ey-1 : ey)/u_local_mat(:, ey-w+2 : ey)$ is sent to the eastern neighbor that receives data in $u_local_mat(:, sy-2 : sy-1)/u_local_mat(:, sy-w+1 : sy-1)$;

(e) $u_local_mat(sx : sx+1, ey-1 : ey)$ is sent to the northeast neighbor that receives data in $u_local_mat(ex+1 : ex+2, sy-2 : sy-1)$;

(f) $u_local_mat(ex-1 : ex, ey-1 : ey)$ is sent to the southeast neighbor that receives data in $u_local_mat(sx-2 : sx-1, sy-2 : sy-1)$;

(g) $u_local_mat(ex-1 : ex, sy : sy+1)$ is sent to the southwest neighbor that receives data in $u_local_mat(sx-2 : sx-1, ey+1 : ey+2)$;

(h) $u_local_mat(sx : sx+1, sy : sy+1)$ is sent to the northwest neighbor that receives data in $u_local_mat(ex+1 : ex+2 :, ey+1 : ey+2)$.

For subdomains with at least one edge included in the image domain boundary, diagonal communications do not occur and are replaced by communications with the ghost cells of the involved contiguous subdomain.
Created function : **void communication(double ** u,double ** v1_local_mat, double ** v2_local_mat,double ** g1_local_mat,double ** g2_local_mat,double ** Q_local_mat,int * tab_bounds,MPI_Comm comm2d,int * voisin, int * voisin _diagonale)**

(vii) The values of u^{n+1}, Q^{n+1}, v_1^{n+1}, v_2^{n+1}, g_1^{n+1} and g_2^{n+1} are computed using the above mentioned finite difference schemes (v_1 and v_2 have been initialized to 1, g_1, g_2 and Q to 0, while u has been set to the values of the original image) and the question of boundary conditions is addressed. For the sake of simplicity, we have assumed

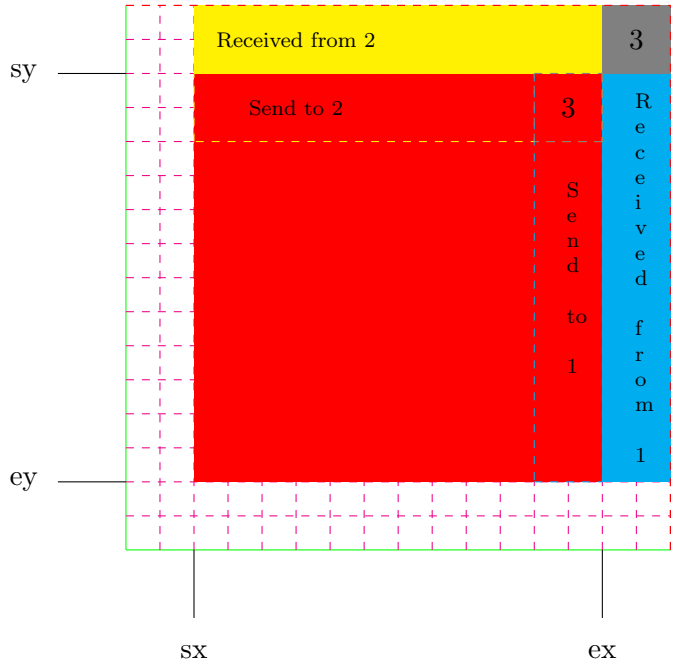

Figure 5.3: Phantom cells and communications, example on process 0 for the local case.

homogeneous Neumann boundary conditions for u, simulating reflection of the array through its boundaries and Dirichlet boundary conditions for $v_1 - 1$, $v_2 - 1$, $\vec{g}$ and Q. We thus identify subdomains with at least one edge included in the image domain boundary. We then replicate the third row of the local matrix in the second one, the fourth row in the first one, similarly for the last two rows and first/last two columns for u. The diagonal components are processed using point symmetry. The newly computed values are then transmitted to neighboring subdomains and a new time step is achieved.

(viii) We finally write the result (component v_2 encoding the fine structure we aim to recover) in a file using again MPI I/O. The general file manipulation function **MPI_File_open** is called. We then create a new datatype describing the two-dimensional subarray extracted from the original local array v2_local_mat when removing the ghost cells. The routine **MPI_File_set_view** changes the process view of the data in the file, while the routine **MPI_File_write_all** writes the file, starting at the locations specified by individual file pointers.
Created function : **void ecrire_mpi(double *v2_local_vect,int ntx,int nty,int * tab_bounds,MPI_Comm comm2d)**

(ix) In the nonlocal case, the computation of the nonlocal weights is done by every process on their associated subdomain.

The computations have been made with the supercomputer Myria operated by the CRIANN (Centre Régional Informatique et d'Applications Numériques de Normandie, `http:`

//www.criann.fr/). Myria is an ATOS BULL solution with 11144 computing cores, with a power of 403 TFlops Xeon, 170 TFlops GPU and 27 TFlops Xeon Phi KNL. Myria also has a fast storage space of about 2.5 Po. Submission of the work is done through the SLURM software.

The local algorithm has been applied to a bituminous surfacing image of size 2248×4000, requiring 500 time step iterations both in the case of the sequential algorithm , execution time : 289.576683 seconds, and parallelized algorithm with 224 tasks, execution time : 1.752749 seconds. The efficiency is of 74% from 1 to 224 tasks and of 100% from 28 to 224 tasks. Below (Figure 5.4) are the statistics obtained for 1 task and 224 tasks. The

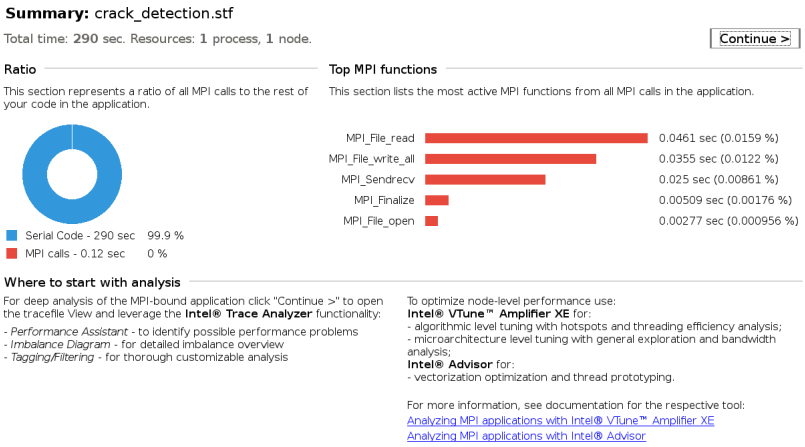

(a) 1 task

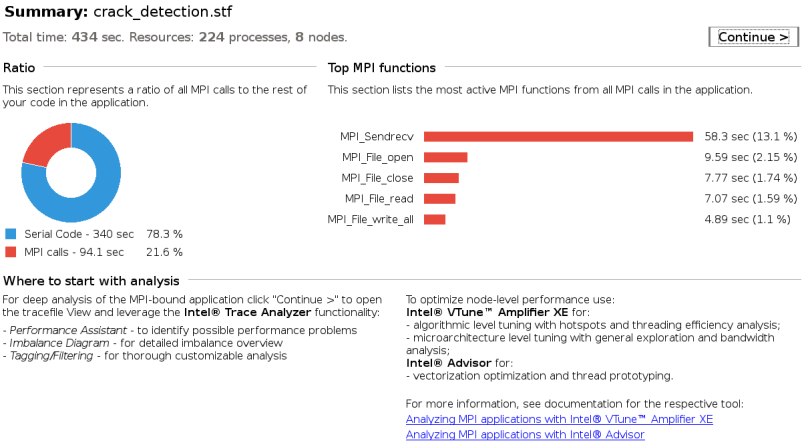

(b) 224 tasks

Figure 5.4: Computational statistics for the local algorithm.

nonlocal algorithm has been applied to a bituminous surfacing image of size 2248×4000, requiring 360 time step iterations both in the case of the sequential algorithm , execution time : 596.582511 seconds, and parallelized algorithm with 224 tasks, execution time : 4.409619 seconds. Below (Figure 5.5) are the statistics obtained for 1 task and 224 tasks.

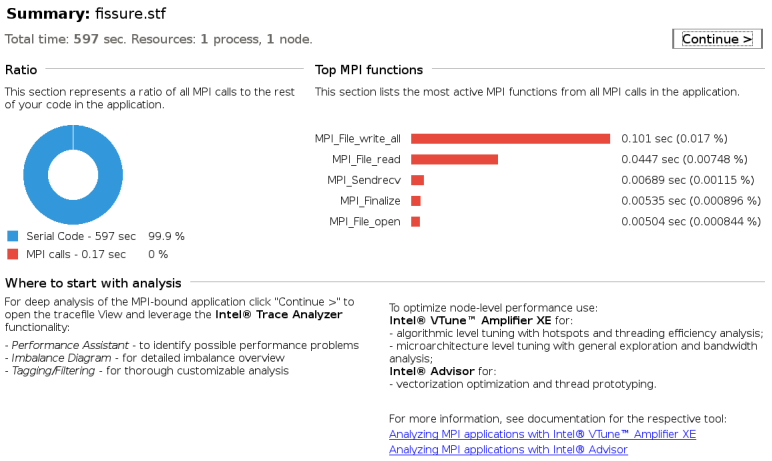

(a) 1 task

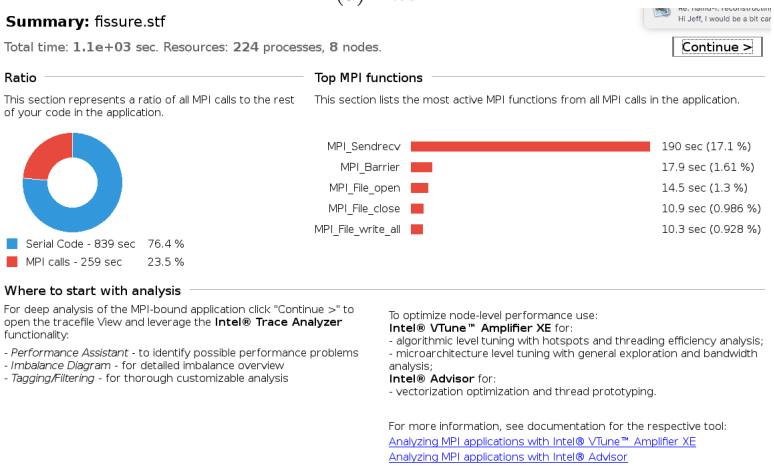

(b) 224 tasks

Figure 5.5: Computational statistics for the nonlocal algorithm.

4.4 Numerical simulations

Experimental results on real datasets are now provided, resulting from the application of the above algorithms (local/nonlocal). The values of the parameters in the functional are chosen on the basis of the results of a number of experiments. We can nevertheless infer the behavior of some of them: less regularization (smaller α, β, ρ and ξ_ε) induces more edges/creases in v_1 and v_2 respectively. Also, a higher parameter μ balancing the L^∞-norm of $|\nabla Q|$ will lead to smaller scale features in the $v = \operatorname{div} \vec{g}$ component. The fine structures appear as contours along which the auxiliary variable v_2 is close to zero, while jumps appear as contours with larger thickness.
We start off with an application dedicated to road network detection on urban scenes.

An aerial urban scene is depicted in Figure 5.6 (A. Drogoul's courtesy, size of the image 652×892), together with its smooth approximation u obtained with our local implementation (u local), with our nonlocal implementation in which we consider only the four closest neighbors (u nonlocal (only 4 closest neighbors)), with our nonlocal implementation in which the weights are computed using the distance based on the comparison of the image gradients (u nonlocal (weights based on gradient) and with our nonlocal implementation in which the weights are computed using the distance comparing the Hessian of the image (u nonlocal (weights based on Hessian)) in which small scale features have been removed (more precisely, u should be piecewise linear since the model involves second order penalization) and the auxiliary function v_2 that maps the fine structures of u. Function v_2 discriminates properly edges (i.e. discontinuities in the image function) that appear in light gray, from creases and filaments (i.e. road network here) that appear in dark gray. Small scale features are assimilated to oscillatory patterns having small G-norm and are thus well-captured in the $v = \operatorname{div} \vec{g}$ component (e.g., the rows in the fields are clearly extracted). The road network is clearly detected, while noise and texture are left in the $v = \operatorname{div} \vec{g}$ component. The most sensitive parameters are those related to regularization, namely ρ, α and β. The smaller parameters α and β are, the more edges/creases are present in the auxiliary function v_2. Parameter ρ acts on the thickness of the contours and on the range of function v_2: the higher ρ is, the closer to the value one contours representing fine structures are. Parameter ε also plays on the thickness and intensity of the contours, and is always set between 0.5 and 1. These elements are exemplified in Figure 5.7 where various sets of parameters have been tested with our local implementation.

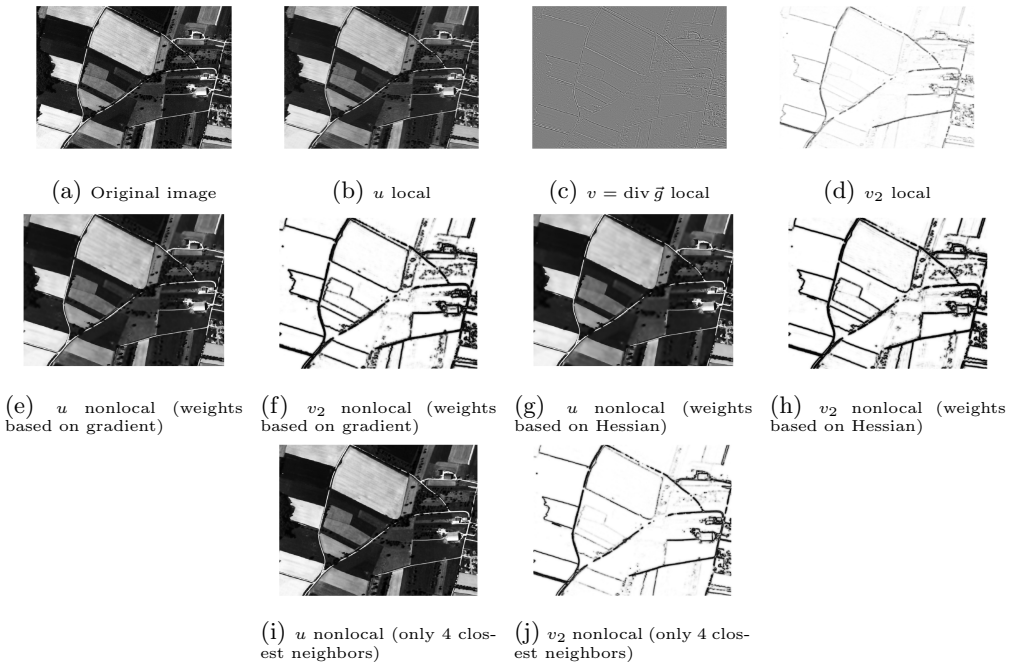

(a) Original image (b) u local (c) $v = \operatorname{div} \vec{g}$ local (d) v_2 local

(e) u nonlocal (weights based on gradient) (f) v_2 nonlocal (weights based on gradient) (g) u nonlocal (weights based on Hessian) (h) v_2 nonlocal (weights based on Hessian)

(i) u nonlocal (only 4 closest neighbors) (j) v_2 nonlocal (only 4 closest neighbors)

Figure 5.6: Road network extraction on an aerial scene: local: $\mu = 8$, $\xi_\varepsilon = 0$, $\alpha = \beta = 0.5$, $\rho = 5$, $\varepsilon = 0.5$, $\gamma = 0.5$, 10 iterations; nonlocal (weights based on Hessian): $\mu = 0.0001$, $\xi_\varepsilon = 3.5$, $\alpha = 0.14$, $\beta = 0.07$, $\rho = 3.5$, $\varepsilon = 1.0$, $\gamma = 1.0$, $w = 15$, $m = 7$, 450 iterations; nonlocal (only 4 closest neighbors): $\mu = 0.0001$, $\xi_\varepsilon = 3.5$, $\alpha = 0.14$, $\beta = 0.07$, $\rho = 3.5$, $\varepsilon = 1.0$, $\gamma = 1.0$, 450 iterations; nonlocal (weights based on gradient): $\mu = 0.0001$, $\xi_\varepsilon = 3.5$, $\alpha = 0.06$, $\beta = 0.03$, $\rho = 3.5$, $\varepsilon = 1.0$, $\gamma = 1.0$, $w = 15$, $m = 7$, 1250 iterations.

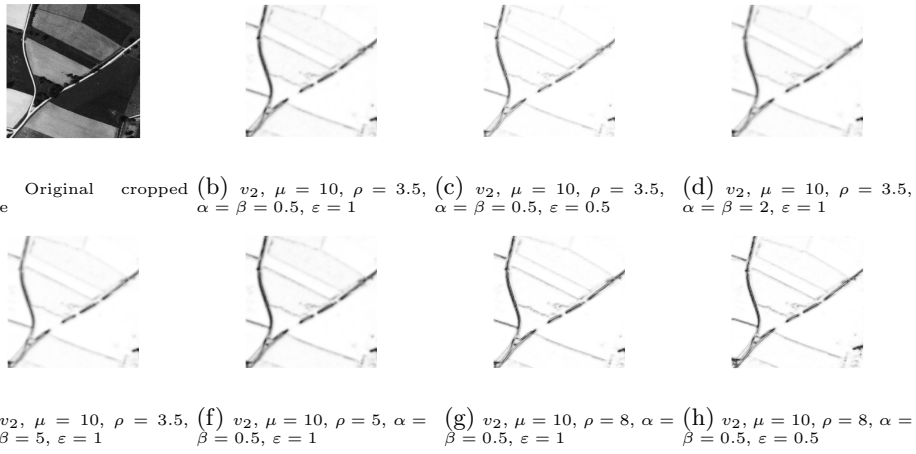

(a) Original image cropped (b) v_2, $\mu = 10$, $\rho = 3.5$, $\alpha = \beta = 0.5$, $\varepsilon = 1$ (c) v_2, $\mu = 10$, $\rho = 3.5$, $\alpha = \beta = 0.5$, $\varepsilon = 0.5$ (d) v_2, $\mu = 10$, $\rho = 3.5$, $\alpha = \beta = 2$, $\varepsilon = 1$

(e) v_2, $\mu = 10$, $\rho = 3.5$, $\alpha = \beta = 5$, $\varepsilon = 1$ (f) v_2, $\mu = 10$, $\rho = 5$, $\alpha = \beta = 0.5$, $\varepsilon = 1$ (g) v_2, $\mu = 10$, $\rho = 8$, $\alpha = \beta = 0.5$, $\varepsilon = 1$ (h) v_2, $\mu = 10$, $\rho = 8$, $\alpha = \beta = 0.5$, $\varepsilon = 0.5$

Figure 5.7: Road network extraction on an aerial scene: effect of the parameters on the component v_2 with the local algorithm.

We compare our results with those obtained by Aubert and Drogoul [8, 30] with the topological gradient (Figure 5.8). We first observe that the topological gradient has the tendency to oversmooth the contours. Second, it does not properly discriminate the edges from the filaments and creases in terms of intensity for instance. At last, even if we tuned the algorithm adequately (in particular, a weighting parameter in their model influences the size of the detected structures), our algorithm detects more accurately the center of the road network. Another illustration devoted to filament/vessel-like structure detection is

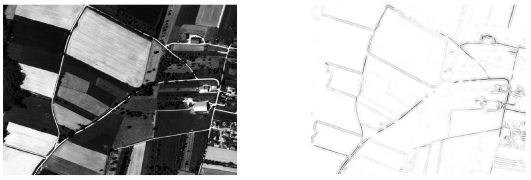

(a) Original image (b) Structures detected by the topological indicator

Figure 5.8: Road network extraction on an aerial scene with Aubert and Drogoul's topological gradient method.

provided on Figure 5.9 (size 338×436) and focuses on dendrite and axon detection (courtesy of A. Drogoul, `https://sites.google.com/site/drogoulaudric/recherche`). The skeleton of the dendrite network is well recovered, with in particular strong intensity in the middle of the dendrites. Also, to emphasize the role of the decomposition, we display the v_2 component when $\vec{g}$ and Q are removed from the local model: we observe that spurious details (not related to filament structures) spoil this constituent. We now apply the proposed algorithm to crack detection, both on Figure 5.10 (size 501×501) and 5.11 (size 285×429), courtesy of A. Drogoul. We depict the three main components of the decomposition/segmentation, i.e., u, $v = \operatorname{div} \vec{g}$, v_2, for the local model and u and v_2, for the three versions of our nonlocal algorithm, as well as the results obtained with Aubert and Drogoul's topological gradient method. The cracks are correctly enhanced, the oscillatory patterns are well captured by the $v = \operatorname{div} \vec{g}$ component. Again, the role of the decomposition part of the algorithm is highlighted (Figure 5.10) by depicting the obtained v_2 component when decomposition is turned off in our local implementation (spurious details are visible on the top of the image). Also, the linear piecewise nature of the component u in Figure 5.11 is properly returned.

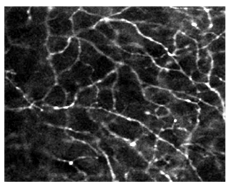

(a) Original image

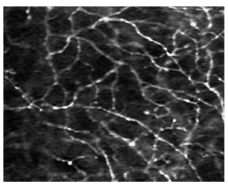

(b) u local

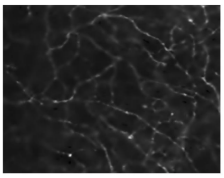

(c) u nonlocal (weights based on gradient)

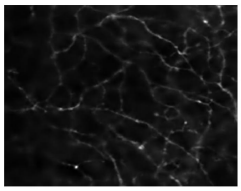

(d) u nonlocal (weights based on Hessian)

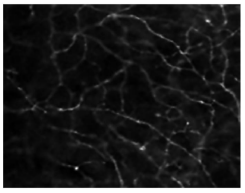

(e) u nonlocal (only 4 closest neighbors)

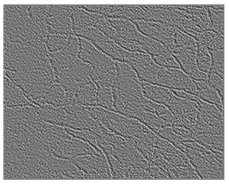

(f) $v = \operatorname{div} \vec{g}$ local

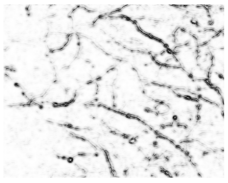

(g) v_2 local

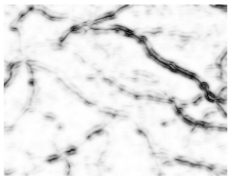

(h) v_2 local, zoom on a region of the image

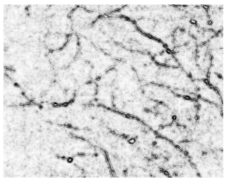

(i) v_2 local, when no decomposition is applied

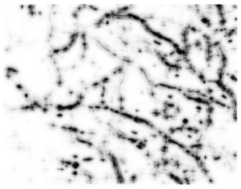

(j) v_2 nonlocal (weights based on gradient)

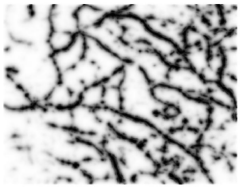

(k) v_2 nonlocal (weights based on Hessian)

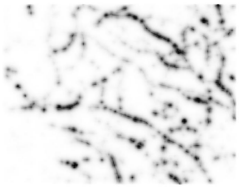

(l) v_2 nonlocal (only 4 closest neighbors)

Figure 5.9: Dendrite and axon extraction: $\mu = 1$, $\xi_\varepsilon = 0$, $\alpha = \beta = 0.1$, $\rho = 3.5$, $\varepsilon = 0.5$, $\gamma = 5$, 20 iterations; nonlocal (weights based on Hessian): $\mu = 0.0001$, $\xi_\varepsilon = 3.5$, $\alpha = 0.016$, $\beta = 0.008$, $\rho = 3.5$, $\varepsilon = 1.5$, $\gamma = 1.0$, $w = 15$, $m = 7$, 330 iterations; nonlocal (only 4 closest neighbors): $\mu = 0.0001$, $\xi_\varepsilon = 3.5$, $\alpha = 0.016$, $\beta = 0.008$, $\rho = 3.5$, $\varepsilon = 1.5$, $\gamma = 1.0$, 330 iterations; nonlocal (weights based on gradient): $\mu = 0.0001$, $\xi_\varepsilon = 3.5$, $\alpha = 0.016$, $\beta = 0.08$, $\rho = 3.5$, $\varepsilon = 1.0$, $\gamma = 1.0$, $w = 15$, $m = 7$, 500 iterations.

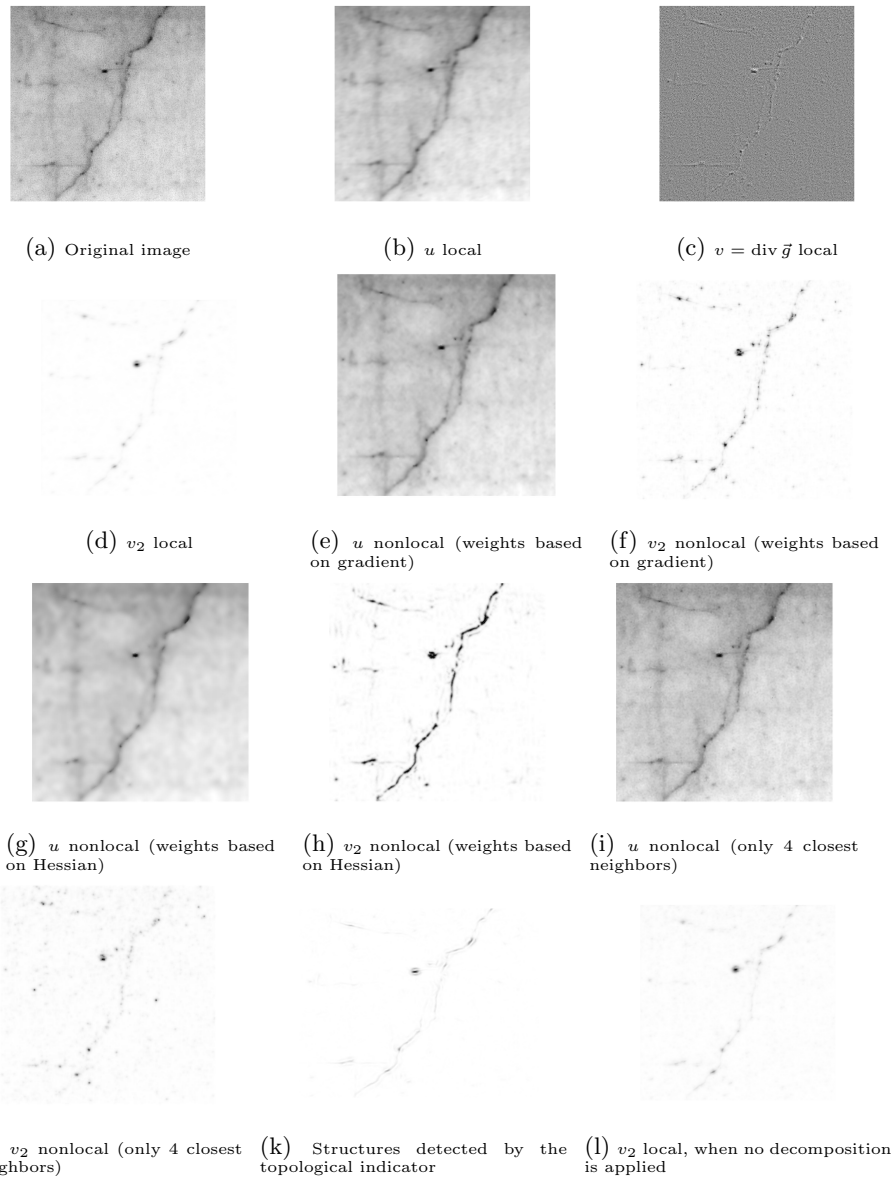

(a) Original image (b) u local (c) $v = \operatorname{div} \vec{g}$ local

(d) v_2 local (e) u nonlocal (weights based on gradient) (f) v_2 nonlocal (weights based on gradient)

(g) u nonlocal (weights based on Hessian) (h) v_2 nonlocal (weights based on Hessian) (i) u nonlocal (only 4 closest neighbors)

(j) v_2 nonlocal (only 4 closest neighbors) (k) Structures detected by the topological indicator (l) v_2 local, when no decomposition is applied

Figure 5.10: Crack detection: $\mu = 0.001$, $\xi_\varepsilon = 3.5$, $\alpha = 0.14$, $\beta = 0.07$, $\rho = 3.5$, $\varepsilon = 1$, $\gamma = 0.5$, 50 iterations; nonlocal (weights based on Hessian): $\mu = 0.0001$, $\xi_\varepsilon = 3.5$, $\alpha = 0.14$, $\beta = 0.07$, $\rho = 3.5$, $\varepsilon = 1.5$, $\gamma = 1.0$, $w = 15$, $m = 7$, 550 iterations; nonlocal (only 4 closest neigbors): $\mu = 0.0001$, $\xi_\varepsilon = 3.5$, $\alpha = 0.06$, $\beta = 0.03$, $\rho = 3.5$, $\varepsilon = 1.5$, $\gamma = 1.0$, 550 iterations; nonlocal (weights based on gradient): $\mu = 0.0001$, $\xi_\varepsilon = 3.5$, $\alpha = 0.06$, $\beta = 0.03$, $\rho = 3.5$, $\varepsilon = 1.0$, $\gamma = 1.0$, $w = 9$, $m = 5$, 1000 iterations.

(a) Original image

(b) u local

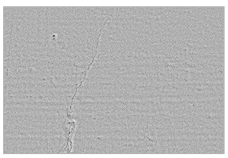

(c) $v = \operatorname{div} \vec{g}$ local

(d) v_2 local

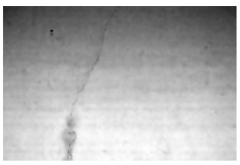

(e) u nonlocal (weights based on gradient)

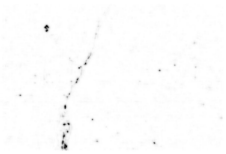

(f) v_2 nonlocal (weights based on gradient)

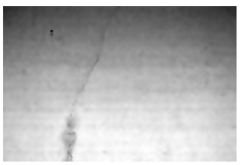

(g) u nonlocal (weights based on Hessian)

(h) v_2 nonlocal (weights based on Hessian)

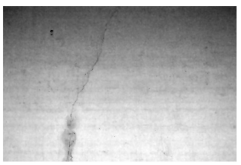

(i) u nonlocal (only 4 closest neighbors)

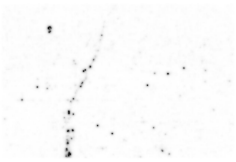

(j) v_2 nonlocal (only 4 closest neighbors)

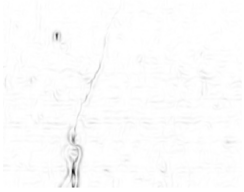

(k) Structures detected by the topological indicator

Figure 5.11: Crack detection: $\mu = 0.001$, $\xi_\varepsilon = 3.5$, $\alpha = 0.14$, $\beta = 0.07$, $\rho = 3.5$, $\varepsilon = 1$, $\gamma = 0.5$, 50 iterations; nonlocal (weights based on Hessian): $\mu = 0.0001$, $\xi_\varepsilon = 1.0$, $\alpha = 0.06$, $\beta = 0.03$, $\rho = 1.0$, $\varepsilon = 1.5$, $\gamma = 1.0$, $w = 15$, $m = 7$, 750 iterations; nonlocal (only 4 closest neighbors): $\mu = 0.0001$, $\xi_\varepsilon = 1.0$, $\alpha = 0.06$, $\beta = 0.03$, $\rho = 1.0$, $\varepsilon = 1.5$, $\gamma = 1.0$, 330 iterations; nonlocal (weights based on gradient): $\mu = 0.0001$, $\xi_\varepsilon = 3.5$, $\alpha = 0.06$, $\beta = 0.03$, $\rho = 3.5$, $\varepsilon = 1.0$, $\gamma = 1.0$, $w = 9$, $m = 5$, 1000 iterations.

We conclude the paper with two applications dedicated to crack detection on bituminous surfacing Figure 5.13 (size 231 × 650) and 5.14 (size 201 × 640), courtesy of CEREMA, France. The two considered slices of bitumen, in addition to long and thin cracks, exhibit high oscillatory patterns and white spots of varying sizes, which makes the straight application of our algorithm difficult. Indeed, in terms of scale, the crack and some of these spots could be comparable and could not be properly discriminated, resulting in superfluous information in the v_2 component. Think for instance of a white spot assimilated to a ball of radius 2 pixels (—if the image domain is the $n \times n$ discretized unit square, then the scale behaves like $\frac{1}{n}$—), and of a long thin crack of width 2 pixels and length k pixels ($k \gg 1$) leading to a similar scale. To circumvent this issue, a pre-processing step is applied. It consists in apprehending the problem first as an inpainting one ([1]), and by considering these white spots as missing parts of the image that need to be filled. This is achieved with the MATLAB® function **imfill** (`https://fr.mathworks.com/help/images/ref/imfill.html` —to fill holes in a grayscale image) applied to the inverse image, yielding an image that serves as input of our algorithm. In both cases, the cracks are well recovered in the v_2 component which does not include superfluous information. The edge detector v_1 also recovers parts of the crack but contains spurious information regarding the problem we address, such as asphalt defect boundaries. It thus justifies the use of a second order method.
Besides, Figure 5.13-(g)-(h)-(i) and 5.14-(g)-(h)-(i) are the results obtained by minimizing the elliptic approximation of the Blake-Zisserman functional that is to say without considering the decomposition part. Thanks to Figure 5.13-(j)-(k)-(l) and 5.14-(j)-(k)-(l) showing the absolute difference between both results, we observe that u is less noisy with our method, v_1 and v_2 also exhibit better contrast with less superfluous information. The results obtained with the three versions of our nonlocal algorithm are comparable with the ones obtained with our local implementation.
We also compare our results with the ones obtained by thresholding the image. It appears that the crack is even more spotty than with our method and there is more superfluous information or the crack is not entirely recovered. Furthermore, the contrast is lower. The value of the threshold t has been chosen to get a compromise between recovering the whole crack and having the least residual noise.

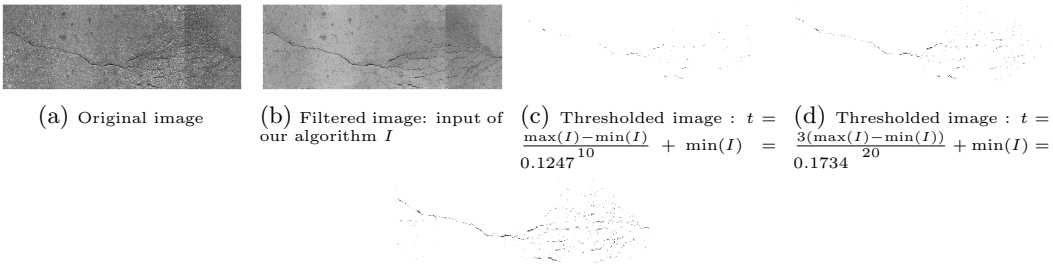

(a) Original image

(b) Filtered image: input of our algorithm I

(c) Thresholded image : $t = \frac{\max(I)-\min(I)}{10} + \min(I) = 0.1247$

(d) Thresholded image : $t = \frac{3(\max(I)-\min(I))}{20} + \min(I) = 0.1734$

(e) Thresholded image : $t = \frac{2(\max(I)-\min(I))}{10} + \min(I) = 0.2221$

Figure 5.12: Crack detection by thresholding the original image.

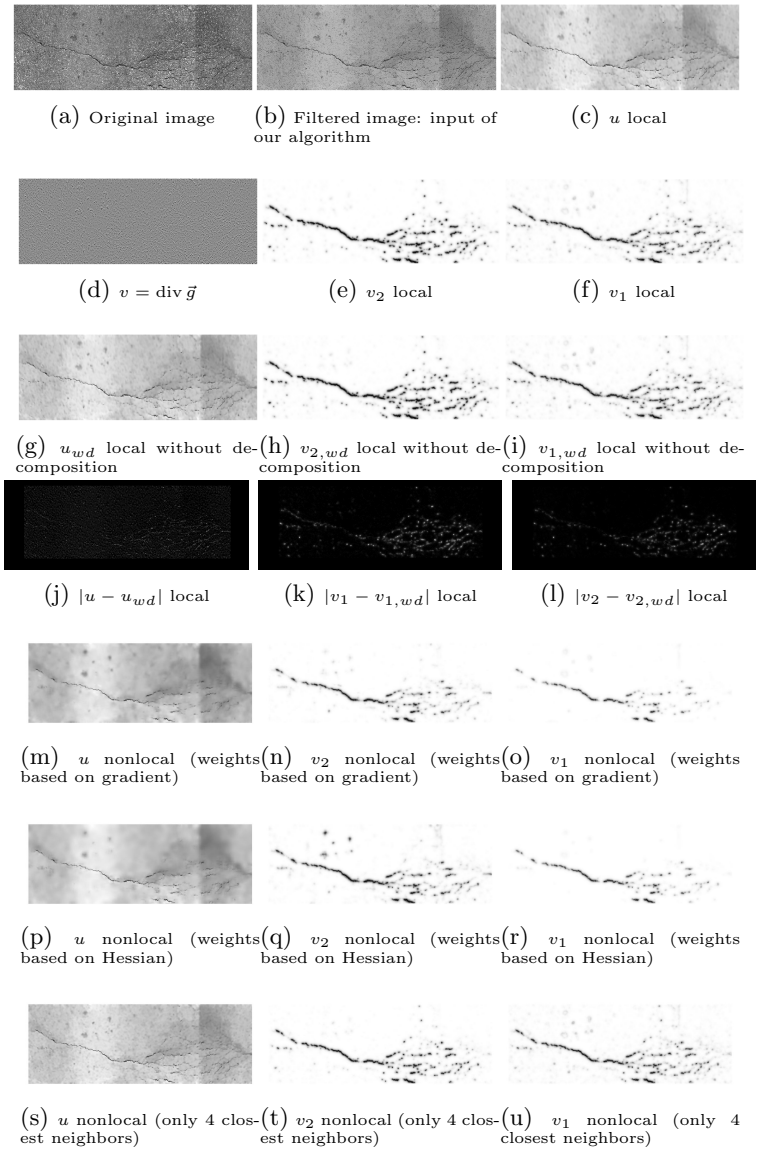

(a) Original image (b) Filtered image: input of our algorithm (c) u local

(d) $v = \operatorname{div} \vec{g}$ (e) v_2 local (f) v_1 local

(g) u_{wd} local without decomposition (h) $v_{2,wd}$ local without decomposition (i) $v_{1,wd}$ local without decomposition

(j) $|u - u_{wd}|$ local (k) $|v_1 - v_{1,wd}|$ local (l) $|v_2 - v_{2,wd}|$ local

(m) u nonlocal (weights based on gradient) (n) v_2 nonlocal (weights based on gradient) (o) v_1 nonlocal (weights based on gradient)

(p) u nonlocal (weights based on Hessian) (q) v_2 nonlocal (weights based on Hessian) (r) v_1 nonlocal (weights based on Hessian)

(s) u nonlocal (only 4 closest neighbors) (t) v_2 nonlocal (only 4 closest neighbors) (u) v_1 nonlocal (only 4 closest neighbors)

Figure 5.13: Crack detection: $\mu = 0.0001$, $\xi_\varepsilon = 3.5$, $\alpha = 0.14$, $\beta = 0.07$, $\rho = 3.5$, $\varepsilon = 1$, $\gamma = 0.9$, 270 iterations; nonlocal (weights based on Hessian): $\mu = 0.0001$, $\xi_\varepsilon = 3.5$, $\alpha = 0.14$, $\beta = 0.07$, $\rho = 3.5$, $\varepsilon = 1.0$, $\gamma = 1.0$, $w = 15$, $m = 7$, 500 iterations; nonlocal (only 4 closest neighbors): $\mu = 0.0001$, $\xi_\varepsilon = 3.5$, $\alpha = 0.14$, $\beta = 0.07$, $\rho = 3.5$, $\varepsilon = 1.0$, $\gamma = 1.0$, 500 iterations; nonlocal (weights based on gradient): $\mu = 0.0001$, $\xi_\varepsilon = 3.5$, $\alpha = 0.14$, $\beta = 0.07$, $\rho = 3.5$, $\varepsilon = 1.0$, $\gamma = 1.0$, $w = 9$, $m = 3$, 500 iterations.

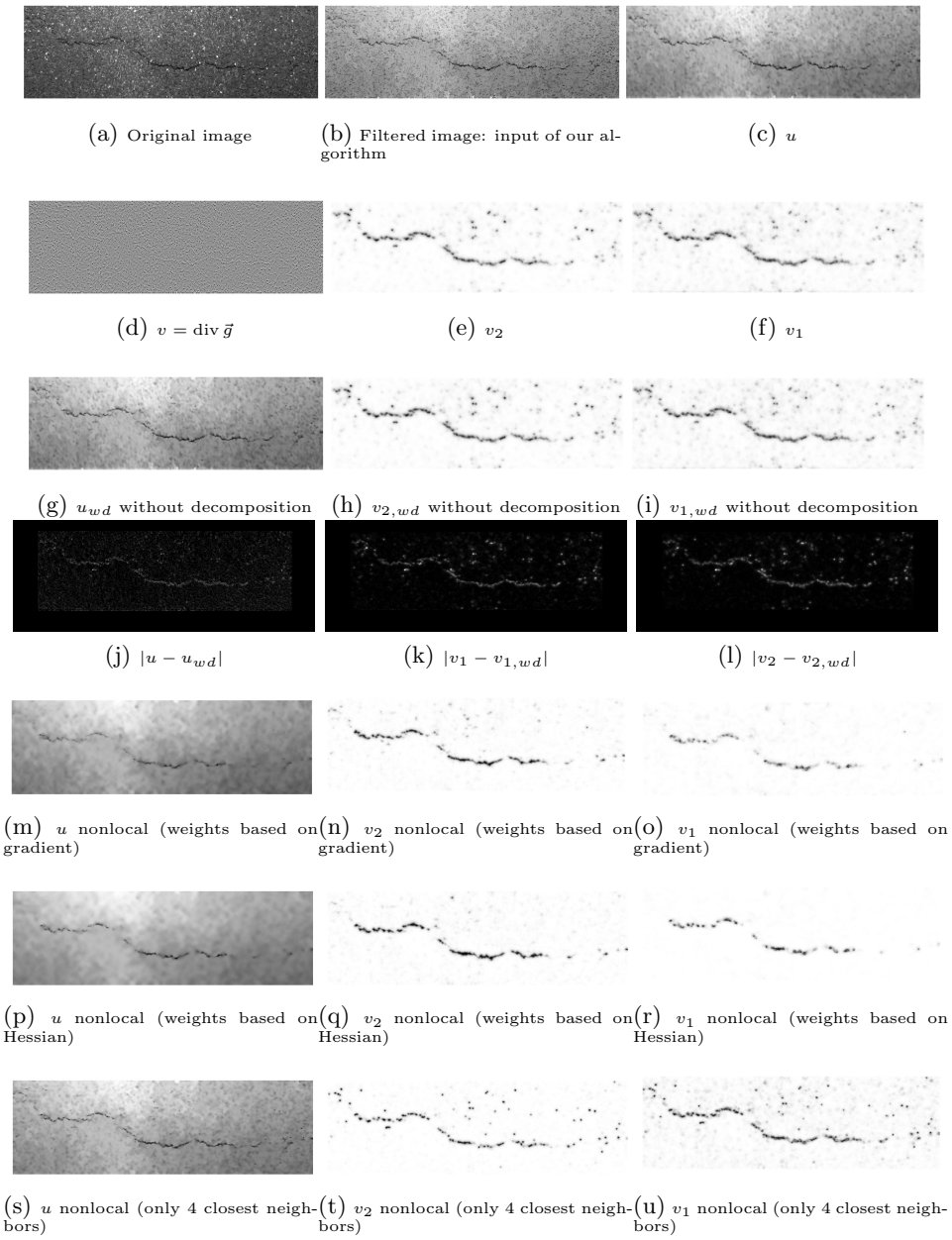

(a) Original image (b) Filtered image: input of our algorithm (c) u

(d) $v = \operatorname{div} \vec{g}$ (e) v_2 (f) v_1

(g) u_{wd} without decomposition (h) $v_{2,wd}$ without decomposition (i) $v_{1,wd}$ without decomposition

(j) $|u - u_{wd}|$ (k) $|v_1 - v_{1,wd}|$ (l) $|v_2 - v_{2,wd}|$

(m) u nonlocal (weights based on gradient) (n) v_2 nonlocal (weights based on gradient) (o) v_1 nonlocal (weights based on gradient)

(p) u nonlocal (weights based on Hessian) (q) v_2 nonlocal (weights based on Hessian) (r) v_1 nonlocal (weights based on Hessian)

(s) u nonlocal (only 4 closest neighbors) (t) v_2 nonlocal (only 4 closest neighbors) (u) v_1 nonlocal (only 4 closest neighbors)

Figure 5.14: Crack detection: $\mu = 0.001$, $\xi_\varepsilon = 2.5$, $\alpha = 0.1$, $\beta = 0.05$, $\rho = 2.5$, $\varepsilon = 1$, $\gamma = 0.9$, 270 iterations; nonlocal (weights based on Hessian): $\mu = 0.0001$, $\xi_\varepsilon = 3.5$, $\alpha = 0.14$, $\beta = 0.07$, $\rho = 3.5$, $\varepsilon = 1.0$, $\gamma = 1.0$, $w = 9$, $m = 3$, 500 iterations; nonlocal (only 4 closest neighbors): $\mu = 0.0001$, $\xi_\varepsilon = 3.5$, $\alpha = 0.14$, $\beta = 0.07$, $\rho = 3.5$, $\varepsilon = 1.0$, $\gamma = 1.0$, 500 iterations; nonlocal (weights based on gradient): $\mu = 0.0001$, $\xi_\varepsilon = 4.5$, $\alpha = 0.14$, $\beta = 0.07$, $\rho = 4.5$, $\varepsilon = 1.0$, $\gamma = 1.0$, $w = 15$, $m = 7$, 2000 iterations.

Bibliography

[1] R. D. Adam, P. Peter, and J. Weickert, *Denoising by inpainting*, in Lauze, F., Dong, Y., Dahl, A. B. (eds) Scale Space and Variational Methods in Computer Vision: 6th International Conference, SSVM 2017, Kolding, Denmark, June 4-8, 2017, 2017, pp. 121–132.

[2] L. Ambrosio, L. Faina, and R. March, *Variational approximation of a second order free discontinuity problem in computer vision*, SIAM J. Math. Anal., 32 (2001), pp. 1171–1197.

[3] L. Ambrosio and V. M. Tortorelli, *Approximation of functionals depending on jumps by elliptic functionals via* Γ*-convergence*, Commun. Pur. Appl. Math., 43 (1990), pp. 999–1036.

[4] L. Ambrosio and V. M. Tortorelli, *On the approximation of free discontinuity problems*, B. Unione Mat. Ital., (1992), pp. 105–123.

[5] G. Aronsson, M. Crandall, and P. Juutinen, *A tour of the theory of absolutely minimizing functions*, B. Am. Math. Soc., 41 (2004), pp. 439–505.

[6] G. Aubert and J.-F. Aujol, *Modeling very oscillating signals. Applications to image processing*, Appl. Math. Opt., 51 (2005), pp. 163–182.

[7] G. Aubert, J.-F. Aujol, and L. Blanc-Féraud, *Detecting codimension–two objects in an image with Ginzburg-Landau models*, Int. J. Comput. Vision, 65 (2005), pp. 29–42.

[8] G. Aubert and A. Drogoul, *Topological gradient for a fourth order operator used in image analysis*, ESAIM: COCV, 21 (2015), pp. 1120–1149.

[9] G. Aubert and P. Kornprobst, *Can the nonlocal characterization of Sobolev spaces by Bourgain et al. be useful for solving variational problems?*, SIAM J. Numer. Anal., 47 (2009), pp. 844–860.

[10] A. Baudour, G. Aubert, and L. Blanc-Féraud, *Detection and completion of filaments: A vector field and PDE approach*, in Sgallari, F., Murli, A., Paragios, N. (eds.) SSVM 2007. LNCS, vol. 4485, 2007, pp. 451–460.

[11] M. Bergounioux and L. Piffet, *A second-order model for image denoising*, Set-valued var. anal., 18 (2010), pp. 277–306.

[12] M. Bergounioux and D. Vicente, *Parameter selection in a Mumford-Shah geometrical model for the detection of thin structures*, Acta Appl. Math., 141 (2016), pp. 17–48.

[13] D. Berkovitz, L., *Lower semicontinuity of integral functionals*, Trans. AMS, 192 (1974), pp. 51–57.

[14] A. Blake and A. Zisserman, *Visual Reconstruction*, MIT Press, Cambridge, 1989.

[15] J. Boulanger, P. Elbau, C. Pontow, and O. Scherzer, *Non-local functionals for imaging*, in Bauschke, H. H., Burachik, R. S., Combettes, P. L., Elser, V., Luke, D. R., Wolkowicz, H. (eds) Fixed-Point Algorithms for Inverse Problems in Science and Engineering, 2011, pp. 131–154.

[16] J. Bourgain, H. Brezis, and P. Mironescu, *Another look at Sobolev spaces*, in Menaldi, J. L., Rofman, E., Sulem, A. (eds) Optimal Control and Partial Differential Equations, in honour of Professor Alain Bensoussan's 60^{th} Birthday, 2001, pp. 439–455.

[17] K. Bredies, K. Kunisch, and T. Pock, *Total generalized variation*, SIAM J. Imaging Sci., 3 (2010), pp. 492–526.

[18] H. Brezis, *Analyse fonctionnelle*, Dunod Paris, 2005.

[19] A. Buades, B. Coll, and J.-M. Morel, *A non-local algorithm for image denoising*, Computer Vision and Pattern Recognition, 2 (2005), pp. 60–65.

[20] X. Cai, *Variational image segmentation model coupled with image restoration achievements*, Pattern Recognit., 48 (2015), pp. 2029–2042.

[21] M. Carriero, A. Leaci, and F. Tomarelli, *A second order model in image segmentation: Blake & Zisserman functional*, in Variational Methods for Discontinuous Structures: Applications to image segmentation, continuum mechanics, homogenization, Birkhäuser Basel, 1996, pp. 57–72.

[22] M. Carriero, A. Leaci, and F. Tomarelli, *Free gradient discontinuity and image inpainting*, J. Math. Sci., 181 (2012), pp. 805–819.

[23] V. Caselles, J.-M. Morel, and C. Sbert, *An axiomatic approach to image interpolation*, IEEE T. Image Process., 7 (1998), pp. 376–386.

[24] A. Chambolle and P. L. Lions, *Image recovery via total variation minimization and related problems*, Numer. Math., 76 (1997), pp. 167–188.

[25] T. Chan, S. H. Kang, and J. Shen, *Euler's elastica and curvature-based inpainting*, SIAM J. Appl. Math., 63 (2002), pp. 564–592.

[26] T. Chan, A. Marquina, and P. Mulet, *High-order total variation-based image restoration*, SIAM J. Sci. Comput., 22 (2001), pp. 503–516.

[27] G. Crandall, M., H. Ishii, and P.-L. Lions, *User's guide to viscosity solutions of second order partial differential equations*, Bulletin of the American Mathematical Society, 27 (1992), pp. 1–67.

[28] J. Dávila, *On an open question about functions of bounded variation*, Calc. Var. Partial Differential Equations, 15 (2002).

[29] F. Demengel and G. Demengel, *Functional Spaces for the Theory of Elliptic Partial Differential Equations*, Springer London, 2012.

[30] A. Drogoul, *Numerical analysis of the topological gradient method for fourth order models and applications to the detection of fine structures in imaging*, SIAM J. Imaging Sci., 7 (2014), pp. 2700–2731.

[31] C. Evans, L. and F. Gariepy, R., *Measure Theory and Fine Properties of Functions*, Studies in advanced mathematics, 1992.

[32] N. Forcadel, *Dislocation dynamics with a mean curvature term: Short time existence and uniqueness*, Differ. Integral Equ., 21 (2008), pp. 285–304.

[33] G. Gilboa and S. Osher, *Nonlocal operators with applications to image processing*, Multiscale Model. Simul., 7 (2008), pp. 1005–1028.

[34] J. Lellman, K. Papafitsoros, C. Schönlieb, and D. Spector, *Analysis and application of a non-local hessian*, SIAM J. Imaging Sci., 8 (2015), pp. 2161–2202.

[35] Y. Meyer, *Oscillating Patterns in Image Processing and Nonlinear Evolution Equations*, vol. 32, Amer. Math. Soc., 2002.

[36] D. Mumford and J. Shah, *Optimal approximations by piecewise smooth functions and associated variational problems*, Commun. Pur. Appl. Math., 42 (1989), pp. 577–685.

[37] O. Nemitz, M. Rumpf, T. Tasdizen, and R. Whitaker, *Anisotropic curvature motion for structure enhancing smoothing of 3D MR angiography data*, J. Math. Imaging Vis., 27 (2007), pp. 217–229.

[38] C. Ponce, A., *A new approach to Sobolev spaces and connections to* Γ*-convergence*, Calc. Var. Partial Differential Equations, 19 (2004), pp. 229–255.

[39] M. Rochery, I. Jermyn, and J. Zerubia, *Higher order active contours*, Int. J. Comput. Vision, 69 (2005), pp. 27–42.

[40] D. Spector, *Characterization of Sobolev and BV Spaces*, PhD thesis, 2011. Carnegie Mellon University.

[41] R. Stoica, X. Descombes, and J. Zerubia, *A Gibbs point process for road extraction from remotely sensed images*, Int. J. Comput. Vision, 57 (2004), pp. 121–136.

[42] G. Strang, *L^1 and L^∞ approximation of vector fields in the plane.*, in Nonlinear Partial Differential Equations in Applied Science, The U.S.-Japan Seminar, 1982, pp. 273–288.

[43] F. Zana and J.-C. Klein, *Segmentation of vesell-like patterns using mathematical morphology and curvature evaluation*, IEEE T. Image Process., 10 (2001), pp. 1010,1019.

[44] M. Zanetti and A. Vitti, *The Blake-Zisserman model for digital surface models segmentation*, in ISPRS Workshop Laser Scanning 2013, ISPRS Annals of the Photogrammetry, Remote Sensing and Spatial Information Sciences, 2013, pp. 355–360.

Chapter 6

Conclusion and perspectives

In this thesis, we have introduced the problems of image registration, image segmentation, and image decomposition/denoising and have proposed to address them jointly into a single framework. As they are closely related, we believe that they can take advantage of each other leading to their reinforcement and to fewer drawbacks than when taken separately.

We have first proposed a registration model guided by topology-preserving segmentation results in a nonlinear elasticity setting. The alignment of the evolving shape implicitly modelled by a level-set function with intermediate topology-preserving segmentation results ([5]) drives the registration process as a fidelity term. Both theoretical results and numerical experiments have been provided. New perspectives have also been suggested to enlarge this work. One is to introduce dynamics into the model and so to consider it as continuous in time instead of taking samples in time. The existence of minimizers for this problem has been proved on a Sobolev space of Banach-space-valued functions but the implementation remains a work in progress. The other one is to couple the segmentation and the registration tasks rather than to consider a segmentation-guided registration model. A substitute for $\Phi_0 \circ \varphi$ is incorporated in the topology-preserving model and the interaction is made through an L^2-penalization involving the mutual influence of both tasks. It inherits good theoretical properties in the context of the viscosity solution theory.

Then, we have developed a joint segmentation/registration model giving additionally a decomposition of the Reference image into a cartoon-like image and an oscillatory part. The fidelity term is composed of three expressions, namely the weighted total variation aiming to align the edges of the deformed Template to the ones of the Reference, a nonlocal shape descriptor inspired by the Chan-Vese model for segmentation matching the homogeneous regions of the deformed Template with the ones of the Reference, and a classical sum of square distances locally comparing the intensity levels of the deformed Template with the ones of the Reference. As for the regularization of the transformation, it relies on the stored energy function of a Saint-Venant Kirchhoff material and a term penalizing large volume changes. Many theoretical results legitimate our model and a thorough comparison of our results with the ones obtained by previous models has been made. However, one

of its main drawback is that it has been designed for 2D images and cannot be extended to 3D images straightforwardly. A perspective of work in this direction would be to replace our regularizer by another one derived from an isotropic, homogeneous, hyperelastic material, such as Cialet-Geymonat or Ogden materials, stored energy function. Indeed, for such materials, the energy appears to be polyconvex and therefore lifts the theoretical limitation of our model. However, the numerical implementation becomes more challenging due to the apparition of $\mathrm{Cof}\,\nabla\varphi$ matrix. Based on Negrón Marrero's work [7], one way of dealing with this highly nonlinear term would be to introduce an auxiliary variable V simulating the Jacobian of the deformation and to solve the problem under the equality constraint $\mathrm{Cof}\,V = \mathrm{Cof}\,\nabla\varphi$.

In the last chapter, we have addressed a slightly different issue but still combining several image processing tasks in a single framework. In order to recover very thin structures, namely cracks on bituminous surface images, we have studied a second order variational model based on the elliptic approximation of the Blake-Zisserman functional ([1]) and on a decomposition model using Meyer's G norm ([6]). We then have looked into a nonlocal version of this model leading to both theoretical and numerical results. We have carried out a comparison of our results with the ones of Drogoul's model [3] designed to detect fine structures in images and showed that including the decomposition part actually gives better results. Then an MPI parallelization of the code has been done to improve the computational efficiency. A perspective of work would be to further investigate the weights to be applied in the nonlocal code. We could consider some weights enabling us to regularize the image far from the crack but not close to it based on the response obtained by the vessel-detection filter developed by Frangi *et al.* [4] for example. We could also think of a slightly different model in which we replace the L^2 norm by an L^1 norm applied to the nonlocal Laplacian. Besides, the CEREMA is interested in a measure of the crack length and so a lead of work in this direction is to connect the fragments of cracks we recover. Indeed, for the time being, our segmentation of the crack is very discontinuous and we would like to do a post-processing step to connect these different pieces. One way of doing that would be to apply a diffusion term along the direction of the crack depicted by the eigen vector associated with the highest eigen value of the Hessian matrix. We would also like to remove the residual noise appearing in v_2. To address this issue, one can think of using a blob-detection like filter and then considering these blobs as missing data in an inpainting algorithm.

Another perspective of work related to the registration problem is to introduce some landmark information given by an expert as hard constraints in order to improve the quality of the registration in the regions of interest. Using Lagrangian multipliers in a finite element setting enables us to exactly interpolate the landmark constraints. We have started some preliminary theoretical investigations, based on [8] and [10], on the existence of Lagrange multipliers, the existence and uniqueness of solutions and the invertibility of the rigidity matrix for both a solely registration-based model and a joint segmentation and registration model. A numerical implementation of these models is still a work in progress.

The last perspective of work I am going to mention here is a theoretically 3D friendly joint segmentation and registration model based on the Potts model for segmentation and the stored energy function of an Ogden material inspired by [9], [12], and [2]. It is meant to be applied on a whole database of medical images. Every single image is registered to the mean image of the database. This Reference is then refined by taking the mean image of the deformed database we have obtained. The last step consists in polishing the segmentation and the registration results by using a model inspired by [13] to register the deformed database to this new Reference. We could also consider a joint segmentation/registration/shape averaging model based on [11, Chapter 4].

Bibliography

[1] L. Ambrosio, L. Faina, and R. March, *Variational approximation of a second order free discontinuity problem in computer vision*, SIAM J. Math. Analysis, 32 (2001), pp. 1171–1197.

[2] A. Chambolle, D. Cremers, and T. Pock, *A convex approach to minimal partitions*, SIAM Journal on Imaging Sciences, 5 (2012), pp. 1113–1158.

[3] A. Drogoul, *Numerical analysis of the topological gradient method for fourth order models and applications to the detection of fine structures in imaging*, SIAM J. Imaging Sci., 7 (2014), pp. 2700–2731.

[4] A. F. Frangi, W. J. Niessen, K. L. Vincken, and M. A. Viergever, *Multiscale vessel enhancement filtering*, in International Conference on Medical Image Computing and Computer-Assisted Intervention, Springer, 1998, pp. 130–137.

[5] C. Le Guyader and L. Vese, *Self-Repelling Snakes for Topology-Preserving Segmentation Models*, Image Processing, IEEE Transactions on, 17 (2008), pp. 767–779.

[6] Y. Meyer, *Oscillating patterns in image processing and nonlinear evolution equations: the fifteenth Dean Jacqueline B. Lewis memorial lectures*, vol. 22, American Mathematical Soc., 2001.

[7] P. Negrón Marrero, *A numerical method for detecting singular minimizers of multidimensional problems in nonlinear elasticity*, Numerische Mathematik, 58 (1990), pp. 135–144.

[8] S. Ozeré, *Modélisation mathématique de problèmes relatifs au recalage d'images*, PhD thesis, 2015. Thèse de doctorat dirigée par Gout, Christian et Le Guyader, Carole Mathématiques Rouen, INSA 2015.

[9] M. Storath and A. Weinmann, *Fast partitioning of vector-valued images*, SIAM Journal on Imaging Sciences, 7 (2014), pp. 1826–1852.

[10] S. Vieira-Teste, *Représentation de structures géologiques à l'aide de modèles déformables sous contraintes géométriques*, PhD thesis, 1997. Thèse de doctorat dirigée par Apprato, Dominique Mathématiques appliquées Pau 1997.

[11] B. Wirth, *Variational Methods in Shape Space*, PhD thesis, Universitäts-und Landesbibliothek Bonn, 2010.

[12] B. Wirth, *On the* Γ*-limit of joint image segmentation and registration functionals based on phase fields*, 18 (2016), pp. 441–477.

[13] Z. Zhang, Q. Xie, and A. Srivastava, *Elastic registration and shape analysis of functional objects*, Geometry Driven Statistics, pp. 218–238.